FOODS and raw materials

Volume 9
Issue 2
2021

ISSN 2308-4057 (print)
ISSN 2310-9599 (online)

FRM

food production technology

food production processes and equipment

biotechnology

economics

food hygiene

chemistry and ecology

standardization, certification, quality and safety

automation and informational support of technological processes

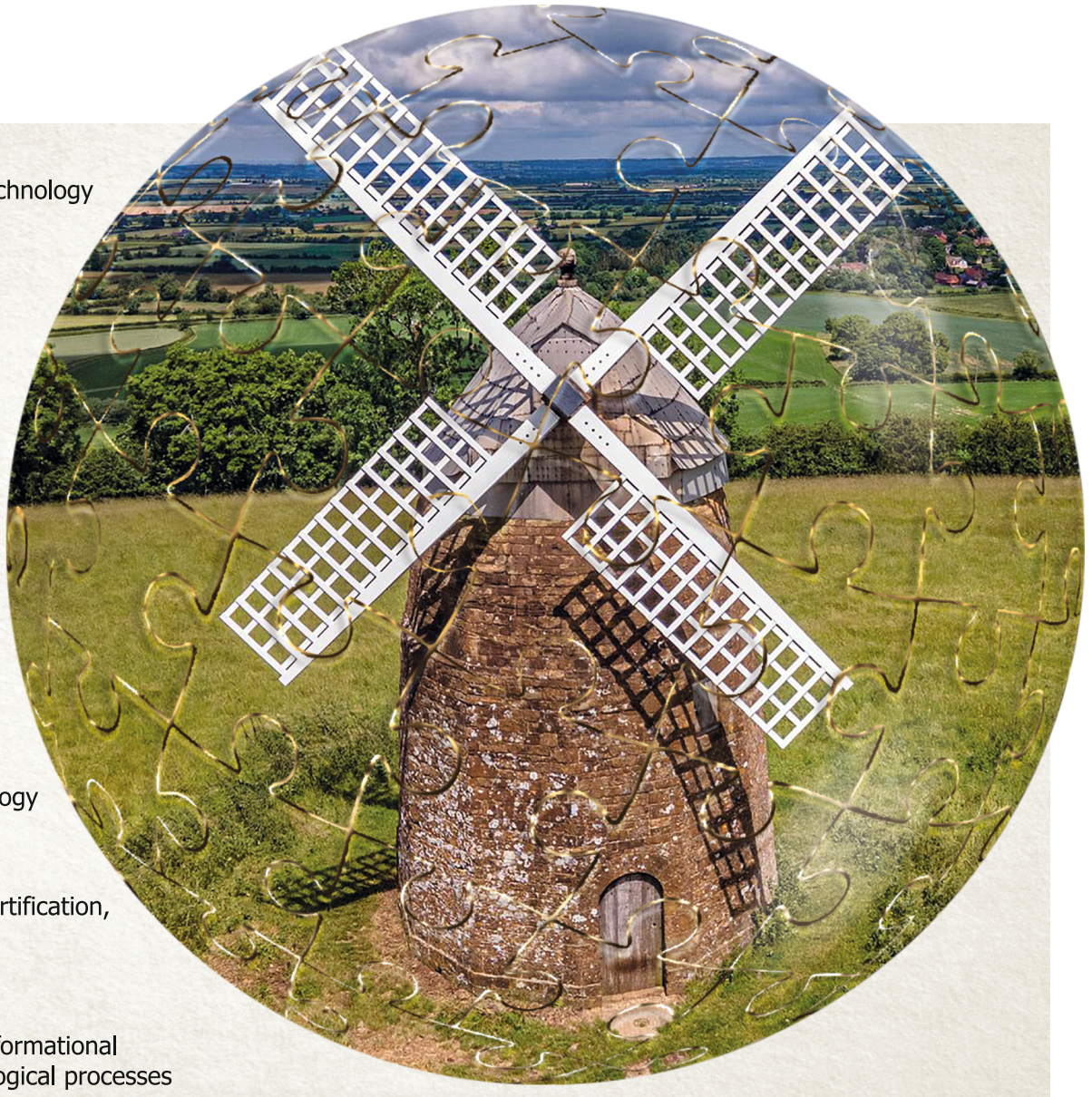

FOODS AND RAW MATERIALS

Kemerovo State University Vol. 9, no. 2, 2021

ISSN 2308-4057 (Print) ISSN 2310-9599 (Online)

The Journal covers pioneering research in the food industry and related branches. The Journal stimulates scientific communication between academia and manufacturers. The Journal publishes theoretical and empirical research papers to promote new technologies and innovative ideas, bridge the gap between regional, federal, and international scientific publications and educate qualified specialists.

The Journal publishes scientific papers, reports, peer reviews, brief scientific communications, letters to the editor, and related news items.

The Journal is included in the International Databases: Emerging Sources Citation Index (Web of Science Core Collection), Scopus, DOAJ, CAS, FSTA, EBSCOhost, ResearchBib, ProQuest, CABI, Agricola, Ulrich's, Google Scholar, OCLC WorldCat, BASE.

The Journal is included in the List of leading Peer-reviewed Scientific Journals recommended by the Higher Attestation Commission of the Russian Ministry of Science and Higher Education of the Russian Federation.

The Journal comes out in print and on-line. It is published in the English language with periodicity of two volumes a year.

All submitted articles are checked for plagiarisms via www.ithenticate.com and www.antiplagiat.ru.

The Journal only publishes the manuscripts recommended by the reviewers. The Journal uses double-blind review.

"Foods and Raw Materials" is included in the Russian index of scientific citation (RISC) and registered in the Scientific electronic library eLIBRARY.RU.

Opinions of the authors of the published materials do not always coincide with the editorial viewpoint. Authors are responsible for the content of their research papers.

The Journal "Foods and Raw Materials" is an open access journal. All articles are made freely available to readers immediatly upon publication. Our open access policy is in accordance with the Budapest Open Access Initiative (BOAI) definition.

For submission instructions, subscription and all other information visit this journals online at http://jfrm.ru/en.

Founder: Kemerovo State University (KemSU), 6 Krasnaya Str., Kemerovo, Kemerovo region – Kuzbass 650000, Russia.

Editorial Office, Publishing Office: 6 Krasnaya Str., Kemerovo, Kemerovo region – Kuzbass 650000, Russia. Phone: +7(3842)58-81-19. E-mail: fjournal@mail.ru.

Printing Office: 73 Sovetskiy Ave., Kemerovo, Kemerovo region – Kuzbass 650000, Russia.

Date of publishing November 09, 2021
Circulation 500 ex. Open price.
Subscription index: for the unified "Russian Press" catalogue – 40539.

The Federal Service for Supervision of Communications, Information Technology and Mass Media (Media Registration Certificate PI no. FS77-72606 dated April 04, 2018).

16+

Foods and Raw Materials, 2021, vol. 9, no. 2
E-ISSN 2310-9599
ISSN 2308-4057

Editorial
Open Access

Available online at http://jfrm.ru/en

Editor's column

In December 2015, the Paris Climate Agreement marked the ultimate need to restructure the global power economy in order to reduce the risks of climate change. The Agreement demanded that every country that signed it should develop a long-term national low carbon strategy. It was not the temperature rise that worried the participants of the Summit, but the anthropogenic effect on the chemical composition of the atmosphere.

Greenhouse gases are a highly researched issue. The increasing concentrations of CO_2 and methane in the air can boost climate warming: it is the unprecedented CO_2 increase that worries the global scientific community, while the current temperature rise is nothing but a canary in the coalmine. And it is man-induced CO_2 emissions from fossil fuel combustion that may send us over the edge.

One of the first actions recommended by the Global Climate Policy is the soft national regulation of greenhouse gas emissions, which is expected to accelerate high-tech development. This implies (1) mandatory carbon reporting, which has been practiced by all London Stock Exchange companies since 2013, (2) restructuring of the economy in order to increase the share of high-tech industries, which requires huge investments few countries can afford, (3) green logistics, i.e. finding ways to minimize the carbon footprint from transport of goods to the end consumer.

On the global agenda, industrial countries might eventually have to be forced to reduce their carbon footprint if the situation changes for the worse by 2030. Of course, such drastic measures will ruin all long-term investment plans.

Most anthropogenic greenhouse gas emissions come from fuel combustion. Therefore, all anti-emission measures can be classified as follows:

– decarbonization, i.e. transition to low-emission fuels, e.g. hydrogen, or renewable energy sources, e.g. solar energy, wind power, etc.;
– higher energy efficiency and lower energy intensity of industries, communal services, etc., which means a decrease in specific fuel consumption;
– new technologies for capturing, storage, utilization, removal, and commercialization of greenhouse gases;
– support and promotion for low carbon footprint products.

A lower carbon footprint will require major efforts from all areas of human activities, from installing expensive and highly efficient wastewater treatment plants to banning plastic bags in supermarkets. Carbon footprint benefits as much from garbage sorting as it does from deep processing of metallurgical raw materials. Every little bit counts. Effective redistribution of raw materials and waste policy can decrease the current man-induced impact on the environment and increase the range of products with high added value.

All these methods pose a threat to Russian economy because they will inevitably lead to a lower demand for fossil fuels and industrial energy-intensive products of metallurgical, chemical, and cellulose industries. In addition, carbon footprint takes into account the greenhouse gas emissions from transporting products to the consumption point.

Many countries are busy switching to carbon-free energy. Unfortunately, such alternative energy sources as solar and wind power require a whole new infrastructure, while the electricity generation they provide relies heavily on the time of day and year. A renewable energy grid will require large energy storage facilities and specific consumer demand management policies, whereas now customers can consume energy without any restrictions, and energy production depends on energy consumption, not the other way round.

Agriculture is another major emitter of greenhouse gases. Carbon footprint reduction has become one of the most important challenges of modern agriculture. The Russian Ministry of Agriculture tries to achieve this goal by building agricultural carbon landfills. This project is likely to increase Russia's agro-industrial export potential as it satisfies the new EU requirements.

Nuclear power is also carbon-free, but few countries can provide the highest safety standards and deal with the nuclear waste problem, all while avoiding nuclear proliferation. More nuclear power plants and hydroelectric power stations mean a serious environmental threat. For instance, should Eastern Siberia one day become a carbon-free zone, it will lose all its major rivers. At this point in history, Siberian nature may have to pay a high price if it abandons coal mining for nuclear and hydroelectric energy.

Editor-in-Chief,
Corresponding Member of the Russian Academy of Sciences,
Professor A. Yu. Prosekov

Foods and Raw Materials, 2021, vol. 9, no. 2

E-ISSN 2310-9599
ISSN 2308-4057

Research Article
Open Access

https://doi.org/10.21603/2308-4057-2021-2-201-206
Available online at http://jfrm.ru/en

Organochlorine pesticide residues and other toxic substances in salted *Tenualosa ilisha* L.: Northeastern part of India

Sanchari Goswami, Kuntal Manna*

Tripura University, Suryamaninagar, India

* e-mail: k_manna2002@yahoo.com

Received March 17, 2021; Accepted in revised form April 12, 2021; Published online July 09, 2021

Abstract:
Introduction. Fish can sometimes be contaminated with several highly toxic substances at once, e.g. heavy metals, pesticides, and preservatives. In this regard, it is essential to determine the presence of these harmful chemicals in fish products. The research objective was to analyze the level of organochlorine pesticide residues and other toxic substances in *Tenualosa ilisha* L.
Study objects and methods. The study featured organochlorine pesticide residues and other toxic substances in raw and cooked samples of fresh and salted *T. ilisha*, which is a popular dish in Northeast India, especially in the state of Tripura. The analysis involved tests for formaldehyde, pesticides, and heavy metals. Formaldehyde content was estimated using high-performance liquid chromatography, pesticides content – by low-pressure gas chromatography/tandem mass spectrometry, and heavy metals – by inductively coupled plasma/mass spectrometry.
Results and discussion. The salted samples had a high content of formaldehyde, though it remained within the normal range. Both fresh and salted samples demonstrated high concentrations of heavy metals such as zinc, copper, and selenium. The salted sample appeared to have a high content of toxic organochlorine pesticide residues. Frying and boiling of fresh and salted fish decreased formaldehyde and organochlorine pesticide residue contents but did not reduce heavy metal content.
Conclusion. T. ilisha was found to be quite safe for human health.

Keywords: *Tenualosa ilisha*, formaldehyde, pesticides, heavy metals, cooking, chromatography, spectrometry

Please cite this article in press as: Goswami S, Manna K. Organochlorine pesticide residues and other toxic substances in salted *Tenualosa ilisha* L.: Northeastern part of India. Foods and Raw Materials. 2021;9(2):201–206. https://doi.org/10.21603/2308-4057-2021-2-201-206.

INTRODUCTION

Fish is a highly nutritive part of human diet. First of all, it is the primary source of polyunsaturated fatty acids (PUFA), especially eicosapentaenoic acid (EPA) and docosahexaenoic acid (DHA). PUFAs are known to decrease the risk of cardiovascular diseases [1]. Additionally, fish provides proteins, fats, amino acids, essential minerals (mainly iron), as well as vitamins A, B group, and D [2].

Northeast India has huge potential for fisheries due to its many rivers, streams, lakes, and ponds [3]. Fish and rice are the basis of the traditional menu in the state of Tripura. Unfortunately, fish can be contaminated with various harmful substances, e.g. salt, dust, organic toxins, heavy metals, microbes, pesticides, preservatives, etc. [4, 5]. As a result, fish may pose a serious threat to human health. For instance, formaldehyde, which is often used as an antimicrobial preservative, is considered to be carcinogenic to humans, which was also confirmed by the International Agency for Research on Cancer (IARC) [6, 7]. Still, this substance is often used to process foods [8]. In small quantities, formaldehyde is involved in human metabolism. However, high doses can cause pain, vomiting, coma, and possible death [9]. According to the United States Environmental Protection Agency, the acceptable daily intake of formaldehyde is about 0.2 mg/kg b.w. [10]. In addition to being used as a preservative, low concentrations of formaldehyde can also serve as an antiseptic solution due to its antibacterial and antifungal properties. If inhaled, it damages respiratory organs and may cause dizziness and suffocation, not to mention eye, nose, and throat irritation [11]. Exposure to formaldehyde increases the incidence of lung and nasopharyngeal cancer. Ingestion of formaldehyde damages the gastrointestinal tract [11]. The normal range of formaldehyde is 2–50 mg/kg, and the maximum can reach 60 mg/kg in fruits and marine fish [8].

Heavy metals, such as lead, chromium, mercury, arsenic, etc., are well-known contaminating chemicals that cause water and soil pollution [12]. These metals have no beneficial effects on human health. On the contrary, they are generally considered as one of the most toxic elements for humans and animals.

Similarly, pesticides in fish products are a sign of contamination and pose a serious threat to human health as they accumulate in human body fats [13]. Acute symptoms of pesticide poisoning include numbness, incoordination, headache, dizziness, tremor, nausea, abdominal cramps, respiratory depression, etc. [14].

Exposure to organochlorine pesticides mainly occurs through contaminated food, especially fish or shellfish obtained from contaminated rivers and streams. A long term exposure to moderate levels of aldrin and dieldrin can cause headache, irritability, vomiting, and uncontrollable muscle movements. Excessive dieldrin has been established as a 2–7-fold higher risk factor for breast cancer. The lethal dose (LD50) of dieldrin per day is approximately 10 mg per 1 kg of body weight [15].

Carbofuran and its major metabolites (3-hydroxy-carbofuran and 3-ketocarbofuran) can cross the placental barrier and affect the maternal-placental-fetal unit [16]. Alachlor is another toxic chemical that dissipates from soil mainly through volatilization, photodegradation, and biodegradation. It is readily absorbed through gastrointestinal tract and distributed to blood, spleen, liver, kidney, brain, stomach, and ovaries. The LD50 of alachlor is between 1.910 and 2.310 mg/kg in mice [17]. Therefore, timely detection of these toxic elements in fish is essential for human health.

Tenualosa ilisha, *Clupeidae* family, is the most popular fish in the Bay of Bengal. *Hilsa*, as they call it in India, occupies the top position among edible fishes due to its unique taste and delicious properties. *T. ilisha* is rich in amino acids, minerals, and fats. In addition, the fish has a high content of high density lipoprotein and a low level of low density lipoprotein, which makes it beneficial for human health [18]. Because of its high lipid content, it cannot be sun-dried. As a result, it is preserved by salting, which is simple and cheap [19]. Both fresh and salted *Hilsa* are very popular among the common people of Tripura. Cooking methods for fresh and salted *Hilsa* include boiling, frying, roasting, etc. Suitable cooking methods minimize the nutrient loss and also improve the digestibility of food [20, 21].

Although some aspects of nutritional composition of *T. ilisha* have already been reported, the estimation of toxic elements in both raw and cooked samples of fresh and salted *T. ilisha* has not yet been explored scientifically [22]. The objective of the present experiment was to analyze the level of organochlorine pesticide residues and other toxic materials in raw and cooked samples of fresh and salted *T. ilisha*.

STUDY OBJECTS AND METHODS

Sample preparation and cooking. Fresh and salted samples of *Tenualosa ilisha* L. were obtained from the local market of Battala, Tripura. The samples were cleaned to remove dust particles. The fresh samples were washed and gutted. In case of fresh samples, the main purpose was to obtain the maximal amount of flesh portion, so the samples were cut approximately parallel to the backbone. The flesh portion was cut into small pieces and prepared for boiling and frying. The salted samples were washed with water and cut into small pieces for further cooking. Fresh and salted samples were boiled for 20 min or deep-fried in vegetable oil for 15 min at 240°C.

Sample preparation to determine formaldehyde. The formaldehyde content was determined according to Claeysa *et al.* [23]. Blank and spiked formalin was added into five-gram samples. After adding 5 mL of acetonitrile, the samples were sonicated for 30 min at 25–30°C and shaken for 30 min in a shaking water bath at 150 rpm at room temperature. Then, they were centrifuged at 6000 rpm at 22°C for 5 min and filtered through a Whatman filter paper (90 mm). After 5 mL of the upper layer of the extract was carefully removed, 2.5 mL DNPH solution (dinitrophenylhydrazine) and vortex were added. Recrystallization of DNPH was carried out by dissolving 10 mL of anhydrous acetonitrile acetate to obtain a saturated solution. The samples were derivatized by shaking at 150 rpm at 40°C for 1 h in a shaking water bath. After incubation, the supernatant was filtered with a syringe micro filter (0.45 μm).

Analytical condition of HPLC. A 10-μL sample solution was analyzed by using a C-18 column (250× 4.6 mm, 5 μm) with a 60% methanol solution as mobile phase and analyzed at 355 nm. The flow rate was 1 mL/min and the operating time was 13 min.

Standard curve preparation. A stock formaldehyde solution (6.2%) was used to prepare standard solutions with concentrations of 0.838, 1.68, 2.51, 3.35, and 5.03 ppm by diluting with distilled water. The absorbance was then measured using a spectrophotometer at 415 nm. The molar concentration of formaldehyde was determined as follows:

$$A = € \cdot C \cdot L \quad (1)$$

where A is absorbance, € is molar absorption coefficient, C is molar concentration, and L is length of the cell.

In case of matrix-free calibration, the limit of detection (LOD) was 0.117 ppm and the limit of quantification (LOQ) was 0.384 ppm.

Recovery test. The known concentration of formaldehyde (5, 10, and 25 mg/L) was spiked in fish matrix. Recovery was calculated as follows:

$$\% \text{ of recovery} = \text{concentration of formaldehyde quantified in the sample} \times 100/\text{spiked concentration} \quad (2)$$

Pesticide determination. The fish samples were homogenized with an Ultra-Turrax T25 homogenizer and stored in a freezer at –20°C. A standard pesticide

Table 1 Formaldehyde content in raw and cooked samples of fresh and salted *Tenualosa ilisha*

Formaldehyde	Fresh *T. ilisha*			Salted *T. ilisha*		
	Raw ± SEM	Boiled ± SEM	Fried ± SEM	Raw ± SEM	Boiled ± SEM	Fried ± SEM
Content, mg/kg	10.32 ± 2.11	9.24 ± 2.40[a]	9.02 ± 1.80[a]	12.14 ± 1.51	11.23 ± 1.10[b]	10.58 ± 3.70[b]

Five samples were taken to calculate the standard error mean

[a] $P < 0.05$ when compared with raw fresh *T. ilisha*

[b] $P < 0.05$ when compared with raw (uncooked) salted *T. ilisha*

mix, 20 µg/mL in 0.05% formic acid in methyl cyanide, was used as a spiking solution for 100 and 50 ng/g spiking levels. A standard pesticide mix, 500 ng/mL in 0.05% formic acid in methyl cyanide, was used for 5 and 1 ng/g spiking levels in the recovery experiments. A mix of atrazine-d5 and fenthion-d6 at 10 µg/mL was prepared in 0.05% formic acid in methyl cyanide.

Sample preparation. Ten grams of homogenized fish sample was put into a 50-mL polypropylene centrifuge tube. Adding 1000 ng of internal standards (ISTDs) yielded 100 ng/mL. After adding 10 mL of methyl cyanide, the tube was vigorously shaken by hand for 30 s. The entire extract, including tissue, was poured into another 50-mL centrifuge tube with 4 g of $MgSO_4$ (anhydrous) and 1 g of NaCl. After that, the tube underwent a vigorous shaking for 1 min and centrifuging at relative centrifugal field of 3250 for 2 min. Subsequently, 1 mL of the extract and 150 mg of $MgSO_4$ were shaken vigorously in a tube for 30 s and centrifuged at 3250 for 2 min. Then, 0.5 mL of the fish extract was transferred into an auto sampler vial for low-pressure gas chromatography/tandem mass spectrometry (LP-GC/MS-MS). 5 mL of distilled water served as a reagent blank sample. The equivalent tissue concentration per sample extract was 1 g/mL [24].

Five replicates of fish samples were prepared for spiking level. Each batch of samples included a reagent blank and a sample blank. Matrix-matched calibration standards at concentration of 0.5, 1, 5, 10, 25, 50, 100, 250, and 400 ng/mL were used to calculate the recoveries of the pesticides. Fenthion-d6 was used as an ISTD for pesticide quantification, and atrazine-d5 was used as a back-up ISTD if needed. The method detection limits were determined as the pesticide's lowest calibrated levels (LCL).

Determination of heavy metals. Fish tissue was weighed (0.3–0.5 g) and placed in a Teflon digestion vessel with 7 mL of concentrated (65%) nitric acid and 1 mL of 30% hydrogen peroxide. The sample in the vessel containing concentrated nitric acid was then subjected to a microwave program:

Step I: 25–200°C for 10 min at 1000 W;

Step II: 200°C for 10 min at 1000 W.

Digests were made up to 25 mL with deionized water. The heavy metal content was analyzed by inductively coupled plasma/mass spectrometry (ICP-MS) (Model X series, Winsford-cheshire UK) [25].

Statistical analysis. The statistical analysis was performed using the Statistical Package for the Social Sciences (SPSS) v. 16.0 for windows (SPSS, SAS Institute Inc. Cary, USA). The data were analyzed to determine the descriptive statistics, such as standard error of mean (SEM), standard deviation (SD), statistic mean, minimum and maximum value, and ranges of variables. A one-way analysis of variance (ANOVA) was performed to determine a 5% level of significance.

RESULTS AND DISCUSSION

Table 1 shows the formaldehyde content in the raw and cooked samples of fresh and salted *Tenualosa*

Table 2 Pesticide residues in raw and cooked samples of fresh and salted *Tenualosa ilisha*

Pesticides	*T. ilisha* (fresh)			*T. ilisha* (salted)		
	Raw ± SEM	Boiled ± SEM	Fried ± SEM	Raw ± SEM	Boiled ± SEM	Fried ± SEM
Aldrin	11 ± 2	10 ± 2*	10 ± 1*	78 ± 9	76 ± 7**	68 ± 8**
Alachlor	n.d.	n.d.	n.d.	88 ± 5	82 ± 6**	78 ± 4**
Carbofuran	17 ± 3	12 ± 2*	10 ± 4*	64 ± 3	62 ± 2**	58 ± 3**
Dieldrin	26 ± 5	22 ± 2*	18 ± 3*	66 ± 4	64 ± 2**	62 ± 4**
Endosulfan sulfate	17 ± 4	15 ± 2*	14 ± 3*	34 ± 9	32 ± 7**	31 ± 8**
o,p′-DDT+ p,p′-DDD	47 ± 8	46 ± 6*	45 ± 8*	118 ± 13	113 ± 17**	112 ± 12**
p,p′-DDT	19 ± 6	17 ± 2*	16 ± 1*	38 ± 4	36 ± 7**	32 ± 8**
Hexachlorobenzene	n.d.	n.d.	n.d.	67 ± 5	65 ± 2**	64 ± 6**

The pesticide values are expressed as spiking level (5 ng/g)

n.d. – not detected

* $P < 0.05$ when compared with raw fresh *T. ilisha*

** $P < 0.05$ when compared with raw (uncooked) salted *T. ilisha*

Table 3 Heavy metal content in raw and cooked samples of fresh and salted *Tenualosa ilisha*

Heavy metals	*T. ilisha* (fresh)			*T. ilisha* (salted)		
	Raw ± SEM	Boiled ± SEM	Fried ± SEM	Raw ± SEM	Boiled ± SEM	Fried ± SEM
Total arsenic, µg/g	11.90 ± 0.005	11.02 ± 0.002	10.98 ± 0.002	11.74 ± 0.005	11.06 ± 0.002	10.85 ± 0.005
Inorganic arsenic, µg/g	0.049 ± 0.0002	0.042 ± 0.0005	0.041 ± 0.0005	0.061 ± 0.0002	0.060 ± 0.0002	0.058 ± 0.0005
Mercury, mg/kg	0.101 ± 0.0005	0.098 ± 0.0002	0.090 ± 0.0002	0.102 ± 0.0005	0.097 ± 0.0005	0.095 ± 0.0002
Lead, mg/kg	0.81 ± 0.002	0.80 ± 0.005	0.80 ± 0.005	0.80 ± 0.005	0.78 ± 0.002	0.78 ± 0.002
Cadmiun, mg/kg	0.51 ± 0.002	0.50 ± 0.002	0.50 ± 0.002	0.52 ± 0.005	0.51 ± 0.002	0.51 ± 0.002
Chromium, mg/kg	< 1.0	< 1.0	< 1.0	< 1.0	< 1.0	< 1.0
Copper, mg/kg	54.02 ± 0.005	54.00 ± 0.002	54.00 ± 0.002	53.88 ± 0.005	54.00 ± 0.002	53.87 ± 0.005
Nickel, mg/kg	1.82 ± 0.005	1.80 ± 0.002	1.81 ± 0.002	1.79 ± 0.005	1.78 ± 0.002	1.78 ± 0.002
Selenium, mg/kg	11.20 ± 0.006	10.88 ± 0.005	10.85 ± 0.005	11.00 ± 0.002	10.98 ± 0.006	10.97 ± 0.005
Zinc, mg/kg	122.0 ± 0.035	121.5 ± 0.032	121.3 ± 0.032	121.6 ± 0.057	121.4 ± 0.057	121.3 ± 0.032

The result is significant at $P < 0.05$

ilisha L. The salted sample contained a higher amount of formaldehyde (12.14 mg/kg) than the fresh sample (10.32 mg/kg), which could be because formaldehyde served as a preservative. However, its content reduced after boiling and frying. Again, cooking had some effect on the formaldehyde content. This toxic element is known to degrade after thermal treatment [26]. The concentration of formaldehyde mainly depends on different levels of trimethylamine n-oxide (TMAO) [27]. Tri-methylamine, di-methylamine, and formaldehyde are formed after the breakdown of TMAO [28].

The normal range of formaldehyde is 2–50 mg/kg, so the formaldehyde content in the present experiment was within the normal range for both fresh and salted fish samples.

Table 2 demonstrates the pesticide content (spiking level 5 ng/g) in the raw and cooked samples of fresh and salted *T. ilisha*. Alachlor and hexachlorobenzene were detected neither in the raw nor in the cooked samples. On the other hand, the levels of aldrin, alachlor, carbofuran, dieldrin, endosulfan sulfate, o,p′-DDT+ p,p′-DDD, p,p′-DDT, and hexachlorobenzene were higher in the salted sample. After cooking, the pesticide content went down. The toxic organochlorine pesticides residue was higher in the salted sample, which may be due to the fact that these substances were added to the fish as preservatives. After cooking, the organochlorine pesticides residue decreased because cooking process increases volatilization, hydrolysis, or other chemical degradation and leads to the decomposition by applying heat [29, 30].

Table 3 shows the heavy metal content in the raw and cooked samples of fresh and salted *Hilsa*. The mercury content was found to be 0.101 mg/kg in the fresh sample and 0.102 mg/kg in the salted sample. However, it went down after cooking. The above result is acceptable for fish, considering that the proposed upper limit for mercury is 0.5 mg per 1 kg of fresh weight. The cadmium content was high in both fresh and processed samples. For general fish muscle, cadmium level is 0.05 mg per 1 kg of fresh weight [30].

Copper is essential for maintaining good health, but a long term exposure may cause toxic effects, e.g. Wilson's disease [31]. In the present experiment, the copper concentration was 54.02 and 53.88 mg/kg in fresh and salted *T. ilisha*, respectively. The chromium content did not exceed 1.0 mg/kg for all raw and cooked samples of fresh and salted *T. ilisha*. Zinc is another essential nutrient. In moderate quantities, it improves immune system and metabolism, whereas a high level of zinc can be harmful. According to FAO, the limit for zinc is 30 mg/kg [32].

The limit of zinc acceptability exceeded the norm in both raw and cooked samples of fresh and salted fish. Selenium is an essential trace element required in small amounts for animals and humans. However, a higher content of selenium is toxic. Cooking appeared to have no significant effect on selenium content. The nickel content was within acceptable limits. Cooking had no significant effect on lead contamination either. Arsenic, another toxic element, can be found as a contaminant in fish, shellfish, and other seafood. In the present experiment, the arsenic content was within the normal range. According to FAO/WHO, the maximal intake of arsenic is 15 µg/kg b.w. Both raw and cooked samples of fresh and salted *T. ilisha* contained a high amount of arsenic [33].

CONCLUSION

The organochlorine pesticide residues were higher in the salted samples of *Tenualosa ilisha* L., but boiling and frying reduced their amounts. The salted samples of *T. ilisha* contained a high amount of such heavy metals as zinc, copper, and selenium. Fresh *T. ilisha* proved to be safe for human health as thermal treatment had some positive effects on the potentially harmful substances.

CONTRIBUTION

Dr. Kuntal Manna designed the research; Sanchari Goswami collected the samples, performed the analysis, and wrote the manuscript.

CONFLICT OF INTEREST

The authors declare no conflict of interests regarding the publication of this article.

ACKNOWLEDGMENTS

The authors are grateful to New Jersey Feed Lab Inc., 1686 Fifth St, Trenton NJ 08638, USA, for providing instrument facility. The authors would like to express their gratitude to State Biotech Hub, Tripura Central University-799022, for providing working facility and to Tripura State Pollution Control Board, Kunjaban, Gorkhabasti, Agartala-799006, for providing the instrumental facility for mineral analysis. The authors are also indebted to Mr. W. Somraj Singh and Mr. Bikash Debnath, Research Scholar, Department of Pharmacy, Tripura Central University, for editing the manuscript.

REFERENCES

1. Njoroge SW, Laposata M, Katrangi W, Seegmiller AC. DHA and EPA reverse cystic fibrosis-related FA abnormalities by suppressing FA desaturase expression and activity. Journal of Lipid Research. 2012;53(2):257–265. https://doi.org/10.1194/jlr.M018101.
2. Roos N, Islam M, Haraksingh Thilsted S. Small fish is an important dietary source of vitamin A and calcium in rural Bangladesh. International Journal of Food Sciences and Nutrition. 2003;54(5):329–339. https://doi.org/10.1080/09637480120092125.
3. Korelat M, Whitten T. Freshwater biodiversity in Asia: With special reference to fish. Washington: The World Bank, 1996. pp. 17–22.
4. Bhuiyan NI, Bhuiyan HR, Nath KK. Incidence of organochlorine insecticides (DDT and heptachlor) in Bangladeshi dry fish: Seasonal trends and species variability. African Journal of Environmental Science and Technology. 2009;3(11):405–411.
5. Siddique MAM, Aktar M. Detection of health hazard insecticide dichlorodiphenyltrichloroethane (DDT) in some common marine dry fish samples from Bangladesh. Health. 2012;4(4):185–189. https://doi.org/10.4236/health.2012.44027.
6. WHO global strategy for food safety: Safer food for better health. Geneva: World Health Organization; 2002. 23 p.
7. IARC monographs on the evaluation of carcinogenic risks to humans. Volume 88. Formaldehyde, 2-butoxyethanol and 1-*tert*-butoxypropan-2-ol. Lyon: International Agency for Research on Cancer; 2006. 278 p.
8. Weng X, Chon CH, Jiang H, Li D. Rapid detection of formaldehyde concentration in food on a polydimethylsiloxane (PDMS) microfluidic chip. Food Chemistry. 2009;114(3):1079–1082. https://doi.org/10.1016/j.foodchem.2008.10.027.
9. Consice International Chemical Assessment Document № 40. Formaldehyde. Geneva: World Health Organization; 2002. 75 p.
10. Additional foods ingredients. Jakarta; 1988.
11. Environmental Health Criteria 89. Formaldehyde. Geneva: World Health Organization; 1989.
12. Sabine M, Wendy G. Human health effects of heavy metals. Environmental Science and Technology Briefs for Citizens. 2009;(15).
13. Kafilzadeh F, Shiva AH, Malekpour R, Azad HN. Determination of organochlorine pesticide residues in water, sediments and fish from lake Parishan, Iran. World Journal of Fish and Marine Sciences. 2012;4(2):150–154.
14. Kumar N, Pathera AK, Saini P, Kumar M. Harmful effects of pesticides on human health. Annals of Agri Bio Research. 2012;17(2):125–127.
15. Ravindran J, Pankajshan M, Puthur S. Organochlorine pesticides, their toxic effects on living organisms and their fate in the environment. Interdisciplinary Toxicology. 2016;9(3–4):90–100. https://doi.org/10.1515/intox-2016-0012.
16. Gupta C. Invited review: Carbofuran toxicity ramesh. Journal of Toxicology and Environmental Health. 1994;43(4):383–418. https://doi.org/10.1080/15287399409531931.
17. Ahrens WH. Herbicide Handbook, Seventh Edition. Champaign: Weed Science Society of America; 1994. pp. 10–59.
18. Alam AKMN, Mohanty BP, Hoq ME, Thilshed S. Nutritional values,consumption and utilization of hilsa Tenualosa ilisha (Hamilton 1822). Collection of conference materials: Proc. Regional workshop on hilsa: Potential for aquaculture; 2012; Dhaka: WorldFish Regional Office; 2012.
19. Majumdar RK, Basu S, Anandan R. Biochemical and microbiological characteristics of salt fermented hilsa (*Tenualosa ilisha*). Fishery Technology. 2005;42(1):67–70.
20. Eriksson CE. Oxidation of lipids in food systems. In: Chan HW-S, editor. Autoxidation of unsaturated lipids. London: Academic Press. 1987. pp. 207–231.

21. Kimura M, Itokawa Y. Cooking losses of minerals in foods and its nutritional significance. Journal of Nutritional Science and Vitaminology. 1990;36:S25–S32. https://doi.org/10.3177/jnsv.36.4-supplementI_S25.
22. Salam KA, Hossain Motahar AKM, Khurshid Alam AHM, Pervin F, Absar N. A comparative analysis on physio-chemical characteristic of oil extracted from six different parts of Hilsa fish (*Hilsa ilisha*). Pakistan Journal of Biological Sciences. 2005;8(6):810–815. https://doi.org/10.3923/pjbs.2005.810.815.
23. Claeys W, Vleminckx C, Dubois A, Huyghebaert A, Höfte M, Daenens P, et al. Formaldehyde in cultivated mushrooms: a negligible risk for the consumer. Food Additives and Contaminants – Part A Chemistry, Analysis, Control, Exposure and Risk Assessment. 2009;26(9):1265–1272. https://doi.org/10.1080/02652030903081929.
24. Anastassiades M, Lehotay SJ, Štajnbaher D, Schenck FJ. Fast and easy multiresidue method employing acetonitrile extraction/partitioning and "dispersive solid-phase extraction" for the determination of pesticide residues in produce. Journal of AOAC International. 2003;86(2):412–431. https://doi.org/10.1093/jaoac/86.2.412.
25. Method 3051. Microwave assisted acid digestion of sediments, sludges, soils, and oils. 1994.
26. Leslie GB, Lunau FW. Indoor air pollution: problems and priorities. Cambridge: Cambridge University Press; 1994. 352 p.
27. Kibria G. Formalin and fish trade in Bangladesh – human and environmental risks. https://doi.org/10.13140/RG.2.1.4994.6087.
28. Tunhun D, Kanont S, Chaiyawat M, Raksakulthai N. Detection of illegal addition of formaldehyde to fresh fish. ASEAN Food Journal. 1996;11(2):74–77.
29. Abou-Arab AAK. Behavior of pesticides in tomatoes during commercial and home preparation. Food Chemistry. 1999;65(4):509–514. https://doi.org/10.1016/S0308-8146(98)00231-3.
30. Holand PT, Hamilton D, Ohlin B, Skidmore MW. Effects of storage and processing on pesticide residue in plant production. Pure and Applied Chemistry. 1994;66(2):335–356.
31. European Commission. Commission regulation (EC) no. 1881/2006 of 19 December 2006 setting maximum levels for certain contaminants in foodstuffs. Official Journal of the European Union. 2006:L364-5/L364-24.
32. Vincent JB. Recent advances in the nutritional biochemistry of trivalent chromium. Proceedings of the Nutrition Society. 2004;63(1):41–47. https://doi.org/10.1079/PNS2003315.
33. Nauen CE. Compilation of legal limits for hazardous substances in fish and fishery products. Rome: Food and Agriculture Organization; 1983. 102 p.

ORCID IDs
Sanchari Goswami https://orcid.org/0000-0003-1362-195X
Kuntal Manna https://orcid.org/0000-0001-5327-365X

Foods and Raw Materials, 2021, vol. 9, no. 2

E-ISSN 2310-9599
ISSN 2308-4057

Research Article
Open Access

https://doi.org/10.21603/2308-4057-2021-2-207-214
Available online at http://jfrm.ru/en

Glycemic properties of soursop-based ice cream enriched with moringa leaf powder

Ayokunle O. Ademosun

Federal University of Technology, Akure, Nigeria

e-mail: ayoademosun@yahoo.com

Received April 15, 2021; Accepted in revised form May 17, 2021; Published online July 09, 2021

Abstract:

Introduction. Diabetes is a common disease all over the world that is often a cause of mortality. Ice cream is popular in many countries. However, sugar and fat in its composition makes ice cream a high-caloric product. Soursop (*Annona muricata* L.) and moringa (*Moringa oleifera* L.), African medicinal plants, contain natural sugars and are rich in phytochemicals. We aimed to produce ice cream with these plants and evaluate its remedial properties.

Study objects and methods. The study featured ice cream purchased in a local store (control sample) and soursop ice cream with moringa leaf powder (experimental samples). The experimental ice cream samples included ice cream with soursop, ice cream with soursop and 0.1 g of moringa, and ice cream with soursop and 1 g of moringa. The antioxidant properties, glycemic indices, amylose and amylopectin contents, as well as α-amylase and α-glucosidase inhibitory properties of the samples were determined using the standard methods.

Results and discussion. Comparing with the other samples, ice cream with 1 g of moringa showed the highest total phenol and flavonoid contents, ABTS scavenging ability, DPPH radical scavenging ability, hydroxyl scavenging ability, ferric reducing antioxidant properties, and lowest glycemic index. Sensory evaluation revealed a lower overall acceptability of the experimental samples compared to the control ice cream. This could be due a peculiar taste of moringa (the formulation did not include sugar).

Conclusion. Ice cream based on soursop and moringa can be a good alternative to sugar-sweetened ice cream due to its antioxidant properties, low glycemic index, and acceptable sensory attributes.

Keywords: Ice cream, diabetes, antioxidant properties, glycemic index, phenolic compounds, *α*-amylase, *α*-glucosidase

Please cite this article in press as: Ademosun AO. Glycemic properties of soursop-based ice cream enriched with moringa leaf powder. Foods and Raw Materials. 2021;9(2):207–214. https://doi.org/10.21603/2308-4057-2021-2-207-214.

INTRODUCTION

The World Health Organization reported that by 2035 the number of people with diabetes, a major cause of mortality worldwide, will account for 471 million [1]. Cheap snacks and products with high energy content are risk factors in diabetes development [2, 3]. One of the most popular high energy snacks is ice cream, which mainly contains milk or cream and sugar. Ice cream is a homogenized mixture of milk, flavorings, colorings, and stabilizers frozen at the temperature that is lower than the freezing point to avoid the formation of large ice crystals.

There are many varieties of ice cream, but generally ice cream contains 10% of milk fat, less than 10% of non-milk fat (caseins, whey proteins, lactose), 13–20% of sweeteners, 0.1–0.7% of stabilizers and emulsifiers, and about 64% of water [4]. Ice cream has become a popular product due to its cooling properties and the enormous amount of energy it supplies. However, a high amount of carbohydrates fats in ice cream can increase bad cholesterol deposition around the belly and have become one of the leading causes of obesity and such diseases as diabetes, atherosclerosis, and hypertension [5]. All these diseases caused by ice cream consumption have been found to result from excess energy deposition, which is a central factor to hyperglycemia. Despite a high demand for ice cream, there has been little effort to improve its nutritional and medicinal properties. Hence, there is a need to develop functional ice cream without the mentioned disadvantages which would treat a wide array of metabolic diseases.

Herbs are widely available, effective, safe, and acceptable raw materials which can be used as functional plants in the food industry [6]. Various types of plants that have been used in the treatment of heart-

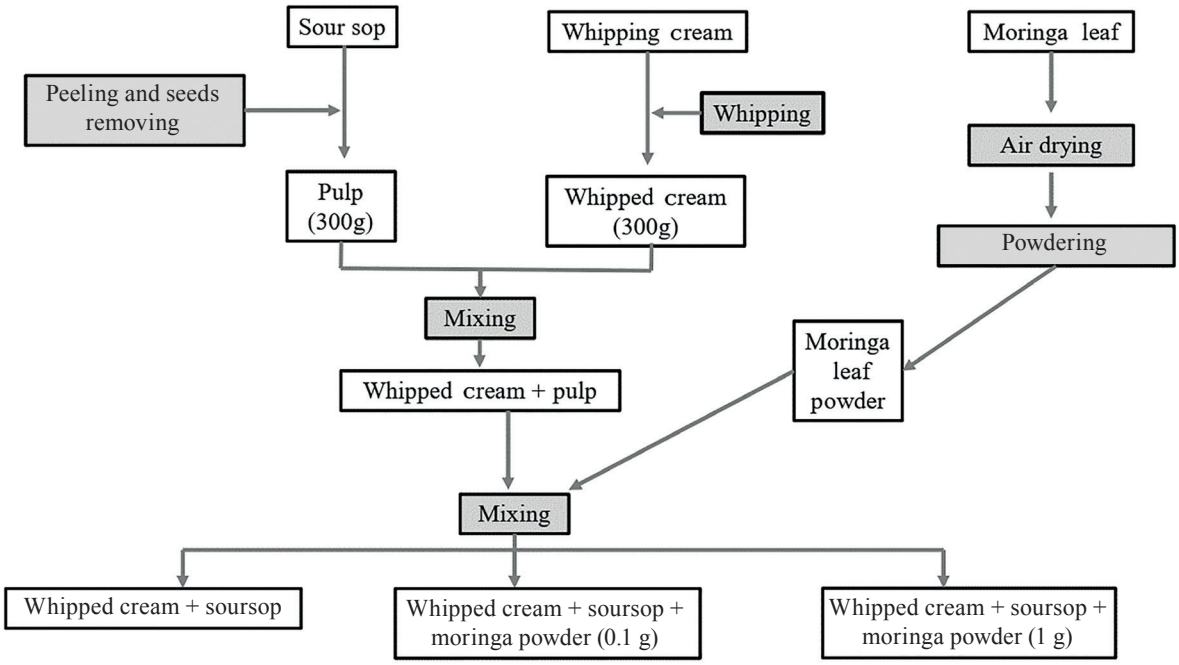

Figure 1 Production process for soursop based ice cream enriched with moringa leaf powder

related diseases have shown promising therapeutic potential. Soursop (*Annona muricata* L.) is a tropical plant popular in ethnomedicine due to its antioxidant properties [7]. Soursop is rich in phytochemicals such as flavonoids, phenolic acids, phytosterols, saponins, and cardiac glycosides [7, 8]. *Moringa oleifera* L. (*Moringaceae* family) is a fast growing plant of economic and medical importance widely distributed in Africa, America, and Asia [9–11]. Some of the phytochemicals present in moringa leaf, which have medicinal potential, are mainly natural antioxidants such as flavonoids, carotenoids, vitamins, and phenolic acids [12–17].

Therefore, this study aimed to produce soursop-based ice cream enriched with moringa leaf powder and then assess its antioxidant properties, glycemic index, amylose and amylopectin contents, as well as α-amylase and α-glucosidase inhibitory properties.

STUDY OBJECTS AND METHODS

Soursop (*Anona muricata* L.) and moringa (*Moringa oleifera* L.) leaves were collected from the botanical garden at the Federal University of Technology, Akure. The moringa leaves were washed, air dried, and finely powdered using a stainless steel blender. The powdered samples were kept dry at room temperature for further analysis.

The soursop was peeled and seeds were separated from the pulp. Whipping cream (600 g) was stirred for 15 min using a mixer. Thereafter, 600 g of the soursop pulp was mixed together with the whipping cream for another 15 min. The mixture was divided into three parts and frozen (Fig. 1). This produced three experimental samples of soursop-based ice cream: with no moringa, with 0.1 g of moringa, and with 1 g of moringa. Ice cream purchased at a local store served as control.

Sensory analyses were conducted in well illuminated odorless laboratory booths. Water was provided for mouth rinsing in between successive evaluation. Sample attributes (color, texture, taste, aroma, etc.) were rated from 1 to 7, where 1 = very poor and 7 = excellent. Panelists made their responses on score sheets which were designed in line with the test procedures [18].

The total phenol content was determined according to the method reported by Singleton *et al*. and calculated as gallic acid equivalent (GAE) [19].

The total flavonoid content was determined using a slightly modified method reported by Meda *et al*. [20]. The absorbance of the reaction mixture was subsequently measured at 415 nm, and the total flavonoid content was subsequently calculated.

DPPH free radical scavenging ability was evaluated as described by Gyamfi *et al*. [21]. Ice cream samples (0.05 mL) were incubated in the dark for 30 min with 1 mL of 0.4 mM DPPH after thorough mixing. The absorbance was measured at 516 nm, and the radical scavenging ability was subsequently calculated as percentage of the control.

ABTS radical scavenging ability was determined according to the method described by Re *et al*. [22]. The radicals were generated by adding 7 mmol/L ABTS aqueous solution to a reaction mixture containing 2.45 mmol/L $K_2S_2O_8$, keeping in the dark for 16 h, and adjusting the absorbance to 0.700 with ethanol at 734 nm. 0.2 mL of appropriate dilution of the ice

cream samples was added to 2.0 mL of ABTS solution and absorbance was measured at 734 nm after 15 min. The radical scavenging ability and Trolox equivalent antioxidant capacity were subsequently calculated.

Ferric reducing antioxidant property of the samples was determined by assessing its ability to reduce $FeCl_3$ solution as described by Pulido *et al*. [23]. The reducing property was subsequently calculated using ascorbic acid equivalent.

Hydroxyl radical scavenging ability was determined using the method of Halliwell and Gutteridge [24]. The reaction mixture contained 1–100 µL of the ice cream samples, 400 µL of 0.1 M phosphate buffer, 120 µL of 20 mM deoxyribose, 40 µL of 20 mM hydrogen, and 40 µL of 500 M $FeSO_4$. The mixture was incubated at 37°C for 30 min. Thereafter, 0.5 mL of 2.8% TCA (trichloroacetic acid) and 0.4 mL of 0.6% TBA (thiobarbituric acid) solution were added. The tubes were subsequently incubated in boiling water for 20 min. The absorbance was measured at 532 nm using a spectrophotometer.

α-amylase activity assay. The reaction mixture contained the sample dilution (500 µL) and 0.5 mg/mL of α-amylase in 500 µL of 0.02 M sodium phosphate buffer (pH 6.9 with 0.006 M NaCl). The mixture was incubated for 10 min at 25°C. 500 µL of a 1% starch solution in 0.02 M sodium phosphate buffer (pH 6.9 with 0.006 M NaCl) was then added to the reaction mixture and incubated for another 10 min at 25°C. Dinitrosalicylic acid (DNSA) was used to stop the reaction before incubating for 5 min at room temperature. Absorbance was measured at 540 nm, and the percentage enzyme inhibitory was calculated [25].

The α-glucosidase inhibitory activity was determined by the method of Apostolidis *et al*. [26]. The reaction mixture contained 100 µL of α-glucosidase solution (EC 3.2.1.20; 1.0 U/mL) in 0.1 M phosphate buffer (pH 6.9). Ice cream samples (50 µL each) were put in the mixture and incubated at 25°C for 10 min. 50 µL of 5 mM pnitrophenyl-α-D-glucopyranoside solution was added, and the reaction mixture was incubated for 5 min at 25°C. The absorbance was read at 405 nm.

Glycemic index and starch hydrolysis rate *in vitro* were determined according to the method of Goni *et al*. [27]. Each ice cream sample (50 mg) was incubated with pepsin (1 mg) in 10 mL of HCl-KCl buffer (pH 1.5) at 40°C for 60 min. 2.5 mL of phosphate buffer (pH 6.9) and 5 mL of α-amylase solution were added to the reaction mixture. The mixture was incubated at 37°C in a shaking water bath. To activate the enzyme, we were taking 0.1 mL of the mixtures every 30 min during three hours and boiled. The residual starch was digested to glucose by the addition of 3 mL of α-glucosidase and incubated at 60°C for 45 min. The glucose concentration was assayed by the addition of 200 mL of DNSA. After stopping the reaction by boiling, 5 mL of distilled water was added and absorbance read at 540 nm.

To determine amylose-amylopectin content, 1 mL of 95% ethanol and 9 mL of 1 N NaOH were added to in volumetric flasks containing 100 mg of each ice cream sample. Thereafter, the reaction mixture was heated in boiling water for 10 min. 1 mL of 1 N acetic acid and 2 mL of iodine solution were added to 5 mL portion of the solution. After thorough shaking, the absorbance was measured at 620 nm. Amylopectin content was derived from the difference between the starch and amylose contents [28, 29].

Statistical analysis. The results were expressed as mean ± standard deviation (SD). One-way analysis of variance (ANOVA) was used to analyze the results followed by Turkey's post hoc test, with levels of significance accepted at $P < 0.05$.

RESULTS AND DISCUSSION

The results of the sensory evaluation of the control (commercial ice cream) and experimental (soursop-based ice cream enriched with moringa leaf powder) samples are presented in Table 1. The control ice cream had higher overall acceptability compared to the soursop-based ice cream samples. The experimental samples had no significant differences in their overall acceptability.

Aroma, taste, color, flavor, texture, and general acceptability of food have a significant effect on its sensory quality, which is one of the major criteria in food selection by consumers [30]. The overall acceptability and aroma of the soursop-based ice cream was not significantly different. However, moringa leaf powder reduced such attributes as texture, taste, and color. The ice cream samples with moringa demonstrated reduced acceptability, which could be due to a peculiar taste of moringa leaf powder (no sugar in the formulation).

The soursop-based ice cream had a high amount of phenolic and flavonoid content compared to the control

Table 1 Sensory attributes of soursop-based ice cream enriched with moringa leaf powder

Ice cream	Texture	Taste	Color	Aroma	Overall acceptability
Commercial ice cream (control)	6.09 ± 0.04^a	6.11 ± 0.03^a	6.12 ± 0.07^a	6.21 ± 0.04^a	6.25 ± 0.05^a
SS	5.37 ± 0.08^b	5.89 ± 0.04^b	5.92 ± 0.11^a	5.91 ± 0.04^b	5.82 ± 0.03^b
SS + MLP (0.1 g)	5.11 ± 0.03^c	5.71 ± 0.03^c	5.71 ± 0.06^b	5.82 ± 0.03^b	5.78 ± 0.05^b
SS + MLP (1g)	4.95 ± 0.04^d	5.28 ± 0.04^d	5.05 ± 0.07^c	5.79 ± 0.06^b	5.79 ± 0.04^b

SS – soursop

MLP – moringa leaf powder

Table 2 Total phenol and flavonoid contents in soursop-based ice cream enriched with moringa leaf powder

Ice cream	Total phenols (mg GAE/g)	Total flavonoids (mg QE/g)
Commercial ice cream (control)	4.13 ± 0.02[d]	0.98 ± 0.04[d]
SS	16.24 ± 0.04[c]	9.13 ± 0.05[c]
SS + MLP (0.1 g)	22.27 ± 0.05[b]	12.21 ± 0.04[b]
SS + MLP (1 g)	30.25 ± 0.05[a]	19.11 ± 0.03[a]

Values represent mean ± SD, n = 3

SS – soursop

MLP – moringa leaf powder

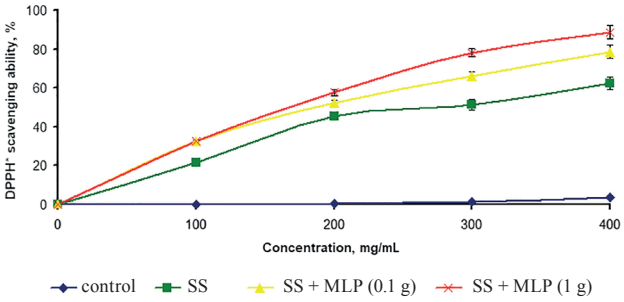

Values represent mean ± SD, n = 3
SS – soursop, MLP – moringa leaf powder

Figure 2 DPPH radical scavenging ability of soursop-based ice cream enriched with moringa leaf powder

sample (Table 2). Our results consistent with the data by Tungmunnithum *et al.* who studied phenolics and flavonoids in medical plants [31]. The authors found that these compounds are responsible for the biological activity of the plants. Phenolic compounds, especially flavonoids, are remarkable antioxidants which have been widely researched for their medicinal properties against various diseases. Phenolic compounds are good iron chelators which scavenge free radicals, preventing oxidative stress [32]. In this study, the sample with moringa leaf powder (1 g) showed the highest total phenol and flavonoid content compared to the other samples.

Figure 2 demonstrates that the ice cream with moringa leaf powder (1 g) had the highest DPPH scavenging ability at all the concentrations (100–400 mg/mL) among all the samples. Also, this ice cream sample showed the highest ABTS scavenging ability compared to the other samples (Fig. 3). The control ice cream sample had the lowest both DHHP and ABST scavenging activities.

The highest ferric reducing antioxidant properties and hydroxyl radical scavenging ability belonged to the experimental sample with moringa leaf powder in the amount of 1 g (Figs. 4 and 5). Among the other samples, these parameters decreased from ice cream with moringa leaf powder (0.1 g) to the control sample (without soursop and moringa powder).

Reducing property of the samples was assessed based on their ability to reduce Fe^{3+} to Fe^{2+}. The results revealed that the control ice cream had significantly lower reducing property compared to the soursop-based samples. Similarly, the ice cream with 1 g of moringa exhibited the highest hydroxyl radical scavenging ability compared to the other soursop-based samples, while the hydroxyl radical scavenging ability of the control ice cream was comparably low.

The antioxidant properties of the sour-sop based ice cream samples was directly proportional to increasing moringa leaf powder proportion (Figs. 2–5). Therefore, the antioxidant properties can be linked to phenolic compounds that majorly present in the moringa and the soursop. Furthermore, the ability of the samples to scavenge DPPH radical could be due to the presence of multiple hydroxyl groups in phenolic compounds, which are able to donate their protons to finally break the chain reaction of the free radicals [32].

ABTS is a water soluble free radical initiator that is oxidized to form a stable green radical ABTS+ in the presence of reactive oxygen [33]. All the soursop-based ice cream samples exhibited a remarkable ABTS radical scavenging ability, with the highest radical scavenging ability in the sample containing 1 g of morings leaf powder. This could also be explained by synergistic effects of phenolic compounds present in moringa and soursop [34, 35]. These results prove that moringa and soursop increased the antioxidant properties of the ice cream samples due to phenolic compounds in their compositions. The correlation between antioxidant properties and phenolic content has been established for many food products [36].

The effect of moringa and soursop on the α-amylase and α-glucosidase inhibitory activity of the ice cream samples are presented in Figs. 6 and 7. The sample with 1 g of moringa leaf powder showed the strongest inhibition of α-amylase activity at the concentrations tested (50–200 mg/mL) and the highest α-glucosidase inhibitory ability compared to the other soursop-based samples. The control sample demonstrated the lowest α-amylase and α-glucosidase inhibitory activities.

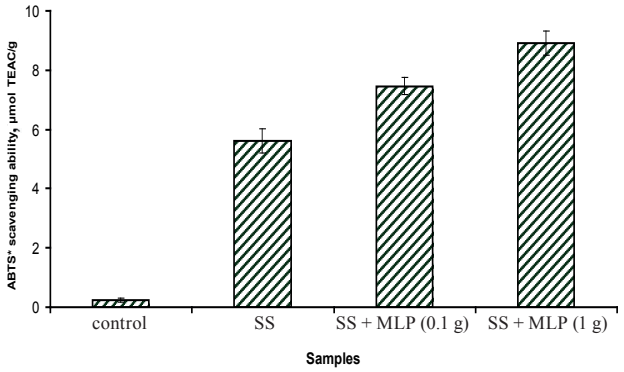

Values represent mean ± SD, n = 3

Figure 3 ABTS scavenging ability of soursop-based ice cream enriched with moringa leaf powder

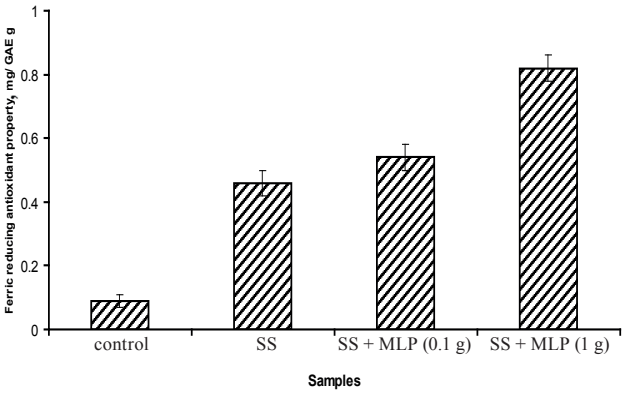

Values represent mean ± SD, n = 3

Figure 4 Ferric reducing antioxidant properties of soursop-based ice cream enriched with moringa leaf powder

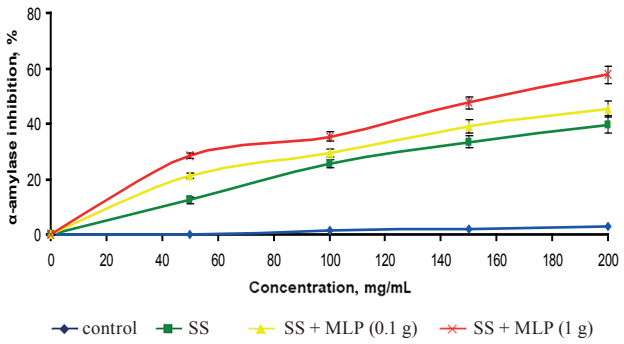

Values represent mean ± SD, n = 3

Figure 6 α-amylase inhibitory ability of soursop-based ice cream enriched with moringa leaf powder

In vitro estimated glycemic indices of the samples are presented in Fig. 8. The results revealed that the control ice cream had the highest glycemic index (61.24) compared to the other samples (27.14–28.61). Figures 6 and 7 revealed that the sour-sop based ice cream samples inhibited carbohydrate hydrolyzing enzymes.

The control ice cream had the lowest amylose content (14.32%) compared to the soursop-based ice cream (32.35–35.34%) (Table 3). There was no significant difference in the amylopectin content of the samples with soursop and moringa leaf powder (64.66–67.65%), while the control ice cream had the highest amylopectin content (85.68%).

A therapeutic and practical way to control postprandial rise of glucose level in blood is the control of carbohydrate hydrolyzing enzymes [37]. Starch is converted to disaccharides and oligosaccharides by pancreatic α-amylase, before further conversion to glucose is catalyzed by intestinal α-glucosidase [38, 39]. Therefore, inhibition of both α-amylase and α-glucosidase activities would result in a reduction of glucose absorbed into the blood. The ability of the sour-sop based ice creams to inhibit the enzymes could be of therapeutic benefit in the management of hyperglycemia.

Interestingly, this tendency for enzyme inhibition by the samples was similar to the tendency for total phenolic and flavonoid contents [40]. In addition, the synergistic contribution of phenolic compounds in soursop and moringa leaves can make ice cream a potent inhibitor of α-amylase and α-glucosidase activities. Our previous studies showed the presence of phenolic compounds, such as gallic acid, elagic acid, rutin, quercetin, kaempferol, epicatechin and chlorogenic acid, in soursop and moringa leaves [34, 35, 41].

The soursop-based ice cream samples had low glycemic indices (Fig. 8) which can be attributed to a number of factors. First, phenolic compounds in soursop and moringa leaves are potent inhibitors of α-amylase and α-glucosidase activities, which results in a slower breakdown of starch into glucose [42]. This is further evidenced by the fact that moringa powder increased phenolic content and reduced glycemic indices. Second, an amylose and amylopectin ratio in food products have a significant effect on postprandial glucose response [43]. Starchy products with a high amylopectin to amylose ratio often digest faster and are absorbed quicker than those with a low amylose to amylopectin ratio and, consequently, produce a high postprandial glucose and insulin response [34]. The control ice cream

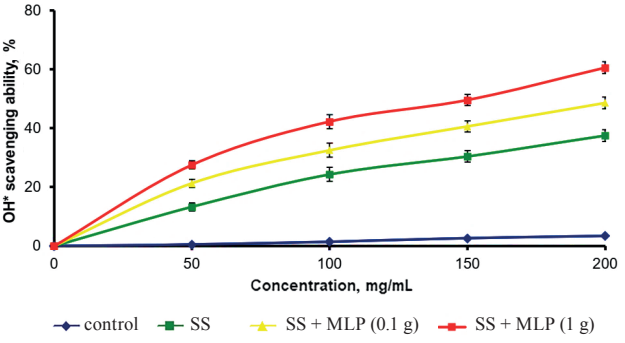

Values represent mean ± SD, n = 3

Figure 5 OH* scavenging abilitiy of soursop-based ice cream enriched with moringa leaf powder

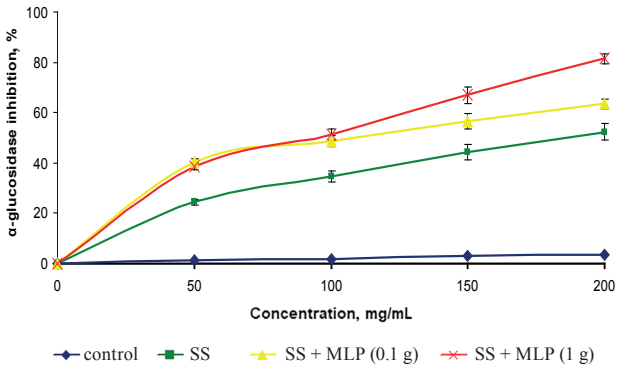

Values represent mean ± SD, n = 3

Figure 7 α-glucosidase inhibitory ability of soursop-based ice cream enriched with moringa leaf powder

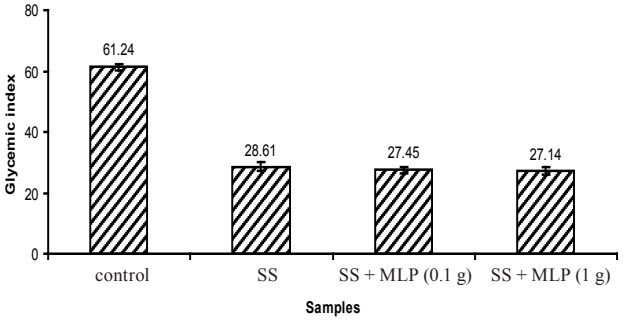

Figure 8 Glycemic indices of soursop-based ice cream enriched with moringa leaf powder

Table 3 Amylose and amylopectin contents of soursop-based ice cream enriched with moringa leaf powder

Ice cream	Amylose, %	Amylopectin, %
Commercial ice cream (control)	14.32 ± 0.11[b]	85.68 ± 0.04[b]
SS	34.36 ± 0.12[a]	65.64 ± 0.16a
SS + MLP (0.1 g)	32.35 ± 0.12[a]	67.65 ± 0.14[a]
SS + MLP (1 g)	35.34 ± 0.09[a]	64.66 ± 0.11[a]

Values represent mean ± SD, n = 3

SS – soursop

MLP – moringa leaf powder

used in this study possessed a low amylose content and high amylopectin content and, thus, the highest glycemic index compared to the experimental ice cream samples, which had a low amylopectin content and a high amylose content.

CONCLUSION

Moringa leaf powder added into soursop-based ice cream improved the antioxidant properties of the final product, reduced its glycemic index, and enhanced inhibition of carbohydrate hydrolyzing enzymes. Soursop-based ice cream with moringa leaf powder can be used to control postprandial hyperglycemia and oxidative stress. The results revealed that moringa-enriched soursop-based ice cream could be an alternative to the sugar-sweetened ice-cream. However, further *in vivo* experiments and clinical trials are recommended.

CONFLICT OF INTEREST

The author declares no conflict of interest regarding the publication of this article.

REFERENCES

1. Global report on diabetes. Geneva: World Health Organization. 2016. 83 p.
2. Nwawuba SU, Nwozo SO, Mohammed KA. Dietary management of diabetes mellitus with focus on Nigeria. International Journal of Diabetes Research. 2019;2(1):26–32.
3. Sami W, Ansari T, Butt NS, Ab Hamid MR. Effect of diet on type 2 diabetes mellitus: A review. International Journal of Health Science. 2017;11(2).
4. Syed QA, Anwar S, Shukat R, Zahoor T. Effects of different ingredients on texture of ice cream. Journal of Nutritional Health and Food Engineering. 2018;8(6):422–435. https://doi.org/10.15406/jnhfe.2018.08.00305.
5. Upadhyay RK. Emerging risk biomarkers in cardiovascular diseases and disorders. Journal of Lipids. 2015;2015. https://doi.org/10.1155/2015/971453.
6. Abubakar AR, Haque M. Preparation of medicinal plants: Basic extraction and fractionation procedures for experimental purposes. Journal of Pharmacy and Bioallied Sciences. 2020;12(1):1–10. https://doi.org/10.4103/jpbs.JPBS_175_19.
7. Agu KC, Okolie NP, Eze I, Anionye JC, Falodun A. Phytochemical analysis, toxicity profile and hemo-modulatory properties of *Annona muricata* (Soursop). Egypt Journal of Haematology. 2017;42(1):36–44. https://doi.org/10.4103/1110-1067.206431.
8. Akomolafe SF, Ajayi OB. A comparative study on antioxidant properties, proximate and mineral compositions of the peel and pulp of ripe *Annona muricata* (L.) fruit. International Food Research Journal. 2015;22(6):2381–2388.
9. Milla PG, Peñalver R, Nieto G. Health benefits of uses and applications of *Moringa oleifera* in bakery products. Plants. 2021;10(2):1–17. https://doi.org/10.3390/plants10020318.
10. Rani NZA, Husain K, Kumolosasi E. *Moringa* Genus: A review of phytochemistry and pharmacology. Frontiers in Pharmacology. 2018;9. https://doi.org/10.3389/fphar.2018.00108.
11. Biel W, Jaroszewska A, Łysoń E. Nutritional quality and safety of moringa (*Moringa oleifera* Lam., 1785) leaves as an alternative source of protein and minerals. Journal of Elementology. 2017;22(2):569–579. https://doi.org/10.5601/jelem.2016.21.3.1249.
12. Vergara-Jimenez M, Almatrafi MM, Fernandez ML. Bioactive components in *Moringa oleifera* leaves protect against chronic disease. Antioxidants. 2017;6(4). https://doi.org/10.3390/antiox6040091.

13. Yassa HD, Tohamy AF. Extract of *Moringa oleifera* leaves ameliorates streptozotocin-induced *Diabetes mellitus*. Acta Histochemica. 2014;116(5):844–854. https://doi.org/10.1016/j.acthis.2014.02.002.
14. Une Hemant D, Pradip S, Patave Tarannum R. A study on the effects of *Moringa oleifera* lam pod extract on alloxan induced diabetic rats. Asian Journal of Plant Science and Research. 2014;4(1):36–41.
15. Al-Malki AL, El-Rabey HA. The antidiabetic effect of low doses of *Moringa oleifera* Lam. seeds on streptozotocin induced diabetes and diabetic nephropathy in male rats. Biomed Research International. 2015;2015. https://doi.org/10.1155/2015/381040.
16. Clement A, Olatunde M, Obigwa P, Orijajogun J. Effect of drying temperature on nutritional content of *Moringa oleifera* leave. World Journal of Food Science and Technology. 2017;1(3):93–96.
17. Talabi JY, Origbemisoye BA, Ifesan BO, Enujuigha VN. Quality characterization of biscuits from blends of Bambara groundnut (Vigna subterranea) Ground bean seed (Macrotyloma) and Moringa seed (Moringa oleifera) flour. Asian Food Science Journal. 2019;12(4):1–12.
18. Olapade AA, Ogunade OA. Production and evaluation of flours and crunchy snacks from sweet potato (*Ipomea batatas*) and maize flours. International Food Research Journal. 2014;21(1):203–208.
19. Singleton VL, Orthofer R, Lamuela-Raventos RM. Analysis of total phenols and other oxidation substrates and antioxidants by means of Folin-Ciocalteau's reagent. Methods in Enzymology. 1999;299:152–178. https://doi.org/10.1016/S0076-6879(99)99017-1.
20. Meda A, Lamien CE, Romito M, Millogo J, Nacoulma OG. Determination of the total phenolic flavonoid and proline contents in Burkina Faso honey as well as their radical scavenging activity. Food Chemistry. 2005;91(3):571–577. https://doi.org/10.1016/j.foodchem.2004.10.006.
21. Gyamfi MA, Yonamine M, Aniya Y. Free-radical scavenging action of medicinal herbs from Ghana *Thonningia sanguinea* on experimentally-induced liver injuries. General Pharmacology 1999;32(6):661–667. https://doi.org/10.1016/S0306-3623(98)00238-9.
22. Re R, Pellegrini N, Proteggente A, Pannala A, Yang M, Rice-Evans C. Antioxidant activity applying an improved ABTS radical cation decolorization assay. Free Radical Biology and Medicine. 1999;26(9–10):1231–1237. https://doi.org/10.1016/S0891-5849(98)00315-3.
23. Pulido R, Bravo L, Saura-Calixto F. Antioxidant activity of dietary polyphenols as determined by a modified ferric reducing/antioxidant power assay. Journal of Agricultural and Food Chemistry. 2000;48(8):3396–3402. https://doi.org/10.1021/jf9913458.
24. Halliwell B, Gutteridge JMC. Formation of a thiobarbituric-acid-reactive substance from deoxyribose in the presence of iron salts: The role of superoxide and hydroxyl radicals. FEBS Letters. 1981;128(2):347–352. https://doi.org/10.1016/0014-5793(81)80114-7.
25. Alpha amylase. In: Worthington enzyme manual. Freehold, NJ: Worthington Biochemical Corp;1993. pp. 36–41.
26. Apostolidis E, Kwon Y-I, Shetty K. Inhibitory potential of herb, fruit, and fungal-enriched cheese against key enzymes linked to type 2 diabetes and hypertension. Innovative Food Science and Emerging Technologies. 2007;8(1):46–54. https://doi.org/10.1016/j.ifset.2006.06.001.
27. Goni L, Garcia-Alonso A, Saura-Calixto F. A starch hydrolysis procedure to estimate glycemic index. Nutrition Research. 1997;17(3):427–437. https://doi.org/10.1016/S0271-5317(97)00010-9.
28. Juliano BO. A simplified assay for milled-rice amylose. Cereal Science Today 1971;16:334–338.
29. Williams VR, Wu W-T, Tasi HY, Bates HG. Varietal differences in amylose content of rice starch. Journal of Agricultural and Food Chemistry. 1958;6(1):47–48. https://doi.org/10.1021/jf60083a009.
30. Tepper BJ, Barbarossa IT. Taste, nutrition, and health. Nutrients. 2020;12(1). https://doi.org/10.3390/nu12010155.
31. Tungmunnithum D, Thongboonyou A, Pholboon A, Yangsabai A. Flavonoids and other phenolic compounds from medicinal plants for pharmaceutical and medical aspects: An overview. Medicines. 2018;5(3). https://doi.org/10.3390/medicines5030093.
32. Jomova K, Valko M. Importance of iron chelation in free radical-induced oxidative stress and human disease. Current Pharmaceutical Design. 2011;17(31):3460–3473. https://doi.org/10.2174/138161211798072463.
33. Phaniendra A, Jestadi DB, Periyasamy L. Free radicals: Properties, sources, targets, and their implication in various diseases. Indian Journal of Clinical Biochemistry. 2015;30(1):11–26. https://doi.org/10.1007/s12291-014-0446-0.
34. Oboh G, Ademosun AO, Akinleye M, Omojokun OS, Boligon AA, Athayde ML. Starch composition glycemic indices phenolic constituents and antioxidative and antidiabetic properties of some common tropical fruits. Journal of Ethnic Foods. 2015;2(2):64–73. https://doi.org/10.1016/j.jef.2015.05.003.
35. Oboh G, Ademiluyi AO, Ademosun AO, Olasehinde TA, Oyeleye SI, Boligon AA, et al. Phenolic extract from *Moringa oleifera* leaves inhibits key enzymes linked to erectile dysfunction and oxidative stress in rats' penile tissues. Biochemistry Research International. 2015;2015. https://doi.org/10.1155/2015/175950.

36. Suleria HAR, Barrow CJ, Dunshea FR. Screening and characterization of phenolic compounds and their antioxidant capacity in different fruit peels. Foods. 2020;9(9). https://doi.org/10.3390/foods9091206.
37. Hiyoshi T, Fujiwara M, Yao Z. Postprandial hyperglycemia and postprandial hypertriglyceridemia in type 2 diabetes. Journal of Biomedical Research. 2017;33(1):1–16. https://doi.org/10.7555/JBR.31.20160164.
38. Oboh G, Ogunsuyi OB, Ogunbadejo MD, Adefegha SA. Influence of gallic acid on α-amylase and α-glucosidase inhibitory properties of acarbose. Journal of Food and Drug Analysis. 2016;24(3):627–634. https://doi.org/10.1016/j.jfda.2016.03.003.
39. Ademosun MT, Omoba OS, Olagunju AI. Antioxidant properties, glycemic indices, and carbohydrate hydrolyzing enzymes activities of formulated ginger-based fruit drinks. Journal of Food Biochemistry. 2021;45(3). https://doi.org/10.1111/jfbc.13324.
40. Mbhele N, Balogun FO, Kazeem MI, Ashafa T. *In vitro* studies on the antimicrobial antioxidant and antidiabetic potential of *Cephalaria gigantean*. Bangladesh Journal of Pharmacology. 2015;10(1):214–221. https://doi.org/10.3329/bjp.v10i1.21716.
41. Oboh G, Ogunsuyi OB, Adegbola DO, Ademiluyi AO, Oladun FL. Influence of gallic and tannic acid on therapeutic properties of acarbose in vitro and in vivo in Drosophila melanogaster. Biomedical Journal. 2019;42(5):317–327. https://doi.org/10.1016/j.bj.2019.01.005.
42. Kalita D, Holm DG, LaBarbera DV, Petrash JM, Jayanty SS. Inhibition of α-glucosidase, α-amylase, and aldose reductase by potato polyphenolic compounds. PLoS One. 2018;13(1).
43. Lafiandra D, Riccardi G, Shewry PR. Improving cereal grain carbohydrates for diet and health. Journal of Cereal Science. 2014;59(3):312–326. https://doi.org/10.1016/j.jcs.2014.01.001.

ORCID IDs
Ayokunle O. Ademosun https://orcid.org/0000-0001-9767-1844

Foods and Raw Materials, 2021, vol. 9, no. 2

E-ISSN 2310-9599
ISSN 2308-4057

Research Article
Open Access

https://doi.org/10.21603/2308-4057-2021-2-215-223
Available online at http://jfrm.ru/en

Grape pomace treatment methods and their effects on storage

Natalia M. Ageyeva*, Anastasia N. Tikhonova, Boris V. Burtsev, Svetlana A. Biryukova, Ekaterina V. Globa

North-Caucasian Federal Scientific Center of Horticulture, Viticulture and Winemaking, Krasnodar, Russia

* e-mail: ageyeva@inbox.ru

Received October 28, 2020; Accepted in revised form November 20, 2020; Published online July 09, 2021

Abstract:
Introduction. Grape pomace is the most important by-product of winemaking that can be used as an additional raw material. There is a need for an optimal storage technology so that pomace can be further processed to obtain new types of products. We aimed to study the effect of grape pomace treatment on its microflora.
Study objects and methods. We identified and quantified microflora on the fresh and one-month-stored pomace samples from white and red grape varieties. The samples were exposed to conventional drying at 60–65°C, infrared drying at 60–65°C, as well as sulfitation with sulfur dioxide and sodium metabisulfite.
Results and discussion. The pomace microflora can be considered a microbial community. Almost all the samples stored for one month in an open area contained *Saccharomyces cerevisiae* yeasts, higher concentrations of filmy yeasts of the *Candida*, *Pichia*, *Hansenula*, *Hanseniaspora*/*Kloeckera*, and *Torulaspora* genera, as well as conidia of *Mucor*, *Aspergillus niger*, and *Penicillium* molds. Prevalent bacteria included acetic acid (mainly *Acetobacter aceti*) and lactic acid (*Lactobacillus plantarum*, *Pediococcus*, *Leuconostoc*) bacteria. These microorganisms significantly changed concentrations of volatile and non-volatile components, decreasing total polysaccharides, phenolic compounds, and anthocyanins 1.7–1.9, 3.7–4.0, and 4.0–4.5 times, respectively. The contents of micromycetes and bacteria in the one-month-stored samples were significantly higher than in the fresh pomace. Pre-drying and sulfitation decreased bacterial contamination, but to a lesser extent compared to micromycetes.
Conclusion. Long-term storage spoiled pomace, leading to significant changes in its chemical composition. Sulfitation reduced microorganism growth during storage, but did not provide long-term preservation (over a month), while pre-drying at 60–65°C promoted longer storage.

Keywords: Winemaking by-products, grape pomace, yeast, bacteria, microflora, storage conditions

Funding: The research was financially supported by the Kuban Science Foundation as part of the scientific project No. MFI-20.1/22 “Studying the mechanisms of biotransformation of winemaking by-products for targeted management of their storage and processing”.

Please cite this article in press as: Ageyeva NM, Tikhonova AN, Burtsev BV, Biryukova SA, Globa EV. Grape pomace treatment methods and their effects on storage. Foods and Raw Materials. 2021;9(2):215–223. https://doi.org/10.21603/2308-4057-2021-2-215-223.

INTRODUCTION

The accumulation of wine production waste has an adverse effect on the environmental situation in grape-growing regions. Grape pomace is a key winemaking by-product that can be used as an additional raw material [1].

Grape pomace is rich in biologically valuable components, including polyphenols, pectin substances, and microelements [2, 3]. About 10–15% of this by-product is used as a biofertilizer to improve the soil structure [4]. Grape pomace can also be a source of dietary fiber, natural food colors, grape alcohol, tartaric acid, as well as extracts and concentrates [5–8]. Grape seeds are used to extract grape oil, which is widely used in cosmetology [9, 10]. Therefore, there is an urgent need for effective methods to process grape pomace.

Pomace can be sweet, fermented, and alcoholized, depending on the technology of grape processing.

Sweet pomace is obtained by pressing the grapes after the juice has separated. Such pomace contains microorganisms and major components of grape berries, including sugars. Sweet pomace is usually derived from white grapes during the production of table wines and

wine base for sparkling wines and champagne, as well as from red grapes processed like white grapes (without maceration or fermentation).

Fermented pomace results from pressing the fermented grapes during red table wine production. It contains ethanol (a product of natural fermentation of grape sugars), organic acids, phenolic, nitrogenous and pectin substances, aromatic components of wine base, as well as wine yeast and malolactic fermentation bacteria used for fermentation and acidity reduction.

Alcoholized pomace is produced through pressing fermented and alcoholized grapes in the production of liqueur wines, especially Kagor (fortified dessert wine) and Muscat wines. The last 15–20 years have seen a significant decrease in these wines due to a need to use grape alcohols in their production. Alcoholized pomace contains ethanol, sugars, and other components of grapes and wine base, including yeast. According to the Russian Ministry of Agriculture, alcoholized pomace accounts for 2.0–3.4% of total pomace, depending on the volume of liqueur wine production.

Various types of pomace differ in their components and microflora. Pomace can rapidly deteriorate during storage due to a combination of nutrients (sugars, nitrogenous compounds, organic acids, vitamins, etc.) and air exposed natural grape microflora (sweet pomace), as well as wine yeast and malolactic bacteria (fermented and alcoholized pomace). As a result, pomace becomes moldy, alcohol turns into acetic acid, and tartaric acid compounds get destroyed by bacteria.

Therefore, pomace needs to be processed immediately after its separation. However, sometimes it has to be stored for a certain time before processing (e.g., in the production of dietary fiber, powders, enocolorants, extracts, etc.). In this case, pomace must be stored under appropriate conditions, depending on the amount, type, and the physiological state of its microflora.

Grape pomace is usually stored on special sites, covered with tarpaulin or other material, if any. However, its surface and inside contain molds (*Aspergillus*, *Penicilium*, *Rhizopus nigricans*, *Cladosprium*, *Fusarium*, *Alternarium*, *Mucor*, *Botritis*, and *Oospora*), yeasts (*Saccharomyces* and *Torula*), bacteria (*Bacillus stearotermophilus*, *Bacillus sudtilis*, and *Staphylococcus aureus*), and many others microorganisms [11–14]. In this regard, the assessment of its microbiological state is an important part of pomace disposal, which depends on grape processing technology and storage conditions.

Our aim was to study the influence of storage conditions on the microflora of white and red grape pomace treated with different methods.

STUDY OBJECTS AND METHODS

Sampling and preparation for microbiological research. We studied fresh and one-month stored pomace from *Vitis vinifera* grapes produced in Krasnodar Krai (Russia), namely: sweet (Chardonnay, Riesling, Sauvignon Blanc, Traminer Rose, and Pinot Noir), fermented (Cabernet Sauvignon, Merlot, and Saperavi), and alcoholized (Traminer Rose, Cabernet Sauvignon, and Saperavi). The pomace came from the production of white and red table and liqueur wines. Some grape processing technologies used pectoproteolytic enzyme preparations – Trenolin Blanc and Trenolin Rouge (Erbsloeh Geisenheim AG, Germany) – in optimal manufacturer-recommended amounts. The storage temperature varied from 14°C (at night) to 26°C (at daytime). An average sample was obtained by mixing equal amounts of samples taken from the surface of the pomace mass. The samples were taken from a depth of 0.5 and 1.0 m, placed in glass flasks, filled with distilled water, and incubated at 22–25°C for two days.

Isolation of microorganisms. The samples were inoculated and passed on yeast-peptone agar containing 10 g yeast extract, 20 g peptone, 20 g agar-agar, and 20 g glucose per 1 L of water (Research Center for Pharmacotherapy, Russia). The elective test was performed on Lysine Medium Base (Himedia, India). Those isolates that were incapable of growing on the elective medium were considered as belonging to the genus *Saccharomyces*.

We also used solid nutrient media, such as grape juice agar (2%) alcoholized with ethanol (14% alcohol) – to identify saccharomycetes, and OFS-agar (Erbsloeh Geisenheim AG, Germany) – to quantify yeast, mold fungi, as well as lactic and acetic acid bacteria.

Chloramphenicol (50 mg/L) was introduced into the media to improve yeast growth and suppress bacterial growth. Yeast colonies were cultivated at 24 ± 2°C for 6–7 days. Some of them were inoculated on selective solid nutrient media. During the cultivation, we monitored the presence of other genera yeast, including *Saccharomyces*, *Pichia*, *Hansenula*, and *Hanseniaspora*.

The colonies were microscoped to identify saccharomycetes and other microorganisms based on their cultural and morphological characteristics [13, 15]. Generic identification of the isolates was based on their morphological and biochemical characteristics.

Physical and chemical parameters. The pomace was extracted with hot water (65–70°C) at a hydromodule of 1:5. The extracts were analyzed to determine:

– organic acids: by capillary electrophoresis State Standard 52841-2007. Wine production. Determination of organic acids by capillary electrophoresis method. Moscow: Standartinform; 2008. 7 p.;

– ethyl alcohol: according to State Standard 32095-2013. The alcohol production and raw material for it producing. Method of ethyl alcohol determination;

– phenolic substances: by the Folin-Ciocalteu colorimetric method [16];

– anthocyanins: by the colorimetric method [16];

– polysaccharides: by the phenol sulfur method [16]; and

– volatile impurities: by gas-liquid chromatography (Crystal 5000, nitrogen carrier gas, flame ionization

detector, PEG-based HP-FFAP column, 50 m, 0.32 mm, dosing device).

Pomace treatment before storage. To study the effect of storage conditions on microbiological parameters, the pomace samples were treated using the following methods:

– drying at 60–65°C to constant weight in a laboratory drying oven with forced air convection (AB UMEGA-GROUP, Lithuania);

– drying at 60–65°C to constant weight in a drying oven with infrared radiation (Radiozavod, Russia);

– exposing to sulfur dioxide (sulfitation) introduced as a concentrated solution (at least 1g SO_2/kg pomace); and

– treating with sodium metabisulfite introduced in tablet form into the lower part of pomace (when decomposed, it produces sulfur dioxide that evenly spreads throughout the pomace).

RESULTS AND DISCUSSION

Microbiological studies of fresh and stored grape pomace. We compared the microbiological indicators for fresh and one-month stored pomace samples from various grape varieties obtained by different methods (Table 1). As we can see, fresh sweet pomace had a significantly smaller amount of micromycetes (including yeast fungi) and bacteria than fermented pomace. This was because the fermented samples contained wine yeast, which is used for alcoholic fermentation, and lactic acid-reducing bacteria, which are often introduced at the final stage of fermentation. The smallest amount of microorganisms was found in the alcoholized pomace, which is associated with the inhibitory effect of ethyl alcohol.

We found that the pomace microflora included microorganisms of various classes, species, and genera. Their metabolic interactions involved the transfer of metabolites between partners, a producer and a metabolizer. For example, yeast converted residual sugars to ethyl alcohol that was consumed by acetic acid bacteria to produce acetaldehyde and acetic acid. Lactic acid bacteria and yeast have a symbiotic relationship. Yeast stimulates growth in lactic acid bacteria, fortifies foods with vitamins, as well as ferments lactose and other sugars to produce antibiotic substances acting against pathogenic microorganisms.

With changes in environmental conditions, some microorganisms can suspend the processes of reproduction and fermentation of other species. Some lactic acid bacteria, mainly rod-shaped (a threat to wine production), can act antagonistically and destroy yeast cells, for example, in nitrogen-depleted media (pH < 6) [17]. Yeast and acetic acid bacteria stimulate growth in lactic acid bacteria. Thus, some biochemical processes that occur during storage can significantly change the chemical composition of grape pomace and make it unsuitable for production. In particular, pomace microorganisms destroy organic acids and polysaccharides, basic components of dietary fiber. Moreover, they consume vitamins and vitamin-like substances, leading to a significant decrease in bioactive components, so important for the production of extracts and concentrates.

Table 1 Microbiological indicators of fresh and stored pomace obtained by pressing, CFU/g

Grape variety, type of pomace / Pressing equipment	Pomace			
	Fresh		Stored for one month	
	micromycetes, incl. yeast	bacteria	micromycetes, incl. yeast	bacteria
Chardonnay, sweet / Diemme, Italy	4.3×10^3	0.6×10^3	6.8×10^5	8.4×10^5
Chardonnay, sweet / Busher Vaslin, France	3.8×10^3	0.4×10^3	6.3×10^5	8.8×10^5
Chardonnay, sweet / Enoventa, Italy	4.6×10^3	0.4×10^3	6.6×10^5	7.8×10^5
Pinot Blanc, sweet / Enoventa, Italy	4.0×10^3	0.5×10^3	7.1×10^5	8.3×10^5
Pinot Blanc, sweet, trenolin blanc / Enoventa, Italy	4.3×10^3	0.4×10^3	6.8×10^5	7.6×10^5
Riesling, sweet / Della Toffola, Italy	3.7×10^3	0.5×10^3	7.1×10^5	7.7×10^5
Riesling, sweet + trenolin blanc / Della Toffola, Italy	3.9×10^3	0.5×10^3	9.5×10^4	5.8×10^4
Traminer Rose, sweet / Enoventa, Italy	3.1×10^3	0.4×10^3	7.4×10^5	7.0×10^5
Traminer Rose, sweet + trenolin blanc / Enoventa, Italy	3.6×10^3	0.4×10^3	7.5×10^4	6.9×10^4
Traminer Rose, alcoholized / Enoventa, Italy	2.1×10^3	0.3×10^3	3.3×10^5	2.4×10^5
Sauvignon B lanc, sweet / Enoventa, Italy	3.6×10^3	0.5×10^3	7.1×10^5	7.7×10^5
Pinot Noir, sweet / Busher Vaslin, France	3.2×10^3	0.2×10^3	4.3×10^5	1.6×10^5
Merlot, fermented / Busher Vaslin, France	7.8×10^4	0.7×10^3	8.7×10^6	6.6×10^5
Merlot, fermented + trenolin rouge / Busher Vaslin, France	8.1×10^4	0.8×10^3	6.8×10^6	6.0×10^6
Saperavi, fermented / Busher Vaslin, France	6.2×10^4	0.6×10^3	3.2×10^6	3.7×10^6
Saperavi, alcoholized / Busher Vaslin, France	3.1×10^3	0.3×10^3	1.8×10^5	2.3×10^5
Saperavi, fermented + trenolin rouge / Busher Vaslin, France	3.7×10^3	0.6×10^3	7.8×10^6	3.1×10^6
Cabernet Sauvignon, fermented/Busher Vaslin, France	6.8×10^4	0.7×10^3	5.4×10^6	2.7×10^6
Cabernet Sauvignon, alcoholized / Busher Vaslin, France	3.7×10^3	0.3×10^3	4.2×10^4	1.1×10^4
Cabernet Sauvignon, fermented + trenolin rouge / Busher Vaslin, France	7.4×10^4	0.5×10^3	5.0×10^5	3.0×10^5

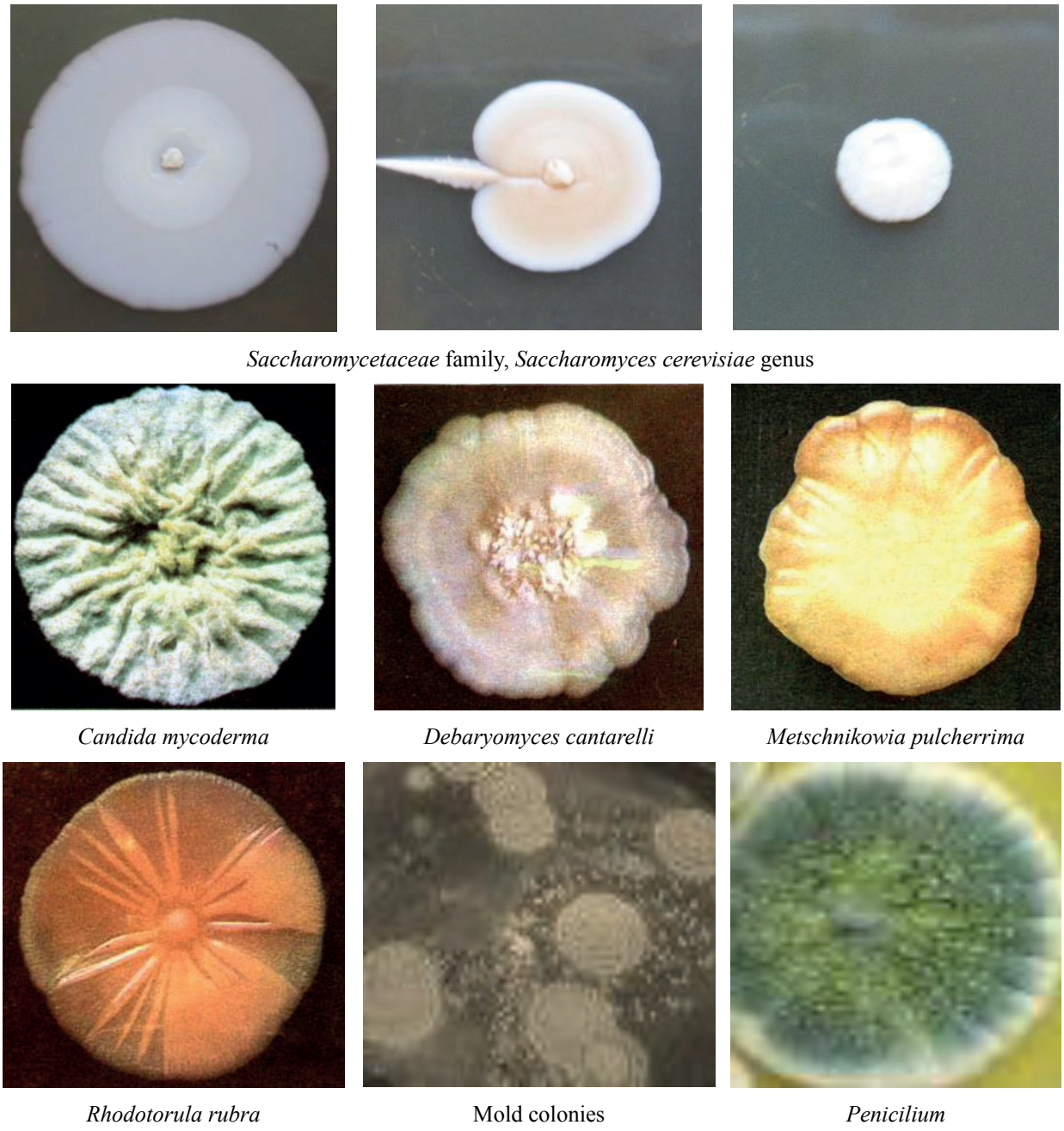

Figure 1 Colonies of microorganisms isolated from grape pomace samples

The Chardonnay samples can be used to show a correlation between the method of pressing and the number of microorganisms (Table 1). Different pressing equipment produces pomace that varies in moisture. The Busher Vaslin press (France) provided a higher degree of pressing and, therefore, a higher mechanical effect on grapes (fresh, fermented or alcoholized) compared to other presses, resulting in less active microorganisms and fewer colonies.

The use of enzyme preparations to produce sweet and fermented pomace led to a decomposition of many high-molecular grape components (proteins, polysaccharides, complex compounds) into low-molecular substances easily assimilated by the microflora. The fermentation increased the concentration of sugars and nitrogenous substances, stimulating the growth of micromycetes and bacteria cells on nutrient media.

Storing the pomace samples in tarpaulin-covered cement pits with air access activated microorganism cells, leading to their significant increase, especially bacteria, in all the experiments.

Figure 1 shows colonies of microorganisms in the pomace samples stored for one month in an open area. They were isolated by inoculation on solid nutrient media. The average pomace sample contained yeast of

the *Saccharomyces cerevisiae* genus, characteristic of wine production. Its colonies varied in shape (round, with or without septa, radial or feathery, some with a well-defined inner ring), appearance (shiny or matte, dry or wet, smooth or wrinkled, with smooth or deformed edges), surface relief, and thickness. Such a variety was due to their belonging to different species [12, 14, 18–20].

Growing on the pomace surface, *Candida mycoderma* consumes extractives and releases volatile compounds that give the pomace a pungent taste and unpleasant odor, making it unsuitable for further processing [12, 14]. Moreover, its enzyme systems can break down high-molecular compounds (including pectin substances), significantly reducing the value of the pomace as a secondary raw material.

Almost all the samples contained filmy yeasts of the *Candida*, *Pichia*, *Hansenula*, *Hanseniaspora*/*Kloeckera*, and *Torulaspora* genera, with their greatest amount in fresh pomace of white grape varieties and the smallest amount in alcoholized pomace. Noteworthily, yeasts of the *Brettanomyces* and *Schizosaccharomyces* genera, which are always present on grape berries, were low in our samples, under 0.7–1.0% [21]. Yeasts of the *Pichia* and *Hansenula* genera were under 1.2%, depending on the technology of pomace production. The growth of these microorganisms in our pomace samples significantly changed their aroma, giving them the tones of fermentation, ethyl acetate, and sour milk.

Debaryomyces yeasts, which we identified in the average pomace sample, have a poor ability to absorb sugars, metabolize tartaric, lactic, and citric acids into esters, synthesize extracellular enzymes, and decompose toxins [22, 23]. They make the pomace unsuitable for further processing.

Molds were clearly visible on the pomace surface (3.5–6.4%), namely *Mucor*, *Aspergillus niger*, and *Penicillium*. They are highly undesirable since they can produce mycotoxins and compounds with unpleasant odors and tastes [24, 25].

Table 2 Physicochemical parameters of fresh and one-month stored pomace extracts

Parameters	Traminer Rose pomace			
	Fresh		Stored for one month	
	Sweet	Sweet fermented	Sweet	Sweet fermented
	Organic acids, g/L extract			
Tartaric	8.8 ± 0.4	9.4 ± 0.6	2.7 ± 0.3	2.5±0.4
Malic	5.6 ± 0.2	6.1 ± 0.4	1.5 ± 0.2	1.3±0.3
Citric	2.0 ± 0.2	2.0 ± 0.2	n.d.	n.d.
Succinic	3.2 ± 0.2	2.4 ± 0.2	n.d.	n.d.
Ascorbic	2.6 ± 0.2	3.0 ± 0.3	n.d.	n.d.
Lactic	n.d.	n.d.	2.76 ± 0.12	2.94 ± 0.08
	Volatile compounds, g/L extract			
Ethanol	8.6 ± 0.2	10.3 ± 0.2	n.d.	n.d.
Acetaldehyde	164 ± 17	182 ± 22	1210 ± 28	1421 ± 32
Acetoin	8.64 ± 0.12	4.26 ± 0.12	124.7 ± 6	88.7 ± 4
Acetone	n.d.	n.d.	44.8 ± 0.3	35.7 ± 0.2
Acetic acid	134 ± 12	146 ± 15	650 ± 22	720 ± 27
Propionic acid	n.d.	n.d.	12.6 ± 0.17	11.8 ± 0.16
Butyric acid	0.24 ± 0.07	0.28 ± 0.07	1.86 ± 0.12	2.15 ± 0.09
Ethyl acetate	246 ± 16	308 ± 22	1264 ± 23	1432 ± 31
Ethyl propionate	n.d.	n.d.	67.6 ± 2.4	65.3 ± 1.8
Methyl acetate	13.8 ± 0.6	10.4 ± 0.6	47.5 ± 1.5	52.8 ± 2.3
Propyl acetate	n.d.	n.d.	144 ± 11	165 ± 13
Butyl acetate	8.4 ± 0.6	6.7 ± 0.6	65 ± 6	78 ± 5
Isoamylacet	28.4 ± 2.2	21.6 ± 2.3	132 ± 8	118 ± 4
Ethyl lactate	44.8 ± 7	42.4 ± 6	187 ± 12	213 ± 13
1-propanol	2.8 ± 0.2	3.0 ± 0.2	43.5 ± 1.3	54.7 ± 2.0
n-propanol	14.7 ± 1.2	23.6 ± 1.6	145 ± 23	127 ± 20
n-butanol	n.d.	n.d.	87 ± 11	94 ± 15
Isoamylol	86 ± 12	78 ± 9	1254 ± 37	1152 ± 27
Glycerol	886 ± 24	935 ± 27	184 ± 11	167 ± 10
	Non-volatile compounds, mg/L extract			
Common polysaccharides	1234 ± 29	1347 ± 33	765 ± 18	684 ± 14
Common phenolic substances	886 ± 21	764 ± 17	237 ± 11	198 ± 9
Common anthocyanins	165 ± 15	144 ± 12	45 ± 6	32 ± 4

n.d. – not detected

Prevailing bacteria included acetic acid bacteria (mainly *Acetobacter aceti*) and lactic acid bacteria (including *Lactobacillus plantarum*, *Pediococcus*, and *Leuconostoc*) amounting to 6–9%, with their greatest increase in sweet pomace during storage.

The greatest growth in microorganisms was in the sweet pomace samples during storage: yeast cells converted sugars to ethanol, which was then used by acetic acid bacteria to synthesize acetic acid. Lactic acid bacteria were especially frequent in fermented pomace. We found that microorganism growth was much greater in white grape pomace compared to red grape pomace, which is rich in phenolic compounds with antiseptic and antibacterial action [26–28].

Microflora also increased in alcoholized pomace, despite 7–10% ethyl alcohol, although not as much as in the other types of samples. With acetic and lactic acid fermentation, alcoholized pomace (e.g. Cabernet-Sauvignon) still retained grape-wine tones in its aroma.

Thus, we found that red grape pomace did better during storage than white pomace due to the presence of polyphenols with antiseptic effects. Alcoholized pomace showed the smallest growth in micromycetes.

Physicochemical parameters of fresh and one-month stored pomace extracts. Changes in the physicochemical parameters of the Traminer Rose pomace extracts (sweet and fermented) are presented in Table 2.

The chemical composition of the extracts (Table 2) showed that microorganism growth in the stored pomace significantly decreased the concentration of tartaric, malic, and citric acids, with succinic and ascorbic acids completely oxidized. Moreover, the microorganisms consumed succinic acid and converted it into fumaric and formic acids, disrupting the pomace aroma. Tartaric acid decomposed under the action of *Debaryomyces* yeast and various lactic acid bacteria (*Lactobacillus brevis*, *Lactobacillus hilgardii*, *Lactobacillus plantarum*, and heterofermentative cocci), producing diacetyl, acetic, propionic, and lactic acids [29].

The above process consumed a large amount of glycerin. The growth in lactic acid bacteria increased the concentration of lactic acid and ethyl lactate ester. Citric acid decomposed under the action of enzymes of lactic acid bacteria and molds, producing acetoin and acetone.

The growth in acetic acid bacteria and molds significantly changed concentrations of volatile components, namely:

– ethanol decomposed under the action of enzyme systems of acetic acid bacteria into acetic acid and its derivatives in the stored pomace extracts, making their further use in wine distillation impossible;

– glycerol, which is used by the pomace microflora in the biochemical processes to synthesize new components, decreased 4.4–6.0-fold;

– acetaldehyde, acetic acid, and ethyl acetate increased 7.3–7.7, 4.2–4.8, and 4.5–5.2 times respectively, all having a smell of acetic acid and thus giving the extracts an unbalanced tangy taste;

– propionic acid and its ethyl ester were identified in the stored pomace extracts, unlike the fresh extracts;

– higher alcohols, especially isoamylol and butanol, significantly increased, making the pomace unsuitable for distilling grape alcohol due to their pronounced fusel tones.

Acetic acid bacteria can oxidize mono- and polyhydric alcohols (as well as ethyl alcohol), carbohydrates and other substances in the extracts. Monohydric alcohols are oxidized to the corresponding acids (e.g., propanol to propionic acid, butyl alcohols to butyric acid), increasing their concentrations (Table 2).

Non-volatile (extractive) components, namely polysaccharides, phenolic compounds, and anthocyanins decreased 1.7–1.9, 3.7–4.0, and 4.0–4.5 times,

Table 3 Microbiological indicators of pomace, CFU/g vs storage conditions

Grape variety, type of pomace	Pomace treatment			
	Drying at 60–65°C	Infrared drying at 60–65°C	Sulfur dioxide	Sodium metabisulfite
	Micromycetes			
Chardonnay, sweet	1.2×10^2	2.8×10^3	3.2×10^3	4.4×10^3
Riesling, sweet	0.8×10^2	1.7×10^3	2.3×10^3	3.7×10^3
Pinot Blanc, sweet	1.2×10^2	1.8×10^3	2.8×10^3	2.9×10^3
Pinot Blanc, sweet, trenolin blanc	1.3×10^2	1.4×10^3	3.0×10^03	2.8×10^3
Cabernet Sauvignon, fermented	0.8×10^2	1.5×10^3	2.7×10^3	2.6×10^3
Cabernet Sauvignon, alcoholized	0.4×10^2	0.2×10^3	1.2×10^3	1.3×10^3
Cabernet Sauvignon, fermented, trenolin rouge	0.8×10^2	0.4×10^3	2.8×10^3	2.5×10^3
	Bacteria			
Chardonnay, sweet	6.3×10^2	2.5×10^3	8.9×10^3	1.2×10^4
Riesling, sweet	6.3×10^2	1.9×10^3	8.9×10^3	2.1×10^4
Pinot Blanc, sweet	7.0×10^2	4.1×10^3	9.1×10^3	4.5×10^4
Pinot Blanc, sweet, trenolin blanc	5.8×10^2	3.8×10^3	1.2×10^4	3.1×10^4
Cabernet Sauvignon, fermented pomace	7.1×10^2	7.2×10^2	6.7×10^3	8.4×10^3
Cabernet Sauvignon, alcoholized	1.3×10^2	5.5×10^2	3.5×10^3	5.1×10^3
Cabernet Sauvignon, fermented, trenolin rouge	3.7×10^2	8.7×10^2	5.1×10^3	8.1×10^3

respectively. This reduced the production of grape dietary fiber and extracts of phenolic compounds from the pomace stored under those conditions, lowering its efficiency 4.5–6.8 times.

Thus, our experimental data showed a need to develop a pomace storage technology that would make pomace suitable for further use in production.

Microbiological pomace parameters versus pre-storage treatment methods. Various methods can be used to prepare pomace for storage. They include drying at various temperatures, treatment with ultraviolet and infrared rays, electromagnetic waves, regulating the gaseous environment, using chemical preservatives, alcoholization, and others [30–32].

Alcoholization is obviously the best preserver of bioactive components in grapes, but it requires large amounts of min 25% ethanol.

Our microbiological assays involved all types of the pomace samples treated by different methods: drying at 60–65°C, infrared drying at 60–65°C, adding sulfur dioxide and sodium metabisulfite (Table 3). We found that all the methods decreased contamination during storage. Drying at 60–65°C was most effective in reducing the activity of micromycetes, especially in red pomace. Infrared drying had the same effect, but to a lesser extent. It may be necessary to work out optimal processing modes, in particular, with higher temperatures.

Sulfur dioxide and its derivatives decreased the growth in micromycetes 75–100 times during one month. Bacterial contamination also decreased, but to a lesser extent. Noteworthily, both drying methods were more efficient than sulfur dioxide and sodium metabisulfite. Most samples, including alcoholized and sulfitized ones, showed an increase in acetic and lactic acid bacteria at the end of the treatments. This indicated that these modes of sulfitation and drying did not ensure complete inhibition of the pomace microflora.

CONCLUSION

Our experimental data led us to the following conclusions. The pomace samples were contaminated with various microorganisms, whose growth spoiled the pomace. Significant changes in its chemical composition during long-term storage can make it unsuitable for further use in food production. Available treatment methods decreased microorganism contamination, but did not ensure long-term preservation of the pomace. Sulfur dioxide or sodium metabisulfite can be used for short-term storage (up to a month). However, thermal treatment is required for longer storage to inhibit microorganism growth.

CONTRIBUTION

The authors were equally involved in writing the manuscript and are equally responsible for plagiarism.

CONFLICT OF INTEREST

The authors declare that there is no conflict of interest.

REFERENCES

1. Beres C, Costa GNS, Cabezudo I, da Silva-James NK, Teles ASC, Cruz APG, et al. Towards integral utilization of grape pomace from winemaking process: A review. Waste Management. 2017;68:581–594. https://doi.org/10.1016/j.wasman.2017.07.017.
2. Zhao X, Zhang S-S, Zhang X-K, He F, Duan C-Q. An effective method for the semi-preparative isolation of high-purity anthocyanin monomers from grape pomace. Food Chemistry. 2020;310. https://doi.org/10.1016/j.foodchem.2019.125830.
3. Minjares-Fuentes R, Femenia A, Garau MC, Meza-Velázquez JA, Simal S, Rosselló C. Ultrasound-assisted extraction of pectins from grape pomace using citric acid: A response surface methodology approach. Carbohydrate Polymers. 2014;106(1):179–189. https://doi.org/10.1016/j.carbpol.2014.02.013.
4. Cortés A, Moreira MT, Domínguez J, Lores M, Feijoo G. Unraveling the environmental impacts of bioactive compounds and organic amendment from grape marc. Journal of Environmental Management. 2020:272. https://doi.org/10.1016/j.jenvman.2020.111066.
5. Sirohi R, Tarafdar A, Singh S, Negi T, Gaur K, Gnansounou E, et al. Green processing and biotechnological potential of grape pomace: Current trends and opportunities for sustainable biorefinery. Bioresource Technology. 2020;314. https://doi.org/10.1016/j.biortech.2020.123771.
6. Tikhonova AN, Ageyeva NM. Deep processing of grapes for obtaining the grape food fibers. Nauchnye trudy Severo-Kavkazskogo federal′nogo nauchnogo tsentra sadovodstva, vinogradarstva, vinodeliya [Scientific works of the North-Caucasian Federal Scientific Center of Horticulture, Viticulture and Winemaking]. 2018;18:180–183. (In Russ.). https://doi.org/10.30679/2587-9847-2018-18-180-183.
7. Kato-Schwartz CG, Corrêa RCG, de Souza Lima D, de Sá-Nakanishi AB, de Almeida Gonçalves G, Seixas FAV, et al. Potential anti-diabetic properties of Merlot grape pomace extract: An *in vitro*, *in silico* and *in vivo* study of α-amylase and α-glucosidase inhibition. Food Research International. 2020;137. https://doi.org/10.1016/j.foodres.2020.109462.

8. Beres C, Freitas SP, Godoy RLDO, de Oliveira DCR, Deliza R, Iacomini M, et al. Antioxidant dietary fibre from grape pomace flour or extract: Does it make any difference on the nutritional and functional value? Journal of Functional Foods. 2019;56:276–285. https://doi.org/10.1016/j.jff.2019.03.014.
9. Glampedaki P, Dutschk V. Stability studies of cosmetic emulsions prepared from natural products such as wine, grape seed oil and mastic resin. Colloids and Surfaces A: Physicochemical and Engineering Aspects. 2014;460:306–311. https://doi.org/10.1016/j.colsurfa.2014.02.048.
10. Dabetic NM, Todorovic VM, Djuricic ID, Antic Stankovic JA, Basic ZN, Vujovic DS, et al. Grape seed oil characterization: A novel approach for oil quality assessment. European Journal of Lipid Science and Technology. 2020;122(6). https://doi.org/10.1002/ejlt.201900447.
11. Mezzasalma V, Sandionigi A, Bruni I, Bruno A, Lovicu G, Casiraghi M, et al. Grape microbiome as a reliable and persistent signature of field origin and environmental conditions in Cannonau wine production. PLoS ONE. 2017;12(9). https://doi.org/10.1371/journal.pone.0184615.
12. Bur′yan NI. Mikrobiologiya vinodeliya [Microbiology of winemaking]. Simferopol′: Tavriya; 2002. 433 p. (In Russ.).
13. Ageeva NM, Suprun II, Prakh AV. Variety of microorganisms groups living on berries of grapes. Polythematic Online Scientific Journal of Kuban State Agrarian University. 2015;(111):1586–1595. (In Russ.).
14. Viziteu G-A, Manoliu A, Andor I. Data concerning the yeasts microbiota from Cotnari vineyard. Romanian Biotechnological Letters. 2008;13(2).
15. Suprun II, Tokmakov SV, Ageeva NM, Prakh AV. Aprobation of genotyping method of wine yeast (genus Saccharomyces) by the analysis of inter-delta genomic region. Polythematic Online Scientific Journal of Kuban State Agrarian University. 2015;(112):484–494. (In Russ.).
16. Gerzhikova VG. Metody tekhnokhimicheskogo kontrolya v vinodelii [Technochemical control methods in winemaking]. Simferopol′: Tavrida; 2009. 304 p. (In Russ.).
17. Dorosh AP, Gregirchak NN. Investigation of thermal resistance and antagonistic properties of the yeast Saccharomyces cerevisiae. Zhivye i biokosnye sistemy. 2015;(11).
18. Bizaj E, Cordente A, Bellon JR, Raspor P, Curtin CD, Pretorius IS. A breeding strategy to harness flavor diversity of *Saccharomyces* interspecific hybrids and minimize hydrogen sulfide production. FEMS Yeast Research. 2012;12(4):456–465. https://doi.org/10.1111/j.1567-1364.2012.00797.x.
19. Li S, Cheng C, Li Z, Chen J, Yan B, Han B, et al. Yeast species associated with wine grapes in China. International Journal of Food Microbiology. 2010;138(1–2):85–90. https://doi.org/10.1016/j.ijfoodmicro.2010.01.009.
20. Settanni L, Sannino C, Francesca N, Guarcello R, Moschetti G. Yeast ecology of vineyards within Marsala wine area (western Sicily) in two consecutive vintages and selection of autochthonous *Saccharomyces cerevisiae*. Journal of Bioscience and Bioengineering. 2012;114(6):606–614. https://doi.org/10.1016/j.jbiosc.2012.07.010.
21. Schopp LM, Lee J, Osborne JP, Chescheir SC, Edwards CG. Metabolism of nonesterified and esterified hydroxycinnamic acids in red Wines by *Brettanomyces bruxellensis*. Journal of Agricultural and Food Chemistry. 2013;61(47):11610–11617. https://doi.org/10.1021/jf403440k.
22. Jara C, Laurie VF, Mas A, Romero J. Microbial terroir in chilean valleys: Diversity of non-conventional yeast. Frontiers in Microbiology. 2016;7. https://doi.org/10.3389/fmicb.2016.00663.
23. Aiko V, Edamana P, Mehta A. Decomposition and detoxification of aflatoxin B_1 by lactic acid. Journal of the Science of Food and Agriculture. 2016;96(6):1959–1966. https://doi.org/10.1002/jsfa.7304.
24. Şen L, Nas S. Identification of ochratoxigenic fungi and contextual change on dried raisins (Sultanas). Journal of Food, Agriculture and Environment. 2013;11(3–4):155–161.
25. Steel CC, Blackman JW, Schmidtke LM. Grapevine bunch rots: Impacts on wine composition, quality, and potential procedures for the removal of wine faults. Journal of Agricultural and Food Chemistry. 2013;61(22):5189–5206. https://doi.org/10.1021/jf400641r.
26. Radovanović VN, Andjelković M, Arsić B, Radovanović A, Gojković-Bukarica L. Cost-effective ultrasonic extraction of bioactive polyphenols from vine and wine waste in Serbia. South African Journal of Enology and Viticulture. 2019;40(2):1–9. https://doi.org/10.21548/40-2-3215.
27. Mewa-Ngongang M, Du Plessis HW, Ntwampe SKO, Chidi BS, Hutchinson UF, Mekuto L, et al. Grape pomace extracts as fermentation medium for the production of potential biopreservation compounds. Foods. 2019;8(2). https://doi.org/10.3390/foods8020051.
28. Friedman M. Antibacterial, antiviral, and antifungal properties of wines and winery byproducts in relation to their flavonoid content. Journal of Agricultural and Food Chemistry. 2014;62(26):6025–6042. https://doi.org/10.1021/jf501266s.

29. Kosel J, Cadež N, Schuller D, Carreto L, Franco-Duarte R, Raspor P. The influence of *Dekkera bruxellensis* on the transcriptome of *Saccharomyces cerevisiae* and on the aromatic profile of synthetic wine must. FEMS Yeast Research. 2017;17(4). https://doi.org/10.1093/femsyr/fox018.
30. Augustine S, Kudachikar VB, Vanajakshi V, Ravi R. Effect of combined preservation techniques on the stability and microbial quality and retention of anthocyanins in grape pomace stored at low temperature. Journal of Food Science and Technology. 2013;50(2):332–338. https://doi.org/10.1007/s13197-011-0325-0.
31. Tseng A, Zhao Y. Effect of different drying methods and storage time on the retention of bioactive compounds and antibacterial activity of wine grape pomace (Pinot Noir and Merlot). Journal of Food Science. 2012;77(9):H192–H201. https://doi.org/10.1111/j.1750-3841.2012.02840.x.
32. Zheng Y, Lee C, Yu C, Cheng Y-S, Simmons CW, Zhang R, et al. Ensilage and bioconversion of grape pomace into fuel ethanol. Journal of Agricultural and Food Chemistry. 2012;60(44):11128–11134. https://doi.org/10.1021/jf303509v.

ORCID IDs
Natalia M. Ageyeva https://orcid.org/0000-0002-9165-6763
Anastasia N. Tikhonova https://orcid.org/0000-0002-3509-3345
Boris V. Burtsev https://orcid.org/0000-0001-9755-5384
Svetlana A. Biryukova https://orcid.org/0000-0001-8182-7429
Ekaterina V. Globa https://orcid.org/0000-0002-6890-3076

Foods and Raw Materials, 2021, vol. 9, no. 2

E-ISSN 2310-9599
ISSN 2308-4057

Research Article
Open Access

https://doi.org/10.21603/2308-4057-2021-2-224-233
Available online at http://jfrm.ru/en

NanoKremny effect on the quality of grapes and wines

Natalia V. Aleinikova[1], Irina V. Peskova[1,*], Elena V. Ostroukhova[1], Yevgenia S. Galkina[1], Pavel A. Didenko[1], Polina A. Probeigolova[2], Nataliya Yu. Lutkova[1]

[1] All-Russian National Research Institute of Viticulture and Winemaking "Magarach" of RAS, Yalta, Russia

[2] JSC "Zolotoye Pole", Zolotoye Pole, Russia

* e-mail: bioxim2012@mail.ru

Received January 31, 2020; Accepted in revised form March 01, 2020; Published online July 09, 2021

Abstract:
Introduction. There is still an urgent need in viticulture for studying the effect of tank mixtures of pesticides and bioactive substances on *Vitis vinifera* and, therefore, the quality and composition of wine. We aimed to study the effect of NanoKremny (silicon fertilizer) treatment of the grapevine on the productivity and quality of grape harvest, as well as the quality of dry wines.
Study objects and methods. Grape varieties from three vineyards in Crimea and the wines produced from them. We applied standard methods used in viticulture, plant protection, and oenological practice. Organic acids and volatile components in grapes and wines were determined by high-performance liquid chromatography and gas chromatography.
Results and discussion. We found that the most effective use of NanoKremny was threefold at 0.15 L/ha during the periods of active growth and formation of vegetative and generative organs in grapevines. It had a positive effect on vegetative development, water balance, productivity of grape plants, as well as yield quality and quantity. Also, NanoKremny decreased the development of mildew and oidium diseases, preserved the content of titratable acids in grapes during their ripening, as well as accumulated phenolic compounds, tartaric and malic acids in grape berries.
Conclusion. We found no negative effect of NanoKremny treatment of the grapevine on the physicochemical parameters and sensory characteristics of wines. Thus, this preparation can be used as a bioorganic additive in viticulture.

Keywords: Grapes, NanoKremny, foliar dressing, tank mixture, productivity, yield parameters, wine, chemical composition, quality

Funding: The study was conducted under Research Agreements No. 67/16 of 12 July 2016, No. 48/17 of 4 April 2017, and No. 54/18 of 7 May 2018.

Please cite this article in press as: Aleinikova NV, Peskova IV, Ostroukhova EV, Galkina YeS, Didenko PA, Probeigolova PA, et al. NanoKremny effect on the quality of grapes and wines. Foods and Raw Materials. 2021;9(2):224–233. https://doi.org/10.21603/2308-4057-2021-2-224-233.

INTRODUCTION

Silicon, whose content in soil is rather high (50–400 g/kg soil), plays a significant role in soil formation and fertility [1, 2]. Back in 1813, Davy established that silicon is concentrated in the epidermal tissues of plants, creating a barrier that protects plants from insect pests. This was the first work on the importance of silicon in plant physiology.

Today, we know a lot about the role of silicon in plant life (Fig. 1). In particular, silicon content determines the level of natural protection against biotic and abiotic stresses [2–8]. Silicon nutrition for plants increases leaf area and creates favorable conditions for photosynthesis [7, 9]. When added to the soil, readily-soluble silica improves the metabolism of nitrogen and phosphorus in tissues, increases the content of phosphates, and facilitates the consumption of boron and other elements. In addition, it reduces the toxicity of excessive heavy metals, neutralizes the negative effects of excessive nitrogen fertilizers, increases the population of ammonifiers, improves nitrification, and helps the soil to absorb mobile forms of nitrogen [10–14].

Silicon fertilizers are increasingly being used in agriculture across the world (the USA, China, India, Brazil, Japan, South Korea, Mexico, Australia, and other countries). Their production increases by 20–30% annually. An ecological alternative to pesticides, they also increase plants' resistance to stress.

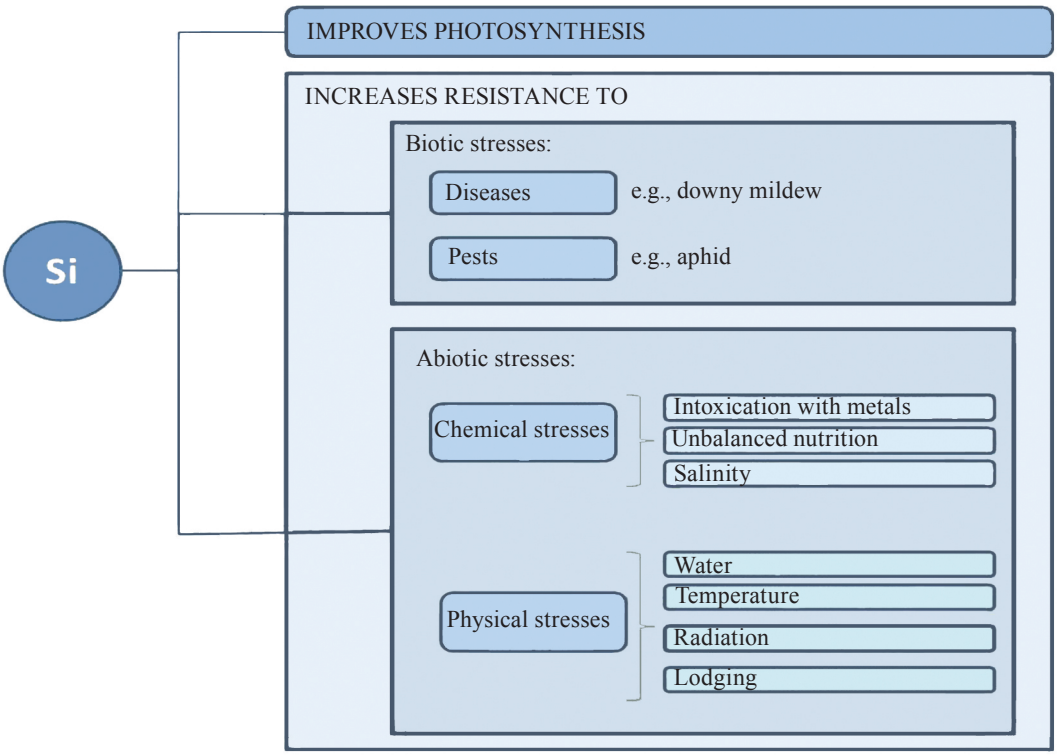

Figure 1 Role of silicon in plant life [12]

Russia-produced silicon fertilizers include natural silicon materials (Diatomite, BIO COMPLEX; Promzeolit, PROMZEOLIT), concentrated monosilicic acid with active colloidal silicon (Akkor, Moscow Region), as well as physiologically active organosilicon biostimulants (FLORA-SI, Moscow). Among them is a unique fertilizer – NanoKremny (NANOCREMNY) – crystalline silicon with a particle size under 0.5 μm, which has no analogues in Russia or other countries.

Silicon fertilizers have a proven positive effect on different soils for the *Leguminosae*, *Gramineae*, *Solanaceae*, *Citrinae*, and *Cruciferae* families, as well as other agricultural crops. However, few studies have looked into tank mixtures of pesticides and bioactive substances in relation to *Vitis vinifera*. In practice, using scientifically unfounded tank compositions often leads to negative phytosanitary and economic consequences [15].

The quantity and quality of grape and wine yield can be increased by using foliar dressing with macro- and microelements. Grape quality is determined primarily by sugar content and acidity of the berry juice. According to State Standard 31782-2012 "Fresh grape of combine and hand harvesting for industrial processing. Specifications", the concentration of sugars in grapes for winemaking must be at least 160 g/L for white varieties and 170 g/L for red varieties. To ensure such high concentrations of sugars and stable grape yield, the grapevine must be provided with sources of microelements [16, 17].

In recent years, scientists have been interested in the role of bioorganic additives in winemaking technology. Silicon-containing preparations, in particular, have a beneficial effect on yeast metabolism and functional activity. They intensify alcoholic fermentation, enrich the wine with volatile components and, therefore, improve its aroma [18–20].

We aimed to substantiate the use of the NanoKremny mineral fertilizer in the Crimean vineyards and to study its effect on crop efficiency, the quality and quantity of grape, as well as the chemical composition and sensory indicators of dry table wines.

STUDY OBJECTS AND METHODS

Our study objects were the grapes of white (Aligoté, Chardonnay) and red (Cabernet Sauvignon) varieties, as well as respective dry wines produced in 2017–2018 in the western piedmont-coastal area of the main viticulture zones of Crimea, namely the South-Western Zone (S. Perovskoy; SVZ-AGRO, Sevastopol), the Central Steppe Zone (Legenda Kryma, Geroyskoye village), and the South Coast zone (Livadiya branch of Massandra Winery, Yalta). Grape cultivation was in line with the technological maps adopted for each variety in each zone.

The technology for dry white table wines (Chardonnay and Aligoté) included the following stages:
– crushing grapes on a manual roll-mill crusher;
– destemming;
– pressing the pulp on a manual basket-type press;

Table 1 Experimental vineyard treatments with NanoKremny

Sample	Number of treatments	Indicators under study
Chardonnay		1. Growth strength and productivity of grapevine bush. 2. Level of disease development. 3. Grape chemical composition and biochemical characteristics. 4. Wine chemical composition and sensory characteristics.
Legenda Kryma, 2017		
Control – vineyard chemical protection system	6	
Experiment – vineyard protection system + NanoKremny treatment during blossom clustering, after florification, and at the beginning of bunch formation	3	
S. Perovskoy, 2017		
Control – vineyard chemical protection system	6	
Experiment – vineyard protection system + NanoKremny treatment during bud pushing, blossom clustering, before and after florification, and at the beginning of bunch formation	5	
Aligoté		
SVZ-AGRO, 2018		
Control – vineyard chemical protection system	6	
Experiment – vineyard protection system + NanoKremny treatment during blossom clustering, before and after florification	3	
Cabernet Sauvignon		
Livadiya branch of Massandra Winery, 2017		
Control – vineyard chemical protection system	6	
Experiment 1 – vineyard protection system + NanoKremny treatment during bud pushing, blossom clustering, and before florification	3	
SVZ-AGRO, 2018		
Control – vineyard chemical protection system	6	
Experiment – vineyard protection system + NanoKremny treatment during blossom clustering, before and after florification	3	

The rate of NanoKremny application – 0.15 L/ha

– sulfitating the must with sulfur dioxide (75–80 mg/L) and stirring;
– clarifying the must at 14–16°C for 18–20 h;
– decanting the clarified must;
– introducing a pure culture of the *Saccharomyces cerevisiae* yeast from the Magarach collection of winemaking microorganisms (strain I-271 for Chardonnay, I-187 and I-525 for Aligoté) and stirring;
– fermenting the must until dry at 20 ± 2°C with stirring 2–3 times a day;
– clarifying the wine; and
– decanting the wine.

The technology for dry red table wines (Cabernet Sauvignon) consisted of the following stages:
– crushing grapes on a manual roll-mill crusher;
– destemming;
– sulfitating the pulp with sulfur dioxide (75–80 mg/L) and stirring;
– introducing a pure culture of the *S. cerevisiae* yeast from the Magarach collection of winemaking microorganisms (strains I-652 and I-250) and mixing;
– fermenting the pulp with a floating cap at 24 ± 2°C, with mixing 7–8 times a day, up to 1/3 of residual sugars;
– pressing the pulp on a manual basket-type press;
– fermenting the must until dry;
– self-clarifying; and
– decanting.

Fieldworks were conducted with common methods of viticulture and plant protection [21, 22]. Foliar dressing was introduced in a tank mixture with pesticides. Experimental treatment schemes are presented in Table 1.

The chemical composition of grapes, must, and wines was analyzed with standard oenological methods [23–25].

The phenolic ripeness of grapes was assessed according to Glories *et al.* [24]. Their method determines the potential amount of anthocyanins that grapes can produce ($ApH_{1.0}$) and the amount of easily extractable anthocyanins ($ApH_{3.2}$). The ratio between these amounts shows the percentage of easily extractable anthocyanins in the grape berry (Ea, %).

The concentration of organic acids was determined in freshly squeezed, centrifuged must (OPN-8 centrifuge, Kyrgyzstan) by HPLC (Shimadzu LC20AD Prominence chromatograph, Japan). The method required preliminary calibration with standard solutions of pure substances on the spectrophotometric detector, taking into account their retention time. Individual components of the organic acid profile were determined at 210 nm. The sample was separated on a Supelcogel C610H column (Supelco®, Sigma-Aldrich) in an isocratic mode of eluent supply (0.1% aqueous solution of phosphoric acid, flow rate 0.5 mL/min). The refractometric detector was additionally calibrated using solutions of carbohydrate standards with the same retention time as organic acids, taking into account their analytical characteristics during analysis.

The concentration of organic acids in the sample was calculated mathematically, using the data obtained on the UV and refractometric detectors.

Volatile components were determined by gas chromatography (Agilent Technology 6890, USA) at an evaporator temperature of 220°C and a thermostat temperature of 50–240°C programmed at 4°C/min. The components were extracted with methylene chloride. The experimental samples were separated on an HP-INNOWAX column (Carbowax 20M or PE-FFAP; 30 m long, 0.25 mm inner diameter). The NIST 2007 database was used to identify the substances.

Experimental data were processed by variational statistical methods using Excel and SPSS Statistica 17 (arithmetic mean, root-mean-square deviation, and error mean square of a singular result). The tables and figures show the mean values of the indicators (standard deviation under 5% at $P \leq 0.005$).

RESULTS AND DISCUSSION

Silicon fertilizers are an innovation in modern intensive agriculture worldwide. NanoKremny is a unique fertilizer that contributes to high-yielding and ecological crops. Its main component is a biologically and chemically active silicon in a chelated form.

Our field experiments showed that NanoKremny produced the best results when applied threefold in the periods of active growth and formation of vegetative and generative organs in grape plants: bud pushing, before florification, after florification, and at the beginning of bunch formation (Table 1). This treatment led to increased stress resistance and yield, as well as reduced fungal diseases. In particular, it contributed to:

– higher productivity of grape plants: for example, the first three spray treatments of Cabernet Sauvignon (Livadiya, Massandra) improved the water balance of grape plants and increased the leaf area (by 13.9%), growth and ripening parameters (by 11.3 and 12.2%), and crop quantity (by 14.7%);
– lower risk of downy mildew disease (1.2–3.6 times, depending on variety) and oidium (protection improved by 10–12%) with threefold spraying during blossom clustering, before florification, and after florification;
– higher crop yield: for example, by 5, 45, and 49% for Aligoté (SVZ-AGRO), Chardonnay (S. Perovskoy), and Cabernet Sauvignon (SVZ-AGRO), respectively [26, 27].

The quality of grapes and young wines was assessed on the basis of their chemical composition and sensory characteristics. The grape batches under study met the requirements of State Standard 31782. The optimal contents of titratable acids are 6–9 and 5–8 g/L and those of sugar are 170–200 and 180–220 g/L for white and red varieties, respectively [28]. These contents are not standardized and recommended for table wines in scientific literature. We compared the carbohydrate-acid composition of the experimental grape batches against the controls and found an up to 5% increase in sugars for Legenda Kryma's Chardonnay and a 5% decrease in sugars for S. Perovskoy's Chardonnay and SVZ-AGRO's Cabernet Sauvignon (Table 2). This might be associated with a significant (by 45–49%) yield growth. The experimental batches of Aligoté and Livadiya's Cabernet Sauvignon had a similar composition to that of the controls.

The concentration of titratable acids in the experimental samples increased by 7 and 9% for Aligoté

Table 2 Chemical composition of the experimental NanoKremny-treated grape varieties vs. controls

Sample	Concentration, g/L		pH	Technological reserve, mg/L		Ea, %
	sugars	titrable acids		phenolic compounds	anthocyanins	
Chardonnay (Legenda Kryma, 2017)						
Control	194.00 ± 8.73	7.80 ± 0.16	3.44 ± 0.07	1234.0 ± 111.1	–	
Experiment	204.00 ± 9.18	7.70 ± 0.15	3.45 ± 0.07	1316.0 ± 118.4	–	
Chardonnay (S. Perovskoy, 2017)						
Control	194.00 ± 6.79	6.50 ± 0.09	3.33 ± 0.05	1505.0 ± 120.4	–	
Experiment	186.00 ± 6.51	6.90 ± 0.10	3.23 ± 0.03	1675.0 ± 134.0	–	
Aligoté (SVZ-AGRO, 2018)						
Control	183.00 ± 9.15	5.80 ± 0.17	3.16 ± 0.03	891.0 ± 84.6	–	
Experiment	188.00 ± 9.40	6.20 ± 0.19	3.16 ± 0.03	999.0 ± 83.9	–	
Cabernet Sauvignon (Livadiya branch of Massandra Winery, 2017)						
Control	271.00 ± 10.84	6.80 ± 0.27	3.61 ± 0.05	2657.0 ± 252.4	703.0 ± 46.4	59.0 ± 3.0
Experiment	271.00 ± 10.84	7.40 ± 0.30	3.41 ± 0.02	2728.0 ± 259.2	726.0 ± 47.9	56.0 ± 2.8
Cabernet Sauvignon (SVZ-AGRO, 2018)						
Control	201.00 ± 9.05	6.10 ± 0.18	3.30 ± 0.03	2434.0 ± 211.8	565.0 ± 49.7	44.0 ± 2.1
Experiment	191.00 ± 8.59	6.40 ± 0.19	3.24 ± 0.05	2516.0 ± 218.9	520.0 ± 45.8	45.0 ± 2.3

Ea – easily extractable anthocyanins

Control – chemical protection system

Experiment – chemical protection system + NanoKremny treatment

and Livadiya's Cabernet Sauvignon, respectively. NanoKremny significantly reduced active acidity (by 0.20) only in the Cabernet Sauvignon samples, compared to the controls. Thus, we did not identify any changes in the carbohydrate-acid complex that would be common for all the experimental samples, regardless of variety or place of growth.

Silicon makes plant more stress-resistant by stimulating the synthesis of phenolic metabolites and the activity of protective enzymes, such as monophenol-monooxygenase (MPMO), peroxidase, and others [29–31]. Important technological characteristics of grapes for winemaking are the content of phenolic compounds, including anthocyanins, phenolic ripeness, and the activity of grape oxidases at the time of their technical ripeness [32].

The experimental treatments increased the technological reserve of phenolic compounds in the experimental samples by 82–170 and 71–82 mg/L for white and red varieties, respectively, compared to the control. We found that the phenolic reserve in the Cabernet Sauvignon and Aligoté samples, both control and experimental, corresponded to the values recommended for table wine production: at least 2000 mg/L for red grapes and under 1000 mg/L for white grapes [28, 32].

We did not find a single trend in the effect of NanoKremny on the accumulation of monomeric anthocyanins in grapes at that stage. For example, Livadiya's Cabernet Sauvignon showed a 3% increase in monomeric anthocyanins, whereas the same variety from SVZ-AGRO had an 8% decrease. Cabernet Sauvignon growing on the South Coast reaches phenolic ripeness when it has at least 45% of easily extractable anthocyanins [32]. We only used phenolically ripe samples of Cabernet Sauvignon (both control and experimental), with 44–56% of easily extractable anthocyanins. The experimental treatment did not have a significant effect on this indicator.

We found that the effect of NanoKremny on the MPMO activity of the must depended largely on the grape variety (Fig. 2). For example, Chardonnay showed a decreasing trend, regardless of the place of its growth, which is a favorable factor for white table wines. Cabernet Sauvignon showed the opposite trend, while the Aligoté samples were not affected at all. However, we registered a correlation between the MPMO activity and the place of growth. For example, Chardonnay showed a decrease in the MPMO activity by 24 and 33% for Legenda Kryma and S. Perovskoy, respectively, while Cabernet Sauvignon had an increase by 91 and 61% for SVZ-AGRO and Livadiya, respectively, compared to the control.

Organic acids determine the sensory characteristics of wines and the intensity of redox processes, as well as protect them from harmful bacterial microflora [33, 34]. Recent studies have proved the relationship between the metabolism of organic acids and plant resistance

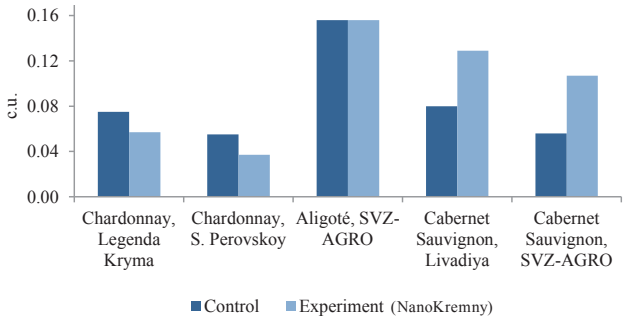

Figure 2 Monophenolmonooxygenase activity of the must obtained with different treatment schemes

to stress [35]. Organic acids are produced during plant respiration due to the incomplete oxidation of carbohydrates, as well as during photosynthesis (mainly in leaves, with further transportation to grape berries). Since silicon fertilizers create favorable conditions for photosynthesis, we can assume that they have an indirect effect on the metabolism of organic acids in the grapevine. As we can see in Fig. 3, NanoKremny contributed to a 9–12% increase in tartaric acid in the grapes, regardless of their variety and growth area. A similar trend was observed with malic acid (especially in Chardonnay), whose concentration increased by 8% in Cabernet Sauvignon and by 25 and 48% in Chardonnay from S. Perovskoy and Legenda Kryma, respectively.

The quality assessment revealed that all the white and red dry table wines produced from the grapes treated in different ways met the requirements of State Standard 32030-2013 "Table wines and table winestocks. General specifications" (Table 3).

The chemical composition of wines and their quality result from a combination of factors, including agricultural methods used in the vineyard. To neutralize technological influence, we used the same technology to produce all the wines. The technologically relevant parameters of grape and wine quality were taken from previous studies [10, 28, 32].

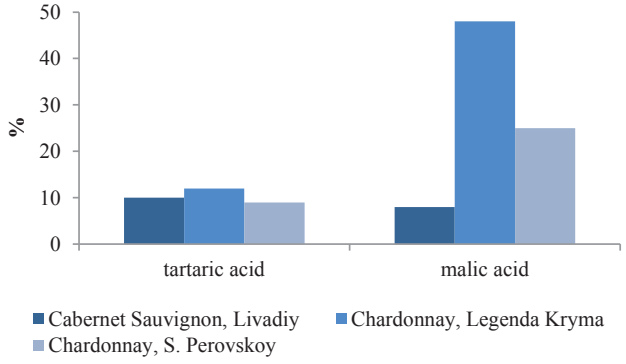

Figure 3 Concentrations of organic acids in NanoKremny-treated grape varieties from different growth areas

Table 3 Chemical composition of dry table wines from grapes exposed to different treatments (average values)

Sample (yeast strain)	Volume rating of ethyl alcohol, %	Concentration, g/L					Concentration, g/L			pH	DE*, point
		sugars	titratable acids	volatile acids	total dry extract	total sulphurous acid	free sulphurous acid	phenolic compounds	anthocyanins		
Values according to State Standard 32030											
	8.5–15	≤ 4	≥ 3.5	≤ 1.1 for white wine; ≤ 1.2 for red wine	≥ 16 for white wine; ≥ 18 for red wine	≤ 200	not standardized				
Chardonnay (Legenda Kryma, 2017)											
Control: chemical protection system (st. I-271)	10.8	1.0	7.2	0.29	20.1	94	50	257	–	3.19	7.60
Experiment: chemical protection system + NanoKremny treatment (st. I-271)	10.6	1.3	7.3	0.79	16.3	100	50	274	–	3.22	7.55
Aligoté (SVZ-AGRO, 2018)											
Control: chemical protection system (st. I-187)	11.9	0.7	6.1	0.43	16.5	86	51	161	–	3.24	7.75
Experiment: chemical protection system + NanoKremny treatment (st. I-187)	10.9	0.5	7.6	0.48	18.3	70	32	114	–	3.24	7.74
Control: chemical protection system (st. I-525)	10.8	0.4	7.2	0.53	16.5	75	33	166	–	3.24	7.78
Experiment: chemical protection system + NanoKremny treatment (st. I-525)	11.5	0.4	7.4	0.34	16.4	68	31	123	–	3.29	7.65
Cabernet Sauvignon (Livadiya branch of Massandra Winery, 2017)											
Control: chemical protection system (st. I-652)	14.8	1.8	5.1	0.43	26.1	120	38	2474	301	4.00	7.69
Experiment: chemical protection system + NanoKremny treatment (st. I-652)	13.9	1.7	5.2	0.26	25.9	110	38	2427	401	3.85	7.57
Cabernet Sauvignon (SVZ-AGRO, 2018)											
Control: chemical protection system (st. I-250)	11.0	1.4	7.2	0.49	20.2	68	27	1563	385	3.50	7.84
Experiment: chemical protection system + NanoKremny treatment (st. I-250)	11.0	1.1	7.9	0.37	20.5	90	45	1446	319	3.38	7.74
Control: chemical protection system (st. I-652)	11.1	0.4	7.6	0.38	21.5	77	35	1322	339	3.40	7.80
Experiment: chemical protection system + NanoKremny treatment (st. I-652)	11.2	1.8	6.7	0.29	20.4	86	43	1593	314	3.54	7.75

*DE – TE – tasting evaluation

We found that the Chardonnay and Aligoté experimental wines showed various trends in relation to titratable acids and active acidity. In the Aligoté wines, the concentration of titratable acids was determined by the yeast strain. For example, strains I-187 and I-525 increased titratable acids by 1.5 and 0.2 g/L, respectively, compared to the control.

Just as the experimental batches of Chardonnay grapes, the experimental wines from them had a high content of phenolic compounds – 7% higher than in the controls. Their technological reserve in the Aligoté wines, however, remained the same. On average, the concentration of phenolic compounds in the experimental wines amounted to 114–123 mg/L, which was 26–29% lower than in the controls (Fig. 4).

It was impossible to determine the exact effect of NanoKremny on the chemical composition of Cabernet Sauvignon wines at that stage of research. Only 33% of the wine samples showed an 0.7 g/L increase in titratable acids. In 33% of the tested wines, the concentration of titratable acids decreased by 0.9 g/L. In other cases, this indicator was the same for both the experimental wines and the controls.

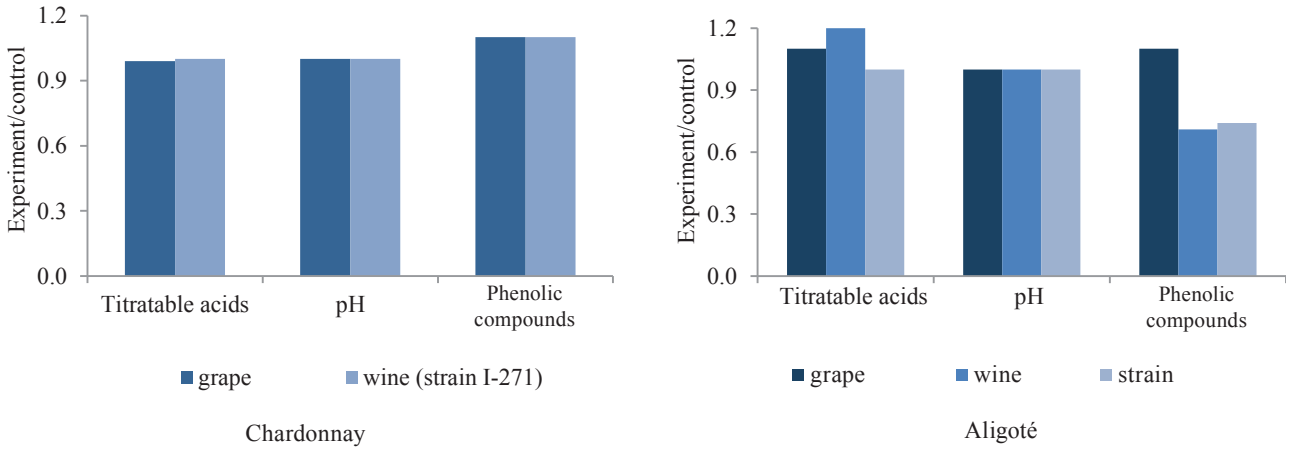

Figure 4 Concentrations of titratable acids, phenolic compounds (technological reserve in grapes), and pH in wines and grapes exposed to different treatments

The profile of organic acids in the "grapes-wine" chain showed the dominance of tartaric acid, whose concentration in the control and experimental samples did not differ, averaging 1.4 g/L (Fig. 5). Malic acid, however, did not show the same increasing trend in the wines as it did in the experimental grape samples. Its average concentration in the experimental wines was 33% lower than in the controls. This might be due to malolactic fermentation, which also led to higher concentrations of lactic and succinic acids, mostly expressed in the experimental wine samples (Fig. 5).

Although NanoKremny contributed to the accumulation of phenolic compounds in the grapes, their concentration averaged 1446–2427 mg/L in 67% of the experimental wines, which was 2–7% lower than in the controls. The only exception was the wines from SVZ-AGRO where the concentration of phenolic compounds averaged 1593 mg/L – 20% higher than in the control. This might be due to the initial composition of raw materials and the physiological and biochemical properties of the strains used. Compounds produced from fermentation can affect the speed of redox processes initiated and mediated by phenolic compounds.

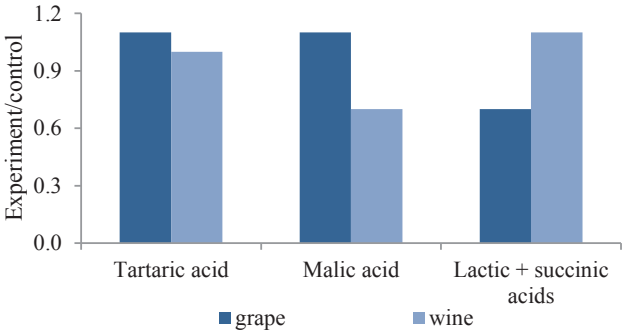

Figure 5 Concentrations of organic acids in the control and experimental samples of grapes and wines (for Cabernet Sauvignon)

The concentration of monomeric anthocyanins was 301–385 and 314–401 mg/L in the control and experimental wines, respectively. In Livadiya's wines, monomeric anthocyanins accounted for 12–17% of phenolic compounds, only half of their proportion in the grapes. In the wines from SVZ-AGRO, they amounted to 20–26%, almost the same as in the grapes (21–23%). This might be due to their ability to bind with other compounds, form complex structures, and precipitate [36]. This assumption could be supported by a lower content of acetaldehyde in the wine materials in 2017 (8–40 mg/L) compared to 2018 (90–133 mg/L).

Aroma is an important characteristic of wine quality. According to the chromatographic analysis, the concentrations of aroma-producing components in the Aligoté and Cabernet Sauvignon wines averaged 104–108 and 120–149 mg/L in the controls, and 96–104 and 112–141 mg/L in the experimental samples, respectively. Aliphatic and aromatic alcohols were predominant among aromatic substances, with the same total concentrations in the experimental and control samples averaging 27–31 and 25–32 mg/L for Aligoté and 35–47 and 27–35 mg/L for Cabernet Sauvignon, respectively.

All experimental wines from Aligoté grapes, regardless of the yeast strain used, showed an increase in ethyl esters 1.2–1.5 times (Fig. 6). They also had high concentrations of acetic acid esters – 2.2 times and 1.6 times higher when treated with the I-187 and I-525 yeast strains, respectively (Fig. 6). The I-525 strain raised the concentration of dioxanes and dioxolans to an average of 3.29 mg/L, which was 2.9 times higher than in the controls.

The experimental wines from Cabernet Sauvignon grapes showed lower (1.2–1.5 times) concentrations of ethyl esters, averaging 7–9 mg/L. As we can see in Fig. 6, the samples treated with the I-652 strain had 1.3 and 2.1 times lower concentrations of lactones

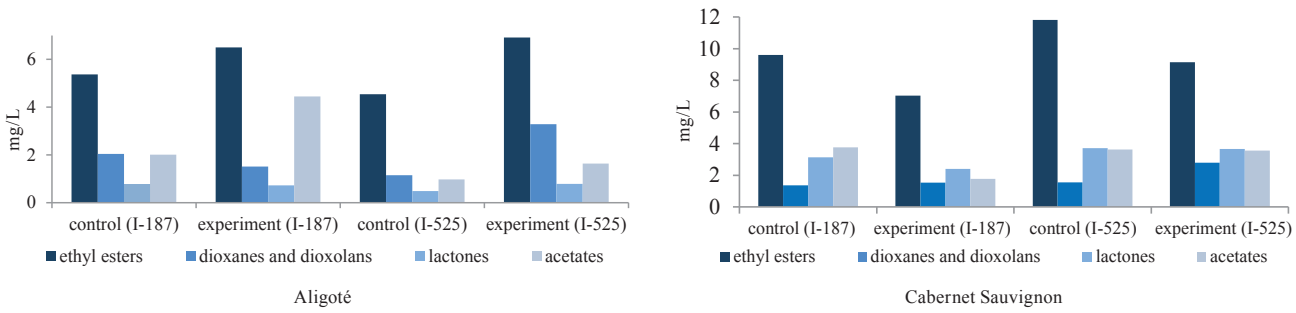

Figure 6 Aroma-producing complexes of the control and experimental wines

and acetates than in the controls, averaging 3.14 and 3.76 mg/L, respectively. The I-250 strain increased the concentration of dioxanes and dioxolans 1.8 times compared to the control. These compositions of the aroma-producing complex might be determined by the physiological and biochemical abilities of the yeast strains used.

The assessment of the influence of grape treatment on the sensory quality of wines showed that young white table wines from Chardonnay grapes contained some shades of medicinal herbs, absent in the control samples. The control Aligoté wines were characterized by a light straw color, a floral aroma, with hints of meadow herbs, candy and spicy tones, and a harmonious taste. In contrast, the experimental wines had a straw color, a fruity aroma, with herbal, spicy and candy tones, as well as a fresh, slightly astringent taste. The average tasting scores of Aligoté wines were 7.70 and 7.77 points for the experimental and control samples, respectively.

The control red table wines from Cabernet Sauvignon grapes had a dark ruby color, a varietal berry aroma with hints of spices, nightshade, morocco leather, and milk cream, as well as a moderate velvety flavor with light astringency. Their average tasting scores were 7.69 and 7.82 points for the 2017 and 2018 grape harvests, respectively. The experimental wines (chemical protection + NanoKremny treatment) had a dark ruby color, a berry aroma with light herbal tints, and a somewhat simple palate with moderate tannins. Their average tasting scores were 7.57 and 7.74–7.75 for the 2017 and 2018 grape harvests, respectively. Different yeast strains had no significant effect on the tasting scores of the experimental red wines.

Thus, the differences in the sensory scores of the control and experimental wines were statistically insignificant ($P < 0.05$).

CONCLUSION

Our study showed that the optimal treatment of grapevines is a threefold application of NanoKremny (0.15 L/ha) during the periods of active growth and formation of vegetative and generative organs in the grape plant. This scheme has a positive effect on vegetative development, water balance, grape plant productivity, as well as yield quality and quantity. Also, it prevents the development of mildew and oidium diseases.

The NanoKremny treatment of the grapevine preserves the content of titratable acids during grape ripening and accumulates phenolic compounds, tartaric and malic acids in the berries. We found no significant differences in the physicochemical parameters of the wines from NanoKremny-treated grapes and the control wines from grapes that underwent standard chemical protection.

The sensory evaluation of young wine samples showed that the NanoKremny treatment enhanced the expression of herbal (grassy) shades in the aroma of both white and red wines. Although it somewhat simplified their taste, NanoKremny did not have a negative effect on the wine quality.

CONTRIBUTION

N.V. Aleinikova studied the effect of NanoKremny on the grape plant and was involved in approving the final version of the manuscript. I.V. Peskova processed experimental data about the effect of NanoKremny on the quality of grapes and wines, and was involved in writing the manuscript. E.V. Ostroukhova studied the effect of NanoKremny on the quality of grapes as raw materials for winemaking and on the quality of wines; she was also involved in approving the final version of the manuscript. Ye.S. Galkina processed experimental data about the effect of NanoKremny on the grape plant. P.A. Didenko conducted fieldworks to identify the effect of foliar dressing on the grape plant. P.A. Probeigolova and N.Yu. Lutkova analyzed the chemical composition of grapes and wines.

CONFLICT OF INTEREST

The authors declare that they have no conflict of interest.

ACKNOWLEDGEMENTS

The authors are grateful to D.Yu. Pogorelov and S.O. Ulyantsev from the Department of Wine Chemistry and Biochemistry at the Magarach All-Russian National Research Institute of Viticulture and Winemaking for their help with chromatographic analysis, as well as all our colleagues involved in the preparation of the manuscript.

REFERENCES

1. Tubana BS, Babu T, Datnoff LE. A review of silicon in soils and plants and its role in us agriculture: History and future perspectives. Soil Science. 2016;181(9–10):393–411. https://doi.org/10.1097/SS.0000000000000179.
2. Sahebi M, Hanafi MM, Akmar ASN, Rafii MY, Azizi P, Tengoua FF, et al. Importance of silicon and mechanisms of biosilica formation in plants. BioMed Research International. 2015;2015. https://doi.org/10.1155/2015/396010.
3. Reynolds OL, Padula MP, Zeng R, Gurr GM. Silicon: Potential to promote direct and indirect effects on plant defense against arthropod pests in agriculture. Frontiers in Plant Science. 2016;7. https://doi.org/10.3389/fpls.2016.00744.
4. Van Bockhaven J, De Vleesschauwer D, Höfte M. Towards establishing broad-spectrum disease resistance in plants: silicon leads the way. Journal of Experimental Botany. 2013;64(5):1281–1293. https://doi.org/10.1093/jxb/ers329.
5. Bakhat HF, Bibia N, Zia Z, Abbas S, Hammad HM, Fahad S, et al. Silicon mitigates biotic stresses in crop plants: A review. Crop Protection. 2018;104:21–34. https://doi.org/10.1016/j.cropro.2017.10.008.
6. Habibi G. Effects of soil- and foliar-applied silicon on the resistance of grapevine plants to freezing stress. Acta Biologica Szegediensis. 2015;59(2):109–117.
7. Haddad R, Kamangar A. The ameliorative effect of silicon and potassium on drought stressed grape (*Vitis vinifera* L.) leaves. Iranian Journal of Genetics and Plant Breeding. 2015;4(2):48–58.
8. Jana S, Jeong BR. Silicon: The most under-appreciated element in horticultural crops. Trends in Horticultural Research. 2014;4(1):1–19. https://doi.org/10.3923/thr.2014.1.19.
9. Song A, Li P, Fan F, Li Z, Liang Y. The effect of silicon on photosynthesis and expression of its relevant genes in rice (*Oryza sativa* L.) under high-zinc stress. PLoS ONE. 2014;9(11). https://doi.org/10.1371/journal.pone.0113782.
10. Zia Z, Bakhat HF, Saqib ZA, Shah GM, Fahad S, Ashraf MR, et al. Effect of water management and silicon on germination, growth, phosphorus and arsenic uptake in rice. Ecotoxicology and Environmental Safety. 2017;144:11–18. https://doi.org/10.1016/j.ecoenv.2017.06.004.
11. Cartes P, Cea M, Jara A, Violante A, Mora ML. Description of mutual interactions between silicon and phosphorus in Andisols by mathematical and mechanistic models. Chemosphere. 2015;131:164–170. https://doi.org/10.1016/j.chemosphere.2015.02.059.
12. Alovisi AMT, Neto AEF, Serra AP, Alovisi AA, Tokura LK, Lourente ERP, et al. Phosphorus and silicon fertilizer rates effects on dynamics of soil phosphorus fractions in oxisol under common bean cultivation. African Journal of Agricultural Research. 2016;11(30):2697–2707. https://doi.org/10.5897/AJAR2016.11304.
13. Veresoglou SD, Barto EK, Menexes G, Rillig MC. Fertilization affects severity of disease caused by fungal plant pathogens. Plant Pathology. 2013;62(5):961–969. https://doi.org/10.1111/ppa.12014.
14. Kulikova AKh. Kremniy i vysokokremnistye porody v sisteme udobreniya sel′skokhozyaystvennykh kul′tur [Silicon and high-siliceous rocks in the fertilization system for agricultural crops]. Ulyanovsk: Ulyanovsk State Agrarian University named after P.A. Stolypin; 2013. 176 p. (In Russ.).
15. Sanin SS. Current phytosanitary problems in Russia. Izvestiya of Timiryazev Agricultural Academy. 2016;(6):45–55. (In Russ.).
16. Serpuhovitina KA, Krasilnikov AA, Russo DE, Khudaverdov EN. Growth, development and productivity of varieties with systemic fertilizer of vineyards. Fruit growing and viticulture of South Russia. 2014;26(2):119–141. (In Russ.).
17. Radchevsky PP, Matuzok NV, Bazoyan SS. Influence of a foliar spraying with new-generation mineral fertilizers on agrobiological and technological indicators of chardonnay grapes. Polythematic Online Scientific Journal Of Kuban State Agrarian University. 2016;(115):665–690. (In Russ.).
18. Panasyuk AL, Kuzmina EI, Kharlamova LN, Babaeva MV, Romanova IP. Influence of bio-organic additives on the ability of yeast to provide biotransformation of pesticides in apple must. IOP Conference Series Materials Science and Engineering. 2019;582(1). https://doi.org/10.1088/1757-899X/582/1/012011.
19. Panasjuk AL, Shishkov YuI, Kuzmina EI, Kharlamova LN, Zaharov MA, Borisova AL. Intensification of process of fermentation of an apple mash with use of the made active biomass of yeast. Vinodelie i vinogradarstvo [Winemaking and viticulture]. 2010;(5):14–15. (In Russ.).
20. Panasjuk AL, Shishkov YuI, Kuzmina EI, Harlamova LN, Zaharov MA. Borisova AL. Change of ultrastructure of cells of wine yeast at use of a bioorganic additive. Vinodelie i vinogradarstvo [Winemaking and viticulture]. 2010;(6): 24–25. (In Russ.).
21. Dolzhenko VI. Metodicheskie ukazaniya po registratsionnym ispytaniyam fungitsidov v sel′skom khozyaystve [Methodological guidelines for registration testing of fungicides in agriculture]. St. Petersburg: VIZR; 2009. 379 p. (In Russ.).
22. Sychev VG, Shapoval OA, Mozharova IP, Verevkina TM, Mukhina MT, Korshunov AA, et al.. Rukovodstvo po provedeniyu registratsionnykh ispytaniy agrokhimikatov v sel′skom khozyaystve [Guidelines for registration testing of agrochemicals in agriculture]. Moscow: Plodorodie; 2018. 193–200 p. (In Russ.).

23. Gerzhikova VG. Methods of technical chemistry control in winemaking. Simferopol: Tavrida; 2009. 304 p. (In Russ.).
24. Cagnasso E, Rolle L, Caudana A, Gerbi V. Relationship between grape phenolic maturity and red wine phenolic composition. Italian Journal of Food Science. 2008;20(3):365–380.
25. Lee J, Durst RW, Wrolstad RE. Determination of total monomeric anthocyanin pigment content of fruit juices, beverages, natural colorants, and wines by the pH differential method: Collaborative study. Journal of AOAC International. 2005;88(5):1269–1278. https://doi.org/10.1093/jaoac/88.5.1269.
26. Aleinikova NV, Galkina ES, Berezovskaya SP, Radionovskaya YaE, Didenko PA, Shaporenko VN, et al. Biological regulation on the use of domestic antidote "Nanokremnyi" (Nano-Silicon) in the vineyards with winemaking grapes in Crimea. Magarach. Viticulture and Vinemaking. 2017;(4):35–37. (In Russ.).
27. Aleinikova NV, Galkina ES, Didenko PA, Didenko LV. Determination of the impact of the use of domestic fertilizer NanoSilicon on the productivity of grapes in the soil and climatic conditions of the Crimea. Science Almanac. 2018;49(11–2):176–179. (In Russ.).
28. Valuyko GG, Kosyura VT. Spravochnik po vinodeliyu [Winemaking guidelines]. Simferopol: Tavrida; 2000. 624 p. (In Russ.).
29. Kulbat K. The role of phenolic compounds in plant resistance. Biotechnology and Food Sciences. 2016;80(2):97–108.
30. Wang M, Gao L, Dong S, Sun Y, Shen Q, Guo S. Role of silicon on plant-pathogen interactions. Frontiers in Plant Science. 2017;8. https://doi.org/10.3389/fpls.2017.00701.
31. Fortunato AA, Rodrigues F, do Nascimento KJT. Physiological and biochemical aspects of the resistance of banana plants to Fusarium wilt potentiated by silicon. Phytopathology.2012;102(10):957–966. https://doi.org/10.1094/PHYTO-02-12-0037-R.
32. Ostroukhova EV, Peskova IV, Probeigolova PA, Verik GN. A study of the interrelationship between the carbohydrate and acid maturity and the phenolic maturity of the grape "Cabernet Sauvignon". Magarach. Viticulture and Vinemaking. 2012;(1):30–32. (In Russ.).
33. Danilewicz JC. Role of tartaric and malic acids in wine oxidation. Journal of Agricultural and Food Chemistry. 2014;62(22):5149–5155. https://doi.org/10.1021/jf5007402.
34. Chidi BS, Bauer FF, Rossouw D. Organic acid metabolism and the impact of fermentation practices on wine acidity: A review. South African Journal for Enology and Viticulture. 2018;39(2):315−329. https://doi.org/10.21548/39-2-3172.
35. Drincovich MF, Voll LM, Maurino VG. Editorial: On the diversity of roles of organic acids. Frontiers in Plant Science. 2016;7. https://doi.org/10.3389/fpls.2016.01592.
36. Oliveira J, de Freitas V, Mateus N. Polymeric pigments in red wines. In: Morata A, editor. Red wine technology. Academic Press; 2019. pp. 207–218. https://doi.org/10.1016/B978-0-12-814399-5.00014-1.

ORCID IDs
Natalia V. Aleinikova https://orcid.org/0000-0003-1167-6076
Irina V. Peskova https://orcid.org/0000-0002-5107-518X
Elena V. Ostroukhova https://orcid.org/0000-0003-0638-9187
Yevgenia S. Galkina https://orcid.org/0000-0003-4322-4074
Pavel A. Didenko https://orcid.org/0000-0001-6170-2119
Polina A. Probeigolova https://orcid.org/0000-0003-4442-8538
Nataliya Yu. Lutkova https://orcid.org/0000-0002-8126-7596

Foods and Raw Materials, 2021, vol. 9, no. 2

E-ISSN 2310-9599
ISSN 2308-4057

Research Article
Open Access

https://doi.org/10.21603/2308-4057-2021-2-234-243
Available online at http://jfrm.ru/en

Fresh and processed wild *Cantharellus cibarius* L. growing in West Siberia: food value

Valentina I. Bakaytis*, Olga V. Golub, Yuliya Yu. Miller

Siberian University of Consumer Cooperation, Novosibirsk, Russia

* e-mail: proscien@sibupk.nsk.su

Received March 27, 2020; Accepted in revised form April 22, 2020; Published online July 09, 2021

Abstract:

Introduction. *Cantharellus cibarius* L. is a wild mushroom that has been part of human diet for many centuries. However, there is little reliable information about its nutritional value, storage conditions, shelf life, and processing. The research objective was to study the nutritional value of *C. cibarius* growing in West Siberia, as well as to define its storage and processing conditions.

Study objects and methods. The research featured fresh and processed (boiled and salted) wild chanterelles (*C. cibarius*) obtained from the forests of the Novosibirsk region. The mushrooms were tested for amino acids, fatty acids, nutrients, reducing sugars, trehalose, mannit, glycogen, fiber, mucus, squalene, ash, minerals, vitamins, trypsin inhibitor, chlorides, mesophilic and facultative anaerobes, etc. The samples also underwent sensory evaluation.

Results and discussion. The samples of *C. cibarius* proved to have a high nutritional value. The samples contained 3.6% proteins, including essential amino acids; 3.9% carbohydrates, including sugars and dietary fiber; and 0.7% lipids, including saturated, monounsaturated, and polyunsaturated acids. In addition, *C. cibarius* appeared to be rich in biologically active substances. It contained trypsin inhibitors that reduce the absorption of protein compounds. Purchasing centers can be recommended to use 70–80% relative air humidity. At 0–2°C, the storage time was five days; at 5–10°C – three days; at 15–20°C – two days; at 20–30°C – one day. Before processing, the mushrooms were washed twice in non-flowing water. *C. cibarius* also proved to be a valuable raw material for boiled and salted semi-finished products. The optimal boiling time was 5–10 min. Lightly-, medium-, and strong-salted semi-finished mushrooms were ready for consumption after the fermentation was complete, i.e. after day 15, 10, and 3, respectively.

Conclusion. Boiled and salted semi-finished products from Siberian *C. cibarius* demonstrated excellent sensory qualities and can become part of various popular dishes.

Keywords: Edible mushrooms, *Cantharellus cibarius*, nutrients, sensory properties, microbiological safety

Please cite this article in press as: Bakaytis VI, Golub OV, Miller YuYu. Fresh and processed wild *Cantharellus cibarius* L. growing in West Siberia: food value. Foods and Raw Materials. 2021;9(2):234–243. https://doi.org/10.21603/2308-4057-2021-2-234-243.

INTRODUCTION

Mushrooms have typical taste and aroma, high nutritional value, and relatively low calorie content. As a result, they have always been an integral part of human diet. However, the advantageous properties of mushrooms depend on their chemical composition, processing method, etc. Mushrooms owe their antibacterial, anti-inflammatory, wound healing, tonic, immunomodulating, and other therapeutic properties due to various biologically active substances in their composition [1–4]. The chemical composition of mushrooms depends on the season, area, ecology, size, and age [5]. Their chemical composition includes 50–65% carbohydrates, 19–35% proteins, 2–6% fats. They are rich in palmitic, oleic, and linoleic acids, with unsaturated fatty acids prevailing over saturated acids. In addition, mushrooms contain a lot of vitamins, especially fat-soluble, e.g. ergosterol [3, 5, 6].

Food scientists are busy developing new processing technologies to optimize mushroom production, improve the quality of mushroom products, and increase demand [7–10].

For instance, Taiwan experts studied the taste profile of canned *Agaricus bisporus*, *Volvariella volvacea*, and *Flammulina velutipes*. The content of soluble sugars and polyols was 22.9–30.9 μg/g in the fruiting body and 5.6–14.2 μg/g in the canning brine. Canned samples of *F. velutipes* appeared to have the largest amount of total free amino acids, i.e. 247 μg/g in the fruiting body and 146 μg/g in the brine, closely followed by *A. bisporus* (42.8 and 33.3 μg/g). *V. volvacea* had the lowest content of soluble sugars and polyols, i.e. 27.2 and 12.4 μg/g [11].

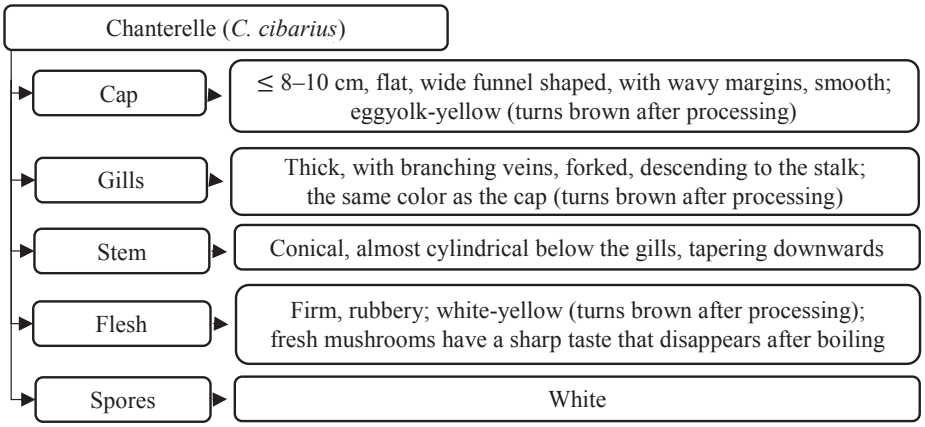

Figure 1 Identification criteria for raw and processed chanterelle (*Cantharellus cibarius*)

Some studies featured the effect of freezing and such pretreatments as blanching, soaking in water / solutions of sodium metabisulfite and/or citric acid and/ or low-methylated pectin, etc. [12]. Polish scientists proved the effect of freezing and thermal treatment on the amino acid content of *A. bisporus*, *Boletus edulis*, and *Pleurotus ostreatus*. Processed samples of *B. edulis* contained more amino acids than *A. bisporus* and *P. ostreatus*. The content of alanine, arginine, proline, cysteine, methionine, and tyrosine depended on the processing method. Limiting amino acids were detected in *B. edulis*, both frozen (leucine) and canned (lysine) [13].

Chinese and American scientists found that frozen, canned, and salted *A. bisporus* are a good source of vegetable protein (16.54–24.35 g/100 g). The content of free amino acids dropped during six months of storage, especially that of tyrosine, alanine, glutamine, and cysteine. Salting and thermal treatment led to a decrease in 5'-nucleotides [14].

Increasing the shelf life of fresh mushrooms is one of the most popular tasks of food research. Spanish scientists investigated the effect of various active substances on the shelf life of mushrooms, their color, and consumer appeal. Sodium metabisulfite in combination with citric acid and green tea extract increased the shelf life, while cinnamon essential oil and purple carrot extracts did not have enough antioxidant properties to inhibit spoilage and/or prolong the shelf life of the mushrooms [15]. Portuguese researchers proved that gamma-, electron beam, and UV irradiations increase the shelf life of fresh *A. bisporus*, *Lentinus edodes*, and *P. ostreatus* [16].

Scientists have always been concerned about the safety of mushroom products [17, 18]. American and British researchers proposed to assess the safety of mushrooms by DNA methods, which is a promising alternative to traditional toxicological tests on animals [19].

A recent research featured five macro- and microelements in 14 species of mushrooms cultivated in China and Poland (*A. bisporus*, *Amauroderma rude*, *Auricularia auricula-judae*, *Auricularia nigricans*, *Ganoderma lucidum*, *Lentinula edodes*, *Lignosus P. ostreatus*, *Sparassis crispa*, *Tremella fuciformis*, *Wolfiporia cocos*, and *V. volvacea*). The samples demonstrated a high content of such toxic elements as aluminum, arsenic, and platinum. In fact, the content of platinum, nickel, erbium, and neodymium exceeded all previously published data. The quantity of the chemical elements did not make the samples toxic, but scientists will have to find a way to reduce the nickel content [20].

As a highly demanded product with high safety and quality standards, mushrooms are bound to be subject to geographical tracking by all international market members, e.g. by using the method of stable isotopes, bar coding, etc. [21, 22].

Chanterelle (*Cantharellus cibarius* L.) is a mycorous symbiotroph of birch, spruce, pine, fir, and oak. This wide-spread mushroom grows alone or in rings all over Russian mixed forests. It can be found in Europe, America, Africa, China, Japan, and Australia [5]. Consumers like *C. cibarius* for its good transportability, storage capacity, and processing options [5, 23]. *C. cibarius* is less prone to damage from larvae, slugs, and other pests [5, 24]. The average weight of one mushroom is 7 g [24]. *C. cibarius* is wild and edible. Its fruiting bodies appear in summer and autumn, and their structure and hymenophore location make them lamellar (Fig. 1) [5]. In Russia, *C. cibarius* belongs to the third category of nutritional value, as stated in Sanitary Regulations SP 2.3.4.009-93 "Sanitary Rules for the Procurement, Processing, and Sale of Mushrooms", approved by the State Committee for Sanitary and Epidemiological Supervision of the Russian Federation No. 10 on August 20, 1993.

The chemical composition of *C. cibarius* is diverse. It includes proteins (eight amino acids), carbohydrates

(monosaccharides, trehalose, mannit, glycogen, fiber, etc.), lipids (phospholipids, monoglycerides, sterols, free fatty acids, triglycerides, waxes, etc.), organic acids (malic, succinic, etc.), and biologically active substances (ascorbic acid, thiamine, riboflavin, niacin, beta-carotene, potassium, sodium, calcium, magnesium, phosphorus, sulfur, etc.) [5, 24, 25]. The list of medicinal substances that can be isolated from mushrooms includes quinomannose, ergosterol, and trametonolinic acid. These substances are used in medicines that treat helminthic infestations, liver diseases, viral hepatitis, etc. [24, 26]. Fruiting bodies contain polyozellin that possesses antitumor properties as it inhibits the activity of prolyl endopeptidase, an enzyme involved in protein metabolism of the precursor of *β*-amyloid [24]. Chinese scientists used *C. cibarius* to isolate a new linear 3-O-methylated galactan (WCCP-Nb), which enhances macrophage phagocytosis, NO release, and secretion of TNF-*α*, IL-6, and IL-1*β*. In addition, it activates macrophages through Akt/NF-κB and mitogen-activated protein kinase through TLR2 [27].

Polish scientists studied the health-improving properties of polysaccharides in *C. cibarius*. Mushroom poly-saccharides consist of one monosaccharide in a repeating unit →6)-*α*-D-Manp-(1→; they inhibit COX-1 and COX-2, decrease the proliferation of colon cancer cells, and stimulate the growth of *Lactobacillus* [28]. Blanching appeared to decrease antioxidant activity and the content of polyphenols. When *Lactobacillus plantarum* was used for lactic acid fermentation of fruiting bodies, it decreased the pH value and the formation of highly concentrated single phenolic acids, e.g. gallic, homogenous, and ferulic [29]. The Polish team also studied the mineral composition of *C. cibarius*, which included silver, aluminum, barium, calcium, cadmium, cobalt, chromium, copper, iron, mercury, potassium, magnesium, manganese, sodium, nickel, lead, phosphorus, rubium, strontium, and zinc. The mineral profile of *C. cibarius* depended on the area where the mushroom was harvested [30]. A Polish-Chinese research revealed that some elements depend not only on the geographical location, but also on anthropogenic factors. For example, the Chernobyl disaster increased the cesium content in *C. cibarius* growing in Poland, compared to samples from Yunnan [31].

Blanching and pickling led to a 77–91% decrease in cadmium content in *C. cibarius*. Blanching of fresh mushrooms decreased cadmium content by 11–36%, while in frozen mushrooms it fell by about 40%. A similar rate of cadmium reduction was observed after blanching with drinking or deionized water for 5–15 min. After pickling the blanched mushrooms in diluted vinegar marinade, cadmium dropped by 37–71% [32]. Convective or freeze drying also affected the aromatic composition and sensory qualities of *C. cibarius*. Fresh and dried mushrooms contained 39 volatile compounds in various concentrations, the largest being 1-hexanol, 1-octene-3-ol, and 2-octene-1-ol [33, 34].

Russian scientists proved that 20 min of thermal treatment detoxifies heavy metals in mushrooms [35].

American scientists found out that *C. cibarius* and *Morchella esculenta* have the lowest folate content (≤ 6 μg/100 g), compared to *P. ostreatus* (44.2 μg/100 g), *B. edulis*, *L. edodes*, *Grifola frondosa*, *F. velutipes*, *A. bisporus* (cream strain), *A. bisporus* "Portobello", and UV-treated samples of *A. bisporus* [36].

German scientists identified several taste-affecting C18-acetylenic acids in *C. cibarius*: (9Z,15E)-14,17,18-trihydroxy-9,15-octadecadien-12-ynoic acid, (9Z,15E)-14-oxo-9,15-octadecadien-12-ynoic acid, (10E,15E)-9-hydroxy-14-oxo-10,15-octadecadien-12-ynoic acid, (10E,15E)-9-hydroperoxy-14-oxo-10,15-octadecadien-12-ynoic acid, (10E,15E)-9,14-dioxo-10,15-octadecadien-12-ynoic acid, (9Z,15E)-14-oxo-9,15-octadecadien-12-ynoic acid methyl ester, (9Z,15E)-17(18)-epoxy-14-oxo-9,15-octadecadien-12-ynoic acid methyl ester, (10E,14Z)-9-hydroperoxy-10,14-octadecadien-12-ynoic acid [37].

German and Swedish scientists studied the content of sterols and vitamin D_2 in wild and cultivated *Cantharellus tubaeformis*. Cultivated samples had a greater content of provitamin D_2 (ergosterol) (4.0–5.0 mg/g) than wild mushrooms (1.7–3.5 mg/g). *C. tubaeformis* also contained ergosta-7,22-dienol, ergosta-5,7-dienol, and ergosta-7-enol. Wild *C. tubaeformis* proved to be a better source of vitamin D_2 (0.7–2.2 μg/g) than cultivated mushrooms (< 0.1 μg/g). UV irradiation of sublimated *C. tubaeformis* led to a slight decrease in the content of ergosterol, while the content of vitamin D_2 increased by nine times [38].

Portuguese scientists discovered that *C. cibarius*, *L. edodes*, *P. ostreatus*, *Craterellus cornucopioides*, and *Lepista nuda* contain insignificant amounts of selenium, compared to *Boletus aestivalis*, *Boletus pinophilus*, *B. edulis*, *Boletus aereus*, *Boletus fragans*, *Boletus spretus*, *Marasmius oreades*, *A. bisporus* "Portobello", *A. bisporus*, and *Russula cyanoxantha* [39].

Available sources reveal no information on the nutritional value of wild Russian *C. cibarius*, while its nutritional value is known to depend on a great number of factors, e.g. climatic zones, environmental impact, etc.

The present research objective was to study the nutritional value of wild *C. cibarius* growing in West Siberia, as well as the qualitative characteristics of semi-finished products from *C. cibarius*.

STUDY OBJECTS AND METHODS

The research featured wild chanterelles (*Cantharellus cibarius* L.): fresh samples (≤ 4 h after mycelium separation) and processed samples (boiled and salted).

The mushrooms were young, mature, and of medium maturity. The age was defined according to the diameter and shape of the cap, the state and color of the hymenophore, and the size and condition of the stem. The mushrooms were harvested in different districts of the Novosibirsk region in 1986–2018. The batch volumes were determined according to standard procedures [5].

The species was established organoleptically [5]: the characteristics of the specimen had to meet the requirements specified in Fig. 1. The mushrooms also met the safety standards in terms of toxicity, pesticides, and radionuclides, namely the mushrooms complied with the Technical Regulation of Customs Union TR CU 021/2011 "On food safety".

The samples of *C. cibarius* were tested for:

– total protein content using dye amide black 10B [40]; amino acid composition of proteins using an AAA-339M amino acid analyzer; total tryptophan content – by spectrophotometric method developed at the Bakh Institute of Biochemistry; qualitative analysis of proteins – by calculating the coefficient of digestibility and comparable redundancy [41];

– content of reducing sugars and trehalose was defined by the semi-micro Bertrand method [42]; mannit – by the iodine-metric method [43]; glycogen – after extraction with trichloroacetic acid; hydrolysis – by the semi-micro Bertrand method [42]; cellulose – by the Pochinok method [44]; mucus – by the gravimetric method [45];

– lipid content was defined according to the Bligh and Dyer method [46]; fatty acid composition – using a Hewlett Packard gas chromatograph HP 6890 (USA); squalene – by high-performance gas-liquid chromatography in a liquid microcolumn chromatograph Milichrom A-02 (Russia);

– ash content was measured by ashing the sample at 525 ± 25°C; ash weight was defined according to State Standard 25555.4-91 "Fruit and vegetable products. Methods for determination of ash and alkalinity of total ash and water-soluble ash";

– ascorbic acid was measured by the titrimetric method according to State Standard 24556-89 "Products of fruits and vegetables processing. Methods for determination of vitamin C"; thiamine, riboflavin, and niacin – by highly efficient gas-liquid chromatography in a Milichrom A-02 chromatograph according to State Standards 25999-83 "Products of fruits and vegetables processing. Methods of determination of vitamins B_1 and B_2" and State Standards R 50479-93 "Fruit and vegetable products. Method for determination of vitamin PP (niacin) content";

– content of minerals (potassium, sodium, calcium, magnesium, phosphorus, sulfur, iron, manganese, cobalt, zinc, copper, and nickel) was described by atomic absorption in an air-acetylene flame using QUANT AFA equipment;

– content of trypsin inhibitor – by the method developed by Gofman and Vaisblai [47];

– sensory properties were described according to a 100-point scale. The weighting factors for the indicators were as follows: appearance – 4; color – 3; consistency – 7; aroma – 6. Quality categories: excellent (90–100 points), very good (80–89 points), good (60–79 points), fair (40–59 points), and poor (≤ 39 points);

– count of mesophilic aerobes and facultative anaerobes was measured by cultivation on nutrient media with agar according to State Standard 10444.15-94 "Food products. Methods for determination of quantity of mesophilic aerobes and facultative anaerobes";

– chloride content was determined by the argentometric method according to State Standard 26186-84 "Fruit and vegetable products, meat and meat-vegetable cans. Methods for determination of chloride content".

RESULTS AND DISCUSSION

A long-term research revealed that the chemical composition, and, consequently, the nutritional value of chanterelles (*Cantharellus cibarius* L.) growing in the Novosibirsk region was not affected by the climatic conditions over a number of years: the mass fraction of proteins was 3.6%; digestible carbohydrates – 1.8%; mass fraction of dietary fiber – 2.1%; mass fraction of lipids – 0.7%; mass fraction of ash – 1.2% [5].

An adult needs eight amino acids: valine, isoleucine, leucine, lysine, methionine, threonine, tryptophan, and phenylalanine. Figure 2 shows that tryptophan proved to be the limiting amino acid, while methionine + cystine appeared to be predominant.

The amino acid score can be ranked as follows: methionine + cystine (147%) > phenylalanine + tyrosine (128%) > valine (120%) > threonine (119%) > lysine (109%) > isoleucine + leucine (107%). Human body can digest 60% of the amino acids in *C. cibarius* due to the coefficient of digestibility and comparable redundancy. The coefficient of digestibility of the amino acid composition of the protein (0.607 CU) reflects the balance of essential amino acids in relation to the standard [41]. The indicator of comparable redundancy (22.2%) describes the total amount of unused amino acids in an amount equivalent to their potentially digestible content in 100 g of the reference protein [41]. Therefore, *C. cibarius* is a potential source of methionine, phenylalanine, valine, and threonine. The amino acids are responsible for the specific aroma and taste: methionine, phenylalanine, tyrosine, valine, isoleucine, and leucine add bitterness while threonine adds sweetness [48].

The qualitative composition of carbohydrates in *C. cibarius* is highly variable [49]. The carbohydrate composition of *C. cibarius* is represented by 1.5% mono- (glucose) and oligosaccharides (trehalose),

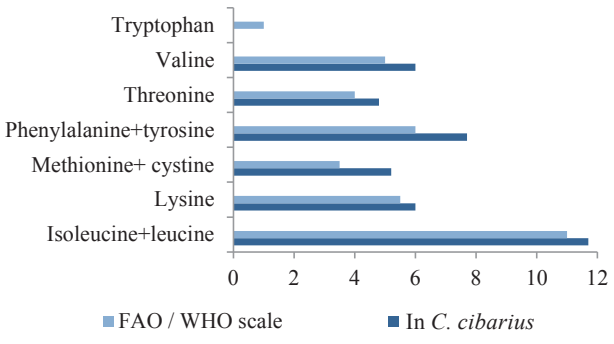

Figure 2 Content of essential amino acids in *Cantharellus cibarius*, g/100 g of protein

0.3% polyols (mannit), 0.1% glycogen, 2% fiber, and 0.8% mucus. Mono- and oligosaccharides, as well as polyols, are responsible for the typical taste of *C. cibarius*. This mushroom owes its physiological value due to trehalose. It consists of two molecules of D-glucose, mannit, glycogen, insoluble fiber, and soluble mucus. Trehalose and mannitol perform mainly a protective function in stress-induced situations. Glycogen performs the accumulative function; for example, it stores energy, which, if necessary, replenishes the lack of glucose. Insoluble fiber and branched sulfated arabinoxylans perform the protective function as they bind and remove toxic and radioactive elements.

The research revealed that 100 g of *C. cibarius* contained about 3.6 g of lipids. Lipids define sensory properties of fresh and processed products and also determine their stability during storage. Figure 3 demonstrates that the lipids of *C. cibarius* include fatty acids with 14–24 carbon atoms in the carbon chain.

The fatty acid composition of fresh *C. cibarius* is represented by the following fatty acids: linoleic (C18:2) – 62.2% of the total fatty acids; palmitic (C16:0) – 16.9%; oleic (C18:1) – 15.2%; stearic (C18:0) – 4.4%; palmitoleic (C16:1) – 0.7%; pentadecanoic acid (C15:0) – 0.3%; and heptadecanoic (C17:0) – 0.2%. The samples revealed no myristic, arachidic, behenic, lignoceric, and eicosadienic fatty acids. The samples also demonstrated high biological effectiveness, since the amount of polyunsaturated acids was 62.2%; monounsaturated – 15.9%; saturated – 21.8%; the ratio of polyunsaturated acids to saturated ones was 2.9%. The obtained results were consistent with the data published by Bengu, who conducted comparative studies of cultivated and wild mushrooms in Turkey [50]. However, the content of unsaturated fatty acids in *C. cibarius* should be taken into account during processing since mushrooms are prone to oxidation. The lipids of *C. cibarius* contained squalene ($C_{30}H_{50}$), a hydrocarbon that is not only a mother substance in sterol synthesis, but also possesses a high physiological

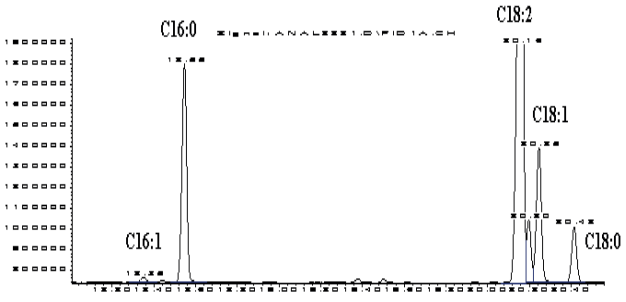

Figure 3 Chromatogram of fatty acid composition of *Cantharellus cibarius*

activity as it normalizes blood cholesterol, has antioxidant properties, etc.

The fresh samples contained a significant amount of vital biologically active substances, such as vitamins, macro- and microelements, etc. [51].

The fresh samples of *C. cibarius* were rich in ascorbic acid (15.05–34.92 mg/100 g), thiamine (0.01–0.03 mg), riboflavin (0.09–0.37 mg) (Fig. 4), and niacin (13.0 mg). Niacin consisted of nicotinic acid and nicotinamide (Fig. 5), the amount of which was 9.94 and 3.10 mg/100 g, respectively.

Micro- and macroelement analysis of the samples showed a significant amount of potassium (450.0–622.2 mg/100 g), sodium (0.0–33.4 mg), calcium (4.0–8.9 mg), magnesium (7.0–7.8 mg), phosphorus (44.0–48.9 mg), sulfur (44.4 mg), iron (0.7–8.6 mg), manganese (0.31–0.55 mg), cobalt (0.03–0.08 mg), zinc (0.34–0.64 mg), copper (0.51 mg), and nickel (0.06 mg).

The samples also demonstrated a trypsin inhibitor in the amount of 0.44–0.67 mg/g, which blocks the activity of enzymes in the digestive tract and also reduces the absorption of protein compounds.

Fresh mushrooms are conditionally-live products because of the ongoing irreversible biological and biochemical processes as they consist mainly of water

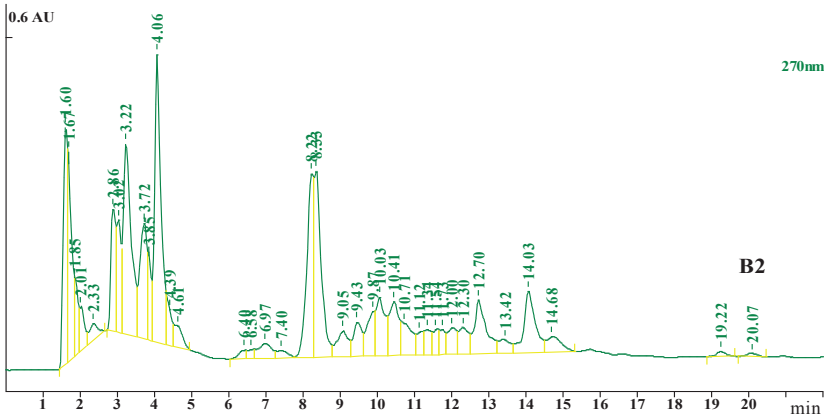

Figure 4 Chromatogram of the riboflavin release area in *Cantharellus cibarius*

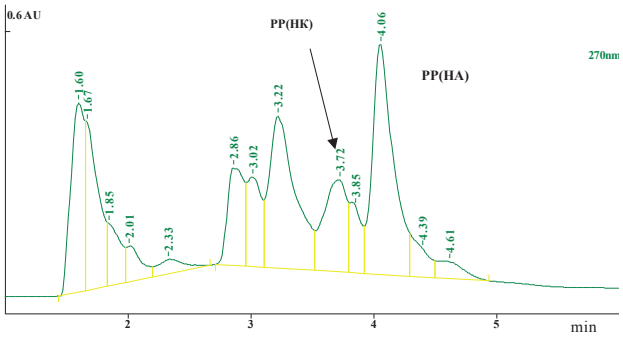

Figure 5 Chromatogram of the niacin release area in *Cantharellus cibarius*

Table 2 Effect of washing on the total microbial count of *Cantharellus cibarius*

Washing conditions	QMAFAnM, CFU/g	Effectiveness, %
Before washing	$(1.5 \pm 1.1) \times 10^6$	–
After double washing in non-flowing water	$(2.1 \pm 1.1) \times 10^5$	86.0
After washing in flowing water	$(9.6 \pm 2.8) \times 10^4$	93.6

(about 89.1%), proteins, and carbohydrates. High temperature, relative humidity, and long-term storage spoil the sensory properties of mushrooms, release cell juice, etc. As a result, scientists have to define shelf life for each type of mushroom, before processing under controlled and unregulated conditions. Table 1 shows the results of sensory evaluation of *C. cibarius* after 72 h of storage under different conditions.

When harvested, the mushrooms were fresh, undamaged, with well-developed hymnephors, uniform in size, and the number of stems matched the number of caps. After a while, some specimen became slightly wilted and/or crushed. After longer storage, the wilting increased, as did the number of crashed specimen. Eventually, all the mushrooms become wilted and slimy and demonstrated signs of tissue maceration.

The uniform yellow color of the fresh mushrooms gradually became heterogeneous and then browned slightly. The browning became more and more pronounced over time. The initial consistency was firm but gradually turned semi-firm and soft. The smell of the fresh mushrooms was typical for *C. cibarius* and pronounced; over time, the smell began to disappear and became weakly expressed, insignificant, musty, and even putrid.

The optimal storage time for fresh *C. cibarius* was 25 days at 0–2°C; ≤ 3 days at 5–10°C; ≤ 2 days at 15–20°C; and ≤ 1 day at 25–30°C.

Fresh mushrooms are hardly ever consumed raw. As a rule, they are served only after processing. Washing is the first procedure to prepare raw materials for processing. It removes impurities and microorganisms. Double washing in non-flowing water proved optimal for *C. cibarius* (Table 2).

Boiling in salt water is one of the processing methods for *C. cibarius*. The concentration of food salt in the finished product was 2.0–3.0%. After 5–10 min of boiling, the mushrooms maintained their typical color and aroma but did not retain the required tough-elastic consistency (Table 3). When the boiling time exceeded 15 min, the mushrooms developed atypical rubbery consistency, smell, and browning.

During boiling, *C. cibarius* underwent some chemical changes. After 10 min of boiling, water-soluble carbohydrates dropped by 50%, proteins – by 4%, ash – by 38%, riboflavin and nicotinic acid – by 34%. However, the content of fiber, glycogen, and nicotinamide increased by 1.5, 6.5, and 32.3%, respectively. Boiling triggered the extraction of free amino acids, especially phenyalanine (63.9%) and aspartic acid (45.7%) (Table 4).

Table 5 shows that boiling affected the content of palmitic, stearic, and oleic acids: their losses were 18.8, 9.1, and 1.3%, respectively. The content of polyunsaturated fatty acids increased by 7.4%, following the increase in linoleic acid.

Boiled mushrooms were used to prepare semi-finished products with different salt content: lightly-salted – 3.5–6.0%, medium-salted – 7.0–1.0%, and strong-salted – 25.0–30.0%. The salt penetration rate

Table 1 Sensory properties of *Cantharellus cibarius* after 72 h of storage, depending on weighting factors (n = 5)

Indicator	Storage temperature, °C			
	0[a]	10[a]	20[b]	30[b]
Appearance	18.4 ± 2.0	16.8 ± 1.6	11.2 ± 1.6	5.6 ± 2.0
Color	13.2 ± 1.5	12.6 ± 1.2	6.6 ± 1.2	3.6 ± 1.2
Consistency	33.6 ± 2.8	30.8 ± 3.4	15.4 ± 2.8	8.4 ± 2.8
Aroma	26.4 ± 3.0	25.2 ± 2.4	12.0 ± 0.0	9.6 ± 2.9
Total score	91.6 ± 4.7	85.2 ± 4.6	45.2 ± 3.4	27.2 ± 4.7
Quality category	excellent	very good	fair	poor

[a] – relative humidity 80–90 %

[b] – relative humidity 70–80 %

Table 3 Sensory properties of *Cantharellus cibarius* after boiling, depending on weighting factors (n = 5)

Indicator	Boiling time, min			
	5	10	15	20
Appearance	15.2 ± 1.6	13.6 ± 2.0	12.8 ± 1.6	10.4 ± 2.0
Color	12.0 ± 0.0	11.4 ± 1.2	10.2 ± 1.5	6.6 ± 1.2
Consistency	26.6 ± 2.8	23.8 ± 3.4	19.6 ± 2.8	14.0 ± 0.0
Aroma	24.0 ± 0.0	20.4 ± 2.9	18.0 ± 0.0	14.4 ± 2.9
Total score	77.8 ± 3.2	69.2 ± 5.1	60.6 ± 3.5	45.4 ± 3.7
Quality category	good	good	good	fair

from the brine at 10 ± 5°C made it possible to obtain ready-to-use lightly-salted or medium-salted products after 10–15 days. Strong-salted mushrooms needed 3-4 days at 25 ± 5°C with two or three replacements of brine. As a result of diffusion processes, the semi-finished products lost some amount of water-soluble substances (Fig. 6).

The concentration of sodium chloride affected the amount of free amino acids, saturated and monounsaturated fatty acids, riboflavin, nicotinic acid, and nicotinamide, which dropped to 25.0, 18.5, 50.8, 37.5, 3.7 and 19.8%, respectively. The proportion of polyunsaturated fatty acids reached 20.3%.

Lightly- and medium-salted semi-finished products retained their quality characteristics for six months of storage at ≤ 25°C and a relative humidity of ≤ 75% in the dark in hermetically sealed glass jars. Strong-salted mushrooms retained their quality for 12 months under the same conditions.

At the beginning of storage, the salted semi-finished products had microbial count of 2.6×10^3 to 4.5×10^3, e.g. micrococci, spore bacteria and bacteria without spores, and yeast. The number of microorganisms gradually increased, especially that of yeasts and molds, which caused a sour and/or musty odor, softening, whitish or green coating, etc. The number of thermophilic bacteria with spores of the *Clostridium butyricum* kind, which caused a putrid odor and gas release.

During storage, the protein content in the salted semi-finished products decreased gradually under the effect of hay bacillus, mold, and butyric acid bacteria. The hydrolytic breakdown of protein increased the amount of free amino acids by 25–30% of the initial content.

The content of saturated and monounsaturated fatty acids increased by an average of 21 and 142%,

Table 4 Content of amino acids in *Cantharellus cibarius* after 10 min of boiling

Amino acid	Content, μg/g	
	fresh	boiled
Aspartic Acid	138.4 ± 10.2	75.1 ± 5.8
Threonine	112.9 ± 9.5	78.0 ± 6.3
Serine	83.0 ± 6.6	61.2 ± 4.9
Glutamic Acid	127.3 ± 11.3	98.5 ± 7.6
Proline	549.1 ± 38.6	421.2 ± 36.5
Glycine	87.5 ± 6.1	83.6 ± 6.9
Alanine	99.6 ± 8.9	103.5 ± 9.1
Valine	121.8 ± 10.5	96.1 ± 8.2
Methionine	8.9 ± 0.6	7.1 ± 0.5
Isoleucine	73.1 ± 5.9	63.9 ± 5.7
Isoleucine	127.3 ± 11.1	112.0 ± 10.9
Tyrosine	77.5 ± 6.5	76.0 ± 5.7
Phenylalanine	155.0 ± 13.9	55.9 ± 4.3
Histidine	66.4 ± 5.5	40.6 ± 3.8
Lysine	60.9 ± 5.9	63.6 ± 5.2
Arginine	135.1 ± 10.8	93.1 ± 8.9
Total	2023.8	1529.4

Table 5 Content of fatty acids in *Cantharellus cibarius* after 10 min of boiling

Fatty acid	Content, % total	
	Fresh	Boiled
Pentadecanoic	0.3	0.3
Palmitic	16.9	13.0
Heptadecanoic	0.2	0.2
Stearic	4.4	4.0
Palmitoleic	0.7	0.7
Oleic	15.2	15.0
Linoleic	62.2	66.8
Total saturated fatty acids	21.8	17.5
Sum of monounsaturated fatty acids	15.9	15.7
Sum of polyunsaturated fatty acids	62.2	66.8

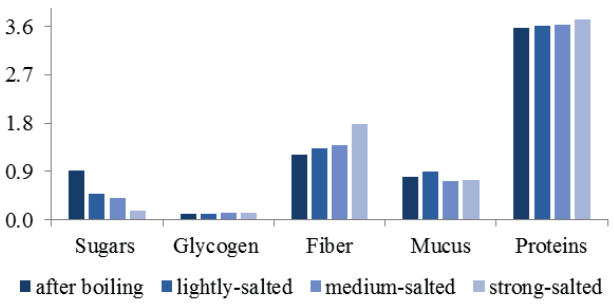

Figure 6 Basic nutrients in the semi-finished product from *Cantharellus cibarius*, depending on the sodium chloride content, %

respectively, while the amount of polyunsaturated acids decreased by 34%. These changes resulted from oxidative and hydrolytic processes, e.g. under the effect of mold and butyric acid bacteria, which were responsible for the typical mushroom smell.

By the end of the shelf life, the salted semi-finished products had almost no riboflavin left, and the amount of niacin dropped by 50%. No trypsin-inhibiting activity was detected in the canned samples.

CONCLUSION

In the Novosibirsk Region of West Siberia, chanterelles (*Cantharellus cibarius* L.) are still harvested in the wild, and no efforts are being made for their industrial cultivation. *C. cibarius* proved to be a good source of such nutrients as proteins, carbohydrates, lipids, vitamins, macro- and microelements, etc. The mushrooms contained a significant amount of amino acids, e.g. methionine, phenylalanine, valine, threonine, etc., squalene, trypsin inhibitors, and other bioactive substances.

The sensory evaluation revealed the optimal storage time for *C. cibarius* in marketing centers, depending on the temperature. The microbiological tests showed that *C. cibarius* has to be double-washed in non-flowing water before processing. The sensory evaluation showed that boiled lightly-, medium-, and strong-salted semi-finished products from *C. cibarius* should be consumed within 15, 10, and 3 days after the end of fermentation, respectively. Further research into the nutritional value of fresh and processed *C. cibarius* can improve the quality of mushroom products.

CONTRIBUTION

V.I. Bakaytis supervised the research. O.V. Golub and Yu.Yu. Miller performed the experiments, processed the data, and wrote the manuscript.

CONFLICT OF INTEREST

The authors declare that there is no conflict of interests regarding the publication of this article.

REFERENCES

1. Ma G, Yang W, Zhao L, Pei F, Fang D, Hu Q. A critical review on the health promoting effects of mushrooms nutraceuticals. Food Science and Human Wellness. 2018;7(2):125–133. https://doi.org/10.1016/j.fshw.2018.05.002.
2. Niksic M, Klaus A, Argyropoulos D. Safety of foods based on mushrooms. In: Prakash V, Martin-Belloso O, Keener L, Astley SB, Braun S, McMahon H, et al. editors. Regulating safety of traditional and ethnic foods. Academic Press; 2016. pp. 421–439. https://doi.org/10.1016/B978-0-12-800605-4.00022-0.
3. Rathore H, Prasad S, Sharma S. Mushroom nutraceuticals for improved nutrition and better human health: A review. PharmaNutrition. 2017;5(2):35–46. https://doi.org/10.1016/j.phanu.2017.02.001.
4. Valverde ME, Hernández-Pérez T, Paredes-López O. Edible mushrooms: Improving human health and promoting quality life. International Journal of Microbiology. 2015; 2015. https://doi.org/10.1155/2015/376387.
5. Kutaf′eva NP, Bakaytis VI, Tsapalova IEh, Poznyakovskiy VM. Ehkspertiza gribov. Kachestvo i bezopasnost′ [Expertise of mushrooms. Quality and safety]. Novosibirsk: Sibirskoe universitetskoe izdatel′stvo; 2007. 288 p. (In Russ.).
6. Aisala H, Sola J, Hopia A, Linderborg KM, Sandell M. Odor-contributing volatile compounds of wild edible Nordic mushrooms analyzed with HS–SPME–GC–MS and HS–SPME–GC–O/FID. Food Chemistry. 2019;283:566–578. https://doi.org/10.1016/j.foodchem.2019.01.053.
7. Aisala H, Laaksonen O, Manninen H, Raittola A, Hopia A, Sandell M. Sensory properties of Nordic edible mushrooms. Food Research International. 2018;109:526–536. https://doi.org/10.1016/j.foodres.2018.04.059.
8. Aisala H, Manninen H, Laaksonen T, Linderborg KM, Myoda T, Hopia A, et al. Linking volatile and non-volatile compounds to sensory profiles and consumer liking of wild edible Nordic mushrooms. Food Chemistry. 2020;304. https://doi.org/10.1016/j.foodchem.2019.125403.
9. Paudel E, van der Sman RGM, Westerik N, Ashutosh A, Dewi BPC, Boom RM. More efficient mushroom canning through pinch and exergy analysis. Journal of Food Engineering. 2017;195:105–113. https://doi.org/10.1016/j.jfoodeng.2016.09.021.
10. Kozhedub TI. Wild macromycetes as a source of phosphorus in the diet of the population of Belarus. Health and Ecology Issues. 2016;48(2):86–89. (In Russ.).
11. Chiang P-D, Yen C-T, May J-L. Non-volatile taste components of canned mushrooms. Food Chemistry. 2006;97(3):431–437. https://doi.org/10.1016/j.foodchem.2005.05.021.
12. Jaworska G, Bernaś E, Mickowska B. Effect of production process on the amino acid content of frozen and canned *Pleurotus ostreatus* mushrooms. Food Chemistry. 2011;125(3):936–943. https://doi.org/10.1016/j.foodchem.2010.09.084.
13. Bernaś E, Jaworska G. Effect of preservation method on amino acid content in selected species of edible mushroom. LWT – Food Science and Technology. 2012;48(2):242–247. https://doi.org/10.1016/j.lwt.2012.03.020.

14. Liu Y, Huang F, Yang H, Ibrahim SA, Wang Y-F, Huang W. Effects of preservation methods on amino acids and 5′-nucleotides of *Agaricus bisporus* mushrooms. Food Chemistry. 2014;149:221–225. https://doi.org/10.1016/j.foodchem.2013.10.142.
15. Wrona M, Bentayeb K, Nerín C. A novel active packaging for extending the shelf-life of fresh mushrooms (*Agaricus bisporus*). Food Control. 2015;54:200–207. https://doi.org/10.1016/j.foodcont.2015.02.008.
16. Fernandes Â, Antonio AL, Oliveira MBPP, Martins A, Ferreira ICFR. Effect of gamma and electron beam irradiation on the physico-chemical and nutritional properties of mushrooms: A review. Food Chemistry. 2012;135(2):641–650. https://doi.org/10.1016/j.foodchem.2012.04.136.
17. Chiaravalle AE, Mangiacotti M, Marchesani G, Bortone N, Tomaiuolo M, Trotta G. A ten-year survey of radiocontamination of edible Balkan mushrooms: Cs-137 activity levels and assessed dose to the population. Food Control. 2018;94:263–267. https://doi.org/10.1016/j.foodcont.2018.05.045.
18. Zou H, Zhou C, Li Y, Yang X, Wen J, Hu X, et al. Occurrence, toxicity, and speciation analysis of arsenic in edible mushrooms. Food Chemistry. 2019;281:269–284. https://doi.org/10.1016/j.foodchem.2018.12.103.
19. VanderMolen KM, Little JG, Sica VP, El-Elimat T, Raja HA, Oberlies NH, et al. Safety assessment of mushrooms in dietary supplements by combining analytical data with in silico toxicology evaluation. Food and Chemical Toxicology. 2017;103:133–147. https://doi.org/10.1016/j.fct.2017.03.005.
20. Mleczek M, Rzymski P, Budka A, Siwulski M, Jasińska A, Kalač P, et al. Elemental characteristics of mushroom species cultivated in China and Poland. Journal of Food Composition and Analysis. 2018;66:168–178. https://doi.org/10.1016/j.jfca.2017.12.018.
21. Chung I-M, Han J-G, Kong W-S, Kim J-K, An M-J, Lee J-H, et al. Regional discrimination of *Agaricus bisporus* mushroom using the natural stable isotope ratios. Food Chemistry. 2018;264:92–100. https://doi.org/10.1016/j.foodchem.2018.04.138.
22. El Sheikha AF, Hu D-M. How to trace the geographic origin of mushrooms? Trends in Food Science and Technology. 2018;78:292–303. https://doi.org/10.1016/j.tifs.2018.06.008.
23. Vlasova MV, Akhmedova TP. Influence of products of processing of mushrooms on baking properties of wheat flour. OrelSIET Bulletin. 2017;40(2):79–84. (In Russ.).
24. Galushchak IP. Lesnye griby: do evrostandartov eshche daleko [Forest mushrooms: a long way from European standards]. Standards and Quality. 2012;(9):58–60. (In Russ.).
25. Nyman AAT, Aachmann FL, Rise F, Ballance S, Samuelsen ABC. Structural characterization of a branched (1→6)-α-mannan and β-glucans isolated from the fruiting bodies of *Cantharellus cibarius*. Carbohydrate Polymers. 2016;146:197–207. https://doi.org/10.1016/j.carbpol.2016.03.052.
26. Gerasimenko AN. Grib lisichka v protivoopukholevykh i protivoparazitarnykh kompozitsiyakh “Blastaps” i “Vermostoping” [Chanterelle mushroom in antitumor and antiparasitic compositions “Blastaps” and “Vermostoping”]. Prakticheskaya fitoterapiya [Practical Phytotherapy]. 2013;(4):9–15. (In Russ.).
27. Yang G, Qu Y, Meng Y, Wang Y, Song C, Cheng H, et al. A novel linear 3-O-methylated galactan isolated from *Cantharellus cibariu*s activates macrophages. Carbohydrate Polymers. 2019;214:33–43. https://doi.org/10.1016/j.carbpol.2019.03.002.
28. Nowacka-Jechalke N, Nowak R, Juda M, Malm A, Lemieszek M, Rzeski W, et al. New biological activity of the polysaccharide fraction from *Cantharellus cibarius* and its structural characterization. Food Chemistry. 2018;268:355–361. https://doi.org/10.1016/j.foodchem.2018.06.106.
29. Jablonska-Rys E, Sławińska A, Szwajgier D. Effect of lactic acid fermentation on antioxidant properties and phenolic acid contents of oyster (*Pleurotus ostreatus*) and chanterelle (*Cantharellus cibarius*) mushrooms. Food Science and Biotechnology. 2016;25(2):439–444. https://doi.org/10.1007/s10068-016-0060-4.
30. Drewnowska M, Falandysz J. Investigation on mineral composition and accumulation by popular edible mushroom common chanterelle (*Cantharellus cibarius*). Ecotoxicology and Environmental Safety. 2015;113:9–17. https://doi.org/10.1016/j.ecoenv.2014.11.028.
31. Falandysz J, Chudzińska M, Barałkiewicz D, Drewnowska M, Hanć A. Toxic elements and bio-metals in *Cantharellus* mushrooms from Poland and China. Environmental Science and Pollution Research. 2017;24(12):11472–11482. https://doi.org/10.1007/s11356-017-8554-z.
32. Drewnowska M, Hanć A, Barałkiewicz D, Falandysz J. Pickling of chanterelle *Cantharellus cibarius* mushrooms highly reduce cadmium contamination. Environmental Science and Pollution Research. 2017;24(27):21733–21738. https://doi.org/10.1007/s11356-017-9819-2.
33. Falandysz J, Widzicka E, Kojta AK, Jarzyńska G, Drewnowska M, Dryałowska A, et al. Mercury in common Chanterelles mushrooms: *Cantharellus* spp. update. Food Chemistry. 2012;133(3):842–850. https://doi.org/10.1016/j.foodchem.2012.01.102.

34. Politowicz J, Lech K, Sánchez-Rodríguez L, Szumny A, Carbonell-Barrachina ÁA. Volatile composition and sensory profile of *Cantharellus cibarius* Fr. as affected by drying method. Journal of the Science of Food and Agriculture. 2017;97(15):5223–5232. https://doi.org/10.1002/jsfa.8406.
35. Che SN, Bakaytis VI, Tsapalova IE. Influence of heat treatment on macromycete physical characteristics and the content of heavy metals in them. Food Processing: Techniques and Technology. 2015;37(2):138–143. (In Russ.).
36. Phillips KM, Ruggio DM, Haytowitz DB. Folate composition of 10 types of mushrooms determined by liquid chromatography – mass spectrometry. Food Chemistry. 2011;129(2):630–636. https://doi.org/10.1016/j.foodchem.2011.04.087.
37. Mittermeier VK, Dunkel A, Hofmann T. Discovery of taste modulating octadecadien-12-ynoic acids in golden chanterelles (*Cantharellus cibarius*). Food Chemistry. 2018;269:53–62. https://doi.org/10.1016/j.foodchem.2018.06.123.
38. Teichmann A, Dutta PC, Staffas A, Jägerstad M. Sterol and vitamin D_2 concentrations in cultivated and wild grown mushrooms: Effects of UV irradiation. LWT – Food Science and Technology. 2007;40(5):815–822. https://doi.org/10.1016/j.lwt.2006.04.003.
39. Costa-Silva F, Marques G, Matos CC, Barros AIRNA, Nunes FM. Selenium contents of Portuguese commercial and wild edible mushrooms. Food Chemistry. 2011;126(1):91–96. https://doi.org/10.1016/j.foodchem.2010.10.082.
40. Buzun GA, Dzhemukhadze KM, Meleshko LF. Opredelenie belka v rasteniyakh s pomoshch′yu amido-chernogo [Determination of protein in plants using dye amide black]. Fiziologiya Rastenij. 1982;29(1):198–204. (In Russ.).
41. Lipatov NN. Nekotorye aspekty modelirovaniya aminokislotnoy sbalansirovannosti pishchevykh produktov [Some aspects of modeling amino acid balance of food products]. Pishchevaya i pererabatyvayushchaya promyshlennost′ [Food and Processing Industry]. 1986;(4):48–52.
42. Lisitsyn DI. Polumikrometod dlya opredeleniya sakharov v rasteniyakh [Semi-micromethod for the determination of sugars in plants]. Biokhimiya [Biochemistry]. 1950;15(2):165–167. (In Russ.).
43. Opredelenie mannita (mannitola) v biologicheskikh lekarstvennykh preparatakh [Determination of mannit in biological medicinal products] [Internet]. [cited 2020 Feb 25]. Available from: http://docs.cntd.ru/document/554199329.
44. Pochinok KhN. Metody biokhimicheskogo analiza rasteniy [Methods of biochemical analysis of plants]. Kiev: Naukova dumka; 1976. 334 s. (In Russ.).
45. Ermakov AI. Metody biokhimicheskogo issledovaniya rasteniy [Biochemical research methods of plants]. Leningrad: Agropromizdat; 1987. 429 p. (In Russ.).
46. Keyts M. Tekhnika lipidologii. Vydelenie, analiz i identifikatsiya lipidov [Technique of lipidology. Isolation, analysis, and identification of lipids]. Moscow: Mir; 1975. 322 p. (In Russ.).
47. Gofman YuYa, Vaysblay IM. Opredelenie ingibitorov tripsina v semenakh gorokha [Determination of trypsin inhibitors in pea seeds]. Applied Biochemistry and Microbiology. 1975;11(5):777–783. (In Russ.).
48. Manninen H, Rotola-Pukkila M, Aisala H, Hopia A, Laaksonen T. Free amino acids and 5′-nucleotides in Finnish forest mushrooms. Food Chemistry. 2018;247:23–28. https://doi.org/10.1016/j.foodchem.2017.12.014.
49. Li X, Guo Y, Zhuang Y, Qin Y, Sun L. Nonvolatile taste components, nutritional values, bioactive compounds and antioxidant activities of three wild *Chanterelle* mushrooms. International Journal of Food Science and Technology. 2018;53(8):1855–1864. https://doi.org/10.1111/ijfs.13769.
50. Bengu AS. The fatty acid composition in some economic and wild edible mushrooms in Turkey. Progress in Nutrition. 2020;22(1):185–192. https://doi.org/10.23751/pn.v22i1.7909.
51. Muszynska B, Grzywacz-Kisielewska A, Kala K, Gdula-Argasinska J, et al. Anti-inflammatory properties of edible mushrooms: A review. Food Chemistry. 2018;243:373–381. https://doi.org/10.1016/j.foodchem.2017.09.149.

ORCID IDs
Valentina I. Bakaytis https://orcid.org/0000-0002-6873-6263
Olga V. Golub https://orcid.org/0000-0003-2561-9953
Yuliya Yu. Miller https://orcid.org/0000-0001-5490-4804

Foods and Raw Materials, 2021, vol. 9, no. 2

E-ISSN 2310-9599
ISSN 2308-4057

Research Article
Open Access

https://doi.org/10.21603/2308-4057-2021-2-244-253
Available online at http://jfrm.ru/en

Effect of organic compounds on cognac sensory profile

Mikhail N. Eliseev[1], Irina N. Gribkova[2,*], Olga A. Kosareva[3], Olga M. Alexeyeva[1]

[1] Plekhanov Russian University of Economics, Moscow, Russia

[2] All-Russian Research Institute of Brewing, Non-alcoholic and Wine Industry, Moscow, Russia

[3] Moscow University for Industry and Finance "Synergy", Moscow, Russia

* e-mail: beer_institut@mail.ru

Received March 22, 2021; Accepted in revised form April 24, 2021; Published online July 09, 2021

Abstract:
Introduction. The present research featured the effect of carbonyls, phenols, furans, fatty alcohols, ethers, and other chemical compounds on the sensory properties of cognac distillates of different ages. The research objective was to identify additional criteria of sensory evaluation by measuring the effect of various compounds on perception intensity.
Study objects and methods. The study featured cognac samples of different ages. The experiment involved standard methods, including high-performance liquid and gas chromatography and a mathematical analysis based on Microsoft software.
Results and discussion. The content of fatty alcohols, ethers, and carbonyl compounds that formed as a result of fermentation demonstrated little change during the aging period in oak casks. A longer extraction increased the content of phenolic and furan compounds and sugars. The content of terpene compounds decreased due to their high lability. The study revealed the effect of organic compounds on taste descriptors. The article introduces multivariate equations that calculate the dependences of the descriptor intensity on the content of organic compounds. A correlation and regression analysis revealed that phenolic compounds had a significant effect on the taste formation of cognac samples, depending on the aging time.
Conclusion. Organic compounds proved to affect the taste profiles of cognac samples of different ages, as well as sensory evaluation descriptors.

Keywords: Sensory profile, cognac, organic compounds, fatty alcohols, ethers, volatile compounds, polyphenolic compounds, descriptors

Please cite this article in press as: Eliseev MN, Gribkova IN, Kosareva OA, Alexeyeva OM. Effect of organic compounds on cognac sensory profile. Foods and Raw Materials. 2021;9(2):244–253. https://doi.org/10.21603/2308-4057-2021-2-244-253.

INTRODUCTION

Formation of the flavor profile of cognac and brandy is a complex multistage process. Their aroma, taste, and color depend on too many factors, including the quality of raw materials, the technology of fermentation and distillation, etc. One of the most important factors is the aging in oak casks: its time and conditions are responsible for the numerous transformations of organic compounds, such as extraction, synthesis, biosynthesis, oxidation, etc. [1].

Different classes of compounds contribute to the formation of the sensory profile of cognacs with different aging periods (Tables 1 and 2) [2–9].

Figure 1 shows descriptors that make up the sensory profile of cognac [15].

The gustatory sensation formation is a complex process, where a single shade of flavor may result from a whole complex of compounds [16]. People are able to perceive five basic tastes: sweet, sour, bitter, salty, and "umami", which was discovered in the early XX century.

In fact, the taste sensation forms in the brain as protein structures trigger its response to a combination of external stimuli. Several sensory stimuli shape perceptions from several descriptors. For instance, spicy tones are formed by compounds of mustard and pepper because carbon dioxide is responsible for this taste. Fresh tones depend on several compounds of plant raw materials, e.g. mint, or on individual substances, e.g. xylitol. A sense of astringency appears when saliva proteins interact with food polyphenols. How panelists evaluate one particular descriptor depends on a complex of organic compounds that enhance or minimize their effect on taste receptors due to spatial stereoisomerism, etc. [17].

Table 1 Compounds that affect the sensory profile of cognacs

Compounds	Source	Effect on cognac quality
Fatty alcohols	Amino acids of raw materials during fermentation	Resinous, honey, floral, and ripe fruity tones
Ethers	Raw materials; fermentation and aging in oak casks	Fruity tones; ethyl acetate is responsible for floral and anis aroma
Aldehydes and ketones	Raw materials; fermentation and aging in oak casks	Unpleasant unripe tones; nutty and floral tones
Norizoprenoids and terpenes	Fermentation of plant raw materials	Resinous tones, e.g. myrcene; fruity and floral tones; caryophylenes are responsible for the tone of cedar pine nuts
Polyphenols and phenols	Oak wood during aging	A wide range of flavors and colors

Therefore, the present research objective was to study the effect that compounds in cognacs of different ages produce on the intensity of perception of individual descriptors in order to reveal extra quality assessment criteria.

STUDY OBJECTS AND METHODS

The present research featured cognac samples of various ages purchased in a network supermarket. Cognacs were stored in a dark room at 20 ± 1°C.

The reduced extract was analyzed by distillation followed by a pycnometric analysis of solids [18].

The pH of the samples was measured in sevenplicates using a pH meter (METTLER TOLEDO, USA).

The list of phenolic and furan compounds included gallic, syringic, vanilla and sinapic acids, vanillin, syringaldehyde, coniferaldehyde, sinapaldehyde, 5-hydroxymetifurfural, furfural, and 5-methylfurfural. Their content was analyzed by high performance liquid chromatography (HPLC) using a diode array detector Agilent Technologies 1200 (Agilent, USA). We also used a Hypersil 5 um C18 250×4.6 mm column (Thermo, USA) with wavelengths of 270 and 310 nm. The test

Table 2 Polyphenolic compounds extracted from oak wood

Compounds	Effect on cognac
Low molecular benzoic phenolic acids: gallic, p-hydroxybenzoic, protocatechuic, syringic, vanilla	Bitterness and astringency
Low molecular hydroxycinnamic phenolic acids: ellagic, trans-caffeic, ferulic, coniferic, p-coumaric, sinapic, caffeic	Color stabilization [10]
Furan compounds: 5-OH-methyl-furfural, furfural	Pentoses and hexoses, thermal transformation products; almond, grainy, spicy-alcoholic taste during aging in oak casks
Low molecular phenolic aldehydes: syringaldehyde, coniferaldehyde, sinapaldehyde, protocatechuic aldehyde	Woody and roasted tones that appear due to thermal transformation of oak wood lignin by decarboxylation, followed by breaking the aryl-alkyl ether bonds of the end links [6]
Oxidation products of simple acids: vanillin	Vanilla tone
Oxycoumarins: scopoletin	New extract tones due to intermediate products of conversion of lignin to coniferyl alcohol
Ellagotannins: vescalagin, castalagin, grandinin, Roburin A, B, C, D, E	Orange color that appear as anthocyano-ellagitannin compounds react with purple or red pigments of grape raw materials [11]
Phenolic compounds: *cis*- and *trans*-p-coumaric acids, *cis*- and *trans*-coumaric acids, derivatives of *cis*- and *trans*-p-coumaric acids	Woody tone
Flavonoids: (+)-catechin, (−)-epicatechin, Myricetin, myricetin 3-o-glycoside; Flavanols: quercetin 3-o-glucuronide, quercetin 3-o-galactoside, quercetin	Yellow and orange shades
Volatile phenolic compounds: guaiacol, ethyl guaiacol, eugenol, methoxyevgenol	Vanilla, nutty, caramel, and spicy-clove tones; guaiacol is responsible for smoky, spicy, clove, and oak tones [12, 13]
Octalactones: *cis*- and *trans*-octalactone	Coconut, fresh wood, sweet, spicy, and celery tones [14]
Phenols: o-, p-cresol, 2,6-dimethoxyphenol	Milder and better taste by interacting with other aromatic components
Polyphenols: resveratrol, trans-resveratrol, *trans*-, *cis*-3-o-glucoside resveratrol	Responsible for antioxidant properties
Gallic acid ethers (tannins): methyl and ethyl gallates	Astringency
Phenolic alcohols: tyrosol, tryptopol	Bitter tones

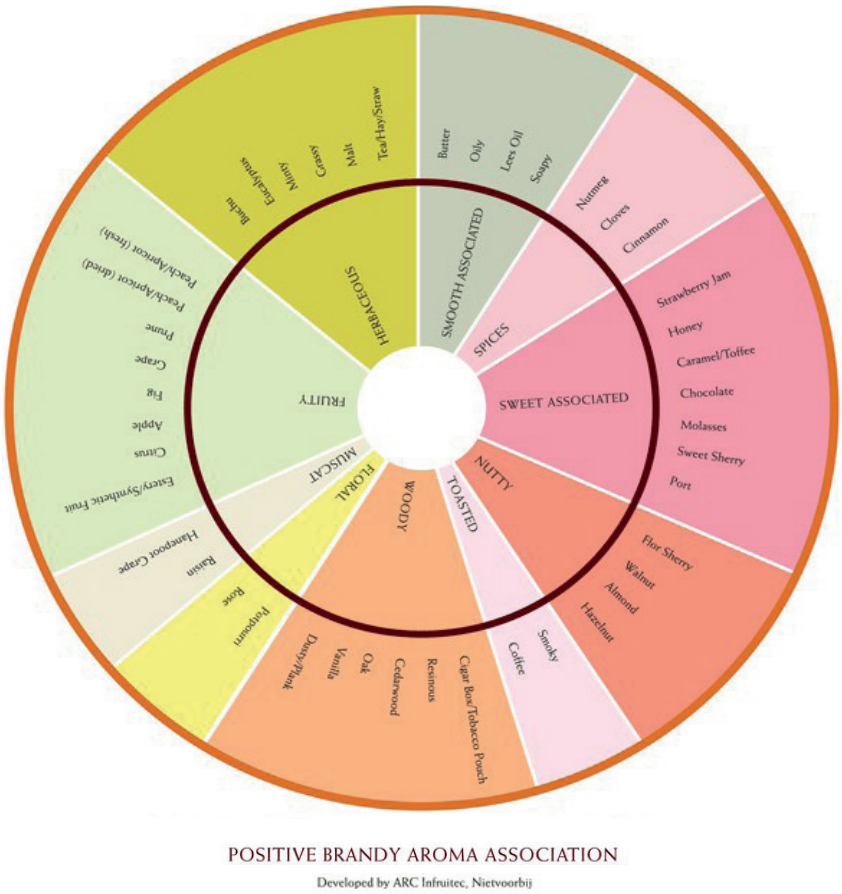

Figure 1 Positive descriptors for brandy and cognacs

samples and standards (0.02 cm^3) were introduced in a reversed-phase column at 40°C. The mobile phase was represented by a 0.025 mol/dm^3 solution of potassium dihydrogen phosphate (A) with pH = 2.5, and a solution of acetonitrile (B) in the ratio of A:B = 87:13. The elution rate was 1.3 cm^3/min.

The mass concentration of sugars, i.e. fructose, glucose, and sucrose, was analyzed by HPLC using an Agilent Technologies 1200 diode array detector (Agilent, USA). A Hypersil 5 um C18 250×4.6 mm column (Thermo, USA) had wavelengths of 440 and 540 nm. The test samples and standard solutions were injected in a volume of 0.02 cm^3 of a reversed-phase column at 40°C. The mobile phase was represented by distilled water (A) and acetonitrile solution (B) in the ratio of A:B = 87:13. The elution rate was 600 cm^3/min.

The mass concentration of higher alcohols, ethers, and hydrocarbons was assessed using gas chromatography (HPHC). A flame ionization detector (GC-FID) was used to detect various volatile components, including methanol, ethanol, 1-, 2-propanol, 1-, 2-butanol, isobutanol, isoamilol, hexanol, phenylethyl alcohol, acetaldehyde, isobutyl aldehyde, acetone, ethyl formate, diethyl formate, ethyl acetate, isoamyl acetate, ethyl caproate, ethyl lactate, ethyl caprylate, ethyl caprate, guaiacol, and eugenol. The analysis also involved such non-volatile components as o-cresol, tyrosol, myrcene, and β-terpineol.

All measurements were conducted in sevenplicates, standard deviation ≤ 5%. Each sample in the volume of 5 cm^3 (40% vol.) was added to 0.25 cm^3 of internal standard solution and placed in 2 cm^3 vials. Each component was introduced at a concentration of 2 g/dm^3 in absolute alcohol. The vials were hermetically sealed. A sample of 0.002 cm^3 was introduced into the chromatograph inlet. The column thermostat

Table 3 Indicators of cognac samples of different ages

Indicator	Content (reliability limit $P \geq 0.95$)		
	3 years	5 years	7 years
Ethanol, g/dm^3	4.0 ± 0.1	4.0 ± 0.1	4.0 ± 0.1
Reduced extract, g/dm^3	2.80 ± 0.03	4.00 ± 0.04	4.70 ± 0.50
Active acidity (pH)	3.70 ± 0.04	3.50 ± 0.35	3.60 ± 0.36

Table 4 Volatile components in cognacs of different ages

Compound	Mass concentration, mg/dm³ (reliability limit p ≥ 0.95)		
	3 years	5 years	7 years
Higher alcohols			
methanol	107.40 ± 11.00	101.80 ± 10.00	100.60 ± 10.00
1-propanol	101.50 ± 10.00	103.60 ± 10.00	101.50 ± 10.10
1-butanol	1.20 ± 0.01	1.30 ± 0.01	1.20 ± 0.01
2- butanol	0.20 ± 0.01	0.20 ± 0.01	0.10 ± 0.01
2-propanol	5.50 ± 0.55	5.70 ± 0.55	4.60 ± 0.04
isobutanol	394.60 ± 40.00	428.90 ± 43.00	394.60 ± 40.00
isoamylol	1138.00 ± 100.00	1168.60 ± 120.00	1138.00 ± 115.00
hexanol	8.80 ± 0.90	10.80 ± 1.00	10.80 ± 1.10
phenylethyl alcohol	17.10 ± 2.00	20.00 ± 2.00	26.50 ± 3.00
Aldehydes and ketones			
acetaldehyde	31.40 ± 3.00	36.30 ± 4.00	59.30 ± 6.00
isobutyraldehyde	20.30 ± 2.00	19.80 ± 2.00	18.30 ± 2.00
acetone	6.90 ± 0.70	9.30 ± 1.00	18.70 ± 2.00
Carboxylic acid ethers			
ethyl formate	4.70 ± 0.50	6.90 ± 0.70	12.80 ± 1.30
diethylformal	0.70 ± 0.01	1.10 ± 0.10	4.10 ± 0.40
ethyl acetate	120.30 ± 12.00	142.70 ± 14.00	261.40 ± 25.00
isoamyl acetate	2.60 ± 0.30	2.40 ± 0.25	2.30 ± 0.25
ethylcaproate	4.40 ± 0.40	5.10 ± 0.50	6.40 ± 0.65
ethyl lactate	74.40 ± 7.00	98.90 ± 10.00	81.10 ± 8.00
ethyl caprylate	16.00 ± 2.00	28.80 ± 3.00	43.70 ± 4.50
ethyl caprate	86.70 ± 9.00	96.20 ± 10.00	155.20 ± 15.00

temperature was 220°C, and the carrier gas velocity was 1.3 cm³/min.

The sensory evaluation of the cognac samples involved seven panelists with an extensive experience in cognac industry and sensory tests. The panelists worked in separate booths, isolated from external factors. The cognac samples were served chilled to 18 ± 1°C in testing glasses at room temperature 20 ± 1°C under white diffused light. The samples were evaluated according to set of descriptors in comparison with the reference sample. The result was expressed in points from 0 to 10 (0 – impossible to evaluate; 1–2 – unsatisfactory (demonstrates a severe flaw); 3–4 – satisfactory (demonstrates an obvious flaw); 5–6 – satisfactory (violates the quality standard); 7–8 – very satisfactory (slightly violates the quality standard); 9–10 – excellent (corresponds with the quality standard).

The statistical analysis was performed in sevenplicates. The descriptive statistics and values were expressed as mean ± standard deviation (SD). The Student-Fisher method provided multivariate models of the correlation and regression dependence of the parameters. The reliability limit of the obtained data ($P \geq 0.95$) was used to assess various factors that affected the content of polyphenols in all the experiments. The obtained statistical data were processed using the Statistics program (Microsoft Corporation, Redmond, WA, USA, 2006).

RESULTS AND DISCUSSION

Tables 3–5 show the content of ethanol, reduced extract, carbohydrates, volatiles, furans, and phenols in the cognac samples of different ages.

The data are representatives of seven independent experiments, and values are expressed in mean (± SD).

Table 3 shows that the content of ethanol stayed within the permissible values for cognac products specified in State Standard 31732-2014 "Brandy. General specifications" and did not fall below 40.0 ± 0.3% or 4.00 ± 0.03 g/dm³. The content of volatile compounds in the samples increased together with the aging time, which correlates with the previously published scientific data [19, 20].

Table 3 clearly demonstrates that the active acidity decreased insignificantly as the aging time increased. The total acidity index depended on the origin of the wood. However, it increased as a result of long-term aging in oak casks due to the oxidation of ethanol as compounds passed from the wood to the cognac [21, 22].

The pH value is known to depend on the amount of acids and the strength of the distillate. As the content of alcohol in the distillate increases, the dissociation of carboxyl groups decreases, and acidity drops. As tannins dissolve, volatile acids appear, and the strength decreases during aging, the pH decreases [23]. The pH value also depends on the amount of dissolved tannins with an acidic pH, which increases the acidity of the distillates [23]. The experimental data in Table 5 confirmed these trends.

The data are representatives of seven independent experiments, and values are expressed in mean (± SD).

Table 5 Phenols, furans, and carbohydrates in cognac samples of different ages

Compound	Mass concentration, mg/dm³ (reliability limit $P \geq 0.95$)		
	3 years	5 years	7 years
Phenolic acids			
gallic acid	3.00 ± 0.30	4.60 ± 0.45	8.30 ± 0.80
syringic acid	0.80 ± 0.01	1.50 ± 0.15	3.30 ± 0.30
vanilla acid	0.50 ± 0.05	0.80 ± 0.08	1.50 ± 0.15
sinapic acid	0.10 ± 0.01	0.40 ± 0.04	0.60 ± 0.05
Phenolic aldehydes			
syringaldehyde	2.50 ± 0.25	4.00 ± 0.40	7.70 ± 0.80
vanillin	1.00 ± 0.10	1.60 ± 0.15	3.30 ± 0.30
sinapaldehyde	2.20 ± 0.20	2.90 ± 0.30	3.00 ± 0.30
coniferaldehyde	0.80 ± 0.08	1.30 ± 0.10	1.70 ± 0.15
Furan compounds			
5-hydroxymethylfurfural	37.00 ± 4.00	47.90 ± 5.00	57.40 ± 6.00
furfural, mg/100 cm³ of anhydrous alcohol	2.30 ± 0.20	2.70 ± 0.30	2.90 ± 0.30
5-methylfurfural	0.30 ± 0.03	0.40 ± 0.04	0.50 ± 0.05
syringaldehyde vs. vanillin	2.50 ± 0.25	2.50 ± 0.25	2.40 ± 0.25
Phenols			
o-cresol	0.038 ± 0.001	0.050 ± 0.005	0.065 ± 0.006
Phenolic alcohols			
tyrosol	0.150 ± 0.001	0.235 ± 0.002	0.345 ± 0.004
Volatile phenolic compounds			
guaiacol	1.460 ± 0.010	2.000 ± 0.020	3.420 ± 0.003
eugenol	0.020 ± 0.001	0.118 ± 0.001	0.200 ± 0.002
Volatile terpenoids			
myrcenol	0.255 ± 0.006	0.210 ± 0.002	0.147 ± 0.001
β-terpineol	0.830 ± 0.004	0.645 ± 0.006	0.278 ± 0.003
Carbohydrates			
fructose	1.15 ± 0.10	1.55 ± 0.15	3.02 ± 0.30
glucose	0.99 ± 0.10	1.43 ± 0.15	2.94 ± 0.30
sucrose	6.12 ± 0.60	6.33 ± 0.60	6.45 ± 0.65

Table 4 shows that the content of volatile fractions in the cognac samples increased together with the aging period, as reported in [19]. The total of higher alcohols was 1.774–2.092 mg/dm³. A longer aging period triggered the process of oxidation in higher alcohols (Table 4). Since the content of these alcohols in the cognac distillate was low, the oxidation of each alcohol was insignificant, in comparison with the oxidative processes of ethyl alcohol. The amounts of aldehydes, acids, and ethers formed by higher alcohols were also insignificant. Nevertheless, even in such small quantities that are elusive for conventional analysis methods, these substances still affect the taste of cognac due to the sheer fact of their existence [24–26]. If the cognac composition is well-balanced, higher alcohols form the basis of its sensory profile [27].

Undesirable tones may result from excessive acetaldehyde that form during oxidation, especially in the samples with a longer aging period, depending on the characteristics of oak wood [22, 28]. However, if other volatile compounds are present, the excessive acetaldehyde in these samples does not disrupt the taste balance.

Ethers also affect the flavor profile of cognacs. Their content depends on the aging time [29]. If ethyl acetate exceeds the sensitivity threshold (180 mg/dm³), it affects the sensory profile of the distillate, giving it undesirable tones [30].

The data are representatives of seven independent experiments, and values are expressed in mean (± SD).

Table 5 shows that the cognac samples contained typical phenolic acids and aldehydes in quantities that did not exceed those featured in research publications for cognacs of 2.5–15 years of aging [31–33]. The content of syringaldehyde is a marker of aging time. It was in the range of 2.5–7.7 mg/dm³ and increased with aging time, which corresponded with scientific publications on this chemical substance and other simple phenolic acids and aldehydes [31].

Table 5 illustrates the ratio of syringaldehyde and vanillin, which is also a marker of aging time. This ratio stayed within the range of 2–4, established for collection samples, and was 2.4–2.5 [31, 34].

Phenolic acids are involved in the complex biochemical processes of aging and affect the sensory profile of cognacs [35]. For instance, gallic acid, a product of hydrolysis of soluble gallotannins and eluggotannins of oak wood, affects the aging processes, acts as an oxidation catalyst, and removes sulfides [36, 37].

As alcohol comes in contact with oak bark during aging, it triggers solubilization with the subsequent cleavage of the covalent alkylaryl ether. This reaction leads to the cleavage of lignins and produces vanillin, syringaldehyde, and their acids, which affect the taste profile of cognac distillates [38]. Table 5 shows that phenolic acids and aldehydes increased with aging, which is consistent with the previously published research data [38].

Furan compounds appear as the temperature increases during the decomposition of non-starch polysaccharides of oak bark or during distillation from five-membered sugars [39]. The amount of furan compounds is known to affect the number of distillations [26]. The content of furan compounds increased after a prolonged contact of oak bark and cognac distillate.

Reducing sugars, i.e. glucose, arabinose, and fructose, were also registered in the distillate samples. During aging, the contact of alcohol and oak wood led to the hydrolysis of hemicelluloses and hydrolyzable tannins [40]. Sugars affected the sensory profile of cognacs, and their quantity increased with aging (Table 5).

Volatile phenolic compounds, phenols, and terpene compounds are responsible for some characteristic tones in the cognac bouquet. The content of phenolic compounds increases with aging, while the concentration of terpene compounds decreases as a result of their lability (Table 5).

The cognac samples underwent a sensory evaluation (Table 6) using the descriptors presented in Fig. 2, which demonstrates how certain organic compounds compose particular descriptors.

In low alcohol drinks, bitterness is known to depend on alcohol content [41]. This study proved that bitterness depends not only on aliphatic alcohols, but also on phenolic compounds.

Aldehydes are responsible for mildness [42]. However, aliphatic alcohols with their different tones also might help make the taste of cognac milder, and the content of o-cresol might also produce a certain effect on the mildness [2]. Astringency appears when phenolic compounds are released during aging as a result of contact with oak wood, depending on the aging time and pH [5, 6].

The resinous tones result from the combined action of organic compounds in the distillate; it defines the quality of the finished product [33]. This descriptor is formed during fermentation, distillation, and aging [1, 33]. As a result, resinousness may depend on the content of aliphatic alcohols, phenolic compounds, and terpenoids [5, 7, 33].

Oiliness, another cognac descriptor, appears mainly due to secondary fermentation products that remain after distillation, and partly due to the contact of alcohol with oak [33]. Fruity tones depend on such secondary fermentation products as aldehydes and alcohols, as well as on terpene compounds, which is associated with the fermentation of fruit raw materials [9].

Chocolate tones are more difficult to form than the rest of the descriptors. Chocolate tones are known to depend on secondary fermentation products, volatile phenolic compounds, vanillin, and methylfurfural, the latter also being responsible for sweet-nutty tones [26].

The intensity indicators for each descriptor were quantitatively correlated with the results of the sensory evaluation (Tables 3–5). They were processed in order to obtain correlation and regression equations that made it possible to calculate the dependence of the tones on particular compounds (Table 7).

The values of the coefficients were analyzed in modulus in each group of the dependencies (Y_1, Y_2, Y_3, Y_4, Y_5, Y_6 and Y_7) and the variables. In group Y_1, the variables at X_3 had a larger coefficient because o-cresol had a greater effect on descriptor Y_1; in groups Y_2 and Y_3, phenolic alcohols contributed; in Y_4 – volatile phenolic compounds and aldehydes; in Y_5 – oxymethylfurfural; in Y_6 – terpene compounds, and in Y_7 – vanillin.

Table 8 demonstrates equations for the dependence of the compounds (X) on the aging period (Y_x) obtained by the method of pair linear correlation.

The greatest value belonged to variable X_3. Therefore, the change in the content of volatile phenolic compounds affected the sensory profile of the cognac samples more than other compounds. Probably, descriptor groups Y_4 (resinousness) and Y_7 (chocolate tone) had a greater affect on the taste perception in comparison with other descriptor groups. Phenolic compounds, i.e. acids, aldehydes, alcohols, and volatile compounds, were especially important for the development of the sensory profile of the cognac samples.

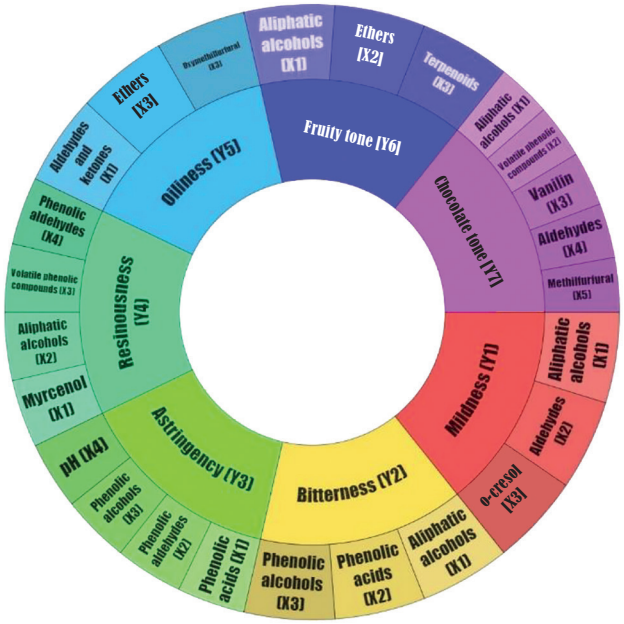

Figure 2 Descriptors for sensory evaluation of cognac samples

CONCLUSION

The correlation and regression analysis made it possible to assess the role of various organic compounds

Table 6 Sensory evaluation of cognac samples of different aging

Aging time, years	Descriptor (point ± 0.2)									
	Palate fullness	Balance	Aftertaste	Mildness	Bitterness	Astringency	Resinousness	Oiliness	Fruity tones	Chocolate tones
3	7.8	6.4	4.8	6.5	0.4	0.7	3.8	2.2	5.2	0.2
5	8.2	8.2	7.2	7.2	1.0	0.8	5.8	5.8	6.4	3.4
7	9.4	9.4	8.4	8.4	0.4	1.6	6.4	6.6	7.0	4.6

Table 7 Mathematical assessment of the effect of various compounds on the formation of sensory profiles of cognac samples

Descriptor (Y)	Equation of multivariate variable dependence (X_n) on descriptor (Y) depending on the aging time, years		
	3	5	7
Mildness (Y_1)	$Y_{1/3}=3\times10^{-3}+2.45\times10^{-7}\times X_1-6\times10^4\times X_2+1{,}703\times X_3$	$Y_{1/5}=11\times10^{-4}\times X_1-0.23\times X_2-7.4\times X_3+7\times10^{-3}$	$Y_{1/7}=42\times10^{-5}\times X_1+0.1\times X_2-22.9\times X_3-0.05$
Bitterness (Y_2)	$Y_{2/3}=2.8\times X_3-1\times10^{-5}\times X_1-7.4\times10^{-4}\times X_2+12.9\times10^{-5}$	$Y_{2/5}=5\times10^{-3}\times X_1+0.1\times X_2-2.85\times X_3-2\times10^{-5}$	$Y_{2/7}=2\times10^{-6}\times X_1-4\times10^{-6}\times X_2+X_3+17\times10^{-4}$
Astringency (Y_3)	$Y_{3/3}=-0.3\times X-0.25\times X_2+17.3\times X_3+0.25\times X_4+0.011$	$Y_{3/5}=3\times10^{-3}+0.31\times X_1-0.12\times X_2+0.66\times X_3-0.13\times X_4$	$Y_{3/7}=-75\times10^{-4}\times X_1+0.133\times X_2-0.403\times X_3-0.07\times X_4-0.01$
Resinousness (Y_4)	$Y_{4/3}=-10\times10^{-4}\times X_1+16.9\times10^{-4}\times X_2+0.98\times X_4-0.75$	$Y_{4/5}=2\times10^{-2}+27.4\times X_1-36\times10^{-4}\times X_2+0.65\times X_4$	$Y_{4/7}=89\times10^{-4}-4.5\times X_1+44\times10^{-4}\times X_2-0.128\times X_4$
Oiliness (Y_5)	$Y_{5/3}=11.7\times10^{-5}-16.5\times10^{-6}\times X_1-20.8\times10^{-6}\times X_2+0.6\times X_3$	$Y_{5/5}=-72.6\times X_1+37.6\times X_2-214\times X_3-1.57$	$Y_{5/7}=8\times10^{-2}+84\times10^{-4}\times X_1-7\times10^{-6}\times X_2-0.162\times X_3$
Fruity tone (Y_6)	$Y_{6/3}=0.265-6.85\times10^{-3}\times X_1+6\times10^{-3}\times X_2-0.734\times X_3$	$Y_{6/5}=8.25\times10^{-3}+2.6\times10^{-3}\times X_1-0.7\times10^{-3}\times X_2+2.25\times X_3$	$Y_{6/7}=26\times10^{-3}-0.12\times X_1+0.44\times X_2+1.42\times X_3$
Chocolate tone (Y_7)	$Y_{7/3}=41\times10^{-3}+25\times10^{-4}\times X_1+24\times10^{-4}\times X_2+4.4\times X_3-0.17\times X_4$	$Y_{7/5}=17\times10^{-3}-7\times10^{-3}\times X_1-1.42\times X_2+3.8\times X_3+0.23\times X_4$	$Y_{7/7}=46\times10^{-4}\times X_1-2.35\times X_2+2.77\times X_3-0.03\times X_4$

Table 8 Equations of linear correlation of accumulation of organic compounds in cognacs of different ages

Effect of aging period (Y_n) on the content of the compound (X_n)	Equation
o-cresol (X_1) and (Y_1)	$Y_1=4.7+3\times10^{-4}\times X_1$
phenolic alcohols (X_2) and (Y_2)	$Y_2=1.4+13.3\times X_2$
volatile phenolic compounds (X_3) и (Y_3)	$Y_3=2+18\times X_3$
phenolic aldehydes (X_4) и (Y_4)	$Y_4=1.8+0.27\times X_4$
oxymethylfurfural (X_5) и (Y_5)	$Y_5=5\times X_5-1.183$
terpene compounds (X_6) и (Y_6)	$Y_6=-0.05+6\times X_6$
vanillin (X_7) и (Y_7)	$Y_7=82\times10^{-4}+2.35\times X_7$

in the development of taste profiles for cognac samples of different ages. The paper introduced equations of multivariate models that describe the effect of organic compounds on the descriptors of cognac products. Linear regression equations revealed that phenolic compounds of various classes played a major role in the taste profile formation. The obtained data will make it possible to form a list of additional criteria for sensory evaluation of cognac products.

CONTRIBUTION

M.N. Eliseev supervised the research project. O.A. Kosareva developed the research plan, I.N. Gribkova and O.M. Alexeyeva performed the experimental research, obtained the data, and analyzed them.

CONFLICT OF INTEREST

The authors declare that there is not conflict of interests regarding the publication of this article.

REFERENCES

1. Song L, Wei Y, Bergiel BJ. COGNAC consumption: A comparative study on American and Chinese consumers. Wine Economics and Policy. 2018;7(1):24–34. https://doi.org/10.1016/j.wep.2018.01.001.
2. Awad P, Athès V, Decloux ME, Ferrari G, Snakkers G, Raguenaud P, et al. The evolution of volatile compounds during the distillation of cognac spirit. Journal of Agricultural and Food Chemistry. 2017;65(35):7736–7748. https://doi.org/10.1021/acs.jafc.7b02406.
3. Inui T, Tsuchiya F, Ishimaru M, Oka K, Komura H. Different beers with different hops. Relevant compounds for their aroma characteristics. Journal of Agricultural and Food Chemistry. 2013;61(20):4758–4764. https://doi.org/10.1021/jf3053737.

4. Rettberg N, Biendl M, Garbe L-A. Hop aroma and hoppy beer flavor: chemical backgrounds and analytical tools – A review. Journal of the American Society of Brewing Chemists. 2018;76(1):1–20. https://doi.org/10.1080/03610470.2017.1402574.
5. De Simón BF, Martínez J, Sanz M, Cadahía E, Esteruelas E, Muñoz AM. Volatile compounds and sensorial characterisation of red wine aged in cherry, chestnut, false acacia, ash and oak wood barrels. Food Chemistry. 2014;147:346–356. https://doi.org/10.1016/j.foodchem.2013.09.158.
6. Delia L, Jordão AM, Ricardo-Da-Silva JM. Influence of different wood chips species (oak, acacia and cherry) used in a short period of aging on the quality of "Encruzado" white wines. Mittelungen Klosterneuburg. 2017;67(2):84–96.
7. Coldea TE, Socaciu C, Mudura E, Socaci SA, Ranga F, Pop CR et al. Volatile and phenolic profiles of traditional Romanian apple brandy after rapid ageing with different wood chips. Food Chemistry. 2020;320. https://doi.org/10.1016/j.foodchem.2020.126643.
8. Ianni F, Segoloni E, Blasi F, Di Maria F. Low-molecular-weight phenols recovery by eco-friendly extraction from *Quercus spp*. wastes: An analytical and biomass-sustainability evaluation. Processes. 2020;8(4). https://doi.org/10.3390/pr8040387.
9. Ruiz J, Kiene F, Belda I, Fracassetti D, Marquina D, Navascués E et al. Effects on varietal aromas during wine making: a review of the impact of varietal aromas on the flavor of wine. Applied Microbiology and Biotechnology. 2019;103(18):7425–7450. https://doi.org/10.1007/s00253-019-10008-9.
10. Hu Y, Ma Y, Wu S, Chen T, He Y, Sun J, et al. Protective effect of Cyanidin-3-*O*-glucoside against ultraviolet B radiation-induced cell damage in human HaCaT Keratinocytes. Front Pharmacology. 2016;7. https://doi.org/10.3389/fphar.2016.00301.
11. Escudero-Gilete ML, Hernanz D, Galán-Lorente C, Heredia FJ, Jara-Palacios MJ. Potential of cooperage byproducts rich in ellagitannins to improve the antioxidant activity and color expression of red wine anthocyanins. Foods. 2019;8(8). https://doi.org/10.3390/foods8080336.
12. Noestheden M, Thiessen K, Dennis EG, Tiet B, Zandberg WF. Quantitating organoleptic volatile phenols in smoke-exposed *Vitis vinifera* berries. Journal of Agricultural and Food chemistry. 2017;65(38):8418–8425. https://doi.org/10.1021/acs.jafc.7b03225.
13. Del Fresno JM, Morata A, Ricardo-da-Silva JM, Escott C, Loira I, Lepe JAS. Modification of the polyphenolic and aromatic fractions of red wines aged on lees assisted with ultrasound. International Journal of Food Science and Technology. 2019;54(9):2690–2699. https://doi.org/10.1111/ijfs.14179.
14. Călugăr A, Coldea TE, Pop CR, Pop TI, Babeș AC, Bunea CI, et al. Evaluation of volatile compounds during ageing with oak chips and oak barrel of Muscat Ottonel Wine. Processes. 2020;8(8). https://doi.org/10.3390/pr8081000.
15. Tsakiris A, Kallithraka S, Kourkoutas Y. Grape brandy production, composition and sensory evaluation. Journal of Science and Food Agricultural. 2014;94(3):404–414. https://doi.org/10.1002/jsfa.6377.
16. Aprotosoaie AC, Luca SV, Miron A. Flavor chemistry of cocoa and cocoa products – An overview. Comprehensive Reviews in Food Science and Food Safety. 2016;15(1):73–91. https://doi.org/10.1111/1541-4337.12180.
17. Delompré T, Salles C, Briand L. Taste perception: from molecule to eating behaviour. Correspondances en MHND. 2020;24(3):88–92.
18. Peschanskaya VA, Osipova VP, Trofimchenko VA, Tochilina RP, Goncharova SA. On the determination of the total extract and given not less than 35.0 % strength in wine production. Food Industry. 2016;(9):36–38. (In Russ.).
19. Rodríguez-Solana R, Rodríguez-Freigedo S, Salgado JM, Domínguez JM, Cortés-Diéguez S. Optimisation of accelerated ageing of grape marc distillate on a micro-scale process using a Box-Benhken design: influence of oak origin, fragment size and toast level on the composition of the final product. Australian Journal of Grape and Wine Research2017;23(1):5–14. https://doi.org/10.1111/ajgw.12249.
20. Giannetti V, Mariani MB, Marini F, Torrelli P, Biancolillo A. Flavour fingerprint for the differentiation of Grappa from other Italian distillates by GC-MS and chemometrics. Food Control. 2019;105:123–130. https://doi.org/10.1016/j.foodcont.2019.05.028.
21. Herrera P, Durán-Guerrero E, Sánchez-Guillén MM, García-Moreno MV, Guillén DA, Barroso CG, et al. Effect of the type of wood used for ageing on the volatile composition of Pedro Ximénez sweet wine. Journal of the Science of Food and Agriculture. 2020;100(6):2512–2521. https://doi.org/10.1002/jsfa.10276.
22. Viana EJ, de Carvalho Tavares IM, Rodrigues LMA, das Graças Cardoso M, Júnior JCB, Gualberto SA, et al. Evaluation of toxic compounds and quality parameters on the aged Brazilian sugarcane spirit. Research, Society and Development. 2020;9(8). https://doi.org/10.33448/rsd-v9i8.5544.
23. Cherkashina YuA. Identifikatsiya kon′yakov s primeneniem organolepticheskogo analiza i fiziko-khimicheskikh metodov: opredelenie khromaticheskikh pokazateley, dubil′nykh veshchestv i pokazatelya pH [Identification of

cognacs using sensory evaluation and physicochemical methods: determination of chromatic indicators, tannins, and pH]. Bulletin of the Technological University. 2011;(7):198–204. (In Russ.).

24. Botelho G, Anjos O, Estevinho LM, Caldeira I. Methanol in grape derived, fruit and honey spirits: A critical review on source, quality control, and legal limits. Processes. 2020;8(12). https://doi.org/10.3390/pr8121609.
25. Oseledzeva IV, Kirpicheva LS. Assessment of the influence of long factor on variation of parameters of the factions volatile cognac wine materials and young brandy distillate. Agricultural Bulletin of Stavropol Region. 2015;17(1):246–252. (In Russ.).
26. Puentes C, Joulia X, Vidal J-P, Esteban-Decloux M. Simulation of spirits distillation for a better understanding of volatile aroma compounds behavior: Application to Armagnac production. Food and Bioproducts Processing. 2018;112:31–62. https://doi.org/10.1016/j.fbp.2018.08.010.
27. Santos F, Correia AC, Ortega-Heras M, García-Lomillo J, González-SanJosé ML, Jordão AM, et al. Acacia, cherry and oak wood chips used for a short aging period of rosé wines: effects on general phenolic parameters, volatile composition and sensory profile. Journal of the Science of Food and Agriculture. 2019;99(7):3588–3603. https://doi.org/10.1002/jsfa.9580.
28. Fernandes OWB, Silva DF, Sanson AL, Coutrim MX, Afonso RJDCF, Eichler P, et al. Influence of harvest season and maturation of different sugarcane (Saccharum spp.) cultivars on the chemical composition of alembic Brazilian sugarcane spirit. OALib Journal. 2017;4. https://doi.org/10.4236/oalib.1103266.
29. García-Moreno MV, Sánchez-Guillén MM, de Mier MR, Delgado-González MJ, Rodríguez-Dodero MC, García-Barroso C, et al. Use of alternative wood for the ageing of brandy de Jerez. Foods. 2020;9(3). https://doi.org/10.3390/foods9030250.
30. Xu ML, Yu Y, Ramaswamy HS, Zhu SM. Characterization of Chinese liquor aroma components during aging process and liquor age discrimination using gas chromatography combined with multivariable statistics. Scientific Reports. 2017;7. https://doi.org/10.1038/srep39671.
31. Egorova EYu, Morozhenko YuV, Reznichenko IYu. Identification of aromatic aldehydes in the express assessment of quality of herbal distilled drinks. Foods and Raw Materials. 2017;5(1):144–113. https://doi.org/10.21179/2308-4057-2017-1-144-153.
32. Cernîşev S. Analysis of lignin-derived phenolic compounds and their transformations in aged wine distillates. Food Control. 2017;73:281–290. https://doi.org/10.1016/j.foodcont.2016.08.015.
33. Lukanin A, Sidorenko A. Criteria for determination of age of cognac spirits. Bulletin of Agricultural Science. 2016(10):51–60. (In Russ.). https://doi.org/10.31073/agrovisnyk201610-10.
34. Savchuk SA, Vlasov VN, Appolonova SA, Arbuzov VN, Vedenin AN, Mezinov AB, et al. Application of chromatography and spectrometry to the authentication of alcoholic beverages. Journal of Analytical Chemistry. 2011;56(3):214–231. https://doi.org/10.1023/A:1009446221123.
35. Chira K, Anguellu L, Da Costa G, Richard T, Pedrot E, Jourdes M, et al. New C-glycosidic ellagitannins formed upon oak wood toasting; identification and sensory evaluation. Foods. 2020;9(10). https://doi.org/10.3390/foods9101477.
36. Payab M, Chaichi MJ, Nazari OL, Maleki FY. Tannin extraction from oak gall and evaluation of anti-oxidant activity and tannin iron chelation compared with deferoxamine drug. Journal of Drug Design and Medicinal Chemistry. 2019;5(2):18–25. https://doi.org/10.11648/j.jddmc.20190502.11.
37. Marchal A, Pons A, Lavigne V, Dubourdieu D. Contribution of oak wood ageing to the sweet perception of dry wines. Australian Journal of Grape and Wine Research. 2013;19(1):11–19. https://doi.org/10.1111/ajgw.12013.
38. Rasines-Perea Z, Jacquet R, Jourdes M, Quideau S, Teissedre PL. Ellagitannins and flavano-ellagitannins: Red wines tendency in different areas, barrel origin and ageing time in barrel and bottle. Biomolecules. 2019;9(8). https://doi.org/10.3390/biom9080316.
39. Phetxumphou K, Miller G, Ashmore PL, Collins T, Lahne J. Mashbill and barrel aging effects on the sensory and chemometric profiles of American whiskeys. Journal of the Institute of Brewing. 2020;126(2):194–205. https://doi.org/10.1002/jib.596.
40. Kumar V, Joshi VK, Thakur NS, Sharma N, Gupta RK. Effect of artificial ageing using different wood chips on physico-chemical, sensory and antimicrobial properties of apple tea wine. Brazilian Archives of Biology and Technology. 2020;63. https://doi.org/10.1590/1678-4324-2020180413.
41. Paixão JA, Filho ET, Bolini HMA. Investigation of alcohol factor influence in quantitative descriptive analysis and in the time-intensity profile of alcoholic and non-alcoholic commercial pilsen beers samples. Beverages. 2020;6(4). https://doi.org/10.3390/beverages6040073.
42. Cvetković D, Stojilković P, Zvezdanović J, Stanojević J, Stanojević L, Karabegović I. The identification of volatile aroma compounds from local fruit based spirits using a headspace solid-phase microextraction technique coupled

with the gas chromatography-mass spectrometry. Advanced Technologies. 2020;9(2):19–28. https://doi.org/10.5937/savteh2002019C.

ORCID IDs
Mikhail N. Eliseev https://orcid.org/0000-0001-8636-4468
Irina N. Gribkova https://orcid.org/0000-0002-4373-5387
Olga A. Kosareva https://orcid.org/0000-0002-9639-8302
Olga M. Alexeyeva https://orcid.org/0000-0001-8254-6987

Foods and Raw Materials, 2021, vol. 9, no. 2

E-ISSN 2310-9599
ISSN 2308-4057

Research Article
Open Access

https://doi.org/10.21603/2308-4057-2021-2-254-261
Available online at http://jfrm.ru/en

Directed homoenzymatic fragmentation of the plant protopectin complex: Assessment criteria

Vladimir V. Kondratenko*, Tatyana Yu. Kondratenko, Andrey N. Petrov

Russian Research Institute of Canning Technology, Vidnoye, Russia

* e-mail: nauka@vniitek.ru

Received April 01, 2021; Accepted in revised form May 03, 2021; Published online July 09, 2021

Abstract:

Introduction. The functional basis of protopectin complex may be represented as a network of regions that consist of homogalacturonan sequences and a base of rhamnogalacturonans-I, i.e. rhamnosyl-containing branching sites. Enzymatic isolation of these regions is possible only at a certain minimal native degree of polymerization. The research objective was to develop a system of criteria for assessing the potential applicability of the enzymatic transformation of plant protopectin complex.

Study objects and methods. The research featured the polymerization degree of the homogalacturonan regions within the protopectin complex and produced a system of assessment criteria for the enzymatic fragmentation potential of the protopectin complex. The theoretical calculations were based on the values of the mass fractions of rhamnosyl and galacturonide residues in plant cell walls. The result was a new polymerization degree analytical function.

Results and discussion. The ratio of the mass fractions of rhamnosyl and galacturonide residues in the water-insoluble plant tissue served as a dimensionless criterion of applicability. The rational condition for the dimensionless criterion of applicability was based on the fundamental constraint for homogalacturonan regions in the protopectin complex. It was expressed by a fundamental inequation. The rational area for determining the numerical values of the applicability criterion was presented as $\nu \in \left[0; \frac{M_{Rh}}{M_{GalA}}\right)$. The functional dependence was reduced to a two-dimensional criteria space as "width of rhamnosyl branches vs. the criterion of applicability", where each pectin-containing raw material was given a single uniquely defined position. The boundary conditions for the criteria space were determined analytically.

Conclusion. The new approach offers an assessment of the enzymatic fragmentation potential of the plant protopectin complex by homoenzyme preparations. The approach is in fact the second stage of the decision tree in the science-based technology for pectin and its products.

Keywords: Protopectin complex, rhamnogalacturonan-I, homogalacturonan, transformation, criterion assessment

Funding: The research was part of state assignment of the V.M. Gorbatov Federal Research Center for Food Systems of RAS (Russian Academy of Sciences).

Please cite this article in press as: Kondratenko VV, Kondratenko TYu, Petrov AN. Directed homoenzymatic fragmentation of the plant protopectin complex: Assessment criteria. Foods and Raw Materials. 2021;9(2):254–261. https://doi.org/10.21603/2308-4057-2021-2-254-261.

INTRODUCTION

The biopolymer complex of plant tissue cell walls is a complex conglomerate of intertwined branched supramolecular networks of the protopectin complex and the hemicellulose. The complex is permeated with cellulose microfibrils and protein extensin (Fig. 1) [1, 2]. All its components are linked to each other by ester, salt, combined, and hydrogen bonds. Each component possesses valuable physicochemical properties with a good potential for food industry [3–7].

Pectins have the most attractive and numerous functional properties among all the carbohydrates of plant cell walls [5, 8]. They owe these useful properties due to their molecular structure. In their native form, pectins have a water-insoluble supramolecular structure called the protopectin complex. The structure is an extended and highly branched linear and lateral network of polymer fragments (Fig. 2). Lateral branches also have a complex structure and can be interconnected with salt and borate bonds [9–18].

Contemporary science knows eight types of fragments of the protopectin complex: homo-galacturonan, rhamnogalacturonan-I, rhamnogalacturonan-II, xylogalacturonan, apiogalacturonan, and arabinogalacturonan [19].

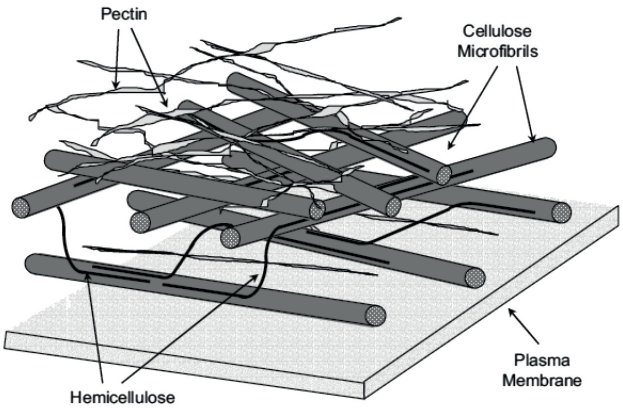

Figure 1 Primary cell wall of higher plants [1]

Homogalacturonans are linear polymeric fragments of α-D(+)-galacturonic acid residues, linked by (1 → 4)-glycosidic bonds (Fig. 3) [19, 20]. Each residue contains a carboxyl group, which naturally may exist in a free, esterified, or amidated state. Free carboxyl groups are capable of dissociation, while acquiring a partial negative charge. Carboxyl groups esterified with methanol demonstrate inactivated charge formation. Amidated carboxyl groups, due to the donor-acceptor bond of the lone-pair electrons, accept cation H+ and acquire a partial positive charge.

In positions C1 and C2, hydroxyl groups can form glycosidic bonds with the residues of xylose, ribose, arabinose, and galactose, as well as ester bonds with carboxylic acids and aromatic compounds. The state and total amount of carboxyl groups in the pectin molecule fragment define the physicochemical properties of pectins, while the degree and the nature of the substitution of hydroxyl groups define the inhibition degree.

The practical use of pectins depends on the chemical structure of homogalacturonans.

Ramnogalacturonan-I is the second most common fragment of pectins. Its content can reach 45% in sugar beet pectin [5, 19, 20]. These fragments include sequences from the residue of α-L-rhamnose and α-D(+)-galacturonic acid, linked by a (1 → 4)-glycosidic bond. In the rhamnosyl residue, the pair can be linked with other pairs or with the end of the homogalacturonan by a rhamnosyl-uronic (1 → 2)-glycosidic bond. In the uronic residue, the pair can be linked with other pair by a rhamnosyl-uronic (1 → 2)-glycosidic bond or with the end of homogalacturonan by a uronic-uronic (1 → 4)-glycosidic bond. As a result, rhamnosyl residues of rhamnogalacturonan-I are the branching zones of the pectin molecule, where free functional groups can form glycosidic bonds with either residues of neutral sugars, or their polymer sequences, i.e. arabinans, galactans, arabinogalactans, and galactoarabinans-I and II (Fig. 4).

The basis of the protopectin complex of plant tissue cell walls is a network of regions formed by linear sequences of homogalacturonans and rhamnogalacturonans-I. Of course, this assumption excludes two types of lateral branches: the rhamnosil-free lateral branches (rhamnogalacturonan-II), which may contain residues of L-rhamnose and/or α-D(+)-galacturonic acid with proportion of ≤ 2–3%, and branches formed by neutral sugars and their oligo- and polymers [16, 19]. Molecular properties of homogalacturonan fragments define the physicochemical properties of plant pectin. Therefore, enzymatic fragmentation is the most effective method for the protopectin complex. It is a selective hydrolytic cleavage of rhamnosyl-uronide (1 → 2) and (1 → 4) glycosidic bonds.

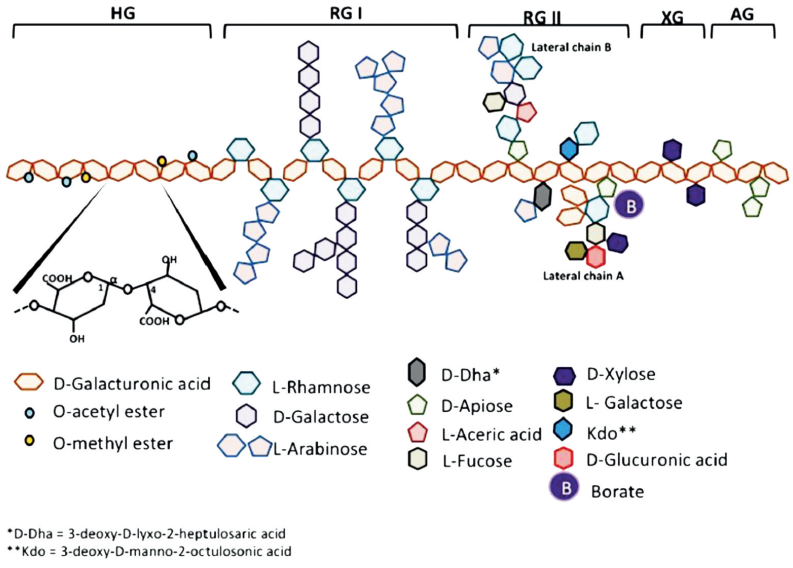

Figure 2 Pectin molecule [16]: HG – homogalacturonan region, RG I – branch region of rhamnogalacturonan I, RG II – rhamnose-free branch region, XG – xylogalacturonan region, AG – arabinogalacturonan region

[4)-αGalA-(1,4)-αGalA-(1,4)-αGalA-(1,4)-αGalA-(1,4)-αGalA-(1,4)-αGalA-(1,4)-αGalA-(1,]$_n$

Figure 3 Homogalacturonan fragment of pectin molecule [20]

However, the physicochemical properties of pectin also depend on the polymerization degree of the fragmentation products [21]. The maximal possible degree of polymerization depends on the polymerization degree of the native homogalacturonan fragments in the protopectin complex. In each specific case, the experimental determination of this indicator is a difficult resource- and time-consuming task.

Therefore, a criteria assessment would be the optimal approach to evaluate the potential efficiency of the directed enzymatic fragmentation of a particular plant protopectin complex. Such assessment can also define the boundary conditions that determine the degree of the targeted physicochemical properties of the fermentolysis products. This approach could also determine the conditions for processing any plant tissue or its derivatives. The approach consists of some step-by-step stages. The first stage was a system of criteria for assessing the transformation potential of a plant biopolymer complex [22].

As a next stage, the present research objective was to develop a system of criteria for assessing the enzymatic transformation potential of a plant biopolymer complex as in the case of pectin substances. The research included the following tasks:

– developing the abovementioned assessment criteria system, based on the use of zoned criteria space;

– developing a system of boundary conditions for the classification of plant raw materials according to the applicability of the enzymatic transformation of its protopectin complex.

STUDY OBJECTS AND METHODS

The protopectin complex of the plant tissue consists of three main types of fragments: homogalacturonan, rhamnogalacturonan-I, and rhamnogalacturonan-II. The latter type was disregarded as its mass fraction in the protopectin complex is ≤ 2%.

Rhamnogaracturonan-I has linear polynalacturonan sites. As a result, the homogalanic component of the protopectin complex can be considered as part of rhamnogalacturonan-I fragments.

A pectin molecule can be classified as rhamnogalacturonan-I only if, in addition to the homogalacturonan component, it contains at least one branch formed by at least one rhamnosyl residue. Consequently, a polymer molecule has at least two homogalacturonan regions with at least one terminal link (rhamnosyl residue) each.

Linear and homogalacturonan regions of the molecular network alternate in the protopectin complex in a particular order. This order presumably depends on the taxonomy of the raw material and the function

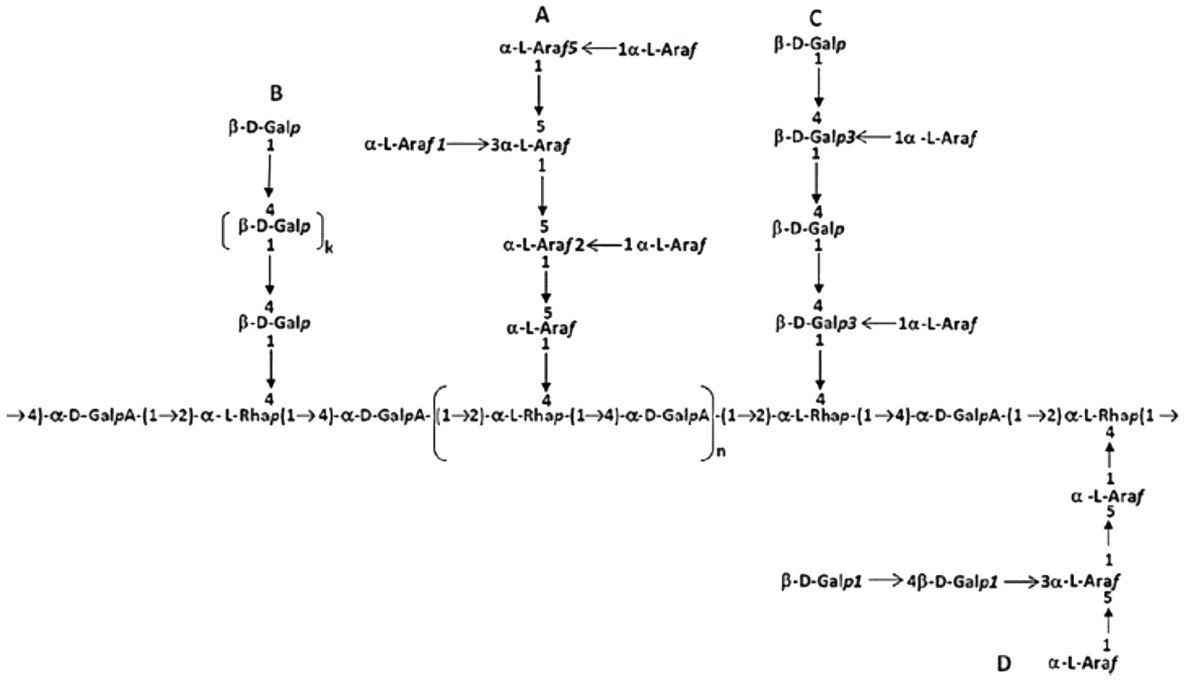

Figure 4 Fragment of rhamnogalacturonan-I of pectin molecule [19]. Lateral branches: A – arabinan, B – galactan, C – arabinogalactan, D – galactoarabinan

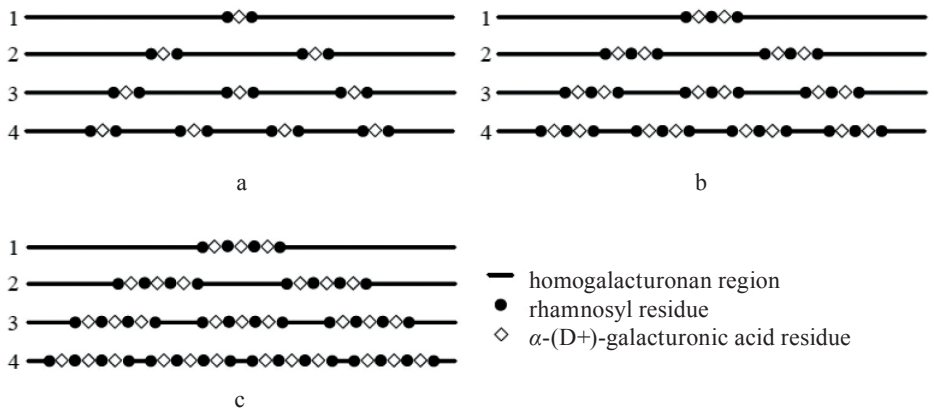

Figure 5 Distribution of homogalacturonan and branching sites in rhamnogalacturonan-I at b_r = 1–4. Not to scale. a) $z_{Rh} = 2$; b) $z_{Rh} = 3$; c) $z_{Rh} = 4$

of the plant parts. The structural features of the fragments of rhamnogalacturonan-I are such that the natural boundaries of the homogalacturonan regions are L-rhamnose residues connected to the terminal uronid links (1 → 2) and (1 → 4) by glycosidic bonds. The fragment can be roughly described by the following sequence: "terminal link of homogalacturonan – rhamnose residue (the branching starts) – branching site – rhamnose residue (the branching ends) – homogalacturonan region – … – section of homogalacturonan – rhamnose residue (the branching starts) – branching site – rhamnose residue (the branching ends) – terminal link of homogalacturonan".

In the simplest case, the rhamnogalacturonan-I fragment has only one branching site ($b_r = 1$). Depending on its structure, the rhamnogalacturonan-I can include only one rhamnosyl residue ($z_{Rh} = 1$). In a more complex case, the rhamnogalacturonan-I may contain several rhamnosyl residues ($z_{Rh} = q$, where $q = 1, 2, 3, ...$), which alternate with galacturonid residues (Fig. 5).

The number of branching sites may also depend, to some extent, on the plant species and the functional type of the plant tissue.

Figure 5 features no fragments of rhamnogalacturonan-I as their lateral branches are represented mainly by the nonuronic component.

The conditional assumption is that the uronide-containing part of rhamnogalacturonan-I is completely determined by the following variables: n_{HG} is total homogalacturonan sites, n_{Rh} is total rhamnosyl units in the branching sites, $n_{GalA(b)}$ is total uronid residues in the branching sites, z_{Rh} is number of rhamnosyl residues per branching site, $z_{GalA(b)}$ is number of uronid residues per branching site, and n_{br} is total branch sites. Table 1 demonstrates the numerical values of the variables in particular cases of the distribution of homogalacturonan and branching sites in Fig. 5.

The ratios in Table 1 can be expressed by the following formulae:

$$n_{Rh} = (n_{HG} - 1) \cdot z_{Rh}, \quad (1)$$

Table 1 Particular cases of the distribution of variables that determine the structure of rhamnogalacturonan-I, at different values of b_r

Number of branching sites, b_r	Cases								
	A			B			C		
	n_{HG}	n_{Rh}	$n_{GalA(b)}$	n_{HG}	n_{Rh}	$n_{GalA(b)}$	n_{HG}	n_{Rh}	$n_{GalA(b)}$
1	2	2	1	2	3	2	2	4	3
2	3	4	2	3	6	4	3	8	6
3	4	6	3	4	9	6	4	12	9
4	5	8	4	5	12	8	5	16	12
…	…	…	…	…	…	…	…	…	…
n_{br}	$n_{Rh} = (n_{HG} - 1) \cdot 2$ $n_{GalA(b)} = (n_{HG} - 1) \cdot 1$ $n_{GalA(b)} = \frac{n_{Rh} \cdot 1}{2}$			$n_{Rh} = (n_{HG} - 1) \cdot 3$ $n_{GalA(b)} = (n_{HG} - 1) \cdot 2$ $n_{GalA(b)} = \frac{n_{Rh} \cdot 2}{3}$			$n_{Rh} = (n_{HG} - 1) \cdot 4$ $n_{GalA(b)} = (n_{HG} - 1) \cdot 3$ $n_{GalA(b)} = \frac{n_{Rh} \cdot 3}{4}$		

$$n_{GalA(b)} = (n_{HG} - 1) \cdot z_{GalA(b)} \quad (2)$$

The structure of the rhamnogalacturonan-I fragments suggests that the main structural unit is the amount of rhamnosyl residues in the branching sites. As a result, formulae (1) and (2) take the following form:

$$n_{HG} = \frac{n_{Rh}}{z_{Rh}} + 1 = \frac{n_{Rh} + z_{Rh}}{z_{Rh}}, \quad (3)$$

$$n_{GalA(b)} = \frac{n_{Rh} \cdot z_{GalA(b)}}{z_{Rh}} \quad (4)$$

Based on the data in Table I,

$$z_{GalA(b)} = z_{Rh} - 1 \quad (5)$$

Thus, the final formula (4) is:

$$n_{GalA(b)} = \frac{n_{Rh} \cdot (z_{Rh} - 1)}{z_{Rh}} \quad (6)$$

These dependences give an approximate quantitative idea of the structure of rhamnogalacturonan-I. For their practical use, they have to be linked to the real chemical composition of a particular raw material.

The line of reasoning follows the next path.

Considering that the molecular weight of the rhamnosyl residue is M_{Rh} (Da) and the mass fraction of rhamnose in the composition of the natively insoluble part of the raw material is ω_{Rh} (%), the amount of rhamnosyl residues in the mass of the natively insoluble part of the raw material m (g) can be calculated according to the formula below:

$$n_{Rh} = \frac{m \cdot \omega_{Rh}}{100 \cdot M_{Rh} \cdot a} \quad (7)$$

where a is the atomic mass unit ($1.66053892 \times 10^{-24}$ g/Da).

A combination of formulae (6) and (7) gives the number of moles of α-D(+)-galacturonic acid residues in the branch sites:

$$n_{GalA(b)} = \frac{\frac{m \cdot \omega_{Rh}}{100 \cdot M_{Rh} \cdot a} \cdot (z_{Rh} - 1)}{z_{Rh}} = \frac{m \cdot \omega_{Rh} \cdot (z_{Rh} - 1)}{100 \cdot M_{Rh} \cdot z_{Rh} \cdot a} \quad (8)$$

Consequently, the mass fraction of α-D(+)-galacturonic acid residues in the insoluble part of the raw material in the branching sites is:

$$\omega_{GalA(b)} = \frac{M_{GalA} \cdot n_{GalA(b)} \cdot a \cdot 100}{m} = \frac{M_{GalA} \cdot a \cdot 100}{m} \times \times \frac{m \cdot \omega_{Rh} \cdot (z_{Rh} - 1)}{100 \cdot M_{Rh} \cdot z_{Rh} \cdot a} \Rightarrow \frac{M_{GalA} \cdot \omega_{Rh} \cdot (z_{Rh} - 1)}{M_{Rh} \cdot z_{Rh}} \quad (9)$$

where M_{GalA} is the molar mass of α-D(+)-galacturonic acid residue, Da.

The conditional assumption is that all the residues of α-D(+)-galacturonic acid in the insoluble part belong exclusively to the protopectin complex and are present only in the composition of homogalacturonan fragments and branch points of rhamnogalacturonan-I. Then, the mass fraction of α-D(+)-galacturonic acid residues in homogalacturonan fragments can be calculated as follows:

$$\omega_{GalA(HG)} = \omega_{GalA} - \omega_{GalA(b)} = = \omega_{GalA} - \frac{M_{GalA} \cdot \omega_{Rh} \cdot (z_{Rh} - 1)}{M_{Rh} \cdot z_{Rh}} \quad (10)$$

As the plant tissue grows, the protopectin complex of cell walls and intercellular spaces changes continuously. As a result, the structure of the complex becomes heterogeneous. Assuming that all homogalacturonan regions of the protopectin complex are a native component of rhamnogalacturonan fragments, the whole protopectin complex can be represented as consisting almost entirely of rhamnogalacturonan-I fragments. The length of the homogalacturonan regions differs in different parts of the protopectin complex. Consequently, a particular homogalacturonan molecular mass is in fact a certain mean value. The molecular weight of any arbitrarily taken (i-th) homogalacturonan region of the protopectin complex is related to its polymerization degree by the following ratio:

$$M_{HG(i)} = M_{GalA} \cdot k_i \quad (11)$$

where k_i is the polymerization degree of the i-th homogalacturonan region.

Consequently, the formula for the average molecular weight of homogalacturonan sites is as follows:

$$M_{HG(av)} = \frac{\sum_{i=1}^{N} M_{HG(i)}}{N} = \frac{\sum_{i=1}^{N} M_{GalA} \cdot k_i}{N} = = M_{GalA} \cdot \frac{\sum_{i=1}^{N} k_i}{N} = M_{GalA} \cdot k_{av} \quad (12)$$

where k_{av} – average polymerization degree of homogalacturonan regions and N – total homogalacturonan regions amount.

The mass fraction of the homogalacturonan component in the insoluble part can be expressed as follows:

$$\omega_{HG} = \frac{M_{HG(av)} \cdot n_{HG} \cdot a \cdot 100}{m} \quad (13)$$

A combination of formulae (3) and (13) gives the following result:

$$\omega_{HG} = \frac{M_{HG(av)} \cdot \frac{n_{Rh} + z_{Rh}}{z_{Rh}} \cdot a \cdot 100}{m} = = \frac{M_{HG(av)} \cdot (n_{Rh} + z_{Rh}) \cdot a \cdot 100}{z_{Rh} \cdot m} \Rightarrow \Rightarrow \frac{M_{HG(av)} \cdot \left(\frac{m \cdot \omega_{Rh}}{100 \cdot M_{Rh} \cdot a} + z_{Rh} \right) \cdot a \cdot 100}{z_{Rh} \cdot m} \Rightarrow \Rightarrow \frac{M_{HG(av)} \cdot \left(\omega_{Rh} + \frac{100 \cdot M_{Rh} \cdot a \cdot z_{Rh}}{m} \right)}{M_{Rh} \cdot z_{Rh}} \quad (14)$$

However, the following inequation occurs at $m \geq 10^{-6}$ g and $z_{Rh} \leq 10^3$:

$$\frac{100 \cdot M_{Rh} \cdot a \cdot z_{Rh}}{m} << 10^{-10}$$

which makes it possible to disregard the sum of $\frac{100 \cdot M_{Rh} \cdot a \cdot z_{Rh}}{m}$ as insignificant, in which case formula (14) can be simplified as follows:

$$\omega_{HG} \approx \frac{M_{HG(av)} \cdot \omega_{Rh}}{M_{Rh} \cdot z_{Rh}} \quad (15)$$

The mass fraction of homogalacturonan fragments and the mass fraction of α-D(+)-galacturonic acid residues that make up the homogalacturonan fragments are the same, which leads to the following identical equation:

$$\frac{M_{HG(av)} \cdot \omega_{Rh}}{M_{Rh} \cdot z_{Rh}} \cong \omega_{GalA} - \frac{M_{GalA} \cdot \omega_{Rh} \cdot (z_{Rh} - 1)}{M_{Rh} \cdot z_{Rh}} \quad (16)$$

Added to formula (12), the equation assumes the following form:

$$\frac{M_{GalA} \cdot k_{av} \cdot \omega_{Rh}}{M_{Rh} \cdot z_{Rh}} \cong \omega_{GalA} - \frac{M_{GalA} \cdot \omega_{Rh} \cdot (z_{Rh} - 1)}{M_{Rh} \cdot z_{Rh}} \quad (17)$$

Applying formula (17) to k_{av} makes it possible to calculate the average polymerization degree of homogalacturonan regions in the protopectin complex:

$$k_{av} = \frac{M_{Rh} \cdot \omega_{GalA} \cdot z_{Rh} - M_{GalA} \cdot \omega_{Rh} \cdot (z_{Rh} - 1)}{M_{GalA} \cdot \omega_{Rh}} =$$

$$= \left(\frac{M_{Rh} \cdot \omega_{GalA}}{M_{GalA} \cdot \omega_{Rh}} - 1 \right) \cdot z_{Rh} + 1 \quad (18)$$

Thus, the mass fractions of galacturonide and rhamnosyl residues in the plant cell can help to determine the average polymerization degree of the homogalacturonan regions in the protopectin complex.

RESULTS AND DISCUSSION

Let the dimentionless criterion ν is uniquely determined on the basis of chemical analysis of the native water-insoluble plant tissue component:

$$\nu = \frac{\omega_{Rh}}{\omega_{GalA}} \quad (19)$$

As a result, formula (18) looks as follows:

$$k_{av} = \left(\frac{M_{Rh}}{M_{GalA} \cdot \nu} - 1 \right) \cdot z_{Rh} + 1 \quad (20)$$

In (20), constituent $\frac{M_{Rh}}{M_{GalA}}$ is constant. Subsequently, formula (20) is a mathematical description of functional dependence $k_{av} = f(\nu, z_{Rh})$ (Fig. 6). Thus, analytically obtained ω_{Rh} and ω_{GalA} can define the weighted average degree of polymerization of homogalacturonan regions of pectins.

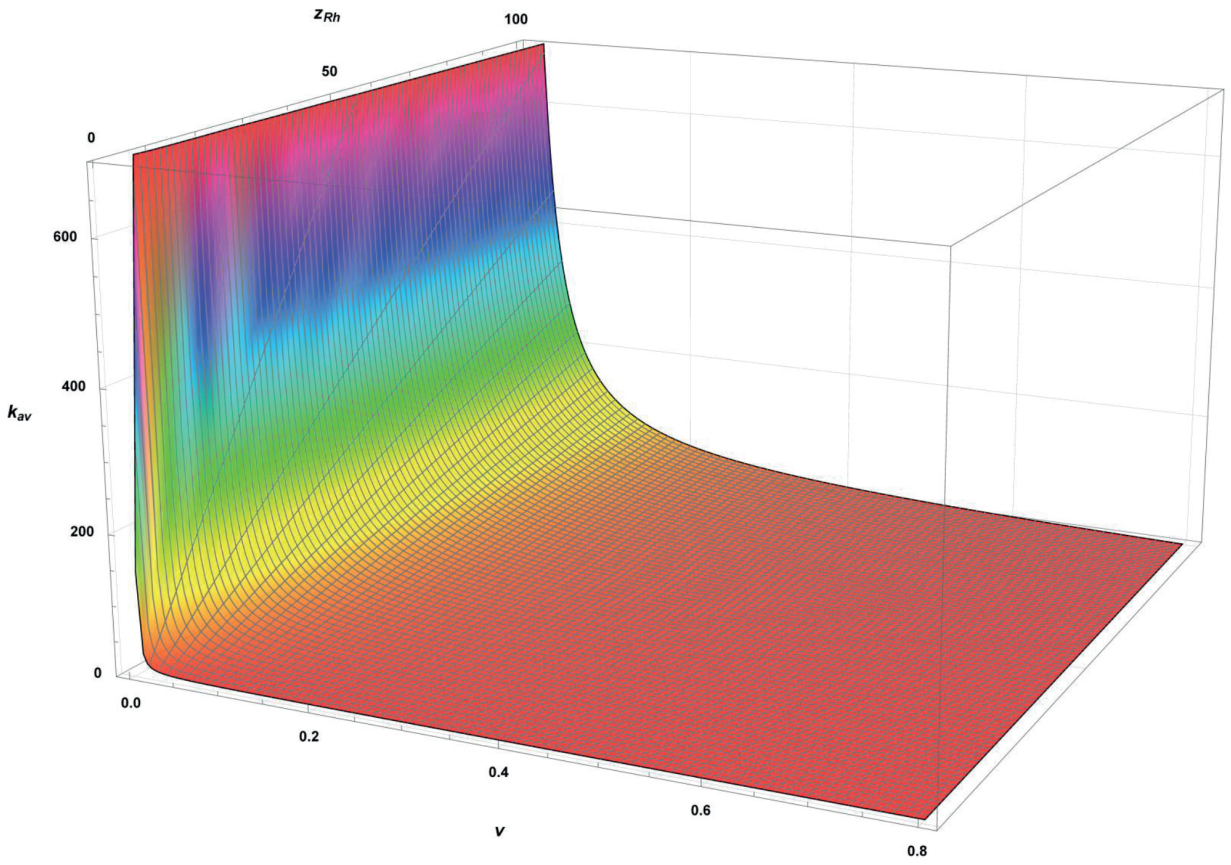

Figure 6 Weighted average polymerization degree of homogalacturonan sites of the rhamnogalacturonan fraction in pectins: functional dependence

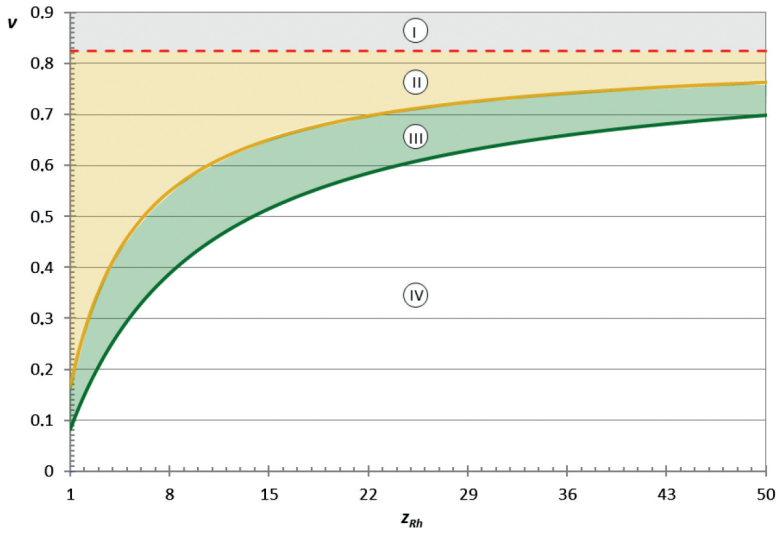

Figure 7 Zoned criteria space of molecular characteristics of homogalacturonan fractions in pectins

In a same time, homogalacturonan regions in the rhamnogalacturonan fraction of pectin are possible only at $k_{av} \geq 1$.

As a result, the rational condition for criterion ν is:

$$\nu \leq \frac{M_{Rh} \cdot z_{Rh}}{M_{GalA}\left[\left(k_{av}-1\right)+z_{Rh}\right]} \qquad (21)$$

Provided that there are homogalacturonan regions in the rhamnogalacturonan fraction of pectin substances, the range for determining the numerical values of this criterion can be represented as $\nu \in \left[0; \frac{M_{Rh}}{M_{GalA}}\right)$. The functional dependence can be reduced to a criterion space in coordinates ν and z_{Rh}, where k_{av} is boundary zoning conditions (Fig. 7).

Within this criterion space, zone I is the absence of homogalacturonan regions in pectins. Zone II is the presence of regions with the weighted average polymerization degree of homogalacturonan region in the range of 1–5; zone III – 5–10; and zone IV – ≥ 10.

Homogalacturonan regions with $k_{av} > 10$ are of their own practical importance. Therefore, the use of homoenzyme preparations for fragmentation of the native protopectin complex makes sense only for plant tissues in zone IV. In other cases, the use of homogalacturonan-specific enzyme preparations for protopectin complex fragmentation has no sense.

The new criteria-based approach makes it possible to unambiguously define the effectiveness of targeted enzymatic fragmentation of the plant protopectin complex within the boundary conditions that determine the degree of the targeted physicochemical properties of the final product. This approach is universal and represents the second stage of the decision tree started in [22] as a science-based technology for pectin production.

CONCLUSION

The research produced a criteria space to assess the potential effectiveness of the homoenzymatic transformation of a plant biopolymer complex as in the case of pectin substances. The method was based on a two-dimensional criteria space, zoned according to the key factor, i.e. the targeted polymerization degree of homogalacturonan fragments in the native protopectin complex.

We found that the compliance with the first criteria zone (at $k_{av} \geq 10$) determined the feasibility of using homogalacturonan-specific enzyme preparations to isolate of homogalacturonan (targeted) regions of the plant protopectin complex. The compliance with the second criteria zone (at $1 \leq k_{av} < 10$) determined the expediency of non-enzymatic fragmentation of the protopectin complex. The compliance with the third zone (at $k_{av} < 1$) meant that the fragmentation of the protopectin complex would neither increase the mass fraction of pectin substances in the medium, nor release pectins.

The new criteria approach is an integral part of the technologies for obtaining pectin and its products with targeted physical and chemical properties.

CONTRIBUTION

All authors contributed equally to the manuscript and are equally responsible for any possible plagiarism.

CONFLICT OF INTEREST

The authors state that there is no conflict of interests related to the publication of this article.

REFERENCES

1. O'Neill MA, York WS. The composition and structure of plant primary cell walls. In: Rose JKC, editor. The plant cell wall. Annual plant reviews. Volume 8. Oxford: CRC Press; 2003. pp. 1–54.
2. Tian L. Influence of pectin supplementation on feed fermentation characteristics in rats and pigs. Dr. sci. diss. Wageningen: Wageningen University; 2016. 144 p. https://doi.org/10.18174/370098.
3. Moreno FJ, Sanz ML. Food oligosaccharides: production, analysis and bioactivity. Wiley-Blackwell; 2014. 552 p.
4. Ramawat KG, Mérillon J-M. Polysaccharides: bioactivity and biotechnology. Cham: Springer; 2015. 2241 p. https://doi.org/10.1007/978-3-319-16298-0.
5. Donchenko LV, Firsov GG. Pektin: osnovnye svoystva, proizvodstvo i primenenie [Pectin: main properties, production, and application]. Moscow: DeLi print; 2007. 275 p. (In Russ.).
6. Lisovitskaya EP, Patieva SV, Tymoshenko NV, Patieva AM. Evaluation of analytical characteristics of the different types of pectin in canned technologies for preventive human nutrition. Vsyo o myase. 2016;(3):32–35. (In Russ.).
7. Galstyan AG, Aksyonova LM, Lisitsyn AB, Oganesyants LA, Petrov AN. Modern approaches to storage and effective processing of agricultural products for obtaining high quality food products. Herald of the Russian Academy of Sciences. 2019;89(2):211–213. https://doi.org/10.1134/S1019331619020059.
8. Bush PL. Pectin: Chemical properties, uses and health benefits. Nova Science; 2014. 268 p.
9. May CD. Industrial pectins: Sources, production and applications. Carbohydrate Polymers. 1990;12(1):79–99. https://doi.org/10.1016/0144-8617(90)90105-2.
10. Thakur BR, Singh RK, Handa AK. Chemistry and uses of pectin – A review. Critical Reviews in Food Science and Nutrition. 1997;37(1):47–73. https://doi.org/10.1080/10408399709527767.
11. Caffall KH, Mohnen D. The structure, function, and biosynthesis of plant cell wall pectic polysaccharides. Carbohydrate Research. 2009;344(14):1879–1900. https://doi.org/10.1016/j.carres.2009.05.021.
12. Ovodov YuS. Current views on pectin substances. Russian Journal of Bioorganic Chemistry. 2009;35(3):269–284. https://doi.org/10.1134/S1068162009030017.
13. Harholt J, Suttangkakul A, Scheller HV. Biosynthesis of pectin. Plant Physiology. 2010;153(2):384–395. https://doi.org/10.1104/pp.110.156588.
14. Sato MF, Rigoni DC, Canteri MHG, Petkowicz CLO, Nosueira A, Wosiacki G. Chemical and instrumental characterization of pectin from dried pomace of eleven apple cultivars. Acta Scientarium – Agronomy. 2011;33(3):383–389. https://doi.org/10.4025/actasciagron.v33i3.7125.
15. Srivastava P, Malvia R. Sources of pectin, extraction and its application in pharmaceutical industry – An overview. Indian Journal of Natural Products and Resources. 2011;2(1):10–18.
16. Leclere L, Cutsem PV, Michiels C. Anti-cancer activities of pH- or heat-modified pectin. Frontiers in Pharmacology. 2013;4. https://doi.org/10.3389/fphar.2013.00128.
17. Muller-Maatsch J, Bencivenni M, Caligiani A, Tedeschi T, Bruggeman G, Bosch M, et al. Pectin content and composition from different food waste streams. Food Chemistry. 2016;201:37–45. https://doi.org/10.1016/j.foodchem.2016.01.012.
18. Lara-Espinoza C, Carvajal-Millán E, Balandrán-Quintana R, López-Franco Y, Rascón-Chu A. Pectin and pectin-based composite materials: Beyond food texture. Molecules. 2018;23(4). https://doi.org/10.3390/molecules23040942.
19. Yapo BM, Gnakri D. Pectic polysaccharides and their functional properties. In: Ramawat KG, Mérillon J-M, editors. Polysaccharides: bioactivity and biotechnology. Cham: Springer; 2015. pp. 1729–1749. https://doi.org/10.1007/978-3-319-16298-0_62.
20. Mohnen D. Pectin structure and biosynthesis. Current Opinion in Plant Biology. 2008;11(3):266–277. https://doi.org/10.1016/j.pbi.2008.03.006.
21. Kondratenko VV, Kondratenko TYu. Influence of molecular weight on sorption properties display of pectin substances. New Technologies. 2011;(2):20–26. (In Russ.).
22. Kondratenko VV, Kondratenko TYu, Petrov AN, Belozerov GA. Assessing protopectin transformation potential of plant tissue using a zoned criterion space. Foods and Raw Materials. 2020;8(2):349–361. http://doi.org/10.21603/2308-4057-2020-2-348-361.

ORCID IDs

Vladimir V. Kondratenko https://orcid.org/0000-0002-0913-5644
Tatyana Yu. Kondratenko https://orcid.org/0000-0001-8237-0774
Andrey N. Petrov http://orcid.org/0000-0001-9879-482X

Foods and Raw Materials, 2021, vol. 9, no. 2

E-ISSN 2310-9599
ISSN 2308-4057

Research Article
Open Access

https://doi.org/10.21603/2308-4057-2021-2-262-270
Available online at http://jfrm.ru/en

Antioxidant properties of edible sea weed from the Northern Coast of the Sea of Japan

Anton V. Tabakaev[1], Oksana V. Tabakaeva[1,*], Wojciech Piekoszewski[1,2], Tatyana K. Kalenik[1], Valery M. Poznyakovsky[3]

[1] Far Eastern Federal University, Vladivostok, Russia

[2] Jagiellonian University, Krakow, Poland

[3] Kemerovo State Medical University, Kemerovo, Russia

* e-mail: yankovskaya68@mail.ru

Received January 21, 2021; Accepted in revised form February 22, 2021; Published online July 09, 2021

Abstract:

Introduction. New natural antioxidants remain a relevant research task of food science. Natural antioxidants neutralize free radicals in food systems, as well as in human body. The antioxidant properties of seaweed have attracted scientific attention for many years. However, most experiments featured non-polar extracts while aqueous extracts still remain understudied. The present research objective was to evaluate the antioxidant properties of hydrothermal extracts of edible seaweed from the Northern Coast of the Sea of Japan.

Study objects and methods. The study featured hot-water and autoclave (30 and 60 min) extracts of three edible seaweed species from Russia's Far East. The research focused on dry matter yield, total phenol content, phenolic profile, antiradical properties, hydroxyl-ion ($OH^{\bullet}$) scavenging activity, and superoxide radical ($O_2^{\bullet-}$) scavenging activity.

Results and discussion. The hot-water extracts appeared to have a higher yield than the autoclave extracts. The hot-water extract of red-purple seaweed *Gracilaria verrucosa* had the highest yield – 15.90%. The extract of brown seaweed *Sargassum miyabei* demonstrated the highest total phenol content. The phenolic profile of the extracts revealed 10 compounds, syringic acid and epicatechin being the major ones. The radical scavenging activity of the extracts varied from 48.2 to 88.9%, the highest value was observed in the hot-water extract of *S. miyabei*. The autoclave *S. miyabei* extracts also had a high radical scavenging activity, which exceeded other samples by 5.0–13.3%. The hot-water (30 min) extract of *G. verrucosa* had the lowest antiradical activity. Hot-water and autoclave extracts of *S. miyabei* showed the best $OH^{\bullet}$ scavenging activity. Only the samples of *G. verrucosa* demonstrated signs of superoxide radical scavenging.

Conclusion. The extracts of brown seaweed *S. miyabei* proved to be the most active. The hot-water and autoclave extracts had the highest total phenol content and the strongest DPPH and $OH^{\bullet}$ inhibitory activity.

Keywords: Marine plants, phenols, extract, antioxidant activity, radicals, Sea of Japan

Funding: The research was supported by the Presidential grant No. MK-4715.2021.4.

Please cite this article in press as: Tabakaev AV, Tabakaeva OV, Piekoszewski W, Kalenik TK, Poznyakovsky VM. Antioxidant properties of edible sea weed from the Northern Coast of the Sea of Japan. Foods and Raw Materials. 2021;9(2):262–270. https://doi.org/10.21603/2308-4057-2021-2-262-270.

INTRODUCTION

Modern science associates many diseases with the destructive effect of oxidants, or free radicals. Peroxidation is the most grievous consequence of free radicals entering the cell. Lipid oxidation in biological membranes is a highly destructive process that triggers liver damage, carcinogenesis, and aging. Lipid peroxidation is a major cause of the defective cell proliferation [1, 2]. Oxidized lipid compounds react with proteins, thus lowering enzymatic activity, causing cleavage of polypeptide chains, initiating DNA damage, accelerating aging, and aggravating such diseases as cancer and atherosclerosis. The aldehyde groups of these compounds form intermolecular crosslinks, which violate the structure of macromolecules and disorganize their functioning. By oxidizing lipids, free radicals cause glaucoma, cataracts, cirrhosis, ischemia, etc. [3].

The negative effects of oxidative stress can be mitigated by antioxidants, which neutralize potentially harmful reactive free radicals in the body cells before they cause lipid and protein oxidation. As a result, they can reduce potential mutations and prevent cancer and heart disease [4, 5].

Plants contain effective antioxidant substances. Polyphenols or bioflavonoids of plant origin, when they work in tandem, are extremely efficient against free radicals. Therefore, any study of vegetables, fruits, and spices as an alternative source of antioxidants will be highly relevant, considering that synthetic antioxidants are potentially toxic and carcinogenic. The past two decades have seen a lot of studies in phytochemicals from various types of terrestrial plant materials [6–8].

In this respect, seaweed attracts much less scientific attention than higher plants. Seaweed makes up a significant part of the marine flora. It contains compounds of various structures and bioactivities, which provide antioxidant, antibacterial, anti-inflammatory, and anticarcinogenic properties [9–11]. Although seaweed is rich in polysaccharides and minerals, it is seldom used in food technology. A science-based proof of its antioxidant activity could increase its value as a food or supplement and expand its market. When exposed to light and oxygen, seaweed produces free radicals and other strong oxidants. However, the absence of oxidative damage in its structural components and its resistance to oxidation during storage suggest that seaweed has a good antioxidant system. Seaweed extracts are known to be rich in such hydrophilic components as polyphenols and soluble polysaccharides [9, 12–15]. In particular, brown seaweed is rich in natural antioxidants, e.g. such phenolic compounds as phlorotannins and such carotenoids as fucoxanthin and isoprenoids [16].

Many seaweed extracts possess strong antioxidant properties [17–21]. However, there have been no publications on the antioxidant activity of seaweed from the Northern Coast of the Sea of Japan. Moreover, the antioxidant activity of seaweed has been studied mainly in non-polar extracts and very seldom – in aqueous extracts [22, 23]. Seaweed owes its antioxidant properties due to its hydrophilic and hydrophobic compounds. Therefore, its antioxidant activity in hydrothermal extracts needs more research because hydrothermal treatment is an integral part of processing.

This study featured three species of seaweeds that are part of human and animal diet in the Primorye Territory of Russia's Far East.

Codium flagile from the family of *Codiaceae* is a species of green seaweed found in the Indo-Pacific and the Atlantic. In Russia, it grows on the Northern Coast of the Primorye Territory. Its thallus is prostrate, branched, pillow-shaped or upright. It can be 5–30 cm long. In Oceania and Asia, and especially in Korea and Russia's Primorye, *C. flagile* is usually served raw or boiled. *C. flagile* extracts are widely used in medical cosmetology as it synthesizes water-retaining substances.

Gracilaria verrucosa, *Gracilariaceae* family, is a species of red-purple seaweed found in the low-boreal-tropical Atlantic-Indo-Pacific. In Russia, this seaweed grows in the Far East, in the Sea of Japan and the Sea of Okhotsk. It has branched, cylindrical or flat, gristly thallus, which is purple-red or fading to green. *G. verrucosa* is 20–40 cm long, sometimes reaching up to 100 cm. It grows in the littoral and sublittoral sea zones at a depth of up to 2 m. The species prefers estuarine and sheltered coastal areas and stony, silty-sandy and sandy bottom, interspersed with stones and shell rock. Classified as a potentially commercial species, *G. verrucosa* is a fast-growing seaweed with a biomass of 4.5 kg/m^2, which makes it convenient for cultivation. In Southeast Asia, it is used for food and as a tonic substance in folk medicine. *G. verrucosa* can serve as a raw material for agar and various food and feed additives. It is known to contain minerals, proteins with antibiotic properties, B vitamins, phycocolloids, etc. However, agar remains the only commercial product related to this raw material.

Sargassum miyabei, *Sargassaceae (Decne) Kutz*. family, is a species of brown seaweed that thrives in cold waters in the low-boreal-subtropical areas of Asian. Its thallus is branched, rough, and thick, 2.0–2.5 m in length, olive green. It grows in the littoral and sublittoral at a depth of 11 m on rocky, stony, and silty-sandy bottom, near semi-sheltered and open coastal areas, in separate bushes or small clusters, clustering with kelp seaweeds and sea grasses. It is a potentially commercial perennial species, with the biomass up to 15 kg/m^2, the mass of one thallus up to 7 kg, and population density of 2–6 specimens per 2 m^2. In the Russian Far East, it grows in the Sea of Japan and the Sea of Okhotsk. It is used in the food industry and as a raw material for therapeutic and prophylactic medications, food and feed additives. *S. miyabei* is known to contain vitamins A, B_1, B_6, B_{12}, minerals, polysaccharides with immunostimulating and antitumor activity, etc. [24].

The research objective was a comparative analysis of hydrothermal extracts of the following seaweeds: green *C. flagile*, brown *S. miyabei*, and red *G. verrucosa*, obtained by hot-water or autoclave methods for 30 and 60 min. The extracts were compared according to the following parameters: total phenols, phenolic profile, and antioxidant activity, i.e. DHHP radicals, $OH^{\bullet}$ scavenging activity, and $O_2^{\bullet-}$ scavenging activity.

STUDY OBJECTS AND METHODS

Materials. All samples of *Codium flagile*, *Gracilaria verrucosa*, and *Sargassum miyabei* were harvested in the coastal sea waters of the Sea of Japan in the northern Primorye Territory in May-July 2018 (Table 1).

Chemicals and reagents. 1,1-diphenyl-2-picrylhydrazyl (DHHP), BHT-2,6-di-tert-butyl-4-methylphenol (ionol), and tannic acid were purchased from Sigma-Aldrich (USA). The Folin-Ciocalteu phenolic reagent was purchased from Fluka (Switzerland). All the other reagents were of analytical grade.

Table 1 Place and time of harvest

Seaweed	Place	Time
Codium flagile	Olga Bay of the Sea of Japan, Primorye Territory, Russia	May 2018
Gracilaria verrucosa	Valentina Bay of the Sea of Japan, Primorye Territory, Russia	June 2018
Sargassum miyabei	Valentina Bay of the Sea of Japan, Primorye Territory, Russia	July 2018

Extract samples. After harvesting, the samples were placed in plastic bags, cooled with ice, and immediately transported to the laboratory. They were washed with flowing tap water to remove salt, sand, and epiphytes. After that, the samples were soaked twice in distilled water for 30 min, dried on filter paper, and ground using a Waring mill. The samples were stored in an airtight container at –20°C. Hot water extraction procedures followed the methods described in [25, 26]. To obtain hot-water extracts, 10 g of crushed seaweed was added to 300 mL of deionized water and boiled for 30 and 60 min. Then, the suspension was filtered through three layers of gauze. The resulting filtrate underwent freeze-drying and subsequent grinding to obtain a dry extract. To obtain autoclave extracts, 10 g of crushed seaweed was autoclaved in 100 mL of deionized water at 120°C for 30 and 60 min. The hot aqueous solution was filtered through three layers of gauze. The residue was freeze-dried and crushed.

Total phenol content. A spectrophotometric method with the Folin-Ciokalteu reagent was used to determine the total content of phenolic compounds: a mix of phosphotungstic and phosphoromolybdic acids was reduced in an alkaline medium. It is the main method for determining the total content of phenols in medicine and food industry [27]. The experiment featured a UV-1800 scanning spectrophotometer (Shimadzu, Kyoto, Japan). The quantity of polyphenolic compounds was determined in terms of tannic acid.

Phenolic compounds were identified by HPLC in a high pressure liquid chromatograph LC-20A (Shimadzu, Kyoto, Japan) at 30°C on a reverse phase column (Phenomenex RPC18 250×4.6 mm, 5 µm, Torrance, California, USA). The extracts went through a 0.45 µm filter (Millipore, Westboro, MA, USA) before being put into the chromatograph. The total run time was about 50 min at a flow rate of 0.6 mL/min. The mobile phase included methanol (B) with water (A) and 0.2% acetic acid (B:A = 65:35, w/w). The gradient elution looked as follows: 0–2 min, 5% of isocratic B; 2–10 min, linear gradient 5–25% of B; 10–20 min, linear gradient 25–40% of B; 20–30 min, linear gradient 40–50% of B; 30–40 min, linear gradient 50–100% of B; 40–45 min, 100% of isocratic B, 45–55 min, linear gradient 100% of B. Individual phenolic compounds were identified by comparing retention times of phenolic compounds and original standards (Sigma, USA) under the same conditions. The simultaneous detection wavelength control was 324 nm for chlorine, caffeic, 2,5-dihydroxybenzoic, coumaric, ferulic, and salicylic acids and 277 nm for epigalocatechin gallate, epicatechin, epicatechin gallate, and syringic acid. Each compound was quantified based on its peak area.

Antioxidant activity. The antiradical properties of the extracts were assessed by their ability to interact with a stable free 2,2-diphenyl-1-picrylhydrazyl (DPPH) radical *in vitro*. The reaction mix contained 3 mL of 0.3 mM DPPH in ethanol, 1 mL of 50 mMtris-HCl buffer (pH 7.4), and 1 mL of extract [28].

After a 30-min incubation at room temperature, the optical density values were recorded at λ = 517 nm using a UV-1800 scanning spectrophotometer (Shimadzu, Japan) in l×1 cm cuvettes at 25°C.

The radical scavenging properties were described using the following indicators: radical scavenging activity; the effective concentration of the substance which restores 50% of DPPH (EC_{50}), mg/mL; recovery time for one half of the radical ($T_{EC_{50}}$), min; and anti-radical effectiveness.

The radical scavenging activity (RSA) was calculated as follows:

$$RSA(\%)=[A_0-A_1]/A_0\times100 \quad (1)$$

where A_0 is optical density of the control solution and A_1 is optical density of the extract.

Antiradical efficacy (AE) links the half-recovery time of the radical ($T_{EC_{50}}$) and the required substrate concentration (EC_{50}), which was calculated by the formula:

$$AE=1/[EC_{50}\times T_{EC_{50}}] \quad (2)$$

The antiradical properties were compared with the effect of the synthetic antioxidant ionol (2,6-di-tert-butyl-4-methyl-phenol), which was preliminarily recrystallized from ethanol. Tthe obtained crystals were dried and sublimated in vacuum.

OH• scavenging activity. The OH• scavenging activity was determined according to [29]: 1.5 mM $FeSO_4$ (0.5 mL) was mixed with 6 mM H_2O_2 (0.35 mL), 20 mM sodium salicylate (0.15 mL), and various concentrations (0.2–1.0 mg/mL) of 1 mL of each sample. The mix was kept at 37°C for 1 h. The optical density of the hydroxylated salicylate complex was determined spectrophotometrically at a wavelength of 562 nm. Ascorbic acid was used as positive control. The OH• scavenging activity was calculated using the following formula:

$$OH^{\bullet} \text{ scavenging activity } (\%) = 1-[A_1-A_2]/A_0\times100 \quad (3)$$

where A_1 is optical density of the extract; A_0 is optical density of the control solution; and A_2 is optical density of the reagent blank without sodium salicylate.

$O_2^{\bullet-}$ scavenging activity. The $O_2^{\bullet-}$ scavenging activity was determined according to the method developed by Ruch *et al.* [30]: 40 mM H_2O_2 was dissolved in phosphate buffer (pH 7.4). Various

concentrations (0.1–1.0 mg/mL) of extracts in MeOH (3.0 mL) were added to a 40 mM H_2O_2 solution (3.0 mL). The optical density was measured at 230 nm after 10 min of incubation against an empty solution of phosphate buffer without H_2O_2.

The $O_2^{\bullet-}$ scavenging activity was determined by the formula:

$$O_2^{\bullet-} \text{ scavenging activity (\%)} = [A_0 - A_1/A_0] \times 100 \quad (4)$$

where A_1 is optical density of the extract and A_0 is optical density of the control solution.

Calculation of EC_{50} (mg/mL) was the next step.

Statistical analysis. The data were obtained as mean and standard deviation (SD) and analyzed by one-way ANOVA using SPSS 11.5 for Windows. The difference in mean values was significant at $P < 0.05$.

RESULT AND DISCUSSION

The hot-water and autoclave hydrothermal extracts obtained from three edible seaweeds from the Northern Coast of the Sea of Japan demonstrated different dry matter yields. Figure 1 shows the effect of processing time and method on the extraction yield.

A comparative analysis of the quantitative yield resulted in the following descending order: *Gracilaria verrucosa* > *Codium flagile* > *Sargassum miyabei*.

The hot-water extract of the red-purple seaweed *G. verrucosa* had the highest yield – 15.90%, which was 1.17–1.58 times higher than that in the autoclave samples. The extraction time increased the yield by 55–57% for hot-water extracts and by 16.3–47.5% for autoclave extracts. The hot-water *G. verrucosa* extract and the autoclave *C. flagile* and *S. miyabei* extracts experienced the greatest effect of extraction time. However, a high yield did not equal high antioxidant activity, which depends on strong antioxidants, e.g. polyphenols.

Figure 2 illustrates the content of phenols in the seaweed extracts.

A comparative analysis of the total phenols showed that *S. miyabei* had the hot-water extract with the highest phenolic level, about 3–4 times higher than the other hot-water extracts. The autoclave extract of *S. miyabei* had similar level of total phenols. The extract of *C. flagile* had the lowest total phenols among the hot-water extracts, while *G. verrucosa* had the lowest total phenols among the autoclave samples. The fact that brown seaweeds proved richer in fenols than green and red seaweeds confirms the data obtained by other scientists [31]. However, the methods were slightly different. The total phenol content in the autoclave *C. flagile* extract was twice as high as in the hot-water extract, while in the autoclave extract of *S. miyabei* it was lower than in the respective hot-water extracts (Fig. 2).

Such hydrophilic polyphenols as phlorotanins, which are bipolar and occur in brown seaweeds, can act as antioxidant components and thus help the seaweed overcome oxidative stress [32, 33].

Identification of phenolic compounds. Individual phenolic compounds were tested using HPLC in extracts obtained after 60 min of hydrothermal treatment because a longer processing time provided a higher level of total phenols. Table 2 shows the content of the main phenolic compounds in the extracts.

Table 2 demonstrates 10 phenolic compounds in the composition of edible seaweed extracts from the Northern Coast of the Sea of Japan. Chlorogenic acid was the first of the phenolic compounds to elute; it was not detected in the hot-water *C. flagile* extract. Similarly, 2,5-dihydroxybenzoic acid was not detected in both extracts of *G. verrucosa* and the autoclave extract of *C. flagile*. Caffeic, coumaric, ferulic, salicylic, and

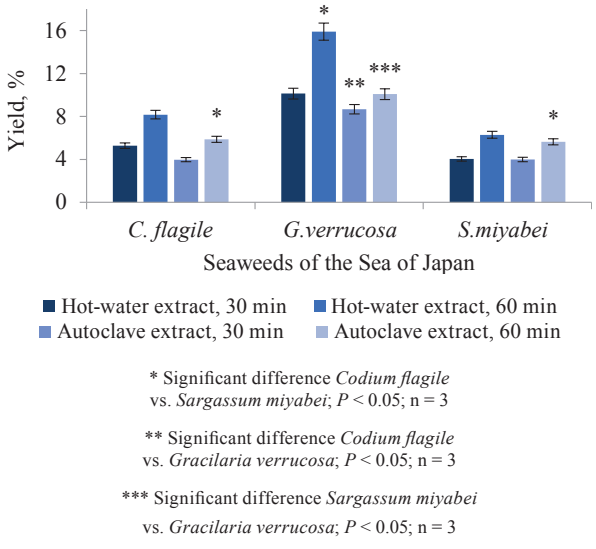

Figure 1 Yield of seaweed extracts from the Northern Coast of the Sea of Japan

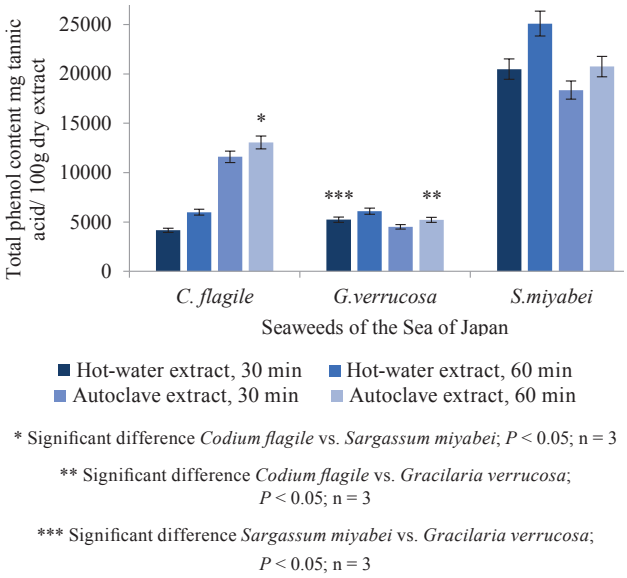

Figure 2 Total phenols in the seaweed extracts from the Northern Coast of the Sea of Japan

Table 2 The main phenolic compounds in the seaweed extracts from the Northern Coast of the Sea of Japan

Compound	Retention time, min	Content, mg/g					
		Sargassum miyabei		*Codium flagile*		*Gracilaria verrucosa*	
		Hot-water extract	Autoclave extract	Hot-water extract	Autoclave extract	Hot-water extract	Autoclave extract
		324 nm					
Chlorogenic Acid	8.12	2.48 ± 0.01	4.12 ± 0.02	n.d.	0.15 ± 0.00	6.78 ± 0.23	10.82 ± 0.33
Caffeic Acid	10.49	1.69 ± 0.05	2.80 ± 0.12	2.69 ± 0.01	5.09 ± 0.02	4.51 ± 0.14	3.09 ± 0.09
2,5-dihydroxybenzoic Acid	17.43	0.12 ± 0.01	0.45 ± 0.02	0.85 ± 0.00	n.d.	n.d.	n.d.
Coumaric Acid	20.56	6.02 ± 0.21	8.71 ± 0.29	10.28 ± 0.32	9.04 ± 0.03	11.64 ± 0.48	8.47 ± 0.29
Ferulic Acid	24.19	8.83 ± 0.43	7.12 ± 0.30	15.21 ± 0.56	10.27 ± 0.40	3.15 ± 0.09	2.70 ± 0.08
Salicylic Acid	44.92	11.05 ± 0.42	10.58 ± 0.37	6.87 ± 0.02	7.18 ± 0.03	8.48 ± 0.30	12.48 ± 0.55
		277 nm					
Epigallocatechin Gallate	8.13	15.19 ± 0.59	10.48 ± 0.43	35.89 ± 0.97	20.17 ± 0.79	18.29 ± 0.75	14.50 ± 0.59
Epicatechin	10.11	33.52 ± 0.98	31.84 ± 0.83	20.15 ± 0.86	24.76 ± 0.95	30.48 ± 1.07	26.53 ± 1.08
Epicatechin Gallate	13.00	4.07 ± 0.15	2.11 ± 0.07	8.97 ± 0.25	9.15 ± 0.38	12.07 ± 0.43	14.20 ± 0.56
Syringic Acid	14.78	57.40 ± 2.14	63.18 ± 2.46	17.67 ± 0.54	28.94 ± 1.05	25.76 ± 0.90	30.87 ± 1.14

n.d. – not detected

syringic acids, epigallocatechin gallate, epicatechin gallate, as well as epicatechin were registered in all the samples. Syringic acid and epicatechin appeared to be the major phenolic compounds for all the extracts.

All the autoclave extracts showed higher levels of chlorogenic and syringic acids compared to the hot-water samples, which had a higher content of ferulic acid and epigallocatechin gallate.

A comparative analysis of individual phenolic compounds showed that *S. miyabei* extracts had the highest content of epicatechin, which was maximal in the hot-water sample, and syringic acid, which was maximal in the autoclave sample. The *C. flagile* extracts demonstrated the highest content of ferulic acid and epigallocatechin gallate, which were the most abundant in the hot-water sample. The *G. verrucosa* extracts had the highest content of chlorogenic acid, especially in the autoclave sample, coumaric acid (hot-water sample), salicylic acid (autoclave sample), and epicatechin gallate (autoclave sample). Thus, the phenolic profile of the extracts depended on the type of seaweed and the method of hydrothermal treatment. Phenolic acids, which are the main class of phenolic compounds, are found in seaweed in significant quantities. Typical phenols are known to possess antioxidant properties. Other publications prove that seaweed is rich in phenolic compounds, e.g. catechin, caffeic acid, epicatechin, epicatechin gallate, etc. [34, 35].

Antioxidant activity. Radical scavenging properties. DPPH possesses a nitrogen free radical

Table 3 Antiradical properties of the seaweed extracts from the Northern Coast of the Sea of Japan

Seaweed	Antiradical properties							
	Radical scavenging activity,%		EC_{50}, μg/mL		T_{EC50}, min		Antiradical efficacy, μg/L·c	
	30 min	60 min	30 min	60 min	30 min	60 min	30 min	60 min
				Hot-water extract				
Codium flagile	58.9 ± 2.8	72.8 ± 3.5	25.69 ± 1.20	20.04 ± 0.67*	22.01 ± 1.00	17.89 ± 0.80	0.0018 ± 0.0000	0.0028 ± 0.0001
Gracilaria verrucosa	48.2 ± 2.3	76.1 ± 3.7**	28.06 ± 1.30	21.29 ± 0.96	36.21 ± 1.70	27.12 ± 1.30	0.0010 ± 0.0000	0.0017 ± 0.0001
Sargassum miyabei	72.6 ± 3.5	88.9 ± 4.4	14.53 ± 0.60	10.39 ± 0.09	10.59 ± 0.50	8.09 ± 0.40	0.0065 ± 0.0003	0.0120 ± 0.0005***
				Hot-water extract				
Codium flagile	65.3 ± 3.2	80.6 ± 4.0	14.59 ± 0.21	11.23 ± 0.36	17.23 ± 0.36	15.52 ± 0.60	0.0040 ± 0.0002	0.0057 ± 0.0003
Gracilaria verrucosa	50.1 ± 2.5	78.4 ± 3.8**	30.83 ± 0.58	22.36 ± 1.47	32.36 ± 1.47	20.04 ± 1.00	0.0010 ± 0.0000	0.0022 ± 0.0006
Sargassum miyabei	75.2 ± 3.6***	85.6 ± 4.1	12.12 ± 0.15*	11.15 ± 0.08	12.30 ± 0.08	9.08 ± 0.40	0.0067 ± 0.0003	0.0099 ± 0.0005
Ionol	94.0 ± 4.5		8.75 ± 0.3		8.0 ± 0.4			0.0160 ± 0.0700

* Significant difference *Codium flagile* vs. *Sargassum miyabei*; $P < 0.05$; n = 3

** Significant difference *Codium flagile* vs. *Gracilaria verrucosa*; $P < 0.05$; n = 3

*** Significant difference *Sargassum miyabei* vs. *Gracilaria verrucosa*; $P < 0.05$; n = 3

and is easily destroyed by a free radical scavenger. The DPPH radical assay was used to test the ability of the antioxidant compounds found in the extracts to act as proton radical scavengers or hydrogen donors. Table 3 demonstrates the antiradical properties of the extracts.

The autoclave extracts appeared to be more active than the hot-water extracts. The radical scavenging activity varied within wide limits of 39.6–88.9%. The maximal value was observed in the hot-water *S. miyabei* extract, and its radical scavenging activity was 12.8–28.4% higher than that of the other extracts and only 10.4% lower than that of ionol. The autoclave extracts of *S. miyabei* also had a high radical scavenging activity, which exceeded that of the other extracts by 5.0–13.3%. A comprehensive assessment of the antiradical activity showed that the hot-water (30 min) extract of *G. verrucosa* had the lowest values. The hot-water extract of *S. miyabei* had the most pronounced antiradical properties. Its EC_{50} concentration was 1.89–2.41 times lower than the other extracts, its T_{EC50} time was 2.21–9.79 times shorter, and its antiradical efficiency was 4.29–24.00 times higher.

The extract of *S. miyabei*, which had the highest total phenol content, also had a much lower effective concentration of EC_{50}. The autoclave extracts demonstrated a strong correlation between the level of total phenols (Fig. 2) and the effective concentration of EC_{50}. When the total phenol level was high, the effective EC_{50} concentration was low. Therefore, the polyphenolic components in the seaweed extracts were capable of acting as free radical scavengers. For hot-water extracts, however, this ratio was weak. Since the DPPH radical analysis was not specific for any particular antioxidants, the antiradical activity of these extracts result not only from phenols, but also from various other water-soluble antioxidants, e.g. polysaccharides, folic acid, thiamine, and ascorbic acid [36, 37].

The $OH^{\bullet}$ scavenging activity and absorption of superoxide radicals. Antioxidant activity was determined according to the ability of the antioxidant components to inhibit the oxidation of deoxyribose by the reactive hydroxyl-ion radical ($OH^{\bullet}$), formed as a result of the Fenton-type reaction. The reaction involves two antioxidant defense mechanisms: suppression of the generation of $OH^{\bullet}$ from H_2O_2 by binding with metal ions and the direct transfer of one electron to the generated radical. Figure 3 illustrates the $OH^{\bullet}$ scavenging activity of the seaweed extracts.

Both autoclave and hot-water *S. miyabei* extracts demonstrated the highest $OH^{\bullet}$ scavenging activity, while that of the other extracts was significantly lower. A comparative analysis showed similar E_{C50} values and ranking. A longer extraction time increased the $OH^{\bullet}$ scavenging activity, but the increase was insignificant. Brown seaweeds are known to contain floratanins, which chelate heavy metals [32, 38]. Probably, the high content of floratanins predetermined the high $OH^{\bullet}$ scavenging activity of *S. miyabei* extracts. However, seaweeds have a complex composition, and its phenols are not the only compounds that exhibit antioxidant activity, which is also typical of carotenoids and polysaccharides [39]. Hydrothermal extracts of some green and brown seaweeds contain sulfated heteropolysaccharides, which strongly inhibit $OH^{\bullet}$ activity *in vitro* [40–42].

Figure 4 demonstrates the $O_2^{\bullet-}$ scavenging activity of the extracts.

Although $O_2^{\bullet-}$ is a relatively weak oxidizing agent, it decomposes into stronger oxidative forms, such as singlet oxygen and $OH^{\bullet}$. The autoclave extract of *G. verrucosa* was the only sample to demonstrate $O_2^{\bullet-}$ scavenging activity. All hot-water extracts showed $O_2^{\bullet-}$ inhibitory activity. Figure 4 shows that the maximal inhibitory activity belonged to the *C. flagile* extract. Surprisingly, *S. miyabei* revealed no signs of $O_2^{\bullet-}$ scavenging. The extraction time only slightly increased the $O_2^{\bullet-}$ absorption.

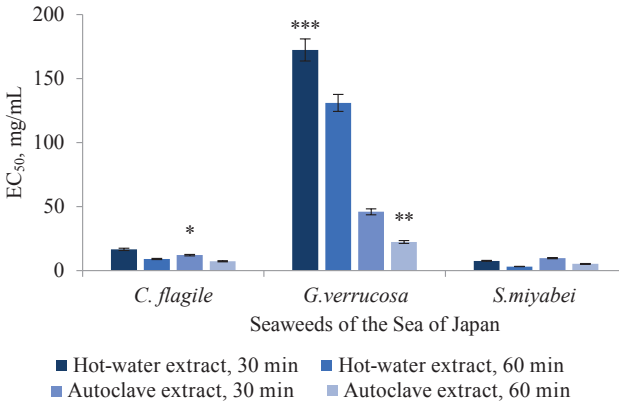

* Significant difference *Codium flagile* vs. *Sargassum miyabei*; $P < 0.05$; n = 3

** Significant difference *Codium flagile* vs. *Gracilaria verrucosa*; $P < 0.05$; n = 3

*** Significant difference *Sargassum miyabei* vs. *Gracilaria verrucosa*; $P < 0.05$; n = 3

Figure 3 $OH^{\bullet}$ scavenging activity of the seaweed extracts from the Northern Coast of the Sea of Japan

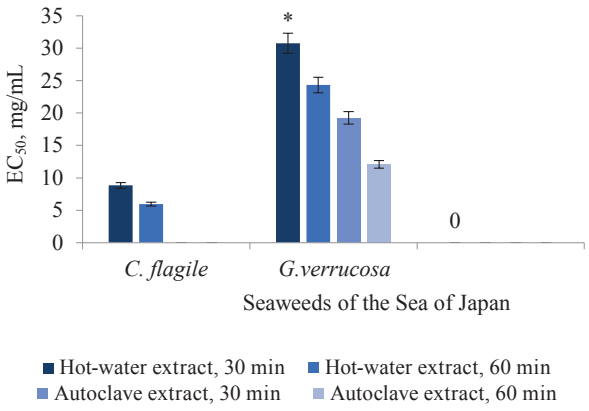

* Significant difference *Codium flagile* vs. *Gracilaria verrucosa*; $P < 0.05$; n = 3

Figure 4 $O_2^{\bullet-}$ scavenging activity of the seaweed extracts from the Northern Coast of the Sea of Japan

The established difference in the $O_2^{\bullet-}$ absorption between the hot-water and autoclave extracts proved that the two methods extracted different types of antioxidants. The lack of correlation between the total content of phenols and $O_2^{\bullet-}$ inhibition means that such activity demonstrated by all three species could not be explained solely by the presence of phenolic antioxidants. Sulfated polysaccharides obtained from the hot-water extracts of green and brown seaweeds inhibited the activity of $O_2^{\bullet-}$ *in vitro* [40–42].

CONCLUSION

The hot-water extraction proved more effective than the autoclave extraction in terms of $OH^{\bullet}$ and $O_2^{\bullet-}$ scavenging activity. However, the autoclave extracts had better antiradical properties. The extracts of the brown seaweed *Sargassum miyabei* showed significantly higher antiradical and antioxidant activity than the extracts of the red seaweed *Gracilaria verrucosa* and the green seaweed *Codium flagile*. The relationship between $OH^{\bullet}$ scavenging and antioxidant activities in these samples indicated that it came from the hydrophilic polyphenolic antioxidants. The hydrothermal extracts of the seaweeds proved to be a promising source of antioxidants for human consumption.

CONTRIBUTION

The authors contributed equally to the manuscript and are equally responsible for any potential plagiarism.

CONFLICT OF INTEREST

The authors declare that there is no conflict of interests related to the publication of this article.

REFERENCES

1. Tan BL, Norhaizan ME. Liew W-P-P. Nutrients and oxidative stress: Friend or foe? Oxidative Medicine and Cellular Longevity. 2018;2018. https://doi.org/10.1155/2018/9719584.
2. Sies H. Hydrogen peroxide as a central redox signaling molecule in physiological oxidative stress: Oxidative eustress. Redox Biology. 2017;11:613–619. https://doi.org/10.1016/j.redox.2016.12.035.
3. Mazon JN, de Mello AH, Ferreira G, Rezin GT. The impact of obesity on neurodegenerative diseases. Life Sciences. 2017;182:22–28. https://doi.org/10.1016/j.lfs.2017.06.002.
4. Noufou O, Sawadogo WR, Tibiri A, Lompo M, Dijoux MG, Diederich M, et al. Phenolic contents and *in vitro* pharmacological activities of methanolic extract of *Pterocarpus erinaceus* Poir. Stem bark (Fabaceae). Journal of Pharmaceutical Research International. 2016;10(2). https://doi.org/10.9734/BJPR/2016/23149.
5. Halliwell B, Aeschbach R, Löliger J, Aruoma OI. The characterization of antioxidants. Food and Chemical Toxicology. 1995;33(7):601–617. https://doi.org/10.1016/0278-6915(95)00024-V.
6. Wang S, Zhu F. Chemical composition and biological activity of staghorn sumac (*Rhus typhina*). Food Chemistry. 2017,237:431–443. https://doi.org/10.1016/j.foodchem.2017.05.111.
7. Li Y, Jiang J-G. Health functions and structure-activity relationships of natural anthraquinones from plants. Food and Function. 2018;9(12):6063–6080. https://doi.org/10.1039/c8fo01569d.
8. Fierascu RC, Ortan A, Fierascu IC, Fierascu I. *In vitro* and *in vivo* evaluation of antioxidant properties of wild-growing plants. A short review. Current Opinion in Food Science. 2018;24:1–8. https://doi.org/10.1016/j.cofs.2018.08.006.
9. Meresse S, Fodil M, Fleury F, Chenais B. Fucoxanthin, a marine-derived carotenoid from brown seaweeds and microalgae: A promising bioactive compound for cancer therapy. International Journal of Molecular Sciences. 2020;21(23). https://doi.org/10.3390/ijms21239273.
10. Jesumani V, Du H, Aslam M, Pei P, Huang N. Potential use of seaweed bioactive compounds in skincare – a review. Marine Drugs. 2019;17(12). https://doi.org/10.3390/md17120688.
11. Gerasimenko NI, Martyyas EA, Busarova NG. Composition of lipids and biological activity of lipids and photosynthetic pigments from algae of the families Laminariaceae and Alariaceae. Chemistry of Natural Compounds. 2012;48(5):737–741. https://doi.org/10.1007/s10600-012-0371-5.
12. Liu Z. Gao T, Yang Y, Meng F, Zhan F, Jiang Q, et al. Anti-cancer activity of porphyran and carrageenan from red seaweed. Molecules. 2019;24(23). https://doi.org/10.3390/molecules24234286.
13. Salehi B, Sharifi-Rad J, Seca AML, Pinto DCGA, Michalak I, Trincone A, et al. Current trends on seaweeds: Looking at chemical composition, phytopharmacology, and cosmetic applications. Molecules. 2019;24(22). https://doi.org/10.3390/molecules24224182.
14. Amosova AS, Ivakhnov AD, Skrebets TE, Ulyanovskiy NV, Bogolitsyn KG. Supercritical fluid extraction of carotenoids from *Shantane carrot*. Russian Journal of Physical Chemistry B. 2014;8(7):963–966. https://doi.org/10.1134/S1990793114070021.
15. Rosa GR, Barreto MC, Seca AML. Pharmacological effects of *Fucus spiralis* extracts and phycochemicals: A comprehensive review. Botanica Marina. 2019;62(2):167–178. https://doi.org/10.1515/bot-2018-0047.

16. Sukhoveeva MV, Podkorytova AV. Promyslovye vodorosli i travy morey Dal′nego Vostoka: biologiya, rasprostranenie, zapasy, tekhnologiya pererabotki [Commercial seaweeds and sea grasses of the Far East: biology, distribution, reserves, and processing technology]. Vladivostok: TINRO-Tsentr; 2006. 243 p. (In Russ.).
17. Cao L, Lee SG, Lim KT, Kim H-R. Potential anti-aging substances derived from seaweeds. Marine drugs. 2020;18(11). https://doi.org/10.3390/md18110564.
18. Hentati F, Tounsi L, Djomdi D, Pierre G, Delattre C, Ursu AV. Bioactive polysaccharides from seaweeds. Molecules. 2020;25(14). https://doi.org/10.3390/molecules25143152.
19. Viji P, Venkateshwarlu G, Ravishankar CN, Gopal TKS. Role of plant extracts as natural additives in fish and fish products – A review. Fishery Technology. 2017;54(3):145–154.
20. Oucif H, Benaissa M, Ali Mehidi S, Prego R, Aubourg SP, Abi-Ayad S-ME-A. Chemical composition and nutritional value of different seaweeds from the west Algerian coast. Journal of Aquatic Food Product Technology. 2020;29(1):90–104. https://doi.org/10.1080/10498850.2019.1695305.
21. Rajauria G. In-vitro antioxidant properties of lipophilic antioxidant compounds from 3 brown seaweed. Antioxidants. 2019;8(12). https://doi.org/10.3390/antiox8120596.
22. Chakraborty K, Joseph D. Antioxidant potential and phenolic compounds of brown seaweeds Turbinaria conoides and Turbinaria ornata (class: Phaeophyceae). Journal of Aquatic Food Product Technology. 2016;25(8):1249–1265. https://doi.org/10.1080/10498850.2015.1054540.
23. Chakraborty K, Maneesh A, Makkar F. Antioxidant activity of brown seaweeds. Journal of Aquatic Food Product Technology. 2017;26(4):406–419. https://doi.org/10.1080/10498850.2016.1201711.
24. Dzizyurov VD, Kulepanov VN, Shaposhnikova TV, Sukhoveeva MV, Gusarova IS, Ivanova NV. Atlas massovykh vidov vodorosley i morskikh trav rossiyskogo Dal′nego Vostoka [Atlas of mass species of seaweeds and sea grasses of the Russian Far East]. Vladivostok: TINRO-Tsentr; 2008. 328 p. (In Russ.).
25. Hou W-Y, Chen J-C. The immunostimulatory effect of hot-water extract of *Gracilaria tenuistipitata* on the white shrimp *Litopenaeus vannamei* and its resistance against *Vibrio alginolyticus*. Fish and Shellfish Immunology. 2005;19(2):127–138. https://doi.org/10.1016/j.fsi.2004.11.009.
26. Huang R, Lee H-T. Immunological properties of the marine brown alga *Endarachne binghamiae* (Phaeophyceae). International Journal of Applied Science and Engineering. 2005;3(3):167–173.
27. FFS 1.5.3.0008.15. The determination of tannins in herbal drugs and medicinal plant preparations [Internet]. [cited 2020 Dec 20]. Available from: https://193.232.7.120/feml/clinical_ref/pharmacopoeia_2/HTML/#417/z.
28. Molyneux P. The use of the stable free radical diphenylpicrylhydrazyl (DPPH) for estimating antioxidant activity. Songklanakarin Journal of Science and Technology. 2004;26(2):211–219.
29. Smirnoff N, Cumbes QJ. Hydroxyl radical scavenging activity of compatible solutes. Phytochemistry. 1989;28(4):1057–1060. https://doi.org/10.1016/0031-9422(89)80182-7.
30. Ruch RJ, Cheng S-J, and Klaunig E. Prevention of cytotoxicity and inhibition of intercellular communication by antioxidant catechins isolated from Chinese green tea. Carcinogenesis. 1989;10(6):1003–1008. https://doi.org/10.1093/carcin/10.6.1003.
31. Garicano Vilar E, O'Sullivan MG, Kerry JP, Kilcawley KN. Volatile compounds of six species of edible seaweed: A review. Algal Research. 2020;45. https://doi.org/10.1016/j.algal.2019.101740.
32. Papitha R, Selvaraj CI, Palanichamy V, Arunachalam P, Roopan SM. In vitro antioxidant and cytotoxic capacity of Kappaphycus alvarezii successive extracts. Current Science. 2020;119(5):790–798.
33. Phenolic content and antioxidant capacity in algal food products Sathya R, Kanaga N, Sankar P, Jeeva S. Antioxidant properties of phlorotannins from brown seaweed *Cystoseira trinodis* (Forsskal) C. Agardh. Arabian Journal of Chemistry. 2017;10:S2608–S2614. https://doi.org/10.1016/j.arabjc.2013.09.039.
34. Alkhalaf MI. Chemical composition, antioxidant, anti-inflammatory and cytotoxic effects of Chondrus crispus species of red algae collected from the Red Sea along the shores of Jeddah city. Journal of King Saud University Science. 2021;33(1). https://doi.org/10.1016/j.jksus.2020.10.007.
35. Machu L, Misurcova L, Ambrozova JV, Orsavova J, Mlcek J, Sochor J, et al. Phenolic content and antioxidant capacity in algal food products. Molecules. 2015;20(1):1118–1133. https://doi.org/10.3390/molecules20011118.
36. Wang L, Oh JY, Hwang J, Ko JY, Jeon Y-J, Ryu B. In vitro and in vivo antioxidant activities of polysaccharides isolated from celluclast-assisted extract of an edible brown seaweed, *Sargassum fulvellum*. Antioxidants. 2019;8(10). https://doi.org/10.3390/antiox8100493.
37. Gomez-Zavaglia A, Prieto Lage MA, Jimenez-Lopez C, Mejuto JC, Simal-Gandara J. The potential of seaweeds as a source of functional ingredients of prebiotic and antioxidant value. Antioxidants. 2019;8(9). https://doi.org/10.3390/antiox8090406.

38. Valdes FA, Gabriela Lobos M, Diaz P, Saez CA. Metal assessment and cellular accumulation dynamics in the green macroalga *Ulva lactuca*. Journal of Applied Phycology. 2018;30(1):663–671. https://doi.org/10.1007/s10811-017-1244-x.

39. Tabakaeva OV, Tabakaev AV. Carotenoid profile and antiradical properties of brown seaweed *Sargassum miyabei* extracts. Chemistry of Natural Compounds. 2019;55(2):364–366. https://doi.org/10.1007/s10600-019-02692-w.

40. Jridi M, Mezhoudi M, Abdelhedi O, Boughriba S, Elfalleh W, Souissi N, et al. Bioactive potential and structural characterization of sulfated polysaccharides from Bullet tuna (*Auxis Rochei*) by-products. Carbohydrate Polymers. 2018;194:319–327. https://doi.org/10.1016/j.carbpol.2018.04.038.

41. Bogolitsyn K, Dobrodeeva L, Druzhinina A, Ovchinnikov D, Parshina A, Shulgina E. Biological activity of a polyphenolic complex of Arctic brown algae. Journal of Applied Phycology. 2019;31(5):3341–3348. https://doi.org/10.1007/s10811-019-01840-7.

42. Layana P, Xavier KAM, Lekshmi S, Deshmukhe G, Nayak BB, Balange AK. Antioxidant and antimicrobial potential of hydroethanolic extracts of *Padina tetrastromatica* from North-west Coast of India. Fishery Technology. 2019;56(3):199–204.

ORCID IDs
Anton V. Tabakaev https://orcid.org/0000-0001-5658-5069
Oksana V. Tabakaeva https://orcid.org/0000-0002-7068-911X
Wojciech Piekoszewski https://orcid.org/0000-0001-5718-9797
Tatyana K. Kalenik https://orcid.org/0000-0003-2288-8613
Valery M. Poznyakovsky https://orcid.org/0000-0001-7034-4675

Foods and Raw Materials, 2021, vol. 9, no. 2

E-ISSN 2310-9599
ISSN 2308-4057

Review Article
Open Access

https://doi.org/10.21603/2308-4057-2021-2-271-281
Available online at http://jfrm.ru/en

Continuous hydrolysis of milk proteins in membrane reactors of various configurations

Ksenia A. Ryazantseva*, Evgeniya Yu. Agarkova, Olga B. Fedotova

All-Russian Scientific Research Institute of the Dairy Industry, Moscow, Russia

* e-mail: k_riazantseva@vnimi.org

Received July 20, 2020; Accepted in revised form September 24, 2020; Published online July 09, 2021

Abstract:

Introduction. The article provides a review of technologies for membrane fractionation of various hydrolyzed food substrates in membrane bioreactors (MBR). In food industry, MBRs are popular in functional food production, especially in the processing of whey, which is a very promising raw material due to its physicochemical composition.

Study objects and methods. The research was based on a direct validated analysis of scientific publications and featured domestic and foreign experience in MBR hydrolysis of protein raw material.

Results and discussion. The MBR hydrolysis of proteins combines various biocatalytic and membrane processes. This technology makes it possible to intensify the biocatalysis, optimize the use of the enzyme preparation, and regulate the molecular composition of hydrolysis products. The paper reviews MBRs based on batch or continuous stirring, gradient dilution, ceramic capillary, immobilized enzyme, etc. Immobilized enzymes reduce losses that occur during the production of fractionated peptides. Continuous MBRs are the most economically profitable type, as they are based on the difference in molecular weight between the enzyme and the hydrolysis products.

Conclusion. Continuous stirred tank membrane reactors have obvious advantages over other whey processing reactors. They provide prompt separation of hydrolysates with the required biological activity and make it possible to reuse enzymes.

Keywords: Milk proteins, whey proteins, hydrolysis, membranes, enzymes, membrane reactor, substrate

Please cite this article in press as: Ryazantseva KA, Agarkova EYu, Fedotova OB. Continuous hydrolysis of milk proteins in membrane reactors of various configurations. Foods and Raw Materials. 2021;9(2):271–281. https://doi.org/10.21603/2308-4057-2021-2-271-281.

INTRODUCTION

Balanced diet and natural food quality are the most important issues of contemporary food science [1–4]. Environmental pollution and such diet-related diseases as hypertension, diabetes, allergies, etc., require new types of diet and functional products [5–8]. Modified milk and whey proteins can serve as basic components of functional foods [9–13]. Enzymatic hydrolysis of dairy proteins is the most popular method of whey modification, which makes it possible to impart additional functional and technological properties, e.g. emulsifying, foaming, antioxidant, antihypertensive, immunomodulatory, etc. [14, 15].

Whey proteins and their hydrolysates possess high nutritional value, which makes them the most promising components for diet therapy products. Whey proteins owe their useful functional properties to bioactive peptides [16, 17]. Bioactive peptides are amino acid sequences, encoded in the primary structure of native proteins. A protein hydrolyzate contains a mix of biologically active and inactive peptides, in addition to non-hydrolyzed proteins. Fractioning can isolate certain biologically active peptide fractions from hydrolysates. Fractioning relies on such membrane separation processes as ultrafiltration and microfiltration [18–22].

Membrane separation means that two or more components are separated through a membrane that acts as a selective semipermeable barrier that partially or completely stops one or more substances. The retained components produce retentate, while those that pass through the membrane form permeate [23, 24]. Membrane processes have several advantages over other separation methods. First of all, they require less energy than evaporation or distillation. Second, they demonstrate high selectivity and are easy to scale. Finally, they are material friendly, which is a very important factor for food industry [24].

Development and design of new membrane bioreactors (MBR) is one of the most promising and dynamic areas of industrial biotechnology. MBR technology combines various membrane and biochemical separation processes, the latter being induced by a catalyst of biological origin, i.e. an enzyme. The main advantage of MBR enzymatic hydrolysis is that it saves expensive enzyme preparations and regulates the molecular composition of hydrolysis products by combining membranes with a recommended molecular weight cut-off [18].

Unfortunately, contemporary food industry uses only about 50% of the whey produced worldwide, which means that the task of whey recycling is yet to be solved. This issue remains controversial and requires comprehensive research. The present review describes how various whey processing MBRs can increase the value of whey components [25].

STUDY OBJECTS AND METHODS

The present research was based on a direct validated analysis and featured the most recent domestic and foreign publications on protein hydrolysis in various membrane reactors.

RESULTS AND DISCUSSION

Figure 1 illustrates two most common membrane reactors (MBR). In the first type, the membrane controls the mass transfer of the substrate and enzyme preparation to and from the reactor module, thus producing an indirect effect on the hydrolytic degradation of the substrate (Fig. 1a). In the other type, the reaction occurs at the membrane level and complements the regulation of substrate and enzyme mass transfer [26, 27]. Complex as it is, MBRs of the second type makes it possible to control proteolysis at the cellular level (Fig. 2b) [26, 27].

Such MBRs are called biocatalytic because the membrane itself acts as a catalyst. They are based on continuous stirring: the product either passes through the membrane, which retains the enzyme and returns it to the reactor, or remains in the membrane module. The biocatalyst is immobilized and separated by a membrane in the reaction vessel [26, 28]. As a rule, the membrane immobilizes the enzymes on membranes because biomolecules are covalently attached to the surface of the carrier. As a result, the system is more stable, and the microreactor can be reused while the enzyme is no longer active. The covalent attachment of enzymes to solid substrates is very strong and increases the service life of the microreactor and immobilized enzymes [29].

The numerous advantages of these MBRs make them an alternative to simple bioreactors. The most important advantage is that the catalyst (enzyme) can be recovered and reused in a continuous system, which increases the efficiency of the process. The yield rises, while the expensive enzyme preparation is spared, which lowers the cost of the final product. In addition, the selective removal from the reaction medium is continuous, and the supply of the reagent to the catalytic reaction medium is easy to control [26].

Ultrafiltration is the most common separation process used in this type of MBR. Unfortunately, polarization remains its main disadvantage: eventually, the membrane pores get clogged. Nearly all membrane filtration processes gradually decrease, as trapped particles accumulate on the surface of the

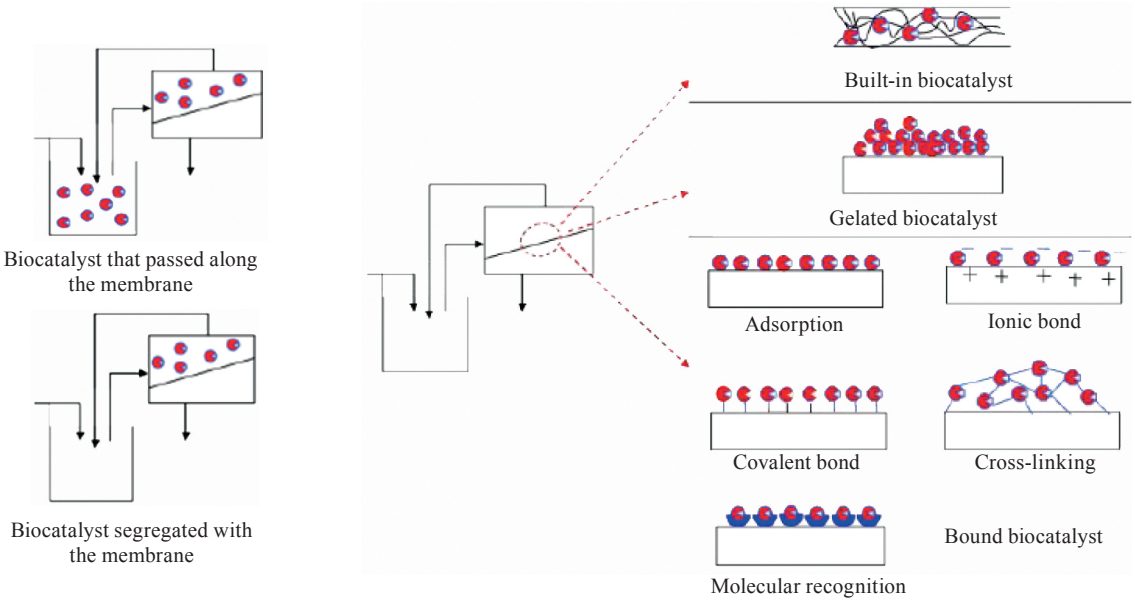

а) membrane bioreactor

б) biocatalytic membrane reactor

Figure 1 Schematic illustration of membrane reactors

membrane. The rate depends on the operation type of the membrane, the nature of the flow, the pore size, and charge of the membrane. The flow decreases because of certain physical or chemical interactions that occur between the interface of the membrane and the components of the feed stream. The formation rate of the surface layer has to be controlled, as it keeps accumulating on the side of the membrane that experiences excess pressure. No pre-treatment can prevent clogging, and the membrane has to be cleaned regularly [26].

In a biocatalytic MBR, the membrane not only separates but also catalyzes. The enzyme enters the membrane matrix and is immobilized there (Fig. 1b), increasing its stability, which is another advantage of this type of MBR [30]. Immobilization increases the stability of enzymes during storage, namely, their resistance to changes in temperature and pH [31].

In their study of continuous MBRs, Wang *et al.* focused on transglutaminase, which was covalently bound to the surface of the polyethersulfone membrane. The enzyme cross-linked α-lactalbumin and β-lactoglobulin, thereby retaining them on the membrane [32]. Using transglutaminase for enzymatic modification of milk protein can prevent protein loss during whey processing and increase the biological value of the product [33]. During whey ultrafiltration, α-lactalbumin and β-lactoglobulin can pass through the membrane under transmembrane pressure, in which case they block the pores or penetrate into the filtered solution. As a result, β-lactoglobulin is the main cause of membrane clogging during whey filtration [34–36].

Wang *et al.* studied an enzymatic MBR with transglutaminase, its efficiency, the catalysis of protein crosslinking, and its separation from whey. The protein recovery rate reached 85%, but it decreased over time, as did the relative membrane flow, probably, following the decrease in enzymatic activity on the membrane surface after 1365 min of continuous operation. The overall specific performance of the enzyme bound membrane was about 50% less than that of the pure polyethersulfone membrane. Wang *et al.* concluded that the efficiency failed because of the repulsion forces that appeared between the cross-linked proteins and the membrane [32].

Vasileva *et al.* studied β-galactosidase that was covalently bound by glutaraldehyde to the surface of the modified polypropylene membrane. They determined the optimal hydrolysis conditions for lactose in a batch MBR: enzyme activity 13.6, temperature 40°C, pH 6.8, time 10 h. The scientists compared the resulting degree of hydrolysis with that obtained by a free non-immobilized enzyme. The immobilized enzyme method proved 1.6 times more effective than the one based on a free enzyme, as the immobilized enzyme itself was twice as stable as the free enzyme. The resulting immobilized β-galactosidase/polypropylene membrane system was used to obtain glucose-galactose syrup from whey waste. Vasileva *et al.* carried out hydrolysis of whey lactose in a MBR using an immobilized enzyme and a spiral membrane. The optimal membrane surface and the whey flow rate were 100 cm^2 and 1.0 mL/min, respectively. After 10 h, the lactose hydrolysis reached 91%. After cycle 20, the yield was 69.7% [37].

Sen *et al.* focused on skim milk hydrolysis in a batch MBR using β-galactosidase immobilized on a polyethersulfone membrane with a pore diameter of 30 kDa. The study featured aqueous solutions of skim milk in the concentration range of 30–80 kg/m^3. The solutions underwent deproteinization through two membrane ultrafiltration modules with pore sizes 30 kDa and 5 kDa. As a result, 95–97% of lactose became permeate. The permeates obtained were subjected to hydrolysis in a batch MBR equipped with an enzyme-immobilized membrane. The enzyme was immobilized by cross-linking on an ultrafiltration membrane using 3 and 4% glutaraldehyde. The 4% glutaraldehyde solution provided a greater enzyme activity retention (94.2%) and enzyme loading (98%). The final conversion of lactose was 45.2 and 21.4% when β-galactosidase was immobilized with 4 and 3% glutaraldehyde, respectively. The control experiment with an immobilized enzyme showed a significant decrease in the flow of pure water: 27.5 for 3% glutaraldehyde and 67.5 for 4% glutaraldehyde [38]

When the biocatalyst is confined to the membrane module, not the reservoir with the reagents, it is not recirculated into the outlet flow; with that, low molecular weight products and inhibitors leave the system directly through the membrane. This type of MBR finds application in bio-artificial pancreas or extracorporeal detoxification devices [26].

Biocatalytic MBRs are undoubtedly more efficient, since both the reaction and the separation occur in the same membrane module. However, current knowledge about the nanoscale processes within the microenvironment of the membrane remains insufficient. Equally lacking is the knowledge about the control of continuous hydrolysis at the macroscopic level. As a result, biocatalytic MBRs cannot be used for commercial production [39–41].

Biocatalytic MBRs, or bioreactors, are integrated with such membrane processes as microfiltration, ultrafiltration, reverse osmosis, membrane extraction, etc. They are especially effective for food and beverage production, e.g. wine, fruit juices, milk, etc. [42, 43]. In the dairy industry, MBRs were first used to produce low lactose milk [43]. Such MBRs are still widely used to produce functional products for patients with lactase deficiency. However, lactose is not the only substance that causes milk intolerance: some people cannot absorb high molecular proteins ($\geq$ 5 kDa) due to inadequate immune response. MBRs are also used to produce low-allergenic milk [44].

MBRs are getting more popular in food industry as a result of industrial demand for functional foods, e.g. hypoallergenic, nutraceutical, or alternative foods, ingredients that are part of dietary and preventive

menus, etc. MBRs are actively used in whey processing. The physicochemical composition of whey makes it a very promising raw material for functional food production. Whey contains 0.4–0.8% of protein and 4.4–5.5% of lactose. Whey proteins possess a good latent potential of biofunctional properties [43].

Batch MBRs are simple enough to gain extensive use in the production of protein hydrolysates. However, they need a lot of enzyme, energy, and labor, which makes it expensive [19]. American scientists from the Department of Food Science (Pennsylvania, USA) attempted to process food substrates using batch-type enzyme reactors with an immobilized enzyme. They identified a number of additional disadvantages, e.g. high losses in the activity of the biocatalyst, the expensive enzyme immobilization, etc. [44].

Continuous stirred tank membrane reactors (CSTMR) are an alternative to batch MBRs. They are based on the difference in molecular weight between the enzyme and the hydrolysis products. CSTMRs can separate products from the reaction medium to increase the yield. The soluble enzyme is confined to the retentate side of the membrane, where it comes in contact with the substrate. CSTMRs make it possible to reuse the enzyme and select a suitable membrane pore size, which facilitates the control of the molecular weight of the final product [44].

Ewert *et al*. used a two-stage enzymatic membrane bioreactor (EMBR) to obtain sodium caseinate hydrolyzate with improved antioxidant capacity and reduced bitterness (Fig. 2) [44]. At the first stage, sodium caseinate was hydrolyzed at 65°C and pH 6.7 using endopeptidase Sternzym BP 25201. The stage took 12 h and involved hydrolysis and filtration through a ceramic ultrafiltration membrane made of hollow fiber with a molecular weight cut-off of 10 kDa. The antioxidant activity of the resulting permeate increased by 33%, compared to sodium caseinate. The volume of permeate that left EMBR-1 was automatically compensated for by adding a new substrate to the reactor vessel.

At the second stage, the main objective was to remove bitterness. The hydrolysis was carried out in EMBR-2 using Flavorzyme at 50°C and pH 6.7. After 12 h of hydrolysis, it was filtered through a UV polyethersulfone membrane with a molecular weight cut-off of 10 kDa. EMBR-2 also increased the antioxidant capacity of the permeate to its half-maximal inhibition concentration (IC_{50}) of 13.8 μg/mL, which was 39% more than that of sodium caseinate. The experiment made it possible to avoid the mutual effect of peptidases by separating endo- and exopeptidases at the two stages of hydrolysis. The selected conditions proved optimal and ensured a stable production for three days. The research featured the degree of hydrolysis of biocatalysis products. The hydrolyzate obtained in EMBR-1 had the following parameters: degree of hydrolysis – 8.0 ± 0.2%, permeate – 8.7 ± 0.4%, sediment fraction – 2.9 ± 0.3%. The permeate hydrolyzed in EMBR-2 had a degree of hydrolysis of 21.8 ± 0.8%. The loss of enzymatic activity in both reactor vessels was compensated by the daily addition of the corresponding enzyme. The whole process took 110 h [45].

Due to the applied temperature, the relative activity of peptidase in EMBR-1 decreased to 82 ± 6.9% of its initial value during the preliminary hydrolysis. As for EMBR-2, its initial activity remained the same during the preliminary hydrolysis (26–38 h) and decreased to 82% after 24 h of filtration (38–62 h). The two reactors maintained stable conditions because the activities were adjusted every 24 h. The experiment proved that CSTMRs can be used for commercial production of functional antioxidant ingredients based on sodium caseinate [45].

Guadix *et al.* studied hydrolyzate production of hypoallergenic whey [44]. The research objective was

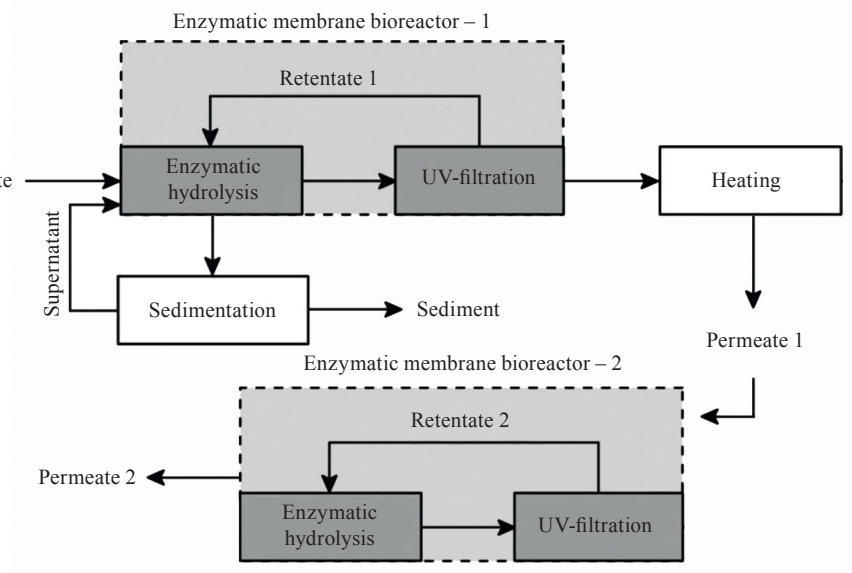

Figure 2 Block diagram of a two-stage installation of a two-stage enzymatic membrane bioreactor with continuous hydrolysis

to create a stable long-term process for the production of whey protein hydrolysates with low antigenicity. The study was based on other scientific schools of continuous hydrolysis. For instance, specialists from the University of Illinois (USA) studied continuous hydrolysis of soy protein from Promin-D in a CSTMR with hollow membrane fibers. At the initial stage, the conversion rate was 90%, which dropped to 60% after 10 h because of the leakage of the enzyme through the membrane and thermal deactivation. The Illinois team also studied milk protein hydrolysis. They hydrolyzed casein with alkalase, also in a CSTMR with hollow fibers. Their experiments determined the efficiency of the reactor at 50 and 37°C. After a 15-h fermentative treatment, the degree of conversion dropped from 96 to 62% at 50°C and from 75 to 51% at 37°C. Like in the first case, the efficiency fell down because of enzyme leakage, thermal deactivation, and enzyme-membrane interactions.

French scientists studied the effect of operating variables on the performance of hollow fiber CSTMRs for hydrolysis of blood plasma proteins using alcalase. After 35 h of operation, the permeate flow dropped due to membrane clogging, which occurred as a result of the polarizing layer that accumulated on the membrane surface. Spanish and Colombian biochemists hydrolyzed whey proteins with alcalase using the same CSTMRs with hollow fibers. They managed to maintain an uninterrupted process only for 7 h because of the rapid clogging and the inactivation of enzymes. Both the proteolysis regimes and the design features of the membranes obviously needed correction.

A team from Taiwan managed to maintain uninterrupted operation for 16 h. In addition to alcaslase, they also included Flavuerzyme into the enzyme preparation. The Laboratory of New Dairy Technologies (France) used CSTMRs to obtain specific bioactive peptides by hydrolysis of casein-macropeptide.

Cow's milk whey is not the only type of whey in such studies. Cambridge specialists studied hydrolysates of goat whey from the point of view of the formation of biologically active peptide compounds. Goat whey was hydrolyzed with pepsin in an enzymatic reactor. The ultrafiltration polymer membrane was combined with a mineral membrane with a cut-off of 30 kDa. Peptides in the permeate were separated by reversed-phase HPLC, which is the most common method for separating milk peptides [46, 47]. As β-lactoglobulin is resistant to pepsin, most opioid and antihypertensive peptides were derived from α-lactalbumin. Pepsin exhibited a considerable substrate specificity; the molecular weights of the obtained peptides ranged from dipeptides to very large peptides with disulfide bridges (150–6900 Da). As a result of the α-lactalbumin hydrolysis, the amount of peptides with a molecular weight of $\leq$ 600 Da was 36%, 600–2000 Da – 24%, and $\geq$ 2000 Da – 40%.

Guadix *et al.* hydrolyzed diluted milk whey concentrate (50 g protein/L) in a CSTMR at 50°C and pH 8.5 using Protex 6L bacterial protease obtained from *Bacillus licheniformis*. The design of the membrane reactor included a 3-L vessel, an automatic controller of pH and temperature, a recirculation pump, and a frame membrane ultrafiltration module with a polyethersulfone plate with an effective area of 0.07 m^2 and a molecular weight cut-off of 3 kDa. The reaction mix was continuously recirculated at a rate of 1.5 L/min with a pump at a rate of 0–15 L/min. The pump was installed between the reaction vessel and the inlet of the membrane module.

As a result of membrane clogging, the permeate flow dropped from 10 mL/min to 6.3 mL/min after 16 h. After 10 h of operation, the degree of hydrolysis stabilized at about 80%, while the permeate flow stabilized after 13 h. As the permeate flow decreased during the first 13 h, the enzymes demonstrated signs of thermal inactivation. The resulting hydrolyzate contained peptides that consisted of four amino acids. The content of antigenic whey protein decreased by 99.97% in the final product, which means that it can be used in hypoallergenic diets, baby food, and enteral feeding. However, the authors had to compensate for the loss of enzymatic activity by feeding small amounts of fresh enzyme [44].

O'Halloran *et al.* developed an EMBR in which the whey protein isolate was subjected to enzymatic hydrolysis to obtain antidiabetic peptides that inhibit dipeptidyl peptidase-IV (DPP-IV). The efficiency grew

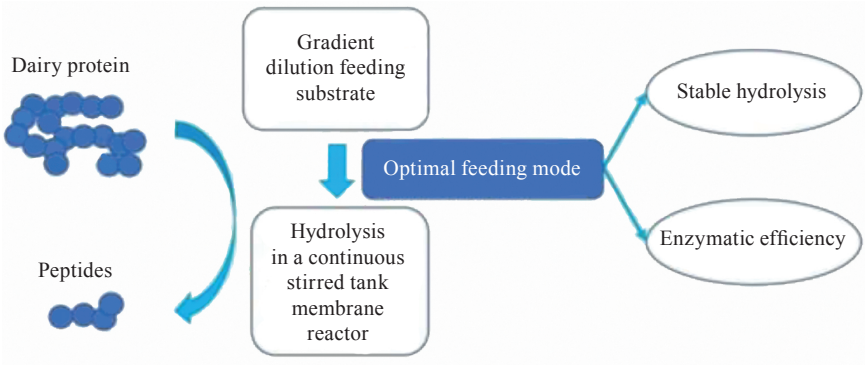

Figure 3 Method of gradient dilution feeding substrate in an enzymatic membrane reactor

by 7.2 and 8.7% when using Protamex and Korolase 2TS, respectively, compared to the standard method of batch processing. Previously, neither of the enzymes was considered effective for obtaining peptides with antidiabetic activity. Protamex and Korolaza 2TS proved capable of producing peptides that inhibit DPP-IV. The permeate hydrolyzate obtained with Protamex showed a 33.7% higher DPP-IV inhibition value compared to the hydrolyzate obtained using Korolase 2TS. J. O'Halloran and colleagues proved that Protamex can be used to produce protein substrates with antidiabetic activity [48].

Huang *et al*. used a CSTMR to improve the yield of peptides that inhibit angiotensin-converting enzyme from milk protein. The research employed a new method of gradient dilution feeding substrate (GDFS) (Fig. 3) [49]. The scientists compared the stability of the hydrolysis process, enzymatic efficiency, and kinetics of the method with the traditional modes of feeding, when adding water after feeding the substrate, or feeding the substrate with a constant concentration. The GDFS method showed the highest membrane flow rate and the lowest fluctuations in the protein concentration in the reactor. GDFS also had a higher rate of protein hydrolysis, which increased by 67.58%. The yield of peptides reached 138.51 g/g neutrase, and the angiotensin-converting enzyme inhibitory activity of hydrolysates was 0.74 mg/mL. The optimal operating time was 720 min. The GDFS method can serve as an alternative method for obtaining highly efficient bioactive peptides [49].

German researchers developed a stable process for obtaining specific hydrolysates with selected biological properties. They developed and tested a continuous reactor system with a ceramic capillary module with various combinations of enzymes and protein substrates (Fig. 4) [49]. Alcalase was immobilized on the surface of capillaries modified with aminosilane with a pore size of 1.5 µm. The loading capacity was 0.3 µg of enzyme per 1 mg of capillary with a residual enzyme activity of 43%. They tested controlled hydrolysis of casein, sunflower, and lupine isolates. Casein hydrolysates proved to possess the largest amount of peptides with enhanced biological properties [50].

A continuous reactor consists of a ceramic capillary with one enzymatic filler. The filler is made of yttrium-stabilized zirconium oxide. It is fixed in a special stainless steel casing (Fig. 4). In a way, this system is a plug flow reactor system. The protein solution is pumped through the capillary module with a peristaltic pump. The capillary module is part of the column oven, which makes it possible to keep the temperature at 37°C. The end of the capillary is sealed with cyanoacrylate cement to inject the flow from the intracapillary space into the extracapillary space. The enzyme is immobilized on the activated surface of the ceramic capillary with an APTES linker. The protein moves through ceramic capillaries by forced convective flow. The immobilization makes it possible to use the entire available capillary surface. As a result, enzymes can be immobilized on the inner and outer surfaces, as well as on the pore walls. One capillary is 10 cm long and has an outer diameter of 1.8 mm, an inner diameter of 1 mm, and an average pore size of 1.5 µm. The ceramic capillary was replaced with a new immobilized enzyme to prevent protein contamination. The residence time of the substrate appeared to be inversely proportional to the flow rate: the longer the residence time of the substrate in the capillary filled with the enzyme, the higher the continuous yield. These continuous reactors produced specific peptides with the desired biologically active properties [50].

New combined hypoallergenic functional products need new methods of gluten reduction. For example, MBRs can be used for wheat processing to create dairy products fortified with vegetable protein, but with hypoallergenic proteins and a low content of lactose and gluten.

Merz *et al*. developed a 96-h continuous hydrolysis of wheat gluten with flavurzim in an EMBR [51].

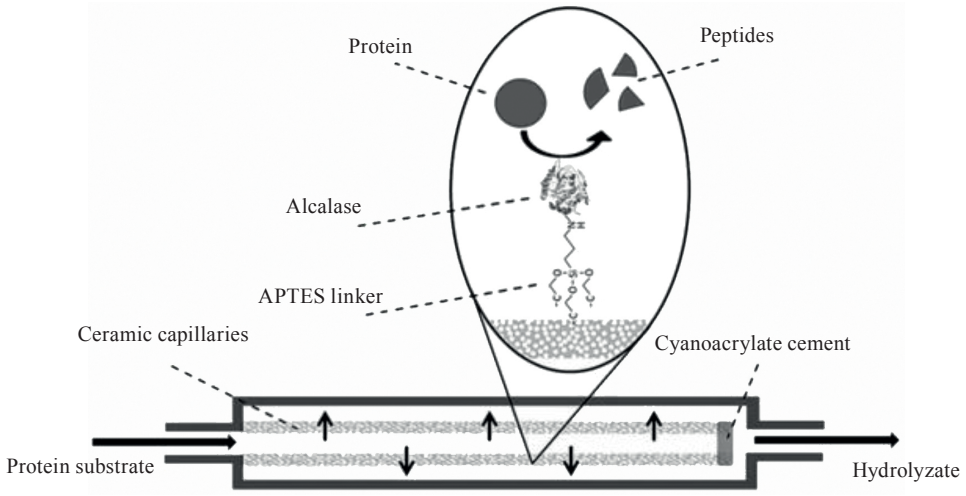

Figure 4 Capillary module that immobilizes enzymes on a ceramic substrate APTES

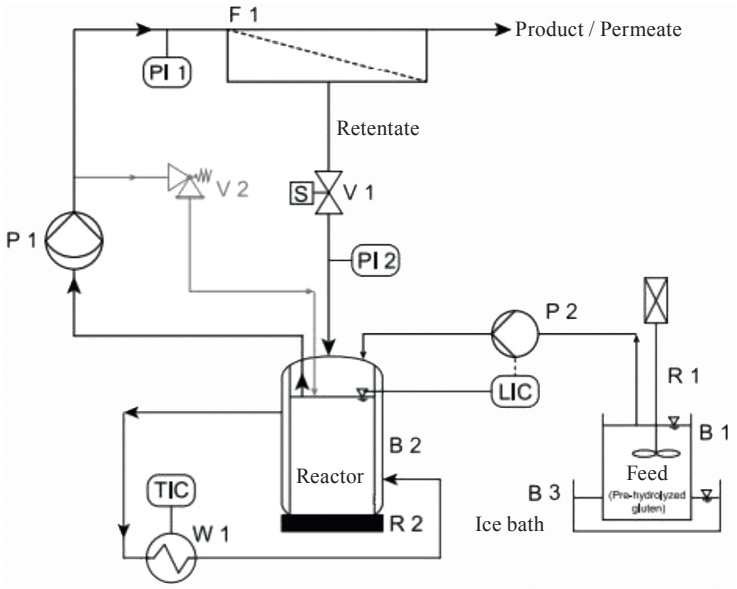

* – the gray line indicates a membrane restart, which is activated if the pressure exceeds 6 bar

Figure 5 Enzymatic membrane reactor with two stirred reactors (B 1, B 2), a water bath (W 1) with a thermostat (TIC), a membrane pump (P 1), a feed pump (P 2), a transverse filtration unit flow (F 1), two barometers (PI 1, PI 2), level indicator (LIC), and valves (V 1, V 2)

Temperature, pump load, and enzyme flow through the membrane were the main criteria for hydrolysis stability and direction. The scientists optimized the hydrolysis to maximize the space-time yield. For microbial stability, they included 8% ethanol with a substrate concentration of 100 g/L at 37°C and pH 7.5 for 96 h (Fig. 5) [51].

A diaphragm pump (P 1) circulated one liter of substrate. The flow rate was 3.3 L/min. Hollow fiber ceramic membranes were 45 mm in length, 6 mm in diameter, and 0.0085 m^2 in surface area. They performed cross-flow ultrafiltration of hydrolysates (F 1) on a membrane with a pore size of 1, 5, or 10 kDa. The hydrolyzate inside the reactor was stirred using a magnetic stirrer (R 2). A constant transmembrane pressure of 2 Bar was adjusted with a ball valve (V 1) and measured with barometers (PI 1, PI 2). The substrate was fed continuously using a tubular pump (P 2). The feed container was kept in an ice bath during the entire test [51]. This EMBR hydrolysis scheme can be cost-effective in the industrial production of hydrolysates from grain proteins.

Russian specialists also developed a CSTMR that produced a hydrolyzate of whey proteins with low residual antigenicity. The installation was based on enzyme preparation alcalase 2.4 L (Fig. 6) [52]. Hydrolysis products were accumulated in an enzymatic medium, which was followed by membrane separation into a purified hydrolyzate (permeate) and an insoluble residue (retentate). The experiment aimed at complete separation of the enzyme to keep it active inside the reactor core.

The scientists reproduced the process described in foreign publications, i.e. protein hydrolysis, combined with the separation of hydrolysis products on ultrafiltration membranes. The resulting hydrolyzate had a low solids content (1.5%). The technology proved commercially unprofitable and expensive. The low solids content resulted from the low cut-off of membranes (5 and 10 kDa). In this case, a portion of hydrolysis products was retained by the elective membranes and remained in the concentrate. Another disadvantage of membranes with a low molecular weight cut-off (≤ 10 kDa) was the low filtration rate and high transmembrane pressure. The latter triggered the formation of a polarization layer and, eventually, membrane clogging [52].

The molecular weight of the enzyme used for protein biocatalysis is the most important parameter for determining the cut-off threshold of membranes. Alcalase, which we used for hydrolysis of whey proteins in our research, has a molecular weight of 24–27 kDa. Membranes with a cut-off threshold of 20 kDa could easily separate an enzyme with such a molecular weight [22]. Such membranes could significantly reduce the transmembrane pressure, thus minimizing the formation of a polarization layer and subsequent membrane clogging.

Separate hydrolysis and filtration made it possible to provide optimal conditions for each of the processes (Fig. 6).

The hydrolysis was carried out under the previously established conditions: substrate concentration – 4.5%; enzyme concentration – 0.5%, hydrolysis temperature –

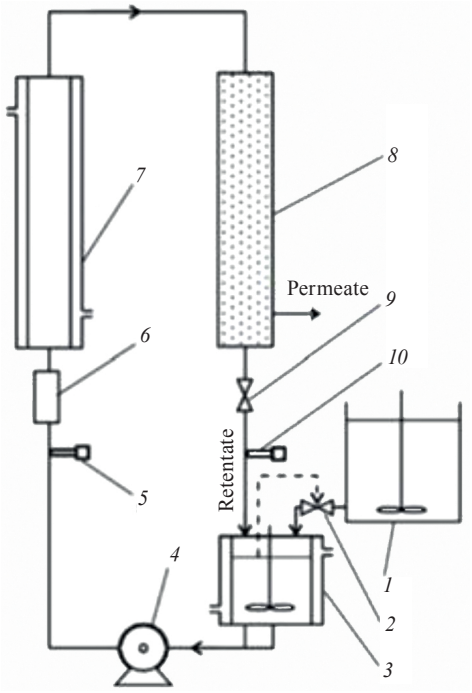

Figure 6 Enzymatic membrane reactor: *1* – container with a substrate for hydrolysis; *2* – tap with an overflow valve, *3* – fermentation reactor, *4* – recirculation pump; *5*, *10* – manometers; *6* – flow meter; *7* – heat exchanger; *8* – membrane module; *9* – retentate dump valve

65°C; hydrolysis time – 1 h. The proteolysis did not include pH-statisation. The initial active acidity of the reaction mix was 10. As for the molecular weight distribution of hydrolysis products, the residues of unhydrolyzed protein were retained during fractionation, which decreased the hydrolyzate yield. However, a double filtration made it possible to increase the yield of the finished product by an average of 6%.

The whey protein hydrolyzate had the following parameters: degree of hydrolysis – 18–25%; mass fraction of ash – 6.5–6.9%; osmolality of a 10% solution – 280–300 mmol/L of water; residual antigenicity – $\leq 2\times10^{-5}$ of the protein mass. The resulting hydrolyzate in the form of a 10% aqueous solution had a clear, moderately bitter taste, without off-flavors. Its antigenic properties make it possible to use it in therapeutic and prophylactic functional foods based on enzymatic protein hydrolysates [30].

CONCLUSION

In addition to batch enzymatic reactors, bioactive peptides are obtained by a semi-continuous reaction or a continuous reaction in an enzymatic membrane reactor (EMBR) [31, 39, 40, 42–45].

Considering the enzymatic efficiency and cost of enzymatic hydrolysis, continuous reaction has obvious advantages. Hydrolysates can promptly be separated from the substrate, the yield of biological peptides can be significantly increased, and enzymes can be used more than once. In addition, the production process is quite simple, which reduces labor costs [47, 48]. As a result, this method is popular in food industry.

Membrane reactors can process a variety of protein food media of plant and animal origin. They have good prospects for whey processing in functional food production. Bioreactors can also be used for the proteolysis of whey proteins with maximal antigenic, antihypertensive, and antidiabetic properties.

Protein hydrolysis in continuous EMBRs is attracting scientific attention because it can simplify the technological process and reduce the cost of the final product while increasing the yield, despite high operating costs. Therefore, the need to improve and develop these technologies is obvious.

CONTRIBUTION

K.A. Ryazantseva supervised the project. E.Yu. Agarkova and O.B. Fedotova conducted the theoretical research, processed the data, and prepared the manuscript.

CONFLICT OF INTEREST

The authors declare that there is no conflict of interests regarding the publication of this article.

REFERENCES

1. Bogatyrev AN, Pryanichnikova NS, Makeeva IA. Natural food – health of the nation. Food Industry. 2017;(8):26–29. (In Russ.).
2. Haritonov VD. Priority directions of food technologies developments. Dairy Industry. 2014;(5):4–5. (In Russ.).
3. Zobkova ZS, Fursova TP, Zenina DV, Gavrilina AD, Shelaginova IR. Fermented milk products as a component of functional nutrition. Dairy Industry. 2019;(2):44–46. (In Russ.).
4. Zobkova ZS, Fursova TP, Zenina DV, Gavrilina AD, Shelaginova IR. Development of the technology for receiving curds product fortified with functional ingredients. Dairy Industry. 2019;(5):44–46. (In Russ.). https://doi.org/10.31515/1019-8946-2019-5-44-46.
5. Zobkova ZS. Funktsional′nye tsel′nomolochnye produkty [Functional whole milk products]. Dairy Industry. 2006;(3):46–52. (In Russ.).
6. Asafov VA, Haritonov VD. New technologies and quality of milk products. Dairy Industry. 2018;(10):39–41. (In Russ.).

7. Minj S, Anand S. Developing a dairy-based health formulation by combining the bioactive properties of whey protein hydrolysates and probiotic organisms. Journal of Dairy Science. 2019;102.
8. Hafeez Z, Cakir-Kiefer C, Roux E, Perrin C, Miclo L, Dary-Mourot A. Strategies of producing bioactive peptides from milk proteins to functionalize fermented milk products. Food Research International. 2014;63:71–80. https://doi.org/10.1016/j.foodres.2014.06.002.
9. Zolotaryov NA, Fedotova OB, Agarkova EYu. Development of the technology of the aerated curds product with whey proteins hydrolysate. Dairy Industry. 2018;(8):52–54. (In Russ.). https://doi.org/10.31515/1019-8946-2018-8-52-54.
10. Donskaya GA, Zaharova EV. Antioxidant properties of milk whey. Dairy Industry. 2010;(9):72–73. (In Russ.).
11. Haritonov VD. Deep processing of raw milk materials and secondary resources. Dairy Industry. 2018;(6):30–31. (In Russ.).
12. Asafov VA, Tankova HL, Iskakova EL. Functional high protein drink with casein hydrolysate and protein fractions of colostrum. Innovations and Food Safety. 2018;20(2):51–54. (In Russ.).
13. Donskaya GA, Drojjyn VM, Morozova VV, Bryzgalina VV. Fermented milks fortified with whey proteins. Dairy Industry. 2017;(6):68–70. (In Russ.).
14. Zobkova ZS. The page of a technologist. Innovative functional milk products. Dairy Industry. 2019;(2):63–64. (In Russ.).
15. Nasri M. Protein hydrolysates and biopeptides: production, biological activities, and applications in foods and health benefits. A review. Advances in Food and Nutrition Research. 2017;81:109–159. https://doi.org/10.1016/bs.afnr.2016.10.003.
16. Dullius A, Goettert MI, de Souza CFV. Whey protein hydrolysates as a source of bioactive peptides for functional foods – Biotechnological facilitation of industrial scale-up. Journal of Functional Foods. 2018;42:58–74. https://doi.org/10.1016/j.jff.2017.12.063.
17. Torkova AA, Ryazantseva KA, Agarkova EYu, Kruchinin AG, Tsentalovich MYu, Fedorova TV. Rational design of enzyme compositions for the production of functional hydrolysates of cow milk whey proteins. Applied Biochemistry and Microbiology. 2017;53(6):580–591. (In Russ.). https://doi.org/10.7868/S0555109917060137.
18. Abd El-Salam MH, El-Shibiny S. Separation of bioactive whey proteins and peptides. In: Grumezescu AM, Holban AM, editors. Ingredients extraction by physicochemical methods in food. A volume in handbook of food bioengineering. Academic Press; 2017. pp. 463–494. https://doi.org/10.1016/B978-0-12-811521-3.00012-0.
19. Ryan MP, Walsh G. The biotechnological potential of whey. Reviews in Environmental Science and Biotechnology. 2016;15(3):479–498. https://doi.org/10.1007/s11157-016-9402-1.
20. Arunkumar A, Molitor MS, Etzel MR. Comparison of flat-sheet and spiral-wound negatively-charged wide-pore ultrafiltration membranes for whey protein concentration. International Dairy Journal. 2016;56:129–133. https://doi.org/10.1016/j.idairyj.2016.01.012.
21. Das B, Sarkar S, Sarkar A, Bhattacharjee S, Bhattacharjee C. Recovery of whey proteins and lactose from dairy waste: A step towards green waste management. Process Safety and Environmental Protection. 2016;101:27–33. https://doi.org/10.1016/j.psep.2015.05.006.
22. Rjazanceva KA, Kruchinin AG, Agarkova EYu, Kharitonov VD. Usage of baromembrane processes in the production technology of yoghurt of functional orientation for dietary-prophylactic nutrition. Storage and Processing of Farm Products. 2015;(5):36–41. (In Russ.).
23. Aita OA, Saad SA, El-Sayed HS. Utilization of sweet whey and ultra filtration-milk permeate in manufacture of yoghurt drink. Middle East Journal of Agriculture Research. 2019;8(4):1091–1102. https://doi.org/10.36632/mejar/2019.8.4.12.
24. Lobasenko BA, Kotlyarov RV, Sazonova EK, Vagaytseva EA, Skomorokov AV. Improvement of low-waste technology of dairy raw material processing using new type membrane equipment. Food Processing: Techniques and Technology. 2019;49(4):587–593. (In Russ.). https://doi.org/10.21603/2074-9414-2019-4-587-593.
25. Argenta AB, Scheer ADP. Membrane separation processes applied to whey: A review. Food Reviews International. 2020;36(5):499–528. https://doi.org/10.1080/87559129.2019.1649694.
26. Brunetti A, Zito PF, Giorno L, Drioli E, Barbieri G. Membrane reactors for low temperature applications: An overview. Chemical Engineering and Processing – Process Intensification. 2018;124:282–307. https://doi.org/10.1016/j.cep.2017.05.002.
27. Bazzarelli F, Piacentini E, Poerio T, Mazzei R, Cassano A, Giorno L. Advances in membrane operations for water purification and biophenols recovery/valorization from OMWWs. Journal of Membrane Science. 2016;497:402–409. https://doi.org/10.1016/j.memsci.2015.09.049.

28. Erdős B, Grachten M, Czermak P, Kovács Z. Artificial neural network-assisted spectrophotometric method for monitoring fructo-oligosaccharides production. Food and Bioprocess Technology. 2017;11(2):305–313. https://doi.org/10.1007/s11947-017-2011-3.
29. Meller K, Szumski M, Buszewski B. Microfluidic reactors with immobilized enzymes – characterization, dividing, perspectives. Sensors and Actuators B: Chemical. 2017;244:84–106. https://doi.org/10.1016/j.snb.2016.12.021.
30. Li NA, Giorno L, Drioli E. Effect of immobilization site and membrane materials on multiphasic enantiocatalytic enzyme membrane reactors. Annals of the New York Academy of Sciences. 2003;984(1):436–452. https://doi.org/10.1111/j.1749-6632.2003.tb06018.x.
31. Giorno L, Zhang J, Drioli E. Study of mass transfer performance of naproxen acid and ester through a multiphase enzyme-loaded membrane system. Journal of Membrane Science. 2006;276(1–2):59–67. https://doi.org/10.1016/j.memsci.2005.09.031.
32. Wang W, Han X, Yi H, Zhang L. The ultrafiltration efficiency and mechanism of transglutaminase enzymatic membrane reactor (EMR) for protein recovery from cheese whey. International Dairy Journal. 2018;80:52–61. https://doi.org/10.1016/j.idairyj.2017.12.012.
33. Zobkova ZS, Fursova TP, Zenina DV, Fedulova LV. The use of transglutaminase to increase the biological value of cottage cheese. Food Industry. 2017;(8):16–19. (In Russ.).
34. Steinhauer T, Hanély S, Bogendörfer K, Kulozik U. Temperature dependent membrane fouling during filtration of whey and whey proteins. Journal of Membrane Science. 2015;492:364–370. https://doi.org/10.1016/j.memsci.2015.05.053.
35. Steinhauer T, Marx M, Bogendörfer K, Kulozik U. Membrane fouling during ultra- and microfiltration of whey and whey proteins at different environmental conditions: The role of aggregated whey proteins as fouling initiators. Journal of Membrane Science. 2015;489:20–27. https://doi.org/10.1016/j.memsci.2015.04.002.
36. Kuzina JI, Manevich BV, Haritonova EB. Enzymes cleaning for regeneration of the ultra-filtration plants. Dairy Industry. 2016;(12):63–65. (In Russ.).
37. Vasileva N, Ivanov Ya, Damyanova S, Kostova I, Godjevargova T. Hydrolysis of whey lactose by immobilized β-galactosidase in a bioreactor with a spirally wound membrane. International Journal of Biological Macromolecules. 2016;82:339–346. https://doi.org/10.1016/j.ijbiomac.2015.11.025.
38. Sen P, Choudhury N, Dutta M, Bhattacharya R. Studies on hydrolysis of skimmed milk using immobilized β-*galactosidase* in a membrane reactor. Materials Today: Proceedings. 2016;3(10):3403–3417. https://doi.org/10.1016/j.matpr.2016.10.021.
39. Mazzei R, Giorno L, Piacentini E, Mazzuca S, Drioli E. Kinetic study of a biocatalytic membrane reactor containing immobilized β-glucosidase for the hydrolysis of oleuropein. Journal of Membrane Science. 2009;339(1–2):215–223. https://doi.org/10.1016/j.memsci.2009.04.053.
40. Giorno L, D'Amore E, Drioli E, Cassano R, Picci N. Influence of OR ester group length on the catalytic activity and enantioselectivity of free lipase and immobilized in membrane used for the kinetic resolution of naproxen esters. Journal of Catalysis 2007;247(2):194–200. https://doi.org/10.1016/j.jcat.2007.01.021.
41. Nath A, Mondal S, Chakraborty S, Bhattacharjee C, Chowdhury R. Production, purification, characterization, immobilization, and application of β-galactosidase: A review. Asia-Pacific Journal of Chemical Engineering, 2014;9(3):330–348. https://doi.org/10.1002/apj.1801.
42. Eş I, Vieira JDG, Amaral AC. Principles, techniques, and applications of biocatalyst immobilization for industrial application. Applied Microbiology and Biotechnology. 2015;99(5):2065–2082. https://doi.org/10.1007/s00253-015-6390-y.
43. Prazeres AR, Carvalho F, Rivas J. Cheese whey management: A review. Journal of Environmental Management. 2012;110:48–68. https://doi.org/10.1016/j.jenvman.2012.05.018.
44. Guadix A, Camacho F, Guadix EM. Production of whey protein hydrolysates with reduced allergenicity in a stable membrane reactor. Journal of Food Engineering. 2006;72(4):398–405. https://doi.org/10.1016/j.jfoodeng.2004.12.022.
45. Ewert J, Claaßen W, Stressler T, Fischer L. An innovative two-step enzymatic membrane bioreactor approach for the continuous production of antioxidative casein hydrolysates with reduced bitterness. Biochemical Engineering Journal. 2019;150. https://doi.org/10.1016/j.bej.2019.107261.
46. Yurova EA. Present day approach to the methods of assessing indices. Dairy Industry. 2016;(4):43–44. (In Russ.).
47. Yurova EA, Denisovich EYu, Mel′denberg DN. Otsenka belkovogo i solevogo sostava molochnoy syvorotki v zavisimosti ot stepeni ee obrabotki [Evaluation of the protein and salt composition of whey depending on the processing degree]. Molochnaya Reka. 2019;76(4):36–38. (In Russ.).
48. O'Halloran J, O'Sullivan M, Casey E. Production of whey-derived DPP-IV inhibitory peptides using an enzymatic membrane reactor. Food and Bioprocess Technology. 2019;12(5):799–808. https://doi.org/10.1007/s11947-019-02253-7.

49. Huang S, Gong Y, Li Y, Ruan S, Roknul Azam SM, Duan Y, et al. Preparation of ACE-inhibitory peptides from milk protein in continuous enzyme membrane reactor with gradient dilution feeding substrate. Process Biochemistry. 2020;92:130–137. https://doi.org/10.1016/j.procbio.2020.02.030.
50. Sewczyk T, Hoog Antink M, Maas M, Kroll S, Beutel S. Flow rate dependent continuous hydrolysis of protein isolates. AMB Express. 2018;8(1). https://doi.org/10.1186/s13568-018-0548-9.
51. Merz M, Eisele T, Claaßen W, Appel D, Rabe S, Stressler T, et al. Continuous long-term hydrolysis of wheat gluten using a principally food-grade enzyme membrane reactor system. Biochemical Engineering Journal. 2015;99:114–123. https://doi.org/10.1016/j.bej.2015.03.019.
52. Sviridenko YuYa, Myagkonosov DS, Abramov DV, Ovchinnikova EG. Development of manufacturing processes of whey protein hydrolyzates using membrane technology. Part 2. Optimizing process conditions for producing whey protein hydrolysates in an enzymatic membrane reactor. Food Industry. 2017;(8):40–43. (In Russ.).

ORCID IDs
Ksenia A. Ryazantseva https://orcid.org/0000-0003-3207-2837
Evgeniya Yu. Agarkova https://orcid.org/0000-0001-8967-7074
Olga B. Fedotova https://orcid.org/0000-0002-7348-6019

Foods and Raw Materials, 2021, vol. 9, no. 2

E-ISSN 2310-9599
ISSN 2308-4057

Research Article
Open Access

https://doi.org/10.21603/2308-4057-2021-2-282-289
Available online at http://jfrm.ru/en

Nutritional, textural, and sensory quality of bars enriched with banana flour and pumpkin seed flour

Umme Habiba[1], Md. A. Robin[1], Md. M. Hasan[1], Maria A. Toma[1], Delara Akhter[2], Md. A. R. Mazumder[1,*]

[1] Bangladesh Agricultural University, Mymensingh, Bangladesh

[2] Sylhet Agricultural University, Sylhet, Bangladesh

* e-mail: anis_engg@bau.edu.bd

Received April 08, 2021; Accepted in revised form May 13, 2021; Published online July 09, 2021

Abstract:

Introduction. Nowadays, health-conscious consumers attend to nutritional, health, and easy-to-use products. Demand for healthy snacks is significantly increasing. Our study aimed to develop high protein nutrition bars by incorporating pumpkin seed flour and banana flour and assess their quality.

Study objects and methods. We analyzed three bar samples for nutritional, textural, and sensory quality. The bars contained banana flour, pumpkin seed flour, and the mixed flour. Proximate analysis was performed following the AOAC method. The mineral content and antioxidant properties of the bars were determined by using emission spectrophotometry and the 2,2-Diphenyl-1-picrylhydrazyl (DPPH) free radical scavenging modified method, respectively.

Results and discussion. The mixed flour nutrition bar had significantly higher total phenolic content and antioxidant activity than the bar with banana flour and the bar with pumpkin seed flour. Textural analysis demonstrated that the mixed flour sample had significantly ($P < 0.05$) higher hardness and color parameters compared to the other bar samples. Nutritional analysis indicated that mixed flour bar contained significantly higher amounts of protein, fat, and calcium; while pumpkin seed flour bar had higher ash, iron, and magnesium contents. The mixed flour sample also had better sensory parameters.

Conclusion. The mixed flour demonstrated good quality. Hence, both banana and pumpkin seed flour have a potential to be used in bar formulations.

Keywords: Nutrition bar, banana, pumpkin seed, flour, nutritional value, textural properties, sensory analysis

Please cite this article in press as: Habiba U, Robin MA, Hasan MM, Toma MA, Akhter D, Mazumder MAR. Nutritional, textural, and sensory quality of bars enriched with banana flour and pumpkin seed flour. Foods and Raw Materials. 2021;9(2):282–289. https://doi.org/10.21603/2308-4057-2021-2-282-289.

INTRODUCTION

Lifestyle changes and dietary habits of human all over the world may affect nutrient intake. Therefore, a healthy and balanced diet is important to meet the basic needs of human body. Accordingly, nutrition bars/cereal bars are the most sophisticated ready-to-eat products due to the natural ingredients and health concerns [1].

Nowadays, a special attention has been given to by-products to utilize raw materials as much as practical and avoid economic losses and environmental pollution. Nutrition or energy bars are getting popular among health aware consumers, school goers, and weight watchers [2] due to its nutritive value and easy-to-use. The increasing demand of consumers for nutritious snacks, results the fastest outgrowth in cereal bars market more than 20% per year [3] that provide nutrition and convenience [4].

Health-conscious consumers prefer nutritious foods to conventional sweets. This tendency driven to the development of several ready-to-eat, nutritious, and energy bars containing different fruits and nuts [5–6]. Incorporation of fruit and vegetable by-products in nutrition bars not only adds the value to products but also contributes to newly formulated food products and minimize losses of raw materials by utilizing peels, seeds, etc. [7].

Modern consumers prefer snacks not only to satisfy their hunger but also to provide themselves with essential nutrients. In this regard, food scientists today are aiming to develop formulations of cereal bars with various highly nutritious ingredients. Thus, Russian scientists have developed a cereal bar with rolled oat flakes, bee honey, walnut, dried cranberry, sunflower seeds, peanut butter, dates, and prunes [8].

Snacks satisfy hunger, replace a meal, and provide the body with essential nutrition, including protein, carbohydrates, fats, and vitamins [9–10]. One of the popular fruits in Bangladesh is banana [11], which is a rich source of energy (90 kcal/100 g) [12]. In addition, banana contains health benefiting antioxidants, crude fiber, and minerals [13]. Health beneficiary effect of banana pulp is due to bioactive compounds [14] such as phenolic acid compounds, flavonoids, carotenoids, sterols, and antimicrobial compounds. The compounds make banana a perfect functional food [15].

Russian researchers revealed that main sources of vegetable protein are seeds of legumes and oilseeds [16]. Pumpkin (*Cucurbita pepo* L.) seed has also received considerable attention due to its nutritional value (200 calories) and high content of amino acids, such as palmitic, oleic, linoleic, and stearic, as well as dietary fiber [17]. Pumpkin seed also shows pharmacological activities including anti-fungal [18], anti-cancer [19], anti-bacterial, anti-inflammation, and anti-oxidant effects [20]. The robust flavor of pumpkin seed allows using it as a valuable ingredient in cooking [21]. Pumpkin seed oil obstructs changes in plasma lipids and blood pressure together with inadequate estrogen availability [22].

Recent research on pumpkin seed flour indicated that it increased reducing sugars, vitamin C, and carotenoid content in bread [23]. 10% of pumpkin seed flower in a cake formulation had strong effects on physicochemical and organoleptic properties of the cake [24]. Replacement of refined wheat flower with pumpkin seed flower improved the textural and sensory qualities of cookies [25]. Addition of 15% of pumpkin seed flower into biscuit dough had a significant effect on the rheological and sensory characteristics of the final product [26].

Searching safe methods to extend the shelf life of food products is a relevant task for the food industry. Banana and pumpkin seed demonstrate significant anti-oxidant properties. Natural antioxidants can be an alternative to existing preservatives due to its ability to inhibit oxidation of the main nutrients [27]. An increasing growth of metabolic diseases and obesity worldwide is a global problem that makes food scientists and researchers develop not only tasty but also health beneficial snacks.

In Bangladesh, mango or peanut bars with glucose syrup are popular among the population, however, their nutritional value is low and energy value is high. We did not find research on the quality of bars enriched with pumpkin seed flour. The findings of this work will be beneficial for the local food industry and will reduce malnutrition problems.

Our work aimed to formulate bars with banana flour and pumpkin seed flour and evaluate their nutritional, textural, and sensory quality.

STUDY OBJECTS AND METHODS

Our research featured nutritional bars with banana flour, pumpkin seed flour, and the mix of banana and pumpkin seed flours.

Materials. Raw materials, such as brown sugar, sunflower oil, oats, corn flakes, chickpea, nuts, and raisins, were purchased from the local supermarket. All the ingredients were purchased evaluated for safety standards. The following technical and food safety information was evaluated: name of the products with batch number, physicochemical composition, information about recognized food allergens, sensory properties (appearance, flavor, and aroma), microbial information, and shelf life. To store the ingredients, we used high-density polyethylene and low-density polyethylene as a packaging material.

Pumpkin seed flour preparation. Pumpkin seed was collected from the local market as a by-product of pumpkin processing. Seeds were cleaned with potable water and sun dried to remove extra water from the surface of the seeds. After that, the pumpkin seed with shell was dried in a cabinet dryer (M-1816, Modern Laboratory Equipment, USA) at 55°C for 4 h, ground using a grinder (Panasonic Mixer Grinder MX-AC555, India), and finally sieved through 20 mesh (0.841 mm) to get fine pumpkin seed flour. Then the pumpkin seed flour was weighed and vacuum packed for further use.

Banana flour preparation. Ripe banana (Sagor variety) was collected from the Horticulture center of Bangladesh Agricultural University, Bangladesh. Banana was sorted to remove defected banana and washed with running water. Banana was sliced into 0.5 cm thick pieces with peel. To reduce enzymatic browning, the slices were then dipped in 10% citric acid solution for 10 min. The peel was removed and sliced banana was air dried to remove extra water. Banana then was dried in a cabinet dryer (M-1816, Modern Laboratory Equipment, USA) at 60°C for 5 h, ground using a grinder (Panasonic Mixer Grinder MX-AC555, India), and sieved through 30 mesh (0.595 mm) to get fine flour. The banana flour was vacuum packed for further use.

Bar preparation. Three nutrition bars were formulated: with banana flour, with pumpkin seed flour, and with the mixed flours (Table 1). Amounts of banana flour, pumpkin seed flour, salt, and lecithin were chosen based on trial and error methods to find the optimum color and texture of the bars. Similarly, the other ingredients were chosen based on consumer interest by survey (data not shown).

Figure 1 demonstrates the production process of nutrition bars. At first, all the dry ingredients, such as oats, corn flakes, pumpkin seed flour and/or banana flour, nuts, raisins, chickpea, and skim milk powder, were weighed and mixed gently. The heated sugar syrup, sunflower oil, and lecithin were added into the dry mixture and mixed. The mixture was heated in a water bath at 70°C. The mixture then was compressed, dried in an oven at 110°C for 15 min, and cut into uniform pieces (12×2.5×2.0 cm) and cooled at room temperature (25°C) for 30 min. The bars were packed in low and high density package and then kept in a sealed container at ambient temperature for further analysis.

Table 1 Formulation of nutrition bars with banana flour, pumpkin seed flour, and mixed flour, g/100 g

Ingredient	Bars with:		
	Banana flour	Pumpkin seed flour	Mixed flour
Oats	10	10	10
Corn flakes	10	10	10
Pumpkin seed flour	0	15	10
Banana flour	15	0	5
Sunflower oil	10	10	10
Nuts	7	7	7
Raisins	6	6	6
Water	6	6	6
Salt	0.2	0.2	0.2
Lecithin	0.8	0.8	0.8
Glucose syrup	10	10	10
Brown sugar	10	10	10
Chickpea	5	5	5
Skim milk powder	10	10	10

The proximate analysis of pumpkin seed flour, banana flour and newly formulated bars were determined by Tasnim *et al.* [28] using the guidelines and methods of AOAC (Association of Official Analytical Chemists): moisture content – method 950.46; crude protein, 981.10; crude fat, 922.06; crude fiber, 978.10; and ash, 920153.00. Total carbohydrate contents in the both flours and nutrition bar were estimated according to the methods of Food and Agriculture Organization (FAO) [29]. Mineral contents were determined following the procedures described in [30]. Inductively coupled plasma emission spectrophotometer was used to analyze calcium, iron, magnesium, phosphorus, and potassium in the samples.

The antioxidant activities of flours and nutrition bars were determined by using the 2,2-Diphenyl-1-picrylhydrazyl (DPPH) free radical scavenging modified method, as described by Brand-Williams *et al.* [31]. In methanol, DPPH in oxidized form gives a deep violet color. However, antioxidant compounds usually denote an electron to DPPH, thus causing reduction. In reduction form, DPPH turns to yellow. A 0.002% DPPH solution was prepared in methanol and measured at 517 nm. Sample extracts (50 µL) were mixed with 3 mL of the DPPH solution and kept for 15 min in the dark. Then the absorbance was measured again at 517 nm.

The total phenolic content in the banana flour, pumpkin seed flour, and nutrition bar was determined using the modified method of Odabasoglu *et al.* [32]. The total phenolic content of the samples was calculated as gallic acid equivalents (mg GAE/g) and every experiment was performed in triplicate. Peroxide value, free fatty acids, and thiobarbuturic acid (MA/kg sample), which are generally used to evaluate lipid oxidation in food products, were measured in accordance with Rukunudin *et al.*, Sallam *et al.* and Schmedes and Holmer, respectively [33–35].

The color characteristics of the nutrition bar were determined using a Minolta colorimeter (Cr-400/410, Japan). The CIELB scale with L^*, a^* and b^* was used to analyze the results, where L^* showed the lightness ($L^* = 0$, black and $L^* = 100$, white) of the product, a^* showed red-green color (+60 to –60), and b^* showed yellow-blue color (+60 to –60) [36].

The textural parameters of the nutrition bar under the study (12×2.5×2.0 cm) were determined using a texture analyzer (Stable Micro Systems, UK) and the modified method described by Momin *et al.* [37]. The cutting probe and compression platen of the texture

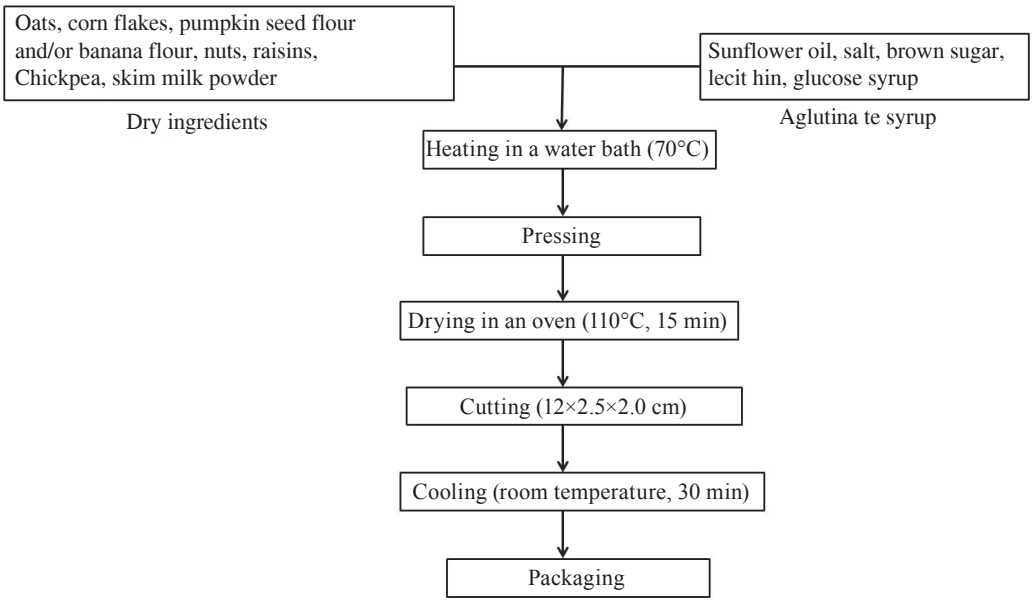

Figure 1 Flowchart of nutrition bar production process

Table 2 Nutrient content of pumpkin seed flour and banana flour (per 100 g)

Ingredients	Pumpkin seed flour	Banana flour
Moisture, %	1.20[b] ± 0.05	3.00[a] ± 0.75
Carbohydrate, %	14.47[b] ± 1.00	78.30[a] ± 1.50
Protein, %	29.54[a] ± 1.50	3.9[b] ± 0.50
Fat, %	47.6[a] ± 2.35	1.8[b] ± 0.45
Crude fiber, %	2.13[b] ± 0.25	9.9[a] ± 1.15
Calcium, mg	30.07[a] ± 2.00	22.96[b] ± 2.50
Magnesium, mg	1103.19[a] ± 10.50	108.05[a] ± 5.25
Phosphorus, mg	3205.13 [a] ± 11.20	74.54 [a] ± 3.50
Iron, mg	0.31 [a] ± 0.01	1.22 [a] ± 0.04
Potassium, mg	809.03 [a] ± 3.25	1491.88 [a] ± 8.50
Energy, kcal	604.44	385.00

Values are expressed as mean ± SD. Means in the same row with different superscripts were significantly different ($P \leq 0.05$)

analyzer were calibrated at a 20 cm distance using data acquisition software. The following parameters were used for the analysis: pre-test speed 1.0 mm/s, trigger 5 g, and post-test speed 10 mm/s. Each sample was texted in three replications.

Three different types of the nutrition bars were evaluated by 10 semi-trained panelists for color, flavor, texture, and overall acceptability. For statistical analysis, the 9-point hedonic rating test [38] was used to access the sensory quality of the newly nutrition bar. The analysis was performed three times. The significant difference of mean values was assessed by the analysis of variance (ANOVA) using a software STATISTIC version 8.1. For the significant difference, DMRT was applied.

RESULTS AND DISCUSSION

Table 2 shows the nutrient composition of pumpkin seed flour and banana flour. It is remarkable that the pumpkin seed flour contained significantly ($P < 0.5$) higher amount of protein and fat but lower amount of water, crude fiber, and carbohydrate, compared to the banana flour. Among the minerals, calcium, magnesium, and phosphorus concentrations were higher in the pumpkin seed flour and iron and potassium was higher in the banana flour (Table 2). The energy value of the pumpkin seed flour (604.44 kcal/100 g) was also higher than that of the banana flour (385 kcal/100 g).

a b c

Figure 2 Appearance of nutrition bars with banana flour (a), pumpkin seed flour (b), and the mix of banana and pumpkin flour (c)

The nutrition bars developed (Fig. 2) were analyzed to determine their nutritional value (Table 3). Dietary protein is one of the vital nutrients for human due to its functional properties, including the improving of health growing of muscles [28, 39]. All the nutrition bars under study may easily supply recommended daily allowance for protein. The mixed nutrition bar contained significantly higher amount of protein compared to the others.

The fat content of the mixed bar sample was significantly higher than of the sample with banana flour and the bar with the pumpkin seed flour. The ash content was higher in the pumpkin seed flour bar, which did not significantly differ from the mixed flour sample.

The total carbohydrate content solely depends on the other nutrient components of the nutrition bars. The mixed flour nutrition bar had the lowest carbohydrate (66.11%) content compared to the pumpkin seed flour (73.19%) and banana flour (80.20%) nutrition bar. The banana flour and mixed flour nutrition bars had the lowest and highest energy values, respectively (398.60 and 424.94 kcal/100 g).

Table 3 Nutritional composition of nutrition bars with banana flour, pumpkin seed flor, and mixed flour

Composition	Banana flour	Pumpkin seed flour	Mixed flour
Moisture content, %	6.94[a] ± 1.0	6.61[a]±1.25	6.82[a] ± 1.55
Ash content, %	1.16[b] ± 0.05	1.46[a] ± 0.35	1.32[a] ± 0.50
Protein content, %	5.50[c] ± 0.75	9.74[b] ± 1.15	14.25[a] ± 1.55
Fat content, %	6.20[c] ± 0.50	9.05[b] ± 0.45	11.50[a] ± 0.75
Carbohydrate content, %	80.20[a] ± 2.50	73.19[b] ± 3.05	66.11[b] ± 3.00
Energy content, kcal	398.60[b] ± 3.00	412.72[a] ± 2.75	424.94[a] ± 1.80
Calcium (Ca), mg	3.75[b] ± 0.05	3.10[c] ± 0.25	4.90[a] ± 0.75
Iron (Fe), mg	0.04[b] ± 0.02	0.2[a] ± 0.05	0.05[b] ± 0.03
Magnesium (Mg), mg	15.20[c] ± 0.05	153.45[a] ± 5.00	118.25[b] ± 4.25
Phosphorus (P), mg	10.20[c] ± 1.10	450.75[a] ± 2.55	345.20[b] ± 2.35
Potassium (K), mg	115.20[c] ± 5.20	220.45[a] ± 5.55	150.79[b] ± 4.75

Values are expressed as mean ± SD. Means in the same row with different superscripts were significantly different ($P \leq 0.05$)

Table 4 Total phenolic content, antioxidant activity, and textural properties of nutrition bar with different types of flour

Nutrition bar	Total phenolic content, mg GAE	DPPH inhibition, %	Texture analysis	
			Hardness, gf	Fracturability, s
Banana flour	$7.10^{b} \pm 0.03$	$40.50^{b} \pm 0.35$	$41254.00^{b} \pm 210.80$	$17.85^{b} \pm 2.10$
Pumpkin seed flour	$6.45^{c} \pm 0.07$	$38.25^{c} \pm 0.45$	$39806.00^{c} \pm 205.07$	$17.50^{b} \pm 1.35$
Mixed flour	$8.55^{a} \pm 0.05$	$45.35^{a} \pm 0.10$	$47453.00^{a} \pm 195.70$	$18.95^{a} \pm 2.45$

Values are expressed as mean ± SD. Means in the same column with different superscripts were significantly different ($P \leq 0.05$)

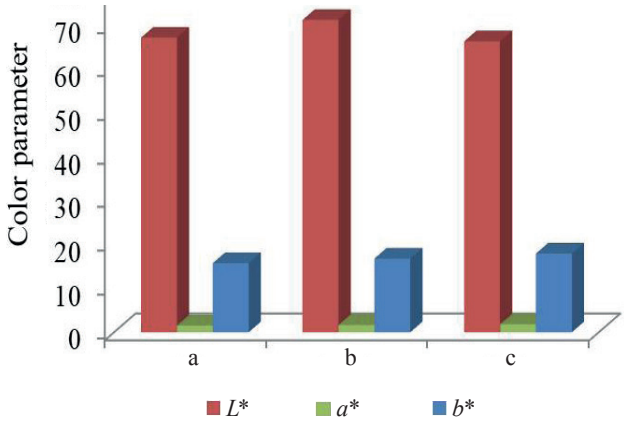

Figure 3 Color parameter of nutrition bar with banana flour (a), pumpkin seed flour (b), and the mix of the flour (c)

Iron is an essential element whose deficiency causes anemia [40]. According to Institute of Medicine, Food and Nutrition Board, iron and calcium contents in 100 g of the nutrition bars would contribute less than 4 and 10%, respectively, of recommended daily allowance for men aged 19–50 years reported in 2001 [41]. Our results also indicated that 100 g of the nutrition bars with pumpkin seed flour, banana flour, and mixed flours would provide more than 45, 32, and 10% of phosphorus, respectively [42].

The total phenolic content was found to be highest in the mix flour bar (8.55 ± 0.05 mg GAE/g), compared to that in the banana flour and pumpkin seed flour samples (7.10 ± 0.03 and 6.45 ± 0.07 mg GAE/g, respectively (Table 4). Phenolics combat with free radicals, which are harmful to human, and stop their further activity [43]. DPPH inhibition level indicates free radical scavenging property and is a measure of antioxidant potential. The DPPH radical scavenging activity of the nutrition bars depended on an amount of phenolics in the banana flour, pumpkin seed flour, chickpea, and raisins. Food materials rich in phenolics exhibit a high DPPH inhibition level as reported by Abu El-Baky, who studied phenolic compounds in spirulina and their protective properties [44]. In our research, the mixed flour nutrition bar demonstrated the highest DPPH inhibition level (45.35 ± 0.10%) and, consequently, better antioxidant activity. The lowest one was found to be 38.25 ± 0.45% (pumpkin seed flour).

The textural properties of the bar samples were measured using a texture analyzer and included hardness and fracturability (Table 4). The mix sample had the highest hardness, while the pumpkin seed flour bar showed the lowest hardness. Fracturability of banana flour bar was the lowest but it did not significantly differ from that of the banana sample, so their textural properties were close. Among the other samples, the pumpkin seed flour bar had the least hardness.

The color of food products is a critical parameter, especially for bars, which are potentially targeted on children and women. Figure 3 shows the color parameters for the nutrition bars. There was a significant difference ($P < 0.05$) in L^* values among all the samples. This could be due to the presence of polyphenols in banana flour, pumpkin seed flour, and chick pea. The pumpkin seed flour bar showed a lower L^* value than the other bars.

All the nutrition bars demonstrated positive a^* (redness) and b^* values (yellowness). The pumpkin seed flour sample had significantly ($P < 0.5$) higher a^* value than the other nutrition bars, which can be explained by the presence of higher polyphenol concentrations in the raw materials such as pumpkin seed flour and chick pea. The positive b^* value of all the nutrition bars could be due to the presence of cornflakes, chickpea, and pumpkin seed flour.

Table 5 Sensory evaluation of nutrition bars

Nutrition bars	Sensory attributes				
	Color	Flavor	Texture	Taste	Overall acceptability
Banana flour	$6.60^{a} \pm 0.50$	$5.80^{a} \pm 0.65$	$5.80^{a} \pm 0.85$	$5.20^{a} \pm 0.50$	$5.20^{a} \pm 0.85$
Pumpkin seed flour	$6.90^{b} \pm 0.43$	$7.20^{b} \pm 0.50$	$6.80^{b} \pm 0.65$	$6.20^{a} \pm 0.80$	$6.60^{b} \pm 0.95$
Mixed flour	$7.80^{c} \pm 0.72$	$8.20^{c} \pm 0.95$	$7.20^{b} \pm 0.45$	$7.60^{b} \pm 0.75$	$7.80^{c} \pm 0.55$
LSD value	0.96	0.94	0.94	1.16	0.96

Values are expressed as mean ± SD. Means in the same column with different superscripts were significantly different ($P \leq 0.05$)

Table 6 Changes in moisture, peroxide value, free fatty acids, and thiobarbuturic acid in the bar with banana and pumpkin seed flours stored at 25°C and packed in low density polyethylene (LDP) and high density polyethylene (HDP)

Attributes	Packaging materials	Storage periods, days		
		0	30	60
Moisture, %	LDP	6.82^{c}	7.37^{bA}	7.76^{aA}
	HDP		6.93^{cdB}	7.01^{cB}
Peroxide value, meq O_2/kg fat	LDP	0.9^{e}	4.2^{cA}	7.5^{aA}
	HDP		3.8^{B}	6.7^{bB}
Free fatty acids, % oleic acid	LDP	1.7^{c}	2.1^{bA}	2.5^{aA}
	HDP		2.0^{bA}	2.1^{bB}
Thiobarbituric acid value, MA/kg sample	LDP	0.19^{d}	0.25^{bA}	0.30^{aA}
	HDP		0.23^{cB}	0.26^{bB}

Different uppercases in columns lowercases in rows indicate significant difference ($P \leq 0.05$). Values are mean ± SD of three measurements

Sensory assay of the newly nutrition bars included color, flavor, texture, taste, and overall acceptability (Table 5). The analysis showed that there was a significant ($P < 0.5$) difference in the sensory attributes among banana flour, pumpkin seed flour, and mixed flour bars. However, the sample with mixed flour demonstrated better sensory properties compared to the other nutrition bars.

We assessed changes in lipid peroxidation in the nutrition bar with the mix of banana flour and pumpkin seed flour during two months of storage at room temperature (25°C). Peroxide value, free fatty acids, and thiobarbuturic acid values of the bar sample are demonstrated in Table 6.

On day 60, the moisture content in the sample slightly increased, regardless of the packaging material used. Between the packaging materials (low-density polyethylene and high-density polyethylene), a significant difference ($P < 0.5$) was observed in the moisture content. Chemical changes in the mixed bar were found low in the samples packed in the high-density polyethylene compared to those packed in the low-density polyethylene. After two months of storage, peroxide value, free fatty acids, and thiobarbuturic acid in the mixed nutrition bar became 7.5, 2.1., and 1.5 times higher, respectively.

CONCLUSION

We evaluated the quality of nutrition bars containing banana flour, pumpkin seed flour, and mixed flour. The samples with both banana flour and pumpkin seed flour (mixed flour) showed good nutritional quality, with higher amount of protein (14.25 ± 1.55%), fat (11.50 ± 0.75%), and calcium (4.90 ± 0.75 mg/100 g) content compared to the other bars. However, the sample based on pumpkin seed flour demonstrated higher amount of ash (1.46 ± 0.35 mg/100 g), magnesium (153.45 ± 5.00 mg/100 g), potassium (450.75 ± 2.55 mg/100 g), and phosphorus (220.45 ± 5.55 mg/100 g) content.

Antioxidant activity (45.35 ± 0.10% DPPH inhibition), total phenolic content (8.55 ± 0.05 mg GAE/bar), and textural properties (47453 ± 195.70 gf hardness and 18.95 ± 2.45 s fracturability) were significantly the highest in the mixed flour nutrition bar. Sensory analysis found that the mixed flour nutrition bar was attributed as the best formulation.

Thus, banana flour and pumpkin seed flour showed considerable potential as ingredients in the formulation of nutrition bars and improved their nutrient value. Further studies are needed to determine the shelf life and *in vivo* metabolism of nutrition bars enriched with banana flour and/or pumpkin seed flour.

CONTRIBUTION

U. Habiba: conceptualization, methodology, investigation, visualization, and drafting manuscript. M.A. Robin: conceptualization, investigation, visualization, and drafting manuscript. M.M. Hasan: conceptualization, investigation, and drafting manuscript. M.A. Toma: data analysis, methodology, drafting manuscript, and writing. D. Akhter: data analysis and writing. M.A.R. Mazumder: conceptualization, methodology, project administration, writing, and supervision.

CONFLICT OF INTEREST

The authors declare no conflict of interest.

ACKNOWLEDGMENTS

The authors gratefully acknowledge Department of Food Technology and Rural Industries, Bangladesh Agricultural University, Bangladesh for project work research grants.

REFERENCES

1. Grden L, Oliveira CS, Bortolozo EAFQ. Elaboration of a cereal bar as a compensating food for physical activity practitioners and athletes. Brazilian Journal of Agroindustrial Technology. 2008;2(1):87–94. (In Port.). https://doi.org/10.3895/S1981-36862008000100008.
2. Rawat N, Darappa I. Effect of ingredients on rheological, nutritional and quality characteristics of fibre and protein enriched baked energy bars. Journal of Food Science and Technology. 2015;52(5):3006–3013. https://doi.org/10.1007/s13197-014-1367-x.
3. Lin P-H, Miwa S, Li Y-J, Wang Y, Levy E, Lastor K, et al. Factors influencing dietary protein sources in the PREMIER trial population. Journal of the American Dietetic Association. 2010;110(2):291–295. https://doi.org/10.1016/j.jada.2009.10.041.

4. Izzo M, Niness K. Formulating nutrition bars with inulin and oligofructose. Cereal Foods World. 2001;46(3):102–106.
5. da Silva EP, Siqueira HH, do Lago RC, Rosell CM, Vilas Boas EVDB. Developing fruit-based nutritious snack bars. Journal of the Science of Food and Agriculture. 2014;94(1):52–56. https://doi.org/10.1002/jsfa.6282.
6. Sun-Waterhouse D, Teoh A, Massarotto C, Wibisono R, Wadhwa S. Comparative analysis of fruit-based functional snack bars. Food Chemistry. 2010;119(4):1369–1379. https://doi.org/10.1016/j.foodchem.2009.09.016.
7. Naves LP, Corrêa AD, de Abreu CMP, dos Santos CD. Nutrients and functional properties in pumpkin seed (*Cucurbita maxima*) submitted to different processings. Ciencia e Tecnologia de Alimentos. 2010;30(1):185–190. (In Port.). https://doi.org/10.1590/S0101-20612010000500028.
8. Laricheva K, Mikhailova O. Development of scientifically-based recipe and technology for the production of natural honey-based muesli bar. IOP Conference Series: Earth and Environmental Science. 2020;613(1). https://doi.org/10.1088/1755-1315/613/1/012067.
9. Hogan AS, Chaurin V, O'Kennedy BT, Kelly PM. Influence of dairy proteins on textural changes in high-protein bars. International Dairy Journal. 2012;26(1):58–65. https://doi.org/10.1016/j.idairyj.2012.02.006.
10. Anitha G, Rajyalakshmi P. Value added products with popular low-grade rice varieties of Andhra Pradesh. Journal of Food Science and Technology. 2014;51(12):3702–3711. https://doi.org/10.1007/s13197-012-0665-4.
11. Parvin MM, Islam N, Islam F, Habibullah M. An analysis of cost of production of banana and profitability at Narsingdi and Gazipur district in Bangladesh. International Journal of Research in Commerce, IT and Management. 2013;3(5):113–118.
12. Emaga TP, Bindelle J, Agneesens R, Buldgen A, Wathelet B, Paquot M. Ripening influences banana and plantain peels composition and energy content. Tropical Animal Health and Production 2011;43(1):171–177. https://doi.org/10.1007/s11250-010-9671-6.
13. Kumar KPS, Bhowmik D, Duraivel S, Umadevi M. Traditional and medicinal uses of banana. Journal of Pharmacy and Phytochemistry. 2012;1(3):51–63.
14. Ovando-Martinez M, Sáyago-Ayerdi S, Agama-Acevedo E, Goñi I, Bello-Pérez LA. Unripe banana flour as an ingredient to increase the undigestible carbohydrates of pasta. Food Chemistry. 2009;113(1):121–126. https://doi.org/10.1016/j.foodchem.2008.07.035.
15. Boua BB, Ouattara D, Traoré L, Mamyrbekova-Békro JA, Békro Y-A. Effect of domestic cooking on the total phenolic, flavonoid and condensed tannin content from plantain of Côte d'Ivoire. Journal of Materials and Environmental Sciences. 2020;11(3):396–403.
16. Zverev SV, Nikitina MA. Balance of protein supplements according to the criterion of convertible protein. Food Systems. 2019;2(1):16–19. https://doi.org/10.21323/2618-9771-2019-2-1-16-19.
17. Nkosi CZ, Opaku AR. Antioxidative effects of pumpkin seed (*Cucurbita pepo*) protein isolate in CCl_4-induced liver injury in low-protein fed rats. Phototherapy Research. 2006;20(11):935–940. https://doi.org/10.1002/ptr.1977.
18. Xie JM. Induced polarization effect of pumpkin protein on B16 cell. Fujian Medical University Acta. 2004;38: 394–395.
19. Jian L, Du C-J, Lee AH, Binns CW. Do dietary lycopene and other carotenoids protect against prostate cancer? International Journal of Cancer. 2005;113(6):1010–1014. https://doi.org/10.1002/ijc.20667.
20. Stevenson DG, Eller FJ, Wang L, Jane J-L, Wang T, Inglett GE. Oil and tocopherol content and composition of pumpkin seed oil in 12 cultivars. Journal of Agriculture and Food Chemistry. 2007;55(10):4005–4013. https://doi.org/10.1021/jf0706979.
21. Herbst ST. The new food lover's companion: Comprehensive definitions of nearly 6,000 food, drink, and culinary terms. Barrons Educational Series; 2001. 772 p.
22. Gossell-Williams M, Lyttle K, Clarke T, Gardner M, Simon O. Supplementation with pumpkin seed oil improves plasma lipid profile and cardiovascular outcomes of female non-ovariectomized and ovariectomized Sprague-Dawley rats. Phytotherapy Research. 2008;22(7):873–877. https://doi.org/10.1002/ptr.2381.
23. Rakcejeva T, Galoburda R, Cude L, Strautniece E. Use of dried pumpkins in wheat production. Procedia Food Science. 2011;1:441–447. https://doi.org/10.1016/j.profoo.2011.09.068.
24. Jesmin AM, Ruhul AM, Chandra MS. Effect of pumpkin powder on physico-chemical properties of cake. International Research Journal of Biological Sciences. 2016;5(4):1–5.
25. Sudipta D, Soumitra B, Jayanti P. Utilization of foam mat dried pumpkin powder as a source of nutraceuticals content in cookies. Annals Food Science and Technology. 2015;16(2):338–346.
26. Khan MA, Mahesh C, Vineeta P, Sharma GK, Semwal AD. Effect of pumpkin flour on the rheological characteristics of wheat flour and on biscuit quality flours. Journal of Food Processing and Technology. 2019;10(10). https://doi.org/10.35248/2157-7110.19.10.814.

27. Kupaeva NV, Kotenkova EA. Search for alternative sources of natural plant antioxidants for food industry. Food Systems. 2019;2(3):17–19. https://doi.org/10.21323/2618-9771-2019-2-3-17-19.
28. Tasnim T, Das PC, Begum AA, Nupur AH, Mazumder MAR. Nutritional, textural and sensory quality of plain cake enriched with rice rinsed water treated banana blossom flour. Journal of Agriculture and Food Research. 2020;2. https://doi.org/10.1016/j.jafr.2020.100071.
29. Food energy – methods of analysis and conversion factors. Rome: Food and Agriculture Organization; 2003. 93 p.
30. Poitevin E. Determination of calcium, copper, iron, magnesium, manganese, potassium, phosphorus, sodium, and zinc in fortified food products by microwave digestion and inductively coupled plasma-optical emission spectrometry: Single-laboratory validation and ring trial. Journal of AOAC International. 2012;95(1):177–185. https://doi.org/10.5740/jaoacint.CS2011_14.
31. Brand-Williams W, Cuvelier ME, Berset C. Use of a free radical method to evaluate antioxidant activity. LWT – Food Science and Technology. 1995;28(1):25–30. https://doi.org/10.1016/S0023-6438(95)80008-5.
32. Odabasoglu F, Aslan A, Cakır A, Suleyman H, Karagoz Y, Halici M, et al. Comparison of antioxidant activity and phenolic content of three lichen species. Phytotherapy Research. 2004;18(11):938–941. https://doi.org/10.1002/ptr.1488.
33. Rukunudin IH, White PJ, Bern CJ, Bailey TB. A modified method for determining free fatty acids from small soybean sample sizes. JAOCS, Journal of the American Oil Chemists' Society. 1998;75(5):563–568. https://doi.org/10.1007/s11746-998-0066-z.
34. Sallam KhI, Ishioroshi M, Samejima K. Antioxidants and antimicrobial effects of garlic in chicken sausage. LWT – Food Science and Technology. 2004;37(8):849–855. https://doi.org/10.1016/j.lwt.2004.04.001.
35. Schmedes A, Homer G. A new thiobarbituric acid (TBA) method for determining free malondialdehyde (MDA) and hydroperoxides selectively as a measure of lipid peroxidation. Journal of the American Oil Chemists Society. 1989;66(6):813–817. https://doi.org/10.1007/BF02653674.
36. Mapari SAS, Meyer AS, Thrane U. Colorimetric characterization for comparative analysis of fungal pigments and natural food colorants. Journal of Agricultural and Food Chemistry. 2006;54(19):7027–7035. https://doi.org/10.1021/jf062094n.
37. Momin MA, Jubayer MF, Begum AA, Nupur AH, Ranganathan TV, Mazumder MAR. Substituting wheat flour with okara flour in biscuit production. Foods and Raw Materials. 2020;8(2):422–428. https://doi.org/10.21603/2308-4057-2020-2-422-428.
38. Mazumder MAR, Ranganathan TV. Encapsulation of isoflavone with milk, maltodextrin and gum acacia improves its stability. Current Research in Food Science. 2020;2:77–83. https://doi.org/10.1016/j.crfs.2019.12.003.
39. Drummen M, Tischmann L, Gatta-Cherifi B, Adam T, Westerterp-Plantenga M. Dietary protein and energy balance in relation to obesity and co-morbidities. Frontiers in Endocrinology. 2018;9. https://doi.org/10.3389/fendo.2018.00443.
40. McLean E, Cogswell M, Egli I, Wojdyla D, de Benoist B. Worldwide prevalence of anaemia, WHO vitamin and mineral nutrition information system, 1993–2005. Public Health Nutrition. 2008;12(4):444–454. https://doi.org/10.1017/S1368980008002401.
41. Dietary reference intakes for vitamin A, vitamin K, arsenic, boron, chromium, copper, iodine, iron, manganese, molybdenum, nickel, silicon, vanadium, and zinc: A report of the panel on micronutrients external link disclaimer, Washington: National Academy Press; 2001. 800 p. https://doi.org/10.17226/10026.
42. Dietary reference intakes for calcium, phosphorus, magnesium, vitamin D, and fluoride. Washington: National Academies Press; 1997. 448 p. https://doi.org/10.17226/5776.
43. Chaiklahan R, Chirasuwan N, Loha V, Tia S, Bunnag B. Separation and purification of phycocyanin from *Spirulina* sp. using a membrane process. Bioresource Technology. 2011;102(14):7159–7164. https://doi.org/10.1016/j.biortech.2011.04.067.
44. Abu El-Baky HH, El Baz FK, El-Baroty GS. Production of phenolic compounds from Spirulina maxima microalgae and its protective effects. African Journal of Biotechnology. 2009;8(24):7059–7067.

ORCID IDs
Umme Habiba https://orcid.org/0000-0003-2924-4335
Md. A. Robin https://orcid.org/0000-0002-4194-9576
Md. M. Hasan https://orcid.org/0000-0001-9352-0424
Maria A. Toma https://orcid.org/0000-0001-5892-030X
Delara Akhter https://orcid.org/0000-0003-3886-4245
Md. A. R. Mazumder https://orcid.org/0000-0002-0964-5521

FRM

Foods and Raw Materials, 2021, vol. 9, no. 2

E-ISSN 2310-9599
ISSN 2308-4057

Research Article
Open Access

https://doi.org/10.21603/2308-4057-2021-2-290-301
Available online at http://jfrm.ru/en

Yeast race effect on the quality of base and young sparkling wines

Alexander S. Makarov, Igor P. Lutkov*

All-Russian National Research Institute of Viticulture and Winemaking "Magarach" of RAS, Yalta, Russia

* e-mail: igorlutkov@mail.ru

Received June 25, 2020; Accepted in revised form August 12, 2020; Published online July 30, 2021

Abstract:

Introduction. A disadvantage of the ancestral method (la méthode ancestrale), which is widely used in the production of sparkling wine, is that it is difficult to control fermentation. We aimed to identify the optimal yeast race for obtaining high-quality young sparkling wines with varietal aroma without yeast tones.

Study objects and methods. Our study objects were base and young sparkling wines from Cabernet-Sauvignon prepared on various yeast races. Organic acids, sugars, and ethanol contents were determined by high performance liquid chromatography. Phenolic and coloring substances were measured by colorimetric method. Foaming properties were determined by air barbotage of a wine sample in a measuring cylinder; sparkling properties, by measuring the CO_2 desorption rate; CO_2 content, by volumetric method; viscosity, with a viscometer. Sensory evaluation was carried out according to standard methods.

Results and discussion. The wines produced on the Odesskiy Chernyi-SD13 yeast race received the highest tasting scores of 7.82 and 9.05 points for base wine and young sparkling wines, respectively. They contained larger amounts of phenolic substances (1103 mg/dm^3) and coloring agents (275 mg/dm^3) and had higher color intensity (1.614). The panelists rated them highly on their complex varietal aroma and harmonious, velvety flavor, as well as their foaming and sparkling properties. This yeast race ensured intensive fermentation of sugars and a great amount of bound CO_2 (up to 24.93%).

Conclusion. The Odesskiy Chernyi-SD13 yeast race is optimal for making base and young sparkling wines by the bottle method. This technology can be used to produce high-quality sparkling wines in the crop year by large and small enterprises.

Keywords: Fermentation, descriptors, color, aroma, acids, carbon dioxide, foaming properties, sparkling properties

Please cite this article in press as: Makarov AS, Lutkov IP. Yeast race effect on the quality of base and young sparkling wines. Foods and Raw Materials. 2021;9(2):290–301. https://doi.org/10.21603/2308-4057-2021-2-290-301.

INTRODUCTION

Russian sparkling wines enjoy a well-deserved popularity among consumers. Despite the growing demand, Russia has a shortage of raw materials for their production. Grapes suitable for sparkling wines can only be cultivated in certain parts of the country, mainly in the southern regions. Local agricultural lands have different forms of ownership and many landowners have lost interest in grape cultivation due to a long payback period. Yet, most large producers of sparkling wines do not have their own source of raw materials and therefore have to import cheap base wines, often of poor quality. The long production cycle (over 9 months for the bottle method) holds back increased production of domestic sparkling wines. The need to purchase expensive equipment for pressure operations limits the use of the acratophoric method by small farms.

The solution is to produce young sparkling wines (aged 2–3 months) by the bottle method. They can be made during one wine-making season and delivered to the consumer by the New Year. The EU countries make sparkling wine by the ancestral method (la méthode ancestrale), i.e., incomplete fermentation of grape must on spontaneous microflora. Fermentation is suspended by cooling and the stuck must is stored until spring. Then it is bottled and sealed for complete fermentation and saturation with carbon dioxide [1]. This method has two disadvantages: it is difficult to control fermentation when using spontaneous microflora and the finished wine has a tendency to cloudiness.

In Russia, a similar method is used to produce "Tsymlyanskoe Igristoe" red sparkling wine. It is also based on subsequent fermentation of stuck must in bottles, but this process may stop spontaneously and result in varying contents of sugars, ethanol, and carbon dioxide in the finished wines.

Hypothetically, the optimal yeast race should provide young sparkling wines with the desired properties. Most importantly, it should be suitable for primary and secondary fermentation, have no yeast tones and preserve the varietal aroma.

The yeast used in the production of bottled sparkling wines must meet a number of requirements. In particular, it must have autolytic and flocculating power and be resistant to high ethanol concentration and pressure, as well as low fermentation temperature and pH [2, 3]. For this, yeast is preliminarily acclimatized and fertilized with nitrogen compounds [4]. After fermentation, when aging on yeast, the wine is saturated with yeast autolysis products (e.g., amino acids) and phenolic compounds (e.g., catechins, caffeic and gallic acids in rosé wines) [5, 6]. The technology for young sparkling wines excludes yeast aging, thus preserving the original varietal aroma. Also, there is only one fermentation process and therefore yeast does not need to adapt.

We aimed to study the effect of yeast race on the quality of base and young sparkling wines produced by the bottle fermentation method.

STUDY OBJECTS AND METHODS

Our study objects were base and young sparkling wines produced with various yeast races from Cabernet-Sauvignon grapes grown on the South Coast of Crimea in 2019. The grapes were processed in micro-vinification conditions in line with the relevant standards and guidelines. The mass concentration of sugars was 202 g/dm^3 and titratable acids amounted to 10.0 g/dm^3. Must was fermented with glucosophilic, fructosophilic, S-sensitive, and killer factor yeast races. The latter significantly increased the dominance of this species during fermentation [7]. In total, we selected five races from the Magarach Collection of Winemaking Microorganisms (Table 1).

Wine-making. Rosé must was obtained by pressing pulp on a basket press, yielding 50 daL per 1 ton of grapes. Then it was sulfurized (75 mg/dm^3 SO_2), sedimented at 15°C, and decanted. To obtain red must, grapes were crushed on a roller crusher and destemmed, with the pulp sulfurized (75 mg/dm^3 SO_2). The pulp and must were fermented at 15°C. The pulp was fermented (2/3 of sugars) and pressed, with the resulting must fermented in separate tanks. At a residual sugar concentration of 22–24 g/dm^3, one part of each batch of stuck must was bottled for champagnization, with the other part fermented dry. After introducing bentonite (0.2 g/dm^3), the bottles were stoppered, stacked, and stored at 12–14°C. After 60 days, the sediment was reduced to the neck (remuage) and discharged (degorgeage). The resulting rosé and red base wines met the requirements of State Standard 32030-2013 "Table wines and table winestocks. General specifications."

The physicochemical parameters of the base and sparkling wines were determined in accordance with the current standards. Phenolic substances were measured colorimetrically by the Folin-Ciocalteu reaction. Optical characteristics were determined by measuring optical density at 420 and 520 nm. The dynamic viscosity was measured with a viscometer. Foaming properties (maximum foam volume and time of foam break) were determined according to Standard STO 01580301.015-2017 "Table base wines for sparkling wines and drinks saturated with carbon dioxide. Determination of foaming properties." A 200 cm^3 sample of degasified wine was poured in a 1 dm^3 measuring cylinder. Barbotage was carried out using a portable compressor and a sprayer lowered to the bottom of the measuring cylinder. Foaming took place at the same time. The maximum foam volume was determined visually using the cylinder scale, and the time of foam break was measured with a timer. This method, as well as Mosalux, provided an accurate determination of the wine's foaming properties [9].

Table 1 Yeast species used in making young sparkling wines

No.	Race title	Yeast species (V. Kudryavtsev taxonomy)	Phenotype	Properties
I-25	Cabernet 5	*Saccharomyces vini* Meyen, 1838 syn. *Saccharomyces cerevisiae* (Kreger-van Rij N.J.W., 1984)	Sensitive (S)	Resistant to cold, SO_2, alcohol, and acid (pH 2.8); glucosophilic; does not form H_2S
I-523	Bastardo 1965	*Saccharomyces oviformis* Osterwalder, 1924 syn. *S. cerevisiae* (Kreger-van Rij N.J.W., 1984)	Sensitive (S)	Resistant to SO_2, alcohol, tannin and polyphenols; fructosophilic
I-525	Sevasto-polskaya 23	*S. oviformis* Osterwalder, 1924 syn. *S. cerevisiae* (Kreger-van Rij N.J.W., 1984)	Sensitive (S)	Resistant to cold, SO_2, and alcohol; glucosophilic; does not form H_2S
I-527	47-K	*S. vini* Meyen, 1838 syn. *S. cerevisiae* (Kreger-van Rij N.J.W., 1984)	Killer (K)	Effective in fermenting non-sterile grape must; high degree of protein hydrolysis; resistant to acid, SO_2, alcohol; forms H_2S in small amounts; glucosophilic; low iron sensitivity index [8]. Recommended for table base wines for sparkling wines.
I-652	Odesskiy Chernyi-SD13	*S. oviformis* Osterwalder, 1924 syn. *S. cerevisiae* (Kreger-van Rij N.J.W., 1984)	Sensitive (S)	Strong ability to form alcohols, esters and lactones; synthesizes β-phenylethanol and aliphatic alcohols; enhances spicy tones in the aroma of base wines. Recommended for red table wines with berry-spicy aroma.

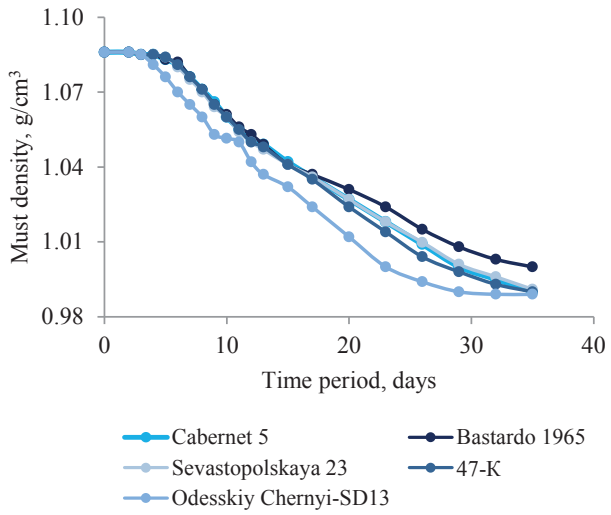

Figure 1 Must fermentation with different yeast races for rosé base wines

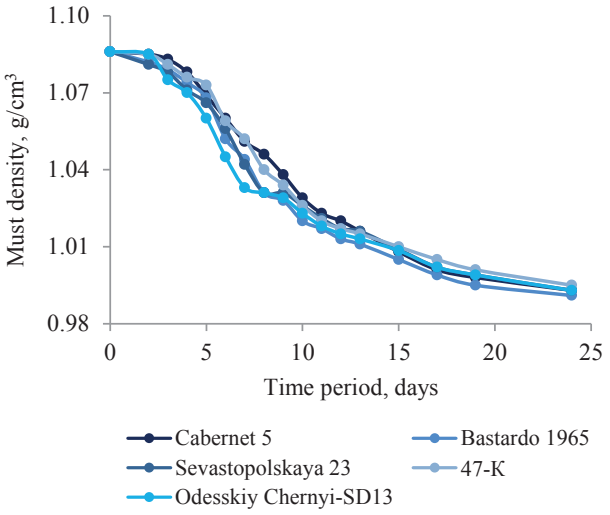

Figure 2 Must fermentation with different yeast races for red base wines

Table 2 Organic acids, sugars, and ethanol contents in experimental base wine samples

Race title	C	T	M	S	L	A	TA	Su	Glu	F	Gly	Ethanol, vol. %
						g/dm³						
					Rosé							
Cabernet 5	0.35	4.04	3.15	1.51	0.09	0.21	9.4	0.26	0.42	3.22	7.80	12.41
Bastardo 1965	0.34	3.93	2.93	1.63	0.35	0.03	9.3	0.24	0.32	0.76	7.81	12.54
Sevastopolskaya 23	0.31	3.87	2.96	1.68	0.11	0.20	9.5	0.19	0.33	1.99	8.05	12.44
47-K	0.31	4.09	3.17	1.58	0.10	0.24	9.6	0.23	0.50	6.88	7.96	12.12
Odesskiy Chernyi-SD13	0.45	3.96	3.18	1.20	0.09	0.14	8.6	0.24	0.38	1.01	5.23	12.95
					Red							
Cabernet 5	1.08	2.11	0.41	1.62	1.14	0.27	5.2	0.65	0.25	0.06	8.04	11.41
Bastardo 1965	0.87	2.68	0.36	1.77	1.39	0.20	5.9	0.31	0.30	0.02	8.02	11.28
Sevastopolskaya 23	0.71	2.74	0.39	1.71	1.51	0.20	6.2	0.25	0.31	0.02	7.65	10.63
47-K	0.70	3.16	0.33	1.78	1.97	0.18	7.4	0.26	0.32	2.26	7.81	10.92
Odesskiy Chernyi-SD13	1.06	2.84	2.76	1.75	0.08	0.09	7.9	0.33	0.47	0.41	6.88	12.38

Where: C – citric, T – tartaric, M – malic, S - succinic, L – lactic, A – acetic, TA – sum of titratable acids, Su – sucrose, Glu – glucose, F – fructose, Gly – glycerol

Table 3 Physicochemical parameters of experimental base wines

Race title	pH	Eh	V_{max}, cm³	t_{br}, s	V, mm²/s	TPh, mg/dm³	MPh, mg/dm³	PPh, mg/dm³	C, mg/dm³	I	T
					Rosé						
Cabernet 5	3.1	215	900	30	1.697	266	233	32	4	0.594	1.101
Bastardo 1965	3.1	214	800	28	1.684	286	238	48	4	0.607	1.010
Sevastopolskaya 23	3.1	214	920	30	1.684	269	233	36	6	0.630	1.007
47-K	3.1	214	950	31	1.723	275	231	44	4	0.607	1.000
Odesskiy Chernyi-SD13	3.1	214	1000	42	1.674	233	180	53	14	0.656	1.033
					Red						
Cabernet 5	3.6	180	1100	> 300	1.640	911	535	376	183	0.855	0.611
Bastardo 1965	3.5	193	1250	> 300	1.633	974	598	376	202	0.864	0.716
Sevastopolskaya 23	3.5	193	1250	> 300	1.581	1027	609	418	207	0.964	0.563
47-K	3.4	199	1250	> 300	1.620	826	503	323	188	0.963	0.573
Odesskiy Chernyi-SD13	3.1	203	1250	> 300	1.692	1101	635	466	287	1.959	0.529

Where: Eh – value of redox potential, V_{max} – max foam volume, t_{br} – time of foam break, V – value of dynamic viscosity, TPh – total content of phenolic substances, MPh – content of monomeric fraction of phenolic substances, PPh – content of polymeric fraction of phenolic substances, C – content of coloring agents, I – value of color intensity (D_{420}+ D_{520}), T – value of color shade (D_{420}/ D_{520})

Table 4 Sensory evaluation of experimental base wines

Yeast race	General characteristics of aroma and flavor	Score
	Rosé	
Cabernet 5	Aroma – complex, berry. Flavor – soft, pure, complete, varietal, with "spicy bitterness."	7.76
Bastardo 1965	Aroma – neutral, with berry and fruit notes and passing "choking." Flavor – pure, complete, too fresh, plain.	7.67
Sevastopolskaya 23	Aroma – delicate, berry, with light notes of nightshade. Flavor – fresh, well-formed, varietal.	7.75
47-K	Aroma – subtle, berry-fruit, with spicy and cherry notes. Flavor – complete, with residual sugars and inharmonious acidity.	7.70
Odesskiy Chernyi-SD13	Aroma – bright, complex, berry and fruit, with noes of nightshade. Flavor – pure, fresh, harmonious, varietal.	7.83
	Red	
Cabernet 5	Aroma – bright, complex, berry and fruit, with noes of nightshade. Flavor – soft, complete, harmonious, varietal.	7.81
Bastardo 1965	Aroma – mild, varietal, of berry direction. Flavor – harmonious, complete, varietal, velvet.	7.78
Sevastopolskaya 23	Aroma – less expressed, berry, with light notes of nightshade. Flavor – fresh, velvet.	7.77
47-K	Aroma – mild, of berry direction, with notes of nightshade. Flavor – complete, insufficiently velvet.	7.76
Odesskiy Chernyi-SD13	Aroma – bright, complex, berry, with notes of nightshade. Flavor – deep, velvet, with long coffee and spicy finish.	7.82

Table 5 Physicochemical parameters of experimental young sparkling wines

Race title	pH	Eh	V_{max}, cm^3	t_{br}, s	V, mm^2/s	TPh, mg/dm^3	MPh, mg/dm^3	PPh, mg/dm^3	C, mg/dm^3	I
				Rosé						
Cabernet 5	2.92	218	10.3	1.741	214	212	2	3	0.576	0.974
Bastardo 1965	2.92	217	10.0	1.735	195	186	9	4	0.510	0.927
Sevastopolskaya 23	2.92	218	10.4	1.715	247	235	12	5	0.579	0.989
47-K	2.95	218	10.4	1.735	210	210	0	2	0.512	0.961
Odesskiy Chernyi-SD13	2.93	217	9.6	1.735	217	211	6	6	0.499	0.974
				Red						
Cabernet 5	3.55	182	6.5	1.620	757	474	283	164	0.771	0.523
Bastardo 1965	3.33	197	8.4	1.633	916	524	392	170	0.790	0.681
Sevastopolskaya 23	3.33	198	8.0	1.594	847	540	307	171	0.928	0.540
47-K	3.23	202	9.0	1.620	794	498	296	152	0.908	0.574
Odesskiy Chernyi-SD13	3.18	205	8.7	1.601	1103	675	428	275	1.614	0.491

Where: Eh – value of redox potential, V_{max} – max foam volume, t_{br} – time of foam break, V – value of dynamic viscosity, TPh – total content of phenolic substances, MPh – content of monomeric fraction of phenolic substances, PPh – content of polymeric fraction of phenolic substances, C – content of coloring agents, I – value of color intensity (D_{420}+ D_{520}), T – value of color shade (D_{420}/ D_{520})

Organic acids, residual sugars, and ethyl alcohol were determined by HPLC using a Shimadzu LC 20AD chromatograph (Japan) equipped with a spectrophotometric detector. Sample separation was performed on a Supelcogel C610H column (Supelco®, Sigma-Aldrich, USA). We used a sorbent based on sulfurized divinyl-polystyrene (column size 300×7.8, sorbent granules less than 10.0 μm). An aqueous solution of phosphoric acid (1 g/dm^3) was used as an eluent. Concentrations of substances were determined with a detector at 210 nm by the retention time and the signal quantity.

Total carbon dioxide content in sparkling wines was determined according to Standard STO 01580301.016–2017 "Drinks saturated with carbon dioxide. Determination of mass concentration of carbon dioxide by the modified volumetric method." According to this method, CO_2, which evolved from wine under the action of ultrasound, displaced the barrier fluid from the graduated container. The volume of the displaced barrier fluid corresponded to the volume of carbon dioxide contained in the bottle with sparkling wine. The content of related forms of carbon dioxide was calculated according to Merzhanian method [10], based

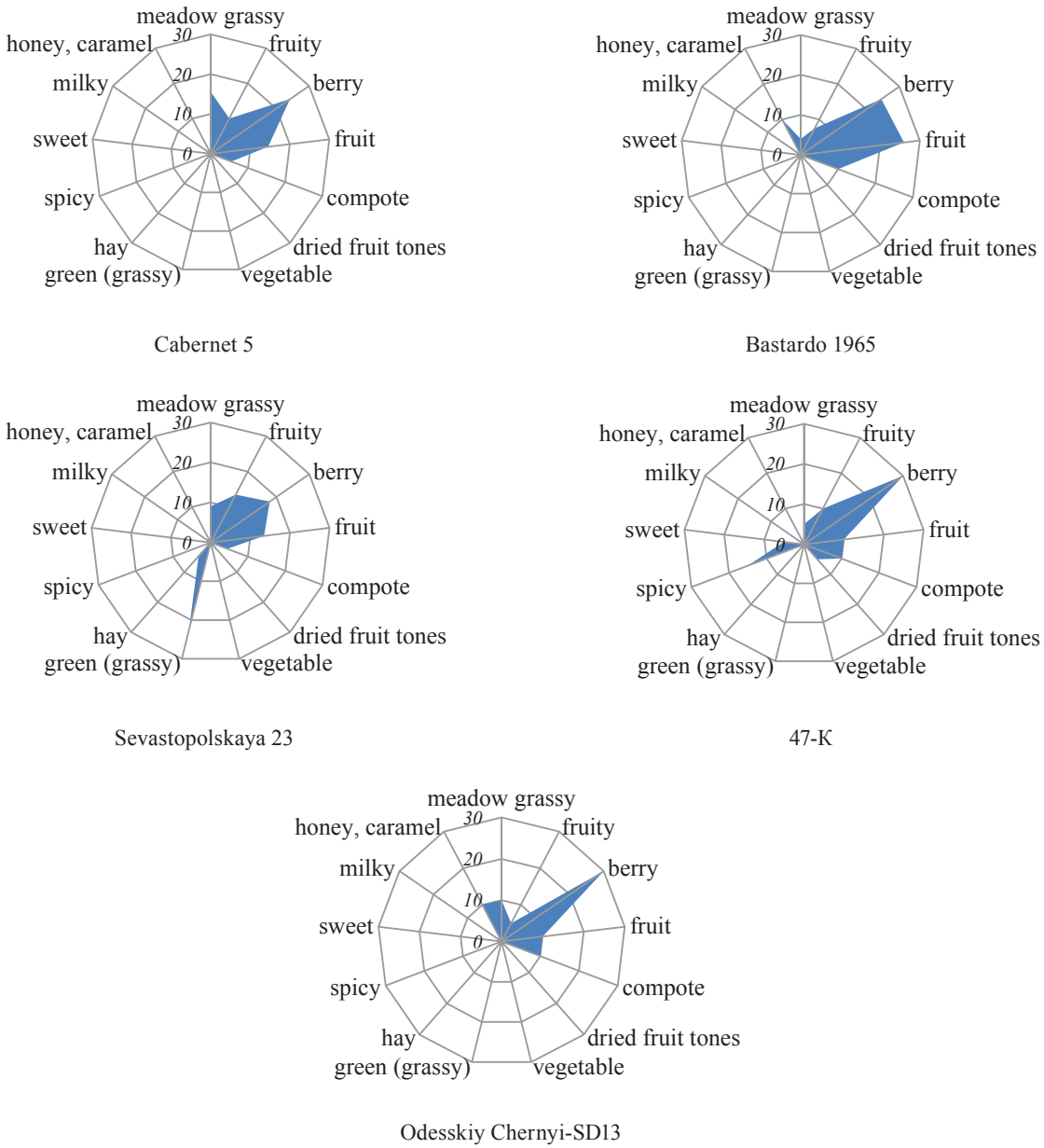

Figure 3 Aromatic profile of rosé base wines on various yeast races

on the difference between the measured CO_2 content and the CO_2 solubility at a certain pressure and ethanol concentration. Sparkling properties were determined according to Standard STO 01586301.022–2019 "Sparkling wines, carbonated wines, and carbonated drinks. Determination of sparkling properties by gravimetric method." In particular, we measured the CO_2 desorption rate from the bottle of wine when depressurizing to the atmospheric level.

Sensory evaluation of base and sparkling wines followed State Standard 32051-2013 "Wine products. Methods of Organoleptic Analysis," ISO 5492:2008 "Sensory analysis – Vocabulary," and ISO 11035:1994 "Sensory analysis – Identification and selection of descriptors for establishing a sensory profile by a multidimensional approach." Sensory evaluation was carried out by trained panelists on a 10-point system, by quantifying the contribution of individual descriptors to the composition of color, flavor, and aroma of wines. The descriptors were selected in accordance with ISO 5492, ISO 11035 and [11, 12, 13].

RESULTS AND DISCUSSION

At the first stage, we assessed the effects of different yeast races on must fermentation (Figs. 1 and 2).

We found that the period of must fermentation using the red method was 10–14 days shorter than that with the white method. This was due to the thermal protective effect of the pomace "cap" and the concentration of yeast cells on the solid parts of pomace, increasing the contact area for yeast and must sugars.

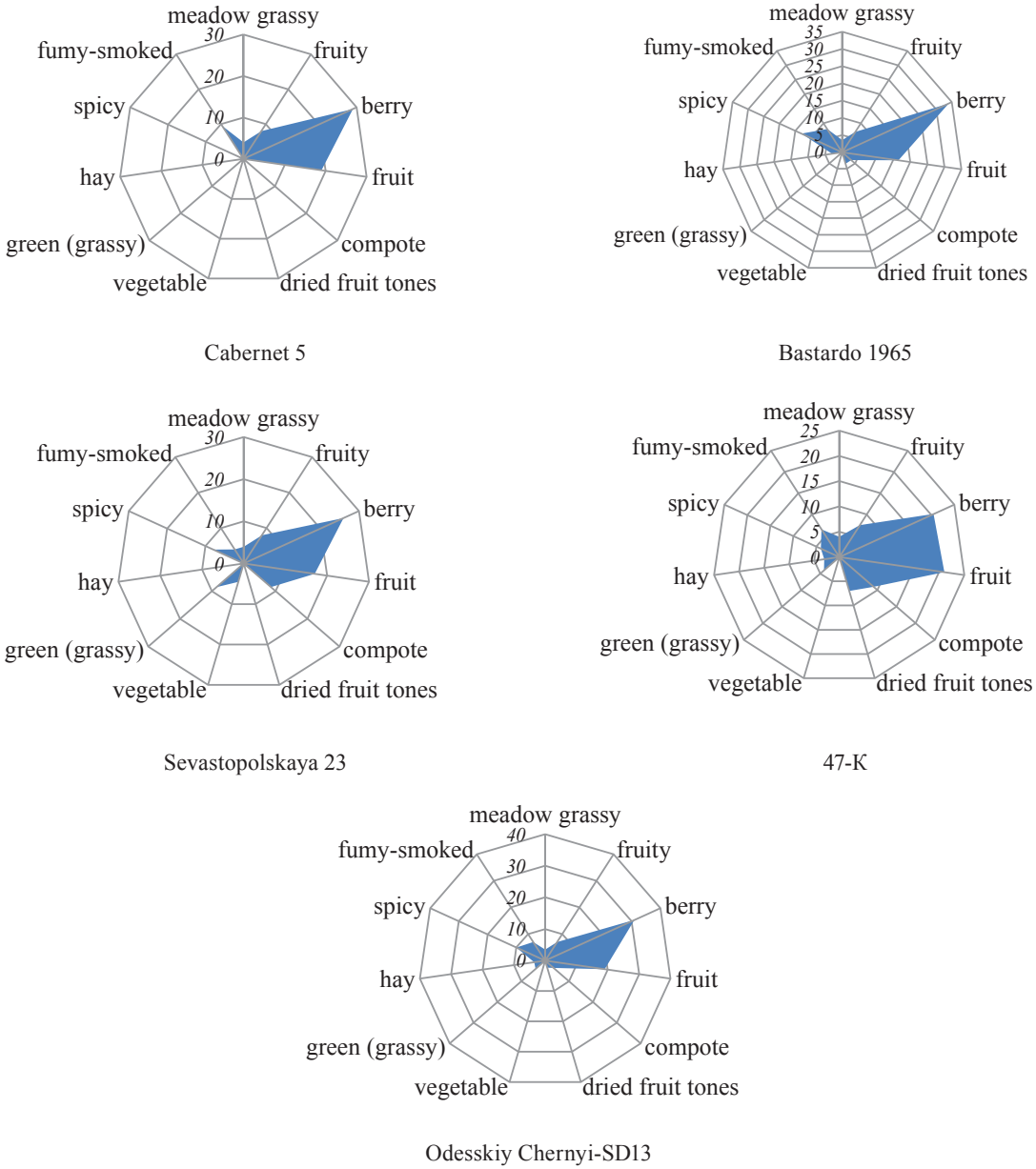

Figure 4 Aromatic profile of red base wines on various yeast races

The fermentation of the rosé must (Fig. 1) was most intensive on the Odesskiy Chernyi-SD13 race and slowest on the Bastardo 1965 race. The red must (Fig. 2) fermented faster on the Bastardo 1965 race and slower on the 47-K race. A slight curvature in the density range of 1.030 g/cm^3 was associated with pulp pressing, which slowed down the fermentation.

Next, we determined the physicochemical parameters of the base wines (Tables 2 and 3).

Among the rosé base wines, the sample fermented on the Bastardo 1965 race had the lowest amount of residual sugars (glucose – 0.32 g/dm^3, fructose – 0.76 g/dm^3), although its fermentation lasted longer than on the other races (41 days). The minimum fructose content in this sample confirmed the fructosophilic properties of this culture. Sugar fermentation proceeded faster (29 days) and more intensively with the Odesskiy Chernyi-SD13 race, with a large volume fraction of ethyl alcohol accumulated at the lowest glycerol content. It indicated that this yeast race fermented a smaller fraction of sugars by the glyceropyruvic path, which was also confirmed by the lower contents of succinic, acetic, and titratable acids. Malolactic fermentation did not take place in the rosé base wine samples. The pH and Eh values were practically the same.

The best foaming properties were shown by the rosé base wines prepared on the Odesskiy Chernyi-SD13 race (max. foam 1000 cm^3), with the lowest values (800 cm^3) found in the wines on the Bastardo 1965 race. In addition, we found an inverse correlation between the maximum foam volume and the total content of phenolic substances (K = –0.80). Noteworthily, the sample

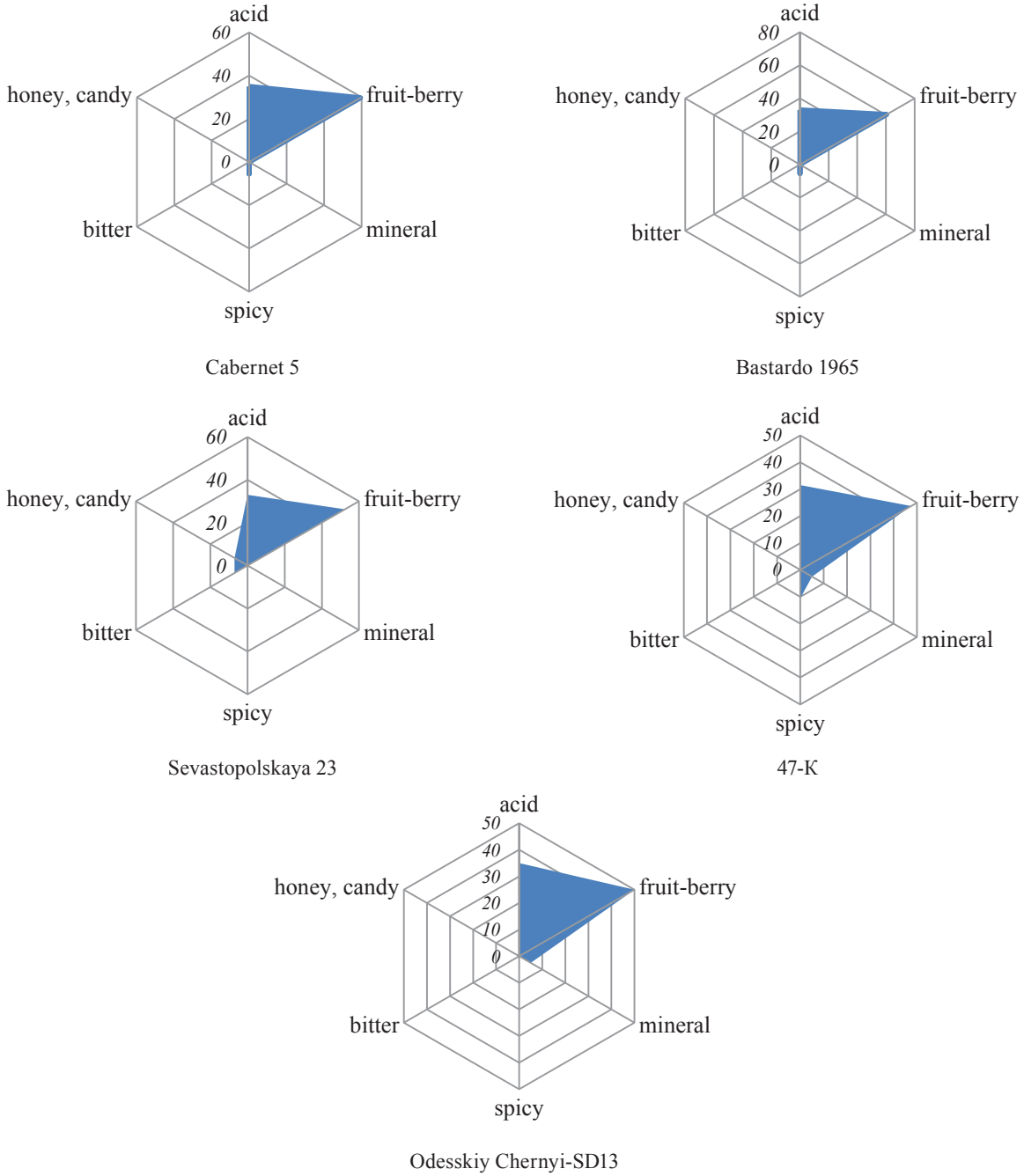

Figure 5 Flavor profile of rosé base wines on various yeast races

prepared on the Odesskiy Chernyi-SD13 race contained the smallest amount of phenolic substances and the highest contents of polyphenols and coloring agents, as well as the highest value of color intensity. The highest dynamic viscosity was shown by the sample prepared on the 47-K race. This was due to the concentration of residual sugars (the correlation coefficient between viscosity and fructose concentration was 0.97).

In the red base wines, the Bastardo 1965 race was the fastest to ferment sugars, while the 47-K race was the slowest. Moreover, the latter race did not ferment about 2 g of fructose. As in the rosé samples, the Odesskiy Chernyi-SD13 race synthesized more alcohol and less glycerin. Malolactic fermentation followed alcoholic fermentation in all the samples, except for the one fermented by the Odesskiy Chernyi-SD13 race. It decreased the Eh value and the concentrations of malic and titratable acids, and increased the pH value and the lactic acid content. In addition, lactic acid bacteria did not utilize residual amounts of fructose in the sample fermented on the 47-K race.

The values of foaming properties were high in all the red base wines (1100–1250 cm^3). The dynamic viscosity was the highest in the sample fermented on the Odesskiy Chernyi-SD13 race, correlating with the concentration of ethyl alcohol (K = 0.98). This sample contained the

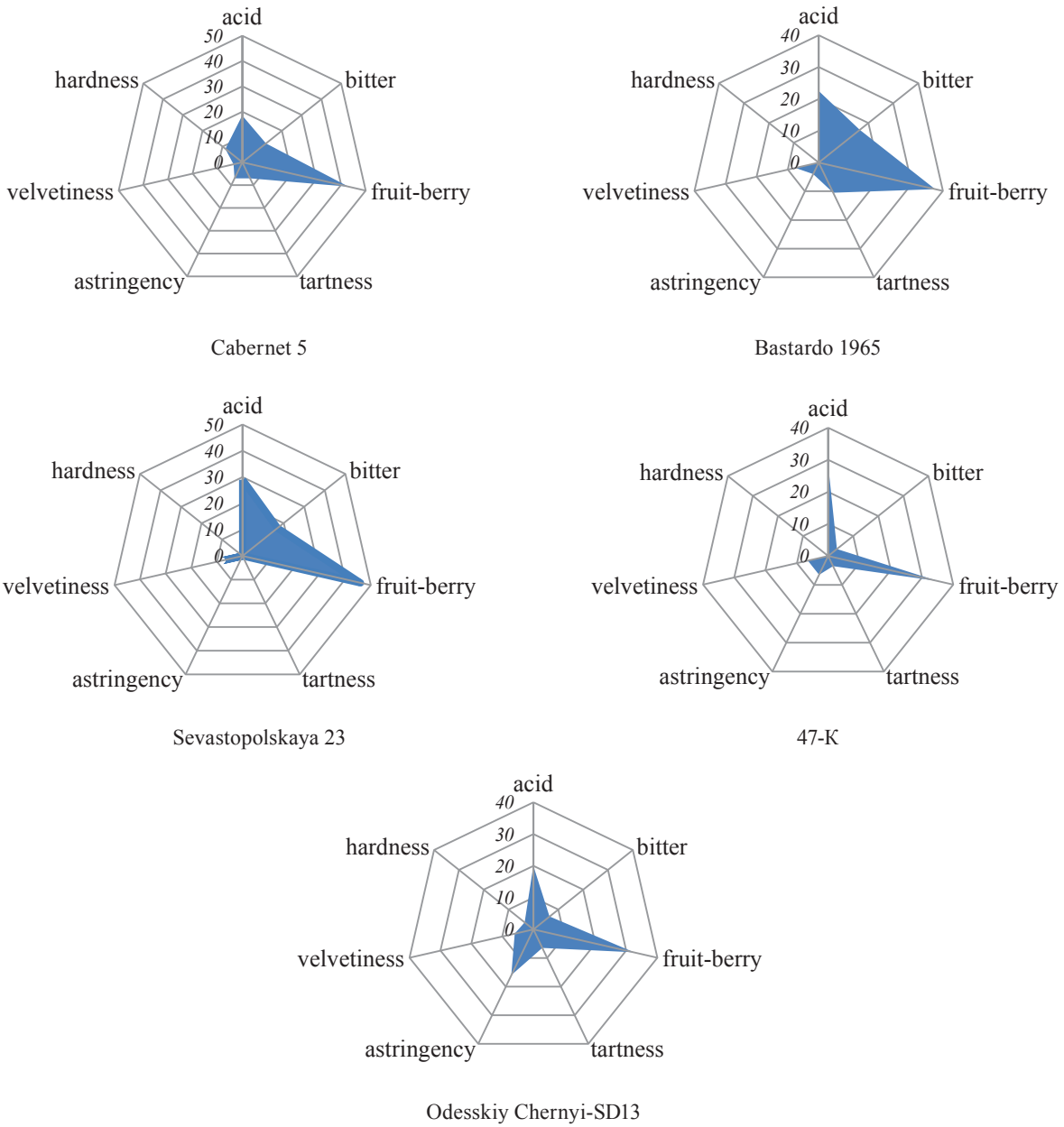

Figure 6 Flavor profile of red base wines on various yeast races

largest amount of phenolic substances (including their polymeric forms) and coloring agents, as well as the highest color intensity. The parameter of color in all the red base wines was less than unity, corresponding to the values for young base wines. This indicated the contribution of anthocyanins and brown condensation products of phenolic substances to the color intensity.

The volume fractions of ethanol in the red base wines were lower than in the rosé samples (on average, by 1 vol. %). This might be due to the partial evaporation of ethyl alcohol from the pomace "cap" during fermentation.

The next stage of our study involved the sensory evaluation of young base wines. Table 4 shows the general characteristics of aroma and flavor, as well as the panelists' scores on a 10-point scale (minimum 7.5 points).

Of the rosé base wines, the sample prepared on the Odesskiy Chernyi-SD13 race was rated highest due to its complex, bright aroma and harmonious flavor. The Bastardo 1965 sample received the lowest score, mainly due to the extraneous note in its aroma associated with long post-fermentation. Among the red wines, the sample prepared on the Odesskiy Chernyi-SD13 race received the higher score due to its rich aroma and velvety flavor.

While tasting, the panelists determined the main descriptors for color and aroma (Fig. 3 and 4), as well as flavor (Figs. 5 and 6). Red (67.5–87.5%) and violet (12.5–32.5%) shades took part in the color composition of rosé

base wines. Red (60.5–65.0%), violet (29.5–35.0%), and brown (0–7%) shades took part in the color composition of red base wines.

Berry tones in aroma and flavor are varietal features of Cabernet-Sauvignon rosé and red base wines. The strongest berry tones were observed in the samples prepared on the Odesskiy Chernyi-SD13 and 47-K races. Fruit tones were significant contributors to the aromatic composition of the remaining samples due to complex esters forming during enzymatic processes during fermentation [14, 15]. In addition to berry and fruit tones, the red base wines featured fume-smoky tones and those of dried fruits, which were most pronounced in the 47-K sample. Vegetable notes (green pepper) were identified in the Sevastopolskaya 23 sample, possibly due to the influence of 3-isobutyl-2-methoxypyrazine [16].

The flavor of rosé base wines was based on fruit-and-berry and acid descriptors. The sample prepared on the Sevastopolskaya 23 race expressed honey and candy hints, as well as light bitterness. The Cabernet 5, 47-K, and Bastardo 1965 samples had distinct spicy notes.

The flavor of red base wines was based on the same fruit-and-berry and acid descriptors, with additional velvetiness, astringency, and tartness. Their astringency could be associated with the content of polymeric forms of phenolic substances, usually with an average degree

Table 6 Sensory evaluation of experimental young sparkling wines

Yeast race	General characteristics of aroma and flavor	Score
	Rosé	
Cabernet 5	Transparent. Color: light rosé. Bouquet: pure, varietal, berry with fruit tones. Flavor: fresh, mild, berry with nightshade notes, well-saturated with CO_2.	8.99
Bastardo 1965	Transparent. Color: light rosé. Bouquet: pure, of berry direction, with candy tones. Flavor: fresh, harmonious, berry-candy, with piquant bitterness, well-saturated with CO_2.	8.93
Sevastopolskaya 23	Transparent. Color: light rosé. Bouquet: berry-fruit. Flavor: fresh, harmonious, of berry direction, well-saturated with CO_2.	8.97
47-K	Transparent. Color: light rosé. Bouquet: pure, berry-fruit. Flavor: fresh, mild, plain, well-saturated with CO_2.	8.90
Odesskiy Chernyi-SD13	Transparent. Color: light rosé. Bouquet: pure, fresh, with candy tones. Flavor: pure, fresh, light, well-balanced, well-saturated with CO_2.	9.03
	Red	
Cabernet 5	Transparent. Color: dark ruby. Bouquet: fresh, varietal, berry, with nightshade note. Flavor: harmonious, varietal, well-formed, well-saturated with CO_2.	8.99
Bastardo 1965	Transparent. Color: dark ruby. Bouquet: varietal, of berry direction, with light "choking." Flavor: fresh, full-bodied, tannin, with piquant bitterness, well-saturated with CO_2.	8.91
Sevastopolskaya 23	Transparent. Color: dark ruby. Bouquet: pure, of berry-fruit direction, with morocco leather noes. Flavor: fresh, velvet, with piquant bitterness, averagely saturated with CO_2.	8.92
47-K	Transparent. Color: dark ruby. Bouquet: varietal, fruit-berry, with light "choking." Flavor: mild, velvet, with light bitterness, averagely saturated with CO_2.	8.87
Odesskiy Chernyi-SD13	Transparent. Color: dark ruby. Bouquet: pure, bright, varietal, berry-fruit direction. Flavor: mild, well-balanced, fresh, full-bodied, tannin, well-saturated with CO_2.	9.05

Table 7 Carbon dioxide contents and foaming properties of young sparkling wines

Race title	Equilibrium pressure of CO_2, kPa	CO_2 content per bottle (0.75 dm^3), g				Weight ratio of bound CO_2, %	Foaming properties	
		Total in bottle	Gasi-form	Dis-solved	Bound		Maximum volume of foam, cm^3	Time of foam break, s
				Rosé				
Cabernet 5	610	8.233	0.195	7.026	1.012	12.28	660	112
Bastardo 1965	650	9.330	0.213	7.310	1.808	19.38	585	43
Sevastopolskaya 23	460	6.861	0.143	5.624	1.094	15.94	780	180
47-K	540	7.547	0.188	6.364	0.995	13.19	640	57
Odesskiy Chernyi-SD13	650	10.062	0.170	7.383	2.509	24.93	900	320
				Red				
Cabernet 5	810	10.520	0.284	8.800	1.435	13.64	820	> 300
Bastardo 1965	750	9.696	0.225	8.274	1.197	12.35	1200	> 300
Sevastopolskaya 23	810	10.611	0.336	8.892	1.383	13.04	1100	> 300
47-K	600	8.416	0.152	7.121	1.142	13.57	1000	> 300
Odesskiy Chernyi-SD13	790	10.245	0.337	8.517	1.392	13.59	1150	> 300

Table 8 Sparkling properties of young rosé wines on different yeast races

Yeast race	$V_{1–300}$, mg/min	Angle of deflection of CO_2 desorption curve, °
Cabernet 5	4.097	0.2347
Bastardo 1965	3.559	0.2039
Sevastopolskaya 23	3.662	0.2098
47-K	4.027	0.2307
Odesskiy Chernyi-SD13	3.358	0.1924

Where: $V_{1–300}$ is the average CO_2 desorption rate on the timespan of 1–300 min

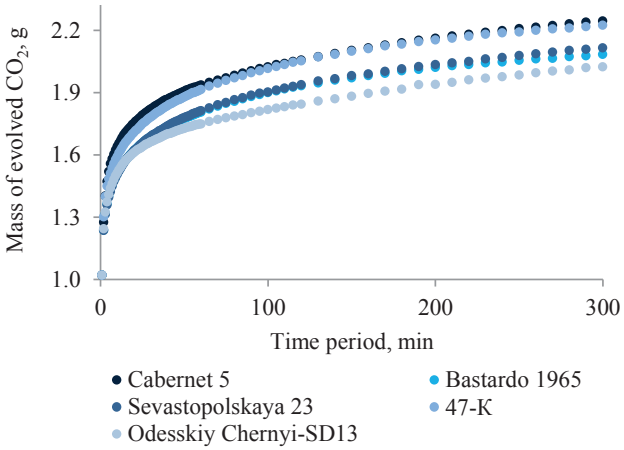

Figure 7 CO_2 desorption from young rosé sparkling wines prepared on different yeast races

of polymerization of ten or more small anthocyanin pigment derivatives (tetramers) [17]. The sample developed on the Odesskiy Chernyi-SD13 race had a richer and more complex flavor.

The physicochemical parameters of experimental young sparkling wines are presented in Table 5.

The samples of young rosé sparkling wines showed similar physicochemical characteristics. Their fermentation process was complete. Their pH was lower than in similar base wines, primarily due to a higher mass concentration of titratable acids.

In young red wines produced on the Cabernet 5 race, alcoholic fermentation was followed by malolactic fermentation, as evidenced by a decreased mass concentration of titratable acids and an increased pH. We found a correlation between the value of redox potential (Eh) and the concentration of titratable acids in young red sparkling and base wines. The correlation coefficient was 0.939 and 0.957 for base and sparkling wines, respectively. This indicated that malolactic fermentation led to a decrease in Eh.

The wine produced on the Odesskiy Chernyi-SD13 race contained the largest amount of phenolic and coloring substances and had higher color intensity compared to the other wines. This might be due to the ability of this race to improve the extraction of phenolic substances during pulp fermentation, with yeast pectolytic enzymes producing a stronger effect on the grape skin [18, 19].

Table 6 shows the results of the sensory evaluation of young sparkling wines, as well as the panelists' scores on a 10-point scale (minimum 8.8 points)

The rosé wines had a distinct varietal berry aroma with various notes. Higher scores were given to the samples prepared on the Odesskiy Chernyi-SD13, Cabernet 5, and Sevastopolskaya 23 yeast races, primarily due to their balanced flavor. The red wines also had a strong berry aroma with various notes. The panelists gave higher scores to the samples prepared on the Odesskiy Chernyi-SD13, Cabernet 5, and Sevastopolskaya 23 yeast races, primarily due to their pure aroma. The samples prepared on the 47-K and Bastardo 1965 races had slight off-tones (H_2S).

The samples of young sparkling wines were tested for their foaming and sparkling properties, as well as CO_2 content and desorption (Tables 7, 8 and Fig. 7).

The best foaming properties were exhibited by the young rosé sparkling wines prepared on the Odesskiy Chernyi-SD13 and Sevastopolskaya 23 races, as well as the young red sparkling wines on the Bastardo 1965 and Odesskiy Chernyi-SD13 races. The red wines showed a direct correlation between the maximum foam volume and the polyphenol content (K = 0.78). The excess CO_2 pressure corresponded to the standard rate (at least 300 kPa), ranging from 460 to 810 kPa. The CO_2 content totaled 6.861–10.520 g in a 0.75 dm^3 bottle, depending on the concentration of sugars and dissolved CO_2 in the must with incomplete fermentation when preparing a tirage mixture. The weight ratio of bound CO_2 ranged from 12.28 to 24.93%, depending on the total CO_2 content in the sample and the peculiarities of fermentation on this yeast race in the bottle. The red wine samples had similar contents of bound CO_2, compared to rosé wines, which affected their sparkling properties. The correlation coefficient between $V_{1–300}$ and the weight ratio of bound CO_2 was –0.95. This confirmed the assumption that higher contents of bound CO_2 in sparkling wines improve their sparkling properties [20–25]. The lowest CO_2 desorption rate and angle of curve deflection (hence the best sparkling properties) were determined in the sample produced on the Odesskiy Chernyi-SD13 race (Table 8, Fig. 7). Slightly higher CO_2 desorption rates were also found in the samples on the Bastardo 1965 and Sevastopolskaya 23 races.

CONCLUSION

Yeast races produce a significant effect on the quality of base and young sparkling wines. Odesskiy Chernyi-SD13 is the best race for rosé and red base wines and young sparkling wines produced from Cabernet-Sauvignon grown in the South Coast of Crimea. This yeast race contributes to a pure varietal aroma and a harmonious flavor (panelists score: 9.03–9.05 points), as well as the best properties (maximum foam volume:

900–1150 cm^3, weight ratio of bound CO_2: 13.59–24.93%). The bottle method of making wines from must with incomplete fermentation ensures original products of high quality. This technology can increase the production of domestic sparkling wines in the crop year. It is especially suitable for small farms since it does not require any complex equipment. Research in this direction is planned to be continued with the aim of introducing this type of product in the regulatory standard documentation.

CONTRIBUTION

A.S. Makarov supervised the research, edited the manuscript, and formulated the conclusions. I.P. Lutkov formulated the hypothesis, set the aim and objectives, conducted the research, and wrote the manuscript.

CONFLICTS OF INTEREST

The authors declare that they have no conflict of interest.

ACKNOWLEDGEMENTS

The authors thank E. Slastye, V. Maksimovskaya, N. Lutkova, and N. Shmigelskaya for their assistance with the study.

REFERENCES

1. Jeandet P, Vasserot Y, Liger-Belair G, Marcha R. Sparkling wine production. In: Joshi VK, editor. Handbook of enology: principles, practices and recent innovations. API; 2011.
2. Di Gianvito P, Arfelli G, Suzzi G, Tofalo R. New trends in sparkling wine production: Yeast Rational Selection. In: Alcoholic beverages. Volume 7: The science of beverages. Woodhead Publishing; 2019. pp. 347–386. https://doi.org/10.1016/B978-0-12-815269-0.00011-8.
3. Borrull A, López-Martínez G, Miró-Abella E, Salvadó Z, Poblet M, Cordero-Otero R, et al. New insights into the physiological state of *Saccharomyces cerevisiae* during ethanol acclimation for producing sparkling wines. Food Microbiology. 2016;54:20–29. https://doi.org/10.1016/j.fm.2015.11.001.
4. Martí-Raga M, Marullo P, Beltran G, Mas A. Nitrogen modulation of yeast fitness and viability during sparkling wine production. Food Microbiology. 2016;54:106–114. https://doi.org/10.1016/j.fm.2015.10.009.
5. Bozdogan A, Canbas A. Influence of yeast strain, immobilization and ageing time on the changes of free amino acids and amino acids in peptides in bottle fermented sparkling wines obtained from *Vitis vinifera* cv. Emir. International Journal of Food Science and Technology. 2011;46(6):1113–1121. https://doi.org/10.1111/j.1365-2621.2011.02550.x.
6. Sartor S, Toaldo IM, Panceri CP, Caliari V, Luna AS, de Gois JS, et al. Changes in organic acids, polyphenolic and elemental composition of rosé sparkling wines treated with mannoproteins during over-lees aging. Food Research International. 2019;124:34–42. https://doi.org/10.1016/j.foodres.2018.11.012.
7. Velázquez R, Zamora E, Álvarez ML, Ramírez M. Using *Torulaspora delbrueckii* killer yeasts in the elaboration of base wine and traditional sparkling wine. International Journal of Food Microbiology. 2019;289:134–144. https://doi.org/10.1016/j.ijfoodmicro.2018.09.010.
8. El'darov MA, Avdanina DA, Shalamitskii MY, Ivanova EV, Tanashchuk TN, Kishkovskaya SA, et al. Polymorphism of the iron homeostasis genes and iron sensitivity in *Saccharomyces cerevisiae* flor and wine strains. Microbiology. 2019;88(2):200–205. https://doi.org/10.1134/S0026261719020036.
9. Cilindre C, Liger-Belair G, Villaume S, Jeandet P, Marchal R. Foaming properties of various Champagne wines depending on several parameters: Grape variety, aging, protein and CO_2 content. Analytica Chimica Acta. 2010;660 (1–2):164–170. https://doi.org/10.1016/j.aca.2009.10.021.
10. Merzhanian AA. Fiziko-khimiya igristykh vin [Physical chemistry of sparkling wines]. Moscow: Pishchevaya promyshlennost′; 1979. 271 p. (In Russ.).
11. Arroyo BL, Roberts RP. How specific wine tasting descriptors are? Procedia – Social and Behavioral Sciences. 2015;198:287–299. https://doi.org/10.1016/j.sbspro.2015.07.447.
12. Niimi J, Boss PK, Bastian SEP. Sensory profiling and quality assessment of research Cabernet Sauvignon and Chardonnay wines; quality discrimination depends on greater differences in multiple modalities. Food Research International. 2018;106:304–316. https://doi.org/10.1016/j.foodres.2017.12.060.
13. Sánchez-Palomo E, Trujillo M, García Ruiz A, González Viñas MA. Aroma profile of malbec red wines from La Mancha region: Chemical and sensory characterization. Food Research International. 2017;100:201–208. https://doi.org/10.1016/j.foodres.2017.06.036.
14. Lytra G, Franc C, Cameleyre M, Barbe J-C. Study of substituted ester formation in red wine by the development of a new method for quantitative determination and enantiomeric separation of their corresponding acids. Journal of Agricultural and Food Chemistry. 2017;65(24):5018–5025. https://doi.org/10.1021/acs.jafc.7b00979.

15. Kemp B, Herve A, Robillard B, Marchal R. Effect of production phase on bottle-fermented sparkling wine quality. Journal of Agricultural and Food Chemistry. 2015;63(1):19–38. https://doi.org/10.1021/jf504268u.
16. Liang C, Ristic R, Jiranek V. Jeffery DW. Chemical and sensory evaluation of magnetic polymers as a remedial treatment for elevated concentrations of 3-Isobutyl-2-methoxypyrazine in Cabernet sauvignon grape must and wine. Journal of Agricultural and Food Chemistry. 2018;66(27):7121–7130. https://doi.org/10.1021/acs.jafc.8b01397.
17. Sáenz-Navajas M-P, Arias I, Ferrero-del-Teso S, Fernández-Zurbano P, Escudero A, Ferreira V. Chemo-sensory approach for the identification of chemical compounds driving green character in red wines. Food Research International. 2018;109:138–148. https://doi.org/10.1016/j.foodres.2018.04.037.
18. Ageyeva NM, Avanesyants RV. Influence of ferment preparations of new generation the wine biopolymer. Fruit growing and viticulture of South Russia. 2017;46(4):129–140. (In Russ.).
19. Fedosova AN, Kaledina MV, Shevchenko NP, Voloshenko LV, Baydina IA, Trubchaninova NS. Research of the pectolytic ability of saccharomyces cerevisiae yeast. Storage and Processing of Farm Products. 2019;(3):78–89. (In Russ.).
20. Malakhov AA, Naberegnykh IA. Regulation the quality of sparkling wines with structurally destroyed autolysis of yeast. News of institutes of higher education. Food technology. 2010;316(4):57–59. (In Russ.).
21. Kotenko STs, Islammagomedova EA, Khalilova EA, Abakarova AA. Biotechnological properties of new strain of yeast *Saccharomyces cerevisiae Y-3980*. Bulletin of Higher Educational Institutions. North Caucasus Region. Natural Sciences. 2016;192(4):45–50. (In Russ.).
22. Makarov AS, Lutkov IP, Peskova IV, Probeygolova PA, Shalimova TR. Influence of strain of yeast chemical composition and quality of red sparkling wines. Fruit growing and viticulture of South Russia. 2018;50(2):111–122. (In Russ.). https://doi.org/10.30679/2219-5335-2018-2-50-111-122.
23. Gnetko LV, Zolotarev IO, Arutyunova GYu, Khachaturov VN. The effect of yeast race on the composition of a high-molecular fraction and physical and chemical properties of sparkling wines. New Technologies. 2019;(1):29–37. (In Russ.). https://doi.org/10.24411/2072-0920-2019-10103.
24. Mishin MV, Talanyan OR. Assessment of the qualities of sparkling sparkling wines. Scientific works of the Kuban State Technological University. 2015;(8):61–63. (In Russ.).
25. Ageeva NM, Guguchkina TI, Kashkara KE, Kashkara GG, Burda VE. Method of production a young red sparkling wine. Patent RU 2662961C1. 2018.

ORCID IDs
Alexander S. Makarov https://orcid.org/0000-0001-8497-5056
Igor P. Lutkov https://orcid.org/0000-0001-9515-4341

Foods and Raw Materials, 2021, vol. 9, no. 2

E-ISSN 2310-9599
ISSN 2308-4057

Research Article
Open Access

https://doi.org/10.21603/2308-4057-2021-2-302-309
Available online at http/jfrm.ru/en

Macro- and microelements in some species of marine life from the Sea of Okhotsk

Evgenia M. Stepanova*, Elena A. Lugovaya

Scientific Research Center "Arktika" Far Eastern Branch of the Academy of Sciences, Magadan, Russia

* e-mail: at-evgenia@mail.ru

Received November 05, 2020; Accepted in revised form December 25, 2020; Published online July 30, 2021

Abstract:
Introduction. Residents of northern regions have a diet low in essential macro- and microelements. The Sea of Okhotsk is an enormous source of fish and non-fish products. We aimed to determine mineral contents in marine fish, shellfish, and algae in order to assess if they could satisfy the daily requirement for these elements through fish and non-fish consumption.
Study objects and methods. Our study objects were saffron cod (*Eleginus gracilis* L.), blue-headed halibut (*Reinhardtius hippoglossoides* L.), commander squid (*Berryteuthis magister* L.), northern shrimp (*Pandalus borealis* L.), salted pink salmon caviar (*Oncorhynchus gorbuscham* L.), and kelp (*Laminaria* L.). The contents of 25 macro- and microelements were determined by atomic emission spectrometry and mass spectrometry with inductively coupled argon plasma.
Results and discussion. The absolute contents of macro- and microelements in the marine species were used to assess the proportion of the recommended daily requirement that they account for. Also, we performed a thorough comparative analysis of mineral quantities in the studied species of marine fish, pink salmon caviar, shellfish, and algae from the Sea of Okhotsk. Finally, we examined the elemental status of the coastal residents belonging to the "northern type" and identified their deficiencies of vital chemical elements.
Conclusion. Some chemical elements in the studied marine species from the Sea of Okhotsk (Magadan Region) satisfy over 100% of the daily human requirement for these minerals. Therefore, their products can be recommended as part of a northern diet in order to compensate for the deficiencies of certain minerals.

Keywords: Marine life, the Sea of Okhotsk, macro- and microelements, diet, toxic elements, shellfish

Funding. This study was carried out at the Scientific Research Center "Arktika" Far Eastern Branch of the Academy of Sciences as part of the state-funded project.

Please cite this article in press as: Stepanova EM, Lugovaya EA. Macro- and microelements in some species of marine life from the Sea of Okhotsk. Foods and Raw Materials. 2021;9(2):302–309. https://doi.org/10.21603/2308-4057-2021-2-302-309.

INTRODUCTION

There is growing concern about chronic diseases such as obesity, diabetes, hypertension, hypercholesterolemia, cancer, and cardiovascular disease resulting from lifestyle changes worldwide [1]. According to a study by S. Shab-Bidar and A. Jayedi, an increase in fish consumption of 100 g/day can reduce overall and cardiovascular mortality, as well as the risk of coronary heart disease, myocardial infarction, stroke, heart failure, depression, and liver cancer. It has no effect on other kinds of cancer. Therefore, fish can be considered a healthy source of animal protein [2].

Oceans cover over 70% of the earth's surface and provide an enormous ecosystem for a wide variety of marine species. These species are a rich source of bioactive compounds that can be used in medicine, pharmacology, and food industry [3].

A number of recent foreign studies have focused on using the by-products of processing fish, marine invertebrates, and plants. These by-products are often discarded as waste, although they contain such valuable components as high-quality proteins, lipids, minerals, vitamins, enzymes, and other bioactive compounds that can be used to fight cancer and some cardiovascular diseases [1, 3, 4].

Nutrition affects our general health and the state of our individual functional systems. Therefore, it should not only be balanced and adequate to gender, age, and the degree of one's physical and mental activity, but also take into account the climatic and geographic conditions, as well as national characteristics and habits. It is especially relevant to the northern regions of Russia.

Fish is an essential component of human diet that provides more than 3 billion people worldwide with

about 20% of animal protein [5]. The global fish catch is 182 million tons per annum, of which 2.6–4.5% is produced in Russia [6]. The Far Eastern basin accounts for 64% of the all-Russian catch. Its white fish, salmon, shrimp, squid, and sea kale are the most popular products among consumers. The global production of pink salmon caviar is 173,000 tons, of which 27% (46 700 t) is produced in Russia (30 900 t in the Sea of Okhotsk). Russia boasts its saffron cod (40 500 t/year), commander squid (150 000 t/year), blue-throated halibut (400 kg/year), and kelp (3800–9800 t/year). Shrimp dominates among the crustaceans, but its annual production of 10 000–20 000 tons only satisfies 20% of the Russian demand [6].

Fishing is the leading industry in many coastal regions of Russia, especially in the North and the Far East, where it is the main source of income. Primorsky Krai produces about 50% of all fish in the Far East, followed by Kamchatka and Sakhalin that equally share 2/5 of the total catch. The Magadan Region is also becoming an important player in the Russian fish market. The Far Eastern Basin has 26 million tons of aquatic biological resources, producing 3 million tons of fish per year. An average Russian consumes 16.1 kg fish per year.

Frozen, lightly salted, and smoked fish, as well as cheap canned fish, are among the most popular products in Russia. There is a growth in the consumption of ultra-processed products, which is associated with the standard of living in the country. There is a growing demand for fish delicacies, valuable species of fish, shrimp, crabs, and other invertebrates, as well as caviar, among high-income population [7].

According to the federal statistics of 2000 vs. 2019, the annual capita consumption of fish and fish products grew from 14.3 to 21.9 kg and from 12.7 to 22.3 kg in urban and rural areas, respectively. In 2019, the urban citizen consumed 13.9 kg of live and frozen fish and seafood, 4.1 kg of salted, smoked, and dried fish and seafood, 2.1 kg of canned fish, and 1.0 kg of semi-finished and finished fish products. These indicators for a rural consumer were 14.8, 4.6, 1.8, and 0.6 kg, respectively. The data for 2018 were almost identical to those for 2019 [8].

Fish has a more diverse mineral composition than meat, mainly due to microelements [9, 10]. While fish and meat have similar amounts of macronutrients (0.2% phosphorus, 0.3% potassium, 0.1% calcium), the content of some microelements in fish is 10 times higher (20–150 μg/g iodine, 140–700 μg% fluorine, 40–50 μg% bromine). Fish is only low in iron (1 mg%). Other microelements in fish include cobalt (about 20 mg%; 3–4 times more than in meat), zinc (1 mg%), copper (0.1 mg%), nickel (6 mg%), and molybdenum (4 mg%). Its average contents of sodium (100 mg%) and chlorine (165 mg%) are 2–3 times higher than in meat. The total content of minerals in marine fish is about 1.5 times as high as meat. Thus, fish and fish products are an essential source of minerals in human diet. We should also note that fish, especially predatory fish, can accumulate some toxic elements – mercury (up to 0.7 mg/kg), lead (up to 2.0 mg/kg), and cadmium (up to 0.2 mg/kg). However, these concentrations are within permissible levels and, when fish is consumed in generally accepted amounts, they do not pose any health hazard [7].

Non-fish species – crustaceans (crabs, shrimps, lobsters, crayfish), cephalopods (squid, octopus), bivalves (oysters, mussels, scallops), as well as algae (kelp, or sea kale) – contain potassium, sodium, calcium, magnesium, chlorine, sulfur, iron, manganese, phosphorus, aluminum, zinc, and many other macro- and microelements [11]. There is scientific evidence that fish species from tropical areas contain high concentrations of calcium, iron, and zinc, while those from cold seas or pelagic seas and oceans are rich in omega-3 fatty acids [12].

Earlier, we determined the contents of macro- and microelements in muscle tissue and testes of anadromous fish of the salmon (*Salmoidae* L.), chum salmon (*Oncorhynchus keta* L.), coho salmon (*Oncorhynchus kisutch* L.), and pink salmon (*Oncorhynchus gorbuscha* L.) caught in the coastal Sea of Okhotsk, Magadan Region. These species are most frequently eaten by the local population [13]. We found that the interspecific differences in the levels of elements in their biosubstrates were within the permissible standards for food products. However, chum salmon had larger amounts of arsenic, cobalt, copper, sodium, tin, antimony, and zinc than coho salmon. The level of iron in chum salmon and coho salmon was similar to that in freshwater fish. The contents of potassium and phosphorus were quite high, while the contents of lead, mercury, antimony, cadmium, arsenic, and cobalt were significantly below the standards. We also found that the element system of the indigenous small-numbered peoples, who have a traditional way of life in the Magadan Region, was in a better state than the element system of the Caucasian group, despite the imbalance in chemical elements seen in all the groups. This was probably due to the genetic adaptation of the northerners' mineral metabolism to the chronically insufficient intake of macro- and microelements, as well as their diet.

In this work, we determined the contents of chemical elements in the muscle tissue of some species of fish and seafood, as well as in algae, native to the Sea of Okhotsk. These products are the most essential components in the diet of the indigenous northern peoples and general inhabitants of the coastal northern regions. The population of the Magadan Region has a "northern" profile of macro- and microelements with a deficiency of calcium, cobalt, magnesium, zinc, selenium, and iodine [13]. Therefore, we aimed to analyze (qualitatively and quantitatively) the mineral composition of some species of marine life in order to

determine whether the consumption of marine fish and seafood can satisfy the recommended daily requirement for minerals.

STUDY OBJECTS AND METHODS

The objects of research were: Far Eastern or Pacific saffron cod (*Eleginus gracilis*, n = 10), black or blue-headed halibut (*Reinhardtius hippoglossoides*, n = 10), commander squid (*Berryteuthis magister*, n = 10), cooked and frozen northern shrimp (*Pandalus borealis*, n = 10), salted pink salmon caviar (*Oncorhynchus gorbuscha*, n = 10), and kelp (*Laminaria*, n = 10) or sea kale. All the objects were caught in the Sea of Okhotsk, the Magadan Region. Each sample of 50 g was packed in a polypropylene container. The contents of macro- and microelements were determined threefold and averaged.

Our study methods included the inductively coupled plasma atomic emission spectrometry (ICP-AES) and the inductively coupled plasma mass spectrometry (ICP-MS) applied with Optima 2000 DV and Agilent 8900 ICP-MS instruments (Perkin Elmer, USA). The study was carried out in line with Guidelines No. 4.1.985-00 "Determination of toxic elements in food products and raw materials. The autoclave sample preparation technique" and in cooperation with the Micronutrients Company (Moscow).

The study objects were analyzed for the following macro- and microelements: aluminum (Al), arsenic (As), boron (B), calcium (Ca), cadmium (Cd), cobalt (Co), chromium (Cr), copper (Cu), iron (Fe), mercury (Hg), iodine (I), potassium (K), lithium (Li), magnesium (Mg), manganese (Mn), sodium (Na), nickel (Ni), phosphorus (P), lead (Pb), selenium (Se), silicon (Si), tin (Sn), antimony (Sr), vanadium (V), and zinc (Zn).

For statistical analysis, we calculated the average measurement error (M ± m) and tested the normality of frequency distribution. When testing null hypotheses, the critical level of statistical significance was $P < 0.05$. Raw product portions of 100 g were used to determine the degree to which the fish and seafood species satisfied the daily adult requirement for macro- and microelements. For this, we referred to the "Standard physiological requirements for energy and nutrients for various population groups in the Russian Federation" (Methodological Guidelines 2.3.1.2432-08).

The macro- and microelement status of the working-age population in Magadan was examined in compliance with the Declaration of Helsinki and the principles of biomedical ethics. Each participant (study subject) voluntarily provided a written informed consent in line with Federal Law No. 323 "On Health Protection in the Russian Federation" of November 21, 2011 and Federal Law No. 152 "On personal data" of July 27, 2006.

We examined a total of 111 men (70 men aged 22–35 and 41 men aged 36–60) and 270 women (120 women aged 21–35 and 150 women aged 36–55). Hair samples from the back of the head were used as biomaterial for elemental analysis. They were exposed to inductively coupled argon plasma mass spectrometry on an Agilent 8900 ICP-MS instrument in the same laboratory to determine the contents of 25 macro- and microelements: Al (aluminum), As (arsenic), B (boron), Be (beryllium), Ca (calcium), Cd (cadmium), Co (cobalt), Cr (chromium), Cu (copper), Fe (iron), Hg (mercury), I (iodine), K (potassium), Li (lithium), Mg (magnesium), Mn (manganese), Na (sodium), Ni (nickel), P (phosphorus), Pb (lead), Se (selenium), Si (silicon), Sn (tin), V (vanadium), and Zn (zinc).

The data were statistically processed with IBM SPSS Statistics 21.

RESULTS AND DISCUSSION

Table 1 shows the average concentrations of essential (vital) macro- and microelements determined in the aquatic organisms and algae sampled from the Sea of Okhotsk.

We found that macronutrients differed significantly across almost all the studied species. Yet, kelp had a significantly higher ($P < 0.05$) content of calcium, potassium, and magnesium, accounting for 18, 50, and 37% of the daily requirement, respectively. Our calculations were based on 100 g portions of fresh (raw) products, since mineral loss during cooking was outside our study objectives. According to literature, however, the loss of minerals in cooked products is less than 10% [9]. Salted pink salmon caviar showed the highest ($P = 0.01$) concentrations of sodium and phosphorus of 10 040 and 4763 μg/g, respectively, amounting to 77 and 60% of the daily intake.

Our macroelement values slightly differed from the Handbook on the Chemical Composition and Caloric Content of Russian Foodstuffs published by the Institute of Nutrition, the Russian Academy of Medical Sciences (hereinafter "Handbook") [9]. Below are the values from the Handbook (with our values in brackets) for 100 g portions of the following species:

– saffron cod: sodium – 70 mg% (114.4 mg%), potassium – 335 mg% (302.7 mg%), calcium – 40 mg% (22.4 mg%), magnesium – 40 mg% (21.5 mg%), phosphorus – 240 mg% (200.6 mg%);

– halibut: sodium – 55 mg% (140.5 mg%), potassium – 450 mg% (188.6 mg%), calcium – 30 mg% (11.4 mg%), magnesium – 60 mg% (18.5 mg%), phosphorus – 220 mg% (131.1 mg%);

– pink salmon caviar: sodium – 2245 mg% (1004 mg%), potassium – 85 mg% (130.8 mg%), calcium – 75 mg% (60.9 mg%), magnesium – 141 mg% (69.6% mg%), phosphorus – 426 mg% (476.3 mg%);

– boiled and frozen shrimp: sodium – 540 mg% (494.3 mg%), potassium – 220 mg% (143.4 mg%), calcium – 70 mg% (89.6 mg%), magnesium – 50 mg% (63.4 mg%), phosphorus – 225 mg% (128.2 mg%); and

– squid: sodium – 110 mg% (468.4 mg%), potassium – 280 mg% (160.5 mg%), calcium – 40 mg% (23.2 mg%), magnesium – 90 mg% (97.9 mg%), phosphorus – 250 mg% (201.4 mg%).

The differences might be associated with the particular species [14] (in some cases, the Handbook only gives the generic name without specifying the

Table 1 Essential macro- and microelements (M ± m) in the muscle tissue of some species of marine life (the Sea of Okhotsk, Magadan)

ME, mcg/g	Pacific saffron cod *Eleginus gracilis*	Black-headed halibut *Reinhardtius hippoglossoides*	Commander squid *Berryteuthis magister*	Northern shrimp *Pandalus borealis*	Pink salmon caviar *Oncorhynchus gorbuscha*	Kelp *Laminaria*	Daily requirement	% of daily adult requirement (in 100 g)					
					Macroelements								
Ca	224 ± 22 1–2, 1–4, 1–5, 1–6	114 ± 11 2–3,2–4, 2–5, 2–6	232 ± 23 3–4, 3–5, 3–6	896 ± 90 4–5, 4–6	609 ± 61 5–6	2210 ± 221	1250 mg	1.8	0.9	1.9	7.2	4.9	17.7
K	3027 ± 303 1–2, 1–3, 1–4, 1–5, 1–6	1886 ± 189 2–4, 2–5, 2–6	1605 ± 161 3–6	1434 ± 143 4–6	1308 ± 131 5–6	12508 ± 1251	2500 mg	12.1	7.5	6.4	5.7	5.2	50.0
Mg	215 ± 22 1–3, 1–4, 1–5, 1–6	185 ± 18 2–3, 2–4, 2–5, 2–6	979 ± 98 3–4, 3–5, 3–6	634 ± 63 4–6	696 ± 70 5–6	1482 ± 148	400 mg	5.4	4.6	24.5	15.9	17.4	37.1
Na	1144 ± 114 1–3, 1–4, 1–5, 1–6	1405 ± 140 2–3, 2–4, 2–5, 2–6	4684 ± 468 3–5, 3–6	4943 ± 494 4–5, 4–6	10040 ± 1004 5–6	7982 ± 798	1300 mg	8.8	10.8	36	38	77.2	61.4
P	2006 ± 201 1–2, 1–4, 1–5, 1–6	1311 ± 131 2–3, 2–5, 2–6	2014 ± 201 3–4, 3–5, 3–6	1282 ± 128 4–5, 4–6	4763 ± 476 5–6	547 ± 55	800 mg	25.1	16.4	25.2	16.0	59.5	6.8
					Microelements								
Cu	0.392 ± 0.047 1–2, 1–3, 1–4, 1–5, 1–6	0.181 ± 0.022 2–3, 2–4, 2–5	2.52 ± 0.25 3–4, 3–6	8.26 ± 0.83 4–5, 4–6	2.99 ± 0.30 5–6	0.190 ± 0.023	1.0 mg	3.9	2.0	25.2	83.0	29.9	1.9
Fe	3.42 ± 0.34 1–2, 1–3, 1–4, 1–5, 1–6	0.981 ± 0.118 2–3, 2–4, 2–5, 2–6	6.01 ± 0.60 3–4, 3–5, 3–6	1.72 ± 0.17 4–5, 4–6	21.46 ± 2.15 5–6	80.72 ± 8.07	Male – 10 mg	3.4	1.0	6.0	1.7	21.5	80.72
							Female –15 mg	2.3	0.7	4.0	1.1	14.3	53.8
I	6.0 ± 0.6 1–2, 1–3, 1–4, 1–5, 1–6	0.841 ± 0.101 2–3, 2–5, 2–6	0.385 ± 0.046 3–4, 3–5, 3–6	0.773 ± 0.093 4–5, 4–6	7.81 ± 0.78 5–6	2319 ± 278	150 mcg	> 100%	56.1	25.7	51.5	> 100%	> 100%
Mn	0.122 ± 0.015 1–2, 1–3, 1–4,1–5, 1–6	0.042 ± 0.006 2–3, 2–4, 2–5, 2–6	0.553 ± 0.066 3–4, 3–5, 3–6	0.186 ± 0.022 4–5, 4–6	1.07 ± 0.11 5–6	0.960 ± 0.115	2.0 mg	0.6	0.2	2.8	0.9	5.4	4.8
Se	0.509 ± 0.061 1–2, 1–3, 1–4, 1–5, 1–6	0.338 ± 0.041 2–5, 2–6	0.327 ± 0.039 3–5, 3–6	0.265 ± 0.032 4–5, 4–6	2.12 ± 0.21	0.020 ± 0.004	70 mcg	72.9	48.3	46.7	37.9	> 100%	2.9
Zn	10.64 ± 1.06 1–2, 1–5, 1–6	3.58 ± 0.36 2–3, 2–4, 2–5, 2–6	10.65 ± 1.06 3–5, 3–6	12.27 ± 1.23 4–5, 4–6	23.40 ± 2.34 5–6	2.78 ± 0.28	12 mg	8.9	3.0	8.9	10.2	19.5	2.3

Note: ME – macro- and microelements; daily requirements were taken from the "Standard physiological requirements for energy and nutrients for various population groups in the Russian Federation" (Methodological Guidelines 2.3.1.2432-08); [1–2] – reliably significant differences in the amounts of macro- and microelements ($P < 0.05$) among the samples

Table 2 Conditionally essential microelements (M ± m) in the biosubstrates of some species of marine life (the Sea of Okhotsk, Magadan)

ME, mcg/g	Pacific saffron cod *Eleginus gracilis*	Blue-headed halibut *Reinhardtius hippoglossoides*	Commander squid *Berryteuthis magister*	Northern shrimp *Pandalus borealis*	Pink salmon caviar *Oncorhynchus gorbuscha*	Kelp *Laminaria*	Daily requirement
B	0.119 ± 0.014 [1–2, 1–3, 1–4, 1–5, 1–6]	0.314 ± 0.038 [2–3, 2–4, 2–5, 2–6]	1.83 ± 0.18 [3–5,3–6]	1.82 ± 0.18 [4–5, 4–6]	<0.021 [5–6]	21.15 ± 2.12	2.0 mg
Co	0.0062 ± 0.00124 [1–2, 1–4, 1–5, 1–6]	0.0019 ± 0.00039 [2–3, 2–4, 2–5, 2–6]	0.0063 ± 0.00126 [3–4, 3–5, 3–6]	0.011 ± 0.002 [4–6]	0.015 ± 0.002	0.020 ± 0.003	10 mcg
Cr	0.103 ± 0.012 [1–2]	0.156 ± 0.019 [2–4, 2–6]	0.128 ± 0.015 [3–4]	0.08 ± 0.012 [4–5]	0.117 ± 0.014	0.10 ± 0.012	50 mcg
V	0.0073 ± 0.00146 [1–2, 1–3, 1–6]	0.0015 ± 0.00031 [2–3, 2–4, 2–5, 2–6]	0.0033 ± 0.00066 [3–4, 3–5, 3–6]	0.010 ± 0.002 [4–5, 4–6]	0.0058 ± 0.00117	0.38 ± 0.046	15 mcg
Si	20.25 ± 2.03 [1–2, 1–3, 1–4, 1–6]	12.55 ± 1.25 [2–3, 2–4, 2–5]	27.42 ± 2.74 [3–5, 3–6]	33.33 ± 3.33 [4–5, 4–6]	20.83 ± 2.08 [5–6]	12.66 ± 1.27	5.0 mg
Li	0.012 ± 0.002 [1–2, 1–3, 1–4, 1–5, 1–6]	0.023 ± 0.004 [2–3, 2–4,2–5,2–6]	0.080 ± 0.012 [3–5, 3–6]	0.079 ± 0.012 [4–5, 4–6]	0.0051 ± 0.00102 [5–6]	0.130 ± 0.015	100 mcg
Ni	0.054 ± 0.008 [1–6]	0.048 ± 0.007 [2–4, 2–5, 2–6]	0.044 ± 0.007 [3–4, 3–5, 3–6]	0.074 ± 0.011	0.062 ± 0.009	0.080 ± 0.012	n.a.

Note: ME – macro- and microelements; [1–2] – reliably significant differences in the amounts of macro- and microelements ($P < 0.05$) among the samples; n.a. – not available

species). Additional factors include their habitat, production season, and the methods used to determine macro- and microelements.

The significantly highest content of copper was recorded in the boiled and frozen shrimp sample (83% of the daily requirement). The maximum contents of iron and iodine were found in the kelp sample (54–81% and over 100%, respectively). The highest concentrations of manganese, selenium, and zinc were determined in pink salmon caviar (5%, over 100%, and 19.5%, respectively).

Of all aquatic products, pink salmon caviar was analyzed in a ready-to-eat salted form, since raw caviar is not stored or frozen. Its sodium content was extremely high (10 040 µg/g vs. the recommended intake of 1300 mg/day), as can be seen in Table 1. However, even if a daily diet includes other sodium-containing foods, one caviar sandwich a day will not pose any health risk. On the contrary, it will benefit health since caviar is rich in phosphorus, iron, iodine, zinc, and valuable bioactive substances, such as omega-3-polyunsaturated fatty acids and vitamins.

The contents of conditionally essential elements are presented in Table 2.

The highest boron content was recorded in the kelp sample (21.15 µg/g or 106% of the daily requirement in 100 g). This trace element plays a significant role in the formation of bone tissue by regulating the activity of parathyroid hormone and, therefore, the metabolism of calcium, magnesium, and phosphorus [15, 16]. This makes kelp an essential component in the northerners' diet. Also, kelp had higher concentrations of cobalt (2 µg or 20% of the daily requirement), vanadium (38 µg or 95%), and lithium (13 µg or 13%) than any other of the studied samples. The maximum amount of chromium was determined in the muscle tissue of blue halibut (15.5 µg or 31% of the daily requirement). Northern shrimp was rich in silicon (3333 mcg or 67% of the daily requirement).

Table 3 Toxic microelements (M ± m) in the biosubstrates of some species of marine life (the Sea of Okhotsk, Magadan)

ME, mcg/g	Pacific saffron cod *Eleginus gracilis*	Blue-headed halibut *Reinhardtius hippoglossoides*	Commander squid *Berryteuthis magister*	Northern shrimp *Pandalus borealis*	Pink salmon caviar *Oncorhynchus gorbuscha*	Kelp *Laminaria*	TPL mg/kg, max.*		
							1,2	3–5	6
Al	1.20 ± 0.12	0.864 ± 0.104	1.0 ± 0.1	0.867 ± 0.104	0.42 ± 0.05	1.82 ± 1.18	–		
As	27.19 ± 2.72	2.07 ± 0.21	0.849 ± 0.102	4.71 ± 0.47	0.294 ± 0.035	6.89 ± 0.69	5.0	5.0	5.0
Cd	0.0024 ± 0.00048	0.0008 ± 0.00023	0.069 ± 0.010	0.075 ± 0.011	0.0016 ± 0.00033	0.130 ± 0.016	0.2	2.0	1.0
Hg	0.034 ± 0.005	0.039 ± 0.006	0.027 ± 0.004	0.028 ± 0.004	<0.0036	0.05 ± 0.008	0.5	0.2	0.1
Pb	0.0043 ± 0.00087	0.0045 ± 0.0009	0.0042 ± 0.00084	0.0031 ± 0.00061	0.0025 ± 0.00051	0.04 ± 0.006	1.0	10.0	0.5
Sn	0.038 ± 0.006	0.004 ± 0.0008	0.0049 ± 0.00097	0.0052 ± 0.00104	0.0092 ± 0.00185	0.008 ± 0.0017	–		
Sr	0.817 ± 0.098	0.636 ± 0.076	4.37 ± 0.44	20.68 ± 2.07	5.42 ± 0.54	193 ± 19	–		

Note: ME – macro- and microelements; TPL – temporarily permissible level

* "Unified sanitary, epidemiological and hygienic requirements for products (goods) subject to sanitary and epidemiological surveillance (control)" (effective from June 1, 2019)

Table 4 Macro- and microelements in the hair samples of working-age residents of Magadan (25–75 percentile)

ME, mcg/g	Male study subjects		Female study subjects		Significance level (*P*)			
	Aged 22–35 (n = 70)	Aged 36–60 (n = 41)	Aged 21–35 (n = 120)	Aged 36–55 (n = 150)	1–2	3–4	1–3	2–4
Al	10.00 (6.59–14.62)	11.69 (5.82–20.73)	7.62 (4.39–13.73)	7.85 (4.69–14.15)	0.50	0.52	**0.02**	**0.04**
As	0.081 (0.046–0.117)	0.079 (0.046–0.185)	0.042 (0.042–0.062)	0.042 (0.027–0.072)	0.73	0.73	**0.00**	**0.00**
Ca	265.42 (187.85–333.54)	310.60 (221.17–405.60)	449.47 (258.10–750.45)	473.00 (282.48–937.98)	0.07	0.17	**0.00**	**0.00**
Cd	0.027 (0.013–0.052)	0.040 (0.013–0.122)	0.008 (0.004–0.016)	0.012 (0.006–0.034)	**0.03**	**0.00**	**0.00**	**0.00**
Co	0.010 (0.006–0.018)	0.014 (0.008–0.074)	0.012 (0.007–0.022)	0.014 (0.008–0.033)	**0.01**	0.11	0.10	0.41
Cr	0.73 (0.47–1.01)	0.56 (0.24–1.03)	0.35 (0.23–0.54)	0.36 (0.18–0.58)	0.10	0.88	**0.00**	**0.00**
Cu	10.98 (9.87–12.28)	9.89 (8.57–12.54)	10.02 (8.41–11.61)	10.23 (8.99–11.56)	0.31	0.35	0.10	0.66
Fe	18.22 (9.87–12.28)	22.42 (14.52–38.68)	20.35 (14.38–31.04)	18.39 (13.08–26.17)	0.19	0.07	0.37	0.06
K	110.40 (44.76–170.75)	171.00 (73.92–515.07)	38.59 (17.27–77.09)	74.64 (32.62–200.12)	**0.01**	**0.00**	**0.00**	**0.00**
Li	0.015 (0.012–0.027)	0.016 (0.010–0.036)	0.012 (0.012–0.017)	0.012 (0.011–0.022)	0.90	0.16	**0.00**	0.38
Mg	26.85 (19.76–35.93)	27.01 (19.18–40.17)	33.75 (21.61–67.33)	49.41 (26.75–104.32)	0.69	**0.01**	**0.00**	**0.00**
Mn	0.43 (0.28–0.69)	0.71 (0.42–0.95)	0.87 (0.43–1.67)	1.18 (0.48–2.31)	**0.01**	**0.01**	**0.00**	**0.01**
Na	198.51 (62.81–413.94)	392.00 (189.99–866.15)	82.05 (40.52–180.23)	170.20 (79.57–575.95)	**0.00**	**0.00**	**0.00**	**0.00**
Ni	0.22 (0.15–0.35)	0.29 (0.17–0.48)	0.18 (0.11–0.31)	0.17 (0.11–0.30)	0.24	0.94	0.07	**0.02**
P	159.72 (143.80–173.99)	163.00 (149.50–186.12)	151.38 (137.55–165.90)	156.56 (140.38–180.53)	0.19	0.07	0.08	0.170
Pb	0.48 (0.31–0.85)	1.12 (0.48–4.68)	0.16 (0.08–0.33)	0.25 (0.11–0.53)	**0.00**	**0.00**	**0.00**	**0.00**
Se	0.38 (0.30–0.51)	0.51 (0.38–0.80)	0.34 (0.26–0.49)	0.46 (0.27–0.74)	**0.00**	**0.00**	0.22	0.30
Si	32.98 (20.59–48.22)	21.33 (13.83–31.30)	28.81 (17.46–49.81)	23.92 (15.28–40.71)	**0.00**	**0.05**	0.58	0.30
Sn	0.09 (0.06–0.18)	0.12 (0.07–0.20)	0.08 (0.04–0.20)	0.08 (0.04–0.17)	0.21	0.59	0.47	**0.04**
V	0.12 (0.04–0.19)	0.04 (0.01–0.09)	0.04 (0.02–0.08)	0.05 (0.02–0.09)	**0.01**	0.73	**0.00**	0.74
Zn	190.80 (166.86–217.14)	177.00 (131.79–208.30)	176.75 (154.51–211.83)	174.42 (147.13–200.36)	**0.02**	0.17	0.08	0.68
I	0.67 (0.32–1.11)	0.74 (0.38–3.46)	0.49 (0.30–1.00)	0.55 (0.30–1.47)	0.34	0.89	0.37	0.14
Hg	0.53 (0.20–0.89)	0.60 (0.37–0.99)	0.48 (0.30–0.67)	0.51 (0.35–0.68)	0.27	0.28	0.07	0.14
B	0.81 (0.58–1.64)	0.89 (0.56–3.72)	0.56 (0.33–1.29)	0.76 (0.29–1.81)	0.29	0.33	0.20	0.12
Be	0.003 (0.003–0.004)	0.003 (0.001–0.009)	0.003 (0.001–0.003)	0.003 (0.001–0.006)	0.27	0.14	0.27	0.70

Note: ME – macro- and microelements; significant differences are highlighted in bold ($P < 0.05$).

We analyzed the concentrations of toxic microelements in the studied biosubstrates against the "Unified sanitary, epidemiological and hygienic requirements for products (goods) subject to sanitary and epidemiological surveillance (control)" (effective from June 1, 2019) and the hygienic safety requirements for food products established in the Technical Regulations of the Customs Union "On food safety" (TR CU 021/2011). Excessive levels were only found for arsenic: 5.4 times as high in the Pacific saffron cod and 1.4 times as high in the kelp sample (Table 3).

Some studies report fluctuations in the content of total arsenic in various species of fish and shellfish from 5 to 200 μg/g (or mg/kg) [17, 18]. The Russian regulations specify certain contents of total arsenic in food products and materials without differentiating between its inorganic (toxic) and organic (low-toxic) forms, which explains excess concentrations determined in marine hydrobionts. Yet, we know that arsenic is mainly present in the tissues of marine life in its organic, low-toxic forms, such as arsenobetaine, arsenocholine, and arsenosugar [19]. This problem could be solved by introducing an additional maximum permissible concentration for inorganic arsenic in marine hydrobionts into the regulatory documents, such as the Technical Regulations of the Customs Union "On food safety" (TR CU 021/2011) [19].

Besides, our long-term studies of the elemental status did not find any excessive contents of heavy and toxic metals (including arsenic) in the population of the Magadan Region [13, 20].

Thus, since the regulatory documents establish maximum permissible concentrations of total, rather than organic, arsenic in marine life, we can conclude that the population of the Magadan Region is not exposed to a toxic load of arsenic.

Rational nutrition involves a variety of foods in the diet, including those produced in other biogeochemical regions that may have a negative impact on the local population. Thus, the consumption of local food with a significant proportion of essential macro- and microelements is an effective way to prevent regional deficiency or excess of certain chemicals.

According to our data, over 50% of the working-age residents of Magadan have a deficiency of calcium and magnesium (most essential macroelements), as well as cobalt and iodine (microelements). This deficiency, which is typical of the "northern" elemental profile, can decrease the northerners' adaptive reserves. Moreover, a chronic deficiency of basic vital elements in extreme northern conditions can cause dysfunctions in many physiological systems and a wide range of pathologies.

The statistical data for the mineral metabolism in the study subjects are presented in Table 4.

The studied cohorts showed obvious differences related to both age and gender. In a linear approximation, reliably significant (at $P < 0.05$)

differences can be schematically represented as follows (common groups of elements are highlighted in bold).

Gender-related differences:

men (**Si,** V, Zn) ♂ 22–35 > < ♂ 36–60 (**Cd**, Co, **K, Mn, Na, Pb, Se**);

women (**Si**) ♀ 21–35 > < ♀ 36–55 (**Cd**, **K,** Mg, **Mn, Na, Pb, Se**).

Age-related differences:

younger age (**Al, As, Cd, Cr, K**, Li, **Na, Pb,** V) ♂ 22–35 > < ♀ 21–35 (**Ca, Mg, Mn**);

older age (**Al, As, Cd, Cr, K, Na,** Ni, **Pb,** Sn) ♂ 36–60 > < ♀ 36–55 (**Ca, Mg, Mn**).

Noteworthily, age-related differences in mineral metabolism were common for men and women. Younger subjects of both sexes had a significantly higher median of Si concentration. The hair samples of older subjects contained significantly higher contents of toxic cadmium and lead, while no excess of these elements was detected in any of the studied cohorts. In addition, older subjects had higher concentrations of essential potassium, manganese, sodium, and selenium. Thus, we can consider these elements age-related. At the same time, they tended to be in excess at different degrees and frequency of detection, which can be considered as mineral pre-deficiency caused by its increased excretion from the body.

Hormone-determined gender differences in metabolism can be seen in the elemental status of men and women. The female subjects of both age groups had significantly higher concentrations of essential calcium, magnesium, and manganese, while their male counterparts had higher contents of aluminum, arsenic, cadmium, chromium, potassium, sodium, and lead. Our data were in line with some literature sources and our earlier studies [13 , 20–22].

Thus, every individual has unique mineral metabolism that differs between men and women and changes with age. We find it extremely important to regularly monitor the elemental status of the working-age population in the North as a socially significant group. This measure will ease the growing pressure on functional reserves, maintain the immune system, and prevent various pathologies related to mineral imbalance and severe deficiencies. People should support their health, individually or under medical supervision, by rationalizing their nutrition and consuming preventative supplements of macro- and microelements, taking into account the specific features of the "northern" mineral metabolism.

The most common "northern" diseases of a biogeochemical nature include iron deficiency states (deficiency of iron, cobalt, magnesium, and calcium), immunodeficiency conditions (deficiency of selenium, zinc, iodine, and calcium), arthrosis (deficiency or excess of calcium and silicon), urolithiasis (excess calcium or silicon), hypertension (deficiency of magnesium or calcium), dental diseases (imbalance of calcium, fluoride, and magnesium), and thyroid pathologies, most commonly endemic goiter (iodine deficiency and imbalance of selenium, copper, manganese, cobalt, calcium, magnesium, and other elements).

CONCLUSION

We determined the absolute contents of macro- and microelements in some species of marine life and assessed the degree to which they could satisfy the recommended daily requirement for these minerals if included in the daily diet. We compared mineral quantities in the studied species of marine fish, pink salmon caviar, shellfish, and algae from the Sea of Okhotsk. In addition, we examined the elemental status of the coastal residents and specified deficiencies of essential chemical elements common for this "northern" profile.

We found that the studied species of marine life native to the Sea of Okhotsk in the Magadan Region are a valuable source of macro- and microelements that, in some cases, satisfy over 100% of the daily requirement for adult humans. However, the amounts of calcium and manganese in the studied fish and non-fish products (100 g) were lower than required. Therefore, we recommend replenishing their deficiencies with other foods that are rich in these minerals (dairy products and meat), as well as bioactive supplements or pharmaceuticals under medical supervision.

Since the indigenous small-numbered northerners, who lead a traditional way of life, have minimum elemental imbalance and no clinical signs of endemic goiter, we recommend that "outsiders" coming to live in the area optimize their daily nutrition with local foods, mainly marine fish and non-fish products.

CONTRIBUTION

The authors were equally involved in writing the manuscript and are equally responsible for plagiarism.

CONFLICT OF INTEREST

The authors declare no conflict of interest.

REFERENCES

1. López-Pedrouso M, Lorenzo JM, Cantalapiedra J, Zapata C, Franco JM, Franco D. Aquaculture and by-products: Challenges and opportunities in the use of alternative protein sources and bioactive compounds. Advances in Food and Nutrition Research. 2020;92:127–185. https://doi.org/10.1016/bs.afnr.2019.11.001.
2. Jayedi A, Shab-Bidar S. Fish consumption and the risk of chronic disease: An umbrella review of meta-analyses of prospective cohort studies. Advances in Nutrition. 2020;11(5):1123–1133. https://doi.org/10.1093/advances/nmaa029.

3. Abhari K, Mousavi Khaneghah A. Alternative extraction techniques to obtain, isolate and purify proteins and bioactive from aquaculture and by-products. Advances in Food and Nutrition Research. 2020;92:35–52. https://doi.org/10.1016/bs.afnr.2019.12.004.
4. Al Khawli F, Martí-Quijal FJ, Ferrer E, Ruiz M-J, Berrada H, Gavahian M, et al. Aquaculture and its by-products as a source of nutrients and bioactive compounds. Advances in Food and Nutrition Research. 2020;92:1–33. https://doi.org/10.1016/bs.afnr.2020.01.001.
5. Sustainable fisheries and aquaculture for food security and nutrition. A report by the High Level Panel of Experts on Food Security and Nutrition of the Committee on World Food Security. Rome: Food and Agriculture Organization. 2014. 119 p.
6. Kleshchevsky YuN, Nikolaeva MA, Ryazanova OA. Current state and prospects of the fish and fish goods market development in Russia. Bulletin of Kemerovo State University. Series: Political, Sociological and Economic Sciences. 2017;(3):34–42. (In Russ.).
7. Rakut′ko SYu, Denisevich EI. Osnovnye napravleniya razvitiya rybnoy otrasli Dal′nego Vostoka [The main directions of fishing development in the Far East]. Innovation Science. 2019;(4):115–118. (In Russ.).
8. Russian Statistical Yearbook. 2019. Statistical handbook. Moscow: Rosstat; 2019. pp. 429–432. (In Russ.).
9. Skurikhin IM, Tutel′yan VA. Tablitsy khimicheskogo sostava i kaloriynosti rossiyskikh produktov pitaniya [Tables of the chemical composition and calorie content in Russian food products]. Moscow: DeLi print; 2008. 275 p. (In Russ.).
10. Shcherbakova EI. The use of seafood in order to improve the nutritional value of fish dishes. Bulletin of the South Ural State University. Series: Food and Biotechnology. 2015;3(1):83–89. (In Russ.).
11. Lopatin SA, Yuvanen EI. On the problems of sea-food consumption in the context of the present-day ecological situation and the growth of international tourism (Russia, St. Petersburg). Problems of Modern Economics. 2018;65(1):166–169. (In Russ.).
12. Hicks CC, Cohen PJ, Graham NAJ, Nash KL, Allison EH, D'Lima C, et al. Harnessing global fisheries to tackle micronutrient deficiencies. Nature. 2019;574(7776):95–98. https://doi.org/10.1038/s41586-019-1592-6.
13. Lugovaya EA, Stepanova EM. Assessment of the north resident''s nutrition supply with view of the content of macro and microelements in food. Problems of Nutrition. 2015;84(2):44–52. (In Russ.).
14. Steblevskaya NI, Polyakova NV, Zhad'ko EA, Chusovitina SV. Microelement composition of tissues of some species of aquatic organisms of Peter the Great Bay (Northern Bay). Vestnik of the Far East Branch of the Russian Academy of Sciences. 2013;171(5):127–132. (In Russ.).
15. Suslikov VL. Geokhimicheskaya ehkologiya bolezney: v 4 t. T. 2: Atomovity [Geochemical ecology of diseases: in 4 volumes. Vol. 2: Atomovites]. Moscow: Gelios ARV. 2000. pp. 322–330. (In Russ.).
16. Skal′nyy AV. Mikroehlementy: bodrost′, zdorov′e, dolgoletie [Microelements: vigor, health, longevity]. Moscow: Pero; 2019. 158 p. (In Russ.).
17. Fattorini D, Notti A, Regoli F. Characterization of arsenic content in marine organisms from temperate, tropical and polar environments. Chemistry and Ecology. 2006;22(5):405–414. https://doi.org/10.1080/02757540600917328.
18. Šlejkovec Z, Kápolna E, Ipolyi I, van Elteren JT. Arsenosugars and other arsenic compounds in littoral zone algae from the Adriatic Sea. Chemosphere. 2006;63(7):1098–1105. https://doi.org/10.1016/j.chemosphere.2005.09.009.
19. Aminina NM, Yakush EV, Blinov YuG. On methods of arsenic determination in marine organisms. Fisheries. 2015;(5):38–39. (In Russ.).
20. Lugovaya EA, Stepanova EM. Features of the content of drinking water in the city of Magadan and population health. Hygiene and Sanitation. 2016;95(3):241–246. (In Russ.). https://doi.org/10.18821/0016-9900-2016-95-3-241-246.
21. Demidov VA, Skalny AV. Men's and women's hair trace element concentrations in Moscow region. Trace Elements in Medicine. 2002;3(3):48–51. (In Russ.).
22. Salnikova EV, Detkov VYu, Skalny AV. Accumulation of essential and conditionally essential trace elements in hair of inhabitants of Russia. Trace Elements in Medicine. 2016;17(2):24–31. (In Russ.). https://doi.org/10.19112/2413-6174-2016-17-2-24-31.

ORCID IDs
Evgenia M. Stepanova http://orcid.org/0000-0002-2223-1358
Elena A. Lugovaya https://orcid.org/0000-0002-6583-4175

Foods and Raw Materials, 2021, vol. 9, no. 2

E-ISSN 2310-9599
ISSN 2308-4057

Research Article
Open Access

https://doi.org/10.21603/2308-4057-2021-2-310-316
Available online at http://jfrm.ru/en

Vinegar extraction from unripe shikuwasa (*Citrus depressa* L.), an Okinawan citrus fruit

Takashi Hanagasaki

Okinawa Agricultural Research Center, Itoman, Okinawa, Japan

e-mail: hangskit@yahoo.co.jp

Received April 14, 2021; Accepted in revised form May 18, 2021; Published online July 30, 2021

Abstract:
Introduction. Nakamoto Seedless, a variety of shikuwasa (*Citrus depressa* L.) in Okinawa, can be used to produce vinegar extracts because it has no seeds causing bitter taste. However, Nakamono Seedless is hardly cultivated commercially in Okinawa. This research was aimed to develop vinegar extract from Ogimi Kugani, another major variety of shikuwasa, and compare its characteristics with those of extracts from Nakamoto Seedless.
Study objects and methods. The study featured vinegar extracts from the whole shikuwasa of Nakamoto Seedless (20% fruit) and Ogimi Kunagi (5, 10, and 20% of fruit) varieties. The fruit was harvested in June, July, and August. We tested the samples for limonin and polymethoxyflavones content and sensory attributes, especially bitterness.
Results and discussion. Vinegar extracts with 20% of Ogimi Kugani harvested in June and July tasted bitter compared to those from Nakamoto Seedless harvested in August, but extracts from Ogimi Kugani harvested in August were not bitter. In addition, 5 and 10% vinegar extracts from Ogimi Kugani harvested in June had lower bitterness. The vinegar extracts from both shikuwasa varieties contained polymethoxyflavones – bioactive compounds – and similar flavor.
Conclusion. The whole shiluwasa fruit can be used to produce vinegar drinks, Ponzu soy sauce, salad dressings, etc.

Keywords: Okinawan citrus, Ogimi Kugani, Nakamoto Seedless, vinegar extract, polymethoxyflavones, sinensetin, nobiletin, tangeretin

Funding: This research was conducted as a part of the project on climate-smart fruit farming, which is funded from Okinawa's economic development budget.

Please cite this article in press as: Hanagasaki T. Vinegar extraction from unripe shikuwasa (*Citrus depressa* L.), an Okinawan citrus fruit. Foods and Raw Materials. 2021;9(2):310–316. https://doi.org/10.21603/2308-4057-2021-2-310-316.

INTRODUCTION

Shikuwasa (*Citrus depressa* L.) is a common citrus fruit in Okinawa, the southernmost prefecture of Japan. Shikuwasa is very sour and also called Hirami lemon or thin-skinned flat lemon. In Okinawan dialect, shikuwasa means "to eat vinegar", however it does not contain vinegar, and the name refers to its strong sour taste. This native Okinawan citrus fruit became popular all over Japan and is used to garnish dishes as well as to make juices and jams.

As it grows, shikuwasa changes color from dark green to yellow or orange. Unripe (green) fruit is extremely sour and is used to make condiments. Ripe (yellow) shikuwasa has better taste from December to the end of January. Shikuwasa harvested from August to September is usually used as an acidifying agent in vinegar substitution. Fruit harvested from September to December is used in juice production and from December to January can be eaten in the raw form.

Shikuwasa is mainly cultivated in the northern part of Okinawa. In 2017, 3398 t of shikuwasa were produced, with the fruiting area of shikuwasa being 363 ha. Shikuwasa contains high levels of nutritional components, including polymethoxyflavones [1], which are well known for their biological activities. Polymethoxyflavons demonstrate anti-tumor, anti-inflammation, and anti-hyperglycemic properties [1–4]. Therefore, extracting polymethoxyflavones and other functional components from shikuwasa can contribute to healthy food products.

Among known varieties of shikuwasa in Okinawa, Ogimi Kugani (hereinafter Kugani) is the most popular. Kugani is a commercially available superior landrace which is widely used in the food industry,

fresh or processed [5]. Nakamoto Seedless (hereinafter Seedless) is a seedless variety of shikuwasa that is becoming popular, due to its characteristics, which are similar to those of Kugani [6].

Citrus tree cultivation involves thinning young fruits to improve fruit size and quality. Thinning is performed from June to July because shikuwasa is not typically used during this period. Thinned fruits as well as normally harvested fruits unsuitable for sale, for example bruised fruits, should be effectively utilized to obtain processed food products such as vinegar extracts.

To produce a vinegar extract with low bitterness, Hirose *et al*. used only the peels of residual substances from Kugani, and Hanagasaki *et al*. used residual substances from Tankan (*Citrus tankan* Hayata) [7, 8]. Using this technology, Ponzu sauce (Japanese citrus vinegar soy sauce) production is already being commercialized in Okinawa. In addition, the whole Seedless fruit harvested from June to August is useful to produce vinegar extract because it has no seeds, contains low levels of limonin, and has low bitterness [9]. In spite of the fact that vinegar extract from the whole Kugani fruit is expected to be bitter because it typically contains 14 seeds per fruit, the potential use of the whole unripe Kugani should be explored to avoid wastes [6].

The aim of the present study was to develop vinegar extract from the whole unripe Kugani fruit and compare the characteristics of this extract with those of Seedless vinegar extracts to improve the profitability of the fruit.

STUDY OBJECTS AND METHODS

Shikuwasa (Nakamoto Seedless and Ogimi Kugani varieties) has been cultivated in Okinawa Agricultural Research Center (26º37’ N, 127º59’ E; 40 masl) since 2005. The Seedless and Kugani fruit under study were harvested in June 8, July 6, and August 3 (2018), respectively.

The objectives of the study were vinegar extracts made from Seedless (20% fruit) and Kugani (5, 10, and 20%). The fruit weight was defined by averaging the weights of 70~450 fruits, equal to approximately 1 kg. The fruit diameter was determined by averaging the diameters of 20 fruits. Moisture content was determined by calculating the weight difference before and after freeze-drying.

Production of vinegar extract. As for shikuwasa of Kugani variety harvested in different months, the fruit was broken down using a Bamix M200 mixer (Bamix, Switzerland). Afterwards, a 20% sample was prepared by stirring 10 g of the fruit and 40 mL of spirit vinegar (Kraft heinz, USA). Stirring was performed with a 4 cm stirrer bar at 2.0×g for 10, 30, 60, and 90 min.

Similarly, we prepared 20% Seedless vinegar samples. To compare vinegar extracts from Kugani and Seedless harvested in July and August, the samples were stirred for 60 min. The mixed samples were centrifuged at 1190×g for 20 min and filtered using No. 2 qualitative filter paper (Advantec Co. Ltd., Japan).

To compare vinegar extracts from shikuwasa harvested in June, we used 20% Seedless as well as 5 and 10% Kugani vinegar samples. The Kugani samples were obtained by mixing 2.5 or 5 g of Kugani fruit with 47.5 and 45 mL of vinegar and stirring for 60 min.

Freeze-dried powder process. To analyze polymethoxyflavone and limonin levels in shikuwasa, the samples were freeze-dried using an FD-550 freeze-drier (Tokyo rikakikai Co. Ltd., Japan). After drying, the samples were crushed in an IFM-800 mill (Iwatani Corp, Japan) using a 1.4 mm mesh.

Titratable acidity determination. A volume of 10 mL of the vinegar extracts was mixed with 100 mL of pure water and titrated with 0.5 mol/L NaOH until pH 8.2 ± 0.3 using a pH meter. We applied acid-base titration [10].

Polymethoxyflavone analysis. Polymethoxyflavone extraction was performed as described by Ichinokiyama *et al.* [11]. To extract polymethoxyflavones from shikuwasa, 100 mg of freeze-dried powder samples with 1 mL of methanol:DMSO (1:1) were subjected to ultrasonic wave for 10 min (M1800-J, Japan) and centrifuged at 2000×g for 2 min. We performed it three times. Extract solutions were obtained by diluting to a volume of up to 5 mL.

To obtain polymethoxyflavones from vinegar extracts, 1 mL of the vinegar extracts with 1 mL of ethanol were subjected to ultrasonic wave for 30 min. The insoluble component was removed by centrifugation at 2000×g for 2 min. The solutions were prepared for HPLC, namely filtered using a 0.20 μm hydrophilic PTFE (Advantec Co. Ltd.).

Sinensetin (Wako Pure Chemical Corp., Japan), as well as nobiletin, and tangeretin (Sigma-Aldrich, Japan) were dissolved in ethanol to a concentration of 0.1 mg/mL and used as standards. Quantitative analysis of each polymethoxyflavone was performed as described by Hirose *et al.* [7]. The sample solutions (5 μL) were injected onto a Union UK-C18 HPLC column (3×100 mm, 0.4 mL/min flow rate, Japan) at 40ºC. The solvent was acetonitrile/water/trifluorasetic acid (50/50/0.05). Analyses were performed at 340 nm using an LC-20A UV detector (Shimadzu corp., Japan). Amounts of polymethoxyflavones were calculated as the sum of sinensetin, nobiletin, and tangeretin.

Limonoid analysis. To extract limonoid from shikuwasa, 100 mg of the freeze-dried sample was mixed with 2 mL of acetic acid and 5 mL of ethyl acetate and then vortexed for 1 min. To obtain limonoid from vinegar extracts, 0.4 mL of the vinegar extracts was mixed with 1 mL of ethyl acetate and then vortexed for 1 min. Both ethyl acetate phases were collected after centrifugation at 2000×g for 2 min. These steps were repeated three times, and the supernatant was completely evaporated under reduced pressure.

Extract solutions were obtained by reconstituting the powdered samples with 2 and 0.4 mL of acetonitrile for shikuwasa and vinegar extract, respectively. The

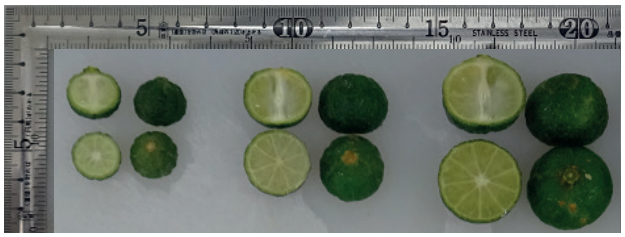

a

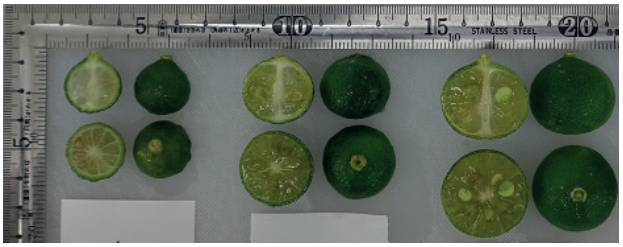

b

Figure 1 Nakamoto Seedless (a) and Ogimi Kugani (b) harvested from June to August (from left to right)

Table 1 Characteristics of Nakamoto Seedless and Ogimi Kugani harvested in different months

Harvesting date	Variety	Fruit weight, g	Fruit diameter, cm	Moisture content, %
June 8, 2018	Nakamoto Seedless	2.27	1.67	75.9
	Ogimi Kugani	3.51	1.92	80.4
July 6, 2018	Nakamoto Seedless	5.48	2.18	82.0
	Ogimi Kugani	8.81	2.58	82.0
August 3, 2018	Nakamoto Seedless	10.07	2.81	83.6
	Ogimi Kugani	15.31	3.24	82.9

solutions were prepared for HPLC by filtering. Limonin and nomilin (Wako Pure Chemical Corp., Japan) were each dissolved in acetonitrile to a concentration of 0.1 mg/mL and used as standards.

Quantitative analysis of limonin and nomilin was performed as described by Hirose *et al*. [7]. A volume of 2 μL of the sample solutions was injected into Cadenza CD-C18 HPLC column (0.4 mL/min, 40ºC). The solvent was acetonitrile/water/formic acid (40/60/0.1). The analyses were carried out at a wavelength of 210 nm using an LC-20A UV detector (Shimadzu corp., Japan).

Sensory evaluation. Vinegar extracts were diluted 10 times with distilled water, and 4% (w/w) caster sugar was added. Six men and six women aged 20–50 evaluated aroma, bitterness, green smell, and overall acceptability of the samples using a 5-point scale. For the shikuwasa aroma, 5 represented the strongest shikuwasa aroma and 1 represented the weakest aroma or the strongest vinegar aroma. For bitterness, 5 represented the lowest bitterness and 1 represented the strongest bitterness. For green smell, 5 represented the lowest green smell and 1 represented the strongest green smell. For overall acceptability, 5 represented "like" and 1 represented "dislike".

RESULTS AND DISCUSSION

Figure 1 demonstrates shikuwasa (Nakamoto Seedless and Ogimi Kugani varieties) harvested from June to August. The weight, diameter, and moisture of both fruit varieties were increasing during the time (Table 1). The characteristics of Seedless were lower than those of Kugani.

Changes in chemical components of Seedless and Kugani with time are shown in Table 2, changes in chemical components of both extracts with time are shown in Tables 3 and 4. In both varieties, the content of polymethoxyflavones was the highest in June and decreased with time ($P < 0.01$ for Seedless and $P < 0.001$ for Kugani). Comparing polymethoxyflvones content in both varieties, there was no significant

Table 2 Chemical components of Nakamoto Seedless and Ogimi Kugani harvested in different months

Component	Nakamoto Seedless			Ogimi Kugani		
	June	July	August	June	July	August
Polymethoxyflavones, mg/g d.w.	19.18 ± 1.46^{a}	12.33 ± 0.06^{b}	$10.81 \pm 0.14^{b*}$	17.89 ± 0.66^{a}	12.44 ± 0.08^{b}	7.87 ± 0.04^{c}
Sinensetin	1.50 ± 0.12^{a}	$1.04 \pm 0.01^{b*}$	$0.90 \pm 0.02^{b*}$	1.21 ± 0.05^{a}	0.90 ± 0.01^{b}	0.56 ± 0.01^{c}
Nobiletin	11.01 ± 0.89^{a}	7.31 ± 0.04^{b}	$6.22 \pm 0.08^{b*}$	11.03 ± 0.42^{a}	$7.94 \pm 0.05^{b*}$	4.81 ± 0.03^{c}
Tangeretin	6.66 ± 0.47^{a}	$3.98 \pm 0.02^{b*}$	$3.69 \pm 0.05^{b*}$	5.65 ± 0.20^{a}	3.60 ± 0.03^{b}	2.50 ± 0.02^{c}
Limonin, mg/g d.w.	0.29 ± 0.04	0.18 ± 0.04	0.28 ± 0.03	$1.55 \pm 0.09^{a*}$	$0.94 \pm 0.03^{b*}$	$0.68 \pm 0.05^{c*}$
Nomilin, mg/g d.w.	n.d.	n.d.	n.d.	n.d.	n.d.	n.d.

Data represent mean ± SE (n = 3)

Different letters among the same variety indicate significant differences by Tukey–Kramer's test ($P < 0.05$)

Asterisks indicate high significance by Tukey–Kramer's test ($P < 0.05$), compared with the other variety in the same month

Polymethoxyflavones represent the sum of sinensetin, nobiletin, and tangeretin

n.d. – not detected

Table 3 Characteristics of vinegar extracts from Nakamoto Seedless and Ogimi Kugani harvested in June

Parameter	Nakamoto Seedless	Ogimi Kugani		
Material/vinegar (w/w)	20%	20%	10%	5%
Vinegar volume, mL	31.5 ± 0.4^{c}	31.9 ± 0.2^{c}	38.4 ± 0^{b}	42.2 ± 0.2^{a}
Titratable acidity, %	4.70 ± 0.10^{c}	4.82 ± 0^{b}	4.87 ± 0.10^{b}	4.99 ± 0.10^{a}
Polymethoxyflavones, mg/100 mL	33.48 ± 0.13 (25.6)^{a}	27.14 ± 0.30 (26.6)^{b}	13.01 ± 0.19 (12.7)^{c}	7.76 ± 0.02 (7.6)^{d}
Sinensetin	2.89 ± 0.04 (38.2)^{a}	2.20 ± 0.03 (44.0)^{b}	1.10 ± 0.02 (22.1)^{c}	0.63 ± 0.01 (12.7)^{d}
Nobiletin	22.80 ± 0.10 (40.9)^{a}	19.15 ± 0.21 (42.1)^{b}	8.63 ± 0.13 (19.0)^{c}	5.03 ± 0.01 (11.1)^{d}
Tangeretin	7.78 ± 0.02 (23.1)^{a}	5.80 ± 0.07 (24.9)^{b}	3.27 ± 0.05 (14.0)^{c}	2.09 ± 0.01 (9.0)^{d}
Limonin, mg/100 mL	0.79 ± 0.04 (45.7)^{c}	2.73 ± 0.09 (42.9)^{a}	2.55 ± 0.02 (40.1)^{a}	1.31 ± 0.05 (20.1)^{b}
Shikuwasa aroma	2.75 ± 0.21	3.17 ± 0.20	2.83 ± 0.26	2.58 ± 0.25
Green smell	4.08 ± 0.33	3.75 ± 0.24	3.75 ± 0.36	4.25 ± 0.34
Bitterness	3.67 ± 0.30^{a}	2.42 ± 0.33^{b}	3.42 ± 0.28^{ab}	4.25 ± 0.27^{a}
Overall acceptability	3.83 ± 0.20^{a}	2.83 ± 0.24^{b}	3.50 ± 0.19^{ab}	3.67 ± 0.14^{a}

Data represent mean ± SE, n = 3 (except sensory evaluation)

Different letters among each sample indicate significant differences by Tukey–Kramer's test ($P < 0.05$)

Polymethoxyflavones represent the sum of sinensetin, nobiletin, and tangeretin

Values in parentheses indicate the recovery ratio of fruit

Table 4 Characteristics of vinegar extracts from Nakamoto Seedless and Ogimi Kugani harvested in July and August

Parameter	July		August	
	Nakamoto Seedless	Ogimi Kugani	Nakamoto Seedless	Ogimi Kugani
Material/vinegar (w/w)	20%			
Vinegar volume, mL	29.8 ± 1.1^{b}	36.4 ± 1.1^{a}	21.8 ± 0.6^{b}	27.5 ± 0.4^{a}
Titratable acidity, %	5.04 ± 0.10^{a}	4.66 ± 0^{b}	5.01 ± 0.10^{a}	4.78 ± 0^{b}
Polymethoxyflavones, mg/100 mL	19.60 ± 0.51 (31.7)	21.42 ± 1.22 (35.7)	17.95 ± 0.06 (48.9)^{a}	15.47 ± 0.12 (55.7)^{b}
Sinensetin	1.71 ± 0.05 (43.9)	1.74 ± 0.10 (55.1)	1.46 ± 0.01 (47.8)^{a}	1.04 ± 0.01 (52.7)^{b}
Nobiletin	13.32 ± 0.34 (48.7)	15.11 ± 0.87 (54.3)	12.12 ± 0.04 (57.5)^{a}	10.32 ± 0.08 (60.8)^{b}
Tangeretin	4.56 ± 0.11 (30.7)	4.57 ± 0.26 (36.2)	4.37 ± 0.02 (34.9)^{a}	4.10 ± 0.04 (46.5)^{b}
Limonin, mg/100 mL	0.58 ± 0.01 (70.9)^{b}	1.26 ± 0.15 (27.3)^{a}	0.92 ± 0.03 (78.8)^{b}	2.85 ± 0.02 (98.2)^{a}
Shikuwasa aroma	2.54 ± 0.18	3.00 ± 0.27	2.46 ± 0.33	2.85 ± 0.35
Green smell	4.08 ± 0.34	3.69 ± 0.30	4.31 ± 0.27	4.65 ± 0.18
Bitterness	3.92 ± 0.23^{a}	3.15 ± 0.27^{b}	4.31 ± 0.28	4.31 ± 0.22
Overall acceptability	3.85 ± 0.15	3.54 ± 0.14	3.62 ± 0.28	3.54 ± 0.22

Data represent mean ± SE, n = 3 (except sensory evaluation)

Different letters among each sample from the same harvest date indicate significant differences by Tukey–Kramer's test ($P < 0.05$)

Polymethoxyflavones represent the sum of sinensetin, nobiletin, and tangeretin

Values in parentheses indicate the recovery ratio of fruit

difference in June, but in August it was significantly higher in Nakamoto Seedless compared with Kugani (Table 2). Additionally, polymethoxyflavones in the vinegar extracts from both varieties significantly decreased with time (Seedless: $P < 0.001$, Kugani: $P < 0.001$) (Tables 3, 4). However, the recovery ratio of polymethoxyflavones from material increased with time. Hence, earlier harvested fruit contain higher amounts of polymethoxyflavones, which possess bioactive properties.

Limonin content did not show a decreasing trend in Seedless, but decreased in Kugani with time ($P = 0.217$ for Seedless and $P < 0.001$ for Kugani). Limonin level was significantly higher in the Kugani than in Seedless variety. Nomilin was not detected in both varieties. In general, the Seedless vinegar extract contained lower concentrations of limonin than the extract from Kugani.

Changes in polymethoxyflavone and limonin levels during the stirring process are demonstrated in Figs. 2 and 3.

The amount of polymethoxyflavones in vinegar extracts from Kugani harvested from June to August significantly increased ($P < 0.001$ in June, $P < 0.01$ in July, and $P < 0.001$ in August) during the stirring process (Fig. 2). Limonin levels in the extracts significantly decreased in July but increased in August

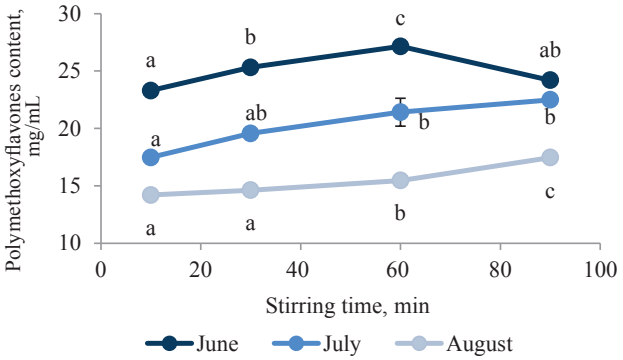

Figure 2 Levels of polymethoxyflavones in Ogimi Kugani vinegar extracts depending on harvest month and stirring time

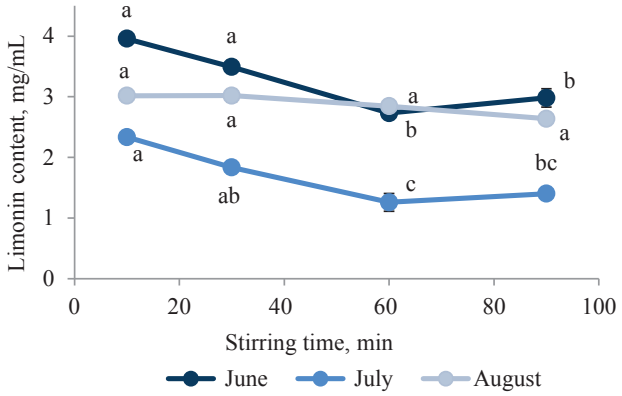

Figure 3 Levels of limonin in Ogimi Kugani vinegar extracts depending on harvest month and stirring time

($P < 0.001$ in June, $P < 0.001$ in July, and $P < 0.05$ in August) during the process (Fig. 2).

Limonin levels in the vinegar extract from Kugani harvested in August were not changed during the stirring time, whereas those in the extract from the fruit harvested in June and July significantly decreased (Fig. 3).

The stirring time of 10–60 min decreased but that of 60–90 min slightly increased the limonin concentration in the vinegar extracts from Kugani harvested in June and July. Thus, 60 min was selected as the optimal stirring time, and this time we used to compare the limonin level in Kugani extracts with that in Seedless.

We also analyzed 5 and 10% vinegar extracts from Kugani harvested in June. The obtained vinegar volumes and titratable acidity significantly increased with the decreasing fruit concentration. As for polymethoxyflavones and limonin, their levels depended directly on the fruit amount (Table 3).

Comparison of the vinegar extracts from Seedless and Kugani are shown in Tables 3 and 4. There was no significant difference in vinegar volume in 20% extracts from Seedless and Kugani harvested in June. However, the 5 and 10% Kugani extracts demonstrated significantly higher vinegar volume than the Seedless extracts in all the months.

The titratable acidity of the 5% Kugani vinegar extract was the highest in June, whereas that of the Seedless extract was the lowest (Table 3). In July and August, the Seedless extract showed higher titratable acidity compared to Kugani (Table 4). Total polymethoxyflavone levels in the vinegar extract from Seedless in June were the highest, while the 5% Kugani extract contained the lowest amount of polymethoxyflavones.

Furthermore, there was a similar tendency for each polymethoxyflavone, namely sinensetin, nobiletin, and tangeretin. In July, there was no significant difference in each polymethoxyflavone between the Seedless and Kugani vinegar extracts. In August, the Seedless vinegar extract demonstrated higher level of these polymethoxyflavones than the Kugani extract.

Sensory evaluation showed no significant difference in aroma and green smell among all the samples. The 20% extract from Seedless fruit had significantly higher bitterness than the 20% Kugani sample in July, but there was no significant difference in August (Table 4). As for June, there was no significant difference between the 20% Seedless extract and the 5 and 10% Kugani samples (Table 3).

Overall acceptability of the Seedless vinegar extracts was significantly higher than that of the 20% Kugani samples, but there was no significant difference between the 5 and 10% Kugani extracts in June. Overall acceptability of the Seedless and Kugani vinegar extracts in July and August showed no significant differences.

As mentioned above, limonin levels in the Kugani vinegar extract decreased during the stirring process in June and July but did not change in August (Fig. 3). This implies that limonin was protected from volatilizing or other enzymatic reactions during the stirring process. This can also explain the increasing level of some components in Kugani harvested from July to August. In addition, it may also be associated with the fact that the vinegar extract from Kugani harvested in August was not bitter despite a high content of limonin, which is a bitter compound present in the vinegar extract.

Hirose *et al*. reported that vinegar extract from waste peel of shikuwasa harvested in October and obtained by the direct pulverizing method tasted bitter and contained high levels of limonin [7]. Dea *et al*. found that increasing levels of sucrose or citric acid decreased the perception of bitterness induced by limonin in orange juice [12].

In our study, sucrose or citric acid contained in Kugani fruit juice could have masked the bitter taste of limonin in the vinegar extract from Kugani harvested in August. Therefore, the whole Kugani fruit harvested after August can be used as a raw material for vinegar extracts production by the stirring method. Not all the vinegar extracts made from Seedless fruit tasted bitter

as expected. However, the 20% Kugani extract was bitter, especially in June. Therefore, we developed a method to reduce bitterness of Kugani harvested in June.

There are other methods to diminish bitterness. Hirose *et al*. reported that limonin was not detected in vinegar extract from only Kugani peel [7]. In other words, segment membranes and seeds contain limonin but removing them is laborious and time-consuming. In the present study, the 5 and 10% Kugani extracts did not taste bitter and there was no significant difference in bitterness among them and the Seedless vinegar extract in June. Moreover, there were no significant differences in shikuwasa aroma and green smell. Thus, the flavor of the Kugani (5 and 10%) and Seedless vinegar extracts was considered to be the same.

Incidentally, some locals in Okinawa prefer the bitter taste of shikuwasa products, such as juice and jam. Demand for bitter-tasting vinegar extract can be met by using 20% Kugani fruit harvested in June. Seedless is hardly cultivated commercially in Okinawa. To produce vinegar extracts with lower bitterness, it is possible to use only Kugani, as showed in this study. It is also desirable to effectively use thinned or bruised Seedless and Kugani, which are not suitable for sale.

CONCLUSION

We produced vinegar extracts from the whole unripe fruit of Ogimi Kugani and Nakamoto Seedless harvested from June to August. The stirring method was applied to obtain the extracts. The 20% extract from Kugani harvested in June and July was bitter compared to the Seedless extract. However, the 5 and 10% Kugani samples did not differ in bitterness from the 20% Seedless extract in June

In addition, the 20% extracts from Kugani and Seedless fruit harvested in August showed similar bitterness, in spite of the fact that limonin levels in the Kugani extract were higher than those in the Seedless sample. Both vinegar extracts from Kugani and Seedless contained polymethoxyflavones, which decreased from June to August. The flavor of both vinegar extracts was similar.

The extraction technique applied in this study is easy to use and requires simple equipment, which minimize hygienic problems. Producing vinegar extracts from shikuwasa would allow creating a broad range of products such as Ponzu soy sauce, salad dressings, and fruit vinegar drinks. Moreover, vinegar extracts from shikuwasa can be applied to any type of citrus fruit worldwide.

CONFLICT OF INTEREST

The author declares that there is no conflict of interest.

ACKNOWLEDGMENTS

I thank Mr. N. Hirose, Senior supervisor of Okinawa Industrial Technology Center for his valuable idea and advice. I also thank Mr. F. Mitsube, Researcher, for providing shikuwasa fruits. I appreciate the technical supports by Ms. K. Kyan and Mr. T. Kadekawa.

REFERENCES

1. Kawaii S, Tomono Y, Katase E, Ogawa K, Yano M. Antiproliferative activity of flavonoids on several cancer cell lines. Bioscience, Biotechnology and Biochemistry. 1999;63(5):896–899. https://doi.org/10.1271/bbb.63.896.
2. Hirata T, Fujii M, Akita K, Yanaka N, Ogawa K, Kuroyanagi M, *et al*. Identification and physiological evaluation of the components from Citrus fruits as potential drugs for anti-corpulence and anticancer. Bioorganic and Medicinal Chemistry. 2009;17(1):25–28. https://doi.org/10.1016/j.bmc.2008.11.039.
3. Choi SY, Ko HC, Ko SY, Hwang JH, Park JG, Kang SH, *et al*. Correlation between flavonoid content and the NO production inhibitory activity of peel extracts from various citrus fruits. Biological and Pharmaceutical Bulletin. 2007;30(4):772–778. https://doi.org/10.1248/bpb.30.772.
4. Kunimasa K, Kuranuki S, Matuura N, Iwasaki N, Ikeda M, Ito A, *et al*. Identification of nobiletin, a polymethoxyflavonoid, as an enhancer of adiponectin secretion. Bioorganic and Medicinal Chemistry Letters. 2009;19(7):2062–2064. https://doi.org/10.1016/j.bmcl.2009.02.002.
5. Ishikawa R, Badenoch N, Miyagi K, Medoruma K, Osada T, Onishi M. Multi-lineages of Shiikuwasha (*Citrus depressa* Hayata) evaluated by using whole chloroplast genome sequences and its bio-diversity in Okinawa, Japan. Breeding Science. 2016;66(4):490–498. https://doi.org/10.1270/jsbbs.15151.
6. Medoruma K, Higa A, Kinjo H, Zukeyama H, Awaguni Y, Miyagi T, *et al*. Characteristics of seedless *Citrus depressa*, Nakamoto seedless. Bulletin of the Okinawa Prefectural Agricultural Research Center. 2011:5–10.
7. Hirose N, Maeda G, Onda S, Shoda M, Miyagi K, Wada K, *et al*. Development of vinegar extract from the waste peels of Shiikuwasha. Nippon Shokuhin Kagaku Kogaku Kaishi. 2017;64(2):81–89. https://doi.org/10.3136/nskkk.64.81.
8. Hanagasaki T, Hirose N, Maeda G, Onda S, Wada K. Vinegar extract of fruit waste from juice production using Tankan (*Citrus tankan* Hayata) native to Okinawa, Japan. Food Science and Technology Research. 2019;25(5):667–676. https://doi.org/10.3136/fstr.25.667.

9. Hirose N, Maeda G, Miyagi K, Wada K, Ohta H. Characteristics of vinegar extract from immature seedless Shiikuwasha (*Citrus depressa* Hayata, Nakamoto Seedless). Food Preservation Science. 2019;45:215–221. (In Jap.).
10. Hashimoto Y, Chuda Y, Suzuki T, Yasui A. Method validation for determination of total acid in vinegar based on potentiometric titration by interlaboratory study. Bunseki kagaku. 2008;57(6):453–459. https://doi.org/10.2116/bunsekikagaku.57.453.
11. Ichinokiyama H, Maegawa T, Goto M. Flavonoid contents of whole fruit and various tissues of a new acid citrus, 'Niihime'. Horticultural research (Japan). 2012;11(3):387–391. https://doi.org/10.2503/hrj.11.387.
12. Dea S, Plotto A, Manthey JA, Raithore S, Irey M, Baldwin EA. Interactions and thresholds of limonin and nomilin in bitterness perception in orange juice and other matrices. Journal of Sensory Studies. 2013;28(4):311–323. https://doi.org/10.1111/joss.12046.

ORCID IDs
Takashi Hanagasaki https://orcid.org/0000-0002-4151-8506

Foods and Raw Materials, 2021, vol. 9, no. 2

E-ISSN 2310-9599
ISSN 2308-4057

Research Article
Open Access

https://doi.org/10.21603/2308-4057-2021-2-317-323
Available online at http:jfrm.ru/en

Farmed Turkish salmon: Toxic metals and health threat

Levent Bat*, Elif Arici, Ayşah Öztekin, Fatih Şahin

University of Sinop, Sinop, Turkey

* e-mail: leventbat@gmail.com

Received June 20, 2021; Accepted in revised form July 12, 2021; Published online September 09, 2021

Abstract:

Introduction. Toxic metals in fish, even at low levels, have negative consequences for human health. Even essential metals pose a health threat if consumed in certain quantities. Mercury, cadmium, and lead are the most frequent metals containing in fish. The research objective was to inspect the quality of aquaculture fish found in most major grocery chains across Turkey.

Study objects and methods. The present research featured the quantities of Zn, Fe, Cu, Al, Pb, Hg, and Cd in Turkish salmon. The sampling took place between February and June 2019. The cumulative carcinogenic and non-carcinogenic risk for consumers was evaluated based on trace element levels in a prospective health risk assessment using the U.S. EPA model of lifetime exposure.

Results and discussion. Fe proved to be the most abundant element in fish fillets, followed by Zn and Cu. Other elements appeared to be far below the permissible values, namely Al ≤ 0.5, Cd ≤ 0.02, Pb, and Hg ≤ 0.05. All the trace elements detected in Turkish salmon were below the reference dose values. The percent contribution to total risk by Fe, Cu, and Zn were 34.20, 24.80, and 41.01%, respectively. The hazard index was ≤ 1. The contamination of aquaculture fish fillet proved insignificant, and the carcinogenic risk was entirely negligible.

Conclusion. The research revealed no hazardous trace elements, and their cumulative effects were not indicated in the hazardous index.

Keywords: Salmon, heavy metals, estimated daily intake, hazard index

Please cite this article in press as: Bat L, Arici E, Öztekin A, Şahin Fa. Farmed Turkish salmon: Toxic metals and health threat. Foods and Raw Materials. 2021;9(2):317–323. https://doi.org/10.21603/2308-4057-2021-2-317-323.

INTRODUCTION

Rainbow trout from North America is one of the most profitable members of the family in Turkish freshwater farming. Black Sea trout, also known as Turkish salmon, has now taken its place on the Turkish fish market, following the decision of the General Directorate of Fisheries and Aquaculture of the Ministry of Agriculture and Forestry. Turkish salmon grows in dam lakes until its weight reaches 180–220 g. After that, it is put into farms in the cold-water areas of the Black Sea. It is harvested when it weighs 3–4 kg.

In 2019, fish farms produced 116 053 tons of Turkish Salmon in inland waters and 9692 tons in sea farms [1]. This amount is constantly increasing compared to previous years. Farmed trout from Turkey's southern Black Sea littoral proved to be a rich nutritional source of fatty and amino acids, which normalize atherogenicity and thrombogenicity indices of blood [2].

Trout is mobile and prefers clean and oxygen-rich waters. As a result, even a slight contamination affects this fish, long before the water quality deteriorates. Even at low concentrations, metals in contaminated foods have harmful effects on human health [3]. Metal contamination occurs in nature; nevertheless, human activities, such as mining and heavy industry, have severe consequences for ecosystems and aquatic environment. Despite advancements in sewage effluent technology, sewage discharge remains a major challenge in many developing countries [4].

Metals have a strong impact on marine environment and make their way into human food chains. Such toxicants as Hg, Cd, and Pb are associated with fish consumption. Methyl Hg poisoning induced by prenatal ingestion of contaminated fish causes infant mortality and severe birth defects, such as mental retardation, cerebral palsy, and various neurological disorders [5–7]. When Cd is deposited in the proximal tubular cells of the kidney, it causes renal failure because of the decreasing glomerular filtration rates [8]. Pb poisoning affects renal, hematological, cardiovascular, gastrointestinal, and reproductive systems. Moreover, skeletal abnormalities may occur as a result of renal dysfunction and Pb accumulation in the bones [9–11].

Even though some metals are necessary, when their level in the tissues exceeds a certain threshold, they damage both individual organs and the entire organism.

Fish, as an essential aquatic food in the human food chain, has often been tested for metal contamination [3, 12–14]. Several studies have identified metal residues in various fish species, including trout. Rainbow trout has also been subjected to toxicological studies, which detected accumulation in tissues and liver even at low concentrations of Zn [15].

The current research dealt with both cancer and non-cancer hazards associated with trace elements (Fe, Zn, Cu, Al, Pb, Hg, and Cd) in Turkish salmon. Despite the fact that wellness threat assessment models were predominantly created in Europe and the United States, the European model is still in development, getting ever more complex [16]. The American model, according to Gržetić and Ghariani, is detailed and accurate [16]. It is accessible through the Risk Assessment Information System (RAIS), which is backed up by chemical characteristic established and gathered by the U.S. Environmental Protection Agency (U.S. EPA) Integrated Risk Information System [17]. Following [18–22], this research was based on the American model produced by the U.S. EPA [23, 24].

SRUDY OBJECTS AND METHODS

Turkish salmon samples collection. The object of the study was Turkish salmon collected from the Yakakent farm between February and June 2019 (three individual samples per month). The samples were randomly picked from fish offered for sale (Fig. 1). The samples were washed, stored in iceboxes, and transported to the Hydrobiology Laboratory, the Department of Fisheries, to be tested for Fe, Zn, Cu, Al, Pb, Hg, and Cd. Prior to the analysis, the fish samples were documented for the required biological parameters, e.g. wet body weight and total length. The measurements were based on the European Parliament's Animal Care and Use Directive on the Protection of Animals Used for Scientific Purposes [25]. After that, the samples were filleted (Fig. 2), put into polyethylene bags, and stored at 21°C.

Analytical procedures. The trace elements in the Turkish salmon fillets were determined by inductively coupled plasma mass spectrometry (ICP-MS) after applying the pressure digestion method at an environmental food analysis laboratory accredited in Turkey (TÜRKAK Test TS EN ISO IEC 17025 AB-0364-T). European Standard method EN 15763 was used to determine trace elements using acid, wet digestion, and standard reference material. The outputs were presented as mg/kg wet wt.

Daily trace elements intake. Risk evaluations for infants, children, and adults were conducted in order to determine the potential hazards that may arise as a result of consuming heavy metals with Turkish salmon. The risks were defined by calculating the probability of health hazard based on potential exposure. The risk exposure depended on the daily consumption of elements (mg/kg body weight per day). The estimated daily intake (EDI) was calculated using element levels and the amount of the fish consumed. The EDI of trace elements was calculated using the following equation:

$$EDI = \frac{C_{metal}\left(\frac{mg}{kg}\right) X\ W_{fish}\left(\frac{kg}{day}\right)}{BW\ (kg)} \quad (1)$$

where C_{metal} is trace elements levels in the fillet; W_{fish} is the daily mean consumption of the fillet, which was reported as 0.041, 0.027, and 0.013 kg/day for adults, children, and infants, respectively [26]; and BW refers to an average adult's body weight of 70 kg, a child's weight of 30 kg, and an infant's weight of 10 kg.

Carcinogenic and non-carcinogenic risks. The incremental lifetime cancer risk (ILCR) model was used to predict the likelihood of cancer risks in the fish caused by exposure to carcinogenic trace elements:

$$ILCR = CDI \times SF \quad (2)$$

where CDI stands for chronic daily consumption of a carcinogen in mg/kg of body weight per day, and refers the lifetime mean diurnal dose of exposure to the carcinogen. The cancer risk connected with the exposure

Figure 1 Turkish salmon

Figure 2 Fillet of Turkish salmon

to a carcinogenic or potentially carcinogenic material was calculated using slope factors (SF) [17].

If the ILCR was < 10^{-6}, it was regarded negligible; if it was 10^{-6} < ILCR < 10^{-4}, it was assessed as permissible or tolerated; if the ILCR > 10^{-4}, it was acknowledged as substantial. The carcinogenic and non-carcinogenic CDI values were obtained using the following formula [17]:

$$CDI_{car.} = \frac{C_{fish}\left(\frac{mg}{kg}\right) x\ EF\left(\frac{350\ days}{year}\right) x\ ED\ (26\ years)\ x\ FIR\left(\frac{41000\ mg}{day}\right) x\frac{10^{-6}\ kg}{1\ mg}}{AT\left(\frac{365\ days}{year} x\ LT(70\ years)\right) x\ BW\ (70\ kg)} \quad (3)$$

$$CDI_{non-car.} = \frac{C_{fish}\left(\frac{mg}{kg}\right) x\ EF\left(\frac{350\ days}{year}\right) x\ ED\ (26\ years)\ x\ FIR\left(\frac{41000\ mg}{day}\right) x\frac{10^{-6}\ kg}{1\ mg}}{AT_a\left(\frac{365\ days}{year} x\ ED\ (26\ years)\right) x\ BW\ (70\ kg)} \quad (4)$$

where CDI is the chronic daily intake of carcinogen; C_{fish} is the trace element concentrations in the fillet; EF is the exposure frequency; ED is the exposure duration; FIR is the fish ingestion rate for adults; AT is the averaging exposure time for non-carcinogenic effects and 70 years of lifetime (LT) for carcinogenic effect; AT_a is the averaging exposure time for non-carcinogenic effects and 26 years of exposure for carcinogenic effect; BW is the body weight.

Many recent studies used the Target Hazard Quotient (THQ) to peruse the potential non-carcinogenic effect of elements in the edible tissues of fish. In the present study, THQ was computed using the following equation to assess non-carcinogenic risks for trace elements in the fillet for adults [27–33]:

$$THQ = \frac{CDI}{Rf.D.} \quad (5)$$

where Rf.D. is an estimate of daily exposure that is unlikely to have significant adverse effects over the lifetime.

The U.S. EPA oral reference doses for Fe, Zn, Cu, Al, and Cd are 0.7, 0.3, 0.04, 1.00, and 0.001 mg/kg/day, respectively [23, 24]. The Rf.D. value for Hg inorganic salts is 0.0003 in the Risk Assessment Information System (RAIS). However, there is no Rf.D. value for Pb and its compounds [17]. The oral slope factor, on the other hand, is only indicated for Pb and its compounds as 0.0085 mg/kg/day [17]. The Hazard Index (HI) was found by summing up the THQs, as illustrated by the equation below:

$$HI = THQ\ (Fe) + THQ\ (Zn) + THQ\ (Cu) + THQ\ (Al) + \\ + THQ\ (Pb) + THQ\ (Hg) + THQ\ (Cd) \quad (6)$$

In the current study, the term "non-carcinogenic effect" (HI) describes the cumulative non-carcinogenic effect. If HI > 1.0, the CDI of a certain element exceeds Rf.D, which indicates that the element poses a potential risk.

Statistical analysis. The statistical analysis was performed using the statistical software SPSS Version 21.0. The one-way analysis of variance (ANOVA) was used to examine the difference in trace element quantities in the fish samples across months, followed by Duncan's post hoc test. The threshold for significance was set at $P < 0.05$.

RESULTS AND DISCUSSION

Fifteen Turkish salmon were purchased for trace element analysis. The fish had an average length of 51 cm and a weight of 2.90 kg.

Trace elements in the Turkish salmon. The concentrations of the trace elements observed in the samples of Turkish salmon were generally low (Table 1). Fe appeared to be the most abundant element, followed by Zn and Cu. As long as they do not exceed certain concentrations, such essential elements as Fe, Zn, and Cu are not harmful to biota, including fish.

No Al, Pb, Hg, and Cd concentrations were determined in the fillet samples. In both the European Union Commission Regulation and Turkish Food Codex, the maximum allowable values of carcinogenic Pb, Hg, and Cd are 0.3, 0.5, and 0.05 mg/kg wet wt., respectively [34, 35]. However, neither the European Union Commission Regulation nor the Turkish Food Codex gives any permissible values for Fe, Zn, Cu, and Al [34, 35]. These elements were far below the

Table 1 Trace elements content in the fillet of Turkish salmon

Months	Content, mg/kg wet wt.						
	Fe	Zn	Cu	Al	Pb	Hg	Cd
February	3.9[a]	2.2[a]	0.13[a]	< 0.5[a]	< 0.05[a]	< 0.05[a]	< 0.02[a]
March	4.2[a]	2.3[a]	0.11[a]	< 0.5[a]	< 0.05[a]	< 0.05[a]	< 0.02[a]
April	4.8[b]	2.7[b]	0.23[b]	< 0.5[a]	< 0.05[a]	< 0.05[a]	< 0.02[a]
May	5.5[c]	2.6[b]	0.24[b]	< 0.5[a]	< 0.05[a]	< 0.05[a]	< 0.02[a]
June	6.7[d]	3.1[c]	0.33[c]	< 0.5[a]	< 0.05[a]	< 0.05[a]	< 0.02[a]
Mean ± SD	5.02 ± 1.12	2.58 ± 0.35	0.21 ± 0.08	< 0.5	< 0.05	< 0.05	< 0.02

Letters a, b, c, and d show statistically significant differences ($P < 0.05$)

Table 2 Estimated daily intake (EDI) of trace elements in Turkish salmon farmed in Yakakent

Trace elements	Rf.D. Values	EDI (2019) mg/day/ kg body wt.		
		Infants	Children	Adults
Fe	0.7	0.006526	0.004518	0.00294029
Zn	0.3	0.003354	0.002322	0.00151114
Cu	0.04	0.0002704	0.000187	0.00012183
Al	1.00	–	–	–
Pb	–	–	–	–
Hg	0.0003	–	–	–
Cd	0.001	–	–	–

permissible values, namely Al ≤ 0.5, Cd ≤ 0.02, and Pb and Hg ≤ 0.05.

The sequence of trace elements according to contamination was Fe > Zn > Cu > Al > Pb = Hg > Cd. The reason for the low amounts of Al, Pb, Hg, and Cd could be that the fish farms are located in areas not contaminated by urban or rural sewage. The toxic quantities of Fe, Zn, Cu, Al, Pb, Hg, and Cd in seafood may have a negative impact on consumers' health. As a result, fish farms in coastal areas may be heavily contaminated with non-carcinogenic and carcinogenic hazardous materials that pose a substantial risk to human health. Thus, trace element levels in fish from this area should be regularly monitored and assessed.

In fact, the toxic elements in fish depend on water, food, and sediment. However, accumulation of these elements in food and water usually depends on other factors, e.g. metabolic rate, physiology, ecology, contamination tendency of food, sediment, and the temperature, salinity, and solubility of water, as well as on the interaction of these parameters.

In this study, food intake and uncontaminated water column had an important effect on the amount of trace elements in Turkish salmon, which resulted in a considerable decrease in the toxic elements in question. As metabolic activity decreases with growth and a proportionally lower food intake, the accumulation of elements decreases quite naturally. The trace elements in Turkish salmon farmed in Yakakent appeared to be below the permissible thresholds set by international and national organizations, confirming the results obtained by other researchers who studied trace element accumulation in trout [31, 36].

Estimated daily intake of trace elements. Table 2 illustrates the EDI values of Turkish salmon farmed in the Black Sea of Yakakent in 2019 for adults, children, and infants.

The toxicity of trace elements in humans is determined by their daily intake. In Turkey, the average fish consumption per adult is still low and remains at 15–20 g/day, compared to the recommended amount of 41 g/day [1, 26]. However, people who live near the coast consume far more fish than those who live in continental Turkey. As a result, the research relied on the data approved by the UN Scientific Committee on the Effects of Atomic Radiation [26]. The consumption of these contaminated fish parts puts the health of the local population at risk.

The EDI calculated for all chemical elements in the fish samples was compared with the toxicologically acceptable level and the oral reference dosage (Rf.D. values). The intake of all the trace elements was below the Rf.D. limits. Thus, the trace elements in Turkish salmon pose no threat for the population of the region.

Human health risks. The Risk Assessment Information System classifies Cd, Hg, and Pb as carcinogenic agents [17]. Chronic exposure to even low levels of Cd, Hg, and Pb could lead to a variety of cancers. If it exceeds a certain threshold value, it can have a carcinogenic effect. Table 3 demonstrates a lifetime risk analysis for Turkish salmon consumers.

Percent contribution to total risk by Fe, Cu, and Zn was determined as 34.20, 24.80, and 41.01%, respectively. According to U.S. EPA, at ILCR 10^{-6}, cancer threat is insignificant, the threshold risk limit of ILCR > 10^{-4} requires preventive medical measures, while ILCR > 10^{-3} signals that local public health is under threat. In the present study, the samples of Turkish

Table 3 Chronic Rf. D values, oral slope factor (SP), non-carcinogenic and carcinogenic chronic daily intake (CDI), target hazard quotient (THQ), hazard index (HI), and incremental lifetime cancer risk (ILCR) of trace elements in Turkish salmon in 2019

Elements	Chronic Rf.D., mg/kg/day	Oral slope factor (SF), mg/kg/day	Noncarcinogenic CDI, mg/kg/day	Carcinogenic CDI, mg/kg/day	THQ	ILCR
Fe	7.00E-01	–	2.82E-03	1.05E-03	4.03E-03	
Zn	3.00E-01	–	1.45E-03	5.38E-04	4.83E-03	
Cu	4.00E-02	–	1.17E-04	4.34E-05	2.92E-03	
Al	1.00E+00	–	–	–	–	
Pb	–	8.5E-03	–	–	–	–
Hg	3.00E-04	–	–	–	–	
Cd	1.00E-03	–	–	–	–	
HI					1.18E-02	–

salmon posed no cancer risk. Since none of the cancer-causing trace elements were detected, Turkish salmon consumption can be considered beneficial. However, a regular control the contamination levels of farmed fish is essential.

Chemicals can be either non-carcinogenic or carcinogenic in health risk assessments. Non-carcinogenic trace elements have a threshold limit. Therefore, they are regarded as having no adverse health effects at doses below the threshold level computed using the dose-response assessment method based on the specific reference dose for each element. Carcinogenic substances, on the other hand, are believed to have no effective threshold limits. This assumption implies that even low doses of the chemicals mean a low risk of cancer developing over time. As a result, there is no such thing as a safe level of exposure to carcinogenic substances [21]. In this sense, risk analysis and regular follow-ups are essential for human health.

The research also featured non-cancer risks of the trace elements in Turkish salmon. The risk level of hazard quotients (HQ) for adults was monitored for Fe, Zn, Cu, Al, Pb, Hg, and Cd. It revealed that consuming these trace elements through a fish-based diet posed a significant non-cancer risk. Individual ingestion of these trace elements from Turkish salmon in this region, on the other hand, is safe (HQ < 1) for the local population. Bat *et al.* and Yardim and Bat have obtained similar results [31, 35]. The cumulative HI, which is the sum of individual trace element THQs, was also used to describe the non-cancer hazards posed by Turkish salmon. Since the total of hazard quotients was ≤ 1, Turkish salmon revealed no potential risk for human health.

CONCLUSION

The hazard index was < 1, so the concentrations of trace elements (Fe, Zn, Cu, Al, Pb, Hg, and Cd) proved to pose no health threat via consumption. Adults, children, and infants had the same risk ranking, although infants were at a higher risk due to their low body weight. However, since Turkish salmon revealed no carcinogenic trace elements, and the non-carcinogenic trace elements were quite low, no consumer in any group is at risk. Risk within the non-carcinogenic trace elements in Turkish salmon was as follows: Zn (41.01%) > Fe (34.20%) > Cu (24.80%).

Food safety requires an intensive study program and longitudinal studies on the health risk of trace elements in aquaculture products cultivated in Turkey's coastal waters, regardless of how safe the current results are. The practice of health management, according to Bassey *et al*., begins with routine monitoring by regulatory bodies, toxicologically assessment of wastewater using conventional procedures, and raising public awareness of health consequences [21].

CONTRIBUTION

The authors were equally involved in writing the manuscript and are equally responsible for plagiarism.

CONFLICT OF INTEREST

The authors declare no conflict of interests regarding the publication of this article.

ACKNOWLEDGEMENTS

The authors wish to acknowledge the Department of Hydrobiology, Fisheries Faculty, University of Sinop, for providing laboratory facilities.

REFERENCES

1. Republic of Turkey Ministry of Agriculture and Forestry General Directorate of Fisheries and Aquaculture. Fishery Statistics [Internet]. [cited 2021 May 10]. Available from: https://www.tarimorman.gov.tr/BSGM.
2. Kaya Öztürk D, Baki B, Öztürk R, Karayücel S, Uzun Gören G. Determination of growth performance, meat quality and colour attributes of large rainbow trout (*Oncorhynchus mykiss*) in the southern Black Sea coasts of Turkey. Aquaculture Research. 2019;50(12):3763–3775. https://doi.org/10.1111/are.14339.
3. Bat L. The contamination status of heavy metals in fish from the Black Sea, Turkey and potential risks to human health. In: Sezgin M, Bat L, Ürkmez D, Arici E, Öztürk B, editors. Black Sea marine environment: The Turkish shelf. Istanbul: Turkish Marine Research Foundation; 2017. pp. 322–418.
4. Bat L, Gökkurt Baki O. Seasonal variations of sediment and water quality correlated to land-based pollution sources in the middle of the Black Sea coast, Turkey. International Journal of Marine Science. 2014;4(12):108–118.
5. Toxicological profile for mercury. Atlanta: U.S. Department of Health and Human Services; 1999. 20 p.
6. Cadmium dietary exposure in the European population. EFSA Journal. 2012;10(1). https://doi.org/10.2903/j.efsa.2012.2551.
7. Statement on the benefits of fish/seafood consumption compared to the risks of methylmercury in fish/seafood. EFSA Journal. 2015;13(1). https://doi.org/10.2903/j.efsa.2015.3982.
8. Scientific opinion on the risk for public health related to the presence of mercury and methylmercury in food. EFSA Journal. 2012;10(12). https://doi.org/10.2903/j.efsa.2012.2985.
9. Toxicological profile for lead. Atlanta: U.S. Department of Public Health and Human Services; 2007. 573 p.
10. Scientific opinion on lead in food. EFSA Journal. 2010;8(4). https://doi.org/10.2903/j.efsa.2010.1570.

11. Lead dietary exposure in the European population. EFSA Journal. 2012;10(7). https://doi.org/10.2903/j.efsa.2012.2831.
12. Bat L. One health: The interface between fish and human health. Current World Environment. 2019;14(3):355–357. https://doi.org/10.12944/CWE.14.3.04.
13. Bat L, Arici E. Heavy metal levels in fish, molluscs, and crustacea from turkish seas and potential risk of human health. In: Holban AM, Grumezescu AM, editors. Food quality: Balancing health and disease. A volume in handbook of food bioengineering. Academic Press; 2018. pp. 159–196. https://doi.org/10.1016/B978-0-12-811442-1.00005-5.
14. Bat L, Öztekin A, Arici E, Şahin F. Health risk assessment: heavy metals in fish from the southern Black Sea. Foods and Raw Materials. 2020;8(1):115–124. DOI: http://doi.org/10.21603/2308-4057-2020-1-115-124.
15. Gundoğdu A, Yardim Ö, Bat L, Çulha ST. Accumulation of zinc in liver and muscle tissues of Rainbow trout (*Onchorhyncus mykiss* Walbaum 1792). Fresenius Environmental Bulletin. 2009;18(1):40–44.
16. Gržetić I, Ghariani ARH. Potential health risk assessment for soil heavy metal contamination in the central zone of Belgrade (Serbia). Journal of the Serbian Chemical Society. 2008;73(8–9):923–934. https://doi.org/10.2298/JSC0809923G.
17. The Risk Assessment Information System [Internet]. [cited 2021 May 10]. Available from: https://rais.ornl.gov/index.html.
18. Wu B, Zhao DY, Jia HY, Zhang Y, Zhang XX, Cheng SP. Preliminary risk assessment of trace metal pollution in surface water from Yangtze River in Nanjing Section, China. Bulletin of Environmental Contamination and Toxicology. 2009;82(4):405–409. https://doi.org/10.1007/s00128-008-9497-3.
19. Li S, Zhang Q. Risk assessment and seasonal variations of dissolved trace elements and heavy metals in the Upper Han River, China. Journal of Hazardous Materials. 2010;181(1–3):1051–1058. https://doi.org/10.1016/j.jhazmat.2010.05.120.
20. Tepanosyan G, Maghakyan N, Sahakyan L, Saghatelyan A. Heavy metals pollution levels and children health risk assessment of Yerevan kindergartens soils. Ecotoxicology and Environmental Safety. 2017;142:257–265. https://doi.org/10.1016/j.ecoenv.2017.04.013.
21. Bassey OB, Chukwu LO, Alimba GC. Cytogenetics of *Chrysichthys nigrodigitatus* as bioindicator of environmental pollution from two polluted lagoons, South-Western Nigeria. Journal of Genetics and Genome Research. 2019;6. https://doi.org/10.23937/2378-3648/1410047.
22. Mohammadi AA, Zarei A, Majidi S, Ghaderpoury A, Hashempour Y, Saghi MH, et al. Carcinogenic and non-carcinogenic health risk assessment of heavy metals in drinking water of Khorramabad, Iran. MethodsX. 2019;6:1642–1651. https://doi.org/10.1016/j.mex.2019.07.017.
23. Risk assessment guidance for superfund. Volume I. Human health evaluation manual (Part A). Interim Final. Washington: U.S. Environmental Protection Agency; 1989. 291 p.
24. Guidance for assessing chemical contamination data for use in fish advisories. Volume 2. Risk assessment and fish consumption limits. Washington: U.S. Environmental Protection Agency; 2000. 383 p.
25. Directive 2010/63/EU of the European parliament and of the council of 22 September 2010 on the protection of animals used for scientific purposes. Official Journal of the European Union. 2010:33–76.
26. Sources and effects of ionizing radiation: United Nations Scientific Committee on the Effects of Atomic Radiation. 2008 Report. Volume I. New York: United Nations; 2010. 683 p.
27. Bat L, Arici E, Sezgin M, Şahin F. Heavy metal levels in commercial fishes caught in the southern Black Sea coast. International Journal of Environment and Geoinformatics. 2017;4(2):94–102.
28. Bat L, Öztekin A, Şahin F. Trace metals amounts and health risk assessment of *Alosa immaculate* Bennett, 1835 in the southern Black Sea. Discovery Science. 2018;14:109–116.
29. Bat L, Arici E, Öztekin A. Heavy metals health risk appraisal in benthic fish species of the Black Sea. Indian Journal of Geo-Marine Sciences. 2019;48(1):163–168.
30. Bat L, Öztekin A, Arici E, Şahin F. Health risk assessment: heavy metals in fish from the southern Black Sea. Foods and Raw Materials. 2020;8(1):115–124. https://doi.org/10.21603/2308-4057-2020-1-115-124.
31. Yardim Ö, Bat L. Human health risk assessment of heavy metals via dietary intake of Rainbow trout from Samsun fish markets. Journal of Anatolian Environmental and Animal Sciences. 2020;5(2):260–263. https://doi.org/10.35229/jaes.702810.
32. Bat L, Şahin F, Öztekin A, Arici E. Toxic metals in seven commercial fish from the southern Black Sea: Toxic risk assessment of eleven-year data between 2009 and 2019. Biological Trace Element Research. 2021. https://doi.org/10.1007/s12011-021-02684-4.
33. Majlesi M, Malekzadeh J, Berizi E, Toori MA. Heavy metal content in farmed rainbow trout in relation to aquaculture area and feed pellets. Foods and Raw Materials. 2019;7(2):329–338. https://doi.org/10.21603/2308-4057-2019-2-329-338.

34. Commission Regulation (EC) No 1881/2006. Setting maximum levels for certain contaminants in foodstuffs. Official Journal of the European Union. 2006;364:5–24.
35. Communiqué on maximum limits of contaminants in foodstuffs. Official Gazette. 2008;(26879). (In Turkish).
36. Bat L, Öztekin A, Yardım Ö. Metal levels in large sea trout from Sinop fish market. Fresenius Environmental Bulletin. 2018;27(12):8505–8508.

ORCID IDs
Levent Bat http://orcid.org/0000-0002-2289-6691
Elif Arici https://orcid.org/0000-0001-6359-9194
Ayşah Öztekin https://orcid.org/0000-0002-3726-7134
Fatih Şahin https://orcid.org/0000-0003-0605-2672

Foods and Raw Materials, 2021, vol. 9, no. 2

E-ISSN 2310-9599
ISSN 2308-4057

Research Article
Open Access

https://doi.org/10.21603/2308-4057-2021-2-324-334
Available online at http://jfrm.ru/en

Migration of mercury in the food chains of the Beloosipovo biocenosis (part 1)

Alexander Yu. Prosekov

Kemerovo State University, Kemerovo, Russia

e-mail: aprosekov@rambler.ru

Received June 28, 2021; Accepted in revised form July 20, 2021; Published online October 01, 2021

Abstract:
Introduction. Mercury and its compounds are among the most dangerous toxic substances, which makes mercury pollution one of the most urgent environmental issues. The present research objective was to study the accumulation of mercury and its impact on the terrestrial ecosystems in the area of the Beloosipovo mercury deposit (Kemerovo Region, West Siberia, Russia).
Study objects and methods. The study used standard methods to test soil, herbs, herpetobiont insects, and small mammals. The sampling was conducted at 13 points in the cardinal directions at 0.5, 1.5, and 3.0 km from the pollution source. The method of atomic absorption was employed to measure the concentration of mercury in the samples prepared by the wet mineralization method.
Results and discussion. The main components of terrestrial ecosystems revealed no excessive concentration of mercury in the soil. However, the water samples from the Belaya Osipova river demonstrated an excess in the maximum permissible concentration of mercury from 5 to 20% (0.00056–0.00074 mg/L). Further up the food chains, the concentration of mercury in organisms decreased by 1–2 orders of magnitude, depending on the sampling point. The study also revealed Siberian trout lily (*Erythronium sibiricum* (Fisch. et C. A. Mey) Kryl.), which is protected at the federal and regional levels, as well as several nemoral tertiary relics.
Conclusion. The decreasing concentration of mercury in the food chains means the ecosystem is under no severe negative impact.

Keywords: Ecology, mercury, mercury-containing compounds, terrestrial ecosystems, food chains

Funding. The research was conducted on the premises of the Research Equipment Sharing Center of Kemerovo State University, agreement No. 075-12021-694 dated August 5, 2021, between the Ministry of Science and Higher Education of the Russian Federation (Minobrnauka) and Kemerovo State University (KemSU) (contract identifier RF----2296.61321X0032).

Please cite this article in press as: Prosekov AYu. Migration of mercury in the food chains of the Beloosipovo biocenosis (part 1). Foods and Raw Materials. 2021;9(2):324–334. https://doi.org/10.21603/2308-4057-2021-2-324-334.

INTRODUCTION

Mercury is an important safety issue in the environmental, medical, and social aspects. In fact, mercury-related issues are one of the most urgent contemporary challenges. Mercury (Hg) and mercury-containing compounds are toxic substances that pose danger to all living organisms. According to preliminary estimates, about 4700 tons of mercury is discharged worldwide every year [1–3]. Mercury-related water pollution is especially dangerous, since water-soluble toxic methylmercury [CH_3Hg] accumulates in the fish as a result of activity of sediment microorganisms.

Mercury affects land and water plants, animals, fungi, and microorganisms, which constantly interact with each other in food chains, symbiosis, and etc. [4]. Many studies recognize the essential role of terrestrial plants in the biogeochemical cycle of mercury [5–7]. For instance, Leonard *et al.* tested five plant species for absorption, distribution, and subsequent release of mercury into the atmosphere, namely *Lepidium latifolium* L., *Artemisia douglasiana* Bessin Hook, *Caulanthus* sp. Watson, *Fragaria vesca* L., and *Eucalyptus globulus* Labill [8]. The research featured various ecological and physiological profiles of plants in a mercury-contaminated area. In the arid ecosystem, mercury emissions proved dominant in the mercury cycle, while plants functioned as channels for the interphase transfer of mercury from the geosphere to the atmosphere.

Asati *et al.* also examined the effect of heavy metals, including mercury, on plants and their metabolic activity in areas with high anthropogenic pressure [9]. Heavy metals appeared to have a severe toxic effect on plants, animals, and other local living organisms. Jameer Ahammad *et al.* claimed that even low concentrations of mercury has a negative effect on plants, e.g. stunted growth and many other adverse consequences [10].

High levels of mercury in soil demonstrated various adverse effects on plant growth and metabolism, e.g. poor photosynthesis, transpiration, water absorption, chlorophyll synthesis, and high lipid peroxidation [11–15].

In plants, a high content of mercury affects most enzymes. Zhou *et al.* studied the global database for about 35 000 measurements of mercury [16]. They examined the distribution and absorption of mercury in deciduous and coniferous ecosystems. The scientists believe that an effective monitoring of the impact of vegetation on the global mercury cycle requires a better parameterization of models and more consistent observational data, while recording the exchange of mercury in the entire ecosystem is especially important.

Obrist *et al.* investigated the role of sedimentation in the global cycle of mercury [17, 18]. The precipitation of mercury compounds occurs all year round. However, it is much higher in summer because the metal is absorbed by vegetation. Absorption of gaseous mercury by the tundra increases its concentration in the soil. The authors predict an increase in the impact of mercury on various ecosystems and human life, which requires further multifaceted research.

Ranieri *et al.* discovered that phytoextraction is an effective and affordable technological solution for the removal of metals, including mercury, from contaminated soil and water [19]. Jiskra *et al.* confirmed the severe effect of mercury isotopes on mercury absorption by vegetation [20]. Greger *et al.* studied six plant species that translocate and release mercury into the air [21]. They used a transpiration chamber to monitor the absorption of mercury by the roots, its further distribution over the shoots, and the final release through the shoots. The research featured garden peas, spring wheat, sugar beets, oilseed rape, white clover, and willow. All the plants were able to absorb significant amounts of mercury from its nutrient solution (200 μg/L). However, the translocation to the shoots was rather low (0.17–2.50 %).

Juillerat *et al.* examined soil and ground litter in 15 locations covered by northern deciduous trees or mixed deciduous and coniferous forests [22]. Their research objective was to determine how mercury content depended on the tree species, forest type, and soil profile. Twelve tree species from two sites demonstrated significant differences. The research proved that the peculiarities of a particular territory are important for mercury studies. The differences in the mercury pools from ground litter correlated with the differences in carbon pools.

These global issues are relevant for Russia and the Kemerovo Region. Komov *et al.* studied the content of mercury in soil, water sediments, and animals on the banks of the Rybinsk Reservoir [23]. The recorded mercury concentrations varied by more than two orders of magnitude. As for aquatic invertebrates, the concentration of metal appeared to be high in heterotopic species: larvae and adult insects had 0.85 mg of mercury per 1 kg of dry weight. However, homotopic species had a lower concentration of mercury, e.g. for mollusks, it was 0.11 mg per 1 kg of wet weight. As for predatory arachnids, aquatic and semi-aquatic species proved to have higher concentrations of mercury: for hydrocarina, it was ≤ 0.68, and for raft spiders, it was ≤ 0.33 mg per 1 kg of dry weight. On the contrary, spiders that lived far from water sources revealed much lower concentrations of mercury: crab spiders ≤ 0.07 mg per 1 kg of dry weight. Creatures that feed on vegetation or phytophagous animals also demonstrated lower mercury concentrations.

Gremyachikh *et al.* studied the content of mercury in the muscle tissue of river perch fished in different areas of the Rybinsk Reservoir in 1997–2012 and registered an increase in mercury concentration in recent decades [24].

Gorbunov *et al.* assessed the increase in mercury in the tissues of fish caught in the Volga [25]. They focused on how the accumulation of mercury in the muscle tissues of perch, bream, and pike depended on the mass of fish. The research registered a directly proportional dependence for perch (correlation coefficient $r = 0.881$, $p = 0.018$) and an inversely proportional relationship for pike ($r = –0.653$, $p = 0.029$). For bream, no such dependence was revealed.

Komov *et al.* studied the content of mercury in five species of amphibians and seven species of leeches [26]. The average values for amphibians were 0.007–0.101, for leeches – 0.014–0.065 mg per 1 kg of wet weight. The concentration of mercury depended on the taxonomy, habitat, and tissue type. The experiment established some consequences of the alimentary mercury intake on several biological parameters, i.e. metamorphosis rate of toad larvae, behavior pattern of tadpoles of frogs and leeches, etc. The results delivered new data on the mechanisms of migration and distribution of mercury compounds in aquatic, near-water, and terrestrial ecosystems.

Golovanov *et al.* studied *in vivo* the effect of accumulated mercury on the maltase and amylolytic activity of glycosidases in tadpoles of the common toad (*Bufobufo* L.) [27]. The research revealed changes in the activity of glycosidases depending on the level of accumulated mercury and the timing. The activity of the glycosidases decreased, whereas the sensitivity of starch-hydrolyzing enzymes to heavy metal ions (Cu, Zn, Cd, and Pb) increased.

The physicochemical properties of mercury allow it to circulate, accumulate, and redistribute in environment, depending on the particular conditions of aquatic and terrestrial ecosystems. Most of the mercury is dispersed and creates a natural global geochemical background, superimposed on man-induced mercury pollution, thus forming areas of antropogenic pollution.

Until recently, the accumulation of mercury by hydrobionts attracted most scientific attention because aquatic environment is optimal for the formation of

the most toxic organomercury compounds. Methylated mercury compounds accumulate in living organisms more intensively than inorganic ones and are slowly to excrete. As a result, the transport of mercury along the food chain is faster than in cases of direct absorption of the metal from the environment.

The content of mercury in living organisms increases at the tops of food webs and reaches maximal values in predatory fish, fish-eating birds, and mammals.

Terrestrial ecosystems attract less attention regarding the issues of mercury accumulation and distribution. More research is needed to establish the accumulation patterns of mercury compounds by living organisms in terrestrial ecosystems. The best way to establish the patterns is to determine the level of mercury accumulation in organisms of different trophic groups.

The present research objective was to study the mercury accumulation and its effect on various components of terrestrial ecosystems near the Beloosipovo mercury deposit (Kemerovo region, Russia).

STUDY OBJECTS AND METHODS

The research featured such components of the terrestrial ecosystem as soil, herbaceous plants, herpetobiont insects, and small mammals harvested in the vicinity of the Beloosipovo mercury deposit in the Kemerovo region, Russia (55.196730 N, 86.970065 E).

The sampling involved standard methods. Regardless of the wind pattern, all samples were taken at four cardinal points (Fig. 1) at three radii:

1) 0.5 km from the pollution source;
2) 1.5 km from the pollution source;
3) 3.0 km from the pollution source.

The sampling points:

Point 0 (Control) – N 55°10.920', E 087°00.959'
Point North 1 (N1) – N 55°11.180', E 087°00.980'
Point North 2 (N2) – N 55°11.798', E 087°00.954'
Point North 3 (N3) – N 55°12.561', E 087°01.244'
Point South 1 (S1) – N 55°10.654', E 087°00.958'
Point South 2 (S2) – N 55°10.189', E 087°01.146'
Point South 3 (S3) – N 55°09.654', E 087°01.123'
Point West 1 (W1) – N 55°10.915', E 087°00.605'
Point West 2 (W2) – N 55°10.918', E 086°59.920'
Point West 3 (W3) – N 55°10.940', E 086°58.496'
Point East 1 (E1) – N 55°10.866', E 087°01.333'
Point East 2 (E2) – N 55°10.939', E 087°02.427'
Point East 3 (E3) – N 55°10.876', E 087°03.705'

The territory of the Beloosipovo mine was considered as the main source of pollution and marked as Point 0 (C).

The control sampling was carried out at N 55°13.291', E 086°35.294'. It was located more than 30 km away from the Beloosipovo mercury deposit, which means it had no effect whatsoever on the background indicators. The soil sampling followed State Standards R 56157-2014 and State Standards 17.4.3.01-2017 using the

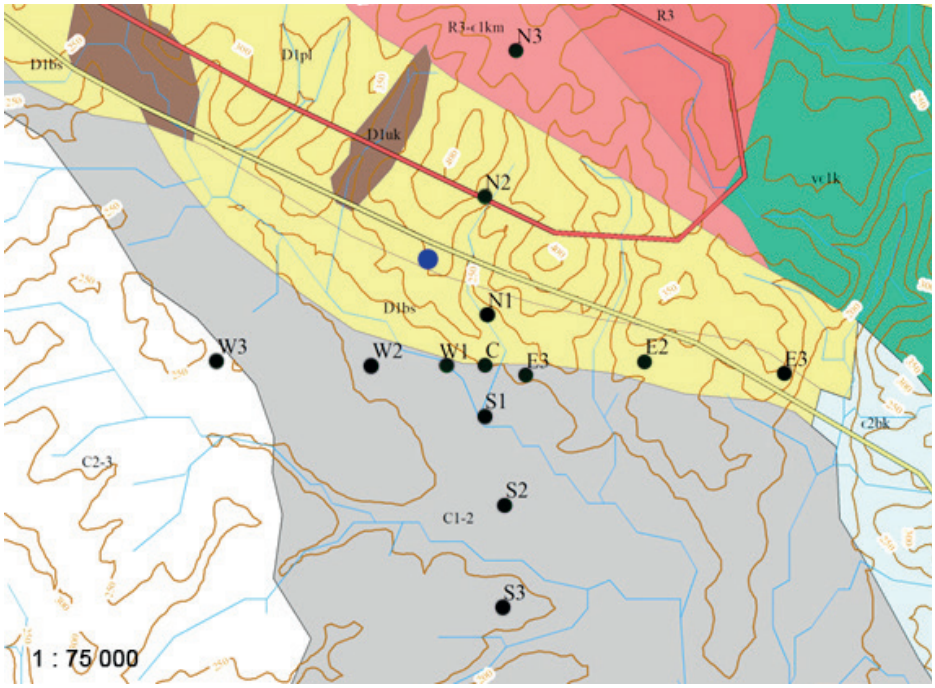

Figure 1 Sampling points and boundaries of mercury zones of the Beloosipovo deposit

Legend:

● – sampling points;
● – adit entrance;
– border of the Beloosipovo mercury deposit;
– border of the Pezass-Beloosipovo mercury ore-bearing zone.

envelope method at a depth of 0–20 cm and 30–60 cm. The total sampling weight was ≥ 2 kg. The soil samples were put in separate plastic containers and labeled.

The eight herb samples were taken in the same areas as the soil samples. The combined sample wet weight was ≥ 2 kg (natural moisture). The plants were removed together with the rhizomes, which were thoroughly cleared of soil. The samples were placed in plastic bags and labeled.

Invertebrates are the main link by which mercury from the environment enters the organisms of vertebrates. Herpetobiont insects inhabit the soil surface and are widespread in terrestrial ecosystems. They play an important role in food and soil chains.

The main group of herpetobiontic insects was represented by four families of Coleoptera (*Coleoptera* L.): dung beetles (*Geotrupidae* L.), lamellar beetles (*Scarabaeidae* L.), ground beetles (*Carabidae* L.), and istafilinids (*Staphylinidae* L.)

The herpetobiont insects were caught using Barber's traps. At one point, 50 traps with a volume of 0.3 l were dug in one line at a distance of 1 m from each other. The traps contained 5% acetic acid solution. The insects collected at each point were packed into containers, labeled, and stored in an automobile refrigerator at –4°C.

The small mammals were represented by insectivores (*Eulipotyphla* L.) and rodents (*Rodentia* L.). They were caught using crushers. At each point, 50 crushers were installed at a distance of 1 m from each other. The captured animals were placed in plastic containers, labeled, and stored in a car refrigerator.

The species composition of the mammals:

Byinsectivores (*Eulipotyphla*)

Shrews (*Soricidae* L.):

– Common shrew (*Sorex araneus* L.);
– Even-toothed shrew (*Sorex isodon* L.);
– Pygmy shrew (*Sorex minutus* L.);
– Masked shrew (*Sorex caecutiens* L.);
– Water shrew (*Neomys fodiens* L.).

Rodents (*Rodentia*)

Hamsters (*Cricetidae* L.):

– Red-backed vole (*Clethrionomys rutilus* L);
– Grey-sided vole (*Clethrionomys rufocanus* L.);
– Bank vole (*Clethrionomys glariolus* L.);
– Root vole (*Microtu oeconomus* L.);
– Common field vole (*Microtus agrestis* L.).

Mice (*Muridae* L.):

– Field mouse (*Apodemus agrarius* L.);
– Jerboa mouse (*Dipodidae* L.);
– Birch mouse (*Sicista betulina* L.).

The sampling of water in the Belaya Osipova river was carried out 0.5–1.0 km above the mouth (Fig. 2) in five replicates in 2018–2021. The samples were poured into two-liter vessels and were delivered to the laboratory within no more than 18 h from the moment of water intake.

The concentration of mercury in soil, plants, herpetobiont insects, and small mammals was carried out in an accredited laboratory of the Kemerovo State University (Russia). The tests followed Federal Environmental standard PNDF 16.1:2:2.2.80-2013 (M 03-09-2013) "Quantitative chemical analysis of soils. Methods for measuring the mass fraction of total mercury in samples of soils and grounds, including greenhouses, clays, and bottom sediments, by the atomic absorption method using a mercury analyzer RA-915M."

The samples were prepared using wet mineralization and concentrated nitric acid, hydrochloric acid, and hydrogen peroxide. The samples were dried to obtain biosubstrates in an EKPS-10 electric chamber furnace at 520°C. The obtained white ash was used to determine the content of mercury.

The method for measuring the mass fraction of total mercury involved thermal decomposition accompanied by the atomization of mercury. After that, the atomic mercury was transferred to the analytical cell of the analyzer by air flow. The atomic absorption

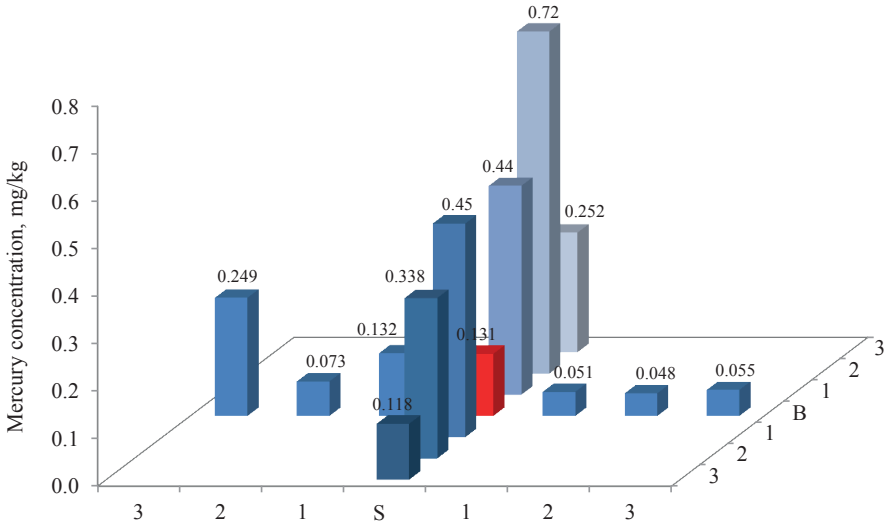

Figure 2 Concentration of mercury in the soil (horizon – 0–20 cm) in the area of the Beloosipovo mercury deposit

of mercury was measured at a resonant wavelength of 253.7 nm. The mass fraction of mercury in the sample was automatically determined by the peak area value (analytical signal). The process was based on the preset calibration characteristic using the software for the analyzer (RAPID software). The calibration was carried out using standard samples of a solution of mercury ions. It involved a calibration sample that contained mercury adsorbed on activated carbon.

RESULTS AND DISCUSSION

According to the e-catalog of geological documents from the Russian Federal Geological Fund, the mercury deposit of 124 tons is located in the river basin of the Belaya Osipova. The ore-bearing mineral is cinnabar (HgS). Mineralization is extremely uneven, and areas of high concentration are replaced by barren ones. The deposit has a hydrothermal low-temperature origin and is confined to the zone of deep and echelon faults. The study area has manifestations and mineralization points, as well as placer and geochemical aureoles of mercury.

The deposit was developed in 1969–1975. A small plant extracted mercury from ore by evaporation. No exact information on the volume of mined mercury is available; according to unofficial data, it mined only several tens of tons.

The area under study is covered by black forests of Siberian fir (*Abies sibirica* Ledeb.), Aspen (*Populus tremula* L.), birch (*Betula pubescens* Ehrh., *Betula pendula* Roth), and tall grasses, which can reach three meters in height.

The lush undergrowth is represented by such shrubs as goat willow (*Salix caprea* L.), cranberry bush (*Viburnum opulus* L.), pea shrub (*Caragana arborescens* Lam.), Siberian mountain ash (*Sorbus sibirica* Hedl.), and bird cherry (*Padus avium* Mill.). Some areas have scarce undergrowth.

The most typical herbaceous plant species are melancholy thistle (*Cirsium heterophyllum* (L.) Hill.), millet grass (*Milium effusum* L.), dissected hogweed (*Heracleum dissectum* Ledeb.), wild chervil (*Anthriscus sylvestris* (L.) L.), Siberian cacalia (*Crepis sibirica* L.), northern wolfsbane (*Aconitum septentrionale* Koelle), black meadowsweet (*Filipendula ulmaria* (L.) Maxim.), Siberian globeflower (*Trollius asiaticus* L.), giant fescue (*Festuca gigantea* (L.) Vill.), etc.

The area has a big population of large ferns, which often dominate the herbaceous cover: adderspit (*Pteridium aquilinum* (L.) Kuhn.), male shield fern (*Dryopteris filix-mas* (L.) Schott), female fern (*Athyrium filix femina* (L.) Roth), and ostrich fern (*Matteuccias truthiopteris* (L.) Tod.).

Nemoral tertiary relics are represented by alfredia (*Alfredia cernua* (L.) Cass.), giant fescue (*F. gigantea* (L.) Vill.), whitespot betony (*Stachys sylvatica* L.), male shield fern (*D. filix-mas* (L.) Schott), sweet woodruff (*Galium odoratum* (L.) Scop.), and slender false brome (*Brachypodium sylvaticum* (Huds.) Beauv.).

The area is dominated by forest phytocenoses, mostly tall-grass forests with a forest stand of birches, aspens, and firs (2Os3B5P): drooping birch (*B. pendula* Roth.), Siberian fir (*A. sibirica* Ledeb.), aspen (*Populus tremula* L.), and Siberian spruce (*Picea obovata* Ledeb.). Siberian fir and silver birch have a good seed reproduction; as a result, the forest canopy is rich in fir undergrowth, while the open areas demonstrate a thick population of young birches. The average diameter of the birch is ≤ 40 cm, the average height is 25 m. The average diameter of the fir is ≤ 30–40 cm, the height is 28–30 m. The average diameter of the aspen is 40–50 cm, the height is about 30 m, and the crown density can reach 0.7–0.8.

The composition of the forest stand differs in the ratio of fir, aspen, and birch: birch-fir-aspen, fir-aspen, or aspen-fir with a few birches, while some areas are entirely fir or birch forests. Some areas have a rich undergrowth: goat willow (*S. caprea* L.), cranberry bush (*V. opulus* L.), pea shrub (*C. arborescens* Lam.), red raspberry (*Rubusidaeus* L.), Siberian mountain ash (*S. sibirica* Hedl.), downy currant (*Ribes spicatum* Robson.), black currant (*Ribes nigrum* L.), and bird cherry (*Padusavium* Mill.).

In the open and birch-dominated areas, raspberries grow in lush thickets. Some forest parts have a steeply-sloping terrain with areas of higher moisture, where willow thickets proliferate. Willow patches and fir- or aspen-predominated areas also host vines, usually represented by wild hop (*Humulus lupulus* L.).

The grass stand is represented by tall grasses. The projective cover is over 85%. The maximal height of the grass standcan reach 3.5 m in cases of alfredia or hogweed, while the average height is 1.5 m. The list of tall grasses includes: melancholy thistle (*C. heterophyllum* (L.) Hill.), millet grass (*M. effusum* L.), northern wolfsbane (*A. septentrionale* Koelle), dissected hogweed (*H. dissectum* Ledeb.), meadow rue (*Thalictrum minus* L.), golden thoroughwax (*Bupleurum aureum* Fisch. ex Hoffm.), great nettle (*Urtica dioica* L.) wild chervil (*A. sylvestris* (L.) Hoffm.), meadowsweet (*F. ulmaria* (L.) Maxim.), cacalia (*Cacalia hastata* L.), and Siberian hawk's beard (*C. sibirica* L.). In some places, especially those dominated by fir trees, the thickets are formed almost entirely by nettle, infested by dodder (*Cuscuta* sp.).

Other perennial herbs also play a significant role in the composition of the phytocenosis: alfredia (*A. cernua* (L.) Cass.), four-leaved Paris herb (*Parisqua drifolia* L.), wood geranium (*Geranium sylvaticum* L.), Dahurian chickweed (*Cerastium davuricum* Fisch. ex Spreng.), Bunge chickweed (*Stellaria bungeana* Fenzl.), wood sorrel (*Oxalisa cetosella* L.), Siberian globeflower (*T. asiaticus* L.), wild leek (*Allium microdictyon* Prokh.), lungwort (*Pulmonaria mollis* Wulf. ex Hornem), spurge (*Euphorbia pillosa* L.), touch-me-not (*Impatiens noli-tangere* L.), Urals peony (*Paeonia anomala* L.), northern bedstraw (*Galium boreale* L.), sedge (*Carex macroura* Meins.), Greek-valerian polemonium (*Polemonium*

caeruleum L.), violet (*Violauni flora* L.), whitespot betony (*S. sylvatica* L.), and snakeflower (*Lamium album* L.).

Ferns make up part of some grass stand areas: female fern (*Athyrium filix-femina* (L.) Roth), adderspit (*P. aquilinum* (L.) Kuhn.), ostrich fern (*Matteuccia struthiopteris* (L.) Tod.), and male shield fern (*D. filix-mas* (L.) Schott). Adderspit and ostrich grow in thickets.

The herbaceous layer also includes species from the spring synusia, which have completed their growing season (*Corydalis*, *Anemone* s. L., etc.), including Siberian trout lily (*Erythronium sibiricum* (Fisch. et C. A. Mey) Kryl.). This flower is endemic to the Altai-Sayan ecoregion and is protected by the federal and regional law.

Herb-dominated patches appear in some open spaces, depending on the moisture and some other factors. They form tall-grass-grassland patches, grass meadows, and motley grass-grasses associations.

The tall-grass-grassland meadows consist of the same species as the herb layer in the forest: melancholy thistle (*C. heterophyllum* (L.) Hill.), northern wolfsbane (*A. septentrionale* Koelle), dissected hogweed (*H. dissectum* Ledeb.), meadow rue (*T. minus* L.), golden thoroughwax (*Bupleurum aureum* Fisch. hastata L.), wild chervil (*C. sibirica* L.), wild leek (*A. microdictyon* Prokh.), soft lungwort (*P. mollis* Wulf. ex Hornem), spurge (*E. pillosa* L.), etc.

The grass meadows and motley grass-grasses associations develop on sunlit and warm areas, e.g. forest edges. Some species grow both in the forest and in the open, e.g. meadow rue (*T. minus* L.), golden thoroughwax (*B. aureum* Fisch. ex Hoffm.), wild chervil (*Anthris cussylvestris* (L.) Hoffm.), meadowsweet (*F. ulmaria* (L.) Maxim.), cock's-foot (*Dactylis glomerata* L.), bluegrass (*Poa* sp.), timothy grass (*Phleum pratense* L.), common tansy (*Tanacetum vulgare* L.), lousewort (*Pedicularis incarnata* L.), bladder campion (*Oberna behen* (L.) Ikonn.), etc. More humid areas are home to other kinds of bluegrass (*Poa remota* Forsell.), water forget-me-not (*Myosotis palustris* (L.), white hellebore (*Veratrum lobelianum* Bernh.), Siberian globeflower (*T. asiaticus* L.), buttercup (*Ranunculus* sp.), marsh orchid (*Dactylorhiza* sp.), wood bulrush (*Scirpus sylvaticus* L.), clump speedwell (*Veronica longifolia* L.), groundsel (*Senecio* sp.), etc.

Many meadows are gradually overgrowing with willow and birch. Willow thickets predominate in the floodplain of the river and represented by goat willow (*S. caprea* L.), woollytwig willow (*Salix dasyclados* Wimm.), basket willow (*Salixvim inalis* L.), almond-leaved willow (*Salix triandra* L.), etc. The list of herbs that proliferate in the willow patches includes fireweed (*Chamerion angustifolium* (L.) Holub), wood horsetail (*Equisetumsyl viaticum* L.), common loosestrife (*Lysim achiavulgaris* L.), sedge (*Carex* sp.), etc.

In addition to willow thickets, floodplain meadows are also widespread along the river banks, where grain grass prevails, e.g. smallweed (*Calamagrostis* sp.), cock's-foot, timothy grass, etc. The floodplain areas also include white hellebore (*V. lobelianum* Bernh.), sorrel (*Rumex* sp.), marsh orchid (*Dactylorhiza* sp.), wood reed (*S. sylvaticus* L.), clump speedwell (*V. longifolia* L.), ragged robin (*Coccyganthe flos-cuculi* (L.), dissected hogweed (*H. dissectum* Ledeb.), marsh cress (*Rorippapalustris* (L.) Bess.), lousewort (*Scrophularia* sp.), scouring horsetail (*Equisetum hiemale* L.), sedge (*Carex* sp.), common loosestrife (*L. achiavulgaris* L.) angelica (*Archangelica decurrens* Ledeb.), and coltsfoot (*Tussilago farfara* L.). Angelica grows in lush thickets. Birch and bird cherry also grow on the floodplain meadows.

In shallow water, there are thickets of butterbur (*Petasites radiatus* (J.F. Gmel.) J. Toman) and rush flower (*Butomusum bellatus* L.).

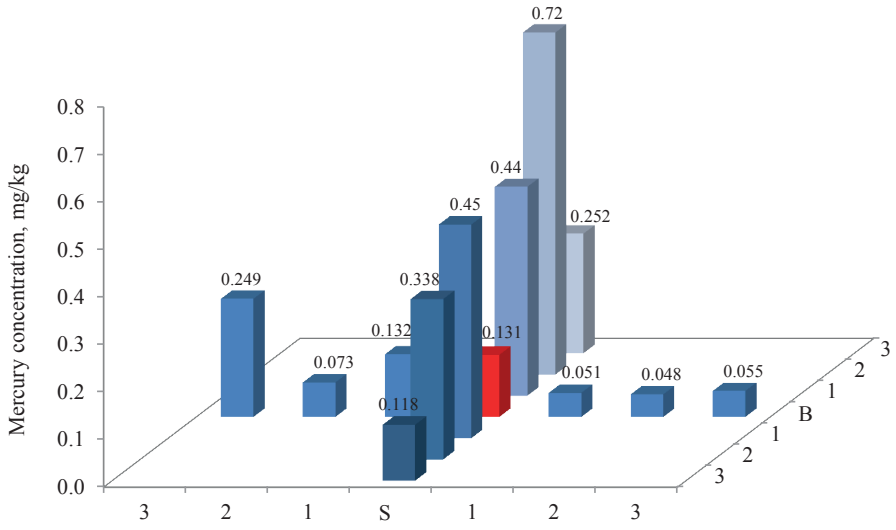

Figure 3 Concentration of mercury in the soil (horizon – 0–20 cm) in the area of the Beloosipovo mercury deposit

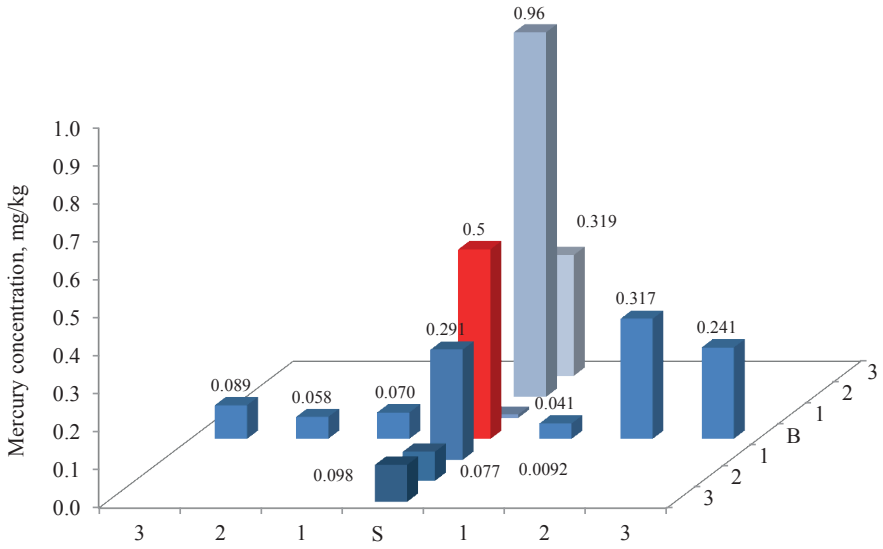

Figure 4 Concentration of mercury in soil (horizon – 30–60 cm) in the area of the Beloosipovo deposit

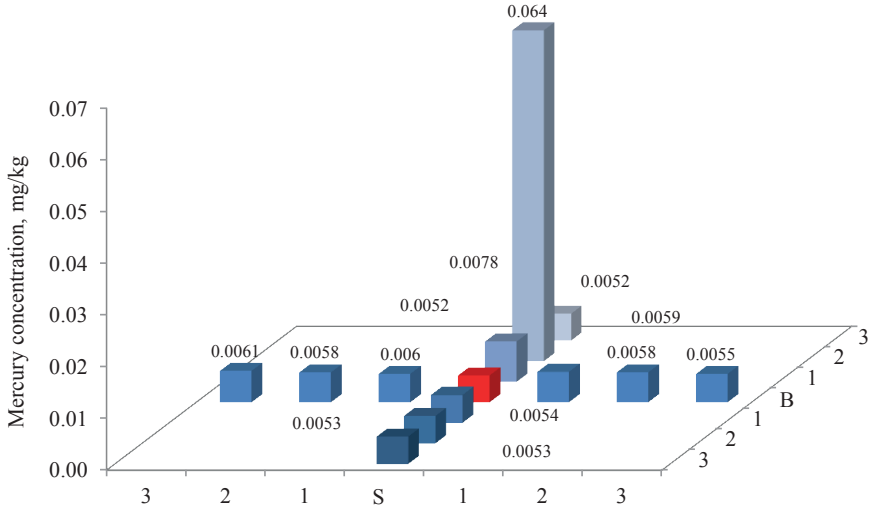

Figure 5 Concentration of mercury in plants in the area of the Beloosipovo deposit

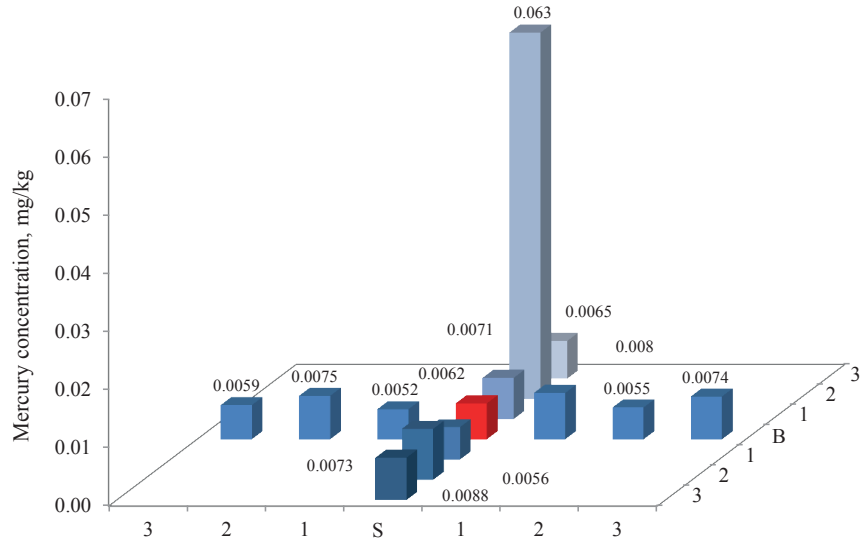

Figure 6 Concentration of mercury in herpetobiont insects in the area of the Beloosipovo deposit

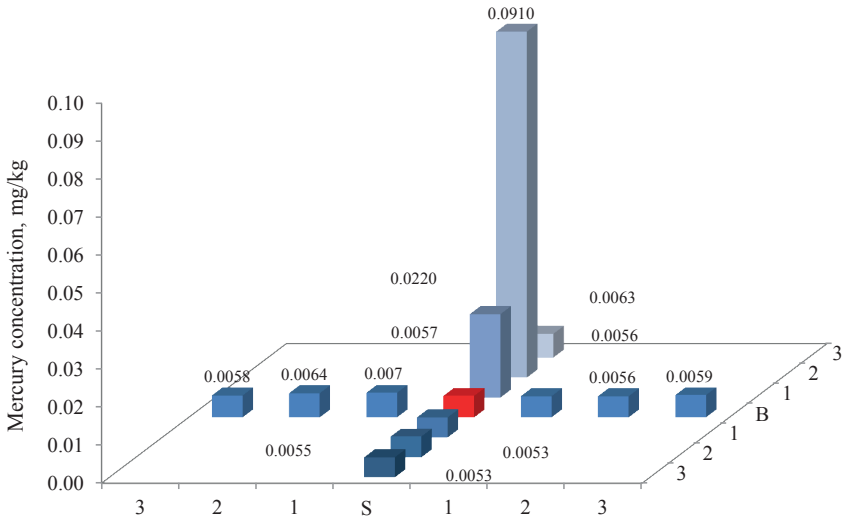

Figure 7 Concentration of mercury in rodents in the area of the Beloosipovo deposit

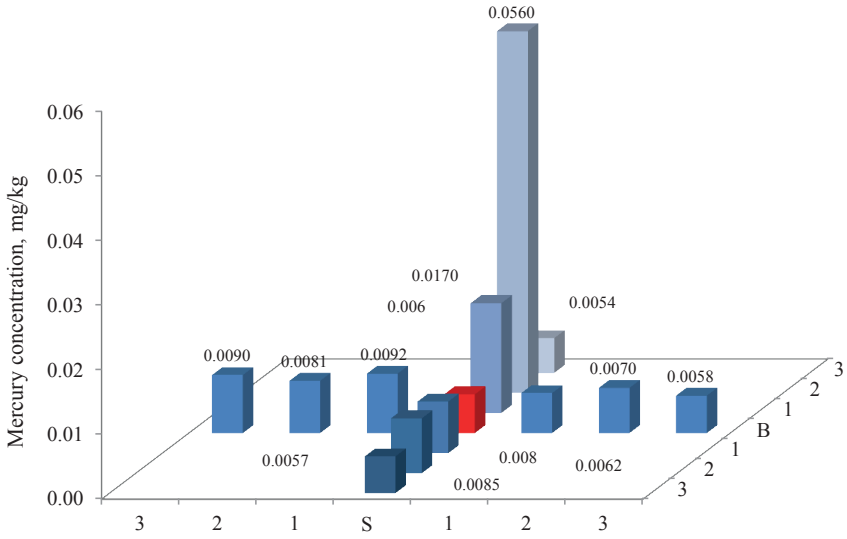

Figure 8 Concentration of mercury in insectivores in the area of the Beloosipovo deposit

Therefore, the study area boasts a significant biological diversity. In addition, it is home to a species protected at the federal and regional levels, namely Siberian trout lily (*E. sibiricum* (Fisch. Et C. A. Mey) Kryl.) and several nemoral tertiary relics, such as alfredia (*A. cernua* (L.) Cass.), giant fescue (*F. gigantea* (L.) Vill.), whitespot betony (*S. sylvatica* L.), male shield fern (*D. filix-mas* (L.) Schott), and slender false brome (*B. sylvaticum* (Huds.) Beauv.). No invasive species were registered.

Figures 3–8 demonstrate the mercury concentration in soil, plants, insects, and small mammals near the Beloosipovo mercury deposit and in the control zone. The highest concentration of mercury was observed at point North 2 (N 2), which was located at 1.5 km north of the deposit: in soil – 0.72 mg/kg and 0.96 mg/kg, in plants – 0.064 mg/kg, in insects – 0.063 mg/kg, in rodents – 0.091 mg/kg, and in insectivores – 0.056 mg/kg.

According to regulatory documents, the maximal permissible concentration of mercury in soil is 2.1 mg/kg. As the maximal value in the soil samples was 0.96 mg/kg, it means that no dangerous concentration of mercury was detected. However, the e-catalog of geological documents specifies the average concentration of mercury in the soils of the Kemerovo Region at the level 0.16–0.22 mg/kg [28]. Thus, the concentrations of mercury in the soil near the Beloosipovo mercury deposit proved to be by 3–4 times higher than the average values, despite the fact that the mine was closed more than 40 years ago.

The high concentration of mercury in the samples taken the north was presumably related to the terrain peculiarities: the altitude decreases from north to south,

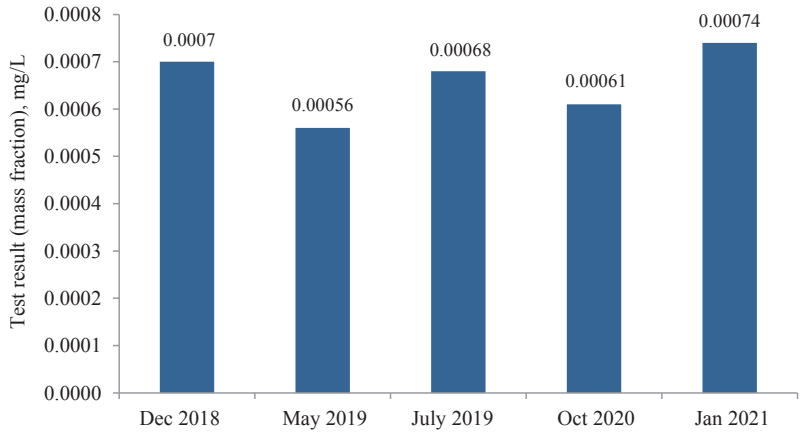

Figure 9 Concentration of mercury in the Belaya Osipova river

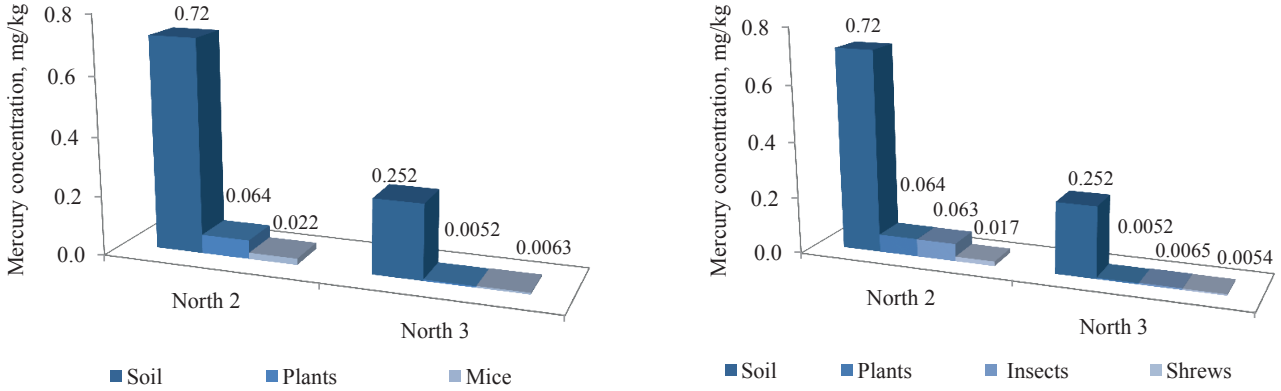

Figure 10 Changes in the concentration of mercury along the food chains

dropping from 407 to 214 m. Points North 2 (N 2) and North 3 (N3) were located directly in the deposit zone, while point North 1 (N 1) was on the borderline.

As for the control point, the concentration of mercury in all components of the ecosystem was much lower than in the area under analysis: in soil and small mammals, it was lower by 1–3 orders of magnitude; in plants and herpetobiontic insects – by 2–4 times.

While the soil samples demonstrated a permissible concentration of mercury, the samples from the Belaya Osipova river exceeded the permissible value (Fig. 9). The maximal permissible concentration of mercury for water bodies is 0.0005 mg/L. In the Belaya Osipova (2018–2021), the concentration exceeded the permissible value by 5–20% and reached 0.00056–0.00074 mg/L.

The high content of mercury in the Belaya Osipova may be associated with the Beloosipovo mercury deposit: mercury compounds might be washed out by groundwater and surface spring floods. Further studies require additional tests of the water biocenosis, which will be one of the tasks of subsequent research.

The concentration of heavy metals is believed to increase up the food chains. To test this presumption, we compared the concentration of mercury in the food chains at points North 2 (N 2) and North 3 (N3) with the highest mercury concentration in the soil. However, it was the soil samples that demonstrated the highest concentration of mercury, and further up the food chains its concentration dropped by one or two orders of magnitude, depending on the collection point (Fig. 10). The greatest drop was observed at North 2, where the concentration of mercury in the soil was the highest: from 0.72 to 0.022 mg/kg in the soil – plants – mice chain and from 0.72 to 0.017 mg/kg in the soil – plants – insects – shrews chain.

CONCLUSION

The mercury concentration in the soil near the Beloosipovo mercury deposit did not exceed the maximal permissible concentrations. The maximal mercury concentration in the soil was 0.96 mg/kg while the permissible value is 2.1 mg/kg. In the control zone, the research registered a decrease in the mercury concentration by 1–3 orders of magnitude for individual components of the terrestrial ecosystem, namely soil and small mammals. However, the water samples from the Belaya Osipova exceeded the maximal permissible

concentration by 5–20% in 2018–2021, which means that mercury compounds may go with groundwater and surface spring floods.

The detected mercury concentrations proved to produce no negative effect on the ecosystem, which was confirmed by the rich biological diversity. The area is home to the critically endangered species of Siberian trout lily (*Erythronium sibiricum* (Fisch. et C.A. Mey) Kryl.) and several nemoral tertiary relics, such as alfredia (*Alfredia cernua* (L.) Cass.), giant fescue (*Festuca gigantea* (L.) Vill.), whitespot betony (*Stachys sylvatica* L.), male shield fern (*Dryopteris filix-mas* (L.) Schott), and slender false brome (*Brachypodium sylvaticum* (Huds.) Beauv.). The research revealed no invasive species.

The mercury content decreased up the food chains, which means that the Beloosipovo mercury deposit has no negative impact on the local ecosystems.

The present article is the first part of a series of related publications. Further publications will feature the impact of technogenic centers on the local ecosystem and its individual representatives.

CONFLICT OF INTEREST

The authors declare no conflict of interests regarding the publication of this article.

REFERENCES

1. Selin H, Keane SE, Wang S, Selin NE, Davis K, Bally D. Linking science and policy to support the implementation of the Minamata Convention on Mercury. Ambio. 2018;47(2):198–215. https://doi.org/10.1007/s13280-017-1003-x.
2. Zhou J, Du B, Shang L, Wang Z, Cui H, Fan X, et al. Mercury fluxes, budgets, and pools in forest ecosystems of China: A review. Critical Reviews in Environmental Science and Technology. 2020;50(14):1411–1450. https://doi.org/10.1080/10643389.2019.1661176.
3. Karimi E, Yari M, Ghaneialvar H, Kazemi HR, Asadzadeh R, Aidy A, et al. Effects of dust phenomenon on heavy metals in raw milk in western Iran. Foods and Raw Materials. 2020;8(2):241–249. http://doi.org/10.21603/2308-4057-2020-2-241-249.
4. Zhu W, Lin C-J, Wang X, Sommar J, Fu X, Feng X. Global observations and modeling of atmosphere-surface exchange of elemental mercury: A critical review. Atmospheric Chemistry and Physics. 2016;16(7):4451–4480. https://doi.org/10.5194/acp-16-4451-2016.
5. Gustin MS, Ericksen JA, Schorran DE, Johnson DW, Lindberg SE, Coleman JS. Application of controlled mesocosms for understanding mercury air-soil-plant exchange. Environmental Science and Technology. 2004;38(22):6044–6050. https://doi.org/10.1021/es0487933.
6. Fantozzi L, Ferrara R, Dini F, Tamburello L, Pirrone N, Sprovieri F. Study on the reduction of atmospheric mercury emissions from mine waste enriched soils through native grass cover in the Mt. Amiata region of Italy. Environmental Research. 2013;125:69–74. https://doi.org/10.1016/j.envres.2013.02.004.
7. Mazur M, Mitchell CPJ, Eckley CS, Eggert SL, Kolka RK, Sebestyen SD, et al. Gaseous mercury fluxes from forest soils in response to forest harvesting intensity: A field manipulation experiment. Science of the Total Environment. 2014;496:678–687. https://doi.org/10.1016/j.scitotenv.2014.06.058.
8. Leonard TL, Taylor GE, Gustin MS, Fernandez GCJ. Mercury and plants in contaminated soils: 1. Uptake, partitioning, and emission to the atmosphere. Environmental Toxicology and Chemistry. 1998;17(10):2063–2071. https://doi.org/10.1002/etc.5620171024.
9. Asati A, Pichhode M, Nikhil K. Effect of heavy metals on plants: An overview. International Journal of Application or Innovation in Engineering and Management. 2016;5(3):56–66.
10. Jameer Ahammad S, Sumithra S, Senthilkumar P. Mercury uptake and translocation by indigenous plants. Rasayan Journal of Chemistry. 2018;11(1):1–12. https://doi.org/10.7324/RJC.2018.1111726.
11. Nagajyoti PC, Lee KD, Sreekanth TVM. Heavy metals, occurrence and toxicity for plants: A review. Environmental Chemistry Letters. 2010;8(3):199–216. https://doi.org/10.1007/s10311-010-0297-8.
12. Cargnelutti D, Tabaldi LA, Spanevello RM, de Oliveira Jucoski G, Battisti V, Redin M, et al. Mercury toxicity induces oxidative stress in growing cucumber seedlings. Chemosphere. 2006;65(6):999–1006. https://doi.org/10.1016/j.chemosphere.2006.03.037.
13. Marrugo-Negrete J, Durango-Hernández J, Pinedo-Hernández J, Enamorado-Montes G, Díez S. Mercury uptake and effects on growth in *Jatropha curcas*. Journal of Environmental Sciences. 2016;48:120–125. https://doi.org/10.1016/j.jes.2015.10.036.
14. Teixeira DC, Lacerda LD, Silva-Filho EV. Foliar mercury content from tropical trees and its correlation with physiological parameters *in situ*. Environmental Pollution. 2018;242:1050–1057. https://doi.org/10.1016/j.envpol.2018.07.120.

15. Fuentes-Gandara F, Herrera-Herrera C, Pinedo-Hernández J, Marrugo-Negrete J, Díez S. Assessment of human health risk associated with methylmercury in the imported fish marketed in the Caribbean. Environmental Research. 2018;165:324-329. https://doi.org/10.1016/j.envres.2018.05.001.
16. Zhou J, Obrist D, Dastoor A, Jiskra M, Ryjkov A. Vegetation uptake of mercury and impacts on global cycling. Nature Reviews Earth and Environment.2021;2(4):269–284. https://doi.org/10.1038/s43017-021-00146-y.
17. Obrist D, Agnan Y, Jiskra M, Olson CL, Colegrove DP, Hueber J, et al. Tundra uptake of atmospheric elemental mercury drives Arctic mercury pollution. Nature. 2017;547(7662):201–204. https://doi.org/10.1038/nature22997.
18. Obrist D, Kirk JL, Zhang L, Sunderland EM, Jiskra M, Selin NE. A review of global environmental mercury processes in response to human and natural perturbations: Changes of emissions, climate, and land use. Ambio. 2018;47(2):116–140. https://doi.org/10.1007/s13280-017-1004-9.
19. Ranieri E, Moustakas K, Barbafieri M, Ranieri AC, Herrera-Melián JA, Petrella A, et al. Phytoextraction technologies for mercury- and chromium-contaminated soil: a review. Journal of Chemical Technology and Biotechnology. 2020;95(2):317–327. https://doi.org/10.1002/jctb.6008.
20. Jiskra M, E. Sonke J, Agnan Y, Helmig D, Obrist D. Insights from mercury stable isotopes on terrestrial–atmosphere exchange of Hg(0) in the Arctic tundra. Biogeosciences. 2019;16(20):4051–4064. https://doi.org/10.5194/bg-16-4051-2019.
21. Greger M, Wang Y, Neuschütz C. Absence of Hg transpiration by shoot after Hg uptake by roots of six terrestrial plant species. Environmental Pollution. 2005;134(2):201–208. https://doi.org/10.1016/j.envpol.2004.08.007.
22. Juillerat JI, Ross DS, Bank MS. Mercury in litterfall and upper soil horizons in forested ecosystems in Vermont, USA. Environmental Toxicology and Chemistry. 2012;31(8):1720–1729. https://doi.org/10.1002/etc.1896.
23. Komov VT, Gremyachikh VA, Udodenko YuG, Shchedrova YeV, Yelizarov MYe. Mercury in abiotic and biotic components of aquatic and terrestrial ecosystems in the urban settlement on the shore of the Rybinsk Reservoir. Transactions of Papanin Institute for Biology of Inland Waters RAS. 2017;77(80):34–56. (In Russ.). https://doi.org/10.24411/0320-3557-2017-10003.
24. Gremyachikh VA, Lozhkina RA, Komov VT. Spatial-temporal variability of mercury content in the river perch *Perca fluviatilis* Linnaeus, 1758 (Perciformes: Percidae) of the Rybinsk Reservoir at the turn of the XX–XXI centuries. Ecosystem Transformation. 2019;2(2):85–95. (In Russ.). https://doi.org/10.23859/estr-180816.
25. Gorbunov AV, Lyapunov SM, Okina OI, Sheshukov VS. Bioaccumulation of mercury in tissues of freshwater fish. Human Ecology. 2018;(11):23–31. (In Russ.). https://doi.org/10.33396/1728-0869-2018-11-26-31.
26. Komov VT, Ivanova ES, Gremyachikh VA, Lapkina LN, Kozlova LV, Zheletok EN, et al. The mercury content in the organism of amphibians and leeches from waterbodies of Vologda and Yaroslavl oblasts and experimental verification of its biological consequences. Transactions of Papanin Institute for Biology of Inland Waters RAS. 2017;77(80):57–76. (In Russ.). https://doi.org/10.24411/0320-3557-2017-10004.
27. Golovanova IL, Filippov AA, Komov VT, Urvantseva GA, Evdokimov EG. Effect of mercury accumulation on the activity of glycosidase and their sensitivity to heavy metals in toad tadpoles. Transactions of Papanin Institute for Biology of Inland Waters RAS. 2015;72(75):60–65. (In Russ.). https://doi.org/10.24411/0320-3557-2015-10012.
28. Ehlektronnyy katalog geologicheskikh dokumentov [Electronic catalog of geological documents] [Internet]. [cited 2021 May 20]. Available from: https://rfgf.ru/catalog/index.php.
29. Doklad o sostoyanii i okhrane okruzhayushchey sredy Kemerovskoy oblasti v 2018 godu [Report on the state and protection of the environment in the Kemerovo region in 2018] [Internet]. [cited 2021 May 20]. Available from: https://www.ecoindustry.ru/gosdoklad/view/523.html.

ORCID IDs
Alexander Yu. Prosekov https://orcid.org/0000-0002-5630-3196

Foods and Raw Materials, 2021, vol. 9, no. 2

E-ISSN 2310-9599
ISSN 2308-4057

Research Article
Open Access

https://doi.org/10.21603/2308-4057-2021-2-335-344
Available online at http://jfrm.ru/en

Erosion potential of ultrasonic food processing

Sergei A. Bredihin[1], Vladimir N. Andreev[1], Alexander N. Martekha[1,*], Matthias G. Schenzle[2], Igor A. Korotkiy[3]

[1] K.A. Timiryazev Russian State Agrarian University, Moscow, Russia

[2] VA GmbH Society for Food Processing, Stuttgart, Germany

[3] Kemerovo State University, Kemerovo, Russia

* e-mail: man6630@rgau-msha.ru

Received April 30, 2021; Accepted in revised form May 21, 2021; Published online October 15, 2021

Abstract:
Introduction. Cavitation is the most significant factor that affects liquid food products during ultrasound treatment. Ultrasonic treatment intensifies diffusion, dissolution, and chemical interactions. However, no physical model has yet been developed to unambiguously define the interaction between ultrasonic cavities and structural particles of liquid food media. Physical models used to describe ultrasonic interactions in liquid food media are diverse and, sometimes, contradictory. The research objective was to study ultrasonic devices in order to improve their operating modes and increase reliability.
Study objects and methods. The present research featured ultrasonic field generated in water by the cylindrical emitter, the intensity of flexural ultrasonic waves and their damping rate at various distances from the emitter.
Results and discussion. The paper offers a review of available publications on the theory of acoustic cavitation in various media. The experimental studies featured the distribution of cavities in the ultrasound field of rod vibrating systems in water. The research revealed the erosion capacity of ultrasonic waves generated by the cylindrical emitter. The article also contains a theoretical analysis of the cavitation damage to aluminum foil in water and the erosive effect of cavitation on highly rigid materials of ultrasonic vibration systems. The obtained results were illustrated by semi-graphical dependences.
Conclusion. The present research made it possible to assess the energy capabilities of cavities generated by ultrasonic field at different distances from the ultrasonic emitter. The size of the contact spot and the penetration depth can serve as a criterion for the erosion of the surface of the ultrasonic emitter.

Keywords: Ultrasound, cavitation, aqueous medium, foil screen, erosion, oscillatory system

Funding: The research was carried out on the premises of the K.A. Timiryazev Russian State Agrarian University (RT SAU), with financial support from the Ministry of Science and Higher Education of the Russian Federation (Minobrnauka) as part of the program for the development of world-class research center "Agrotechnology of the Future" (The grant was delivered as subsidies from the federal budget for state support of world-class research centers, performing R&D in scientific and technological priority areas, No. 075-15-2020-905 (internal number 00600/2020/80682), November 16, 2020).

Please cite this article in press as: Bredihin SA, Andreev VN, Martekha AN, Schenzle MG, Korotkiy IA. Erosion potential of ultrasonic food processing. Foods and Raw Materials. 2021;9(2):335–344. https://doi.org/10.21603/2308-4057-2021-2-335-344.

INTRODUCTION

Ultrasound technologies in the food and processing industries have been the focus of numerous studies. As a result, information about ultrasound treatment of food media is quite abundant. Cavitation is the main process of ultrasound treatment of liquids. Ultrasonic waves accelerate diffusion, chemical reactions, and dissolution processes in liquid foods. The ultrasonic acceleration of chemical interactions results from free ions formed during ultrasonic cavitation.

Contemporary food science knows no universally accepted theory that would unambiguously describe the physical nature of the interaction of ultrasonic cavities and structural particles during food processing. The existing physical models are diverse and often contradictory. They give a very vague explanation of the processes that occur in the ultrasonic field. According to some models, cavities have high pressures and temperatures. According to others, cavitation creates microcavities of deep vacuum and cryogenic temperatures. Both destroy microparticles in liquid

media. For instance, ultrasonic cavities break milk fat globules into smaller fragments [1–5]. Cavitation is the formation of microcavities in a liquid medium, which are called bubbles, voids, or just cavities. These cavities are filled with vapor phase, gas, or a mixture of both. Cavities are formed in local zones of the liquid phase, where the pressure drops to a critical level, which usually coincides with the saturation pressure. Hydrodynamic cavities develop in a flow of fluid; acoustic cavities develop as a result of acoustic treatment [3].

Physical models of cavitation can be contradictory because experimental studies of cavitation are quite complex. To be used in food industry, ultrasonic cavitation requires optimal operating modes of ultrasonic devices. Reliability and safety of ultrasonic devices remain an important issue of food science [6–8].

Cavitation theories. The ability of ultrasound to accelerate food processing was established in the early XX century. For example, such phenomena as the acceleration of water-fat emulsion or finely dispersed suspensions are quite old. In 1960s, ultrasonic treatment began to be used in chocolate production: it provided a more effective mixing, emulsification, and better dispersion. However, these methods found little practical use because of their economic inexpediency. Ultrasound methods and technical means used to be imperfect and expensive [9, 10].

The latest technology of controlled, focused, and highly intensive ultrasonic field had low energy costs, which made it economically feasible. As the technology gained more popularity, it revealed some new opportunities. For example, ultrasound treatment raised the intensity of extraction in cognac production by hundreds of times. Similar beneficial effects were observed in other processes, e.g. extraction of vegetable oils.

However, high-intensity ultrasound technologies erode the device surfaces that come in direct contact with the product. As a result, the processed product might contain some components that are not part of the formulation. Studies of the interaction between the product and the surface of the ultrasonic cavitator (oscillatory system) can help reduce or eliminate erosion [11].

To find out more about various theories of collapse and waves of a single cavity, see [3–5]. The results of these researches made theoretical studies as reliable as actual practical experiments in cavitation.

In its most general form, the equation of motion of the outer wall of the cavity in spherical coordinates looks like this:

$$\frac{\partial u}{\partial t}+u\frac{\partial u}{\partial r}=-\frac{1}{\rho}\frac{\partial p}{\partial r} \quad (1)$$

where t – time, s; r – current radius, m; ρ – liquid density, kg/m^3; p – hydrostatic pressure, Pa.

The continuity equation has the following form:

$$\frac{\partial}{\partial r}\left(r^2u\right)=0 \quad (2)$$

The vortex-free motion of the surface can be considered as a potential with potential φ, i.e.:

$$u=-\frac{\partial\varphi}{\partial r} \quad (3)$$

Provided the bubble surface is $r = R$, $u = U$, then:

$$u=U\left(\frac{R}{r}\right)^2 \quad (4)$$

Equations (3) and (4) produce the following result:

$$\varphi=U\frac{R^2}{r} \quad (5)$$

Integration of (1) from r to $r = \infty$ results in:

$$u-\frac{u^2}{2}+\int_{P_\infty}^{p(r)}\frac{dp}{\rho}=0 \quad (6)$$

The condition of incompressibility of liquid means that $\rho = \rho_0 = const$; therefore, (6) is:

$$u-\frac{u^2}{2}+\frac{1}{\rho_0}\cdot\left[P_\infty-p\left(r\right)\right]=0 \quad (7)$$

Inserting (5) in (7) at $r = R$, we get the following equation for an empty cavity:

$$\frac{1}{r}\left(\frac{R^2}{2}\frac{dU^2}{dR}+2RU^2\right)-\frac{1}{2}U^2\frac{R^4}{r^4}+\frac{1}{\rho_0}\left[P_\infty-p\left(r\right)\right]=0 \quad (8)$$

For cavity surface $r = R$, $U = dR/dt$; thus, equation (8) looks like this:

$$R\frac{d^2R}{dt^2}+\frac{3}{2}\left(\frac{dR}{dt}\right)^2+\frac{1}{\rho_0}\left[P_\infty-P\left(R\right)\right] \quad (9)$$

where $P(R)$ is cavity surface pressure.

The resulting equation describes the motion of the cavity surface depending on the regularity of the pressure change $P(R)$.

Lamb and Rayleigh obtained a solution to equation (9) assuming the simplest boundary conditions: $P(R) = 0$, $P_\infty = P_0$, i.e. pressure at a sufficient distance equals hydrostatic pressure:

$$U^2=\frac{2}{3}\frac{P_0}{\rho_0}\left(\frac{R_m^3}{R^3}-1\right) \quad (10)$$

where R_m is maximal cavity radius early during collapse.

Provided $U = dR/dt$, we get Rayleigh's equation:

$$\tau=0.915R_m\left(\frac{\rho_0}{P_0}\right)^{1/2} \quad (11)$$

where τ is time of cavity collapse, s.

In the middle of the XX century, Nolting and Nepiras obtained an equation for cavity pulsations based on the Laplace surface tension forces and the change in the gas volume in the cavity during adiabatic expansion and compression [5]. They used harmonic pressure fluctuations as a boundary condition at a sufficient distance from the cavity. The equation is:

$$R\frac{d^2R}{dt^2}+\frac{3}{2}\left(\frac{dR}{dt}\right)^2+\frac{1}{\rho_0}\left[P_0-P_s-P_m\sin\left(\omega t\right)+\right.$$
$$\left.+\frac{2\sigma}{R}-\left(P_0+\frac{2\sigma}{R_0}\right)\left(\frac{R_0}{R}\right)^{3\gamma}\right]=0 \quad (12)$$

where P_s – steam pressure in the cavity;

$\omega = 2\pi f$, f – oscillation frequency; σ – Laplace surface tension; γ – adiabatic exponent (4/3), ρ_0 – density of liquid unaffected by fluctuations, P_m – maximal pressure in the cavity attained at its minimal radius.

The numerical solutions proposed in [6, 7] describe the changes in the radius of the cavity. The speed of movement of the cavity surface approaches the speed of sound in a liquid medium. It is the boundary condition for the application of the abovementioned equations. The continuity equation under these conditions has the following form:

$$\frac{\partial \rho}{\partial t} + \frac{1}{r^2}\frac{\partial}{\partial r}\left(r^2 \rho u\right) = 0 \qquad (13)$$

In the considered approximation $u^2/c^2 << 1$, whereas:

$$R\left(1-\frac{2U}{c_0}\right)\frac{d^2R}{dt^2} + \frac{3}{2}\left(1-\frac{4}{3}\frac{U}{c_0}\right)\left(\frac{dR}{dt}\right)^2 + \frac{1}{\rho_0}\left[P_\infty - P(R)\right] + \frac{R}{\rho_0}\frac{U}{c_0}\left(1-\frac{U}{c_0}\right)\frac{dP(R)}{dR} = 0 \qquad (14)$$

where U – the speed of movement of the cavity surface during collapse and pulsation; c_0 – speed of sound in the liquid unaffected by fluctuations.

Flynn supplemented this equation with a term that takes into account the viscosity of the liquid and pressure fluctuations by a harmonic law. As a result, he obtained the following equation:

$$R\left(1-2\frac{U}{c_0}\right)\frac{d^2R}{dR^2} + \frac{3}{2}\left(1-\frac{4}{3}\frac{U}{c_0}\right)\left(\frac{dR}{dt}\right)^2 + \frac{1}{\rho_0}\left[P_0 - P_{\Pi} - P_m \sin(\omega t) + \frac{2\sigma}{R} + \frac{4\eta U}{R} - \left(P_0 + \frac{2\sigma}{R_0}\right)\left(\frac{R_0}{R}\right)^{3\gamma}\right] + \frac{R}{\rho_0}\frac{U}{c_0}\left(1-\frac{U}{c_0}\right)\frac{dP(R)}{dR} = 0 \qquad (15)$$

Kirkwood and Bethe introduced the concept of specific enthalpy h and kinetic enthalpy:

$$\Omega = \frac{\partial \varphi}{\partial t} = h + \frac{u^2}{2} \qquad (16)$$

Thus, they obtained an equation that describes cavity pulsations and takes into account the compression and surface tension of the liquid, as well as the polytropic (adiabatic) character of vapor expansion in the cavity:

$$R\left(1-\frac{U}{c}\right)\frac{d^2R}{dt^2} + \frac{3}{2}\left(1-\frac{1}{3}\frac{U}{c}\right)\left(\frac{dR}{dt}\right)^2 - \left(1-\frac{U}{c}\right)H - \frac{U}{c}\left(1-\frac{U}{c}\right)R\frac{dH}{dR} = 0, \qquad (17)$$

where $c^2 = c_0^2\left(\frac{\rho}{\rho_0}\right)^{n-1}$; $H = \int_{\rho_0}^{\rho}\frac{dp}{\rho} = \frac{c_0^2}{n-1}\left[\left(\frac{\rho}{\rho_0}\right)^{n-1} - 1\right]$;

$c = \left[c_0^2 + (n-1)H\right]$; $c_0^2 = An/\rho_0$

where H – free enthalpy on the sphere surface; A and n – constants for water (A = 3.001×10^8 Pa = 3.001×10^5 MPa; n = 7).

An analysis of the equations of Nolting-Nepiras, Herring-Flynn, and Kirkwood-Bethe showed the similarity of the results, which diverged only at high ultrasound frequencies and in the case of a long collapse time [6].

The theory of shock waves during cavitation. Many researchers performed visual observations and proved that the erosion of the surfaces within the cavitation field occurs due to the high local pressures that take up the form of shock waves when cavities collapse [12, 13].

The analysis of the propagation of spherical shock waves consists in determining function $G\,(R,\,t)$ on the cavity surface with radius R and calculating the time it takes the waves to appear at a distance r from their source:

$$G(R,t) = R(H + \frac{U^2}{2}) \qquad (18)$$

After necessary transformations, equation (18) looks like this:

$$G = rc\left[U\cdot\left(\frac{R}{r}\right)^2\right]\cdot\left\{1+\frac{n+1}{4c}\left[U\cdot\left(\frac{R}{r}\right)^2\right]\right\} \qquad (19)$$

where the speed of the cavity surface U is determined by the following transcendental equation:

$$U^2 = \frac{2}{3}\frac{P_0 + P_m}{\rho_0}\left[\frac{R_m^3}{R^3}\left(1-\frac{U}{3c_0}\right)^{-4} - 1\right] \qquad (20)$$

The pressure along the shock front can be calculated using the formula given in [16]:

$$p = A\left[\frac{2}{n+1} + \frac{n-1}{n+1}\left(1+\frac{n+1}{rc_0^2}G\right)^{1/2}\right]\frac{2n}{n-1} - B \qquad (21)$$

where B – constant for water (3.0×10^5 MPa); constants A and n (see Eq. (17)).

Formula (20) makes it possible to analyze the conditions of cavitation effect on the surface of oscillatory system, which creates ultrasonic waves in liquid.

Theory and practice of erosion studies for solid materials in cavitation field. Erosion of material surfaces in cavitation field occurs following the destruction of bonds in the crystal lattice of the object. Cavitation erosion is determined by the decrease in the mass of the object in the cavitation field, or the state of the photosensitive layer on the glass plate surface. Another variant is to measure the total area of the holes formed in the aluminum foil under the effect of cavitation in a certain period of time. To assess the energy efficiency, Rosenberg introduced the concept of erosion-acoustic efficiency:

$$\eta_{er} = E_m \cdot E \qquad (22)$$

where E_m – energy spent on mechanical erosion; E – ultrasonic vibration energy.

The local rate of cavitation-induced destruction in

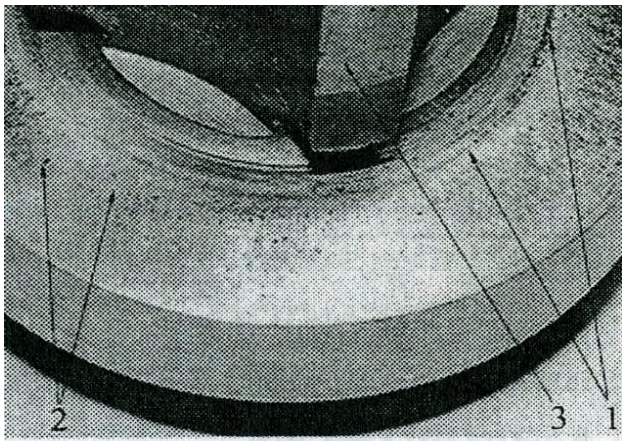

Figure 1 Valve seat of milk homogenizer subjected to cavitation: 1 – erosion canals; 2 – areas of erosion damage to the valve working surface; 3 – guide ways

an inhomogeneous ultrasonic field is determined by the following formula:

$$w_m = \frac{\partial^2 \Delta G}{\partial V dt} \quad (23)$$

where w_m – local rate of erosion in the cavitation field; ΔG – mass of solid particles dispersed in the liquid during erosion that can be separated during analysis; V – the volume of the product (liquid); t – time.

A rather original mathematical apparatus was used to analyze the erosion efficiency of the cavitation field in [6]. Unfortunately, the lack of data makes it impossible to use it for these calculations.

STUDY OBJECTS AND METHODS

This research continues the studies of erosion patterns of cavitation in aquatic environment started at K.G. Razumovsky Moscow State University of Technology and Management [7].

Ultrasound is a promising method of mechanical processing of food masses to produce fine-dispersed systems. However, the product unavoidably comes in contact with the surface of the ultrasonic concentrator, which might result in the diffusion of the solid matter into the liquid medium [8, 9]. This phenomenon is multiplied by vibration, including ultrasound. Figure 1 illustrates erosion on the surface of concentrator (or any other ultrasonic device).

An analytical review of theoretical and experimental studies of cavitation and erosion of solid surfaces in ultrasonic field proved that this process still remains understudied, especially the effect of cavitation on ultrasonic emitters. The theoretical and experimental studies given below represent an initial stage in the research and practical application of data on the interaction between ultrasonic field and ultrasonic emitters, as well as the role of this process in the food safety.

Cavitation produces cavities. When they collapse, they produce an energetic effect on liquid and elements submerged in it. Ertugay and Sengul described an assessment method for the energy impact of cavitation. Evaluation is carried out on a screen of aluminum or tin foil [8]. When the cavity collapses and as it hits the surface of the foil, dents or tears appear on the screen. The erosive capacity of cavitation is defined by the relative size of the area of dents and tears [14].

The generation of harmonic acoustic vibrations by a solid ultrasonic emitter is a convenient and easily controllable method for producing cavities in liquid medium. Wave theory is the basis for the design of solid emitters. It determines the most active areas of emitters of various shapes. However, it cannot describe the cavitation interactions of individual cavities or their groups [15]. Therefore, the cavitation interactions in ultrasonic fields of various intensities, the propagation of ultrasonic waves, and their ability to create cavities are important research and practical tasks in ultrasonic processing of liquid food media for homogenization, suspensions, and emulsions.

The present research featured cavitation in ultrasonic field created by the cylindrical surface of a solid emitter immersed in distilled water to a depth h. An aluminum foil screen was installed at distance x. The number of cavities was calculated at distance h_1 from the liquid surface in the normal vector to this surface.

Laboratory device IL-10-6/2 was used to create ultrasonic waves as described in [16, 17]. Cavities created by the laboratory installation in the liquid deformed the aluminum foil screen, causing either indentations in the foil or tears in the screen. This kind of violation of the integrity of the screen will be called "holes".

RESULTS AND DISCUSSION

The technological effect results from ultrasonic cavitation in liquid media as high-density energy localizes in microvolumes of the treated medium.

After a certain amount of pulsations, cavities collapse and trigger a shock wave, which destroys the nearby solid surfaces. Almost all related studies were focused on the process of cavitation-induced destruction of the medium components as a way to increase its homogeneity [18, 19]. The obtained data on kinetics and thermodynamics of cavity formation, time and forms of their existence, etc. make it possible to describe the kinetic and thermodynamic parameters of both cavities and the medium. The part of the ultrasonic device that comes in contact with the processed product is called the "oscillatory system". The surfaces of oscillatory systems of ultrasonic devices are also subject to cavitation-induced erosion. As a result, a certain amount of the material can mix with the product [20–22].

The present research featured the types and nature of erosion of ultrasonic devices and the safety of the product.

A set of experiments provided foil screens deformed by ultrasonic field. The state of the screen revealed the erosion capabilities of the ultrasonic field generated by

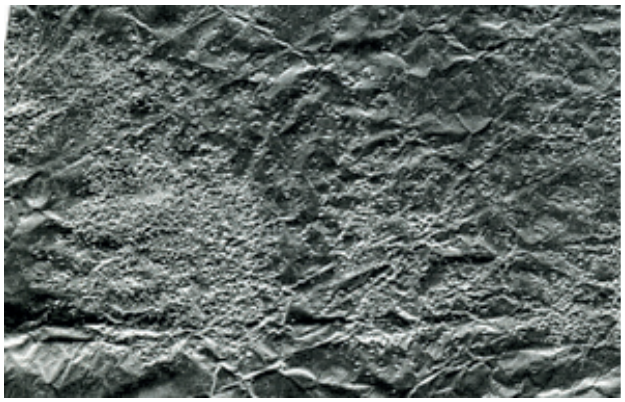

Figure 2 Foil screen deformed by ultrasonic treatment. Processing time – 20 s, distance from the surface of the emitter – 30 mm

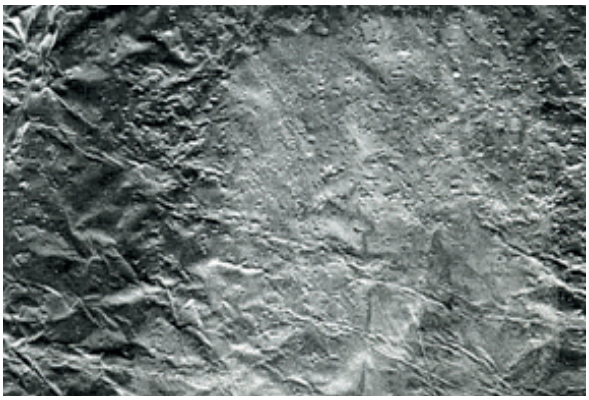

Figure 3 Foil screen deformed by ultrasonic treatment. Processing time – 20 s, distance from the surface of the emitter – 150 mm

Table 1 Distribution of deformations on the screen depending on the distance from the surface of emitter x and the distance from the surface of liquid h_1.

x, mm	h_1, mm	Distribution of screen deformations at ultrasonic treatment time t and distance h_1			
		5 s	10 s	15 s	20 s
30	5	23	129	115	110
	20	50	126	184	172
	40	104	135	202	304
	60	114	110	125	222
	80	32	31	78	40
		Σ 323	Σ 531	Σ 704	Σ 848
45	5	12	76	140	81
	20	52	196	230	74
	40	51	62	126	60
	60	49	124	112	52
	80	17	40	60	40
		Σ 181	Σ 498	Σ 668	Σ 308
60	5	1	34	24	24
	20	24	58	48	56
	40	116	46	44	44
	60	26	44	42	31
	80	35	31	11	110
		Σ 202	Σ 213	Σ 169	Σ 265
75	5	22	29	40	72
	20	49	61	48	86
	40	37	55	36	32
	60	24	55	155	40
	80	12	54	36	24
		Σ 144	Σ 254	Σ 315	Σ 254
150	5	2	27	10	8
	20	30	26	47	17
	40	40	21	41	30
	60	21	33	27	44
	80	10	14	26	41
		Σ 103	Σ 121	Σ 151	Σ 140
250	5	34	8	15	16
	20	32	24	11	16
	40	26	38	30	25
	60	25	24	34	26
	80	4	4	8	11
		Σ 121	Σ 98	Σ 98	Σ 94
320	5	5	16	25	1
	20	21	10	32	8
	40	38	37	50	20
	60	38	20	24	16
	80	2	9	4	6
		Σ 104	Σ 102	Σ 135	Σ51

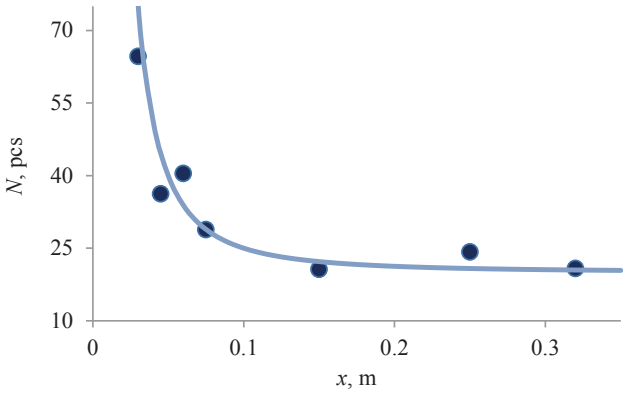

Figure 4 Effect of the distance from the surface of the cylindrical emitter on the amount of screen per 1 s of ultrasonic exposure

a cylindrical acoustic emitter in water. The surface of the screen was also given a cylindrical shape before it was installed in the test medium. The screen was placed in the test medium equidistantly to the surface of the emitter. The exposure of the screen and the curvature of its surface varied in different experiments. Figures 2 and 3 show the aluminum foil screens deformed by ultrasonic treatment.

The surface of the screens indicated a significant inhomogeneity of deformation. However, the agglomeration pattern of acoustic caverns was quite stable in certain areas of the screen surface. The experiments also determined the average value of the density of screen deformations depending on the time of the acoustic impact and the distance from the surface of the emitter (Table 1).

The amount of deformations on the screen decreased as the distance from the surface of the emitter increased.

Figure 4 shows the number of deformations per second (N, pcs) per 0.0004 m^2 of the screen surface, depending on the distance from the surface of the emitter (x, m). The diameter of the emitter was 0.03 m, the depth of immersion was 0.12 m, and the thickness of water layer was 0.25 m.

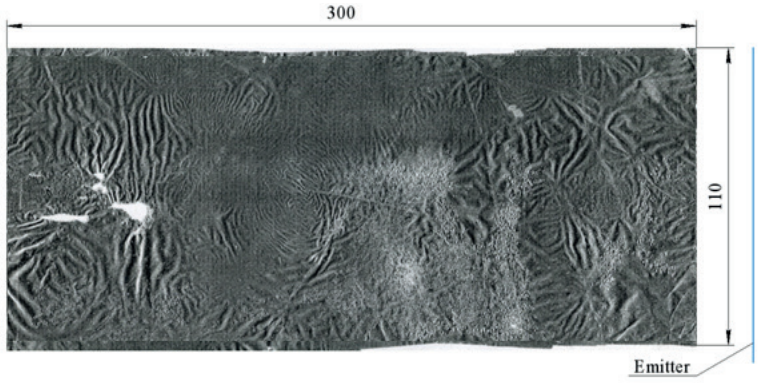

Figure 5 Distribution of cavitation-induced deformations and holes on the screen located equidistantly at distance *x* from the surface of the cylindrical emitter

Figure 4 illustrates that as the distance from the emitter increased, the amount of screen deformations decreased according to the hyperbolic function:

$$N = a{\cdot}x\text{^}b{+}c \quad (24)$$

where a, b, and c are constant: a = 0.05, b = 2, and c = 20.

Figure 6 clearly shows the distribution of cavitation-induced deformations after different acoustic exposure periods.

The difference in the distributions shown in Figures 6 and 8 can be explained by such factors as acoustic wind, Bjerknes force, and Stokes force.

Figure 6 suggests that the holes on the radially arranged screen appear as a result of ultrasound waves in the vessel. Thus, the expression for the wave interference for the number of holes will be the following:

$$N = \psi \left[\frac{\sin\left[\left(\frac{2\pi}{T}\right)\left(\frac{x}{c} - t\right)\right]}{\frac{2\pi}{T}\cdot\left(\frac{x}{c} - t\right)} \right]^2 \quad (25)$$

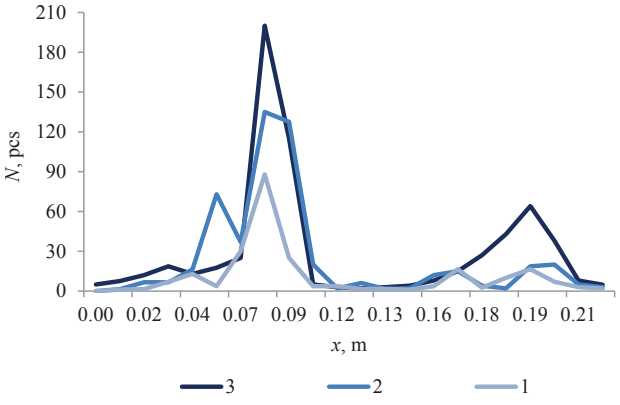

Figure 6 Effect of the distance from the surface of the cylindrical emitter on the distribution of deformations of the radially located screen during 10 s (1), 15 s (2), and 20 s (3)

where ψ – constant equal to the maximum number of cavities on 0.0004 m^2.

Curves 1 and 2 in Fig. 6 can also be simulated, like curve 3. However, in their cases, the speed of sound is somewhat less than it is universally accepted, i.e. instead of c = 1500 m/s, it is c = 1140 m/s because the water flow is intense and contains air bubbles, which obviously reduces the speed of sound in the water.

The number of holes in the foil screen makes it possible to characterize the energy of cavities formed in this volume. In a first approximation, the work of cavities can be calculated by the following formula:

$$A_E = \frac{4}{3}\pi R_{max}^3 PN \quad (26)$$

where A_E – work produced by the collapsing cavities, W·s; R_{max} – maximal size the cavity reaches as it oscillates around the equilibrium state (max 100 μm); P – pressure in the cavity as it collapses (10^3 MPa); N – number of cavities per volume.

As the cavity collapses, it produces spherical shock waves (Fig. 8) at a pressure of thousands of MPa. This pressure is much higher than the tensile strength of aluminum, which begins to flow like an ideally plastic body according to Saint-Venant. Therefore, the theory of plasticity can be applied to the theoretical analysis of the effect of shock wave on aluminum foil.

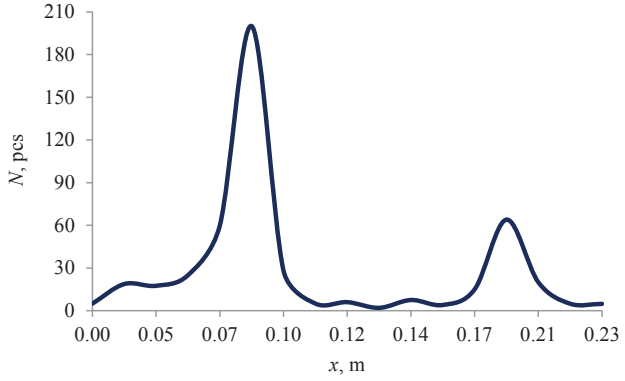

Figure 7 Graphic approximation of curve 3 in Fig. 6

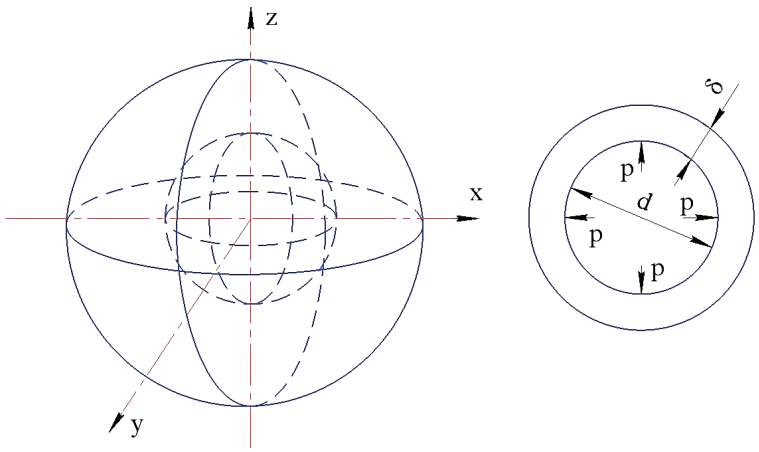

Figure 8 Expansion of hollow sphere made of ideally plastic material under internal pressure

Considering that the area of the foil around the hole formed by the cavity assumes hemispherical shape and that aluminum outside the strength limits behaves like an ideally plastic body, the model of the hole can be represented as the destruction of an ideally plastic sphere by a spherical shock wave (Fig. 9).

The following equation is valid for an ideally plastic body:

$$2\left(\sigma_r - \sigma_t\right) + r\frac{d\sigma_r}{dr} = 0 \qquad (27)$$

where σ_r and σ_t – normal stresses (tangential and along coordinate r), Pa.

Based on the deformation of the sphere:

$$\sigma_t - \sigma_r = \sigma_f \qquad (28)$$

where σ_f – yield stress, Pa.

Considering (27) and (28):

$$d\sigma_r = \pm 2\sigma_f \frac{dr}{r} \qquad (29)$$

at $r = d/2\sigma_f = -p_d$; at $r = (d/2) + \delta\sigma_r = -p_g$

where p_g is the hydrostatic pressure of the liquid, Pa.

By integrating (29) under the indicated boundary conditions, we obtain:

$$-p_d = \pm 2\sigma_f \ln\left(d/2\right) + C \qquad (30)$$

$$-p_g = \pm 2\sigma_f \ln\left[\left(d/2\right) + \delta\right] + C \qquad (31)$$

where C – arbitrary constant.

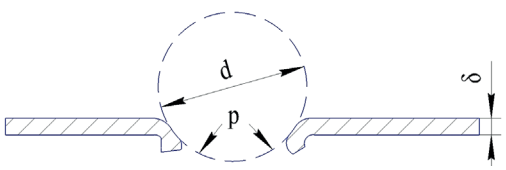

Figure 9 Formation of a hole in the foil under the effect of spherical shock wave as the cavity collapses

Expressing the total pressure of the internal and external hydrostatic (plastic) flow, we get the following equation:

$$p_f = p_d - p_g = \pm 2\sigma_f \ln\frac{\left[\left(d/2\right) + \delta\right]}{d/2} \qquad (32)$$

At $p_d >> p_g$:

$$p_f = 2\sigma_f \ln\frac{\left[\left(d/2\right) + \delta\right]}{d/2} \qquad (33)$$

The resulting formula (33) makes it possible to calculate the pressure inside the sphere formed by the shock wave after the cavity collapses at a distance close enough to the foil for a hole to occur.

The formula was tested using the data on the ultimate strength of aluminum. The ultimate strength, or the yield condition, of aluminum is σ_f = 60–100 MPa.

The size of the holes in the foil varied from 5×10^{-4} to 10^{-6} m. Therefore, the range of pressures in the corresponding cavities can be defined by formula (33).

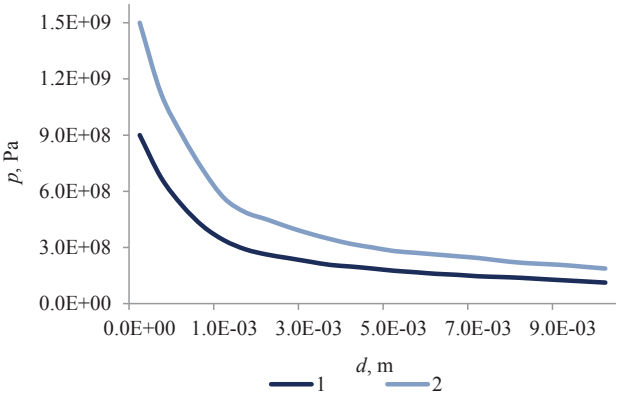

Figure 10 Effect of the diameter of the collapsing cavity on the pressure in spherical shock wave at the strength limits of aluminum = 60 MPa (curve 1) and 100 MPa (curve 2)

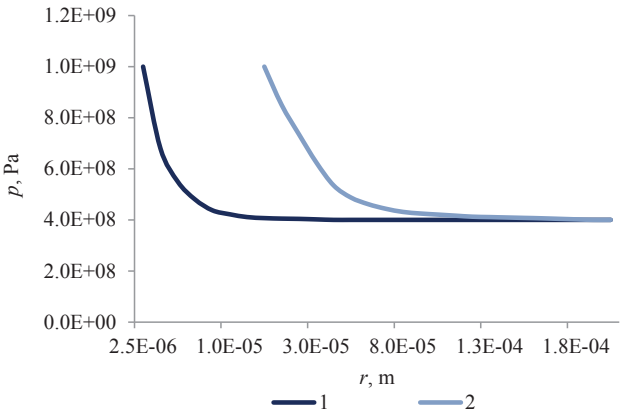

Figure 11 Pressure in the shock wave as calculated by Kirkwood-Bethe formula for distances from the center of the cavity r: the radii of the collapsed cavities – 10–5 m (curve 1) and 10–6 m (curve 2)

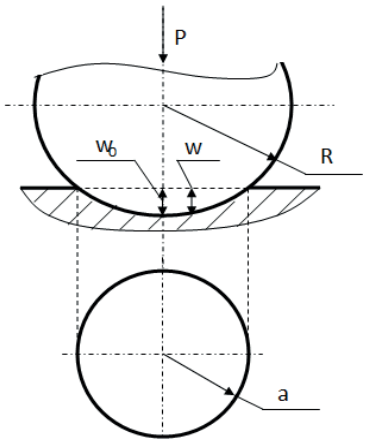

Figure 12 Penetration of an absolutely rigid ball into elastic half-space

Figure 10 shows the dependences of the pressure in spherical shock wave on the diameter of the collapsing cavity at different strength limits of aluminum.

The pressure in the wave calculated by formula (33) was compared to that calculated by Kirkwood-Bethe formula (17). Figure 11 shows the pressure graph in the shock wave calculated by Kirkwood-Bethe formula for the distances from the center of the cavity r under the collapse of the cavities.

Figures 10 and 11 show that the calculations correlate almost entirely. Therefore, the approach to calculating the collapse pressure in collapsing cavities based on comparing this pressure with the strength of solid materials under erosion can be used to assess the intensity of erosion.

CONCLUSION

The present research revealed the following erosive effect of cavitation on highly rigid materials of ultrasonic vibrating systems.

Figure 12 shows how the corresponding problem from the theory of elasticity can be applied to the task in hand. The spherical shock wave from the collapse of the ultrasonic cavity was considered here as an absolutely rigid ball penetrating into the elastic surface of the ultrasonic emitter.

The problem has the following solution:

$$a = \sqrt[3]{\frac{3\pi}{8}\frac{kP}{\beta}} \quad (34)$$

$$q_0 = \sqrt[3]{\frac{24}{\pi^5}\left(\frac{\beta}{k}\right)^2 P} \quad (35)$$

$$w_0 = \sqrt[3]{\frac{9\pi^2}{8}\beta k^2 P^2} \quad (36)$$

where a – radius of the contact spot of the ball with radius R with elastic half-space; q and q_0 – current and maximal (in the center of the spot) contact stresses, respectively; $\beta = 1/2R$; $k = (1–\mu^2)/\pi E$; w, w_0 – current and maximal values of the deflection of the elastic space; P – force pushing the ball into the elastic half-space.

The previous studies defined the range of pressure values in cavities. Using these values, assuming that the maximal pressure in the cavity that erodes the emitter, is $p = q_0$, and expressing the size of the contact spot as a and the penetration depth as w_0 via q_0, we get the following equation:

$$a = q_0 \frac{\pi R\left(1-\mu^2\right)}{2E} \quad (37)$$

$$w_0 = \frac{a^2}{R} = R\left[\frac{q_0\pi\left(1-\mu^2\right)}{2E}\right]^2 \quad (38)$$

The obtained results proved that contact spot size a and penetration depth w_0 can serve as a criterion for the erosion of the surface of the ultrasonic emitter.

CONTRIBUTION

The authors were equally involved in the research and are equally responsible for any potential plagiarism or other unethical issues.

CONFLICT OF INTEREST

The authors declare that there are no conflicts of interests regarding the publication on this article.

REFERENCES

1. Chemat F, Rombaut N, Sicaire A-G, Meullemiestre A, Fabiano-Tixier A-S, Abert-Vian M. Ultrasound assisted extraction of food and natural products. Mechanisms, techniques, combinations, protocols and applications: A review. Ultrasonics Sonochemistry. 2016;34:540–560. https://doi.org/10.1016/j.ultsonch.2016.06.035.
2. Soria AC, Villamiel M. Effect of ultrasound on the technological properties and bioactivity of food: a review. Trends in Food Science and Technology. 2010;21(7):323–331. https://doi.org/10.1016/j.tifs.2010.04.003.
3. Jadhav AJ, Holkar CR, Goswami AD, Pandit AB, Pinjari DV. Acoustic cavitation as a novel approach for extraction of oil from waste date seeds. ACS Sustainable Chemistry and Engineering. 2016;4(8):4256–4263. https://doi.org/10.1021/acssuschemeng.6b00753.
4. Ansari JA, Ismail M, Farida M. Investigation of the use of ultrasonication followed by heat for spore inactivation. Food and Bioproducts Processing. 2017;104:32–39. https://doi.org/10.1016/j.fbp.2017.04.005.
5. Wu H, Hulbert GJ, Mount JR. Effects of ultrasound on milk homogenization and fermentation with yogurt starter. Innovative Food Science and Emerging Technologies. 2000;1(3):211–218. https://doi.org/10.1016/S1466-8564(00)00020-5.
6. Senrayan J, Venkatachalam S. Ultrasonic acoustic-cavitation as a novel and emerging energy efficient technique for oil extraction from kapok seeds. Innovative Food Science and Emerging Technologies. 2020;62. https://doi.org/10.1016/j.ifset.2020.102347.
7. Berezovsky YuM, Shpakov VYu, Andreev VN. Experimental assessment of erosive regularities activity cavitation in water. Tekhnologii 21 veka v pishchevoy, pererabatyvayushchey i legkoy promyshlennosti [Technologies of the XXI century in food, processing, and consumer goods industries]. 2012;(6–1). (In Russ.).
8. Ertugay MF, Sengul M. Effect of ultrasound treatment on milk homogenisation and particle size distribution of fat. Turkish Journal of Veterinary and Animal Sciences. 2004;28(2):303–308.
9. Berezovskii YuM, Dergachev PP, Bliadze VG. Possibilities of milk ultrasonic treatment. Dairy Industry. 2009;(5): 46–47. (In Russ.).
10. Ovsyannikov VYu, Toroptsev VV, Berestovoy AA, Lobacheva NN, Lobacheva MA, Martekha AN. Development and research of new method for juice extracting from sugar beet with preliminary pressing. IOP Conference Series: Earth and Environmental Science. 2021;640(5). https://doi.org/10.1088/1755-1315/640/5/052011.
11. Vasiliev AM, Bredihin SA, Andreev VK. To the question of non-harmonic force oscillations and moment by the vibration generator. IOP Conference Series: Earth and Environmental Science. 2021;640(7). https://doi.org/10.1088/1755-1315/640/7/072011.
12. Wang T, Guo N, Wang S-X, Kou P, Zhao C-J, Fu Yu-J. Ultrasound-negative pressure cavitation extraction of phenolic compounds from blueberry leaves and evaluation of its DPPH radical scavenging activity. Food and Bioproducts Processing. 2018;108:69–80. https://doi.org/10.1016/j.fbp.2018.01.003.
13. Huang L, Zhang W, Ding X, Wu Z, Li Y. Effects of dual-frequency ultrasound with different energy irradiation modes on the structural and emulsifying properties of soy protein isolate. Food and Bioproducts Processing. 2020;123: 419–426. https://doi.org/10.1016/j.fbp.2020.07.021.
14. Chakraborty S, Uppaluri R, Das C. Optimization of ultrasound-assisted extraction (UAE) process for the recovery of bioactive compounds from bitter gourd using response surface methodology (RSM). Food and Bioproducts Processing. 2020;120:114–122. https://doi.org/10.1016/j.fbp.2020.01.003.
15. Zhang L, Zhou C, Wang B, Yagoub AE-GA, Ma H, Zhang X, et al. Study of ultrasonic cavitation during extraction of the peanut oil at varying frequencies. Ultrasonics Sonochemistry. 2017;37:106–113. https://doi.org/10.1016/j.ultsonch.2016.12.034.
16. Scudino H, Silva EK, Gomes A, Guimaraes JT, Cunha RL, Sant'Ana AS, et al. Ultrasound stabilization of raw milk: Microbial and enzymatic inactivation, physicochemical properties and kinetic stability. Ultrasonics Sonochemistry. 2020;67. https://doi.org/10.1016/j.ultsonch.2020.105185.
17. Potoroko I, Kalinina I, Botvinnikova V, Krasulya O, Fatkullin R, Bagale U, et al. Ultrasound effects based on simulation of milk processing properties. Ultrasonics Sonochemistry. 2018;48:463–472. https://doi.org/10.1016/j.ultsonch.2018.06.019.
18. Silva M, Zisu B, Chandrapala J. Influence of low-frequency ultrasound on the physico-chemical and structural characteristics of milk systems with varying casein to whey protein ratios. Ultrasonics Sonochemistry. 2018;49: 268–276. https://doi.org/10.1016/j.ultsonch.2018.08.015.
19. Patil L, Gogate PR. Ultrasound assisted synthesis of stable oil in milk emulsion: Study of operating parameters and scale-up aspects. Ultrasonics Sonochemistry. 2018;40:135–146. https://doi.org/10.1016/j.ultsonch.2017.07.001.

20. Ovsyannikov VYu, Berestovoy AA, Lobacheva NN, Toroptsev VV, Trunov SA. Research of the process of vegetable oil extracting under the influence of a high frequency wave field. IOP Conference Series: Materials Science and Engineering. 2020;941(1). https://doi.org/10.1088/1757-899X/941/1/012052.
21. Krasulya O, Bogush V, Trishina V, Potoroko I, Khmelev S, Sivashanmugam P, et al. Impact of acoustic cavitation on food emulsions. Ultrasonics Sonochemistry. 2016;30:98–102. https://doi.org/10.1016/j.ultsonch.2015.11.013.
22. Shalunov AV, Khmelev VN, Terentiev SA, Nesterov VA, Golykh RN. Ultrasonic dehydration of food products with moisture removal without phase transition. Food Processing: Techniques and Technology. 2021;51(2):363–373. (In Russ.). https://doi.org/10.21603/2074-9414-2021-2-363-373.

ORCID IDs
Sergei A. Bredihin https://orcid.org/0000-0002-6898-0389
Vladimir N. Andreev https://orcid.org/0000-0002-4890-379X
Alexander N. Martekha https://orcid.org/0000-0002-7380-0477
Matthias G. Schenzle https://orcid.org/0000-0001-6334-0481
Igor A. Korotkiy https://orcid.org/0000-0003-4379-9652

Foods and Raw Materials, 2021, vol. 9, no. 2

E-ISSN 2310-9599
ISSN 2308-4057

Research Article
Open Access

https://doi.org/10.21603/2308-4057-2021-2-345-353
Available online at http://jfrm.ru/en

Cooked sausage enriched with essential nutrients for the gastrointestinal diet

Vladimir V. Sadovoy[1,2,*], Tatiana V. Shchedrina[1], Irina A. Trubina[3], Anna V. Morgunova[2], Evgenia P. Franko[4]

[1] North-Caucasus Federal University, Stavropol, Russia

[2] Belgorod University of Cooperation, Economics and Law, Belgorod, Russia

[3] Stavropol State Agrarian University, Stavropol, Russia

[4] Belarusian State Agrarian Technical University, Minsk, Belarus

* e-mail: vsadovoy@yandex.ru

Received June 19, 2020; Accepted in revised form December 03, 2020; Published online October 15, 2021

Abstract:

Introduction. People with gastrointestinal disorders should have a sparing diet with a balanced chemical and amino acid composition including all essential components. Based on formulations of meat products, we identified a number of essential nutritional components that could improve the diet for gastrointestinal pathologies. In this study, we aimed to develop a formulation for cooked sausage enriched with deficient essential nutrients.

Study objects and methods. Our study object was cooked sausage. First, we analyzed the diet for people with gastrointestinal disorders. Then, we formulated a meat-based product (cooked sausage), determined its chemical and amino acid compositions, as well as vitamin and mineral contents, and assessed the balance of amino acids. Finally, we evaluated the biological value and safety of the formulated sausage on laboratory mice.

Results and discussion. The chemical and amino acid compositions of a daily gastrointestinal diet in medical institutions revealed a deficiency of some water-soluble vitamins, vitamin A, calcium, magnesium, and iron, as well as an imbalance of amino acids. To replenish the deficiency, we formulated a meat-based product composed of trimmed beef and pork, beef liver, egg mix, food gelatin, chitosan succinate, rice flour, and soy fortifier. The product was classified as a meat and cereal cooked sausage of grade B, in which most amino acids were used for anabolic purposes. Its daily portion of 100 g eliminated the deficiency of potassium and iron, almost completely replenished magnesium, calcium, and vitamin A, as well as reduced the deficiency of dietary fiber by 4.8 g. The cytological studies of the blood of laboratory animals, whose basic diet contained the formulated sausage, proved its high biological value and safety.

Conclusion. We found that the formulated meat and cereal sausage can be included in the diet for patients with gastrointestinal diseases and used in medical institutions to eliminate the deficiency of essential nutrients.

Keywords: Diet, essential components, raw meat, optimization, formulation, chemical composition, amino acid composition, biological value

Please cite this article in press as: Sadovoy VV, Shchedrina TV, Trubina IA, Morgunova AV, Franko EP. Cooked sausage enriched with essential nutrients for the gastrointestinal diet. Foods and Raw Materials. 2021;9(2):345–353. https://doi.org/10.21603/2308-4057-2021-2-345-353.

INTRODUCTION

According to Russian official statistics, gastroenterological disorders rank third among all diseases. Nutrition is key to their prevention and treatment. Its factors include the chemical composition of the ingredients, the ratios between particular components, the frequency of meals, the calorie content of the daily diet, and others. The treatment of gastrointestinal diseases involves changing the chemical composition of the diet by removing or adding certain components based on their energy value, cooking method, and consistency. Balanced nutrition has a beneficial effect on the metabolism and regulatory systems [1–3].

The development of rational nutrition or adequate diet is still a relevant issue [4, 5]. Such nutrition can include dietary supplements that regulate the chemical composition of foods, stabilize their functional and technological properties, and improve their sensory characteristics and digestibility. The economic indicators are also important, therefore food formulators need to create inexpensive products by adjusting their composition and properties [6, 7].

People with gastrointestinal disorders need a diet that has a balanced composition of micro- and macronutrients, protects the mucous membrane of the gastrointestinal tract, restores natural biocenosis, and reduces gastrointestinal inflammation. Dieticians should take into account the medicinal properties of each food component and their effect on the metabolism and other regulatory systems [1, 3, 5, 8].

Fermented milk products with kefir starter culture, as well as bifidobacteria and lactobacilli, can also benefit people with gastrointestinal diseases. The dietary supplements that maintain and restore the gastrointestinal functions include vitamins, macro- and microelements (Fe, Ca, Zn, etc.), polysaccharides, and dietary fiber. Dietary fiber, which acts as a sorbent, normalizes the motor and evacuation functions of the gastrointestinal tract. Its main feature is high water-retention capacity that accelerates intestinal transit and peristalsis. Dietary fiber also acts as a prebiotic that helps the intestinal microflora by increasing the number of beneficial microorganisms and suppressing the development of coliforms and putrefactive microflora [9, 10].

There is scientific evidence that extracts of bovine abomasum polypeptides, both native and thermally treated, have a therapeutic effect on the damaged gastric mucosa of male Wistar rats, namely gastroprotective and antiulcer effects [11]. Extracts of abomasum polypeptides were also used in the production of pâté for children suffering from gastritis.

It should be noted that bovine abomasum is a potential source of tissue-specific peptides that have a selective effect on the gastric mucosa cells. When formulating a meat product, dieticians should make up for the deficiency of essential components according to the daily requirements for nutraceuticals and dietary fiber, as well as ensure a balanced amino acid composition.

Taking into account the chemical and amino acid composition of meat of slaughter animals, we proposed to formulate a cooked sausage for people with gastrointestinal disorders that can make up the deficiency of essential components.

Cow liver is highly recommended to people with gastrointestinal disorders since it contains significant amounts of vitamin A, iron, copper, and other trace elements and hormonal substances [4, 5, 8, 12]. Beef with a high content of connective tissue and lean pork are also good for their diet [8]. Based on literature, we found the following sources of essential components for our formulation: chitosan succinate, egg mix, soy fortifier, rice flour, and food gelatin [4, 13–15].

Chitosan succinate, a chitin processing product, restores intestinal motility, removes toxic components (cholesterol, heavy metals, bile acids, etc.) from the body, revitalizes lymphatic cells, and helps prevent cancer and diabetes. When using it in cooked sausages, we should take into account that chitosan dissolves in acidic solutions and exhibits its gel-forming and emulsifying properties. It can be used as preliminarily dissolved in milk whey. Chitosan succinate (a complex compound of chitosan and succinic acid) has regions with high and low electron density on the surface of a polymer molecule. Therefore, it is capable of dissolving and exhibiting its functional and technological properties in a wide range of active acidity [12, 13]. When used in meat products, it does not change the active acidity of ground meat.

Rice flour is a source of B vitamins that have a beneficial effect on the nervous system. It contains silicon that normalizes metabolic processes in the human body [14, 15]. Also, rice flour is rich in dietary fiber and biotin, as well as minerals (sodium, potassium, phosphorus), which prevent gastrointestinal diseases [4, 16].

Soy fortifier is a soy milk product that contains a significant amount of dietary fiber, potassium, and ferrous digestible iron. It has a positive effect on the cardiovascular system and stimulates the formation of hemoglobin and certain groups of enzymes [15].

Many cooked sausages contain egg mix that is a source of unsaturated fatty acids, phospholipids, vitamins (A, D, E, B_1, B_2, etc.), phosphorus, iron, and calcium. Also, egg mix enhances the sensory characteristics of the sausage [16, 17].

Gelatin is used as a gelling agent. Up to 30% of connective tissue (primarily collagen-containing) proteins in meat products does not reduce their biological value. Gelatin stimulates blood clotting, acts as dietary fiber, and plays an essential role in the colon motility [18].

Thus, we aimed to develop a balanced meat-based product that could improve the daily intake of essential nutrients for people with gastrointestinal disorders.

STUDY OBJECTS AND METHODS

Our study objects included trimmed beef with connective and adipose tissues under 12%, trimmed pork with fat under 10% (State Standard R 34424-2018 “Meat industry. Classification of trimmed meat for production of meat products for child nutrition”), beef liver (State Standard 32244-2013 “Processed meat by-products. Specification”), soy fortifier (Specification 9146-020-00361809-2001 “Soy food fortifier. Technical conditions”), chitosan succinate (Specification 9284-027-11734126-08 “Chitosan succinate”), egg mix (State Standard 30363-2013 “Products egg dry and liquid food. Specification”), food gelatin (State Standard 11293-89

"Gelatin. Specifications"), and rice flour (State Standard 53495-2009 "Flour for baby's nutrition. Specifications").

The chemical composition of the meat-based product (grade B cooked sausage) was determined on a FoodScan analyzer. The amino acid composition of the sausage samples, which were pre-hydrolyzed in alkaline and acidic solutions, was determined by liquid chromatography on an AAA-400 automatic amino acid analyzer. The mineral composition was studied using a Spectroscan Max GV universal analyzer. The vitamin composition was determined on an LCMS-10EV liquid chromatograph.

The product's biological value was studied on BALB/C white mice (males and females) with an initial weight of 20–30 g. The animals were kept on litter in vivarium cages with standard lighting at about 20°C. The experiment complied with the sanitary, epidemiological, and hygienic regulations for laboratory practice. Lipids, triglycerides, cholesterol, and protein in the blood of experimental animals were determined on an Cobas C-111 biochemical analyzer (Roche Diagnostics) [19–23].

The formulation was optimized using multidimensional scaling and cluster analysis in Statistic (v. 10, 12). Multidimensional data sets were created and processed with the Statistic Neural Networks. To exclude errors, data were obtained in 3–5 repetitions and analyzed in the Error per Case module ($P \leq 0.05$) [24, 25].

RESULTS AND DISCUSSION

Diet therapy for gastrointestinal disorders is based on regular split meals of foods that leave the stomach quickly, do not stimulate gastric secretion, and do not irritate the mucous membrane [3, 5, 8]. To study a daily gastrointestinal diet, we determined the chemical and amino acid compositions and compared the results with the recommended requirements. In particular, we analyzed Diet No. 1 recommended for diseases of the esophagus, stomach, duodenum, and sometimes the small intestine [5, 8, 26, 27].

The calculations were performed in Excel for the diet with and without meat products (Tables 1, 2).

We compared our data for Diet No. 1 (Table 1) with the recommended requirements for people with gastrointestinal disorders and found a number of discrepancies. In particular, the diet had a deficiency of dietary fiber (15.1 g per day – 75.5% of the recommended intake); vitamins: A (0.75 mg – 83.3%), PP (7.8 mg – 39.0%), B_1 (0.7 mg – 46.7%), B_2 (1.0 mg – 55.6%); as well as magnesium (23 mg – 7.7%), potassium (87 mg – 4.0%), calcium (207 mg – 25.9%), and iron (3 mg – 16.7%). Since the deficiency of water-soluble vitamins (B_1, B_2, PP, and C) can be replenished with plant ingredients, and the sodium and

Table 1 Chemical composition of the gastrointestinal diet*

Name of product	Weight, g	Proteins, g	Carbohydrates, g	Fats, g	Dietary fiber, g	Minerals, mg						Vitamins, mg				
						Na	K	Ca	Mg	P	Fe	B_1	B_2	PP	C	A
Breakfast 1																
Rice porridge	250	6.3	65.8	0.5	0.5	973	48	36	25	85	1.0	0.1	0.05	1.2	–	–
Cocoa	200	3.8	25.8	3.9	0.7	50	242	122	18	120	0.6	0	0	0.2	–	–
Cake rusks	60	5.1	31.5	6.5	0.1	264	85	19	25	62	1.1	0.1	0.06	1.1	–	–
Breakfast 2																
Black currant kissel (jelly-drink)	200	0.1	28.0	0	0.2	7	59	8	4	9	0.2	0	0	0.1	24.0	0
Cake rusks	60	5.1	31.5	6.5	0.1	264	85	19	25	62	1.1	0.1	0.1	1.1	0	0
Lunch																
Grain soup	500	6.6	50.1	5.8	1.8	1277	744	75	79	445	2.1	0.2	0.1	2.2	11.5	0
Beef patty	50	5.0	6.8	8.7	0	358	99	11	14	65	0.7	0.04	0.06	1.7	0	0.02
Cranberry jelly	200	2.7	24.1	0	0.1	2	21	44	5	19	0.2	0	0	0.03	1.7	0
Afternoon snack																
Fresh apple	120	0.4	9.8	0	0.6	26	248	16	9	11	0.6	0.03	0.02	0.3	16.0	0
Dinner																
Curd pudding	200	29.8	43.0	8.4	0.7	889	381	201	46	332	1.7	0.03	0.41	1.1	0.4	0.13
Boiled pike perch	75	15.1	0	1.0	0	493	111	26	13	124	1.1	0.07	0.06	0.6	1.5	0.02
Cake rusks	60	5.1	31.5	6.5	0.1	264	85	19	25	62	1.1	0.1	0.06	1.1	0	0
Rosehip drink	200	0.4	31.0	0	0	1.6	4	8	3	2	4.4	0	0	0.2	120	0
Daily total:	–	85.5	378.9	47.8	4.9	4869	2212	604	291	1398	16	0.8	0.9	13.9	175.1	0.17
Daily total without meat products:	–	75.4	372.1	39.1	4.9	4511	2113	593	277	1333	15	0.8	0.8	12.2	175.1	0.15
Recommended daily requirements [25]:	–	85–90	300–330	70–80	20.0	4000–6000	2200–2500	800–1000	300–500	800–2600	18–40	1.5–5.0	1.8–6.0	20–60	90–900	0.9–3.0

* The meat product used for the chemical and amino acid analysis was "Kotlety derevenskiye" (Country-style patties) with connective and adipose tissues under 20% (State Standard 52675-2006. "Semi-prepared meat and meat-contained products. General specifications")

Table 2 Amino acid composition of the daily diet

Indicators \ Essential amino acids	Tryptophan	Leucine	Isoleucine	Valine	Threonine	Lysine	Methionine + cystine	Phenylalanine + tyrosine
Actual amino acid consumption, g per day	0.88	4.57	2.25	2.97	3.22	3.69	2.38	4.66
Amino acid composition of the diet, g/100 g protein	1.03	5.35	2.63	3.47	3.77	4.32	2.78	5.45
FAO/WHO standard, g/100 g protein	1.0	7.0	4.0	5.0	4.0	5.5	3.5	6.0
Amino acid score of the daily diet, %	102.9	76.4	65.8	69.5	94.2	78.5	79.5	90.8

Table 3 Chemical composition of the formulated cooked sausage for people with gastrointestinal disorders

Components	Recommended daily intake for people with gastrointestinal disorders [29]	Actual daily consumption without meat products	Nutrient deficiency in the daily diet	Formulated product
Dietary fiber, g/day	20.0	4.9	15.1	15.1
Vitamin A, mg/day	0.9–3.0	0.15	0.75	0.75–2.85
Calcium, mg/day	800–1000	593.0	207	207.0–407.0
Magnesium, mg/day	300–500	277	23	23–223
Potassium, mg/day	2200–2500	2113	87	87–387
Iron, mg/day	18.0–40.0	15.0	3.0	3.0–25.0

Table 4 Fragment of the planning matrix for the cooked sausage formulation

Experiment No.	Formulation component, %							
	Trimmed beef with connective tissue under 12%	Trimmed pork with fat under 10%	Beef liver	Chitosan succinate	Soy fortifier	Egg mix	Food gelatin	Rice flour
1	1.00	0	0	0	0	0	0	0
---	---	---	---	---	---	---	---	---
37	0.33	0.33	0.33	0	0	0	0	0
---	---	---	---	---	---	---	---	---
93	0.25	0.25	0.25	0.25	0	0	0	0
---	---	---	---	---	---	---	---	---
170	0.20	0.20	0.20	0	0	0.20	0.20	0
---	---	---	---	---	---	---	---	---
240	0	0.17	0.17	0.17	0.17	0.17	0.17	0
---	---	---	---	---	---	---	---	---
254	0	0.14	0.14	0.14	0.14	0.14	0.14	0.14
255	0.13	0.13	0.13	0.13	0.13	0.13	0.13	0.13

phosphorus contents were within the permissible limits, these components were outside our focus during the formulation.

Since we aimed to formulate a meat-based product, we analyzed the chemical composition of Diet No. 1 with the meat product (beef patty) excluded. We found a discrepancy between the amino acid contents in the diet and the recommended requirements based on the FAO/WHO standards.

All essential amino acids in Diet No. 1, except for tryptophan, were below the recommended daily intake (Table 2).

Having compared the recommended and actual daily intake of essential components, we calculated the desired chemical composition of our meat product for people with gastrointestinal disorders (Table 3).

Experimental calculations were performed in the planning matrix. Each factor had a range of action. The plan included 255 experiments, with each factor analyzed according to the mixture design simplex centroid (Table 4).

It was important that our meat product complied with the FAO/WHO standards. The use of essential amino acids for anabolic purposes was based on the limiting amino acid.

The optimal formulation was identified using modern data mining methods based on artificial intelligence. For this, we used the following algorithm:

– calculation of the chemical and amino acid compositions for each planning matrix experiment;
– development of a neural network to adequately describe the process;
– compilation of an array of input variables in the algorithmic Pascal language;
– filling in functional (output) variables using the developed neural network (multilayer perceptron); and
– identification of the optimal variant by multidimensional scaling and cluster analysis.

The formulation parameters were determined using a neural network approximation: the scaled functions were superimposed on the scaled factors (Figs. 1 and 2).

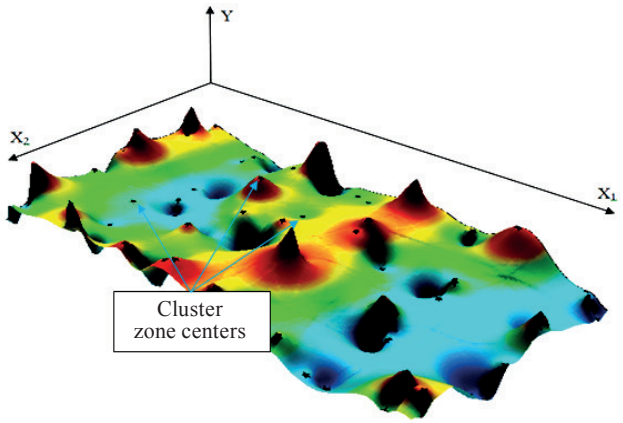

Figure 1 Neural network approximation of cooked sausage formulations

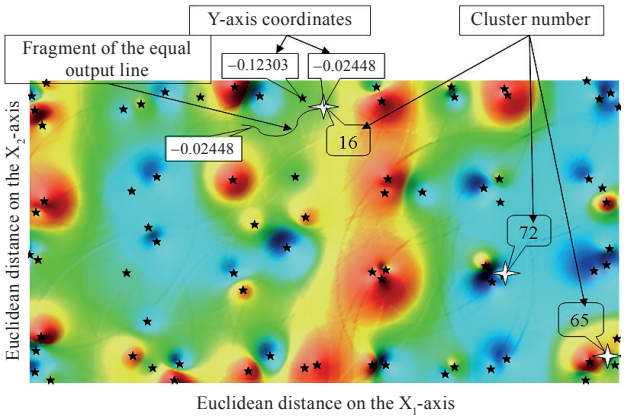

Figure 2 Neural network contour diagram of the cooked sausage composition

Table 5 Fragment of the array of optimal cluster formulations

Experiment No.	Formulation component, %							
	Trimmed beef with connective tissue under 12%	Trimmed pork with fat under 10%	Beef liver	Chitosan succinate	Soy fortifier	Egg mix	Food gelatin	Rice flour
1	56.9	24.4	16.3	0	1.6	0	0.8	0
2	75.7	8.4	12.6	0	2.5	0	0.8	0
3	64.8	32.3	0	0.1	1.6	0.4	0.8	0
4	73.3	8.1	12.2	0	2.4	0	2.4	1.6
- - -	- -	- -	- - -	- - -	- - -	- - -	- - -	- - -
31	69.5	7.0	8.4	0.4	2.7	1.1	4.9	6.0
32	59.8	20	7.1	0.4	2.2	0.8	4.2	5.4
- - -	- -	- -	- - -	- - -	- - -	- - -	- - -	- - -
83	29.2	14.6	24.8	21.9	6.9	0.5	1.6	0.4
84	68.8	0	14.8	0.2	3.9	0.5	3.9	7.9
85	61.0	20.3	6.8	0.1	3.4	0.3	2.7	5.4
86	62.8	12.1	9.6	0.6	2.4	1.2	5.3	6.0
- - -	- -	- -	- - -	- - -	- - -	- - -	- - -	- - -

Table 6 The most optimal composition for the formulated cooked sausage*

Formulation component, %							
Trimmed beef with connective tissue under 12%	Trimmed pork with fat under 10%	Beef liver	Chitosan succinate	Soy fortifier	Egg mix	Food gelatin	Rice flour
63.0	12.0	10.0	0.6	2.4	1.0	5.0	6.0

* The component contents are rounded to whole values

The formulation components (input variables) were scaled in two dimensions, while the functional indicators (chemical and amino acid compositions) were one-dimensional. The color gamut of the functional indicators (Figs. 1 and 2) indicated the diversity of compositions and process complexity. Only modern data mining modules can ensure an optimal formulation with the required parameters.

Having analyzed the clusters in different color zones (Clusters 72, 16, and 65 are given as examples in Fig. 2), we found Cluster 16 to have reference indicators (Y = –0.02448, X = –0.12303).

The compositional analysis of Cluster 16 showed that some options had unacceptable ratios between formulation components, often with insignificant amounts of meat. Also, some options had very similar compositions. Therefore, we analyzed the input variables (components) for Cluster 16 (Table 5).

The most optimal composition of the meat product formulated to prevent gastrointestinal disorders is shown in Table 6. This formulation was based on Experiment 86 (Table 5).

The most optimal composition became a basis for our cooked sausage formulation. Chitosan succinate is readily soluble in water and can be directly added to the ground meat. Soy fortifier is a source of high-grade, easily soluble protein that contains 7.9% of plant-based dietary fiber of origin. Egg mix has good binding and emulsifying properties due to the presence of lecithin. It contains digestible proteins and fat-soluble vitamins and is widely used in cooked sausage formulations.

Lebedeva[1] studied the use of rice flour in cooked sausage formulations. She found that preliminary treatment of rice flour in water heated up to 80°C

[1] Lebedeva LI. Razrabotka tekhnologii ehmul′girovannykh myasnykh produktov s ispol′zovaniem modifitsirovannoy risovoy muki [The development of technology for emulsified meat products with modified rice flour]. Cand. eng. sci. diss. Moscow: V.M. Gorbatov All-Russian Research Institute of the Meat Industry, 2003. 133 p. (In Russ.).

Table 7 Basic formulation of cooked sausage*

Unsalted ingredients, kg/100 kg								
Trimmed beef with connective tissue under 12%	Trimmed pork with fat under 10%	Beef liver	Chitosan succinate	Soy fortifier	Egg mix	Food additive		
48	9	8	0.5	2	1	31,5		
						Gelatin	Rice flour	Water
						Ratio, %		
						1	1.2	6.6

* Additional ingredients included 1.8 kg table salt, 100 g granulated sugar, and 5 g sodium nitrite per 100 kg of unsalted raw materials

Table 8 Amino acid composition of the daily diet and the formulated cooked sausage, $P < 0.05$

Indicator \ Essential amino acids	Tryptophan	Leucine	Isoleucine	Valine	Threonine	Lysine	Methionine + cystine	Phenylalanine + tyrosine
Amino acid composition of cooked sausage, g/100 g protein	0.86	6.56	3.88	5.10	3.92	6.00	3.45	5.82
Amino acid score of cooked sausage, %	86.0	93.7	97.0	102.0	98.0	109.1	98.6	97.0
Amino acid composition of beef patty, g/100 g protein	0.96	8.86	4.94	5.77	4.81	5.29	1.92	3.65
Amino acid score of beef patty, %	96.1	126.5	123.6	115.4	120.2	96.1	55.0	60.9
Daily diet with cooked sausage instead of beef patty:	1.02	4.8	2.40	3.21	3.38	4.04	2.63	5.07
Amino acid composition of the diet, g	1.09	5.60	2.81	3.74	3.95	4.71	3.07	5.92
Amino acid composition of the diet, g/100 g protein	109.0	80.1	70.1	74.9	88.7	85.7	87.8	98.7
Amino acid score of the diet, %								

increases the water-binding, fat-binding, gelling, and stabilizing capabilities of the ground meat emulsion. Gelatin swells but does not dissolve in cold water. It dissolves in hot water (60–80°C) and, when cooled, turns into jelly [10, 18].

Since chitosan succinate, egg mix, and soy fortifier are not exposed to heat treatment, a food additive of gelatin and rice flour (1:1.2) was mixed with 80°C water (1:3) and homogenized for 3–4 min. Then, it was chilled and introduced into the meat at the final stage of cutting. Our formulation of cooked sausage with a food additive is shown in Table. 7.

The sausage yield was 117 kg/100 kg of unsalted raw materials. State Standard 23670-2019. "Cooked meat sausage products. Specifications" classifies the formulated sausage as a hybrid (meat and cereal) product according to the content of meat ingredients (53.6%), and as belonging to grade B according to the content of muscle tissue (43.0%).

The sensory evaluation of the sausage was performed by 10 panelists. The average score was 4.9 points, with slight discrepancies in the color evaluation. The chemical composition of the cooked sausage sample included 60.8% water, 4.4% fat, 10.3% protein, and 3.2% minerals ($P \leq 0.05$). With a beef patty excluded from the diet, the protein deficiency was 9.6–14.6 g/day (Table 1). Therefore, the diet should contain at least 100 g of cooked sausage to replenish the protein deficiency.

To assess the biological value of the formulated sausage, we determined the amino acid composition of a beef patty using the reference book [4] and calculated the daily intake of amino acids for a diet with cooked sausage and a diet with a beef patty (Table 8).

As can be seen in Table 8, the score of the limiting amino acid (isoleucine) in the sausage (70.1%) was higher than the score in the patty (65.8%). This means that in the diet with cooked sausage, more essential amino acids will be used for anabolic purposes. There was no need to assess the balance of amino acids in the daily diet, since it consisted of split meals consumed at different times.

We compared amino acid contents in the cooked sausage and beef patties (Table 8) and found that the formulated meat product had a well-balanced composition of essential amino acids. Based on Table 8 and using the method of Lipatov, we calculated the mutual balance and rationality of essential amino acid contents in the formulated sausage and beef patties (Table 9) [28, 29].

As can be seen in Table 9, the rationality coefficient for cooked sausage was much higher than for a beef patty. Cooked sausage had a low content of amino acids used for the biosynthesis of nonessential amino acids ($\sum^{BS}$EAA), compared to a beef patty. The proportion of essential amino acids used as energogenic material ($\sum^{EG}$EAA) was almost the same for both samples. Thus,

Table 9 Mutual balance and rationality of essential amino acids (EAA) in cooked sausage and beef patties

Limiting amino acid score, % to FAO/WHO standard (C_{min})	Content of essential amino acids in protein, % (ΣEAA)	Utility coefficient (U)	EAA excess indicator, g/100 g protein	EAA not used for anabolic purposes, g/100 g protein	BSEAA used to synthesize non-essential amino acids (Σ^{BS}EAA)	EAA used for energogenic purposes (Σ^{EG}EAA)	Estimated rationality coefficient (R_C)	Desirable rationality coefficient (R_B)
Cooked sausage								
0.86	0.356	0.87	4.63	5.98	0.028	0.14	0.87	1
Beef patty								
0.55	0.362	0.55	15.91	28.9	0.365	0.16	0.55	1

the formulated sausage had a well-balanced amino acid composition.

The contents of some deficient minerals and vitamins in the formulated product are shown in Table 10.

Based on Tables 10 and 3, we found that 100 g of the cooked sausage could replenish a daily deficiency of potassium and iron, and significantly reduced the deficiency of magnesium, calcium, and vitamin A.

The sausage sample contained 1.2% of insoluble plant-based dietary fiber (cellulose, hemicellulose, and lignin) and 3.6% of animal-based dietary fiber (gelatin). Thus, 100 g of the cooked sausage could reduce the deficiency of dietary fiber in people with gastrointestinal disorders by 4.8 g. We find it advisable to recommend including dietary fiber in the formulations of other products in the diet.

The biological value and safety of the developed sausage was determined on BALB/C white mice *in vivo*. The experiments complied with the sanitary, hygienic, and epidemiological standards and requirements. The experimental mice were divided into 3 groups of 5 animals: mice fed on the basic diet (control group A), mice fed on the basic diet + cooked sausage without a preventative supplement (control group B), and mice fed on the basic diet + cooked sausage with a preventative supplement (experimental group).

Table 10 Some minerals and vitamin A in cooked sausage, $P < 0.05$

Content, mg/100 g of product				
K	Ca	Mg	Fe	Vitamin A
290	185	21.8	3.2	0.73

The observations lasted 30 days. The hematological parameters of mice blood at the end of the experiment are given in Table 11.

We found a slight increase in leukocytes, hemoglobin, and erythrocytes in the blood of the experimental mice over the entire feeding period (30 days).

The contents of total protein and albumin increased in the control group B and in the experimental group by 6.6 and 6.0 g/L, respectively. The level of glucose was within the normal range (4.11–4.18 mol/L) for all the animals in the entire period, regardless of the diet.

The activity of aspartaminotransferase (AST) and alanine aminotransferase (ALT) in blood serum is indicative of general health and the state of specific organs. For example, a deviation from the AST norm (26–77 U/L for mice) can indicate liver pathology, heart problems, abnormalities in protein structures and bile production, etc. ALT is responsible for the movement of alanine from one cell to another. Its normal level (54–269 U/L for mice) strengthens the immune system and normalizes metabolic processes. Increased ALT indicates blood disease and disorders in the work of heart, liver, and blood vessels, as well as other pathologies. Decreased ALT is usually caused by a deficiency of vitamin A. Our study showed that the levels of the AST and ALT enzymes were within the normal range in all the groups of mice, and their ratio (de Ritis coefficient) corresponded to the required level (0.91–1.75) [30].

Thus, the hematological parameters pointed to the biological value and safety of the formulated sausage.

CONCLUSION

We analyzed Diet No. 1 used in medical institutions for people with gastrointestinal disorders and found that its daily contents of essential ingredients (proteins,

Table 11 Hematological parameters of mice blood before and after feeding, $P < 0.05$

Name	Erythrocytes, 10^{12}/L	Leukocytes, 10^{9}/L	Hemoglobin, g/L	Total protein, g/L	Albumin, g/L	Glucose, mol/L	AST, U/L	ALT, U/L	ALT/AST (de Ritis coefficient)
A day before feeding (7^{th} day of observations)	8.16	8.64	126.00	59.60	36.62	4.11	51.40	67.85	1.32
30^{th} day: Basic diet	8.64	8.94	128.60	61.40	39.40	4.18	52.00	62.92	1.21
Basic diet + sausage without preventative supplement	8.78	9.32	129.40	66.20	42.80	4.16	57.20	68.068	1.19
Basic diet + sausage with preventative supplement	8.50	9.32	129.01	65.60	42.40	4.16	53.80	62.95	1.17

dietary fiber, vitamins, and some minerals) did not meet the recommended intake. In particular, we identified an imbalance of amino acids in the meat product used in the diet (a beef patty). In order to eliminate this nutritional deficiency, we formulated a meat and cereal product of grade B – cooked sausage. Apart from meat, it contained chitosan succinate, egg mix, soy fortifier, food gelatin, and rice flour. Our product had a well-balanced composition of amino acids, with tryptophan as the limiting amino acid (amino acid score – 86.0%, the utility coefficient – 0.87). 100 g of the formulated cooked sausage can completely eliminate the deficiency of potassium, calcium, and iron, as well as significantly reduce the lack of magnesium and vitamin A. Since it can only reduce, rather than fully replenish, the deficiency of dietary fiber, we recommend that foods rich in dietary fiber are included in the diet.

The experimental studies of the hematological parameters in the laboratory mice confirmed the nutritional value and safety of the formulated cooked sausage. Therefore, it can be included in the diet for people with gastrointestinal disorders and used in medical institutions.

CONTRIBUTION

The authors were equally involved in conducting the research and writing the manuscript.

CONFLICT OF INTEREST

The authors declare that they have no conflict of interest.

REFERENCES

1. Nichipuruk E. The Tract. Moscow: Tochka; 2019. 408 p. (In Russ.).
2. Khan TN, Ansari TH, Zulkifle M. Concept of transformation and incorporation of nutriment in the body: A review. International Journal of Food Science and Nutrition. 2019;4(3):93–96.
3. Nikityuk DB, Pogozheva AV, Sharafetdinov KhKh, Baturin AK, Bogdanov AR, Gapparova KM, et al. Standarty lechebnogo pitaniya [Standards of medical nutrition]. Moscow, 2017. 313 p. (In Russ.).
4. Spisok produktov (Khimicheskiy sostav) [A list of products (chemical composition)] [Internet]. [cited 2020 May 20]. Available from: http://frs24.ru/himsostav.
5. Baranovskiy AYu. Dietologiya. 5-e izd. [Dietology. 5th edition]. St. Petersburg: Piter; 2017. 1104 p. (In Russ.).
6. Sadovoy VV, Selimov MA, Shchedrina TV, Nagdalian AA. Nutritional supplement for control of diabetes. Journal of Excipients and Food Chemicals. 2017;8(2):31–38.
7. Sadovoy VV, Shchedrina TV, Melentyeva VV, Khamitsaeva AS. Forecasting the molecular properties of dietary supplement used in the recipe of foodstuff for diabetes mellitus prevention. Research Journal of Pharmaceutical, Biological and Chemical Sciences. 2018;9(4):1620–1625.
8. Aljutaily T, Huarte E, Martinez-Monteagudo S, Gonzalez-Hernandez JL, Rovai M, Sergeev IN. Probiotic-enriched milk and dairy products increase gut microbiota diversity: a comparative study. Nutrition Research. 2020;82:25–33. https://doi.org/10.1016/j.nutres.2020.06.017.
9. Simpson T, Deleuil S, Echeverria N, Komanduri M, MacPherson H, Suo C, et al. The Australian Research Council Longevity Intervention (ARCLI) study protocol (ANZCTR12611000487910) addendum: Neuroimaging and gut microbiota protocol. Nutrition Journal. 2019;18(1). https://doi.org/10.1186/s12937-018-0428-9.
10. Chernukha IM, Bogatyrev AN, Dydykin AS, Aslanova MA, Fedulova LV. Effect of polypeptides isolated from cattle abomasum on stomach regenerative processes in rats. Problems of Nutrition. 2014;83(5):26–32. (In Russ.).
11. Aslanova MA. Funktsional′nyy pashtet dlya pitaniya detey, stradayushchikh gastritom [Functional pâté for children with gastritis]. Meat Technology. 2016;157(1):39–41. (In Russ.).
12. Zhu J, Zhang Y, Wu G, Xiao Z, Zhou H, Yu X. Inhibitory effects of oligochitosan on TNF-α, IL-1β and nitric oxide production in lipopolysaccharide-induced RAW264-7 cells. Molecular Medicine Reports. 2015;11(1):729–733. https://doi.org/10.3892/mmr.2014.2643.
13. Azuma K, Osaki T, Minami S, Okamoto Y. Anticancer and anti-inflammatory properties of chitin and chitosan oligosaccharides. Journal of Functional Biomaterials. 2015;6(1):33–49. https://doi.org/10.3390/jfb6010033.
14. Ol′khovatov EA, Ponomarenko LV, Kovalenko M.P. Ispol′zovanie soi v pishchevykh i meditsinskikh tselyakh [The use of soy for nutritional and medical purposes]. Young Scientist. 2015; 95(15):231–235. (In Russ.).
15. Antipova LV, Mishchenko AA, Osipova NA. Rastitel′nye istochniki dlya proizvodstva produktov pitaniya funktsional′nogo naznacheniya [Vegetable sources for functional food production]. Molodezhnyy innovatsionnyy vestnik [Youth Innovative Bulletin]. 2018;8(3):37–38. (In Russ.).
16. Korrol′ AE, Drozdova LI. The mélange as a product of the food industry. Molodezh′ i nauka [Youth and science]. 2017;(3):27–32. (In Russ.).

17. Ratushnyy AS, Aminov SS. Vsyo o ede ot A do Ya: Ehntsiklopediya [Everything about food from A to Z: Encyclopedia]. Moscow: Dashkov and K; 2019. pp. 433–434. (In Russ.).
18. Esimbekova EN, Kratasyuk VA, Govorun AE, Lonshakova-Mukina VI. Gelatin and starch: what better stabilizes the enzyme activity? Doklady Rossijskoj Akademii Nauk. Nauki o Zhizni. 2020;491(1):151–154. (In Russ.). https://doi.org/10.31857/S2686738920020110.
19. Sanitarno-veterinarnye pravila soderzhaniya laboratornykh zhivotnykh [Sanitary and veterinary rules for keeping laboratory animals] [Internet]. [cited 2020 May 20]. Available from: https://dommedika.com/medicinskaia_mikrobiologia/soderganie_laboratornix_givotnix.html.
20. Denisov AV, Cheprakova VA, Anisin AV, Bezrukov SI. Ethical aspects of modern use of animals in experimental studies. Bulletin of the Russian Military Medical Academy. 2018;63(3):238–242. (In Russ.).
21. Sadovoy VV, Shchedrina TV, Selimov MA. Biologically active composition for regulation of lipolysis process in the organism under obesity. Problems of Nutrition. 2017;86(6):74–83. (In Russ.).
22. Berezin I, Chupakhina L, Popov A. Modern aspects of sanitary-epidemiological normalization of working conditions at work with laboratory animals. Veterinariya sel′skokhozyaystvennykh zhivotnykh [Veterinary medicine of farm animals]. 2021;(5). (In Russ.).
23. Garber JC, Barbee RW, Bielitzki JT, Clayton LA, Donovan JC, Kohn DF, et al. Guide for the care and use of laboratory animals. Moscow: IRBIS; 2017. 304 p. (In Russ.).
24. Gromyko GL. Teoriya statistiki [Theory of statistics: practical exercises]. Moscow: Infra-M; 2018. 544 p. (In Russ.).
25. Goreeva NM. Statistika v skhemakh i tablitsakh [Statistics in diagrams and tables]. Moscow: Ehksmo; 2017. 414 p. (In Russ.).
26. Kodentsova VM, Vrzhesinskaya OA, Nikityuk DB, Tutelyan VA. Vitamin status of adult population of the Russian Federation: 1987–2017. Problems of Nutrition. 2018;87(4):62–68. (In Russ.). https://doi.org/10.24411/0042-8833-2018-10043.
27. Kodentsova VM, Risnik DV, Nikitiuk DB, Tutelyan VA. Multivitamin-mineral supplementation in medical nutrition. Consilium Medicum. 2017;19(12):76–83. (In Russ.).
28. Yanova MA. Standartizatsiya i sertifikatsiya myasa i myasnykh produktov [Standardization and certification of meat and meat products]. Krasnoyarsk: Krasnoyarsk State Agrarian University; 2020. 51 p. (In Russ.).
29. Borisova T. Quality control of foodstuff and food raw materials. Shimadzu Solutinons. Analytics. 2016;28(3):64–71. (In Russ.).
30. Krasnikova ES, Krasnikov AV, Radionov RV, Artemyev DA, Okolelov VI. Blood biochemical parameters of rats – wistar line under the blv experimental infection. Innovations and Food Safety. 2019;24(2):69–75. (In Russ.). https://doi.org/10.31677/2311-0651-2019-24-2-69-75.

ORCID IDs
Vladimir V. Sadovoy https://orcid.org/0000-0002-0182-9318
Tatiana V. Shchedrina https://orcid.org/0000-0001-5201-7961
Anna V. Morgunova https://orcid.org/0000-0001-6312-7963

Foods and Raw Materials, 2021, vol. 9, no. 2

E-ISSN 2310-9599
ISSN 2308-4057

Research Article
Open Access

https://doi.org/10.21603/2308-4057-2021-2-354-363
Available online at http://jfrm.ru/en

Formulating a functional drink with antiosteoporosis effects

Marietta A. Aslanova*, Anastasia A. Semenova, Olga K. Derevitskaya

V.M. Gorbatov Federal Research Center for Food Systems of Russian Academy of Sciences, Moscow, Russia

* e-mail: m.aslanova@fncps.ru

Received March 23, 2021; Accepted in revised form May 11, 2021; Published online October 15, 2021

Abstract:

Introduction. Osteoporosis is one of the most common diseases of the musculoskeletal system in modern clinical practice. Its prevention and treatment requires a diet with a sufficient intake of calcium, vitamins, and connective tissue proteins that regenerate cartilage and bone tissue. We aimed to formulate a functional product based on collagen fermentolysate to prevent osteoporosis and prove its effects in experiments on laboratory rats.

Study objects and methods. Our study objects were collagen fermentolysate obtained from pork ears and legs (1:1) and the functional product based on it. The biological experiment was carried out on Wistar female rats exposed to osteoporosis through complete ovariectomy. Their femurs were analyzed for the contents of phosphorus, magnesium, and calcium, as well as cytometric and biochemical blood parameters.

Results and discussion. The formulated functional product based on collagen fermentolysate contained 41% of the most easily assimilable peptide fractions with a low molecular weight of 10 to 20 kDa. Other components included pumpkin powder, dietary fiber, calcium, chondroprotectors, and vitamins E, C, and D_3. Compared to the control, the experimental rats that received the functional product had increased contents of calcium and magnesium in the bone tissue (by 25.0 and 3.0%, respectively), a decreased content of phosphorus (by 7.0%), a calcium-to-phosphorus ratio restored to 2.4:1.0, and a higher concentration of osteocalcin in the blood serum (by 15%).

Conclusion. The developed functional product based on collagen fermentolysate can be used as an additional source of connective tissue protein, calcium, vitamins C, E, and D_3, dietary fiber, and chondroprotectors to prevent osteoporosis.

Keywords: Collagen, fermentolysate, osteoporosis, functional foods, raw meat, calcium, oophorectomy

Please cite this article in press as: Aslanova MA, Semenova AA, Derevitskaya OK. Formulating a functional drink with antiosteoporosis effects. Foods and Raw Materials. 2021;9(2):354–363. https://doi.org/10.21603/2308-4057-2021-2-354-363.

INTRODUCTION

Current global trends in food production are aimed at designing healthy foods to improve public health and prevent diseases caused by unbalanced nutrition. In the recent years, the quality and safety of food products has been a strategic priority in Russia. New laws have been passed to regulate and encourage the development and production of a wide range of healthy foods, including functional products.

Diseases of the musculoskeletal system are among the most common in modern clinical practice, especially osteoporosis. According to the World Health Organization, almost 200 million people suffer from osteoporosis worldwide, with over 9 million fractures occurring every year. Women aged 55+ are especially vulnerable to this pathology, which is presumably associated with estrogen deficiency in the postmenopausal period.

Postmenopausal osteoporosis is caused by accelerated bone resorption and systemic calcium imbalance. Osteoporosis caused by hypoestrogenism is commonly treated with drugs that prevent bone resorption or stimulate the formation of bone tissue. These drugs are mainly based on female sex hormones or selective estrogen receptor modulators. However, hormone therapy in postmenopausal women can be a risk factor for stroke, myocardial infarction, thromboembolism, and breast cancer. Moreover, these drugs can cause serious side effects, such as atrial fibrillation, atypical subcutaneous fracture, delayed fracture healing, hypersensitivity reactions, hot flashes, leg cramps, gastrointestinal disorders, etc. Another cause of osteoporosis is deficiency states due to insufficient intake of calcium, magnesium, protein, and vitamin D [1–8].

All these factors determine a need for new ways of osteoporosis prevention and treatment, namely for

alimentary correction with functional foods. Such foods not only meet the intake of essential nutrients, but also benefit certain bodily functions and prevent the negative effects of lifestyle and environmental factors. Our diet – as a whole and its individual components – influences different physiological processes in our body. Therefore, food formulators should introduce physiologically active ingredients with corrective properties, as well as use technology that preserves the nutritional and biological value of raw materials and components during processing and cooking.

Formulation of functional meat products is one of the current trends in modern meat industry. In particular, low-value meat-and-bone material can be used to obtain protein hydrolysates and bone mineral components [9–12].

Protein hydrolysates are commonly used as an alternative protein source in commercial products. They consist of a mixture of proteins and peptides resulting from the hydrolysis of intact proteins. During hydrolysis, peptide bonds of intact proteins get broken, which leads to a range of peptides of different sizes. Protein hydrolysates are used in various products depending on their properties [13, 14]. Numerous studies show that protein hydrolysates can be used in diets due to their high nutritional and therapeutic value – low immunological reactivity, bioactive peptides, and antioxidant activity. Protein hydrolysates are widely used in the diet for people who cannot digest whole protein. Protein hydrolysis can be carried out using enzymes, acids, or alkalis, but enzymatic hydrolysis is preferable for food purposes since it can produce hydrolysates with a well-defined peptide profile [15].

Collagen-containing products of meat processing are the main source of collagen with a unique amino acid composition. Collagen can be transformed into active peptides and amino acids to be used as functional ingredients in food formulations. It is a protein that is present in large quantities in the connective tissue of animal materials. Connective tissue is part of cartilage, tendons, subcutaneous tissue, bone, intercellular substance of muscles, parenchymal organs, and vascular walls. It accounts for about 50% of the animal's body weight. Connective tissue contains proteoglycans, whose polysaccharide group includes glucosamine or galactosamine. One of its main functions is that it takes part in the formation of organs and their restoration. Enzymatic hydrolysis increases the bioavailability of collagen and glycosaminoglycans for the body to assimilate. It produces peptides and amino acids that are absorbed into the bloodstream and then enter the cells of the connective tissue matrix [16].

The content of protein fractions and their amino acid composition in hydrolysates can be regulated by modes of hydrolysis, type of enzyme, processing method, temperature, and other factors.

Pork legs and ears are a valuable source of collagen hydrolysates. They contain 23.5 and 21.0% of protein, respectively, with 15.3 and 12.6% in the connective tissue, respectively. In our previous work, we substantiated hydrolysis parameters for the production of active peptides and free amino acids (10–15%) [17]. In particular, we described a method for obtaining hydrolysate from pork legs and ears using enzyme-containing pancreas homogenate (15% of the raw materials.) at T = 50 ± 2°C, τ = 6 h, and further freeze-drying at –40°C.

Thus, functional foods play a special role in the prevention and nutritional correction of osteoporosis, especially products based on hydrolyzed connective tissue proteins. They contain large amounts of collagen peptides and amino acids that stimulate the synthesis of physiological collagen and other substances creating cartilage and bone matrix. In addition to collagen peptides, the diet should meet the intake of calcium, magnesium, copper, zinc, as well as vitamins D, A, E, C, and group B.

In this regard, we aimed to formulate a functional product based on collagen fermentolysate for osteoporosis prevention and to confirm the identified properties in animal experiments. Our objectives were to substantiate the formulation in terms of its composition and component ratios, evaluate its sensory, microbiological, and toxicological indicators, as well as assess its restorative effect on bone metabolism impaired by oophorectomy in experiments on rats.

STUDY OBJECTS AND METHODS

Our study objects were dried collagen fermentolysate and a functional product based on it.

Collagen fermentolysate was obtained from pork by-products (ears and legs, 1:1) using raw pancreas homogenate as an enzyme-containing material. The resulting hydrolysate was dried under vacuum in an Alpha 1-2 LD freeze-dryer (Germany) at –40°C. Then, it was crushed to a particle size < 0.2 mm. The resulting hydrolysate was a homogeneous fine powder of light beige color, readily soluble in water.

The molecular weight distribution of protein fractions in the collagen fermentolysate was studied by electrophoresis in a 10% polyacrylamide gel with sodium dodecisulfate (SDS) according to Laemmli. The amino acid composition was determined on an Agilent 1260 Infinity LC liquid chromatograph in line with State Standard 34132-2017. The hydroxyproline content was measured in line with State Standard 23041-2015.

Protein content in the product was determined by the Kjeldahl method according to State Standard 25011-2017. Mass fractions of vitamin D_3 and calcium were measured according to State Standard 32307-2013 and State Standard R 55573-2013, respectively (the latter by atomic absorption). The method to determine vitamin C involved the vitamin's extraction (by sequential acid and enzymatic hydrolysis), precipitation of proteins, and high performance liquid chromatography in the ultraviolet (UV) region at a given wavelength. The resulting peak in the chromatogram was compared with the peak of a standard with a known concentration.

The method to determine vitamin E was based on alkaline hydrolysis of the sample and extraction with diethyl ether. The obtained extract was analyzed by high performance liquid chromatography in the ultraviolet (UV) region at a given wavelength. The resulting peak in the chromatogram was compared with the peak of a standard vitamin solution with a known mass concentration.

Microbiological indicators were determined using the following standards:
– State Standard 10444.15-94 for the quantity of mesophilic aerobic and facultative anaerobic microorganisms (QMAFAnM);
– State Standard 31747-2012 for coliform bacteria;
– State Standard 31659-2012 for salmonella bacteria; and
– State Standard 10444.12-2013 for mold.

Toxic elements were determined according to the following standards:
– State Standard 26927-86 for mercury;
– State Standard 26930-86 for arsenic;
– State Standard 26932-86 for lead; and
– State Standard 26933-86 for cadmium.

Biological experiments were carried out on female Wistar rats (n = 42) weighing 340 ± 20 g. The animals were kept and studied in a vivarium in strict accordance with State Standard 33216-2014.

After quarantine (7 days), the rats were randomly divided into two groups: 1) intact rats (n = 10), who were fed on a standard diet throughout the experiment, and 2) rats exposed to experimental osteoporosis modeling (n = 32).

The standard vivarium diet contained 12% casein proteins, 72% soluble carbohydrates, 11.5% saturated and polyunsaturated fatty acids, 1.0% fat-soluble vitamins, 0.1% water-soluble vitamins, and 4.0% minerals [18].

The osteoporosis modeling involved complete oophorectomy under general anesthesia (Zoletil 100, Virbac S.A., France; Xila, Interchemie, Netherlands). After 14 days from the surgery, the ovariectomized female rats were divided into three groups:

1) control animals (control), which daily received intragastrically administered distilled water (0.5 mL/head) for 28 days (n = 10);
2) experimental animals (experiment 1), which daily received an intragastrically administered glucosamine-chondroitin solution in a dose of 0.014 g per 1 kg of live weight (Pharmacor Production, Russia) (0.5 mL/head) for 28 days (n = 11); and
3) experimental animals (experiment 2), which daily received an intragastrically administered functional product based on collagen fermentolysate and dissolved in water (12 g/100 mL) in an amount of 0.5 g per 1 kg of live weight (0.5 mL/head) for 28 days (n = 11).

The rats were kept in IV S cages (Tecniplast, Italy), 5 animals each, under standard vivarium conditions: temperature 20 ± 3°C, humidity 48 ± 2%, day/night lighting (from 6.00 to 18.00), as well as free access to water and feed [18].

Before the study and after administering the functional product, the animals were weighed every 4 days on a laboratory electronic balance (Adventurer Pro AV2101, USA). On the 42nd day of the experiment, the animals were euthanized in a chamber (VetTech, UK), with blood samples extracted from the heart.

The experiments were conducted in compliance with Order No. 267 of the Russian Ministry of Health of June 19, 2003 “On the rules of laboratory practice” and European Community Directive 86/609EEC. The study was approved by the bioethical commission of the V.M. Gorbatov Federal Research Center of Food Systems (protocol No. 01/2019 of May 09, 2019) [18].

Following autopsy, all the animals underwent a thorough examination of their body surface, as well as intracranial, thoracic, and abdominal cavities and their contents. Their internal organs (liver, kidneys, spleen, adrenal glands, thymus, and heart) were separated and wet-weighed immediately after dissection. Femurs were sampled to determine mass fractions of phosphorus (State Standard 32009-2013), magnesium (State Standard 33424-2015), and calcium (State Standard R 55573-2013).

The blood cytometric assay involved counts of lymphocytes (LYM), granulocytes (GRA), and

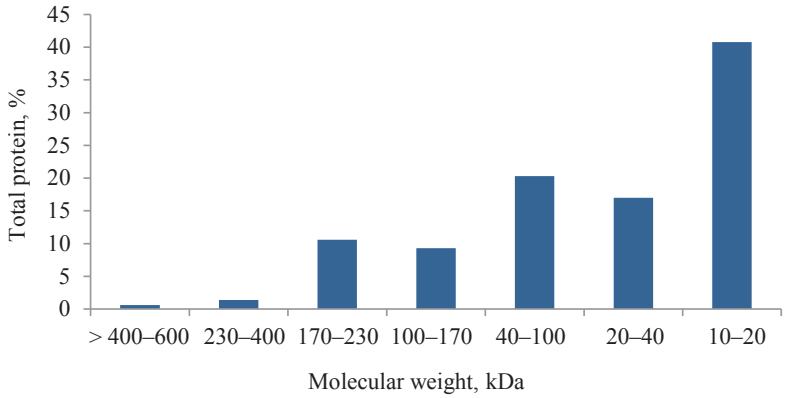

Figure 1 Molecular weight distribution of protein-peptide fractions in collagen fermentolysate

monocytes (MON) according to cell size and granularity on a Guava Easy Cyte flow cytometer (Merck Millipore, Germany). The content of leukocytes was determined as a sum of lymphocytes, granulocytes, and lymphocytes. Relative contents of lymphocytes, granulocytes, and monocytes were calculated using the formulas: LYM/WBC×100%, GRA/WBC×100%, MON/WBC×100%.

Biochemical parameters of blood serum were determined on an automatic BioChem FC-360 analyzer (HTI, USA) using a set of reagents (HighTechnology, USA) [18]. Biochemical analysis measured total protein, albumin, bilirubin (total and direct), urea, creatinine, triglycerides, aspartate aminotransferase (ASAT), alanine aminotransferase (ALAT), alkaline phosphatase (ALP), gamma-glutamyltransferase (GGT), lactate dehydrogenase (LDH), calcium, cholesterol, glucose, phosphorus, and magnesium.

Osteocalcin in blood serum was quantified by enzyme-linked immunosorbent assay (ELISA) using a set of rat-specific reagents on an Immunochem 2100 analyzer (HTI, USA).

Statistical analysis was performed in STATISTICA 10. Statistical significance was determined by the Kruskal-Wallace H-test ($P \leq 0.05$).

RESULTS AND DISCUSSION

First, we studied the physicochemical parameters of collagen fermentolysate. The molecular weight distribution of its fractions is shown in Fig. 1.

As can be seen in Fig. 1, about 41% of fractions weighed from 10 to 20 kDa. Peptides with such a molecular weight should be used as the basis of a functional beverage, since they ensure high bioavailability and good taste characteristics.

The amino acid composition of collagen fermentolysate is shown in Fig. 2.

According Fig. 2, collagen fermentolysate contained relatively high contents of glutamic acid (14.8%), aspartic acid (10.8%), glycine (7.3%), alanine (6.9%), and proline (4.9%). These amino acids are known to stimulate cartilage and bone cells and restore joint tissues. Alanine is the main component of connective tissue, while proline and lysine are precursors of hydroxylysine and hydroxyproline, which are used by the body to form collagen, tendons, and heart muscle. We also found high contents of leucine and threonine. These essential amino acids are important for the biosynthesis of glycine and serine, which are responsible for the production of collagen, elastin, and muscle tissue.

Based on collagen fermentolysate, our functional product with an antiosteoporosis effect also contained dietary fiber, bioactive substances, as well as macro- and microelements.

The formulation was in line with the biomedical requirements for the quality, composition, and safety of functional products with corrective properties. To have a real physiological effect, the product should contain at least 50% of collagen fermentolysate. However, it should also have good consumer appeal. To neutralize the flavor of fermentolysate, pumpkin powder was used as dietary fiber. It has a pleasant taste and, at the same time, contains various carbohydrate components, including pectins, cellulose, fiber, calcium, magnesium, iron, B vitamins, vitamin PP, beta-carotene, and vitamin C.

Our formulation was primarily aimed at normalizing metabolic processes and preventing diseases of the musculoskeletal system. The component quantities met the physiological needs of adult humans.

Increased calcium intake is an integral part of osteoporosis prevention and treatment. To assimilate calcium, we added vitamin D_3, as well as vitamins E and C with antioxidant properties. Products based on collagen hydrolysates in combination with vitamin C are more effective in stimulating collagen fibrils and proteoglycans in the cartilage matrix, thus improving joint mobility [19]. Oxidative stress is an important factor of aging that also contributes to osteoporosis. It induces bone resorption due to superoxide production by osteoclasts, which leads to bone degradation [5, 20, 21].

The dietary fiber included in the formulation is a prebiotic that ensures normal functioning of the gastrointestinal tract and has a beneficial effect on lipid and carbohydrate metabolism. In addition, indigestible oligosaccharides increase the absorption of various minerals, contributing to bone mineralization [22].

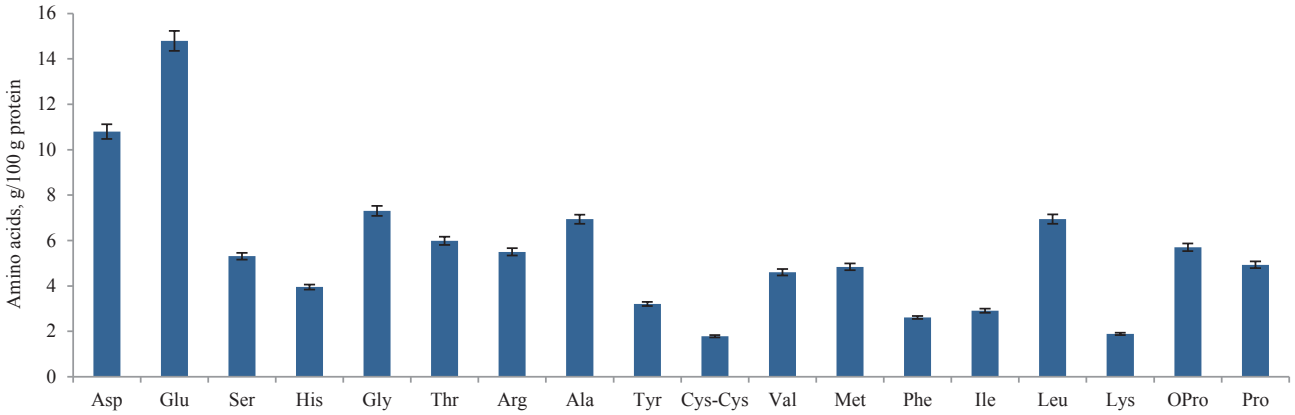

Figure 2 Amino acid contents in collagen fermentolysate

Table 1 Product formulation

Components	Mass fraction, %
Collagen fermentolysate	56.00
Dried pumpkin	20.00
Inulin	11.00
Calcium lactate	7.00
Glucosamine sulfate	3.00
Chondroitin sulfate	1.00
Ascorbic acid (vitamin C)	0.41
Tocopherol acetate (vitamin E)	0.09
Cholecalciferol (Vitamin D_3)	0.13×10^{-4}

Table 2 Nutritional value of the powdered product

Component	Content per 100 g powder	Content per serving (% of daily intake)
Proteins, g	50.0	6.0
Carbohydrates, g	14.0	2.0
Dietary fiber, g	12.0	1.4 (7%)
Ascorbic acid, mg	410.0	49.0 (80%)
Tocopherol, mg	90.0	10.8 (108%)
Cholecalciferol, μg	13.0	1.6 (31%)
Calcium, mg	1100.0	140.0 (15%)
Glucosamine sulfate, mg	3000.0	360.0 (51%)
Chondroitin sulfate, mg	1000.0	120.0 (20%)

Of great importance are chondroprotectors – glucosamine sulfate and chondroitin sulfate. They have a positive effect on metabolic processes in cartilage tissue, slowing down degenerative changes in joints and the spine.

Our choice of ingredients was determined by two main objectives. Firstly, we aimed to formulate an efficient functional product with a high nutritional value. Secondly, we wanted this product to have good sensory characteristics. Both objectives could be achieved with pumpkin powder of the Gribovskaya variety. The pumpkin was peeled, cut into 5–8 mm pieces, blanched for 3–5 min, and placed on racks for 10–15 min to remove water. The pieces were then dried in a convection drying chamber in two stages – first, at 90 ± 5°C to a moisture content of 40–42% and then, at 60 ± 5°C to a moisture content of 3.0–5.0%. The dried pumpkin was crushed to a particle size of 0.2 mm. The resulting powder had a sweetish taste and yellowish color.

To determine an optimal ratio between collagen fermentolysate and dried pumpkin, in both functional and sensory terms, we carried out a sensory experiment. The panelists preferred the taste characteristics of a 80:20 ratio between protein hydrolysate and pumpkin powder. A higher content of hydrolysate gave the product a pronounced bitter taste, which was considered unacceptable.

The amounts of functional ingredients had to meet the standard physiological needs without spoiling the consumer appeal. These ingredients included calcium lactate, glucosamine sulfate, chondroitin sulfate, ascorbic acid (vitamin C), tocopherol acetate (vitamin E), and cholecalciferol (vitamin D_3).

The formulated product is a dry powder for preparing a functional drink (Table 1).

Pre-mixtures based on the compatibility and fineness of ingredients were introduced into a drum-type mixer in two stages to ensure uniformity. The first pre-mixture included fine ingredients in smaller quantities (vitamins D_3, E, and C, chondroitin sulfate, and glucosamine sulfate). At the second stage, they were combined with the remaining components (protein hydrolysate, calcium lactate, dried pumpkin, and dietary fiber). A drink can be prepared by mixing 12 g of the concentrate with 100 mL of water. Three servings per day are needed to provide a good preventative effect.

Next, we studied the sensory, physicochemical, microbiological, and toxicological indicators of the developed product. The nutritional value of the powdered product is shown in Table 2.

When formulating a functional product based on hydrolysates, it is important to crease a characteristic sensory profile. The sensory indicators of our functional product, both in powdered and ready-to-use form, are presented in Table 3.

The microbiological properties and contents of toxic substances (lead, arsenic, cadmium, and mercury) in the

Table 3 Sensory characteristics of the functional product

Indicator	Product characteristics	
	Powder	Drink
Appearance	Fine, light yellow powder consisting of single agglomerated particles	Transparent light yellow liquid without sediment
Consistency	Loose, agglomerated particles disintegrate under light mechanical impact	Liquid, homogeneous, without settling
Color	Light yellow	Light yellow, intense, with no gloss
Aroma	Mild, with a pumpkin note	Mild, with a light pumpkin note
Taste	–	Pleasant, slightly sweet, with a pumpkin flavor, and slight sourness

Table 4 Microbiological indicators of the functional product

Indicator	Content in the powder	Standard content, as in TR CU 021/2011
Mesophilic aerobic and facultative anaerobic microorganisms, CFU/g, max.	8×10^4	1×10^5
Mass of the product in which coliforms are not allowed, g	not detected	0.1
Mass of the product in which pathogenic bacteria, including salmonella, are not allowed, g	not detected	25.0
Mold, CFU/g, max.	30	200

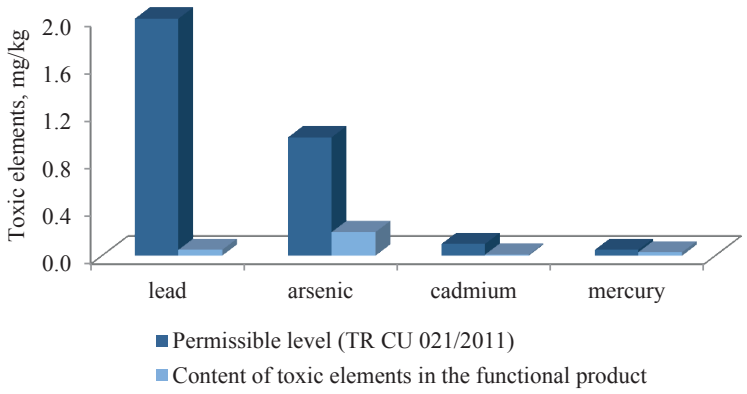

Figure 3 Contents of toxic elements in the functional product

functional product were analyzed against the Technical Regulations of the Customs Union 021/2011 "On food safety" (Table 4 and Fig. 3).

We found that the concentrations of lead and arsenic were significantly below the permissible values, and the contents of cadmium and mercury were within the norms established by TR CU 021/2011. This means that our functional product met the safety requirements of TR CU 021/2011.

Thus, we developed a powdered functional product based on collagen fermentolysate to prevent osteoporosis. Mixed with water, the drink can be used as an additional source of connective tissue protein, calcium, vitamins C, E, and D_3, as well as dietary fiber and chondroprotectors.

Its effectiveness was confirmed in the experiment on laboratory animals with modelled osteoporosis (ovariectomized female rats).

The weight of the intact animals was mostly stable throughout the experiment, with a slight increase from the 9th to the 15th day and from the 19th to the 26th day. The control animals, which received distilled water, gained weight during the entire experiment, especially from the 1st to the 12th day and from the 19th to the 26th day. Two groups of experimental animals, which received glucosamine + chondroitin and the drink based on collagen fermentolysate, also gained weight from the 1st to the 12th day and from the 15th to the 26th day.

By the end of the experiment, the weight gain in the ovariectomized rats treated with distilled water, glucosamine + chondroitin, and the collagen fermentolysate drink was 16.0, 12.5, and 14.3%, respectively. The weight gain in the intact group was 5.3% (Fig. 4). Our data were consistent with the results of other studies [23]. Our findings were associated with a deficiency of estrogen that decreases the secretion of leptin (a hormone with anorexigenic effect) from adipose tissue, thus leading to hyperphagia.

Blood analysis showed a 29.6–60.5% increase in leukocytes in the ovariectomized animals, compared to the intact group. However, statistical significance was only registered in the group that received distilled water. A statistically significant ($P < 0.05$) increase of

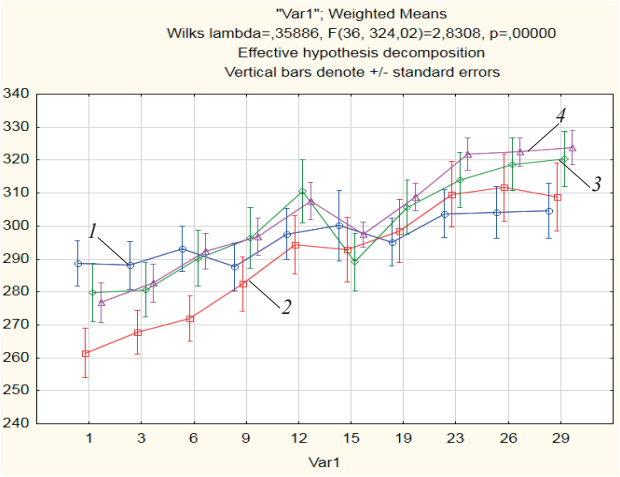

1 – rats on the standard diet (intact), *2* – rats on distilled water (control), *3* – rats on glucosamine + chondroitin (experiment 1), *4* – rats on the collagen fermentolysate drink (experiment 2)

Figure 4 Weight changes in animals throughout the experiment

46.5% in lymphocytes was observed in the rats treated with glucosamine + chondroitin (reference sample), compared to the intact animals. All the ovariectomized animals had an increased content of granulocytes (up to 86.4%), compared to the intact group, although we found significant variation between the experimental rats within the group. Yet, the increased concentrations of lymphocytes and granulocytes did not significantly affect their relative content.

The control rats treated with distilled water had a statistically insignificant increase in monocytes of 27.8% in relation to the intact group. This growth was more pronounced in both experimental groups (1 and 2), averaging 2.3 times ($P < 0.05$) in absolute terms and up to 47.8% ($P < 0.05$) in relative terms (Table 5).

The cytometric analysis showed that both supplements to the diet (glucosamine + chondroitin and the functional drink) contributed to increased contents of leukocytes, granulocytes, lymphocytes, and monocytes, although to a different extent. This meant that they activated the blood immunity.

According to the biochemical blood analysis (Table 6), the control rats had a significant increase, compared to the intact rats, in alkaline phosphatase, phosphorus, and calcium by 36.0, 2.8, and 15.6%, respectively. They also had a significant decrease in magnesium by 15.3%. We know that increased concentrations of these parameters in the blood are among the diagnostic criteria for osteoporosis. However, the supplements of glucosamine + chondroitin and

Table 5 Cytometric blood analysis at the end of the experiment

Parameter	Standard diet (intact)	Supplements to the diet		
		Distilled water (control)	glucosamine + chondroitin (experiment 1)	drink based on collagen fermentolisate (experiment 2)
Lymphocytes, 10^9/L	4.82 ± 1.47	5.48 ± 1.89	7.06 ± 1.47*	7.09 ± 2.73
Leukocytes, 10^9/L	6.68 ± 2.14	8.66 ± 3.56	10.72 ± 2.95*	10.25 ± 4.14
Mixture of monocytes, eosinophils, basophils and immature cells, 10^9/L	0.46 ± 0.22	0.75 ± 0.35	1.04 ± 0.45*	1.01 ± 0.46*
Monocytes, %	6.68 ± 1.20	8.54 ± 1.15	9.34 ± 1.89*	9.89 ± 2.22*
Granulocytes, 10^9/L	1.40 ± 0.59	2.43 ± 2.15	2.61 ± 1.54	2.15 ± 1.22
Lymphocytes, %	72.50 ± 5.23	64.93 ± 11.88	67.85 ± 11.03	69.93 ± 6.78
Relative content of granulocytes, %	20.82 ± 4.73	26.53 ± 11.83	22.81 ± 9.68	20.17 ± 5.97

* – significant difference from the intact group ($P < 0.05$); ** – significant difference from the control group ($P < 0.05$); + – significant difference between the experimental groups ($P < 0.05$)

Table 6 Biochemical analysis of blood serum at the end of the experiment

Parameter		Standard diet (intact)	Supplements to the diet		
			Distilled water (control)	Glucosamine + chondroitin (experiment 1)	Drink based on collagen fermento-lisate (experiment 2)
Proteins	Total protein, g/L	76.50 ± 1.26	76.68 ± 2.62	80.52 ± 5.88	78.65 ± 4.70
	Albumin, g/L	42.18 ± 1.34	42.16 ± 1.91	42.11 ± 2.15	41.95 ± 1.03
Low-molecular-weight nitrogen-containing substances	Creatinine, μmol/L	65.09 ± 4.45	60.41 ± 3.55	60.13 ± 4.68	60.14 ± 2.99
	Urea, mmol/L	8.62 ± 1.60	9.65 ± 1.36	8.80 ± 1.16	8.89 ± 1.52
Pigments	Bilirubin (total), μmol/L	3.02 ± 0.42	2.63 ± 0.54	2.98 ± 0.45	2.77 ± 0.49
	Bilirubin (direct), μmol/L	2.12 ± 0.27	2.22 ± 0.45	2.18 ± 0.36	2.08 ± 0.31
Enzymes	ASAT, U/L	90.63 ± 9.70	95.80 ± 18.74	86.77 ± 9.79	94.86 ± 15.77
	ALAT, U/L	51.06 ± 16.58	48.11 ± 9.19	45.25 ± 6.54	44.48 ± 8.71
	Alkaline phosphatase, U/L	218.0 ± 41.0	339.2 ± 43.4*	194.9 ± 62.4**	208.4 ± 31.5**
	GGT, U/L	3.53 ± 1.30	3.55 ± 0.81	3.51 ± 0.88	3.15 ± 0.56
	LDH, U/L	189.8 ± 114.3	180.2 ± 87.8	186.7 ± 49.9	191.6 ± 85.0
Lipids	Cholesterol, mmol/L	2.18 ± 0.23	2.43 ± 0.58	2.73 ± 0.43*	2.60 ± 0.70
	Triglycerides, mmol/L	1.73 ± 1.23	1.45 ± 0.82	1.71 ± 1.21	1.22 ± 0.37
Carbohydrates	Glucose, mmol/L	11.33 ± 3.81	9.13 ± 2.32	8.66 ± 0.66	8.65 ± 1.61
Inorganic compounds	Calcium, mmol/L	2.82 ± 0.17	3.34 ± 0.19*	2.87 ± 0.17	2.85 ± 0.17
	Magnesium, mmol/L	1.18 ± 0.08	1.00 ± 0.05*	1.02 ± 0.08	1.11 ± 0.10**
	Phosphorus, mmol/L	2.85 ± 0.22	2.93 ± 0.24*	2.90 ± 0.29	2.86 ± 0.32

* – significant difference from the intact group ($P < 0.05$); ** – significant difference from the control group ($P < 0.05$); + – significant difference between the experimental groups ($P < 0.05$)

Table 7 Osteocalcin concentrations in the blood serum of experimental rats

Parameter	Standard diet (intact)	Supplements to the diet		
		Distilled water (control)	Glucosamine + chondroitin (experiment 1)	Drink based on collagen fermentolisate (experiment 2)
Osteocalcin, ng/mL	2.812 ± 0.569	2.618 ± 0.441	2.761 ± 0.522	3.049 ± 0.585

Table 8 Bone mineral metabolism in rats

Parameter	Standard diet (intact)	Supplements to the diet		
		Distilled water (control)	Glucosamine + chondroitin (experiment 1)	Drink based on collagen fermentolisate (experiment 2)
Calcium, mg%	15.3 ± 3.5	10.5 ± 2.6	14.0 ± 3.5	13.7 ± 3.4
Phosphorus, mg%	5.70 ± 0.45	7.30 ± 0.58*	6.80 ± 0.54	5.60 ± 0.44
Magnesium, mg%	7.80 ± 1.56	6.30 ± 1.26	6.80 ± 1.36	6.5 ± 1.3
Ca:P ratio	2.5:1.0	1.5:1.0	2.0:1.0	2.4:1.0

* – significant difference from the intact group ($P < 0.05$); ** – significant difference from the control group ($P < 0.05$); + – significant difference between the experimental groups ($P < 0.05$)

the functional drink decreased the activity of alkaline phosphatase to the intact level. This parameter in the experimental groups was 35.5% ($P < 0.05$) and 31.0% ($P < 0.05$) lower than in the control group. It might indicate a compensatory activation of the collagen-synthetic function of osteoblastic cells in response to increased activity of osteoclasts.

The results of the biochemical analysis were confirmed by the determination of osteocalcin.

Osteocalcin is the main non-collagenous protein of the bone matrix that is synthesized by osteoblasts. Its concentration in the blood reflects the metabolic activity of osteoblasts in bone tissue, since blood osteocalcin is synthesized, rather than released during bone resorption [24].

There were no statistically significant changes in osteocalcin concentrations between the groups (Table 7). However, we found its increase of 15.0% (statistically insignificant) in experimental group 2, which received the functional product based on collagen fermentolysate, compared to the control.

The contents of calcium, phosphorus, and magnesium in the bone tissue of the animals under study are shown in Table 8. As we can see, the control group of ovariectomized rats had decreased contents of calcium and magnesium (by 32.0 and 19.3%, respectively), compared to the intact group. They also had a significant increase in phosphorus levels (by 22.0%).

The experimental rats that received the functional drink had increased amounts of calcium and magnesium (by 25 and 3.0%, respectively), compared to the control group. Although we also found a 7.0% decrease in phosphorus, it was not statistically significant. The ratio between calcium and phosphorus in experimental group 2 was restored to 2.4:1.0 (2.5:1.0 in the intact group).

According to our daily examinations, the general condition of all the animals was satisfactory in terms of appearance, coat quality, and behavior. The experimental animals looked identical to the control group. Their coat was thick, tight, and glossy, with no signs of fur loss. They were physically strong and had no discharge from their natural orifices. Their limbs, motor functions, and behavioral reactions were normal. Their teeth were white, without plaque but with signs of abrasion. Their mucous membranes were pale, shiny, and smooth. The results of necropsy and macroscopic examination did not reveal any hypofunction or displacement in internal organs (lungs, liver, spleen, stomach, kidneys, and pancreas). Their pulmonary pleurae, as well as pericardial and abdominal layers, were thin, shiny, and smooth. The hearts and aortas were unchanged, and the vessels were moderately injected.

Some animals in the control and experimental groups had an enlarged uterus and mucus in the fallopian tubes. This might be associated with the involutional processes in their reproductive organs after surgery.

We weighed the animals' internal organs and determined their percentage in relation to the body weight. The results revealed no significant differences from the physiological norms for the animals of this species and age group.

CONCLUSION

We examined the quality characteristics of dried collagen fermentolysate obtained from low-value by-products of the meat industry (pork legs and ears, 1:1). Collagen fermentolysate contained 41% of peptide fractions with a molecular weight of 10 to 20 kDa. It also had high contents of glutamic acid, aspartic acid, glycine, alanine, proline, leucine, and threonine. These amino acids stimulate cartilage and bone cells, restore joint tissue, and are responsible for the production of collagen, elastin, and muscle tissue.

We developed a technology for a functional product to prevent osteoporosis. Based on collagen fermentolysate, the formulation contained pumpkin powder, dietary fiber, calcium, chondroprotectors, and vitamins E, C, and D_3. The 80:20 ratio between protein hydrolysate and pumpkin powder and the contents of calcium and vitamin D_3 meeting 15 and 30% of the daily intake, respectively, ensured a high nutritional value, functional effects, and good sensory characteristics of the product. The product is a powdered drink designed to mix with water. The microbiological and toxicological analyses confirmed that the product complied with the requirements of TR CU 021/2011.

The experiments on laboratory animals showed that the formulated product had an osteoprotective effect on the ovariectomized female rats. We found that those rats which received the functional product had increased contents of calcium and magnesium in the bone tissue (by 25.0 and 3.0%, respectively) and a decreased content of phosphorus (by 7.0%), compared to the control group. In addition, their calcium to phosphorus ratio was restored to 2.4:1.0 and the concentration of osteocalcin in the blood serum increased by 15%.

Our study makes a theoretical contribution to the concept of safe bone homeostasis correction and proves that a functional drink based on connective tissue protein can be used to prevent postmenopausal osteoporosis associated with hypoestrogenism.

CONTRIBUTION

All the authors were equally involved in, and therefore are equally responsible for, developing the study concept, collecting and analyzing data, writing and editing the manuscript, and approving its final version.

CONFLICTS OF INTEREST

The authors declare that there is no conflict of interest.

REFERENCES

1. Pisani P, Renna MD, Conversano F, Casciaro E, Di Paola M, Quarta E, et al. Major osteoporotic fragility fractures: Risk factor updates and societal impact. World Journal of Orthopedics. 2016;7(3):171–181. https://doi.org/10.5312/wjo.v7.i3.171.
2. Srinivasan V, Martens MG. Hormone therapy in menopausal women with fibroids: is it safe? Menopause. 2018;25(8):930–936. https://doi.org/10.1097/gme.0000000000001105.
3. Muhammad A, Mada SB, Malami I, Forcados GE, Erukainure OL, Sani H, et al. Postmenopausal osteoporosis and breast cancer: The biochemical links and beneficial effects of functional foods. Biomedicine and Pharmacotherapy. 2018;107:571–582. https://doi.org/10.1016/j.biopha.2018.08.018.
4. Rajput R, Wairkar S, Gaud R. Nutraceuticals for better management of osteoporosis: An overview. Journal of Functional Foods. 2018;47:480–490. https://doi.org/10.1016/j.jff.2018.06.013.
5. Pinkerton JV, Aguirre FS, Blake J, Cosman F, Hodis H, Hoffstetter S, et al. The 2017 hormone therapy position statement of the North American Menopause Society. Menopause. 2017;24(7):728–753. https://doi.org/10.1097/gme.0000000000000921.
6. Belyaev NG, Timchenko LD, Rzhepakovsky IV, Piskov SI, Lodygin AD, Gaponov VI, et al. Osteoprotective effect of bread enriched with protein, dietary fiber, calcium, iron and iodine in hypoestrogen-induced osteoporosis among rats. Problems of Nutrition. 2020;89(6):58–69. (In Russ.). https://doi.org/10.24411/0042-8833-2020-10079.
7. Liu J, Liu J, Liu L, Zhang G, Zhou A, Peng X. The gut microbiota alteration and the key bacteria in *Astragalus* polysaccharides (APS)-improved osteoporosis. Food Research International. 2020;138. https://doi.org/10.1016/j.foodres.2020.109811.
8. Honvo G, Lengelé L, Charles A, Reginster J-Y, Bruyère O. Role of collagen derivatives in osteoarthritis and cartilage repair: A systematic scoping review with evidence mapping. Rheumatology and Therapy. 2020;7:703–740. https://doi.org/10.1007/s40744-020-00240-5.
9. Kakimov A, Suychinov A, Mayorov A, Yessimbekov Z, Okuskhanova E, Kuderinova N, et al. Meat-bone paste as an ingredient for meat batter, effect on physicochemical properties and amino acid composition. Pakistan Journal of Nutrition. 2017;16(10):797–804. https://doi.org/10.3923/pjn.2017.797.804.
10. Nasri M. Protein hydrolysates and biopeptides: Production, biological activity, and application in food and health benefits. A review. Advances in Food and Nutrition Research. 2018;81:109–159. https://doi.org/10.1016/bs.afnr.2016.10.003.
11. Kiewiet MBG, Faas MM, de Vos P. Immunomodulatory protein hydrolysates and their application. Nutrients. 2018;10(7). https://doi.org/10.3390/nu10070904.
12. López-Pedrouso M, Borrajo P, Pateiro M, Lorenzo JM, Franco D. Antioxidant activity and peptidomic analysis of porcine liver hydrolysates using alcalase, bromelain, flavourzyme and papain enzymes. Food Research International. 2020;137. https://doi.org/10.1016/j.foodres.2020.109389.

13. Inoue N, Sugihara F, Wang X. Ingestion of bioactive collagen hydrolysates enhance facial skin moisture and elasticity and reduce facial ageing signs in a randomised double-blind placebo-controlled clinical study. Journal of the Science of Food and Agriculture. 2016;96(12):4077–4081. https://doi.org/10.1002/jsfa.7606.
14. Shi P, Liu M, Fan F, Chen H, Yu C, Lu W, et al. Identification and mechanism of peptides with activity promoting osteoblast proliferation from bovine lactoferrin. Food Bioscience. 2018;22:19–25. https://doi.org/10.1016/j.fbio.2017.12.011.
15. Hong H, Fan H, Chalamaiah M, Wu J. Preparation of low-molecular-weight, collagen hydrolysates (peptides): Current progress, challenges, and future perspectives. Food Chemistry. 2019;301. https://doi.org/10.1016/j.foodchem.2019.125222.
16. Yunusov EhSh, Ponomarev VYa, Morozova SA, Ezhkova GO. Izuchenie gidroliza kollagensoderzhashchego syr′ya proteoliticheskimi fermentami [A study of hydrolysis of collagen-containing materials with proteolytic enzymes]. Bulletin of the Technological University. 2016;19(24):168–170. (In Russ.).
17. Aslanova MA, Dydykin AS, Soldatova NE. Preparation of protein hydrolyzate from raw materials of animal origin for the enrichment of products. Food Industry. 2018;(2):16–18. (In Russ.).
18. Chernukha IM, Kotenkova EA, Vasilevskaya ER, Ivankin AN, Lisitsyn AB, Fedulova LV. The study of biological effects of different geographical origin goji berries in rats with alimentary hypercholesterolemia. Problems of Nutrition. 2020;89(1):37–45. (In Russ.). https://doi.org/10.24411/0042-8833-2020-10004.
19. Nikolaeva TI, Shekhovtsov PV. Hydrolysates of collagen concerning prevention and healing joint diseases. Fundamental research. 2014;(12–3):524–528. (In Russ.).
20. Marchenkova LA, Fesyun AD, Gerasimenko MYu, Makarova EV. The effect of administration of dietary supplement with calcium and vitamins D_3 and B_6 on calcium homeostasis and falls incidence in patients with high fracture risk undergoing medical rehabilitation. Problems of Nutrition. 2020;89(5):89–100. (In Russ.). https://doi.org/10.24411/0042-8833-2020-10069.
21. Heaney RP, Bone as the calcium nutrient reserve. In: Weaver CM, Heaney RP, editors. Calcium in human health. Totowa, New Jersey: Humana Press; 2006. pp. 7–12. https://doi.org/10.1007/978-1-59259-961-5_2.
22. Scholz-Ahrens KE, Schaafsma G, Van den Heuvel EGHM, Schrezenmeir J. Effects of prebiotics on mineral metabolism. The American Journal of Clinical Nutrition. 2001;73(2):459S–464S. https://doi.org/10.1093/ajcn/73.2.459s.
23. Puzikov AM. Osteoporosis correction in experiment. Experimental and Clinical Gastroenterology Journal. 2014;102(2):25–31. (In Russ.).
24. Klimova ZhA, Zaft AA, Zaft VB. Modern laboratory diagnosis of osteoporosis. International Journal of Endocrinology. 2014;63(7):75–84. (In Russ.).

ORCID IDs
Marietta A. Aslanova https://orcid.org/0000-0003-2831-4864
Anastasia A. Semenova https://orcid.org/0000-0002-4372-6448
Olga K. Derevitskaya https://orcid.org/0000-0003-1785-7994

Foods and Raw Materials, 2021, vol. 9, no. 2

E-ISSN 2310-9599
ISSN 2308-4057

Research Article
Open Access

https://doi.org/10.21603/2308-4057-2021-2-364-370
Available online at http://jfrm.ru/en

Gliadin proteins from wheat flour: the optimal determination conditions by ELISA

Željka Marjanović-Balaban[1], Vesna Gojković Cvjetković[2,*], Radoslav Grujić[3]

[1] University of Banja Luka, Banja Luka, Bosnia and Herzegovina

[2] University of East Sarajevo, East Sarajevo, Bosnia and Herzegovina

[3] State High School of Medical Science, Prijedor, Bosnia and Herzegovina

* e-mail: vesna.gojkovic@yahoo.com

Received June 13, 2021; Accepted in revised form July 08, 2021; Published online October 15, 2021

Abstract:
Introduction. The number of people with celiac disease is rapidly increasing. Gluten, is one of the most common food allergens, consists of two fractions: gliadins and glutenins. The research objective was to determine the optimal conditions for estimating gliadins by using enzyme-linked immunosorbent assay (ELISA).
Study objects and methods. The experiment involved wheat flour samples (0.10, 0.20, 0.25, 0.50, and 1.0 g) suspended in different solvents (ethanol, methanol, 1-propanol, and isopropanol) of different concentrations (40, 50, 60, 70, 80, and 90% v/v). The samples were diluted with Tris buffer in ratios of 1:50, 1:100, 1:150, and 1:200. The gliadin test was performed using a Gliadin/Gluten Biotech commercial ELISA kit (Immunolab).
Results and discussion. The optimal conditions for determining gliadin proteins that provided the highest gliadin concentration were: solvent – 70% v/v ethanol, extract:Tris buffer ratio – 1:50, and sample weight – 1.0 g.
Conclusion. The obtained results can be of great importance to determine gliadin/gluten concentrations in food products by rapid analysis methods.

Keywords: Extraction, gluten, gliadins, wheat flour, enzyme-linked immunosorbent assay (ELISA)

Please cite this article in press as: Marjanović-Balaban Ž, Gojković Cvjetković V, Grujić R. Gliadin proteins from wheat flour: the optimal determination conditions by ELISA. Foods and Raw Materials. 2021;9(2):364–370. https://doi.org/10.21603/2308-4057-2021-2-364-370.

INTRODUCTION

Gluten is the one of the most common food allergens. According to the Codex Alimentarius, gluten is defined as a protein fraction of wheat, rye, barley, oats, their cross varieties, and derivatives, which some people are sensitive to [1, 2]. Gliadins and glutenins are two fractions present in approximately equal amounts in gluten [3].

Gliadins are respresented by monomers. Due to the high content of glutamine and proline, these proteins are also called "prolamins" [4, 5]. They are not soluble in water as a result of strong hydrophobic interactions and the presence of disulfide bonds, only in aqueous alcohol [6, 7].

Gliadin proteins are divided into four groups (α, β, γ, and ω gliadins) on the basis of mobility in acidic conditions of acid polyacrylamide gel electrophoresis (A-PAGE). Some recent research on amino acid sequences refer α and β gliadins to the same group (α/β) [8, 9]. By amino acid sequences (complete and partial), amino acid composition, and molecular weight, gliadins are divided into: ω5, ω1,2, $\alpha+\beta$, and γ gliadins [10, 11]. As for ω gliadins, they have a high content of glutamine, proline, and phenylalanine. They are divided into ω5 (≈ 50 000 Da) and ω1.2 gliadins (≈ 40 000 Da).

In $\alpha+\beta$ and γ gliadins, the content of glutamine and proline is much lower than in ω gliadins. The molecular weights of these fractions overlap (≈ 28 000–35 000 Da). They differ in the content of several amino acids (tyrosine). Both fractions contain the N- and C-terminal regions [12, 13].

Although the content of total gliadin proteins depends on the type of wheat and growth conditions (soil, climate, fertilization, etc.), $\alpha+\beta$ and γ gliadins are the largest components, while ω gliadins are present in smaller amounts [14, 15].

Table 1 Absorption of gliadin standard solutions at 450 nm

Concentration of gliadin standard solutions, ppm	0	2	6	20	60
Absorbance (450 nm)	0.208 ± 0.02	0.365 ± 0.04	0.598 ± 0.01	1.421 ± 0.08	2.588 ± 0.17

Gluten is a common concern for people around the world, especially in the United States, where nearly one-third of the population have to reduce the intake of this protein. Numerous studies have been conducted on the adverse reactions of gluten and its impact on the health of certain population groups [16–18].

Considering that the number of people with gluten intolerance has been increasing in the last decade, the research objective was to examine the optimal conditions for determining the concentration of gliadin by a rapid enzyme-linked immunosorbent assay method (ELISA).

STUDY OBJECTS AND METHODS

The research featured wheat flour type 500 samples with maximal ash content – 0.55%, maximal moisture – 15%, maximal acidity – 3, and protein content – 9.8 g/100 g. The samples were purchased on the market of the Republic of Srpska, Bosnia and Herzegovina.

The gliadin test involved the following chemicals: ethanol (Refined REAHEM, 96% v/v ethyl alcohol, Srbobran), methanol (Lach-Ner, Czech Republic, high purity, ≥ 99.99%), 1-propanol Lach-Ner, Czech Republic, high purity, ≥ 99.00%), and isopropanol (Lach-Ner, Czech Republic, high purity, 99.90%). The deionized water was obtained in laboratory conditions using a Water Technologies device W3T199551 (Siemens Ultra Clear) at a conductivity of 0.055 mS/cm and temperature of 20°C.

The commercial kit (Immunolab, GmbH, Gliadin/Gluten ELISA, D-Kassel, Germany) contained the following chemicals: a series of gliadin standard solutions (concentrations 0, 2, 6, 20, and 60 ppm), a conjugate (anti-gliadin peroxidase), a substrate (tetramethylbenzidine, TMB), a stop solution (0.5 M H_2SO_4), a buffer (Tris), and a wash solution (PBS + Tween 20), plus 96 wells. According to the manufacturer's instructions, the putty is to be stored in the refrigerator at 2–8°C.

Sample preparation. The wheat flour samples (1.0, 0.5, 0.25, 0.20, 0.10 g ± 0.0001 g) were suspended in 10.0 ml of solvent (ethanol, methanol, isopropanol, and 1-propanol) of different concentrations (40, 50, 60, 70, 80, and 90% v/v). The samples were homogenized with an Ultra-Turrax homogenizer (IKA T25 digital, 10 000 rpm) for 5 min. The samples were then centrifuged (Hettich zentrifugen, rotina 380 R) at 2000 rpm for 10 min. After centrifugation, the supernatant was drained and diluted in a ratio of 1:50 with 10x concentrated Tris buffer, which had been diluted before use.

Determination gliadin proteins by ELISA. The samples and 100 µL of gliadin standard solution (concentrations 0, 2, 6, 20, and 60 ppm) were pipetted into wells, followed by incubation for 20 min at room temperature. The rinsing solution was concentrated (10x) and diluted 1:9 with distilled water. The wells were rinsed with 300 µL of the rinsing solution by adding it into the wells; the procedure was repeated three times. After washing, 100 µL of the conjugate (anti-gliadin peroxidase) was pipetted into the wells and incubated for 20 min. Then, the washing procedure was repeated, and 100 µL of the substrate was put into the wells. To react, they were left in a dark place for 20 min at 20°C until the content of the well turned blue. Upon adding 100 µL of the stop solution (0.5 M H_2SO_4), the blue color turned yellow. After mixing, the absorbance was measured using an ELISA reader (Chromate, Awarenes Technology) at 450 nm. The color was stable after 30 min.

RESULTS AND DISCUSSION

Table 1 shows the absorbance of the gliadin standard solutions at the concentrations of 0, 2, 6, 20, and 60 ppm at a wavelength of 450 nm. The results made it possible to calculate the dependence of the absorbance on the protein solution concentration, as illustrated by the calibration curve (Fig. 1). The correlation coefficient (R^2 = 0.9997) showed a high dependence of the absorbance on the concentration of standard gliadin solutions.

Table 2 shows descriptive indicators of gliadin concentration (ppm) values in extracts obtained from wheat flour samples after extraction with different concentrations of ethanol. During the extraction, which lasted for 20 min, the samples were mixed after every

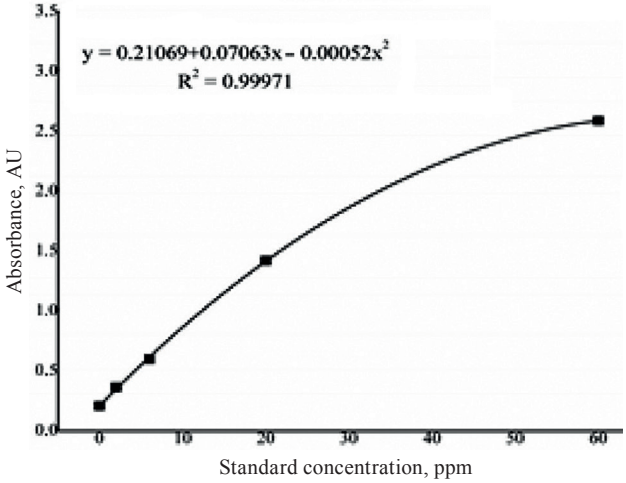

Figure 1 Dependence of absorbance on the concentration of gliadin standard solutions

Table 2 Descriptive indicators of gliadins measured in wheat flour extracts at different solvent concentrations (sample weight 1.0 g ± 0.0001, solvent ethanol)

Ethanol concentration, %	N	Xav	SD	Std. error	95% confidence interval of average		Min	Max
					Lower bound	Upper bound		
40	6	85.42	3.40	1.39	81.86	88.99	78.68	87.61
50	6	88.83	3.33	1.36	85.34	92.32	83.66	93.38
60	6	102.23	2.65	1.08	99.44	105.02	98.71	105.21
70	6	104.15	2.06	0.84	101.99	106.32	100.93	107.21
80	6	75.74	1.63	0.67	74.03	77.45	73.67	78.41
90	6	69.47	3.72	1.52	65.56	73.38	62.92	73.69
ANOVA	F(5.30) = 137.58, Sig. = 0.000, eta square = 5781.29/6033.41 = 0.96							

Table 3 Descriptive indicators of gliadins in wheat flour extracts at different solvent concentrations (sample weight 1.0 g ± 0.0001, solvent methanol)

Methanol concentration, %	N	Xav	SD	Std. error	95% confidence interval of average		Min	Max
					Lower bound	Upper bound		
40	6	83.29	4.85	1.98	78.20	88.38	74.13	88.26
50	6	88.70	2.02	0.83	86.58	90.83	86.65	91.81
60	6	89.51	3.26	1.33	86.09	92.93	83.98	93.41
70	6	95.49	2.69	1.10	92.67	98.31	91.23	99.33
80	6	73.77	2.81	1.15	70.83	76.72	70.52	78.03
90	6	73.81	3.22	1.31	70.43	77.18	69.04	78.33
ANOVA	F(5.30) = 44.48, Sig. = 0.000, eta square = 2360.62/2679.04 = 0.88							

5 min. The obtained extracts were diluted with Tris buffer in a ratio of 1:50.

A descriptive analysis showed that the highest gliadin concentration was obtained after extraction with 70% ethanol (104.15 ppm). Extraction with 90% ethanol demonstrated the lowest gliadin concentration (69.47 ppm). A one-factor analysis of variance of different groups revealed a statistically significant difference in the gliadin concentration at F(5.30) = 137.58 and Sig. = 0.000.

Table 2 shows that the increased solvent concentration between 40 and 70% affected the efficiency of gliadin protein extraction from wheat flour samples: the protein concentration increased. However, a further increase in the solvent concentration (80 and 90%) reduced the extraction efficiency: gliadin protein concentration was lower than in the case of 70% ethanol.

Table 3 illustrates the descriptive indicators of gliadin concentration (ppm) after extraction with methanol of different concentrations.

The highest concentration of gliadins was obtained after extraction with 70% methanol (95.49 ppm), while 80% methanol showed the lowest concentration (73.77 ppm). A one-factor analysis of variance of different groups showed a statistically significant difference in the gliadin concentrations at F(5.30) = 44.48 and Sig. = 0.000 (Table 3).

Under these conditions, the protein extraction was more effective when the methanol concentration was 40–70%, while a further increase in the concentration of methanol (80 and 90%) reduced the extraction efficiency.

Table 4 shows the descriptive indicators of gliadin concentrations (ppm) after extraction with 1-propanol of different concentrations.

Table 4 Descriptive indicators of gliadins in wheat flour extracts at different solvent concentrations (sample weight 1.0 g ± 0.0001, solvent 1-propanol)

1-propanol concentration, %	N	Xav	SD	Std. error	95% confidence interval of average		Min	Max
					Lower bound	Upper bound		
40	6	97.36	1.92	0.78	95.35	99.37	93.59	98.90
50	6	98.40	1.99	0.82	96.30	100.49	95.57	100.98
60	6	101.16	2.01	0.82	99.05	103.27	97.70	103.06
70	6	94.33	1.91	0.78	92.32	96.33	91.19	96.79
80	6	96.40	1.88	0.77	94.43	98.37	93.38	98.70
90	6	84.97	1.75	0.72	83.13	86.81	83.29	88.18
ANOVA	F(5.30) = 51.45, Sig. = 0.000, eta square = 941.55/1051.34 = 0.89							

Table 5 Descriptive indicators of gliadins in wheat flour extracts at different solvent concentrations (sample weight 1.0 g ± 0.0001, solvent isopropanol)

Isopropanol concentration, %	N	Xav	SD	Std. error	95% confidence interval of average		Min	Max
					Lower bound	Upper bound		
40	6	83.65	7.63	3.12	75.64	91.66	73.18	92.36
50	6	92.77	3.80	1.55	88.79	96.75	86.35	97.22
60	6	92.27	3.72	1.52	88.36	96.18	87.31	97.97
70	6	103.35	2.97	1.21	100.23	106.46	98.81	107.23
80	6	93.29	3.69	1.51	89.42	97.17	86.45	97.27
90	6	85.24	3.38	1.38	81.69	88.79	78.80	88.75
ANOVA	F(5.30) = 14.72, Sig. = 0.000, eta square = 1476.98/2079.01 = 0.71							

Table 6 Descriptive indicators of gliadins in wheat flour extracts diluted with different Tris buffer concentrations (sample weight 1.0 g ± 0.0001, solvent 70% ethanol)

Extract:Tris buffer ratio	N	Xav	SD	Std. error	95% confidence interval of average		Min	Max
					Lower bound	Upper bound		
1:50	6	104.15	2.06	0.84	101.99	106.32	100.93	107.21
1:100	6	95.08	0.96	0.39	94.07	96.08	93.29	95.89
1:150	6	89.06	2.88	1.18	86.04	92.09	83.68	91.27
1:200	6	84.35	2.87	1.17	81.33	87.36	79.48	87.88
ANOVA	F(3.20) = 80.62, Sig. = 0.000, eta square = 1314.04/1422.70 = 0.92							

Table 7 Descriptive indicators of gliadins in wheat flour extracts diluted with different Tris buffer concentrations (sample weight 1.0 g ± 0.0001, solvent 70% isopropanol)

Extract:Tris buffer ratio	N	Xav	SD	Std. error	95% confidence interval of average		Min	Max
					Lower bound	Upper bound		
1:50	6	103.35	2.97	1.21	100.23	106.46	98.81	107.23
1:100	6	84.87	1.47	0.60	83.33	86.42	83.69	87.69
1:150	6	74.24	2.23	0.91	71.89	76.58	70.40	76.84
1:200	6	65.95	3.25	1.33	62.53	69.36	61.12	70.30
ANOVA	F(3.20) = 235.73, Sig. = 0.000, eta square = 4691.03/4823.70 = 0.97							

The highest concentration of gliadins was obtained after extraction with 60% 1-propanol (101.16 ppm), while 90% 1-propanol resulted in the lowest concentration (84.97 ppm). A one-factor analysis of variance of different groups revealed a statistically significant difference in the gliadin concentration at F(5.30) = 51.45 and Sig. = 0.000 (Table 4).

A lower solvent concentration of 1-propanol between 40 and 60% increased the efficiency of gliadin protein extraction, while the protein extraction efficiency tended to decrease with a further increase in solvent concentration (70, 80 and 90%), i.e. the concentration decreased.

Table 5 shows the descriptive indicators of gliadin concentrations (ppm) after extraction with isopropanol of different concentrations.

The highest concentration of gliadin was obtained after extraction with 70% isopropanol (103.35 ppm). Extraction with 40% isopropanol showed the lowest concentration of gliadins (83.65 ppm). A one-factor analysis of variance showed a statistically significant difference in gliadin concentrations at F(5.30) = 14.72 and Sig. = 0.000 (Table 5).

A higher solvent concentration of isopropanol for gliadin protein extraction between 40 and 70% increased the extraction efficiency, while further increase in the solvent concentration (80 and 90%) resulted in a lower extraction efficiency, compared to the experiment with 70% isopropanol.

Based on Tables 2–5, the best efficiency of gliadin protein extraction was achieved during the experiments with 70% ethanol and 70% isopropanol as solvents.

Table 6 demonstrates the descriptive indicators of the gliadin concentration (ppm) after extraction with 70% ethanol, followed by dilution of the extract with different Tris buffer concentrations.

The extract:Tris buffer ratios of 1:50 and 1:200 demonatrsted the highest and the lowest concentration of gliadins (104.15 and 84.35 ppm, respectively). A one-factor analysis of variance of different groups showed a statistically significant difference in gliadin concentration at F(3.20) = 80.62 and Sig. = 0.000. An increase in Tris buffer concentration decreased gliadins.

Table 7 shows the descriptive indicators of gliadin concentrations (ppm) in wheat flour extracts obtained after extraction with 70% isopropanol and diluted with different Tris buffer concentrations.

Table 8 Descriptive indicators of gliadins in wheat flour extracts at different sample weights (solvent 70% ethanol, extract:buffer ratio 1:50)

Sample weight, g	N	Xav	SD	Std. error	95% confidence interval of average		Min	Max
					Lower bound	Upper bound		
0.10 ± 0.0001	6	48.41	1.06	0.43	47.30	49.53	46.69	49.73
0.20 ± 0.0001	6	54.67	4.40	1.80	50.05	59.28	51.51	63.30
0.25 ± 0.0001	6	55.80	3.62	1.48	52.01	59.60	52.13	61.72
0.50 ± 0.0001	6	63.94	3.64	1.49	60.12	67.77	60.37	68.91
1.00 ± 0.0001	6	104.15	2.06	0.84	101.99	106.32	100.93	107.21
ANOVA	F(4.25) = 20.85, Sig. = 0.000, eta square = 732.45/966.64 = 0.76							

Table 9 Descriptive indicators of gliadins in wheat flour extracts at different sample weights (solvent 70% isopropanol, extract:buffer ratio 1:50)

Sample weight, g	N	Xav	SD	Std. error	95% confidence interval of average		Min	Max
					Lower Bound	Upper bound		
0.10 ± 0.0001	6	53.59	1.58	0.65	51.93	55.25	51.81	56.14
0.20 ± 0.0001	6	54.96	2.98	1.22	51.84	58.09	52.18	60.33
0.25 ± 0.0001	6	58.77	1.66	0.68	57.02	60.51	56.24	61.12
0.50 ± 0.0001	6	65.58	1.25	0.51	64.27	66.88	64.22	67.79
1.00 ± 0.0001	6	103.35	2.97	1.21	100.23	106.46	98.81	107.23
ANOVA	F(4.25) = 44.05, Sig. = 0.000, eta square = 518.69/597.20 = 0.87							

The highest concentration of gliadins was obtained in the extract diluted with Tris buffer in a ratio of 1:50 (103.35 ppm). The ratio of 1:200 showed the lowest concentration of gliadins (65.95 ppm). A one-factor analysis of variance of different groups demonstrated a statistically significant difference in the concentration of gliadins calculated by the eta square indicator at F(3.20) = 235.73 and Sig. = 0.000 (Table 7). An increase in Tris buffer decreased gliadin protein concentration.

Table 8 shows the descriptive indicators of gliadins (ppm) extracted from wheat flour samples of different weights with 70% ethanol as solvent. The extracts were diluted with Tris buffer in a ratio of 1:50.

The highest and lowest concentration of gliadins was observed in samples with wheat flour weights of 1.00 and 0.10 g (104.15 and 48.41 ppm, respectively). A one-factor analysis of variance of different groups showed a statistically significant difference in gliadin concentration at F(4.25) = 20.85 and Sig. = 0.000 (Table 8).

Table 9 shows descriptive indicators of gliadins (ppm) extracted from wheat flour samples of different weights with 70% isopropanol as solvent. The extracts were diluted with Tris buffer in a ratio of 1:50.

Samples with wheat flour weights of 1.00 and 0.10 g had the highest and the lowest gliadin concentrations (103.35 and 53.59 ppm, respectively). A one-factor analysis of variance of different groups showed a statistically significant difference in gliadin concentration at F(4.25) = 44.05 and Sig. = 0.000 (Table 9). An increase in the weight of the wheat flour increased the gliadin protein concentration value.

Ayob *et al*. developed an enzyme-linked immunosorbent assay (ELISA) in order to determine gliadin proteins in food [19]. They studied three gliadins extracted from wheat flour samples with 70% (v/v) ethanol. The samples were vortexed for 30 min. Prior to the analysis, they were diluted with water in different ratios (1:10, 1:100, 1:1000, and 1:10 000). The highest concentration of gliadin was obtained in the sample diluted 1:10, and the lowest – in the sample diluted 1:10 000.

Allred and Ritter determined the gliadin and glutenin content in flour and in products available on the market, using four commercial ELISA tests [20]. They extracted gliadin with 0.3 M Na-iodide and 7.5% (v/v) 1-propanol. The first test detected gluten in 29 out of 40 analyzed products, the second – in 20 products, the third – in 12 products, and the fourth in 18 products.

Gujral *et al.* determined the gliadin content by ELISA sandwich technique [21]. Gliadins were extracted with 250 mM 2-mercaptoethanol+2M guanidine hydrochloride. The scientists added 7.5 mL of 80% (v/v) ethanol to the solution. Vortex mixing was performed for 30 min. The gliadin content in wheat flour was 7.4 μg/kg.

The results obtained in this work are in conformity with the research by Ayob *et al.*, who also extracted gliadins with 70% (v/v) ethanol and detected the dependance between an increasing dilution and a lowering gliadin concentration [19].

CONCLUSION

To determine the optimal conditions for estimating

gliadin proteins by the ELISA method, we used different solvents (ethanol, methanol, 1-propanol, and isopropanol) at different concentrations (40, 50, 60, 70, 80, and 90%) as well as varied wheat flour weights (0.10, 0.20, 0.25, 0.50 and 1.00 g) and extract:buffer ratios (1:50, 1:100, 1:150, and 1:200).

The experiments demonstrated that 70% ethanol and 70% isopropanol were the optimal solvents, which resulted in the highest gliadin concentrations. However, 70% ethanol had a better financial feasibility. 70% ethanol, a Tris buffer dilution ratio of 1:50, and a wheat flour sample weight of 1.00 g were the optimal conditions that provided the highest concentration of gliadins (104.15 ppm).

Considering the growing number of people with celiac disease, the results obtained can be of great fundamental importance in the study and determination of gliadin/gluten concentrations in food products labeled as gluten or gluten free by ELISA rapid method.

CONTRIBUTION

Ž. Marjanović-Balaban, V. Gojković Cvjetković, R. Grujić conceived, designed, and performed the experiments, analyzed the data, contributed reagents, materials and analytical tools, and wrote the paper.

CONFLICT OF INTEREST

The authors declare no potential conflict of interests regarding the publication of this article.

REFERENCES

1. Standard for foods for special dietary use for persons intolerant to gluten. 2008. 3 p.
2. Scherf KA, Koehler P, Wieser H. Gluten and wheat sensitivities – An overview. Journal of Cereal Science. 2016;67: 2–11. https://doi.org/10.1016/j.jcs.2015.07.008.
3. Shewry P. What is gluten – why is it special? Frontiers in Nutrition. 2019;6. https://doi.org/10.3389/fnut.2019.00101.
4. Shan L, Khosla C. Chemistry and biology of gluten proteins. Immunology, Endocrine and Metabolic Agents in Medicinal Chemistry. 2007;7(3):187–193. https://doi.org/10.2174/187152207780832397.
5. García-Molina MD, Giménez MJ, Sánchez-León S, Barro F. Gluten free wheat: Are we there? Nutrients. 2019;11(3). https://doi.org/10.3390/nu11030487.
6. Delcour JA, Joye IJ, Pareyt B, Wilderjans E, Brijs K, Lagrain B. Wheat gluten functionality as a quality determinant in cereal-based food products. Annual Review of Food Science and Technology. 2012;3(1):469–492. http://doi.org/10.1146/annurev-food-022811-101303.
7. Ortolan F, Steel CJ. Protein characteristics that affect the quality of vital wheat gluten to be used in baking: A review. Comprehensive Reviews in Food Science and Food Safety. 2017;16(3):369–381. https://doi.org/10.1111/1541-4337.12259.
8. Wieser H. Chemistry of gluten proteins. Food Microbiology. 2007;24(2):115–119. https://doi.org/10.1016/j.fm.2006.07.004.
9. Zhang Y, Luo G, Liu D, Wang D, Yang W, Sun J, et al. Genome-, transcriptome- and proteome- wide analyses of the gliadin gene families in *Triticum urartu.* PLoS ONE. 2015;10(7). https://doi.org/10.1371/journal.pone.0131559.
10. Wieser H. Relation between gliadin structure and coeliac toxicity. Acta Paediatrica. 1996;85(412):3–9. https://doi.org/10.1111/j.1651-2227.1996.tb14239.x.
11. Lexhaller B, Colgrave ML, Scherf KA. Characterization and relative quantitation of wheat, rye, and barley gluten protein types by liquid chromatography – tandem mass spectrometry. Frontiers in Plant Science. 2019;10. https://doi.org/10.3389/fpls.2019.01530.
12. Grosch W, Wieser H. Redox reactions in wheat dough as affected by ascorbic acid. Journal of Cereal Science. 1999;29(1):1–16. https://doi.org/10.1006/jcrs.1998.0218.
13. Cebolla Á, Moreno ML, Coto L, Sousa C. Gluten immunogenic peptides as standard for the evaluation of potential harmful prolamin content in food and human specimen. Nutrients. 2018;10(12). https://doi.org/10.3390/nu10121927.
14. Wieser H, Kieffer R. Correlations of the amount of gluten protein types to the technological properties of wheat flours determined on a micro-scale. Journal of Cereal Science. 2001;34(1):19–27. https://doi.org/10.1006/jcrs.2000.0385.
15. Hurkam WJ, Tanaka CK, Vensel WH, Thilmony R, Altenbach S. Comparative proteomic analysis of the effect of temperature and fertilizer on gliadin and glutenin accumulation in the developing endosperm and flour from *Triticum aestivum* L. cv. Butte 86. Proteome Science. 2013;11(1). https://doi.org/10.1186/1477-5956-11-8.
16. Kanny G, Moneret-Vautrin D-A, Flabbee J, Beaudouin E, Morisset M, Thevenin F. Population study of food allergy in France. Journal of Allergy and Clinical Immunology. 2001;108(1):133–140. https://doi.org/10.1067/mai.2001.116427.
17. Zuberbier T, Edenharter G, Worm M, Ehlers I, Reimann S, Hantke T, et al. Prevalence of adverse reactions to food in Germany – a population study. Allergy. 2004;59(3):338–345. https://doi.org/10.1046/j.1398-9995.2003.00403.x.

18. Niland B, Cash BD. Health benefits and adverse effects of a gluten-free diet in non-celiac disease patients. Gastroenterology and Hepatology. 2018;14(2):82–91.
19. Ayob MK, Rittenburg J, Allen JC, Smith CJ. Development of a rapid enzyme-linked immunosorbent assay (ELISA) for gliadin determination in food. Food Hydrocolloids. 1988;2(1):39–49. https://doi.org/10.1016/S0268-005X(88)80036-5.
20. Allred LK, Ritter BW. Recognition of gliadin and glutenin fractions in four commercial gluten assays. Journal of AOAC International. 2010;93(1):190–196. https://doi.org/10.1093/jaoac/93.1.190.
21. Gujral N, Suresh RM, Sunwoo HH. Quantitative double antibody sandwich ELISA for the determination of gliadin. Journal of Immunoassay and Immunochemistry. 2012;33(4):339–351. https://doi.org/10.1080/15321819.2012.655823.

ORCID IDs
Vesna Gojković Cvjetković https://orcid.org/0000-0003-1118-4565

Foods and Raw Materials, 2021, vol. 9, no. 2

E-ISSN 2310-9599
ISSN 2308-4057

Research Article
Open Access

https://doi.org/10.21603/2308-4057-2021-2-371-378
Available online at http://jfrm.ru/en

Sorghum extract: Phytochemical, proximate, and GC-MS analyses

Olayinka O. Ajani[1,*], Taiwo F. Owoeye[1], Kehinde D. Akinlabu[1], Oladotun P. Bolade[2], Oluwatimilehin E. Aribisala[3], Bamidele M. Durodola[1]

[1] Covenant University, Ota, Nigeria

[2] American University of Nigeria, Yola, Nigeria

[3] Olabisi Onabanjo University, Ago-Iwoye, Nigeria

* e-mail: ola.ajani@covenantuniversity.edu.ng

Received July 16, 2021; Accepted in revised form August 06, 2021; Published online October 15, 2021

Abstract:

Introduction. Sorghum is available cereal seeds of African origin belonging to the *Poaceae* family. However, its metabolites and proximate composition have not studied well, which led to the under-utilization of this cereal. This research aimed to investigate the classes of phytochemical and proximate compositions of sorghum extract in order to assess its nutraceutical potential for food chemistry and dietary formulations.

Study objects and methods. We studied the sorghum seed oil extract obtained with the help of a Soxhlet extractor. Sorghum was purchased in Ota, Nigeria. The bioactive compounds were identified by standard methods of phytochemical screening, the nutritional content was investigated with proximate analysis, and the secondary metabolites in the sorghum extract were determined using gas chromatography – mass spectrometry (GC-MS).

Result and discussion. The phytochemical screening showed the presence of steroids, saponins, terpenoids, alkaloids, cardiac glycosides, and quinones in the sorghum extract. The oil yield obtained was 11.00 ± 0.18%. The proximate analysis revealed 5.94% moisture content, 3.05% ash, 0.20% crude fiber, 11.00% fat, 5.54% protein, and 74.27% carbohydrates. The selected physicochemical parameters measured in the sorghum extract included cloud point (0.40°C), specific gravity at 25°C (0.81), and refractive index (1.46). The GC-MS analysis revealed the presence of 9,12-octadecadienoic acid (Z,Z)-, stigmasterol, 8-dodecen-1-ol, acetate, (Z)-, vitamin E, linoleic acid ethyl ester, and 9,12-octadecadienoic acid, methyl ester, which accounted for about 85% in the sorghum composition. Other constituents, presented at lower amounts, included 12-heptadecyn-1-ol, 1H-Imidazole-5-ethanamine, 1-methyl-, and cyclononene.

Conclusion. The findings of this study revealed high nutritive potential of sorghum, which make it a rich source of energy for humans and animals.

Keywords: Sorghum, phytochemicals, nutritional value, chromatography, proximate analysis, bioactive compounds, grain

Please cite this article in press as: Ajani OO, Owoeye TF, Akinlabu KD, Bolade OP, Aribisala OE, Durodola BM. Sorghum extract: Phytochemical, proximate, and GC-MS analyses. Foods and Raw Materials. 2021;9(2):371–378. https://doi.org/10.21603/2308-4057-2021-2-371-378.

INTRODUCTION

Cereals can be defined as classes of grass planted and harvested for food purposes [1]. Different types of cereals are cultivated all over the world and occupy an area of about 60%. They have notable benefits contributing to human health due to nutrients and biologically active substances in their composition [2–4].

In the present study, sorghum was of our interest. Sorghum is also called Jowar in India, Guinea corn in West Africa, and Kaoliang in China. In Nigeria, it is called Oka by the Yorubas, Dawa by the Hausas, and Sorghum by the Igbos. There are also other nomenclatures for sorghum and its role in the food chain is well documented by Sarwar *et al*. [5].

Varoquax *et al*. reported that sorghum is highly resistant towards drought and heat, which allows it to flourish and thrive even under hot and arid environmental conditions [6]. Sorghum is known to be able to boost blood level. This is of tremendous importance to human health. For instance, women who suffer from myoma have anemia due to the excessive blood losses, especially during menstrual period.

Sorghum, with its high nutraceutical value, could help these women [7].

In Africa, where diverse species or cultivars of sorghum are cultivated, this cereal is served as an important food crop. In Nigeria, sorghum is classified into three cultivars depending on the nature and color of their seminal glands and endosperm, namely Guines, Kaura, and Farafara [8]. Nonetheless, small-scale farmers prefer Farafara to Kaura due to the fact that the former is known to have a better storage behaviour and attributes.

Sorghum is classified as a tall grass that often grows to as high as two to eight feet, occasionally being as high as fifteen feet. Generally, a whitish wax coating covers the stalks and leaves of sorghum; while specifically, stalk' piths of some species are juicy and sweet [9, 10]. A well manured sorghum leaf is around 76 cm long and 5 cm wide. Panicle portion of sorghum is responsible for the production of tiny flowers which can be from loose to dense, with clusters containing 800–3000 kernels. The diversity of species is identifiable by the coloration, shape, and size of the seeds, which are smaller than wheat seeds [10].

Statistics in 2016 showed that Nigeria provided 23% of the total sorghum production in African, which made Nigeria the largest producer of sorghum in Africa [11]. Mathur *et al.* documented the emergence of *Sorghum bicolor* as a viable option for producing lignocellulosic biofuel [12]. Vanamala *et al.* reported that sorghum contains bioactive compounds that play a crucial role in its pharmacological potential and immune modulatory properties [13]. Hassan *et al.* studied the effect of ultrasonic waves and microwaves on extraction of the lipid fraction from sorghum. They revealed that these techniques increased the oil yield [14].

Since sorghum seed oil and its defatted extracts are widely used in Africa, the aim of this study was to evaluate the nutraceutical potential, phytochemical components, and secondary metabolites of sorghum from Ota (Nigeria).

STUDY OBJECTS AND METHODS

Sample collection and preparation. Sorghum seeds were purchased from a local market in Ota, Nigeria. The seeds were washed, air-dried, and finally dried in a Thermofisher vacuum oven until constant weight was achieved. The seeds then were finely powdered with a mechanical blender. Prior to extraction, the powdered seeds were protected from sunlight, dust, as well as other particulate matter to avoid oxidation and microbial contamination.

Oil extraction. 200 g of the powdered seeds of sorghum was weighed, carefully wrapped in Whatman filter paper, and mounted up on a Soxhlet extractor. One liter of petroleum ether was transferred into a round bottom flask connected with a thimble with the sample in. When the extraction process completed, the pet-ether solvent was removed with an IKA® RV 10 rotary evaporator, and the sample was stored in a refrigerator.

GC-MS analysis condition. Agilent 7890B GC/5977 MS was utilized for the GC-MS analysis of the extract using the given conditions: column – HP 5 capillary (60 m×0.25 mm×0.25 μm); oven temperature program – the column was held initially at 50°C for 1 min after injection, then ramped to 300°C at 7°C per minute and held for 14 min; injector temperature – 250°C; detector (MS) temperature – 275°C; carrier gas – helium; inlet pressure – 40.65 psi; linear gas velocity – 39 cm/s; column flow rate – 2.7 mL/min; split ratio – 10:1; injection volume – 1 μL. The components were identified by retention time determination on the capillary column as well as by matching mass spectra with the data of the NIST mass spectral library.

Phytochemical tests. *Terpenoids.* 0.30 g of the seed powder was carefully transferred into a 250 mL beaker and extracted with 30 mL of chloroform for 2 h. 2 mL of trichloromethane and 3 mL of concentrated sulphuric acid were added to 5 mL of the extract, thereby forming a layer. Reddish brown color at the interface confirmed the presence of terpenoids [15].

Cardiac glycosides were determined by two methods. According to the Raymond method, 50% C_2H_5OH was gradually added to the extract in a test-tube, followed by 0.10 mL of 1% ethanolic m-dinitrobenzene. The resulting mixture then was titrated with 20% NaOH. Violet coloration confirmed the presence of active methylene group. According to the Killer Killiani method, the extract was solubilized in 1% $FeSO_4$ in 5% glacial acetic acid, followed by the addition of concentrated H_2SO_4. The development of blue coloration indicated the presence of deoxy sugar.

Quinones. Diluted NaOH was added to 1 mL of the sorghum extracted. Blue green or red coloration implied the presence of quinones [16].

Saponins. The extract sample was vigorously mixed with 5 mL of distilled H_2O. The frothing was mixed with few drops of olive oil and shaken vigorously. The appearance of foam demonstrated the presence of saponins.

Steroids. 2 mL of acetic anhydride was introduced into 0.5 mL of the extract, followed by the addition of 2 mL of sulphuric acid. Change in the extract coloration from violet to blue or green indicated the presence of steroids [16].

Tannins. 10 mL of bromine water was introduced into 0.5 g of the extract sample. Decolorization of Br_2/H_2O showed the presence of tannins.

Proximate determination. Proximate analysis was carried out using combination of techniques and methodologies earlier reported. For instance, crude protein and moisture contents were determined using the method by Ajani *et al.*, carbohydrate by Owoeye *et al.*, Molisch's test by Gangwal *et al.*, Biuret test by Suneetha *et al.*, and total ash by Abdulkadir *et al.* [2, 3, 17–19].

RESULTS AND DISCUSSION

Sorghum has been identified and rated as the fifth cereal crop of greatest significance globally [20, 21].

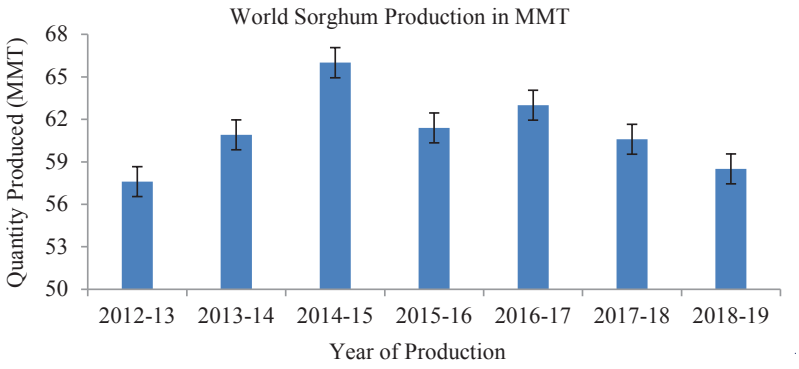

Figure 1 Statistics of world sorghum production from 2012 to 2019 [24]

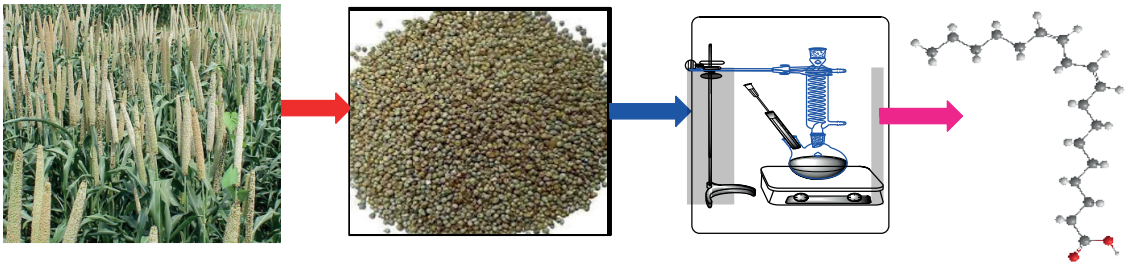

Figure 2 Stages of sorghum processing to identify secondary metabolites

Sorghum is used in food and feed production, in wallboards, fences, biodegradable packing material, as well as for ethanol production [22, 23]. According to the data in [24], before the outbreak of COVID-19, the trend in the world sorghum production from 2012 to 2019 fluctuated between 57 to 59 million tons (Fig. 1). Based on the world sorghum production data, there was a drastic increase in 2015 which was as a result of the increaseв sorghum usage by the Chinese in livestock feed meal. This made them to purchase large volumes of sorghum from the USA.

In our previous works we studied seed oils and their extracts, namely from *Caryota mitis* L., *Adenanthera pavonina*linn L., and sandbox tree (*Hura crepitans* L.) [2, 3, 25]. Continuing our research, this work featured the phytochemical screening, proximate determination, and GC-MS analysis of extract from sorghum from Ota (Nigeria) in order to investigate its nutraceutical potential and add more secondary metabolites to the organic structure database.

Seeds of sorghum were harvested from the plant. It was crushed and mounted on Soxhlet extractor to obtain the oil while the remaining defatted component was herein referred to as the crude extract. The processing stages of the sorghum to identify the secondary metabolites is demonstrated in Fig. 2.

Phytochemical screening. The phytochemical screening of the sorghum extract under study was performed by using standard methods as reported in our previous work [25]. The qualitative phytochemical constituent composition was determined in the sorghum seed oil obtained with the help of two different solvents: petroleum ether and ethanol (Table 1). Saponin availability in the sorghum extracts was established with foam test and Froth test. In the extract obtained with petroleum ether saponins were not detected, while the extract obtained with ethanol contained saponins.

Saponins contain an agent with surface activity due to the sugar units which are very soluble in water. Although, the sapogenin units in saponins have high

Table 1 Phytochemical screening of sorghum extract

Phytochemicals	Type of test	Petroleum ether extract	Ethanol extract
Steroids	Salkowski	–	+
Saponins	Foam test/Froth	–	+
Tannins	Ferric chloride	–	–
Terpenoids	Acidified chloroform	+	+
Alkaloids	Dragendroff	+	–
Cardiac glycosides	Killer Killiani	+	+
Phenol	Ferric chloride	–	–
Oxalates	Acid digestion	–	–
Quinone	Dilute NaOH	+	+

The symbol (–) represents absence, while symbol (+) represents presence

lipophilicity, which make them soluble in fat [26]. DE Bruijn found that a wide variety of leguminous plants contains diverse saponins; for instance, five classes of saponins were reported in soya beans [27]. This explained why the extracts obtained with ethanol had positive saponin test. Saponins play a significant role in the reduction of plasma cholesterol as a result of the effective inhibition of cholesterol absorbing capacity in the intestinal tract of experimentally investigated animals [28].

Cardiac glycosides are present in the both petroleum ether and ethanol extracts. These valuable secondary metabolites are able to enhance myocardial contraction, treating thereby congestive heart failure [29]. Cardiac glycosides also indirectly effect on vascular resistance [30]. Thus, the presence of cardiac glycosides in sorghum could be exploited for their medicinal potential. The presence of cardiac glycosides in the sorghum extracts was detected by Raymond and Killer Killiani tests; the latter effectively transformed 2-deoxy-sugars of cardiac glycoses by distinctive coloration, which made the qualitative and quantitative monitoring easier [29]. Molecules of cardiac glycosides are capable of inhibiting Na^+/K^+- ATPase [31].

Both petroleum ether and ethanol extracts of sorghum contained terpenoids. Terpenoids form a group of compounds, the majority of which occur in the plant kingdom. Simpler mono- and sesquiterpenes are the main constituents of essential oils [32]. Because of their sweet smell, these essential oils are used in perfumery in cosmetic chemistry [33]. Quinone was also present in the tested sorghum extracts. Naturally, quinone plays an important role in transduction and accumulation of energy, which is necessary in such processes as respiration and photosynthesis [34]. Alkaloids were found in the sorghum extracts, while tannins, phenol, and oxalates were not detected in the both ethanol and petroleum ether samples.

Proximate and physico-chemical analyses. The proximate analysis results are presented in Table 2. The importance of oil in human dietary intake cannot be overestimated. Its biological availability and fatty acid profile depends in most cases on environmental, crop, and genetic conditions [35]. The Soxhlet extraction with n-hexane as a solvent revealed the crude fat of the extract of 11.00 ± 0.34%. This was a higher yield than the fat content (9.32%) reported from the distiller dried grain (DDG) sorghum [36].

The ash content in the sorghum extracts under study was 3.05 ± 0.11%, which is in accordance with the results obtained by Mohammed *et al.* who studied nutritional composition of three commonly consumed varieties of sorghum [8]. The ash content may be affected by the nature and amount of ions in the soil from which plants draw nutrients. In our work, the ash content is within acceptable limit (< 5%) [37]. Soil composition has a partial but direct effect on ash content, as the ash content of seeds may partially be a function of the soil composition on which the plants grow [38, 39].

Table 2 Physicochemical and proximate determination of sorghum extract

Parameters	Obtained values
Proximate determination parameters	
Moisture content, %	5.94 ± 0.18
Ash content, %	3.05 ± 0.11
Crude fiber, %	0.20 ± 0.07
Protein, %	5.54 ± 0.15
Crude fat, %	11.00 ± 0.34
Carbohydrates, %	74.27 ± 0.85
Organic matter, %	91.01 ± 0.93
Selected physicochemical parameters	
Refractive index	1.46
Density, g/mL	0.81
Cloudy, °C	0.40

Values are mean ± SD for triplicate measurement

The protein content was determined to be 5.54 ± 0.15%, which was within the range of earlier reported values, namely 4.82 ± 2.39% for white sorghum and 6.06 ± 0.40% for red sorghum. The moisture content of the sorghum tested was 5.94 ± 0.18%, which indicated moderate shelf-life of sorghum [19].

In addition, the investigated sorghum herein had the fiber content of 0.20 ± 0.07%. Dietary fiber is valuable in digestion, hormone production, and cardiovascular health. This also assists in the reduction of low-density lipoprotein cholesterol due to its bile reabsorbed reduction capability in the intestinal tract. Fibers in food prevent excess starch in the body and regulate metabolic conditions such as diabetes and hypercholesterinemia [40].

The carbohydrate content, which generally referred to the readily digested carbohydrates like sugar, starch, as well as organic acids, amounted for 74.27 ± 0.85%. High carbohydrate content supplies energy for the metabolic process, thus stabilizing health status of the consumers [41]. The proximate analysis showed that the studied sorghum extract contained 91.01 ± 0.93% of total organic matter.

The physicochemical parameters of the sorghum extract included its refractive index, density, and cloud point (Table 2). According to the refractive index value, the oil was of a good quality, so it can be used for homogeneous binary mixture formation. In their research, Ospina *et al.* reported that the above mentioned parameters are characteristics for fast and cheap testing of the purity of essential oils [42]. The density of the seed oil of sorghum was 0.81 g/mL, which was lower than that of *C. mitis* (0.93 g/mL) and *A. pavonina* (0.85 g/mL) in our previous works [2, 3]. This also implies that the oil of sorghum was less viscous than that of *A. pavonina* and *C. mitis*.

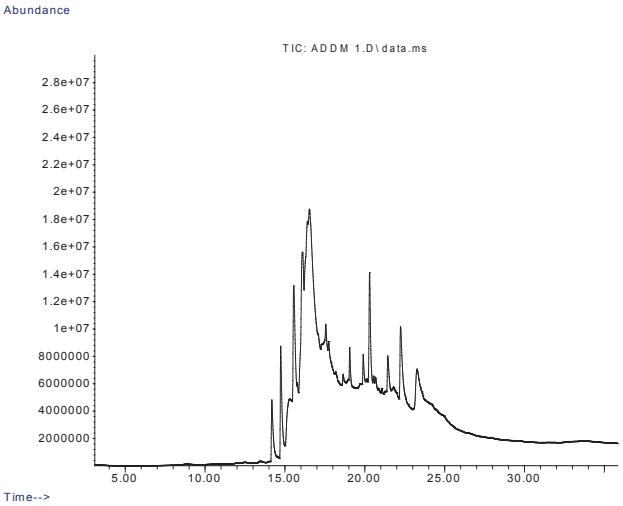

Figure 3 GC-MS chromatogram of sorghum extract

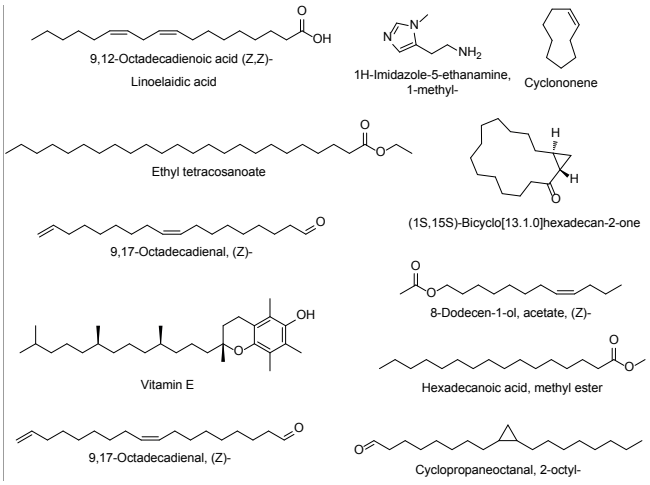

Figure 4 Structural identification of sorghum extract components analyzed chromatographically

GC-MS analysis. Based on the GC-MS analysis, Fig. 3 demonstrates the chromatogram of the sorghum extracts under study. The chromatogram allows us to compare spectra of each composition and the NIST library data. The molecular structures of the identified constituents are shown in Fig. 4, with 9,12-Octadecadienoic acid, methyl ester bring being the predominant fatty acid.

The mass spectrum chromatography assay showed that the major constituents of the sorghum included organic acids, esters, sterols, tocopherols, and fatty aldehyde. Organic acids alone accounted for about 72% of the sorghum composition. Overall, the most abundant compounds are 9,12-Octadecadienoic acid (Z,Z)-, Stigmasterol, 8-Dodecen-1-ol, acetate, (Z)-, vitamin E, Linoleic acid ethyl ester and 9,12-Octadecadienoic acid, and methyl ester, which accounted for about 85% of the sorghum composition.

Among the organic acids, 9,12-Octadecadienoic acid (Z,Z)-, Linoleic acid ethyl ester and hexadecenoic acids were contained in high concentrations. Hexadecanoic acids had three isomers, namely hexadecanoic acid, methyl ester; hexadecanoic acid, ethyl ester; and n-Hexadecanoic acid, making up about 5% of the composition.

9,12-Octadecadienoic acid (Z,Z)-, was the predominant fatty acid. It had two double bonds (C=C), which qualified it as an unsaturated fatty acid. 9,12-Octadecadienoic acid (Z,Z)-, occurs as glycosides in plants, which corroborates the presence of cardiac glycosides in their phyto-constituents. This essential fatty acid is a functional component of human food

Table 3 Identification of sorghum constituents (GC-MS)

Sample №	Retention time	Area Pct	Library (ID)	Molecular formula (molecular weight)
1	12.4708	0.0443	12-Heptadecyn-1-ol	$C_{17}H_{32}O$ (252.44)
2	13.0716	0.0063	1H-Imidazole-5-ethanamine, 1-methyl-	$C_6H_{11}N_3$ (125.17)
3	13.4607	0.0376	Cyclononene	C_9H_{16} (124.22)
4	14.0329	0.018	(1S,15S)-Bicyclo[13.1.0]hexadecan-2-one	$C_{16}H_{28}O$ (236.39)
5	14.1874	0.9545	Hexadecanoic acid, methyl ester	$C_{17}H_{34}O_2$ (270.45)
6	14.7424	1.5527	Hexadecanoic acid, ethyl ester	$C_{18}H_{36}O_2$ (284.48)
7	15.3032	2.3082	n-Hexadecanoic acid	$C_{16}H_{32}O_2$ (256.42)
8	15.5549	4.1409	9,12-Octadecadienoic acid, methyl ester	$C_{19}H_{34}O_2$ (294.47)
9	16.1042	5.17	Linoleic acid ethyl ester	$C_{20}H_{36}O_2$ (308.50)
10	16.5391–31.8454	55.7397	9,12-Octadecadienoic acid (Z,Z)-	$C_{18}H_{32}O_2$ (280.45)
11	19.9093	2.4792	Tetracosanoic acid, methyl ester	$C_{25}H_{50}O_2$ (382.66)
12	20.3042	3.3967	Ethyl tetracosanoate	$C_{26}H_{52}O_2$ (396.69)
13	20.8649 26.4667	3.3824	9,17-Octadecadienal, (Z)-	$C_{20}H_{38}O$ (294.52)
14	22.2496	5.6524	Vitamin E	$C_{29}H_{50}O_2$ (430.71)
15	23.2738	8.2181	Stigmasterol	$C_{17}H_{32}O$ (252.44)
16	24.4526	5.866	8-Dodecen-1-ol, acetate, (Z)-	$C_{14}H_{26}O_2$ (226.36)
17	33.5963	1.0329	Cyclopropaneoctanal, 2-octyl-	$C_{19}H_{36}O$ (280.49)

which takes a part in biosynthesis of prostaglandins and cell membranes. Other polyunsaturated fatty acids have recently been reported to have implication on inflammatory thrombotic condition like COVID-19 [43].

Prominent esters included ethyl tetracosanoate and 8-Dodecen-1-ol, acetate, (Z)-, which accounted for about 9% of the sorghum composition. Sterols (stigmasterol), tocopherols (vitamin E) and fatty aldehyde (9,17-Octadecadienal, (Z)-, linoleate group & Cyclopropaneoctanal, 2-octyl-) were contained in less quantities, accounting for about 8, 6, and 4%, respectively.

CONCLUSION

The sorghum oil extract was analyzed for identification of phytoconstituents, proximate compositions, and physicochemical parameters. It was also characterized spectroscopically for the nature and structures of its secondary metabolites using GC-MS. Proximate determination showed that the sorghum sample contained beneficial amounts of nutrients, while phytochemical screening revealed the presence of bioactive essential phytochemicals.

Thus, sorghum and sorghum-based food could be of high benefit to the population with nutritional deficiencies, for example, to developing countries. This work provided a base for a comparison of nutritional value and therapeutic potential of sorghum extract with other natural food cereal sources. Sorghum requires further research on fortification and functionalization of food with sorghum extract to decrease nutraceutical shortage in the population.

CONTRIBUTION

Olayinka O. Ajani designed the work and wrote the original draft. Taiwo F. Owoeye collected and pretreated the sample, as well as carried out phytochemical screening. Kehinde D. Akinlabu carried out phytochemical screening. Oladotun P. Bolade ran and discussed the GC-MS analysis. Oluwatimilehin E. Aribisala carried out sample pretreatment, Soxhlet extraction, and formal laboratory analysis. Bamidele M. Durodola carried out laboratory testing and editing of the manuscript. All authors read and approved the final manuscript before submission and they are equally responsible for plagiarism.

CONFLICT OF INTEREST

The authors state that there is no conflict of interests related to the publication of this article.

ACKNOWLEDGEMENTS

The authors gratefully acknowledge Covenant University for the support for this work.

REFERENCES

1. McKevith B. Nutritional aspects of cereals. Nutrition Bulletin. 2004;29(2):111–142. https://doi.org/10.1111/j.1467-3010.2004.00418.x.
2. Ajani OO, Owoeye TF, Olasehinde GI, Audu OY, Owolabi FE, Akinlabu DK, et al. Preliminary studies on the seed oil of *Caryota mitis*: Proximate composition, phytochemical screening and evaluation of antimicrobial activity. American Journal of Food Technology. 2016;11(6):253–263. https://doi.org/10.3923/ajft.2016.253.263.
3. Owoeye TF, Ajani OO, Akinlabu DK, Ayanda OI. Proximate composition, structural characterization and phytochemical screening of the seed oil of *Adenanthera pavonina* linn. Rasayan Journal of Chemistry. 2017;10(3):807–814. https://doi.org/10.7324/RJC.2017.1031712.
4. Seal CJ, Brownlee IA. Whole grains and health, evidence from observational and intervention studies. Cereal Chemistry. 2010;87(2):167–174. https://doi.org/10.1094/CCHEM-87-2-0167.
5. Sarwar MH, Sarwar MF, Sarwar M, Qadri NA, Moghal S. The importance of cereals (Poaceae: Gramineae) nutrition in human health: A review. Journal of Cereals and Oilseed. 2013;4(3):32–35. https://doi.org/10.5897/JCO12.023.
6. Varoquax N, Cole B, Gao C, Pierroz G, Baker GR, Patel D, et al. Transcriptomic analysis of field-droughted sorghum from seedling to maturity reveals biotic and metabolic responses. Proceedings of the National Academy of Sciences of the United States of America. 2019;116(52):27124–27132. https://doi.org/10.1073/pnas.1907500116.
7. Oguntola S. Sorghum bicolour, good blood builder for women with fibroid [Internet]. [cited 2021 Apr 27]. Available from: https://tribuneonlineng.com/sorghum-bicolour-good-blood-builder-women-fibroid.
8. Mohammed ZS, Mabudi AH, Murtala Y, Jibrin S, Sulaiman S, Salihu J. Nutritional analysis of three commonly consumed varieties of sorghum (*Sorghum bicolor L.*) in Bauchi State, Nigerian. Journal of Applied Sciences and Environmental Management. 2019;23(7):1329–1334. https://doi.org/10.4314/jasem.v23i7.21.
9. Firdous DH. Health benefits of sorghum, uses and its side effects [Internet]. [cited 2021 Apr 27]. Available from: https://www.lybrate.com/topic/benefits-of-sorghum-and-its-side-effects.
10. Sorghum grain. Encyclopaedia Britannica [Internet]. [cited 2021 Apr 27]. Available from: https://www.britannica.com/plant/sorghum-grain.

11. Ajeigbe HA, Akinseye FM, Ayuba K, Jonah, J. Productivity and water use efficiency of sorghum [*Sorghum bicolor* (L.) Moench] grown under different nitrogen applications in Sudan savanna zone. Nigeria. International Journal of Agronomy. 2018;2018. https://doi.org/10.1155/2018/7676058.
12. Mathur S, Umakanth AV, Tonapi VA, Sharma R, Sharma MK. Sweet sorghum as biofuel feedstock: Recent advances and available resources. Biotechnology for Biofuels. 2017;10(1). https://doi.org/10.1186/s13068-017-0834-9.
13. Vanamala JKP, Massey AR, Pinnamaneni SR, Reddivari L, Reardon KF. Grain and sweet sorghum (*Sorghum bicolor* L. Moench) serves as a novel source of bioactive compounds for human health. Critical Reviews in Food Science and Nutrition. 2018;58(17):2867–2881. https://doi.org/10.1080/10408398.2017.1344186.
14. Hassan S, Imran M, Ahmad N, Khan MK. Lipid characterization of ultrasound and microwave processed germinated sorghum. Lipids in Health and Disease.2017;16(1). https://doi.org/10.1186/s12944-017-0516-4.
15. Ejikeme CM, Ezeonu CS, Eboatu AN. Determination of physical and phytochemical constituents of some tropical timbers indigenous to Niger Delta area of Nigeria. European Scientific Journal. 2014;10(18):247–270.
16. Ramya I, Arunadevi S, Vidhya A. Screening of phytochemicals and testing the antimicrobial activity of different parts of *Erigeon* sp and its essential oil. International Journal of Current Microbiology and Applied Sciences. 2015;4(8):372–378.
17. Gangwal A, Parmar SK, Sheth NR. Triterpenoid, flavonoids and sterols from *Lagenaria siceraria* fruit. Der Pharmacia Lettre. 2010;2(1):307–317.
18. Suneetha V, Mishra B, Gopinath R, Ray SS, Kartik Gaurav KB, Chaubey P, et al. Screening and identification of degradable products by pectin lyase producing Actinomycetes from Katpadi and Chittoor fruit industrial waste enriched soil samples. Asian Journal of Microbiology, Biotechnology and Environmental Sciences. 2012;14(3):405–412.
19. Abdulkadir MN, Amoo IA, Adesina AO. Chemical composition of Hura crepitans seed and antimicrobial activities of its oil. International Journal of Scientific and Research. 2013;2(3):440–445.
20. Cereal production in dryland [Internet]. [cited 2021 Apr 27]. Available from: https://www.fao.org/docrep/012/i0372e/i0372e02.pdf.
21. Adebayo OO, Ibraheem O. The current status of cereals (maize, rice and sorghum) crops cultivation in Africa: Need for integration of advances in transgenic for sustainable crop production. International Journal of Agricultural Policy and Research. 2015;3(3):233–245. https://doi.org/10.15739/IJAPR.035.
22. Iqbal MA, Iqbal A. Overview on sorghum for food, feed, forage and fodder: opportunities and problems in Pakistan's perspectives. American Eurasian Journal of Agriculture and Environmental Sciences. 2015;15(9):1818–1826. https://doi.org/10.5829/idosi.aejaes.2015.15.9.12681.
23. Iqbal A, Sadia B, Khan AI, Awan FS, Kainth RA, Sadaqat HA. Biodiversity in the Sorghum (*Sorghum bicolor* L. Moench) germplasm of Pakistan. Genetics and Molecular Research. 2010;9(2):756–764. https://doi.org/10.4238/vol9-2gmr741.
24. Global trends in sorghum production [Internet]. [cited 2021 Jun 30]. Available from: https://nuseed.com/eu/global-trends-in-sorghum-production/.
25. Ajani OO, Owoeye FT, Owolabi FE, Akinlabu DK, Audu OY. Phytochemical screening and nutraceutical potential of sandbox tree (*Hura crepitans* L.) seed oil. Foods and Raw Materials. 2019;7(1):143–150. https://doi.org/10.21603/2308-4057-2019-1-143-150.
26. Kregiel D, Berlowska J, Witonska I, Antolak H, Proestos C, Babic M, et al. Saponin-based, biological-active surfactants from plants, application and characterization of surfactants. In: Najjar R, editor. Application and characterization of surfactants. IntechOpen; 2017. https://doi.org/10.5772/68062.
27. de Bruijn FJ. Biosynthesis of natural product: introduction. In: de Bruijn FJ, editor. The model legume *Medicago truncatula*. John Wiley and Sons Inc; 2020. p. 207. https://doi.org/10.1002/9781119409144.part4.
28. Liwa AC, Barton EN, Cole WC, Nwokocha CR. Bioactive plant molecules, sources and mechanism of action in the treatment of cardiovascular disease. In: Badal S, Delgoda R, editors. Academic Press; 2017. p. 315–336. https://doi.org/10.1016/B978-0-12-802104-0.00015-9.
29. Morsy N. Cardiac glycosides in medicinal plants. In: El-Shemy H, editor. Aromatic and medicinal plants. Back to nature. IntechOpen; 2017. https://doi.org/10.5772/65963.
30. Ezeonu CS, Ejikeme CM. Qualitative and quantitative determination of phytochemical contents of indigenous Nigerian softwoods. New Journal of Science. 2016;2016. https://doi.org/10.1155/2016/5601327.
31. Cardiac glycosides [Internet]. [cited 2021 Jun 12]. Available from: https://www.amboss.com/us/knowledge/Cardiac_glycosides.
32. Yazaki K, Arimura G-I, Ohnishi T. "Hidden" terpenoids in plants: their biosynthesis, localization and ecological roles. Plant and Cell Physiology. 2017;58(10):1615–1621. https://doi.org/10.1093/pcp/pcx123.

33. Caputi L, Aprea E. Use of terpenoids as natural flavouring compounds in food industry. Recent Patents on Food, Nutrition and Agriculture.2011;3(1):9–16. https://doi.org/10.2174/2212798411103010009.
34. Son EJ, Kim JH, Kim K, Park CB. Quinone and its derivatives for energy harvesting and storage materials. Journal of Material Chemistry A. 2016;4(29):11179–11202. https://doi.org/10.1039/C6TA03123D.
35. Amalfitano C, Golubkina NA, Del Vacchio L, Russo G, Cannoniero M, Somma S, et al. Yield, antioxidant components, oil content, and composition of onion seeds are influenced by planting time and density. Plants. 2019;8(8). https://doi.org/10.3390/plants8080293.
36. Wang L, Weller CL, Hwang KT. Extraction of lipids from grain sorghum DDG. Transactions of the American Society of Agricultural Engineers. 2005;48(5):1883–1888.
37. Chaudhary M, Verma SK. Analysis of the physicochemical properties of the processed fruits and vegetable products. International Journal Pharma and Bio Sciences. 2011;2(4):660–666.
38. Maina CY, Aliyu HM. Extraction and characterisation of Guna oil. International Journal of Food and Agricultural Research. 2009;6:93–100.
39. Umar KJ, Hassan LG, Usman H, Wasagu RSU. Nutritional composition of the seeds of wild melon (*Citrullus ecirrhosus*). Pakistan Journal of Biological Sciences. 2013;16(11):536–540. https://doi.org/10.3923/pjbs.2013.536.540.
40. Bamishaiye EI, Olayemi FF, Awagu EF, Bamishaiye OM. Proximate and phytochemical composition of Moringa oleifera leaves at three stages of maturation. Advance Journal of Food Science and Technology. 2011;3(4):233–237.
41. Bhattacharjee S, Sultana A, Sazzad MH, Islam MA, Ahtashom MM, Asaduzzaman. Analysis of the proximate composition and energy values of two varieties of onion (*Allium cepa* L.) bulbs of different origin: A comparative study. International Journal of Nutrition and Food Science. 2013;2(5):246–253. https://doi.org/10.11648/j.ijnfs.20130205.16.
42. Ospina JD, Tovar CDG, Flores JCM, Orozco MSS. Relationship between refractive index and thymol concentration in essential oils of *Lippia origanoides* Kunth. Chilean Journal of Agricultural and Animal Sciences. 2016;32(2): 127–133. https://doi.org/10.4067/S0719-38902016000200006.
43. Kothapalli KSD, Parka HG, Brenna JT. Polyunsaturated fatty acid biosynthesis pathway and genetics. implications for interindividual variability in prothrombotic, inflammatory conditions such as COVID-19. Prostaglandins, Leukotrienes and Essential Fatty Acids. 2020;162. https://doi.org/10.1016/j.plefa.2020.102183.

ORCID IDs
Olayinka O. Ajani https://orcid.org/0000-0002-3422-3478
Taiwo F. Owoeye https://orcid.org/0000-0002-2055-3919
Kehinde D. Akinlabu https://orcid.org/0000-0001-8580-5868
Oladotun P. Bolade https://orcid.org/0000-0001-9783-8376
Oluwatimilehin E. Aribisala https://orcid.org/0000-0002-6683-5161
Bamidele M. Durodola https://orcid.org/0000-0001-6033-2398

Foods and Raw Materials, 2021, vol. 9, no. 2

E-ISSN 2310-9599
ISSN 2308-4057

Research Article
Open Access

https://doi.org/10.21603/2308-4057-2021-2-379-386
Available online at http://jfrm.ru/en

Cytotoxic effect of *Myrtus communis*, *Aristolochia longa*, and *Calycotome spinosa* on human erythrocyte cells

Leila Gadouche[1,*], Azdinia Zidane[2], Khayra Zerrouki[2], Karima Azouni[2], Saadia Bouinoune[2]

[1] University of Science and Technology Houari Boumediene, Bab Ezzouar, Algeria

[2] Hassiba Benbouali University of Chlef, Chlef, Algeria

* e-mail: gadoucheleila@gmail.com

Received June 21, 2021; Accepted in revised form July 12, 2021; Published online October 15, 2021

Abstract:
Introduction. *Myrtus communis*, *Aristolochia longa*, and *Calycotome spinosa* are medicinal plants frequently used in Algeria. Some plants can cause a fragility of the erythrocyte membrane and lead to hemolysis. Therefore, we aimed to study the cytotoxicity of aqueous extracts from the aerial part of these species against red blood cells.
Study objects and methods. The hemolytic effect was determined spectrophotometrically by incubating an erythrocyte solution with different concentrations of the aqueous extracts (25, 50, 100, and 200 mg/mL) at 37°C during one hour. In addition, we performed phytochemical screening and measured the contents of polyphenols and flavonoids.
Results and discussion. After one hour of incubation of human red blood cells with the aqueous extracts at different concentrations, the hemolysis percentage showed a significant leak of hemoglobin with *A. longa* (68.75 ± 6.11%; 200 mg/mL), the most toxic extract followed by *C. spinosa* (34.86 ± 5.06%; 200 mg/mL). In contrast, *M. communis* showed very low cytotoxicity (20.13 ± 3.11%; 200 mg/mL).
Conclusion. These plants are sources of a wide range of bioactive compounds but their use in traditional medicine must be adapted to avoid any toxic effect.

Keywords: *Myrtus communis*, *Aristolochia longa*, *Calycotome spinosa*, folk medicine, phenolic compounds, alkaloids, hemoglobin, cell toxicity, hemolytic activity

Please cite this article in press as: Gadouche L, Zidane A, Zerrouki K, Azouni K, Bouinoune S. Cytotoxic effect of *Myrtus communis*, *Aristolochia longa*, and *Calycotome spinosa* on human erythrocyte cells. Foods and Raw Materials. 2021;9(2):379–386. https://doi.org/10.21603/2308-4057-2021-2-379-386.

INTRODUCTION

Medicinal plants are an important pool of molecules with therapeutic potential for drug innovation [1]. According to Estella *et al.*, vulgarization of traditional herbal remedies is confronted with many predicaments due to the lack of information on their therapeutic and toxicological properties to guarantee their rational use [2]. According to Calixto [3], plants contain hundreds of phytotherapeutic agents with adverse effects and some of them are very toxic if inappropriately used.

In fact, Kharchoufa *et al.* have identified more than 89 toxic medicinal plants used as treatment in the North-Eastern region of Morocco [4]. These plants contain toxic compounds: alkaloids followed by glucosides, terpenoids, proteins, and phenolics. Their toxicity can lead to serious adverse reactions or interactions with other plants. On the other hand, a misidentification of plants can lead to a toxicity that may also result from an uncontrolled or excessive use [5]. Therefore, before formulating and marketing a herbal medicine, appropriate scientific studies are essential, including those into pharmacological properties, toxicity, and side effects [6].

Algeria has more than 3000 species belonging to several botanical families distributed all along the Mediterranean, Saharan, and tropical regions. *Calycotome spinosa* (L.) belongs to the Fabaceae family, *Aristolochia longa* belongs to the Aristolochiaceae family, and *Myrtus communis* belongs to the *Myrtaceae* family [7]. Algeria is the only country that hosts both species, *M. communis* (L.) in the North and *Myrtus novelli* in the South [8]. For several centuries,

Figure 1 1 – *Myrtus communis*; 2 – *Calycotome spinose*; 3 – *Aristolochia longa*

M. communis has been used in folk medicine as treatment for many diseases due to its broad spectrum of pharmacological and therapeutic effects [9]. Species of *Aristolochia* are known for their toxicity and pose potential health risk associated with their content of aristolochic acids [10].

Since these species are widely used in the littoral zone of Algeria in traditional and folk medicine, there is a need for research into their toxicity. In this context, we aimed to evaluate the hemolytic effect on human erythrocyte cells induced by aqueous extracts of *M. communis* (Rayhan), *A. longa* (Bereztem), and *C. spinosa* (Guendoul). The last two species have been rarely studied.

STUDY OBJECTS AND METHODS

Medicinal plants *Myrtus communis* (L.), *Calycotome spinose* (L.), and *Aristolochia longa* (L.) were collected in many areas in the littoral of Algeria (March 2018), namely Damous (Tipaza), Benni Haoua (Chlef), and Bissa (Chlef) (Fig. 1). These species were identified by Dr. Belhacini, a teacher and researcher at Hassiba Benbouali University of Chlef (Algeria).

Preparation of aqueous extracts. For each species we used dried and powdered plant aerial parts according to traditional use in these areas, namely leaves for *M. communis* and *A. longa* and leaves and flowers for *C. spinosa*. Aqueous extracts were prepared by a decoction of the plant material. In particular, 10 g of the plant material was boiled with 100 mL of distilled water for 15 min and then the solution was filtered and dried at 39°C.

Phytochemical screening. Phytochemical tests were performed on 5% infusion to detect certain secondary metabolites according to Takaidza *et al.* and Behbahani *et al.* [11, 12].

Determination of total phenol contents. A mixture of 250 µL of Folin Ciocalteu phenol reagent, 50 µL of the sample, and 500 µL of 20% Na_2CO_3 was prepared. The volume was adjusted to 5 mL with distilled water while shaking vigorously. After 30 min incubation, absorbance was read at 765 nm. A calibration curve of gallic acid (0–1 mg/mL) was done in parallel. The results were expressed in mg of gallic acid equivalent/g of dry matter (mg EAG/g DM) [13].

Determination of total flavonoid contents. The flavonoid assay was performed according to the method of Hmid *et al.* [14]. 1 mL of each extract was mixed with 1 mL of 2% $AlCl_3$. After 10 min incubation, absorbance was read at 430 nm. The flavonoid concentrations were calculated using a calibration curve established with quercetin (0–40 µg/mL) and expressed in mg of quercetin equivalent/g of dry matter (mg EQ/g DM).

Hemolytic activity determination. A phosphate buffered saline (PBS) solution with pH = 7.4 was prepared by mixing the following compounds in appropriate concentrations: Na_2HPO_4 (10 Mm), KH_2PO_4 (1.8 Mm), KCl (2.7 Mm), and NaCl (137 Mm) [15]. A concentration range for each extract (*M. communis*, *C. spinose*, and *A. longa*) was prepared by diluting in PBS: 25, 50, 100, and 200 mg/mL. An erythrocyte suspension was prepared from the blood of a healthy donor in a heparin tube. After centrifugation at 2400 rpm for 10 min, the plasma was removed and the pellet was washed twice with PBS and then filled up with the same volume of plasma removed. The erythrocyte suspension was diluted 20 times with PBS.

Erythrocyte hemolysis assay. The hemolytic effect test of the species studied was carried out according to the method described by Haddouchi *et al.* and Guo-Xiang and Zai-Qun [16, 17]. We mixed 2950 µL of the erythrocyte suspension with 50 µL of aqueous extract for each species in a hemolysis tube. The operation was repeated three times for each concentration. The tubes were incubated at 37°C for one hour. During this period, 500 µL of each test was taken every 15 min (in 15, 30, 45, and 60 min) and added to 1.5 mL of PBS and then centrifuged again at 2400 rpm for 10 min. The absorbance of the hemoglobin leak in the supernatant was read at 548 nm against a blank containing PBS. A negative control tube was prepared under the same experimental conditions, 2950 µL of the erythrocyte suspension and 50 µL of the PBS buffer solution. On the other hand, a total hemolysis tube was prepared

Table 1 Results of phytochemical screening tests for *Myrtus communis*, *Calycotome spinose*, and *Aristolochia longa*

Samples	Saponoside Test	Tanin Test	Flavonoid Test	Anthocyanin Test	Alkaloid test
 *Myrtus communis* (leaves)	 Foam > 1cm	 Catechin tannins	 Flavonones	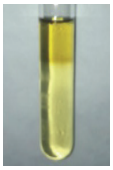 –	 +
 *Calycotome spinose* (leaves and flowers)	 Foam 0.2 cm	 –	 Flavones	 –	 +++
 *Aristolochia longa* (leaves)	 Foam > 1,8 cm	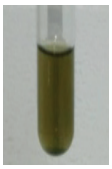 Catechin tannins	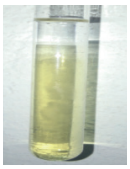 +/–	 +	 –

"+" Present, "++" Moderate presence, "+++" High presence, "+/–" Presence not evident, "–" Absent

containing 250 µL of the erythrocyte suspension and 4750 µL of distilled water. Each test was repeated three times. The hemolysis rate of various extracts was calculated as a percentage (%) of total hemolysis after 15, 30, 45, and 60 min of incubation, according to the following formula:

$$\% \text{ Hemolysis} = A(\text{extract at 60 min}) - A(\text{negative control at 60 min}) / A(\text{Total hemolysis at 60 min}) \quad (1)$$

Statistical analysis. Statistical analysis was done by One Way ANOVA. The data obtained were analyzed using the student's t-test. A P value less than 0.01 was considered statistically significant.

RESULTS AND DISCUSSION

Phytochemical screening. The phytochemical screening allowed us to highlight the presence of some secondary metabolites (saponosides, tannins, alkaloids, flavonoids, and anthocyanins). The phytochemical tests carried out on the infused flowers and leaves of the selected plants are shown in Table 1. The results obtained after shaking the infusion for 15 min showed that *Myrtus communis* and *Aristolochia longa* were rich in saponosides because the foam was greater than 1 cm. In the *Calycotome spinosa* leave and flower infusion, the foam was unstable in the order of a few mm. The appearance of the orange and pink color after the addition of isoamyl alcohol indicated the presence of flavones in the *C. spinosa* leave and flower infusion. The purplish pink color indicated the presence of flavonones in the leaves of *M. communis*. In the *A. longa* infusion, the result was negative. The precipitate in the *C. spinosa* and *M. communis* infusions, which were previously acidified with sulfuric acid, after adding some drops of the Mayer reagent indicated the presence of alkaloids. However, the test was negative for *A. longa*. The appearance of a pink and red coloration after adding ammonia to the HCl-infused *A. longa* and *C. spinosa* indicated the presence of anthocyanins. However, this secondary metabolite was absent in the *M. communis* leave infusion.

Contents of total polyphenols and flavonoids. The amount of polyphenols in the dry matter was expressed in mg gallic acid equivalent (mg EAG/g MS) and determined by the equation: $y = 0.940x + b$; $R^2 = 0.981$. The amount of flavonoids in the dry matter was expressed in mg of quercetin equivalent (mg EQ/g MS) and determined by the equation: $y = 0.055x + b$; $R^2 = 0.996$ (Table 2). The total polyphenol content in the dry matter was 234.89 ± 0.80, 283.68 ± 0.60, and 346.27 ± 2.00 mg GEA/g for *C. spinosa*, *A. longa*, and *M. communis*, respectively. The content of total flavonoids in the dry matter was 10.50 ± 0.03, 34.86 ± 0.06, and 31.02 ± 0.19 mg EQ/g for *A. longa*, *C. spinose*, and *M. communis,* respectively (Table 2).

Hemolytic activity. In the negative control tube (tube containing only PBS and erythrocyte suspension), the hemolysis rate was constant and did not exceed 2.77 ± 0.35% after one hour of incubation. On the

Table 2 Polyphenol and flavonoid content in *Myrtus communis*, *Calycotome spinose*, and *Aristolochia longa*

Species	Polyphenols mg GEA/g DM	Flavonoids mg EQ/g DM
Myrtus communis	346.27 ± 2.00	31.02 ± 0.19
Calycotome spinosa	234.89 ± 0.80	34.86 ± 0.06
Aristolochia longa	283.68 ± 0.60	10.50 ± 0.03

other hand, a total hemolysis of red blood cells was clearly observed in the total hemolysis tube. Indeed, we recorded a hemolysis rate that reached 99.86 ± 10.32% at 60 min.

For the aqueous extract of the *M. communis* leaves, we observed a significantly low hemolysis rate during the first 15 min ($P < 0.01$). The hemolysis rates were 5.07 ± 0.21, 7.85 ± 1.20, and 12.57 ± 2.89% for the concentration of 25 mg/mL; 6.04 ± 1.90 ($P < 0.01$), 6.46 ± 0.77, and 20.42% for 50 mg/mL; 8.05 ± 1.41, 11.32 ± 5.72, and 19.51 ± 6.71 for 100 mg/mL; and 12.01 ± 0.21, 12.22 ± 0.26, and 20.14 ± 3.11% ($P < 0.01$) for 200 mg/mL, respectively, compared to total hemolysis (Fig. 2).

For *C. spinosa*, we found a significant increase in hemolysis rates over time (15, 30, 45, 60 min). Also, the rates were considerably higher with higher concentrations of the extract. For the concentrations of 25 and 50 mg/mL, hemolysis rates ranged between 6.52 ± 3.78 and 17.12 ± 1.50%, as well as 7.50 ± 2.95 and 22.36 ± 2.12%, respectively. However, a significant hemolytic effect was recorded in 100 (45 min) and 200 mg/mL (15, 45, and 60 min) of the *C. spinosa* extract. This rate increased from 8.14 ± 1.23% at 15 min to 23.61 ± 8.94% at 60 min in the presence of a 100 mg/mL concentration and from 24.44 ± 3.95% at 15 min to 34.86 ± 5.05% at 60 min in the presence of a 200 mg/mL concentration (Fig. 3).

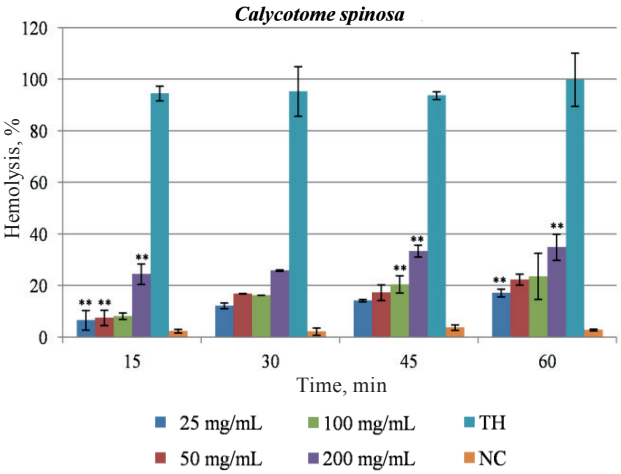

TH: Total Hemolysis. NC: Negative Control.
The means of 3 replicates. $P < 0.01$. ** significant

Figure 3 Hemolytic effect of four concentrations of *Calycotome spinosa* extract at 15, 30, 45, and 60 min

For the extract of the *A. longa* leaves (Fig. 4), we found an increase in hemolysis rates over time (15, 30, 45, and 60 min). As the concentration increased, the percentage of hemolysis increased as well. At concentrations of 25 and 50 mg/mL, a hemolysis percentage ranged from 5 (15 min) to 6.71% (60 min) and from 7.22 (15 min) to 18.47% (60 min), respectively. The hemolysis rate was significant at 15 and 45 min ($P < 0.01$).

On the other hand, we observed an important hemolytic effect of the *A. longa* aqueous extract at concentrations of 100 and 200 mg/mL. This rate went

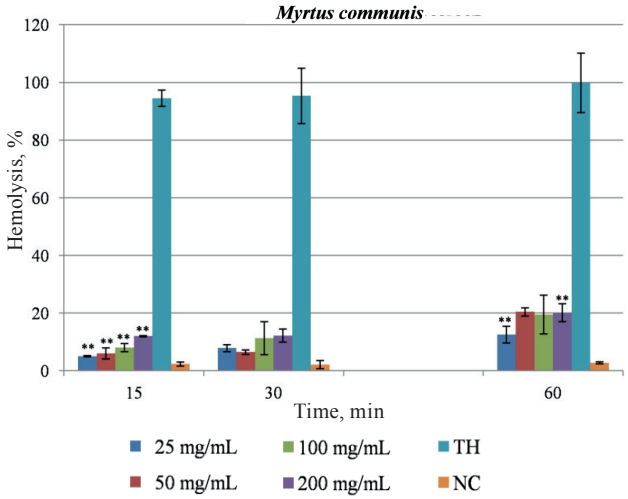

TH: Total Hemolysis. NC: Negative Control.
The means of 3 replicates. $P < 0.01$. ** significant

Figure 2 Hemolytic effect of four concentrations of *Myrtus communis* extract at 15, 30, 45, and 60 min

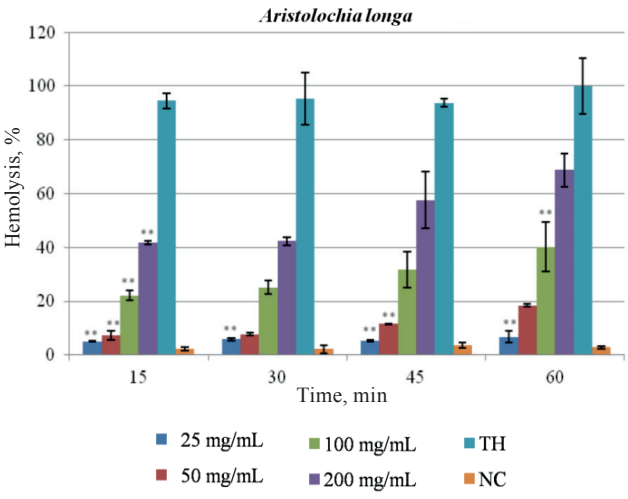

TH: Total Hemolysis. NC: Negative Control.
The means of 3 replicates. $P < 0.01$. ** significant

Figure 4 Hemolytic effect of four concentrations of *Aristolochia longa* extract at 15, 30, 45, and 60 min

from 22.12 ± 1.95 (15 min) to 40.23 ± 9.13% (60 min) and from 41.71 ± 0.75 (15 min) to 68.75 ± 6.11% (60 min), respectively. This increase in hemolytic effect remained inferior to total hemolysis.

Hemolytic effect of the plants studied at 60 min. Figure 5 shows the evolution of the hemolytic effect or the leakage of Hb after 60 min for the *A. longa*, *C. spinose*, and *M. communis* extracts at four concentrations (25, 50, 100, and 200 mg/mL) in a PBS buffer medium (pH 7.4) containing an erythrocyte suspension incubated at 37°C, compared to a negative control tube (PBS + suspension) and a total hemolysis tube (distilled water + suspension).

The *M. communis* species showed a significantly low hemoglobin leakage rate compared to the other species, as well as a 20.14 ± 3.11% total hemolysis. This species had a lesser effect on the cell membrane of erythrocytes ($P < 0.01$). However, *C. spinosa* caused a significant intermediate leakage of hemoglobin, compared to *M. communis* and *A. longa*, at 200 mg/mL (60 min), namely in the range of 34.86 ± 5.06% ($P < 0.01$). Nevertheless, the most important cytotoxic effect on red cells was produced by the aqueous extract of the *A. longa* leaves, where the leakage rate was 68.75 ± 6.11% at 200 mg/mL (60 min) and close to total hemolysis ($P > 0.01$), indicative of the species' high toxicity. These results are phenotypically observable in the supernatant.

For millennia, humans have been searching for drugs in barks, seeds, fruit organs and other parts of plants to heal themselves and alleviate pain [18]. Nowadays, several studies have been conducted on plants to create new drugs and, to some extent, to evaluate their toxicity and identify their components. Polyphenolic compounds of *M. communis* L. extracts are grouped in three major chemical classes: phenolic acids, tannins, and flavonoids [19]. Our results of the phytochemical screening of *C. spinosa* are consistent with those reported by Cherfia *et al.*, who identified polyphenols, flavonoids, alkaloids, tannins, and saponosides [20]. The *Aristolochia* species are a source of various active compounds such as aristolochic acid, alkaloids (aporphines, protoberberines, protopines), quinolines, amides, chlorophylls, terpenoids, lignans, flavonoids, tetralones, and steroids [21].

The polyphenol and flavonoid contents that we found in the *M. communis* leaves were higher than those obtained by Bouaziz *et al.*, who reported 157.70 ± 2.65 mg EAG/g MS and 2.64 ± 0.22 mg EQ/g of dry matter [22]. In another study, the hydromethanolic extract of *C. spinosa* leaves had a polyphenol content of 228.42 ± 8.86 and a flavonoid content of 4.87 ± 0.12 [23]. According to Djeridane *et al.*, the methanolic extract of *A. longa* contained 1.47 ± 0.20 mg/g EAG polyphenols and 0.81 ± 0.02 mg/g EQ flavonoids [24]. Our results were in agreement with Merouani *et al.*, who found 396.88 ± 8.86 mg/g EAG polyphenols and 9.92 ± 0.23 mg/g EQ flavonoids [25].

Plants contain toxic compounds in high doses, which makes the evaluation of their hemolytic power indispensable for their correct use in traditional therapy, as well as for choosing the right mode of administration and preserving the integrity of membranes. According to Haddouchi *et al.*, the hemolysis test should be performed even if a plant has a powerful antioxidant power, since its use in traditional medicine and in pharmacological preparations will be impossible in the presence of their hemolytic effect, which is an indicator of cytotoxicity [16]. "*Free radicals induce several effects on erythrocytes, such as hemolysis, fluidity of the membrane, changes in morphometry and lipid peroxidation, among others. Erythrocytes potentially promoting the oxidative process are extremely sensitive to oxidative damage because of the polyunsaturated fatty acid content in their cell membranes and their high content of oxygen and hemoglobin*" [26].

Many secondary metabolites were revealed in our extracts that may be a cause of cytotoxicity. We found a major lysis of red blood cells treated with *C. spinosa*, which was more prominent when treated with *Aristolchia*, testifying to severe toxicity. We found

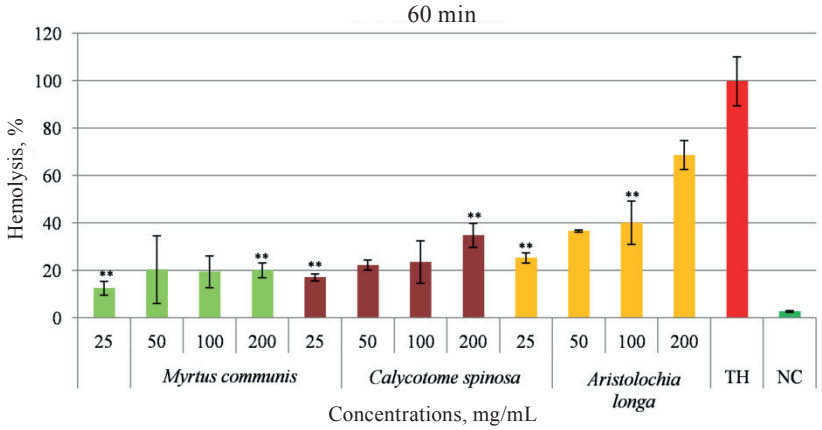

TH: Total Hemolysis. NC: Negative Control. The means of 3 replicates. $P < 0.01$. ** significant

Figure 5 Hemolytic effect of four concentrations of *Myrtus communis*, *Calycotome spinose*, and *Aristolochia longa* extracts at 60 min

very few studies on *A. longa* and *C. spinosa*, trying to examine a relationship between the extracts' chemical composition and toxicity.

According to Bissinger *et al.*, saponins – a secondary metabolite identified in aqueous extracts of the plants under our study – may lead to the stimulation of hemolysis as well as to suicidal erythrocyte death [27]. Alkaloids are present in many plants which may be toxic and affect human health [28]. Mahdeb *et al.* reported that alkaloids are capable of disrupting the permeability of the membranes of erythrocytes [29].

As stated by Galati and O'Brien, many adverse effects were associated with dietary polyphenol consumption or exposures such as hemolytic anemia [30]. The authors added that before using these polyphenols for therapy, they need to be assessed for safety.

According to Grollman *et al.*, the toxicity of *Aristolochia longa* is due to a toxin that is a major component of all *Aristolochia* species, namely the aristolochic acid responsible for nephropathic syndromes, although the therapeutic use of *Aristolochia* has rarely taken into account its intrinsic toxicity before [31]. These findings corroborate the study of Touiti *et al.*, which showed that *Aristolochia longa* was incriminated in nephrotoxicity [32].

CONCLUSION

Some herbs used in traditional therapy in high doses can reveal toxic properties and harm human health. It appears essential to determine their hemolytic capacity as a marker of toxicity for rational adaptation to traditional therapy. We found that *Aristolochia longa* and *Calycotome spinosa* caused significant lyses of red blood cells and a potent leakage of hemoglobin. Therefore, these species cannot be used without control as a therapeutic or pharmacological tool to treat diseases. Furthermore, it is important to perform antitumoral tests on cancer cells with these plant extracts or their chemical compounds to develop anti-cancer drugs.

CONFLICT OF INTEREST

The authors declare no conflict of interest.

CONTRIBUTION

L. Gadouche conceived and designed the analysis, performed the biological experiments, and wrote the paper. A. Zidane and K. Zerrouki contributed to data analysis and revised the paper. K. Azouni and S. Bouinoune performed the biological experiments. All the authors revised the manuscript for publication.

REFERENCES

1. Atanasov AG, Waltenberger B, Pferschy-Wenzig E-M, Linder T, Wawrosch C, Uhrin P, et al. Discovery and resupply of pharmacologically active plant-derived natural products: A review. Biotechnology Advances. 2015;33(8): 1582–1614. https://doi.org/10.1016/j.biotechadv.2015.08.001.
2. Tembe FE, Pougoue KJ, Ngoupayo J, Njunkio BN, Nguidjoe E, Tabi YO, et al. Evaluation of the toxicity of secondary metabolites in aqueous extracts of *Ficus thonningii* Blume in Wistar rats. American Journal of Ethnomedicine. 2018;5(2).
3. Calixto JB. Efficacy, safety, quality control, marketing and regulatory guidelines for herbal medicines (phytotherapeutic agents). Brazilian Journal of Medical and Biological Research. 2000;33(2):179–189. https://doi.org/10.1590/s0100-879x2000000200004.
4. Kharchoufa L, Merrouni IA, Yamani A, Elachouri M. Profile on medicinal plants used by the people of North Eastern Morocco: Toxicity concerns. Toxicon. 2018;154:90–113. https://doi.org/10.1016/j.toxicon.2018.09.003.
5. Forte JS, Raman A. Regulatory issues relating to herbal products – Part 2: Safety and toxicity. Journal of Medicinal Food. 2000;3(1):41–57. https://doi.org/10.1089/jmf.2000.3.41.
6. Subramanian K, Sankaramourthy D, Gunasekaran M. Toxicity studies related to medicinal plants. In: Mandal SC, Mandal V, Konishi T, editors. Natural products and drug discovery: An integrated approach. Elsevier; 2018. pp. 491–505. https://doi.org/10.1016/b978-0-08-102081-4.00018-6.
7. Quézel P, Santa S. Nouvelle flore de l'Algérie et des régions désertiques méridionales. Paris: Centre National de la Recherche scientifique; 1962. 1170 p.
8. Bouzabata A, Casanova J, Bighelli A, Cavaleiro C, Salgueiro L, Tomi F. The genus *Myrtus* L. in Algeria: Composition and biological aspects of essential oils from *M. communis* and *M. nivellei*: A review. Chemistry and Biodiversity. 2016;13(6):672–680. https://doi.org/10.1002/cbdv.201500342.
9. Alipour G, Dashti S, Hosseinzadeh H. Review of pharmacological effects of *Myrtus communis* L. and its active constituents. Phytotherapy Research. 2014;28(8):1125–1136. https://doi.org/10.1002/ptr.5122.
10. Heinrich M, Chan J, Wanke S, Neinhuis W, Simmond MSJ. Local uses of *Aristolochia* species and content of nephrotoxic aristolochic acid 1 and 2 – A global assessment based on bibliographic sources. Journal of Ethnopharmacology. 2009;125(1):108–144. https://doi.org/10.1016/j.jep.2009.05.028.

11. Takaidza S, Mtunzi F, Pilla M. Analysis of the phytochemical contents and antioxidant activities of crude extracts from Tulbaghia species. Journal of Traditional Chinese Medicine. 2018;38(2):272–279. https://doi.org/10.1016/j.jtcm.2018.04.005.
12. Behbahani BA, Shahidi F, Yazdi FT, Mortazavi SA, Mohebbi M. Antioxidant activity and antimicrobial effect of tarragon (*Artemisia dracunculus*) extract and chemical composition of its essential oil. Journal of Food Measurement and Characterization. 2017;11(2):847–863. https://doi.org/10.1007/s11694-016-9456-3.
13. Raafat K, Samy W. Amelioration of diabetes and painful diabetic neuropathy by *Punica granatum* L Extract and its spray dried biopolymeric dispersions. Evidence-based Complementary and Alternative Medicine. 2014;2014. https://doi.org/10.1155/2014/180495.
14. Hmid I, Elothmani D, Hanine H, Oukabli A, Mehinagic E. Comparative study of phenolic compounds and their antioxidant attributes of eighteen pomegranate (*Punica granatum L.*) cultivars grown in Morocco. Arabian Journal of Chemistry. 2017;10:S2675–S2684. https://doi.org/10.1016/j.arabjc.2013.10.011.
15. Mohan C. Buffers. A guide for the preparation and use of bufferd in biological systems. EMD Bioscience; 2006. 38 p.
16. Haddouchi F, Chaouche TM, Halla N. Phytochemical screening, antioxidant activities and hemolytic power of four Saharan plants from Algeria. Phytotherapie. 2018;16(S1):S254–S262. https://doi.org/10.3166/phyto-2019-0140.
17. Li G-X, Liu Z-Q. The protective effects of ginsenosides on human erythrocytes against hemin-induced hemolysis. Food and Chemical Toxicology. 2008;46(3):886–892. https://doi.org/10.1016/j.fct.2007.10.020.
18. Petrovska BB. Historical review of medicinal plants usage. Pharmacognosy Reviews. 2012;6(11):1–5. https://doi.org/10.4103/0973-7847.95849.
19. Aleksic V, Knezevic P. Antimicrobial and antioxidative activity of extracts and essential oils of *Myrtus communis* L. Microbiological Research. 2014;169(4):240–254. https://doi.org/10.1016/j.micres.2013.10.003.
20. Cherfia R, Kara Ali M, Talhi I, Benaissa A, Kacem Chaouche N. Phytochemical analysis, antioxidant and antimicrobial activities of leaves and flowers ethyl acetate and n-butanol fractions from an Algerian endemic plant *Calycotome spinosa* (L.) Link. Journal of Pharmacognosy and Phytotherapy. 2017;9(12):185–196. https://doi.org/10.5897/JPP2017.0471.
21. Tian-Shung W, Amooru GD, Chung-Ren S, Ping-Chung K. Chemical constituents and pharmacology of *Aristolochi* species. Studies in Natural Products Chemistry. 2005;32:855–1018. https://doi.org/10.1016/S1572-5995(05)80071-7.
22. Bouaziz A, Khennouf S, Zarga MA, Abdalla S, Baghiani A, Charef N. Phytochemical analysis, hypotensive effect and antioxidant properties of *Myrtus communis* L. growing in Algeria. Asian Pacific Journal of Tropical Biomedicine. 2015;5(1):19–28. https://doi.org/10.1016/S2221-1691(15)30165-9.
23. Krimat S, Dob T, Lamari L, Boumeridja S, Chelghoum C, Metidji H. Antioxidant and antimicrobial activities of selected medicinal plants from Algeria. Journal of Coastal Life Medicine. 2014;2(6):478–483.
24. Djeridane A, Yousfi M, Nadjemi B, Vidal N, Lesgards JF, Stocker P. Screening of some Algerian medicinal plants for the phenolic compounds and their antioxidant activity. European Food Research and Technology. 2007;224(6):801–809. https://doi.org/10.1007/s00217-006-0361-6.
25. Merouani N, Belhattab R, Sahli F. Evaluation of the biological activity of *Aristolochia longa* L. extracts. International Journal of Pharmaceutical Sciences and Research. 2017;8(5):1978–1992. https://doi.org/10.13040/IJPSR.0975-8232.8(5).1978-92.
26. Martínez V, Mitjans M, Vinardell MP. Cytoprotective effects of polyphenols against oxidative damage. In: Watson RR, Preedy VR, Zibadi S, editors. Polyphenols in human health and disease. Vol. 1. Academic Press; 2014. pp. 275–288. https://doi.org/10.1016/B978-0-12-398456-2.00022-0.
27. Bissinger R, Modicano P, Alzoubi K, Honisch S, Faggio C, Abed M, et al. Effect of saponin on erythrocytes. International Journal of Hematology. 2014;100(1):51–59. https://doi.org/10.1007/s12185-014-1605-z.
28. Beyer J, Drummer OH, Maurer HH. Analysis of toxic alkaloids in body samples. Forensic Science International. 2009;185(1–3):1–9. https://doi.org/10.1016/j.forsciint.2008.12.006.
29. Mahdeb N, Mayouf S, Boukhari F, Souilah S, Bouzidi A. Hemolytic effect of total alkaloids from the seeds of *Peganum harmala in vitro* on erythrocytes of ruminants: Sheep, cattle and goats. Asian Journal of Plant Science and Research. 2013;3(6):53–59.
30. Galati G, O'Brien PJ. Potential toxicity of flavonoids and other dietary phenolics: significance for their chemopreventive and anticancer properties. Free Radical Biology and Medicine. 2004;37(3):287–303. https://doi.org/10.1016/j.freeradbiomed.2004.04.034.
31. Grollman AP, Scarborough J, Jelaković B. Aristolochic acid nephropathy: An environmental and iatrogenic disease. Advances in Molecular Toxicology. 2009;3:211–227. https://doi.org/10.1016/S1872-0854(09)00007-1.

32. Touiti N, Achour S, Iken I, Chebaibi M, Houssaini TS. Nephrotoxicity associated with herbal medicine use, experience from Morroco. Toxicologie Analytique et Clinique. 2019;31(3):145–152. https://doi.org/10.1016/j.toxac.2019.04.001.

ORCID IDs
Leila Gadouche https://orcid.org/0000-0003-1757-1988
Azdinia Zidane https://orcid.org/0000-0003-1575-5994
Khayra Zerrouki https://orcid.org/0000-0002-0217-3138
Karima Azouni https://orcid.org/0000-0002-5662-079X
Saadia Bouinoune https://orcid.org/0000-0003-3780-0178

Foods and Raw Materials, 2021, vol. 9, no. 2

E-ISSN 2310-9599
ISSN 2308-4057

Research Article
Open Access

https://doi.org/10.21603/2308-4057-2021-2-387-396
Available online at http://jfrm.ru/en

RNN- and CNN-based weed detection for crop improvement: An overview

Brahim Jabir*, Loubna Rabhi, Noureddine Falih

Sultan Moulay Slimane University, Beni Mellal, Morocco

* e-mail: ibra.jabir@gmail.com

Received July 22, 2021; Accepted in revised form August 23, 2021; Published online October 15, 2021

Abstract:

Introduction. Deep learning is a modern technique for image processing and data analysis with promising results and great potential. Successfully applied in various fields, it has recently entered the field of agriculture to address such agricultural problems as disease identification, fruit/plant classification, fruit counting, pest identification, and weed detection. The latter was the subject of our work. Weeds are harmful plants that grow in crops, competing for things like sunlight and water and causing crop yield losses. Traditional data processing techniques have several limitations and consume a lot of time. Therefore, we aimed to take inventory of deep learning networks used in agriculture and conduct experiments to reveal the most efficient ones for weed control.

Study objects and methods. We used new advanced algorithms based on deep learning to process data in real time with high precision and efficiency. These algorithms were trained on a dataset containing real images of weeds taken from Moroccan fields.

Results and discussion. The analysis of deep learning methods and algorithms trained to detect weeds showed that the Convolutional Neural Network is the most widely used in agriculture and the most efficient in weed detection compared to others, such as the Recurrent Neural Network.

Conclusion. Since the Convolutional Neural Network demonstrated excellent accuracy in weed detection, we adopted it in building a smart system for detecting weeds and spraying them in place.

Keywords: Digital agriculture, weed detection, machine learning, deep learning, Convolutional Neural Network (CNN), Recurrent Neural Network (RNN)

Please cite this article in press as: Jabir B, Rabhi L, Falih N. RNN- and CNN-based weed detection for crop improvement: An overview. Foods and Raw Materials. 2021;9(2):387–396. https://doi.org/10.21603/2308-4057-2021-2-387-396.

INTRODUCTION

In our growing digital world, machine learning is at the core of data science [1]. Machine learning techniques and computing power play an essential role in the analysis of collected data. They have focused on representing input data and generalizing learned predictive models to future data [2]. Data representation has a dramatic effect on machine learner performance. Proper data representation can lead to high performance even with straightforward machine learning. In contrast, poor representation of data with advanced complex machine learning can lead to decreased performance [3].

Deep learning is an important branch of machine learning that has emerged to achieve impressive results in the field of artificial intelligence. Its strength is in its ability to automatically create powerful data representation through layers of learning without human intervention, thus ensuring great precision of analysis [4]. In comparison with shallow learning algorithms, deep learning uses supervised and unsupervised techniques and machine-learning approaches to automatically learn the hierarchical representation of multi-level data for feature classification [5, 6]. This deep learning composition is inspired by the representation of human brain for processing natural signals. It has attracted the academic community lately due to its performance in different research fields, such as agriculture.

More recently, a number of technologies common in industry have been applied to agriculture, such as remote sensing, the Internet of Things (IoT), and robotic platforms, leading to the concept of "smart agriculture" [7, 8]. Smart agriculture is important to face agricultural production challenges in terms of productivity, environmental impact, and food security. To tackle these challenges, it is necessary to analyze agricultural ecosystems, which involves constant monitoring of different variables. These operations

create data that can be used as input values and processed with varying analysis techniques in deep learning to identify weeds, diseases, etc.

The objects of our study were two neural networks, namely the Convolutional Neural Network (CNN) and the Recurrent Neural Network (RNN). A CNN is an artificial neural network used for image recognition and processing [9]. It is specially intended for handling pixel information. A CNN is viewed as a powerful artificial intelligence (AI) image processing system that employs deep learning to perform generative and descriptive tasks. It commonly uses machine vision, which includes image and video recognition, as well as recommendation systems and natural language processing (NPL) [10]. A RNN, in its turn, is an artificial neural network essentially utilized in discourse identification and programmed regular language treatment. RNNs are intended to perceive successive attributes and information utilization patterns needed to foresee likely scenarios [11]. Therefore, the use of a RNN in image classification requires optimization with the long short-term memory (LSTM) technique to reduce the risk of gradient vanishing [12]. In this study, we compared these two techniques of deep learning with other state of the art techniques in order to create an optimized model and train it to detect weeds. We aimed to create an intelligent system that could detect weeds and spray them locally to avoid wasting herbicides and protect the environment.

STUDY OBJECTS AND METHODS

In this study, we used various methods, devices, techniques, and libraries to study deep learning in crop planting and train the deep learning models on a database that includes images for relevant and smart weed detection. The following sections contain complete descriptions of these methods.

Deep learning. This method came to expand machine learning (ML) and added a lot of complexity and depth to the model based on artificial neural networks (ANNs). A neural network is a system designed to resemble the neural organization of the human brain. A more complex definition would be that a neural network is a computational model made up of artificial neurons connected to each other and resulting in a network architecture. This architecture has specific parameters called weights. Adjusting them, we can enhance the accuracy of our model. This type of networks contains many layers, each with a specific mission. Their number determines the complexity of the network. We can find three layers in a small neural network: the input layer, the hidden layer, and the output layer. Each of these layers is comprised of hubs called “nodes” and has a given assignment, as the name suggests. The input layer is liable for recovering information and giving it to the following layer. The hidden layer plays out all the back-end assignments of the calculation and change of information utilizing different capacities that permit its portrayal in a progressive

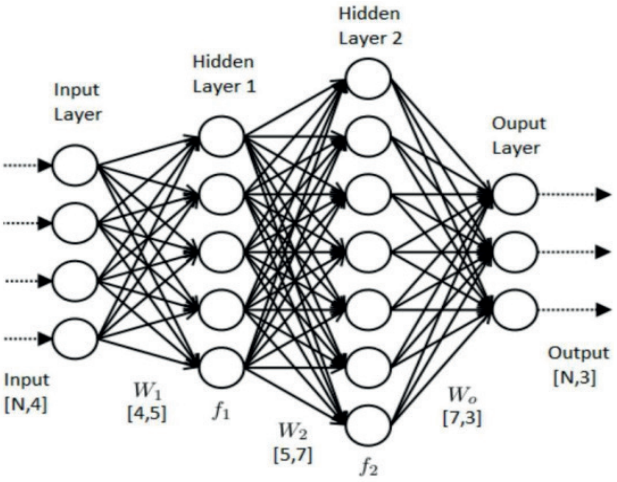

Figure 1 Artificial neural network [14]

manner through a few degrees of abstraction [13]. There can be multiple layers hidden in a neural network as needed. Several parameters influence the laying of various layers, and the goal is always to obtain a high degree of accuracy. The output layer passes the consequence of the hidden layer, as shown in Fig. 1.

Deep learning has various applications ranging from natural language to image processing. Its important advantage is the learning of functionalities, or automatic extraction of functionalities from raw data. Functionalities of more significant levels of a progressive system are framed by the arrangement of lower level functionalities.

Deep learning can tackle more perplexing issues well and rapidly by utilizing more complex layers, which permits enormous parallelization. These complex algorithms increase classification accuracy and reduce errors, provided there are large, well-prepared and sufficient data sets to describe the problem and the layers are well constructed.

The profoundly progressive construction and great learning capacity of deep learning algorithms permit them to perform classification and expectation with high accuracy. They are versatile and adaptable to a wide range of exceptionally complex problems. Deep learning has numerous applications in data management (e.g. video, images), tending to be applied to any type of information, like natural language, speech, and continuous or point data [15].

The main drawbacks of deep learning could be long learning time and a need for powerful hardware suitable for parallel programming (Graphics Processing Unit, Field-programmable Gate Array), while conventional strategies like Scale Invariant Feature Transform (SIFT) or Support Vector Machine (SVM) have less difficult learning measures [16]. In any case, the testing time is quicker in deep learning tools and most of them are more accurate. The subsections below present the most common deep learning techniques.

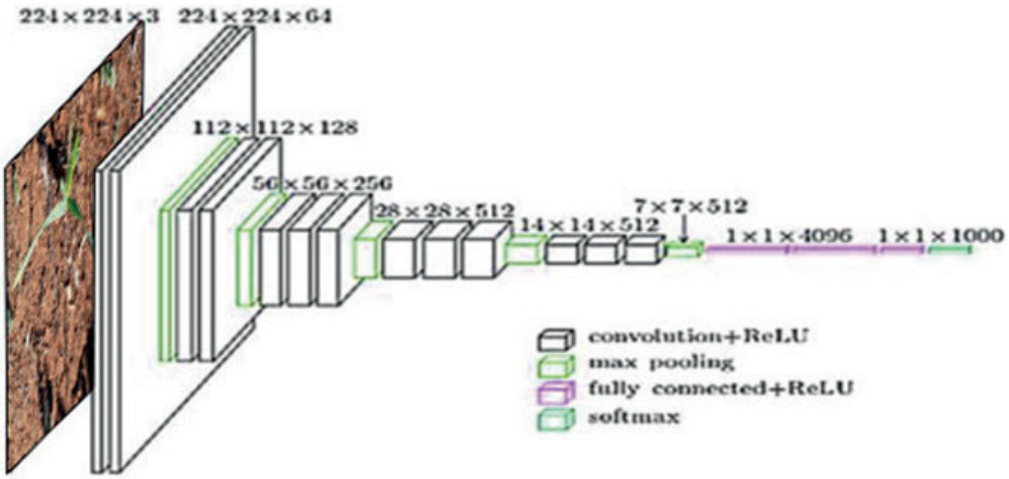

Figure 2 An example of CNN architecture (VGG)

Convolutional Neural Network (CNN). In deep learning, convolutional neural networks (CNNs) are a class of profound feedforward ANNs that has been effectively applied to computer vision. In contrast to an ANN, whose tediously prepared prerequisites may be unfeasible in some huge scope issues, a CNN can learn complex issues quite rapidly because of weight sharing and more complex layers utilized.Convolutional neural networks can increase their likelihood of correct classifications, provided there are sufficiently large data sets (i.e. hundreds to thousands of measurements, depending on the complexity of the problem under investigation) available to describe the problem. They are made up of different convolutional layers, grouped and/or fully connected. Convolutional layers perform operations to extract distinct features from the input images whose dimensionality is reduced by grouping the layers together, while fully connected layers perform classification operations. They usually exploit the learned high-level functionalities at the last layer in order to classify the input images into predefined classes. Many organizations have successfully applied this technique in various fields, such as agriculture where it accounts for 80% of all methods used [17]. An example of CNN architecture is shown in Fig. 2 [18].

Figure 2 shows different representations of the training dataset created by applying various convolutions to certain layers of the network. Training always begins as the most general at the level of the first layers, which are larger, and becomes more specific at the level of the deeper layers.

A combination of convolutional layers and dense layers makes the production of good precision results possible. There are various "successful" architectures that researchers commonly use to start building their models instead of starting from scratch. These include AlexNet, the Visual Geometry Group (VGG) (shown in Fig. 2), GoogleNet, and Inception-ResNet, which uses what we call "transfer learning." Besides, there are various tools and platforms that allow researchers to experience deep learning. The most popular are TensorFlow, Theano, Keras (an application programming interface on top of TensorFlow and Theano), PyTorch, Caffe, TFLearn, Pylearn2, and Matlab. Some of these tools (e.g. Caffe, Theano) integrate popular platforms such as those mentioned above (e.g. AlexNet, VGG, GoogleNet) in the form of libraries or classes [19].

Recurrent Neural Network (RNN). Recurrent neural networks (RNNs) are another type of neural networks that is used to solve difficult machine learning problems involving sequences of inputs. Some RNN architectures for sequence prediction issues are:

1. One-to-Many: sequence yield, for picture captioning;
2. Many-to-One: sequence in input contribution, for sentiment investigation; and
3. Many-to-Many: sequence for synchronized input, machine translation and output sequences, typically processing operations for video classification.

RNNs have connections with loops, adding feedback and memory to networks over time. This memory has come to replace traditional learning that relies on individual patterns. It allows this type of network to learn and generalize through a sequence of inputs. When an out is produced, it is copied and sent back to the recurrent network [20]. To make a decision, it considers the current entry and the exit it learned from the previous entry. An example of RNN architecture is shown in Fig. 3.

Figure 3 shows an RNN for the entire sequence. For example, if a sentence consists of five words, the network will unwind into a neural network of five layers, one layer for each word. The formulas that govern calculations in an RNN are as follows:

– x_t entered at time t.

– U; V; W are the parameters that the network will learn from the training data.

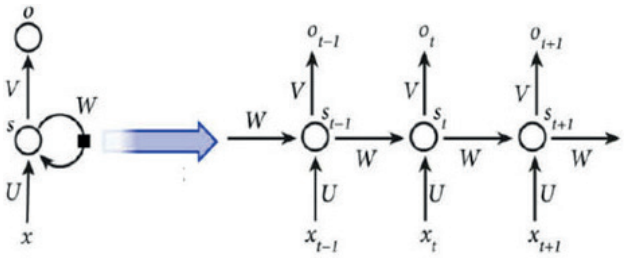

Figure 3 An RNN (left) and its unrolled version (right)

– *St* is the hidden state at time *t*. It is the "memory" of the network. *St* is calculated based on the previous hidden state and the entry to the current step:

$$St = f(Ux_t + Ws_{t-1}) \quad (1)$$

where f is a nonlinear function such as ReLu or Hyperbolic tangent (TanH).

Ot (2) is the exit at time *t*. A well-known example here is the prediction of a word in the sentence. When we want to know the next word in the sentence, it will show a vector of possibilities in the vocabulary.

$$Ot = softmax(Vs_t) \quad (2)$$

Deep learning applications in agriculture. Applications of deep learning in agriculture are spread across several areas, the most popular being weed identification, land cover classification, plant recognition, fruit counting, and crop type classification. According to Fig. 4, which shows deep learning models in crop planting, CNNs and RNNs account for 80% and only 5% of all methods, respectively.

The low ratio of RNNs in agriculture is due to the fact that traditional RNNs have unstable behavior with the vanishing gradient and therefore are not used in image classification. For this reason, we will discuss an advanced RNN in this article that uses the LSTM technique for image classification in weed identification. Weeds are plants that grow spontaneously on agricultural soils where they are unwanted. The growth of these plants causes competition with crops for space, light, and water. Herbicides are the first tool used to fight against weeds, but they present secondary risks for man and nature. Therefore, we need to think about ways to reduce their effects. In this study, we proposed an intelligent system that automatically detects weeds and contributes to localized spraying of infected areas only. To identify weeds, we processed photos of crops and classified them to apply specific herbicides.

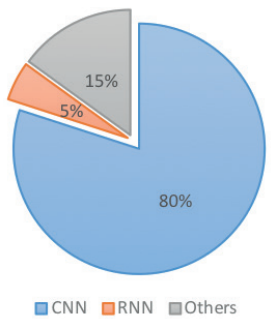

Figure 4 Deep learning methods in crop planting

Weeds can be classified according to the size of their leaves into grass categories (dicot and monocot). This division is adequate since grasses and broadleaf weeds are differentiated in treatment due to the selectivity of some herbicides to the specific group. Herbicide application works best if treatment is targeted at the specific class of weed. Several studies have shown the success of CNNs in comparison with RNNs and other deep learning techniques used for weed identification [21–23].

Technical details. From a technical standpoint, almost all of the research has used popular CNN architectures such as AlexNet, VGG, and Inception-ResNet, or combined CNNs with other procedures. All the experiments that exploited a well-known system also used a deep learning framework, with Caffe being the most famous. Noteworthily, most studies that only had small datasets to train their CNN models exploited the power of data augmentation to artificially increase the number of training images to enhance their accuracy. They used translations, transposition, and reflections, as well as modified the intensities of the RGB Channels, and that is what we did to prepare our dataset.

Also, the majority of related works included image preprocessing steps, where each image in the dataset was scaled down to a smaller size before being used as input into the model, such as 256×256, 128×128, 96×96, 60×60 pixels, or converted to CNN grayscale architectures to take advantage of transfer learning. Transfer learning exploits already existing knowledge of certain related tasks in order to increase the efficiency of learning the problem at hand, refining pre-trained models when it is impossible to train the network on the data from the beginning due to a small set of training data or the resolution of a complex problem. We can get significant results if we rely on weights from other models that were previously trained on big datasets [24]. In our case, these are preformed CNNs that have already been trained on datasets related to different class numbers. The authors of related work mainly used large datasets to train their CNN models, in some cases containing thousands of images. Some of them came from well-known and publicly available sources such as PlantVillage, MalayaKew, LifeCLEF, and UC Merced. In contrast, some authors produced their own datasets for their research needs, as we can see in Table 1. The table also shows whether the authors compared their CNN-based approach with other techniques used to solve the problem under study, as well as the precision of each model. Therefore, conventional precision of the model's response must be exactly the expected response.

Table 1 Application of deep learning in agriculture (weed detection)

Agricultural area	Description of the problem	Data	DL Architecture	DL Model	Accuracy	Comparison with other methods	References
Weed detection	Detection and classification of weeds in soybean crops	400 images of crops captured by the authors with a drone	CNN	CaffeNet (CAFFE FW)	98%	SVM: 98% AdaBoost: 98.2% Random Forest: 96%	[21]
Weed detection	Weed detection and classification by spectral band analysis	200 hyperspectral images with 61 bands	CNN	MatConvnet	94.72 %	HoG: 74.34%	[22]
Weed detection	Accelerate a DL with FPGA approach to classification Weed with 8 classes	18000 weed images from the DeepWeedX dataset	CNN	VGG-16, DenseNet-128-10	90.08%	ResNet: 95.7%	[23]

Application of an optimized RNN in weed detection. All the studies referred to above have used CNN architectures to create deep learning models that detect weeds. Also, they have compared them with other models in terms of accuracy and error. RNNs, however, do not feature much in these works, which means they are hardly used in this field of agriculture, especially for image classification. That is why we aimed to create an optimized RNN model with the long short-term memory (LSTM) technique as an alternative to the traditional RNN [25]. We trained this RNN-LSTM model on our dataset in order to compare the results with those obtained by the CNN above. First, we loaded the dataset that was already used in a previous experiment. This database contained a set of weeds known in our region and spread over four classes. Then, we built an RNN model and trained it on the database created using the following parameters: inputs = 28, step = 28, neuron = 150, output = 10, epoch = 20, Softmax function. LSTMs were introduced in our model in order to improve the RNN standards. The RNN model we created is shown in Fig. 5.

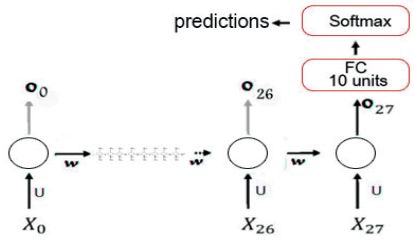

Figure 5 RNN model architecture

To design this deep learning model, we used the python code, as shown in Fig. 6.

```
class ImageRNN(nn.Module):
    def __init__(self, batch_size, n_steps, n_inputs, n_neurons, n_outputs):
        super(ImageRNN, self).__init__()

        self.n_neurons = n_neurons
        self.batch_size = batch_size
        self.n_steps = n_steps
        self.n_inputs = n_inputs
        self.n_outputs = n_outputs

        self.basic_rnn = nn.RNN(self.n_inputs, self.n_neurons)

        self.FC = nn.Linear(self.n_neurons, self.n_outputs)

    def init_hidden(self,):
        return (torch.zeros(1, self.batch_size, self.n_neurons))

    def forward(self, X):
        X = X.permute(1, 0, 2)

        self.batch_size = X.size(1)
        self.hidden = self.init_hidden()

        lstm_out, self.hidden = self.basic_rnn(X, self.hidden)
        out = self.FC(self.hidden)

        return out.view(-1, self.n_outputs)
```

Figure 6 Python code used to create the RNN model

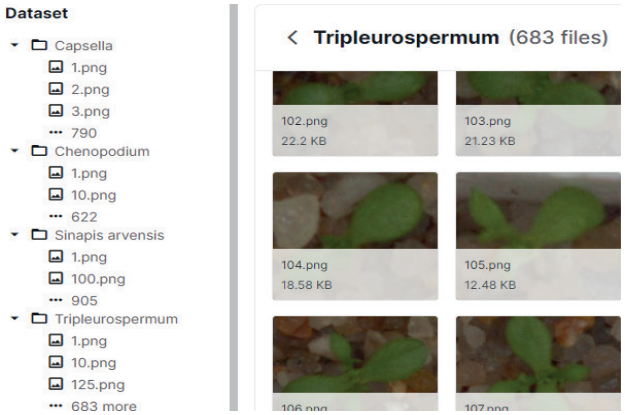

Figure 7 The dataset samples

The above code includes the initialization function *__init__*, which defines some variables. The fully connected layer follows the basic RNN by "*self.FC*" that allows data to flow through the RNN layer and then through the fully connected layer, also using the function "*init_hidden*" that exploits hidden weights with zero values.

The database used to train the proposed RNN and CNN models comprised about 3000 images taken in a wheat field with a digital camera (Sony 6000) under different lighting conditions (from morning to afternoon in sunny and cloudy weather). We combined these images with those from the online Kaggle repository dataset. The images featured four types of weeds that propagate in our region. They corresponded to four classes to be identified by our model (Fig. 7). A well-prepared database is a very important factor in deep learning. We applied preprocessing and data-augmentation techniques on the same data to generate other learning examples through different manipulations (flip, orientation, contrast, crop, exposure, noise, brightness…). These techniques reduced the model's performance.

RESULTS AND DISCUSSION

Before training the model, we added all necessary functions (Fig. 8). Firstly, we specified the device runtime to use during training, determined in the python code by *torch.device(...)*. This function gives commands to the program to use the GPU (Graphics Processing Unit) if it is available. Otherwise the CPU (Central Processing Unit) will be used as a default device. The GPU acts as a specialized microprocessor. It is swift and efficient for matrix multiplication and convolution. Parallelism is often cited as an explanation. The GPU is optimized for bandwidth, while the CPU is optimized for latency. Therefore, the CPU has less latency, but its capacity is lower than that of the GPU. In other words, CPUs are not suited to handle massive amounts of data, while GPUs can provide large amounts

```
import torch.optim as optim

# Device used
device = torch.device("cuda:0" if torch.cuda.is_available() else "cpu")

# instance of Model
model = ImageRNN(BATCH_SIZE, N_STEPS, N_INPUTS, N_NEURONS, N_OUTPUTS)
criterion = nn.CrossEntropyLoss()
optimizer = optim.Adam(model.parameters(), lr=0.001)

def get_accuracy(logit, target, batch_size):
    ''' Obtain accuracy for training round '''
    corrects = (torch.max(logit, 1)[1].view(target.size()).data == target.data).sum()
    accuracy = 100.0 * corrects/batch_size
    return accuracy.item()
```

Figure 8 Addition of necessary functions

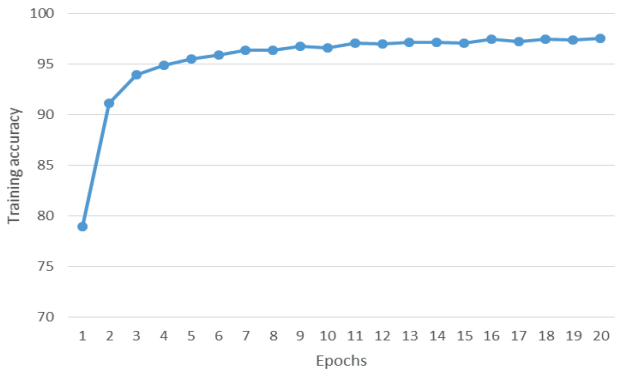

Figure 9 Training accuracy of the RNN model

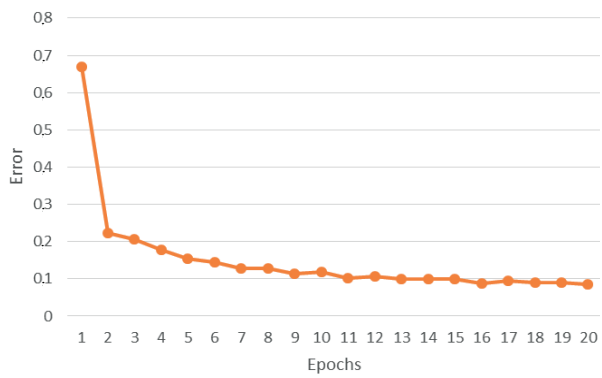

Figure 10 The error rate of the RNN model

```
test_acc = 0.0
for i, data in enumerate(testloader, 0):
    inputs, labels = data
    inputs = inputs.view(-1, 28, 28)

    outputs = model(inputs)

    test_acc += get_accuracy(outputs, labels, BATCH_SIZE)

print('----------------')
print('Test Accuracy of the model: %.2f'%( test_acc/i))
print('----------------')
```

```
PROBLEMS  OUTPUT  DEBUG CONSOLE  TERMINAL

----------------
Test Accuracy of the model: 96,40
----------------
```

Figure 11 Test accuracy of the RNN model

of memory. The CPU is responsible for performing all kinds of calculations, whereas the GPU only handles graphics calculations. Since our dataset was not large, we used an i7 CPU with 2.80GHz and 8G of RAM.

Then, we create an instance of the model with the *ImageRNN(...)* function, with its own configuration and parameters, the criterion represents the function we will use to get the loss of the designed model. To do this process, it is sufficient to use the function: *nn.CrossEntropyLoss()*, which is a softmax function utilized as boundaries log probabilities and followed by a negative log-likelihood loss activity over the output of the model. The code shows how to provide this to the criterion.

We add an optimization function that recalculates the weights based on the current loss and updates it. This is done using the *Optim.adam* function, which requires setting the model parameters and learning rate. To display the results and get the accuracy, we will use the *get_accuracy(...)* function, which computes the accuracy of the model given the log probabilities and target values for each epoch. All these functions are shown in the figure below.

After training the model on 20 epochs, we obtained relevant results (Figs. 9 and 10).

There are different ways and measures to evaluate the performance of a classification model. The performance measures often used are precision, kappa, recall, and others [26]. We were therefore interested in the model's accuracy and error rate. Accuracy is a proportion of genuine expectations in relation to the absolute number of input pictures. The error rate measures the difference between the model's predictions and the real images in the training set [27]. Figures 9 and 10 show the accuracy and error for each epoch. In particular, Fig. 10 shows how the neural network gradually decreased the error to arrive at 0.9. According to Fig. 9, the training accuracy reached 97.58% due to a set of factors, such as the dataset, optimization function, and the adjustment of weights and biases.

Figure 11 shows how the model performed on the test images. The display of predictions on test images is a technique to test the final solution in order to confirm the real predictive power of the network. We computed the accuracy on our dataset to test how well the model performed on the test images. Figure 11 shows a value of 96.40%, which means that the predictions on the test images were well classified.

These results indicated a good performance of the LSTM-RNN on our dataset. According to the three figures above, this model updates with every step, adjusting weights to reduce error and increasing accuracy using a backpropagation algorithm and gradient descent. In addition to the studies that were based on CNNs, we also built a CNN-based model (Fig. 12) and trained it on the same dataset that we used in the RNN experiment.

Our results were close to those reported by the authors referred to above.

The training was run on our local machine and after a few times it reached 98% validation accuracy. The model showed good results after 9 h of training. Figure 13 shows accuracy taken from Tensboard.

To sum up, CNNs are preferred for interpreting visual data, sparse data or data that does not come in sequence. Recurrent neural networks, however, are designed to recognize sequential or temporal data. They make better predictions by considering the order or sequence of data concerning previous or next data nodes. Applications where CNNs are particularly useful include face detection, medical analysis, drug discovery, and image analysis. RNNs are useful for linguistic translation, entity extraction, conversational intelligence, sentiment analysis, and speech analysis. Our experiment also showed that RNNs can be used to classify images if we add the LSTM technique. Based on literature and our

Layer (type)	Output Shape	Param #
conv2d (Conv2D)	(None, 98, 98, 256)	2560
activation (Activation)	(None, 98, 98, 256)	0
max_pooling2d (MaxPooling2D)	(None, 49, 49, 256)	0
conv2d_1 (Conv2D)	(None, 47, 47, 256)	590080
activation_1 (Activation)	(None, 47, 47, 256)	0
max_pooling2d_1 (MaxPooling2	(None, 23, 23, 256)	0
flatten (Flatten)	(None, 135424)	0
dense (Dense)	(None, 64)	8667200
dense_1 (Dense)	(None, 6)	390
activation_2 (Activation)	(None, 6)	0

Total params: 9,260,230
Trainable params: 9,260,230
Non-trainable params: 0

Figure 12 CNN basic configuration

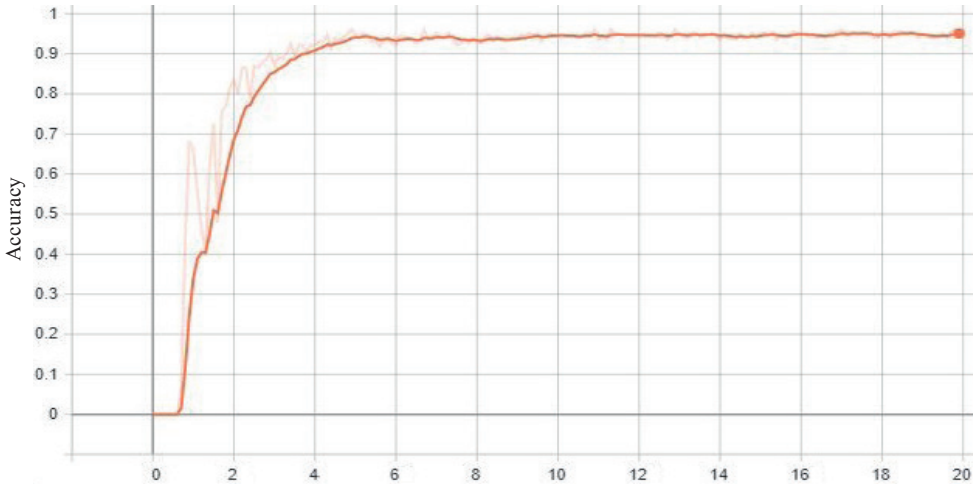

Figure 13 The CNN accuracy

Table 2 Comparison between RNN and CNN

CNN	RNN
Used extensively in agriculture, with over 90% accuracy in weed detection	Although rarely used in weed detection, this model showed the same accuracy as CNN in our experiment.
More powerful than RNN in several areas.	Less captured features compared to CNN.
Ideal for still images and video processing.	Ideal for text and speech analysis (image processing with LSTM).
Appropriate for spatial information.	Used for temporal data, also known as sequential data.
Accepts fixed-size inputs and generates fixed-size outputs.	Can handle arbitrary entry/exit lengths.
Designed to use minimal amounts of pretreatment.	Utilizes its inner memory to deal with discretionary sequences of sources, unlike feedforward neural networks.
Uses models of connectivity between neurons.	Uses time series information.

results, we compared the characteristics of RNNs and CNNs and summarized them in Table 2.

Our experimentation clearly shows why CNNs are so widely used in agriculture despite the abundance of other deep learning techniques. In addition, we proved that a RNN can also be used to detect weeds, but with less efficiency and more effort. Therefore, we recommend the CNN as the best suited deep learning technique for more efficient weed detection as the basis for smarter precision farming.

CONCLUSION

Precision agriculture encompasses several areas of application, such as plant and leaf disease detection, land cover classification, plant recognition, and weed identification to name the most common uses. The development of precision agriculture requires new monitoring, control, and information technologies, including deep learning. This paper presents an overview and a comparative study of deep learning tools in crop planting. First, we looked at agriculture to describe its current problems, specifically weed detection. Then, we listed the technical characteristics of popular deep learning techniques. After that, we created a CNN and a RNN and trained them on our dataset to compare their overall accuracy. The results showed that the optimized RNN model (RNN with LSTM) can also be used to classify images with acceptable accuracy. Hence, a RNN combined with the LSTM is suitable for detecting weeds among other techniques, but a CNN always comes first in terms of speed and accuracy. In future work, we intend to use other metrics to compare the results, such as recall and Kappa. We will also try to develop a platform combining the RNN with the CNN to achieve the best accuracy. These results will be used to build an intelligent system based on Raspberry Pi 4 that can detect weeds in real time and spray them in their area.

CONTRIBUTION

The authors were equally involved in writing the manuscript and are equally responsible for plagiarism.

CONFLICT OF INTEREST

The authors declare no conflict of interest regarding the publication of this article.

ACKNOWLEDGMENTS

This research is part of the Digital Agriculture doctorate project that involves a group of doctors from the Limati Laboratory at Sultan Moulay Slimane University in Morocco.

REFERENCES

1. Ferguson AL. Machine learning and data science in soft materials engineering. Journal of Physics Condensed Matter. 2018;30(4). https://doi.org/10.1088/1361-648X/aa98bd.
2. Momennejad I. Learning structures: Predictive representations, replay, and generalization. Current Opinion in Behavioral Sciences. 2020;32:155–166. https://doi.org/10.1016/j.cobeha.2020.02.017.
3. Peng S, Sun S, Yao Y. A survey of modulation classification using deep learning: Signal representation and data preprocessing. IEEE Transactions on Neural Networks and Learning Systems. 2021. https://doi.org/10.1109/TNNLS.2021.3085433.
4. Salloum SA, Alshurideh M, Elnagar A, Shaalan K. Machine learning and deep learning techniques for cybersecurity: A review. Advances in Intelligent Systems and Computing. 2020;1153:50–57. https://doi.org/10.1007/978-3-030-44289-7_5.
5. Alloghani M, Al-Jumeily D, Mustafina J, Hussain A, Aljaaf AJ. A systematic review on supervised and unsupervised machine learning algorithms for data science. In: Berry MW, Mohamed A, Yap BW, editors. Supervised and unsupervised learning for data science. Cham: Springer; 2020. pp. 3–21. https://doi.org/10.1007/978-3-030-22475-2_1.
6. Nowicki RK, Grzanek K, Hayashi Y. Rough support vector machine for classification with interval and incomplete data. Journal of Artificial Intelligence and Soft Computing Research. 2020;10(1):47–56. https://doi.org/10.2478/jaiscr-2020-0004.
7. Jabir B, Falih N, Sarih A, Tannouche A. A strategic analytics using convolutional neural networks for weed identification in sugar beet fields. Agris On-line Papers in Economics and Informatics. 2021;13(1):49–57. https://doi.org/10.7160/aol.2021.130104.
8. Jabir B, Falih N. Digital agriculture in Morocco, opportunities and challenges. 2020 IEEE 6th International Conference on Optimization and Applications (ICOA); 2020; Beni Mellal. Beni Mellal: Sultan Moulay Slimane University; 2020. https://doi.org/10.1109/ICOA49421.2020.9094450.
9. Duda P, Jaworski M, Cader A, Wang L. On training deep neural networks using a streaming approach. Journal of Artificial Intelligence and Soft Computing Research. 2020;10(1):15–26. https://doi.org/10.2478/jaiscr-2020-0002.
10. Zhang C, Lin Y, Zhu L, Liu A, Zhang Z, Huang F. CNN-VWII: An efficient approach for large-scale video retrieval by image queries. Pattern Recognition Letters. 2019;123:82–88. https://doi.org/10.1016/j.patrec.2019.03.015.
11. Lin JC-W, Shao Y, Djenouri Y, Yun U. ASRNN: A recurrent neural network with an attention model for sequence labeling. Knowledge-Based Systems. 2021;212. https://doi.org/10.1016/j.knosys.2020.106548.
12. Shen J, Ren Y, Wan J, Lan Y. Hard disk drive failure prediction for mobile edge computing based on an LSTM recurrent neural network. Mobile Information Systems. 2021;2021. https://doi.org/10.1155/2021/8878364.
13. LeCun Y, Bengio Y, Hinton G. Deep learning. Nature. 2015;521(7553):436–444. https://doi.org/10.1038/nature14539.
14. Araujo VJS, Guimaraes AJ, Souza PVD, Rezende TS, Araujo VS. Using resistin, glucose, age and BMI and pruning fuzzy neural network for the construction of expert systems in the prediction of breast cancer. Machine Learning and Knowledge Extraction. 2019;1(1):466–482. https://doi.org/10.3390/make1010028.
15. Kulkarni A, Halgekar P, Deshpande GR, Rao A, Dinni A. Dynamic sign language translating system using deep learning and natural language processing. Turkish Journal of Computer and Mathematics Education. 2021;12(10):129–137.
16. Huu PN, Ngoc TP, Manh HT. Proposing gesture recognition algorithm using HOG and SVM for smart-home applications. In: Vo N-S, Hoang V-P, Vien Q-T, editors. Industrial networks and intelligent systems. Cham: Springer; 2021. pp. 315–323. https://doi.org/10.1007/978-3-030-77424-0_26.
17. Kamilaris A, Prenafeta-Boldú FX. A review of the use of convolutional neural networks in agriculture. Journal of Agricultural Science. 2018;156(3):312–322. https://doi.org/10.1017/S0021859618000436.
18. Nash W, Drummond T, Birbilis N. A review of deep learning in the study of materials degradation. npj Mater Degrad. 2018;2(1). https://doi.org/10.1038/s41529-018-0058-x.
19. Bousetouane F, Morris B. Off-the-shelf CNN features for fine-grained classification of vessels in a maritime environment. In: Bebis G, Boyle R, Parvin B, Koracin D, Pavlidis I, Feris R, et al., editors. Advances in visual computing. Cham: Springer; 2015. pp. 379–388. https://doi.org/10.1007/978-3-319-27863-6_35.
20. Ganai AF, Khursheed F. Predicting next word using RNN and LSTM cells: Stastical language modeling. 2019 Fifth International Conference on Image Information Processing (ICIIP); 2019; Shimla. Solan: Jaypee University of Information Technology; 2019. p. 469–474. https://doi.org/10.1109/ICIIP47207.2019.8985885.
21. dos Santos Ferreira A, Freitas DM, da Silva GG, Pistori H, Folhes MT. Weed detection in soybean crops using ConvNets. Computers and Electronics in Agriculture. 2017;143:314–324. https://doi.org/10.1016/j.compag.2017.10.027.

22. Farooq A, Hu J, Jia X. Analysis of spectral bands and spatial resolutions for weed classification via deep convolutional neural network. IEEE Geoscience and Remote Sensing Letters. 2018;16(2):183–187. https://doi.org/10.1109/LGRS.2018.2869879.
23. Lammie C, Olsen A, Carrick T, Azghadi MR. Low-power and high-speed deep FPGA inference engines for weed classification at the edge. IEEE Access. 2019;7:51171–51184. https://doi.org/10.1109/ACCESS.2019.2911709.
24. Harsono IW, Liawatimena S, Cenggoro TW. Lung nodule detection and classification from Thorax CT-scan using RetinaNet with transfer learning. Journal of King Saud University – Computer and Information Sciences. 2020. https://doi.org/10.1016/j.jksuci.2020.03.013.
25. Sherstinsky A. Fundamentals of recurrent neural network (RNN) and long short-term memory (LSTM) network. Physica D: Nonlinear Phenomena. 2020;404. https://doi.org/10.1016/j.physd.2019.132306.
26. Gupta S, Agrawal A, Gopalakrishnan K, Narayanan P. Deep learning with limited numerical precision. Proceedings of the 32 nd International Conference on Machine; 2015; Lille. Lille: JMLR W&CP; 2015. p. 1737–1746.
27. Pak M, Kim S. A review of deep learning in image recognition. 2017 4th International Conference on Computer Applications and Information Processing Technology. Kuta Bali; 2017. p. 367–369. https://doi.org/10.1109/CAIPT.2017.8320684.

ORCID IDs
Brahim Jabir https://orcid.org/0000-0002-8762-9199
Loubna Rabhi https://orcid.org/0000-0002-4617-5223
Noureddine Falih https://orcid.org/0000-0001-7804-5450

Foods and Raw Materials, 2021, vol. 9, no. 2

E-ISSN 2310-9599
ISSN 2308-4057

Research Article
Open Access

https://doi.org/10.21603/2308-4057-2021-2-397-405
Available online at http//jfrm.ru/en

Choline intake effects on psychophysiological indicators of students in the pre-exam period

Olga L. Tarasova[1,*], Vadim I. Ivanov[1], Sergey V. Luzgarev[2], Marya B. Lavryashina[1], Vladimir A. Anan'ev[2]

[1] Kemerovo State Medical University, Kemerovo, Russia

[2] Kemerovo State University, Kemerovo, Russia

* e-mail: tol_66@mail.ru

Received April 26, 2021; Accepted in revised form May 17, 2021; Published online October 15, 2021

Abstract:
Introduction. Choline has a wide range of physiological functions. It has a neuroprotective effect on brain dysfunctions, while its deficiency has a negative effect on antenatal development of the nervous system. We aimed to study the impact of exogenous choline on the psychophysiological indicators in students.
Study objects and methods. 87 students were surveyed by questionnaire to determine their background intake of dietary choline. One month before the exams, we measured their simple and complex visual-motor reaction times, functional mobility and balance of nervous processes, as well as indicators of their short-term memory, attention, health, activity, and mood. Then, we divided the students into a control and an experimental group, regardless of their choline intake. The experimental group took 700 mg choline supplements on a daily basis for one month, followed by a second psychophysiological examination.
Results and discussion. Students with a low choline intake had lower functional mobility and balance of nervous processes, but better attention stability than students with a high choline intake. The second examination showed improved short-term memory, health, and activity indicators in the experimental group, compared to the control. The visual-motor reaction times also increased, but only in students with an initially low level of choline intake.
Conclusion. Choline supplementation can be recommended to students under pre-exam stress to enhance the functional state of their central nervous system.

Keywords: Choline, intake level, choline supplements, students, psychomotor reactions, cognitive functions

Funding: The study was performed at Kemerovo State University (KemSU) (Kemerovo, Russia).

Please cite this article in press as: Tarasova OL, Ivanov VI, Luzgarev SV, Lavryashina MB, Anan'ev VA. Choline intake effects on psychophysiological indicators of students in the pre-exam period. Foods and Raw Materials. 2021;9(2):397–405. https://doi.org/10.21603/2308-4057-2021-2-397-405.

INTRODUCTION

There has been a lot of research into choline over the past few decades. It is a vitamin-like nutrient that takes part in many physiological processes and has a wide range of physiological functions [1, 2].

Choline is ingested with food as part of phosphatidylcholine or formed endogenously. The human need for choline is met mainly through food. Its adequate daily intake is 425 mg for women and 550 mg for men, but not more than 3.5 g/day [3]. Metabolic pathways for the conversion of dietary choline and its endogenous synthesis are genetically heterogeneous. This determines individual sensitivity to a deficiency of choline [4, 5].

Choline has a significant effect on the development and functioning of the nervous system. As part of phosphatidylcholine, it participates in the construction, stabilization, and repair of cell membranes, including neurons. As a component of sphingolipids, it myelinates nerve fibers [6, 7]. As a precursor of betaine (a methyl group donor), choline is a factor in epigenetic regulation of gene expression during neurogenesis [8, 9]. DNA methylation is a dynamic process that can modulate the expression of genes that regulate synaptic plasticity. Since neurogenesis continues throughout life, dietary intake of choline as a source of methyl groups can affect cognitive functions at various stages of ontogenesis [10].

Our special interest is in choline as a precursor of acetylcholine, the most important neurotransmitter of the central and peripheral nervous system. Cholinergic systems of the brain have been in the center of neuroscientific and medical research due to their importance for cognitive functions and motor skills [11–14]. The influence of choline, either ingested or synthesized endogenously, on the effects of cholinergic neurotransmission is determined by a large number of genetic and epigenetic factors. These factors include enzyme systems that transport choline to the presynaptic terminals of neurons, the synthesis of acetylcholine from choline and acetylcoenzyme A and its inactivation after its use in synapses, as well as localization and activity of muscarinic and nicotinic cholinergic receptors. Therefore, it is difficult to interpret experimental data on the relationship between exogenous choline and the effects of acetylcholine.

The effects of choline on the nervous system have also been extensively studied. For example, its deficiency has a negative impact on the intrauterine development of the nervous system. Some studies on animals found that choline-enriched nutrition of pregnant females improved the cognitive functions of their offspring at various stages of ontogenesis and slowed down age-related involution. Its most pronounced effect was found in the study of learning and spatial memory in rodents using the Morris water maze, which indicated the involvement of hippocampal neurons [10]. However, the studies on humans, which examined the effect of a choline-fortified diet for pregnant women on the development of their children's cognitive abilities, produced conflicting data [15–17].

Another area of choline research is its neuroprotective effect and impact on cognitive functions in adults. Pharmaceutical choline-containing drugs are often prescribed for pathologies of the nervous system. The neuroprotective effects of choline alfoscerate and cytidine-5'-diphosphocholine (citicoline) have been proven in treating cognitive impairment associated with trauma, vascular disorders, or neurodegenerative diseases [18–21]. The studies of choline effect on cognitive functions of healthy individuals in postnatal ontogeny have yielded mixed results. For example, memory tests on 1391 adult men and women without cognitive impairment revealed a positive effect of choline consumption, with similar results found for cognitive tests on 2195 people aged 70–74 [22, 23].

Knott *et al.* examined the effect of a single dose of citicoline in low and medium concentrations. They found that the effect was determined by the initial level of choline, i.e., the subjects with initially low levels of choline had improved cognitive functions after citicoline treatment [24].

According to another study, choline bitartrate improved the accuracy (rather than the time) of visual-motor task performance in students [25]. A positive relationship was found between the plasma choline content in 15-year-olds and their school performance [26]. Other researchers, however, did not observe a positive effect of short-term choline bitartrate treatment on the memory function of students [27].

Studies on school and college students are especially relevant. Childhood and adolescence are the periods of life when the morphofunctional maturation of the nervous system is combined with intensive cognitive activity during schooling. Of paramount importance therefore is nutrition that satisfies the plastic and functional needs of the nervous system. Choline is one of such nutrients. However, more research is needed to clarify the relationship between choline and cognitive functions in different age groups, including students.

We should also mention a potential negative effect of high choline intake on human health. This problem has been widely discussed in recent years due to the existence of choline metabolic pathways with the participation of intestinal microflora. A certain composition of intestinal microbiota produces a large amount of trimethylamine (TMA), which is absorbed by the epithelium, entering the liver through the portal vein, where it is converted into trimethylamine N-oxide (TMAO). The cumulative effects of TMAO are currently associated with the risk of atherosclerosis, insulin resistance, stomach and intestinal cancer, as well as kidney pathology [28–30]. Therefore, increasing choline intake should be recommended to adults with caution.

We aimed to expand our awareness of exogenous choline effect on psychophysiological functions under increased nervous stress. For this, we set the following objectives:

– assessing levels of choline intake in university students;
– analyzing the relationship between choline intake levels and psychophysiological characteristics;
– studying the effect of choline supplementation on the functional indicators of the central nervous system in students in the pre-exam period.

STUDY OBJECTS AND METHODS

Study design. First, we formed a cohort of 87 study subjects (13 males and 74 females) aged 19 from the 1st- and 2nd-year students of the Department of Social Work and Psychology at Kemerovo State University (Kemerovo, Russia) and obtained their informed written consent to participate in the study. All the study subjects were surveyed by questionnaire to assess their dietary choline intake. In addition, they underwent a psychophysiological examination to assess their neurodynamic and cognitive functions.

Next, the 2nd-year students were divided into a control and an experimental group, 20 people each (4 males and 16 females) by pairwise selection based on mechanical memory. The experimental group took a mono-component dietary supplement "Choline 350 mg Vegetable Capsules" (Solgar, USA). The supplement was registered under No. RU.77.99.11.003.E.004764.10.18 of 29.10.2018 in the Customs Union's Register of State Registration Certificates. Choline was taken for one

month, one capsule twice a day with a meal. At the end of the intake period, both groups underwent another psychophysiological examination.

Finally, the data were statistically processed and analyzed.

Choline determination methods. Food frequency questionnaire (FFQ) was used to determine the frequency of consumption of choline-containing foods and to estimate the absolute daily intake by portion size [26]. The survey followed the Russian guidelines[I].

The questionnaire included foods with a choline content of at least 10% of the daily intake per 100 g. It also listed dairy products (milk, kefir) which had a choline content of 5–8% of the daily intake per 100 g, but could be consumed in fairly large amounts. The subjects were surveyed in a group, with the interviewer giving explanations about the questionnaire. The respondents were asked to estimate the frequency of consumption of the listed products during the last month, as well as indicate the approximate size of the portions. Then, we analyzed the responses to determine the approximate amount of choline intake using available sources [31, 32] and ranked the results by the quartile method.

Methods for studying psychophysiological functions. The neurodynamic and cognitive indicators were determined with the psychophysiological complex "Status PF"[II]. The testing was carried out in a group in the university computer classroom on Tuesday and Wednesday mornings before classes with minimum extraneous irritants. Prior to the testing, we explained its meaning and significance in order to form a positive attitude among the study subjects. The tests that we selected did not require significant mental strain or much time to perform. In particular, we used the following well-known diagnostic tools.

The latent period of a simple visual-motor reaction is the most common psychomotor indicator that reflects the rate of excitation along the reflex arc and, therefore, the excitability of the central nervous system. This is a rather labile indicator that adequately characterizes its functional state. The general simple visual-motor reaction time is determined by the subject's anatomical features of the sensory system, nervous processes, psychophysiological state, and the motor-coordination potential. The subjects were asked to press a key on the computer keyboard as quickly as possible in response to a light stimulus. The average time of a motor reaction (ms) was determined after 30 light stimuli with various random intervals.

The latent period of a complex visual-motor reaction reflects the time spent on analyzing information in the integrative-triggering cortical zones and making a decision about how to respond. The subjects were asked to react to a red signal with their right hand, to a green signal with their left hand, and not to react to a yellow signal. The average time of a motor reaction (ms) was determined after 30 light stimuli.

Functional mobility of nervous processes was determined by the method of Khilchenko (1958) modified by Makarenko *et al.* (1987). The level of functional mobility is an indicator of neurodynamic constitution that does not depend as much on the actual functional state of the central nervous system as the simple and complex sensorimotor reactions. This method is based on a complex visual-motor differentiation reaction in the feedback mode. In contrast to the previous method, the intervals between signals depended on the correctness of motor reactions, decreasing by 20 ms after a correct reaction and increasing after an incorrect one. The test included 120 standard stimuli. The test time (s) was a quantitative level of functional mobility of the subject's nervous processes – the less time it took to do the test, the more accurate the responses were. The accuracy of responses was determined by the rate of changes between excitation and inhibition, that is, the functional mobility of nervous processes.

Balance of the nervous system in response a moving object reflects the relationship between excitatory and inhibitory processes in the cerebral cortex. This method determines the accuracy of visual-motor reaction to an object moving at the same speed in a circle. When the object overlapped the marker on the circle, the subjects had to press a key and "stop" it, with the time of deviation between the object and the marker recorded up to 1 ms. The subject's reaction was considered accurate if the deviation was within ± 5 ms. We recorded the number of accurate reactions, anticipatory and lagging reactions (total and average), as well as the average deviation time.

Short-term visual memory is a phase of imprinting characterized by a short storage of a limited number of objects in memory. The stimuli on the monitor screen included two-digit numbers (Ebbinghaus method), syllables (Luria method), and unrelated words (Leser method). They were presented one at a time for 1 s with an interval of 2 s. The capacity of short-term memory was determined by the number of correctly reproduced stimuli immediately after presentation.

Attentional capacity was determined by the maximum number of simultaneously perceived objects. The subjects were shown a lined field (5 by 5), with objects (crosses) randomly located in the cells. With every exposure, the number of objects increased by one. After a 500 ms exposure, the objects disappeared and the subjects had to locate them on the field. Attentional capacity was determined by the maximum number of correctly located objects, expressed in points.

[I] Martinchik AN, Baturin AK, Baeva VS. Razrabotka metoda issledovaniya fakticheskogo pitaniya po analizu chastoty potrebleniya pishchevykh produktov: sozdanie voprosnika i obshchaya otsenka dostovernosti metoda [Developing a method to determine nutrition by the frequency of food consumption: creating a questionnaire and assessing the method's reliability]. Problems of Nutrition. 1998;67(3):8–13. (In Russ.).

[II] Ivanov VI, Litvinova NA. Programma dlya EHVM "Otsenka psikhofiziologicheskogo sostoyaniya organizma cheloveka (Status PF)" [Computer program "Assessment of the psychophysiological state of the human body (Status PF)"]; № 2001610233. 2001.

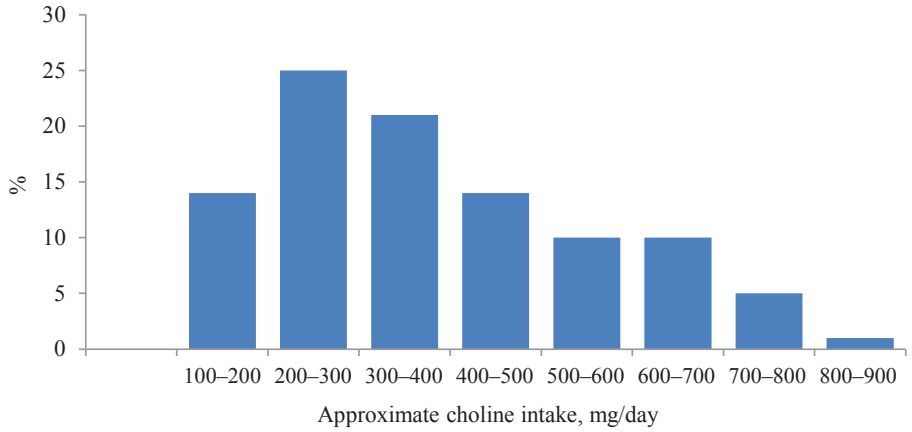

Figure 1 Students distribution by choline intake (according to the food frequency questionnaire)

Attention concentration was assessed with the Schulte table presented on the monitor screen. The subjects were to indicate the numbers from 1 to 25 in ascending order. The time taken to complete the test was an indicator of concentration. The less time one spent, the higher their attention concentration.

Attentional set-shifting was assessed with a red and black Schulte-Gorbov table. The subjects were invited to indicate black numbers in ascending order and red numbers in descending order: 1 – black, 24 – red, 2 – black, 23 – red, 3 – black, etc. The time taken to complete the test was a measure of attentional set-shifting (the less time, the better the indicator).

Attention stability was determined with a computer version of the dot cancellation test. The subjects were asked to look through lines of letters in the table and mark the given four letters for 4 min. The test assessed the speed of performance (number of letters viewed) and its accuracy (number of errors), with their ratio calculated as the total productivity index.

The HAM (health, activity, mood) test[III] was used for the students' additional self-assessment of their functional state. The questionnaire had 30 pairs of subjective characteristics with opposite meanings (for example, "funny-sad", "slow-fast", etc.). The subjects were asked to indicate their current state on a scale between these poles. The neutral state was marked as "0" and the extreme (most pronounced) state as "3" (both poles). The points were added up for each scale (health, activity, and mood).

Statistical processing was carried out in Excel and Statistica 6.0. Mean values and standard errors were determined for all the indicators under study. In addition, we performed the analysis of histograms and the percentile analysis. Normality of the distribution was measured by the Kolomogorov-Smirnov test. Due to the small size of our sample, most indicators did not have a normal distribution. Therefore, we applied the Mann-Whitney test to compare two groups and the median test for multiple comparisons. The Wilcoxon rank test was used to assess changes in indicators. The χ^2 test measured the statistical significance of differences in percentage ratios ($P < 0.05$). Spearman's correlation analysis was also applied.

[III] Doskin VA, Lavrent'eva NA, Miroshnikov MP, Sharay VB. Test differentsirovannoy samootsenki funktsional'nogo sostoyaniya [A test for differentiated self-assessment of the functional state]. Voprosy Psychologii. 1973;19(6):141–145. (In Russ.).

RESULTS AND DISCUSSION

The food frequency questionnaire (FFQ) results showed that the approximate level of choline intake with the products included in the questionnaire ranged from 100 to 900 mg per day (Fig. 1). We found that 60% of the respondents had a choline intake below the recommended value (400 mg). The average choline consumption was 448.7 ± 50.6 mg for males and 373.4 ± 21.6 mg for females, also below the recommended value. Our data were generally consistent with the results of various international studies, as reported by Canadian authors [2]. Their review also emphasized that the reported low intake of total choline did not take into account its form (water-soluble or fat-soluble) and did not always indicate its deficiency in the body. When interpreting our results, we also assumed that the actual intake of choline was higher than the level shown by the FFQ, since the questionnaire did not include all the foods consumed by students. Yet, we had enough grounds for recommending that students who consume less than 400 mg of choline per day adjust their diet by including foods high in choline.

To study the relationship between neurodynamic characteristics and choline intake, the students were divided into three groups based on the quartile analysis: a) low choline intake (under 240 mg/d), quartile 1; b) medium choline intake (240–499 mg/d), quartiles 2 and 3; c) high choline intake (over 500 mg/d), quartile 4. The comparison of the neurodynamic parameters in these groups revealed some statistically significant differences (Tables 1 and 2).

We found that the students with a high choline intake had the best indicators for functional mobility of nervous

Table 1 Neurodynamic parameters in students with different levels of choline intake

Neurodynamic parameters	Choline intake			Mann-Whitney U-test*		
	Low (1)	Medium (2)	High (3)	1–2	1–3	2–3
Latent period of a simple visual-motor reaction, ms	292.3 ± 8.7	303.1 ± 23.3	279.6 ± 7.3			
Latent period of a complex visual-motor reaction, ms	446.5 ± 17.2	444.1 ± 10.6	435.6 ± 9.6			
Functional mobility of nervous processes – time, s	66.6 ± 1.8	65.2 ± 1.2	63.1 ± 1.3		0.04	
Reaction to a moving object: average deviation from accurate reactions, ms	29.8 ± 2.4	27.9 ± 3.3	30.4 ± 5.8			
Reaction to a moving object: total anticipatory reactions, ms	297.1 ± 52.0	246.5 ± 75.4	298.2 ± 62.5			
Reaction to a moving object: total lagging reactions, ms	513.6 ± 66.9	519.5 ± 51.4	340.4 ± 62.6		0.04	0.04

*$P < 0.05$

Table 2 Memory and attention parameters in students with different levels of choline intake

Cognitive functions	Choline intake			Mann-Whitney U-test		
	Low (1)	Medium (2)	High (3)	1–2	1–3	2–3
Short-term memory (numbers), points	6.3 ± 0.4	6.0 ± 0.3	5.8 ± 0.3			
Short-term memory (words), points	7.13 ± 0.2	7.0 ± 0.3	7.1 ± 0.3			
Short-term memory (syllables), points	4.4 ± 0.4	4.6 ± 0.3	4.7 ± 0.4			
Attentional capacity, points	6.7 ± 0.4	6.5 ± 0.4	6.8 ± 0.4			
Attention concentration test completion time, s	45.4 ± 2.7	47.4 ± 2.4	45.0 ± 2.3			
Attentional set-shifting test completion time, s	173.4 ± 7.9	169.7 ± 5.6	167.2 ± 7.0			
Attention stability: total productivity index	62.6 ± 5.5	45.9 ± 5.9	48.9 ± 6.4	0.03		

*$P < 0.05$

processes and the least time of lagging reactions to a moving object.

The assessment of cognitive functions produced quite unexpected results. The integral indicator of attention stability based on the dot cancellation test was the highest among students with a low choline intake (Table 2). There were no other statistically significant differences.

We found no statistically significant correlations between dietary choline intake and psychophysiological indicators in the sample as a whole. However, there were significant differences in the groups with high, medium, and low choline intake.

The group with a low choline intake showed statistically significant correlations between the choline value and the number of anticipatory reactions to a moving object ($r = 0.46$, $P < 0.05$), the number of accurate reactions ($r = –0.68$, $P < 0.01$), the average time of lagging reactions to a moving object ($r = 0.54$, $P < 0.05$), and the short-term memory for numbers ($r = –0.31$, $P < 0.05$). Thus, the best indicators of psychomotor accuracy and short-term memory were found in students with the lowest choline intake.

In the group with a medium choline intake, its daily value had a negative effect on the number of accurate reactions to a moving object ($r = –0.35$, $P < 0.05$) and a positive effect on the average deviation time in the same test ($r = 0.32$, $P < 0.05$), just as in the low choline intake group. We found no statistically significant correlations between choline values and indicators of memory and attention in this group.

The group with a high choline intake revealed an inverse relationship between choline values and the latent period of a simple visual-motor reaction ($r = –0.5$, $P < 0.05$) and the time of completing the attention concentration test ($r = –0.4$, $P < 0.05$), as well as a direct relationship with attention stability ($r = 0.45$, $P < 0.05$). This meant that those students who consumed more choline in this group performed best in the visual-motor reaction and attention tests.

Thus, we found that the level of dietary choline intake had a greater effect on neurodynamic parameters than on cognitive functions. Higher choline values improved the mobility of nervous processes and accuracy in complex visual-motor reactions. However, their effects on cognitive functions were quite contradictory. We assumed that our results should be interpreted with other factors taken into account, which affected the students' choline intake and psychophysiological state. Yet, these additional factors were beyond the scope of this study.

The control and the experimental groups of 20 students in each were formed regardless of the choline

Table 3 Choline intake in the control and experimental groups, mg/day

Group	Median value	25–75 percentiles
Control (no choline treatment)	401	264–652
Experimental (with choline treatment)	416	315–492
P (Mann-Whitney U-Test)	0.91	

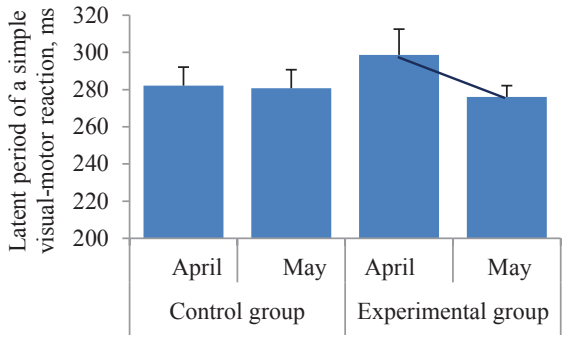

Figure 2 Changes in the simple visual-motor reaction times ($P < 0.05$)

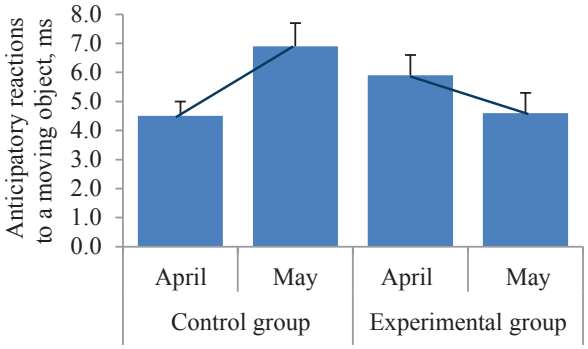

Figure 3 Changes in reactions to a moving object ($P < 0.05$)

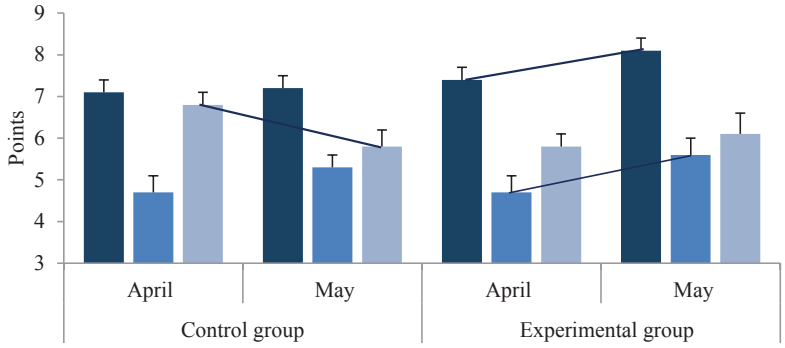

Figure 4 Changes in short-term memory and attention indicators ($P < 0.05$)

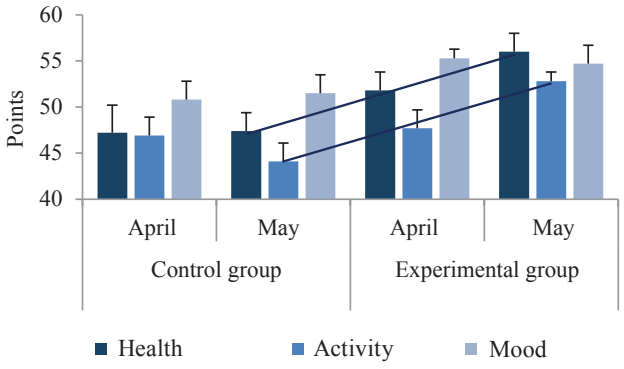

Figure 5 Changes in the HAM (health, activity, mood) test ($P < 0.05$)

values. The analysis of their dietary choline intake did not show any statistically significant differences between the groups (Table 3).

Thus, the control and the experimental groups, which had a homogeneous age and sex composition and similar cognitive indicators at the beginning of the study, were also quite similar in choline intake.

However, we identified some statistically significant changes in their neurodynamic parameters during the observation period (Figs. 2–5).

The experimental group showed significant improvements in the simple visual-motor reaction times (Fig. 2) within a month. The number of anticipatory reactions to a moving object decreased in the experimental group, but increased in the control group (Fig. 3). The students who received choline supplementation had better short-term memory for words and syllables. However, their attentional capacity remained the same, decreasing in the control group (Fig. 4).

The HAM (health, activity, mood) method revealed that during the second examination, the students taking choline supplements had significantly higher indicators of health and activity, compared to the control group (Fig. 5). Thus, the students in the experimental group were in a better state of health.

These changes showed that the pre-exam stress did not affect the functional state of the central nervous system of students in the experimental group – in fact, it improved.

Next, we divided the experimental group into two subgroups, depending on the level of choline intake: students with choline intake below the median value (416 mg) and students with choline intake above the median value. Thus, we could assess the effect of choline supplementation, taking into account the students' dietary choline intake.

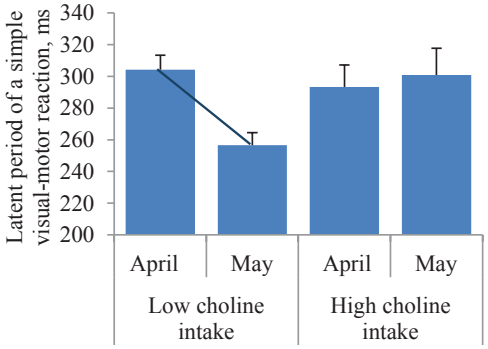

Figure 6 Changes in the simple visual-motor reaction times in students with choline supplementation vs. initial choline intake ($P < 0.05$)

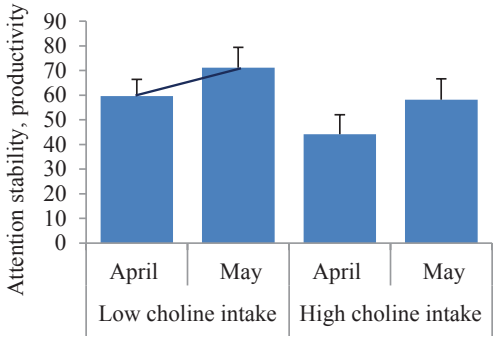

Figure 7 Changes in attention stability in students with choline supplementation vs. initial choline intake ($P < 0.05$)

We found statistically significant changes in neurodynamic parameters among students from the experimental group with a low choline intake. In particular, they showed a shorter simple visual-motor reaction time (Fig. 6) and improved attention stability (Fig. 7).

Changes in cognitive functions indicated better short-term memory for syllables in all experimental students, regardless of their choline intake, and improved performance in the dot cancellation test only in those with a low choline intake (Fig. 8).

The self-assessment with the HAM (health, activity, mood) method did not reveal any significant trends associated with levels of choline intake.

In order to obtain more general information about how choline supplementation affected the functional state of the central nervous system, we analyzed correlations between different psychophysiological parameters throughout the study. The closer connectedness between various neurodynamic, cognitive, and subjective indicators was regarded as a sign of increased psychophysiological adaptation in the pre-exam period.

Figure 9 shows changes in the number of statistically significant correlations between various indicators in the control and experimental groups. We can see a clear difference in the number of correlations between the control and experimental groups, indicating a lesser degree of cognitive stress in the students who took choline supplements.

Thus, we found a positive effect of choline supplementation on the psychophysiological indicators of students in the stressful pre-exam period. Yet, some of the results were quite ambiguous and even conflicting: for example, negative correlations between background choline intake and attention indicators in both the control and the experimental groups, or general uselessness of choline supplementation for cognitive functions. As we know, a human need for choline and sensitivity to its deficiency are highly variable and genetically determined by heterogeneous metabolic pathways of endogenous synthesis and dietary choline conversion.

Our study showed that choline supplementation can be recommended to students, especially those with a low consumption of choline-rich foods.

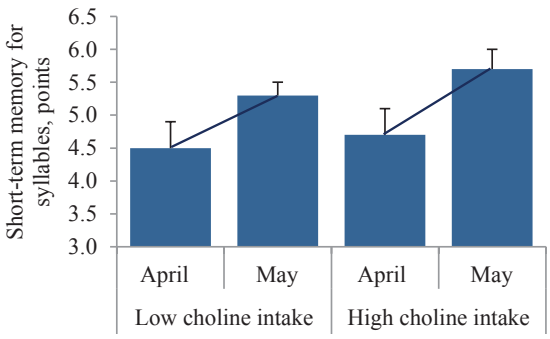

Figure 8 Changes in short-term memory in students with choline supplementation vs. initial choline intake ($P < 0.05$)

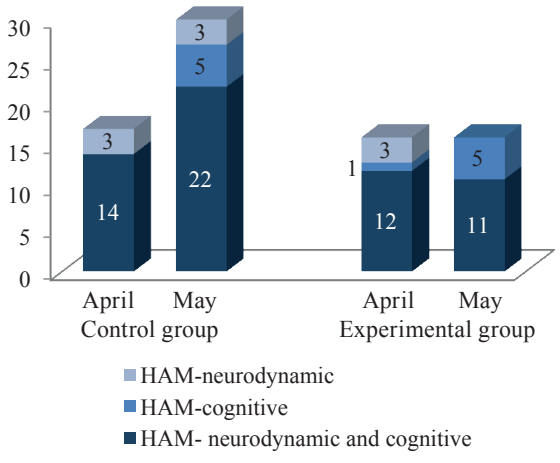

Figure 9 Statistically significant correlations between psychophysiological indicators in different groups

CONCLUSION

Half of the students had a dietary choline intake below the recommended value. The levels of choline intake had a greater effect on the neurodynamic parameters than on the cognitive functions. Increased choline intake correlated with higher functional mobility of nervous processes and faster reactions to a moving object. The students who took choline supplements for one month had positive changes in the functional state of the central nervous system, compared to the control group. Besides, these changes were more pronounced in those students who had a low intake of dietary choline. An additional daily intake of 700 mg choline supplements can be recommended to students under pre-exam stress, especially those with a dietary choline deficiency, to improve the functional state of their central nervous system. However, we did not assess the effectiveness of smaller amounts of choline. We believe there is no need for continuous choline supplementation, since current research indicates possible negative health effects.

CONTRIBUTION

The authors were equally involved in preparing the manuscript.

CONFLICT OF INTEREST

The authors declare that there is not conflict of interest.

REFERENCES

1. Wallace TC, Blusztajn JK, Caudill MA, Klatt KC, Natker E, Zeisel SH, et al. The underconsumed and underappreciated essential nutrient. Nutrition Today. 2018;53(6):240–253. https://doi.org/10.1097/NT.0000000000000302.
2. Wiedeman AM, Barr SI, Green TJ, Xu Z, Innis SM, Kitts DD. Dietary choline intake: Current state of knowledge across the life cycle. Nutrients. 2018;10(10). https://doi.org/10.3390/nu10101513.
3. Dietary Reference Intakes for Thiamin, Riboflavin, Niacin, Vitamin B_6, Folate, Vitamin B_{12}, Pantothenic Acid, Biotin, and Choline. Washington: National Academies Press; 1998. 592 p. https://doi.org/10.17226/6015.
4. Ganz AB, Klatt KC, Caudill MA. Common genetic variants alter metabolism and influence dietary choline requirements. Nutrients. 2017;9(8). https://doi.org/10.3390/nu9080837.
5. Sikalidis AK. From food for survival to food for personalized optimal health: A historical perspective of how food and nutrition gave rise to nutrigenomics. Journal of the American College of Nutrition. 2019;38(1):84–95. https://doi.org/10.1080/07315724.2018.1481797.
6. Bernhard W, Poets CF, Franz AR. Choline and choline-related nutrients in regular and preterm infant growth. European Journal of Nutrition. 2019;58(3):931–945. https://doi.org/10.1007/s00394-018-1834-7.
7. Van Echten-Deckert G, Alam S. Sphingolipid metabolism – an ambiguous regulator of autophagy in the brain. Biological Chemistry. 2018;399(8):837–850. https://doi.org/10.1515/hsz-2018-0237.
8. Zeisel SH. Choline, other methyl-donors and epigenetics. Nutrients. 2017;9(5). https://doi.org/10.3390/nu9050445.
9. Roth ED, Roth TL, Money KM, SenGupta S, Eason DE, Sweatt JD. DNA methylation regulates neurophysiological spatial representation in memory formation. Neuroepigenetics. 2015;2:1–8. https://doi.org/10.1016/j.nepig.2015.03.001.
10. Blusztajn JK, Slack BE, Mellott TJ. Neuroprotective actions of dietary choline. Nutrients. 2017;9*(*8). https://doi.org/10.3390/nu9080815.
11. Haam J, Yakel JL. Cholinergic modulation of the hippocampal region and memory function. Journal of Neurochemistry. 2017;142:111–121. https://doi.org/10.1111/jnc.14052.
12. Romberg C, Bartko S, Wess J, Saksida LM, Bussey TJ. Impaired object-location learning and recognition memory but enhanced sustained attention in M2 muscarinic receptor-deficient mice. Psychopharmacology. 2018;235(12):3495–3508. https://doi.org/10.1007/s00213-018-5065-7.
13. Janeczek M, Gefen T, Samimi M, Kim G, Weintraub S, Bigio E, et al. Variations in acetylcholinesterase activity within human cortical pyramidal neurons across age and cognitive trajectories. Cerebral Cortex. 2018;28(4):1329–1337. https://doi.org/10.1093/cercor/bhx047.
14. Zaharov DV, Mihailov VA, Kotsiubinskaya YuV. Choline Alphoscerat (Gliatilin) in the pathogenetic therapy of Alzheimer's disease. V.M. Bekhterev Review of Psychiatry and Medical Psychology. 2018;(4):93–99. (In Russ.). https://doi.org/10.31363/2313-7053-2018-4-93-99.
15. Cheatham CL, Goldman BD, Fischer LM, da Costa K-A, Reznick JS, Zeisel SH. Phosphatidylcholine supplementation in pregnant women consuming moderate-choline diets does not enhance infant cognitive function: A randomized, double-blind, placebo-controlled trial. American Journal of Clinical Nutrition. 2012;96(6):1465–1472. https://doi.org/10.3945/ajcn.112.037184.
16. Boeke CE, Gillman MW, Hughes MD, Rifas-Shiman SL, Villamor E, Oken E. Choline intake during pregnancy and child cognition at age 7 years. American Journal of Epidemiology. 2013;177(12):1338–1347. https://doi.org/10.1093/aje/kws395.

17. Wiedeman AM, Chau CMY, Grunau RE, McCarthy D, Yurko-Mauro K, Dyer RA, et al. Plasma betaine is positively associated with developmental outcomes in healthy toddlers at age 2 years who are not meeting the recommended adequate intake for dietary choline. Journal of Nutrition. 2018;148(8):1309–1314. https://doi.org/10.1093/jn/nxy108.
18. Gavrilova SI, Kolykhalov IV, Ponomareva EV, Fedorova YaB, Selezneva ND. Clinical efficacy and safety of choline alfoscerate in the treatment of late-onset cognitive impairment. S.S. Korsakov Journal of Neurology and Psychiatry. 2018;118(5):45–53. (In Russ.). https://doi.org/10.17116/jnevro20181185145.
19. Bekdash RA. Choline, the brain and neurodegeneration: insights from epigenetics. Frontiers in Bioscience – Landmark. 2018;23(6):1113–1143. https://doi.org/10.2741/4636.
20. Jasielski P, Piędel F, Piwek M, Rocka A, Petit V, Rejdak K. Application of citicoline in neurological disorders: A systematic review. Nutrients. 2020;12(10). https://doi.org/10.3390/nu12103113.
21. Putilina MV. A personalized selection of choline precursors in evidence – based medicine. S.S. Korsakov Journal of Neurology and Psychiatry. 2020;120(6):144–151. (In Russ.). https://doi.org/10.17116/jnevro2020120061144.
22. Poly C, Massaro JM, Seshadri S, Wolf PA, Cho E, Krall E, et al. The relation of dietary choline to cognitive performance and white-matter hyperintensity in the Framingham Offspring Cohort. American Journal of Clinical Nutrition. 2011;94(6):1584–1591. https://doi.org/10.3945/ajcn.110.008938.
23. Nurk E, Refsum H, Bjelland I, Drevon CA, Tell GS, Ueland PM, et al. Plasma free choline, betaine and cognitive performance: the Hordaland Health Study. British Journal of Nutrition. 2013;109(3):511–519. https://doi.org/10.1017/S0007114512001249.
24. Knott V, de la Salle S, Choueiry J, Impey D, Smith D, Smith M, et al. Neurocognitive effects of acute choline supplementation in low, medium and high performer healthy volunteers. Pharmacology Biochemistry and Behavior. 2015;131:119–129. https://doi.org/10.1016/j.pbb.2015.02.004.
25. Naber M, Hommel B, Colzato LS. Improved human visuomotor performance and pupil constriction after choline supplementation in a placebo-controlled double-blind study. Scientific Reports. 2015;5. https://doi.org/10.1038/srep13188.
26. Nilsson TK, Hurtig-Wennlöf A, Sjöström M, Herrmann W, Obeid R, Owen JR, et al. Plasma 1-carbon metabolites and academic achievement in 15-yr-old adolescents. FASEB Journal. 2016;30(4):1683–1688. https://doi.org/10.1096/fj.15-281097.
27. Lippelt DP, van der Kint S, van Herk K, Naber M. No acute effects of choline bitartrate food supplements on memory in healthy, young, human adults. PLoS One. 2016;11(6). https://doi.org/10.1371/journal.pone.0157714.
28. Egshatyan LV, Tkacheva ON, Boytsov SA. Gut enterobiota – A new player in atherosclerosis pathogenesis. Cardiovascular Therapy and Prevention. 2014;13(6):56–61. (In Russ.). https://doi.org/10.15829/1728-8800-2014-6-56-61.
29. Arias N, Arboleya S, Allison J, Kaliszewska A, Higarza SG, Gueimonde M, et al. The relationship between choline bioavailability from diet, intestinal microbiota composition, and its modulation of human diseases. Nutrients. 2020;12(8). https://doi.org/10.3390/nu12082340.
30. Gatarek P, Kaluzna-Czaplinska J. Trimethylamine N-oxide (TMAO) in human health. EXCLI Journal. 2021;20:301–319. https://doi.org/10.17179/excli2020-3239.
31. Patterson KY, Bhagwat AS, Williams JR, Howe JC, Holden JM. USDA database for the choline content of common foods. Release Two. Washington: U.S. Department of Agriculture; 2008. 37 p.
32. Tutel′yan VA. Khimicheskiy sostav i kaloriynost′ rossiyskikh produktov pitaniya [Chemical composition and calorie content of Russian food products]. Moscow: DeLi plyus; 2012. 283 p. (In Russ.).

ORCID IDs
Olga L. Tarasova https://orcid.org/0000-0002-7992-645X
Vadim I. Ivanov https://orcid.org/0000-0003-2383-9768
Sergey V. Luzgarev https://orcid.org/0000-0002-7259-9089
Marya B. Lavryashina https://orcid.org/0000-0003-1593-0676
Vladimir A. Anan'ev https://orcid.org/0000-0002-3787-9894

Foods and Raw Materials, 2021, vol. 9, no. 2

E-ISSN 2310-9599
ISSN 2308-4057

Review Article
Open Access

https://doi.org/10.21603/2308-4057-2021-2-406-418
Available online at http://jfrm.ru/en

The microorganism-plant system for remediation of soil exposed to coal mining

Margarita Yu. Drozdova, Anna V. Pozdnyakova, Maria A. Osintseva, Nadezhda V. Burova, Varvara I. Minina

Kemerovo State University, Kemerovo, Russia

e-mail: drozdowa.margarita.00@yandex.ru

Received October 05, 2021; Accepted in revised form October 27, 2021; Published online November 02, 2021

Abstract:
Introduction. Coal mining causes a radical transformation of the soil cover. Research is required into modern methods and complementary technologies for monitoring technogenic landscapes and their remediation. Our study aimed to assess soil and rhizosphere microorganisms and their potential uses for the remediation of technogenic soils in Russian coal regions.
Study objects and methods. We reviewed scientific articles published over the past five years, as well as those cited in Scopus and Web of Science.
Results and discussion. Areas lying in the vicinity of coal mines and coal transportation lines are exposed to heavy metal contamination. We studied the application of soil remediation technologies that use sorbents from environmentally friendly natural materials as immobilizers of toxic elements and compounds. Mycorrhizal symbionts are used for soil decontamination, such as arbuscular mycorrhiza with characteristic morphological structures in root cortex cells and some mycotallia in the form of arbuscules or vesicles. Highly important are Gram-negative proteobacteria (*Agrobacterium*, *Azospirillum*, *Azotobacter*, *Burkholderia*, *Bradyrizobium*, *Enterobacter*, *Pseudomonas*, *Klebsiella*, *Rizobium*), Gram-positive bacteria (*Bacillus*, *Brevibacillus*, *Paenibacillus*), and Gram-positive actinomycetes (*Rhodococcus*, *Streptomyces*, *Arhtrobacter*). They produce phytohormones, vitamins, and bioactive substances, stimulating plant growth. Also, they reduce the phytopathogenicity of dangerous diseases and harmfulness of insects. Finally, they increase the soil's tolerance to salinity, drought, and oxidative stress. Mycorrhizal chains enable the transport and exchange of various substances, including mineral forms of nitrogen, phosphorus, and organic forms of C3 and C4 plants. Microorganisms contribute to the removal of toxic elements by absorbing, precipitating or accumulating them both inside the cells and in the extracellular space.
Conclusion. Our review of scientific literature identified the sources of pollution of natural, agrogenic, and technogenic landscapes. We revealed the effects of toxic pollutants on the state and functioning of living systems: plants, animals, and microorganisms. Finally, we gave examples of modern methods used to remediate degraded landscapes and reclaim disturbed lands, including the latest technologies based on the integration of plants and microorganisms.

Keywords: Technogenic landscapes, heavy metals, pollutants, phytoremediation, remediation, mycorrhizal fungi, rhizogenic microorganisms

Funding: This work was part of the state assignment on "Developing approaches to phytoremediation of post-technogenic landscapes using "omix" technology plant growth promoting rhizobacteria (PGPB)"; supplementary agreement No. 075-03-2021-189/4 dated 30.09.2021 (internal No. 075-GZ/H4140/679/4). The research was conducted on the equipment of the Research Equipment Sharing Center of Kemerovo State University.

Please cite this article in press as: Drozdova MYu, Pozdnyakova AV, Osintseva MA, Burova NV, Minina VI. The microorganism-plant system for remediation of soil exposed to coal mining. Foods and Raw Materials. 2021;9(2):406–418. https://doi.org/10.21603/2308-4057-2021-2-406-418.

INTRODUCTION

Areas of anthropogenically transformed soils continue to expand throughout the world. Soil transformation is caused by degradation or complete destruction of topsoil as a result of deforestation, wind and water erosion, pesticide pollution, mining, industrial and civil construction, and growing urbanization [1–6].

Russia accounts for 15% of coal production and export in the world [7]. One of its regions, Kemerovo Oblast-Kuzbass, has about 100 coal mines, of which half are open-pit mines. In the first half of 2021, it produced 116.84 million tons of high-quality coal, up 8% from the previous year.

Extraction of coal and other minerals transforms topsoil drastically, especially in case of opencast mining.

Drilling and blasting are accompanied by enormous dust emissions that contain toxic pollutants, including heavy metals and carcinogenic gas (benzo(a)pyrene) [8–15]. Large amounts of methane and carbon dioxide released into the atmosphere have a greenhouse effect and change the thermal regime, vegetation, and topsoil of the area. All this exacerbates health problems, such as a growth in oncological and cardiovascular diseases, as well as congenital malformations [16].

Active mining causes a serious ecological imbalance. In particular, it transforms or destroys natural landscapes and creates new anthropogenic forms with different physical, chemical, and biological properties. According to Rosprirodnadzor (Russia's environmental watchdog), the country had 194 225 hectares of disturbed lands by 2019. Back in 2015, the Center for Hygiene and Epidemiology in Kemerovo Oblast and the Kemerovo Center for Hydrometeorology and Environmental Monitoring confirmed a strong correlation between increased coal mining, industrial production, and total emission of pollutants into the air. They identified eight ecologically vulnerable districts: Yaysky, Topkinsky, Tisulsky, Leninsk-Kuznetsky, Guryevsky, Prokopyevsky, Novokuznetsky, and Mezhdurechensky.

The above factors call for research that applies modern methods to monitor technogenic landscapes and introduce the latest complementary technologies for their remediation [17–21]. This can be done by using living systems: plants and soil animals and microorganisms. Of great importance are plant-microbial complexes: arbuscular ecto- and endomycorrhizae, symbiotic associations of plants and nitrogen-fixing prokaryotes, as well as rhizobial and cyanobacterial symbioses.

Our aim was to assess the use of soil and rhizosphere microorganisms for remediating technogenic soils in Russia's coal-mining regions.

STUDY OBJECT AND METHODS

We studied the scientific articles published over the past five years, as well as those cited in Scopus and Web of Science.

RESULTS AND DISCUSSION

The Institute of Soil Science and Agrochemistry (Siberian Branch of the Russian Academy of Sciences) has developed theoretical and practical foundations for improving the methods of recultivating technogenic soils [3]. Unfortunately, the geobotanical approach to disturbed territories still prevails, with reclamation of dumps by pine trees or perennial grasses [22]. Along with that, it is important to scientifically substantiate the latest reclamation technologies, taking into account the biosystems of undisturbed soils in a particular geographical zone.

Until 2000, external dumps had been selectively formed during the exploitation of coal deposits. Overburden was selectively placed into the body of the dump. This method of reclamation was used to ensure the rational use of the area's land and develop a harmonious anthropogenic landscape that met the ecological, socioeconomic, and sanitary requirements by using the fertile soil layer and potentially fertile species.

Today, this method is not as common. The biological stage of forest and agricultural reclamation is not effective due to the water regime and, consequently, insufficient moisture supply to the biota. Low moisture in the root layer and the presence of highly toxic heavy metals and other pollutants result in poor survival among trees and poor germination of perennial grass seeds.

Irreversible soil degradation caused by technogenesis may have severe consequences for living systems. Of great concern is chemical pollution of landscapes, especially with heavy metals that are deposited and adsorbed in soil [23–27]. When the contents of metals exceed the ecological capacity or change the redox potential (pH), pollutants are released. The human body contains 81 out of 92 elements found in nature, of which 15 are vital (Fe, I, Cu, Zn, Co, Cr, Mo, Ni, V, Se, Mn, As, F, Si, and Li) and four are conditionally essential (Cd, Pb, Sn, and Rb). They were found in low concentrations in plant and animal tissues, but they are highly dangerous for human health even in the smallest amounts [28]. Almost all regions of the world have a chemically "aggressive" environment. However, biochemical anomalies are more common in the zones of industrial development of natural landscapes, during mineral extraction, and in urban industrial agglomerations. Agrogenic lands are polluted through excessive use of pesticides [29].

According to Li *et al*., mining operations in China resulted in increased copper and cadmium contents in the soil used to grow rice. The environmental load changed in decreasing order from lead to chromium: Pb > Cd > Ni > As > Zn > Cu > Cr [30]. Moreover, lead, chromium, and cadmium exceeded the maximum permissible concentrations in crop production 2–8 times [31, 32]. Lead has the longest period of clearance from the soil-plant system. Plants receive its excessive quantities from soil. As a result, lead inhibits their respiration, suppresses photosynthesis, and sometimes increases the amount cadmium, while decreasing the intake of zinc, calcium, phosphorus, and sulfur.

It has also been found that during coal transportation, many pollutants are deposited on the transport routes along with dust. Heavy metals accumulate in soils for a long time. Their excessive amounts affect plant growth, metabolism, physiology, and aging. Plants have stress control mechanisms responsible for maintaining homeostasis of the basic metals that they require. These mechanisms make plants tolerant to metal contamination by forming less toxic metal complexes with active metabolites excreted through the root system. Other mechanisms are triggered by specific stress [31].

Arsenic is the most dangerous inorganic substance. It does not immediately cause symptoms of poisoning in animals, but its concentrations in their blood, hair, hooves, and urine remain high in contaminated areas. It belongs to a special group of conditionally essential elements since it acts at the ionic level or as part of nonspecific molecules or ions that penetrate the organism of living systems.

Heavy metals in soil have a detrimental effect on living organisms as a result of bioaccumulation and biomagnification [33]. Due to their impact on physiological and biochemical processes, most pollutants are toxic to plants [34]. The extent of toxicity depends on their content in soil, which can vary from 1 to 100 000 mg/kg [35, 36]. Heavy metals are also dangerous because they can replace the ions of the main metals that living systems and humans need [37, 38]. This disturbs metabolic processes and biochemical reactions during food consumption and removes metabolites from the body. Excessive accumulation of heavy metals causes protein compounds to break down at the molecular level, ruptures peptide bonds, increases free radicals, and severely damages vulnerable organs (brain, kidneys, liver, and blood vessels).

Phytoremediation is a well-known method of cleaning contaminated soil by extracting pollutants through the roots of trees, shrubs, and herbaceous plants [17, 39]. The results depend on the plants' tolerance to pollutants, the volume of biomass, and the efficiency of pollutant transportation from roots to shoots. Absorbed by the root system of plants, toxic elements accumulate in their tissues and are subsequently decomposed or converted into safer forms [40].

Russian and foreign researchers have recently developed efficient technologies to improve soil by physical and chemical methods [10–14]. For example, scientists in Kemerovo Oblast have proposed combining a bioorganic remediation agent from industrial waste with a technical agent to improve soil physicochemically and obtain a pollutant-free biomass of perennial grasses [41]. In another study, Altunina *et al.* developed a land reclamation method based on biocryogels. They have high porosity, good mechanical strength, stability in any biotechnological environment, and thermal resistance. Plants in cryostructured soil develop a good root system and do not inhibit soil microflora (www.ipc.tsc.ru).

Soil can also be remediated by sorbents produced from environmentally friendly materials, such as humic acids from naturally oxidized coals [25]. The cleaning mechanism is based on the introduction of reaction centers into the composition of humic acids to bind with metal ions.

A mixture of dry lime and sapropel (5:1) can be used as an active natural sorbent. It is applied evenly to the surface of soil contaminated with heavy metals in an amount of 0.5–1.5 t/ha in early spring. The sorbent improves the redox potential (pH) and the soil's absorbing capacity. Increased amounts of mineral and organomineral colloids contributes to active accumulation and long-term immobilization (3–5 years) of toxicants in the humus horizon, preventing the migration of heavy metals to other ecosystem components (patent RU 2655215C1).

Many studies report using groups of microorganisms with different biological functions to remove heavy metals, radionuclides, and organic compounds from soils. Microbiota used to clean soils, wastewater, bottom sediments, and overburden from pollution are able to extract elements and compounds from adjacent environments, convert them into less hazardous waste products or transport them to plant tissues as nutrition. The most efficient groups of microorganisms are those with high symbiotic activity in relation to plants of different classes, families, genera, and species.

Structurally largest is a group of arbuscular mycorrhiza with characteristic morphological structures in the cells of the root cortex and some mycotallia in the form of arbuscules or vesicles [12]. It has been established that by interacting with arbuscular mycorrhiza, host plants are often actively nourished with nitrogen and phosphorus [11, 13]. Just as important are groups of proteobacteria from the genera *Agrobacterium*, *Azospirillum*, *Azotobacter*, *Burkholderia*, *Bradyrizobium*, *Enterobacter*, *Pseudomonas*, *Klebsiella*, *Rizobium* (Gram-negative), *Bacillus*, *Brevibacillus*, *Paenibacillus* (Gram-positive), as well as Gram-positive actinomycetes (*Rhodococcus*, *Streptomyces*, *Arhtrobacter*).

Mycorrhizal chains can form in soil to transport and exchange various substances, including mineral forms of nitrogen, phosphorus, and organic forms of C3 and C4 plants. Many representatives of the above genera produce phytohormones, vitamins, and bioactive substances that stimulate plant growth, inhibit phytopathogenic diseases and harm from insects, and increase the tolerance to soil salinity, air and soil drought, and oxidative stress [12–16, 22–26]. Mycorrhizal chains are also involved in the removal of toxic elements by precipitating or accumulating them both inside cells and in the extracellular space. The activity of mycorrhizal networks is strongly influenced by soil animals: mites, amoeba, collembola, lumbricids, and others [42, 43].

Mycorrhiza can be identified in plant groups and communities in any ecological zone of the world. Their development depends on abiotic and biotic factors, such as moisture and heat supply of the soil and atmosphere, altitudes above sea level, atmospheric pressure, variety of vegetation, and the presence of phytopathogenic infection or harmful animals (invertebrates and vertebrates). These factors are interdependent and can exert varying degrees of environmental pressure on the development of mycorrhizal networks in the rhizoplane of plants. Mycorrhiza has been identified in 44% of bryophytes, 52% of ferns, 100% of gymnosperms, and 85% of flowering plants. However, it has not been

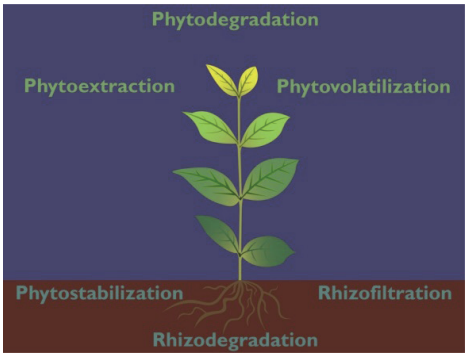

Figure 1 Basic phytoremediation processes [44–50]

found in the families *Caryophyllaceae*, *Cyperaceae*, *Brassicaceae*, *Chenopodiaceae*, and others.

Well studied is the interaction of plants and nitrogen-fixing prokaryotes at the level of symbiotic, associative, and non-symbiotic nitrogen fixation. Lack of nitrogen in the soil limits the bioproductivity of many plant species. Plants absorb nitrogen from the soil in the form of nitrates, ammonium, and amino acids that are available to them as a result of the microbiological destruction of organic litter (leaves, branches, fruits, etc.) or nitrogen fixation. Symbiotic nitrogen fixation occurs in specialized structures of plants. Associative nitrogen fixation takes place in the rhizoplane or rhizosphere of roots and on the surface of leaves. Non-symbiotic nitrogen fixation occurs through external sources of organic matter or photosynthesis in cyanobacteria.

The type of rhizobial symbiosis is associated with prokaryotes of the order *Rhizobiales* and plants from the *Fabaceae* family and *Ulmaceae* family (*Parasponia* ssp.). Thanks to the short-lived nitrogen-fixing nodules on the plant roots, they are able to collect up to 450–550 kg/ha of nitrogen per year. These bacteria are active in wide pH ranges (5.0–8.5). In Siberia, active nitrogen-fixing nodules can be found on many species of clover, astragalus and other plants.

Actinorhizas of the order *Frankia* come into symbiosis with over 200 species of dicotyledonous plants, including woody ones. These long-lived root nodules collect up to 225 kg/ha of nitrogen per year. They can grow on pioneer substrates and easily function even in acidic boggy soils.

Cyanobacteria are mainly of the *Nostoc* genus and sometimes of the *Anabaena* genus. They are localized in the *Azolla* L. cavity, in intercellular spaces of cycad bark, on plant stems, and leaf petioles. Moisture and heat are the main conditions for their activation. Maximum nitrogen fixation is up to 720 kg/ha in Australia and much less in the boreal zone.

Actinorhizal plants are of the families *Betulaceae*, *Elaefgnaceae*, *Rozaceae*, *Datiscaceae*, *Ramnaceae* and other species. Flowering plants that come into symbiosis with cyanobacteria belong to the *Gunneraceae* genus and are common for the southern hemisphere. Cyanobacteria function mainly under aerobic conditions and can use their own photosynthesis or sources of organic matter.

Any type of symbiosis between plants and microorganisms can be used to clean the soil from pollutants. Figure 1 shows the main soil phytoremediation processes using microorganisms as plant symbionts.

Table 1 shows the main stages and processes in the plant during the transformation of toxicants [35, 44–49].

Plants and microorganisms can be mutually beneficial, which gives them an advantage in surviving critical conditions. Microorganisms stimulate the plant's growth and, at the same time, transform soil pollutants into a more accessible form.

Pollutant-resistant bacteria and fungi can be isolated from the rhizosphere of pollution-resistant plants [51]. They are of particular value for biotechnologies to remediate lands contaminated with heavy metals and toxic organic compounds [52]. Table 2 shows strains of microorganisms that are currently of practical interest in the rehabilitation of lands contaminated by active industrial development and are of strategic importance for the economic development of Russian regions [16, 53–67].

In addition to the strains listed in Table 2, more active consortia can be created to produce new soil varieties that are effective and safe for the biota of microbial communities, plants, and soil animals. Such

Table 1 Pollutant transformation processes in plants

Stages	Process description
Rhizofiltration	Pollutants are adsorbed by plant roots with a developed fibrous system. Plants secrete special organic compounds in order to attract microbial communities [44].
Rhizodegradation	Harmful substances are decomposed by various microorganisms, including bacteria, fungi, and yeast, which live in the plant's root system. This process removes such contaminants as pesticides, oil, and PCBs [45, 46].
Phytostabilization	Harmful substances are immobilized in the soil and prevented from entering groundwater and then the food chain. Stabilization is enabled by pollutants sorption in the plant's rhizosphere [47].
Phytovolatilization	Plants convert pollutants into volatile forms that enter the atmosphere [48].
Phytodegradation	Organic substances are biodegraded in the plant under the action of various enzymes such as peroxidase, dehalogenase, nitroreductase, and others [35, 49].
Phytoextraction	The plant's roots accumulate toxicants which then enter its aerial parts [35].

Table 2 Microorganisms for remediation of transformed soils

Microorganisms	Source of extraction	Positive effect on the plant	Reference
Rhizobacteria:			
Cellulosimicrobium 60I1 and *Pseudomonas* 42P4	*Capsicum annuum* L.	Increased growth rate, protection against abiotic stress	[53]
Pseudomonas stutzeri Pr7 and *Bacillus toyonensis* Pr8	*Prunus domestica* L.	Increased growth rate, antifungal activity, improved disease resistance	[54]
Brevibacterium frigoritolerans (AIS-3), *Alcaligenes faecalis* subsp. *Phenolicus* (AIS-8) and *Bacillus aryabhattai* (AIS-10)	*Crocus sativus* L.	Increased growth rate, antifungal activity	[55]
Pseudomonas alcaliphila and *Pseudomonas hunanensis*	*Ocimum basilicum* L.	Improved growth	[56]
B. aryabhattai MS3	Rice root zone	Resistance to salt stress and iron restriction	[57]
Pseudomonas toyotomiensis ND1 (E), *Microbacterium resistens* ND2 (G), and *Bacillus pumilus.* train ND3 (I)	*Lepironia articulata* L.	Biodegradation of polycyclic aromatic hydrocarbons	[58]
Aeromonas taiwanensis isolate 5E, *Bcillus* sp. isolate 7G, *Bacillus cereus* isolate 8H and 3Ca, *Bacillus velezensis* isolate 9I, *Bacillus proteolyticus* isolate 4D, *Bacillus stratosphericus* isolate 14N, *Bacillus megaterium* isolate 11K, *Pseudomonas* sp. isolate 12L, *Enterobacter cloacae*	*Scirpus grossus* L.	Improved disease resistance	[59]
Pseudomonas aeruginosa	Arable land exposed to industrial effluent	Resistance to oxidative stress, increased chlorophyll content, improved growth, zinc resistance	[60]
Enterobacter ludwigii (HG2) and *Klebsiella pneumoniae*	Rhizosphere of plants from contaminated areas	Improved growth, resistance to mercury-caused oxidative stress	[61]
Consortium of cyanobacteria: *Calothrix* sp. and *Anabaena cylindrica* and rhizobacteria: *Chryseobacterium balustinum*, *Pseudomonas simiae*, and *Pseudomonas fluorescens*	Irrigated field horizon	Improved growth	[62]
Rhizobia:			
alpha proteobacteria from the genera *Rhizobium* and *Ensifer*	*Mimosa* spp.	Nitrogen fixation	[63]
Sinorhizobium medicae	*Medicago sativa* L.	Nitrogen fixation	[64]
Rhizobium leguminosarum bv. *Trifolii*	*Trifollium* spp.	Nitrogen fixation	[64]
Mycorrhizal fungi:			
42 genera of endophytic fungi, with a prevalence of *Chaetomium* spp. and *Fusarium* spp.	Blueberry	Improved growth	[65]
Glomus versiforme and *Rhizophagus intraradices*	*Zea mays* L.	Resistance to cadmium-caused oxidative stress	[66
Funneliformis mosseae, *R. intraradices*	*Trifolium repens* L.	Improved growth, resistance to copper-caused oxidative stress	[67]

consortia improve the soil's bioactivity and ecological functions.

Soil bioremediation by plants. All plants assimilate very small quantities of copper, manganese, iron, nickel, and zinc. Along with this, there are plants that are capable of absorbing highly toxic heavy metals, such as cadmium, arsenic, lead, mercury, and others, without serious damage to their growth. They are called hyperaccumulators and are able to accumulate pollutants in large quantities without signs of phytotoxicity in the aerial parts of plants. Metal hyperaccumulators absorb at least 100 mg/kg of arsenic and cadmium and 1000 mg/kg of cobalt, copper, chromium, manganese, nickel, and lead. These plants include *Pteris vittata*, *Bidens pilosa*, *Jatropha curcas*, and *Helianthus annuus* [68–71]. They can resist the harmful effects of heavy metals by accumulating and suppressing them inside cells.

Exposure to toxicants changes the expression of genes responsible for the synthesis of transporter proteins that capture and transfer metals [72]. In Siberia, and Kemerovo Oblast in particular, *H. annuus* is the most available plant of those listed. There are several families of genes responsible for metal transport. These include macrophage proteins (Nramps), heavy metal ATPases, cation diffusion catalysts (CDFS), cationic antiporters, Zn-regulated transporter (ZRT), and the ZIP family [73].

Pollutants are adsorbed by plants in two ways – by symplastic and apoplastic transport. In the case of symplastic transport, heavy metals diffuse into the

roots' endothermal cells through the plasma membrane. Ions can be transported by such carriers as proteins or organic acids, e.g., oxalic acid in combination with aluminum. In the case of apoplastic transport, metals are located in the free space between cells in non-cationic forms [39]. Special carrier proteins help pollutants to diffuse across the plasma membrane. There are special carriers for iron, zinc, and other metals [72, 74]. Various substances produced by plants, such as metallothioneins, glutathione, and phytochelatins, bind metal ions and are transported to vacuoles or shoots [74].

In hyperaccumulator plants, chelates are transported to shoots by membrane proteins: MATE, ATPase, and oligopeptide carrier proteins [72]. There, they are stored in vacuoles of parenchymal and epidermal leaf cells, which occupy 60 to 95% of the cell volume [75].

The problem with toxicant absorption by plants is that not all metals are absorbed in equal amounts. Cadmium and zinc are more readily available, which depends on the mobility of metal ions. Therefore, for better assimilation of elements, the soil conditions need to be adjusted, namely redox potential (pH) and temperature. In addition to these factors, plants themselves create conditions for better absorption of heavy metals. In particular, they secrete phytosiderophores and carboxylates, as well as acidify the rhizosphere for better release of ions from the soil [73].

Soil bioremediation by microorganisms. Microorganisms use various mechanisms for the transformation of pollutants. To survive in toxic environments, they transform compounds into safer substances. Thus, toxicants can be removed both inside and outside the plant's cells and tissues. To neutralize pollutants, microorganisms generate substances that are released into the environment and enhance the processes of cleaning soil from pollutants [76].

Some bacteria (*P. aeruginosa*, *P. fluorescens*, *Haemophilus* spp.) use various cellular enzymes (laccases, peroxidases, phosphatases, nitrilases, nitroreductases, etc.) and are therefore effective in soil remediation [77].

Soil contaminants can be retained through their attachment to the membrane of a microorganism or absorption by inclusions in the form of bodies [78, 79]. At the intra- and extracellular level, toxic chemical compounds can be immobilized through the formation of minerals.

Another important mechanism for soil remediation is using microorganisms to generate exopolymer substances. For example, polysaccharides bind pollutants and they can be simultaneously removed from polluted environments during flocculation. The composition and properties of such polymers depend on the factors listed above, as well as the availability of various useful substances and the contents of salts and heavy metals in the soil [80].

Interaction between plants and microorganisms for bioremediation. An effective mechanism for cleaning transformed landscapes is to use microorganisms that promote plant growth in a polluted environment. They help capture nitrogen and create phytohormones, as well as produce antibiotics for plant protection. For example, introducing *Sinorhizonium meliloti* in the zone of plant roots increases the level of photosynthetic proteins.

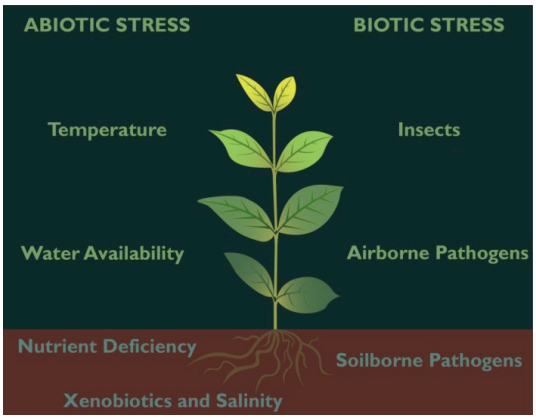

Figure 2 Interaction of plants with biotic and abiotic factors

Figure 2 shows the influence of biotic and abiotic factors on plants.

Bacteria help plants survive under stress conditions (drought, nutritional deficiencies, toxicants). Their survival is facilitated by metabolites such as amino acids, isoflavonoids, flavonoids, and fatty acids. Bacteria can reproduce in mycorrhizal and non-mycorrhizal roots. In a stressful environment, they stimulate the production of special transport proteins and chaperones by plants. For example, the GroEL and DnaK proteins benefit the body under such stress conditions as temperature, drought, and exposure to toxicants [51].

Intensive plant growth is due to bacteria's ability to produce substances such as auxin, cytokinin, gibberellin, hydrogen cyanide, siderophores, indoleacetic acid, and others [81]. In addition, rhizobacteria are able to prevent the effects of unwanted pathogens and insects [79]. Host plants help these bacteria reproduce by providing them with bioactive substances (flavonoids, glycosides, fatty acids, and others) [82].

Prospects for using the microorganism-plant system for soil decontamination. The benefit of the microorganism-plant system is in reducing the anthropogenic impact on both industrially transformed landscapes and agrogenic soils.

Heavy metals pose a great danger to human and animal health. Pinter *et al.* found that phytoremediation was enhanced by a combined use of As-resistant grapevine species and microorganisms such as *Bacillus licheniformis*, *Micrococcus luteus* and *P. fluorescens*. This activated siderophore production, phosphate solubilization, and nitrogen fixation [83].

In another study, Jiang *et al.* isolated microorganisms that improve plant adaptation to the environment from

the rhizosphere of plants growing in polluted areas of chemical and oil refineries. In particular, they isolated *Pseudomonas*, *Cupriavidus*, and *Bacillus* from the rhizosphere of *Boehmeria nivea*. These bacteria are resistant to $Pb^{2+} > Zn^{2+} > Cu^{2+} > Cd^{2+}$ and therefore help plants survive in the soil with high concentrations of heavy metals [84].

Jiang *et al.* studied the effect of arbuscular mycorrhizal fungi *G. versiforme* and *R. intraradices* on the growth, Cd absorption, and antioxidant properties of Japanese honeysuckle (*Lonicera japonica* L.). They found a decreased concentration of cadmium in the plant's shoots and roots. Mycorrhizal fungi increased the biomass of shoots and roots, contributed to the accumulation of phosphorus, and activated such enzymes as catalase (CAT), ascorbate peroxidase (APX), glutathione reductase (GR), and others [85].

A promising symbiosis for soil remediation is between hyperaccumulators, grain crops, and mycorrhizal fungi. Studies by Yang *et al.* showed that a combined use of rice crops, hyperaccumulator *Solanum nigrum* L., and arbuscular mycorrhiza lowered the concentration of cadmium in this strategic culture to 64.5%. Low bioaccumulation was also due to decreased expression of the *Nramp5* gene and decreased activation of the *HMA3* gene in rice roots. In addition, a decline in pH was observed in the plant's rhizosphere. These studies are promising for agricultural production [86].

In another study, pepper (*C. annuum* L.) was inoculated with arbuscular mycorrhizal fungi *F. mosseae* and *R. intraradices* in the soil that contained copper (8 mM). It resulted in a high accumulation of dry biomass and a large leaf area (30 and 50%, respectively) [67].

The presence of arsenic in groundwater can have negative consequences. Mallick *et al.* identified a microbial consortium of resistant halophilic strains *Kocuria flava* AB402 and *Bacillus vietnamensis* AB403 from the rhizosphere of mangrove thickets. These microorganisms were resistant to arsenic concentrations from 20 to 35 mM. Also, the consortium adsorbed arsenic both inside cells and on the surface of biofilms. The strains facilitated better germination of rice seedlings and reduced toxicity [87].

Lyubun and Chernyshova studied the influence of *Aeromonas* sp. MG3, *Alcaligenes* sp. P2, *Acinetobacter* sp. K7, and *Azospirillum brasilense* Sp245 on the growth of, and arsenic absorption by, various plants. In particular, they selected sugar sorghum (*Sorghum saccharatum* L.), Sudan grass (*Sorghum sudanense* L.) and sunflower (*H. annuus* L.). The addition of arsenic had a negative effect of the plants' growth and development, reducing their biomass and height by 30–50%. However, their bioproductivity was restored by the rhizobacteria introduced into the soil. In particular, the use of *A. brasilense* Sp245 and *Acinetobacter* sp. K7 reduced the level of arsenic in the sunflower biomass [88].

Well studied is the positive effect of legumes and rhizobia on plant resistance to pollutants. Current studies are looking for new combinations with rhizobacteria. For example, a combined use of *P. mucilaginosus* rhizobacteria and *S. meliloti* rhizobia resulted in the absorption of copper by alfalfa. The microorganisms decreased lipid peroxidation and radicals accumulation, improving the plant's antioxidant properties and survival rate. In addition, the consortium enhanced the biochemical properties of the soil, contributing to increased contents of nitrogen, available phosphorus, and organic matter. Finally, the rhizosphere microorganisms became more diverse [89].

Shen *et al.*, who used *M. sativa* L. together with rhizobia and urea (nitrogen source) observed the plant's resistance to copper. Nitrogen content was the dominant factor of the pollutant's absorption. The scientists concluded that the combination of rhizobia with urea had a beneficial effect on soil remediation. As a result, copper consumption was 89.3% higher in the shoots and 1.5 times as high in the roots, compared to the control. In addition, rhizobia improved the plant's tolerance to oxidative stress, activated catalase, superoxide dismutase, and peroxidase in the roots and shoots, and increased the content of chlorophyll in the green organs [90].

In another study, castor bean was cultivated on a substrate saturated with lead and zinc, which resulted in a significantly smaller root surface area. The plant's inoculation with a bacterial mix, including phosphate-solubilizing *Actinobacteria*, contributed to its growth and good development of the root system, regardless of the presence of lead or zinc [91].

An association of arbuscular mycorrhizal fungi can also be effective in the phytoremediation of soil contaminated with hexavalent chromium [92]. Kullu *et al.* have found that *Rhizophagus irregularis* promotes the bioaccumulation of chromium by *Brachiaria mutica* (paragrass or buffalo grass). Fungal inoculation decreased the degree of soil contamination and made the pollutant more bioavailable for the plant. Mycorrhiza has a positive effect on plants growing in the soil contaminated with 60 mg/kg of hexavalent chromium. The experiment by Kullu *et al.* showed increased contents of carotenoids, chlorophyll, proline, protein, and protein-enzymes (ascorbate peroxidase, catalase, and glutathione peroxidase). In addition, the plant had improved electron transfer and photosynthetic characteristics. The scientists concluded that *R. irregularis* was compatible with the *B. mutica* population [93].

Islam and Yasmeen evaluated the effect of *P. aeruginosa* on wheat's resistance to oxidative stress caused by 1500 mg/kg of zinc. The study showed that adding the rhizobacteria to the plant's rhizosphere increased the content of antioxidant enzymes, phenolic compounds, and ascorbic acid. This reduced the pollutant's adverse effect on wheat biomass [60].

Another experiment determined the reaction of a consortium of *E. ludwigii* (HG 2) and *K. pneumoniae* (HG 3) to soil contamination with 75 μM of mercury.

This resulted in increased biomass and relative water content in wheat, compared to the control [61].

The above studies have shown the benefits of microbiological associations in remediating natural, agrogenic, and industrial lands destroyed or contaminated with heavy metals and organic toxicants.

CONCLUSION

Anthropogenic impact in industrially developed regions leads to complete transformation of natural landscapes. This has a negative effect on all living systems (plants, animals, and microbocenoses) and causes medical and social problems associated with an increased incidence of all diseases, including the most severe ones.

Our review of scientific literature revealed a variety of methods for soil reclamation and remediation. The most promising and accessible methods are those involving plant communities. Plants can utilize toxicants, convert them into less stable compounds or transfer them to mineral complexes.

Another promising method is to introduce consortia of various microorganisms into the plant's rhizoplane. This approach is effective due to symbiotic interaction. On the one hand, microorganisms convert hard-to-reach minerals and heavy metals into other forms digestible for plants. On the other hand, they actively use plant metabolites for their own life support.

Examples from scientific literature show that consortia can develop bioactive substances, vitamins, and phytohormones for living systems to increase their stress resistance to biotic and abiotic environmental factors.

Rhizobacteria, rhizobia, mycorrhizal fungi, and their consortia have proved to be the most efficient in technogenic land remediation.

CONTRIBUTION

The authors were equally involved in writing the manuscript and are equally responsible for plagiarism.

CONFLICT OF INTEREST

The authors declare that there is no conflict of interest.

REFERENCES

1. Dobrovol′skiy GV. Degradatsiya i okhrana pochv [Soil degradation and protection]. Moscow: Lomonosov Moscow State University; 2002. 654 p. (In Russ.).
2. Kudeyarov VN, Sokolov MS, Glinushkin AP. The soils of agrocenosis in Russia: current status, measures for improvement and rational use. Agrohimia. 2017;(6):3–11. (In Russ.). https://doi.org/10.7868/S0002188117060011.
3. Androkhanov VA, Kulyapina ED, Kurachev VM. The soils of technogenic landscapes: genesis and evolution. Novosibirsk: Siberian Branch of the RAS; 2004. 151 p. (In Russ.).
4. Androkhanov VA. Pochvenno-ehkologicheskoe sostoyanie tekhnogennykh landshaftov: dinamika i otsenka [Ecological state of technogenic landscapes: dynamics and assessment]. Novosibirsk: Siberian Branch of the RAS; 2010. 224 p. (In Russ.).
5. Belozertseva IA, Granina NI. Influence of investigation, extraction and processing of minerals on ground of Siberia. Fundamental research. 2015;(10–2):238–242. (In Russ.).
6. Baltic Sea hot spots – Hazards and possibilities for the Baltic Sea region. Coalition Clean Baltic; 2002. 47 p.
7. Yanovsky AB. Results of structural reorganization and technological reequipment of the coal industry of the Russian federation and objectives for prospective development. Ugol'. 2019;(8):8–16. http://doi.org/10.18796/0041-5790-2019-8-8-16.
8. Baştabak B, Gödekmerdan E, Koçar G. A holistic approach to soil contamination and sustainable phytoremediation with energy crops in the Aegean Region of Turkey. Chemosphere. 2021:276. https://doi.org/10.1016/j.chemosphere.2021.130192.
9. Fichtner A, von Oheimb G, Hardtle W, Wilken C, Gutknecht JLM. Effects of anthropogenic disturbances on soil microbial communities in oak forests persist for more than 100 years. Soil Biology and Biochemistry. 2014;70:79–87. https://doi.org/10.1016/j.soilbio.2013.12.015.
10. Homburg JA, Sandor JA. Anthropogenic effects on soil quality of ancient agricultural systems of the American Southwest. Catena. 2011;85(2):144–154. https://doi.org/10.1016/j.catena.2010.08.005.
11. Pundytė N, Baltrėnaitė E, Pereira P, Paliulis D. Anthropogenic effects on heavy metals and macronutrients accumulation in soil and wood of Pinus sylvestris L. Journal of Environmental Engineering and Landscape Management. 2011;19(1):34–43. https://doi.org/10.3846/16486897.2011.557473.
12. Wall DH, Nielsen UN, Six J. Soil biodiversity and human health. Nature. 2015;528(7580):69–76. https://doi.org/10.1038/nature15744.

13. Ye F, Ma MH, Wu SJ, Jiang Y, Zhu GB, Zhang H, et al. Soil properties and distribution in the riparian zone: the effects of fluctuations in water and anthropogenic disturbances. European Journal of Soil Science. 2019;70(3):664–673. https://doi.org/10.1111/ejss.12756.
14. Chen J, Liu Y-Q, Yan X-W, Wei G-H, Zhang J-H, Fang L-C. Rhizobium inoculation enhances copper tolerance by affecting copper uptake and regulating the ascorbate-glutathione cycle and phytochelatin biosynthesis-related gene expression in Medicago sativa seedlings. Ecotoxicology and Environmental Safety. 2018;162:312–323. https://doi.org/10.1016/j.ecoenv.2018.07.001.
15. Wang Y, Wang R, Fan L, Chen T, Bai Y, Yu Q, et al. Assessment of multiple exposure to chemical elements and health risks among residents near Huodehong lead-zinc mining area in Yunnan, Southwest China. Chemosphere. 2017;174:613–627. https://doi.org/10.1016/j.chemosphere.2017.01.055.
16. Mun SA, Zinchuk SF. Assessment of environmentally dangerous areas and cancer morbidity in the Kemerovo region depending on the air pollution. Modern problems of science and education. 2015;(6). (In Russ.).
17. Gomes HI, Dias-Ferreira C, Ribeiro AB. Electrokinetic remediation of organochlorines in soil: Enhancement techniques and integration with other remediation technologies. Chemosphere. 2012;87(10):1077–1090. https://doi.org/10.1016/j.chemosphere.2012.02.037.
18. Kambo HS, Dutta A. A comparative review of biochar and hydrochar in terms of production, physico-chemical properties and applications. Renewable and Sustainable Energy Reviews. 2015;45:359–378. https://doi.org/10.1016/j.rser.2015.01.050.
19. Trujillo-Reyes J, Peralta-Videa JR, Gardea-Torresdey JL. Supported and unsupported nanomaterials for water and soil remediation: Are they a useful solution for worldwide pollution? Journal of Hazardous Materials. 2014;280:487–503. https://doi.org/10.1016/j.jhazmat.2014.08.029.
20. Wang Y, Luo Y, Zeng G, Wu X, Wu B, Li X, et al. Characteristics and in situ remediation effects of heavy metal immobilizing bacteria on cadmium and nickel co-contaminated soil. Ecotoxicology and Environmental Safety. 2020;192. https://doi.org/10.1016/j.ecoenv.2020.110294.
21. Xu J, Bravo AG, Lagerkvist A, Bertilsson S, Sjöblom R, Kumpiene J. Sources and remediation techniques for mercury contaminated soil. Environment International. 2015;74:42–53. https://doi.org/10.1016/j.envint.2014.09.007.
22. Murzakmatov RT, Shishikin AS, Borisov AN. Specifics of stand formation at coalmine dumps in forest-steppe zone. Siberian Journal of Forest Science. 2018;(1):37–49. (In Russ.). https://doi.org/10.15372/SJFS20180104 .
23. Mandal P. An insight of environmental contamination of arsenic on animal health. Emerging Contaminants. 2017;3(1):17–22. https://doi.org/10.1016/j.emcon.2017.01.004.
24. Pandey P, Dubey RS. Metal toxicity in rice and strategies for improving stress tolerance. In: Hasanuzzaman M, Fujita M, Nahar K, Biswas JK, editors. Advances in rice research for abiotic stress tolerance. Woodhead Publishing; 2019. pp. 313–339. https://doi.org/10.1016/B978-0-12-814332-2.00015-0.
25. Nevedrov NP, Dyukanova EN, Nevedrova NYu. The concentration of heavy metals in the superficial horizons of soils in functional areas in Kursk cenourban agglomeration. Belgorod State University Scientific Bulletin. Natural Sciences. 2016;35(11):139–145. (In Russ.).
26. Nejad ZD, Jung MC, Kim K-H. Remediation of soils contaminated with heavy metals with an emphasis on immobilization technology. Environmental Geochemistry and Health. 2018;40(3):927–953. https://doi.org/10.1007/s10653-017-9964-z.
27. Il′in VB, Syso AI. Mikroehlementy i tyazhelye metally v pochvakh i rasteniyakh Novosibirskoy oblasti [Trace elements and heavy metals in soils and plants of the Novosibirsk Region]. Novosibirsk: Siberian Branch of the RAS; 2001. 231 p. (In Russ.).
28. Pronina NB. Ehkologicheskie stressy (prichiny, klassifikatsiya, testirovanie, fiziologo-biokhimicheskie mekhanizmy) [Environmental stresses (causes, classification, testing, physiological and biochemical mechanisms)]. Moscow: MSKHA; 2000. 310 p. (In Russ.).
29. Selyukova SV. Heavy metals in agrocenoses. Achievements of Science and Technology in Agro-Industrial Complex. 2020;34(8):85–93. (In Russ.). https://doi.org/10.24411/0235-2451-2020-10815.
30. Li H, Xu W, Dai M, Wang Z, Dong X, Fang T. Assessing heavy metal pollution in paddy soil from coal mining area, Anhui, China. Environmental Monitoring and Assessment. 2019;191(8). https://doi.org/10.1007/s10661-019-7659-x.
31. Li F, Li X, Hou L, Shao, A. Impact of the coal mining on the spatial distribution of potentially toxic metals in farmland tillage soil. Scientific Reports. 2018;8(1). https://doi.org/10.1038/s41598-018-33132-4.
32. Xiuzhen T, Changyuan T, Pan W, Chipeng Z, Zhikang W. Distribution and food exposure risk assessment of heavy metals immature rice on the coal mining area Guizhou TAO. Ecology and Environmental Sciences. 2017;(26):1216–1220.

33. Szynkowska MI, Pawlaczyk A, Maćkiewicz E. Bioaccumulation and biomagnification of trace elements in the environment. In: Chojnacka K, Saeid A, editors. Recent advances in trace elements. Wiley Blackwell; 2018. pp. 251–276. https://doi.org/10.1002/9781119133780.ch13.
34. Ghori N-H, Ghori T, Hayat MQ, Imadi SR, Gul A, Altay V, et al. Heavy metal stress and responses in plants. International Journal of Environmental Science and Technology. 2019;16(3):1807–1828. https://doi.org/10.1007/s13762-019-02215-8.
35. Ashraf S, Ali Q, Zahir ZA, Ashraf S, Asghar HN. Phytoremediation: Environmentally sustainable way for reclamation of heavy metal polluted soils. Ecotoxicology and Environmental Safety. 2019;174:714–727. https://doi.org/10.1016/j.ecoenv.2019.02.068.
36. Asati A, Pichhode M, Nikhil K. Effect of heavy metals on plants: An overview. International Journal of Application or Innovation in Engineering and Management. 2016;5(3):56–66.
37. Morcillo P, Esteban MÁ, Cuesta A. Heavy metals produce toxicity, oxidative stress and apoptosis in the marine teleost fish SAF-1 cell line. Chemosphere. 2016;144:225–233. https://doi.org/10.1016/j.chemosphere.2015.08.020.
38. Wijayawardena MAA, Megharaj M, Naidu, R. Exposure, toxicity, health impacts, and bioavailability of heavy metal mixtures. Advances in Agronomy 2016;138:175–234. https://doi.org/10.1016/bs.agron.2016.03.002.
39. Shah V, Daverey A. Phytoremediation: A multidisciplinary approach to clean up heavy metal contaminated soil. Environmental Technology and Innovation. 2020;18. https://doi.org/10.1016/j.eti.2020.100774.
40. Ansari AA, Naeem M, Gill SS, AlZuaibr FM. Phytoremediation of contaminated waters: An eco-friendly technology based on aquatic macrophytes application. Egyptian Journal of Aquatic Research. 2020;46(4):371–376. https://doi.org/10.1016/j.ejar.2020.03.002.
41. Petunkina LO, Zaushintsena AV, Shatilov DI. Optimizatsiya v sootnoshenii rekul′tivantov dlya tselevogo ispol′zovaniya na ugledobyvayushchem predpriyatii [Optimal ratios of recultivators for targeted use at a coal mining enterprise]. Ehkologicheskie problemy promyshlenno razvitykh i resursodobyvayushchikh regionov: puti resheniya. Sbornik trudov Vserossiyskoy molodezhnoy nauchno-prakticheskoy konferentsii [Environmental problems of industrially developed and resource regions: solutions. Proceedings of the All-Russian Youth Scientific and Practical Conference]; 2016; Kemerovo. Kemerovo: T.F. Gorbachev Kuzbass State Technical University; 2016. (In Russ.).
42. Smit SEh, Rid DDzh. Mikoriznyy simbioz [Mycorrhizal symbiosis]. Moscow: Publishing House KMK; 2012. 776 p. (In Russ.).
43. Wang B, Qiu Y-L. Phylogenetic distribution and evolution of mycorrhizas in land plants. Mycorrhiza. 2006;16(5):299–363. https://doi.org/10.1007/s00572-005-0033-6.
44. Patra DK, Pradhan C, Patra HK. Toxic metal decontamination by phytoremediation approach: Concept, challenges, opportunities and future perspectives. Environmental Technology and Innovation. 2020;18. https://doi.org/10.1016/j.eti.2020.100672.
45. Cristaldi A, Conti GO, Jho EH, Zuccarello P, Grasso A, Copat C, et al. Phytoremediation of contaminated soils by heavy metals and PAHs. A brief review. Environmental Technology and Innovation. 2017;8:309–326. https://doi.org/10.1016/j.eti.2017.08.002.
46. Yan L, Le QV, Sonne C, Yang Y, Yang H, Gu H, et al. Phytoremediation of radionuclides in soil, sediments and water. Journal of Hazardous Materials. 2021;407. https://doi.org/10.1016/j.jhazmat.2020.124771.
47. Radziemska M, Gusiatin ZM, Bilgin A. Potential of using immobilizing agents in aided phytostabilization on simulated contamination of soil with lead. Ecological Engineering. 2017;102:490–500. https://doi.org/10.1016/j.ecoleng.2017.02.028.
48. Limmer M, Burken J. Phytovolatilization of organic contaminants. Environmental Science and Technology. 2016;50(13):6632–6643. https://doi.org/10.1021/acs.est.5b04113.
49. Sharma P, Pandey AK, Udayan A, Kumar S. Role of microbial community and metal-binding proteins in phytoremediation of heavy metals from industrial wastewater. Bioresource Technology. 2021;326. https://doi.org/10.1016/j.biortech.2021.124750.
50. Wilson-Kokes L, Skousen J. Nutrient concentrations in tree leaves on brown and gray reclaimed mine soils in West Virginia. Science of the Total Environment. 2014;481:418–424. https://doi.org/10.1016/j.scitotenv.2014.02.015.
51. Sharma M, Sudheer S, Usmani Z, Rani R, Gupta P. Deciphering the omics of plant-microbe interaction: Perspectives and new insights. Current Genomics. 2020;21(5):343–362. https://doi.org/10.2174/1389202921999200515140420.
52. Tabassum B, Khan A, Tariq M, Ramzan M, Khan MSI, Shahid N, et al. Bottlenecks in commercialisation and future prospects of PGPR. Applied Soil Ecology. 2017;121:102–117. https://doi.org/10.1016/j.apsoil.2017.09.030.
53. Ureche MAL, Pérez-Rodriguez MM, Ortiz R, Monasterio RP, Cohen AC. Rhizobacteria improve the germination and modify the phenolic compound profile of pepper (*Capsicum annum* L.). Rhizosphere. 2021;18. https://doi.org/10.1016/j.rhisph.2021.100334.

54. Essalimi B, Esserti S, Rifai LA, Koussa T, Makroum K, Belfaiza M, et al. Enhancement of plant growth, acclimatization, salt stress tolerance and verticillium wilt disease resistance using plant growth-promoting rhizobacteria (PGPR) associated with plum trees (*Prunus domestica*). Scientia Horticulturae. 2022;291. https://doi.org/10.1016/j.scienta.2021.110621.

55. Rasool A, Mir MI, Zulfajri M, Hanafiah MM, Unnisa SA, Mahboob M. Plant growth promoting and antifungal asset of indigenous rhizobacteria secluded from saffron (*Crocus sativus* L.) rhizosphere. Microbial Pathogenesis. 2021;150. https://doi.org/10.1016/j.micpath.2021.104734.

56. AlAli HA, Khalifa A, Al-Malki M. Plant growth-promoting rhizobacteria from *Ocimum basilicum* improve growth of *Phaseolus vulgaris* and *Abelmoschus esculentus*. South African Journal of Botany. 2021;139:200–209. https://doi.org/10.1016/j.sajb.2021.02.019.

57. Sultana S, Alam S, Karim MM. Screening of siderophore-producing salt-tolerant rhizobacteria suitable for supporting plant growth in saline soils with iron limitation. Journal of Agriculture and Food Research. 2021;4. https://doi.org/10.1016/j.jafr.2021.100150.

58. Al Sbani NH, Abdullah SRS, Idris M, Hasan HA, Halmi MIE, Jehawi OH, et al. PAH-degrading rhizobacteria of *Lepironia articulata* for phytoremediation enhancement. Journal of Water Process Engineering. 2021;39. https://doi.org/10.1016/j.jwpe.2020.101688.

59. Kamaruzzaman MA, Abdullah SRS, Hasan HA, Hassan M, Othman AR, Idris M. Characterisation of Pb-resistant plant growth-promoting rhizobacteria (PGPR) from *Scirpus grossus*. Biocatalysis and Agricultural Biotechnology. 2020;23. https://doi.org/10.1016/j.bcab.2019.101456.

60. Islam F, Yasmeen T, Ali Q, Ali S, Arif MS, Hussain S, et al. Influence of *Pseudomonas aeruginosa* as PGPR on oxidative stress tolerance in wheat under Zn stress. Ecotoxicology and Environmental Safety. 2014;104(1):285–293. https://doi.org/10.1016/j.ecoenv.2014.03.008.

61. Gontia-Mishra I, Sapre S, Sharma A, Tiwari S. Alleviation of mercury toxicity in wheat by the interaction of mercury-tolerant plant growth-promoting rhizobacteria. Journal of Plant Growth Regulation. 2016;35(4):1000–1012. https://doi.org/10.1007/s00344-016-9598-x.

62. Kholssi R, Marks EAN, Miñon J, Mate AP, Sacristan G, Montero O, et al. A consortium of cyanobacteria and plant growth promoting rhizobacteria for wheat growth improvement in a hydroponic system. South African Journal of Botany. 2021;142;247–258. https://doi.org/10.1016/j.sajb.2021.06.035.

63. Bontemps C, Rogel MA, Wiechmann A, Mussabekova A, Moody S, Simon MF, et al. Endemic *Mimosa* species from Mexico prefer alphaproteobacterial rhizobial symbionts. New Phytologist. 2016;209(1):319–333. https://doi.org/10.1111/nph.13573.

64. Poole P, Ramachandran V, Terpolilli J. Rhizobia: from saprophytes to endosymbionts. Nature Reviews Microbiology. 2018;16(5):291–303. https://doi.org/10.1038/nrmicro.2017.171.

65. Guo X, Yuan L, Shakeel M, Wan Y, Song Z, Wang D. Screening of the plant growth-promoting mycorrhizal fungi in Guizhou blueberry. Rhizosphere. 2021;19. https://doi.org/10.1016/j.rhisph.2021.100389.

66. Jiang Q-Y, Zhuo F, Long S-H, Zhao H-D, Yang D-J, Ye Z-H, et al. Can arbuscular mycorrhizal fungi reduce Cd uptake and alleviate Cd toxicity of *Lonicera japonica* grown in Cd-added soils? Scientific Reports. 2016;6. https://doi.org/10.1038/srep21805.

67. Ruscitti M, Arango M, Beltrano J. Improvement of copper stress tolerance in pepper plants (*Capsicum annuum* L.) by inoculation with arbuscular mycorrhizal fungi. Theoretical and Experimental Plant Physiology. 2017;29(1):37–49. https://doi.org/10.1007/s40626-016-0081-7.

68. Marrugo-Negrete J, Durango-Hernandez J, Pinedo-Hernandez J, Olivero-Verbel J, Díez S. Phytoremediation of mercury-contaminated soils by *Jatropha curcas*. Chemosphere. 2015;127:58–63. https://doi.org/10.1016/j.chemosphere.2014.12.073.

69. Han Y-H, Liu X, Rathinasabapathi B, Li H-B, Chen Y, Ma LQ. Mechanisms of efficient As solubilization in soils and As accumulation by As-hyperaccumulator *Pteris vittata*. Environmental Pollution. 2017;227:569–577. https://doi.org/10.1016/j.envpol.2017.05.001.

70. Dai H, Wei S, Twardowska I, Han R, Xu L. Hyperaccumulating potential of *Bidens pilosa* L. for Cd and elucidation of its translocation behavior based on cell membrane permeability. Environmental Science and Pollution Research. 2017;24(29):23161–23167. https://doi.org/10.1007/s11356-017-9962-9.

71. Forte J, Mutiti S. Phytoremediation potential of *Helianthus annuus* and *Hydrangea paniculata* in copper and lead-contaminated soil. Water, Air, and Soil Pollution. 2017;228(2). https://doi.org/10.1007/s11270-017-3249-0.

72. Chandra R, Kumar V, Singh K. Hyperaccumulator versus nonhyperaccumulator plants for environmental waste management. In: Chandra R, Dubey NK, Kumar V, editors. Phytoremediation of environmental pollutants. New York: CRC Press; 2017. pp. 43–80. https://doi.org/10.4324/9781315161549.

73. Thakur S, Singh L, Wahid ZA, Siddiqui MF, Atnaw SM, Din MFM. Plant-driven removal of heavy metals from soil: uptake, translocation, tolerance mechanism, challenges, and future perspectives. Environmental Monitoring and Assessment. 2016;188(4). https://doi.org/10.1007/s10661-016-5211-9.

74. Pinto E, Aguiar AARM, Ferreira IMPLVO. Influence of soil chemistry and plant physiology in the phytoremediation of Cu, Mn, and Zn. Critical Reviews in Plant Sciences. 2014;33(5):351–373. https://doi.org/10.1080/07352689.2014.885729.

75. Sharma SS, Dietz K-J, Mimura T. Vacuolar compartmentalization as indispensable component of heavy metal detoxification in plants. Plant Cell and Environment. 2016;39(5):1112–1126. https://doi.org/10.1111/pce.12706.

76. Alvarez A, Saez JM, Davila Costa JS, Colin VL, Fuentes MS, Cuozzo SA, et al. Actinobacteria: Current research and perspectives for bioremediation of pesticides and heavy metals. Chemosphere. 2017;166:41–62. https://doi.org/10.1016/j.chemosphere.2016.09.070.

77. Kotoky R, Rajkumari J, Pandey P. The rhizosphere microbiome: Significance in rhizoremediation of polyaromatic hydrocarbon contaminated soil. Journal of Environmental Management. 2018;217:858–870. https://doi.org/10.1016/j.jenvman.2018.04.022.

78. Thavamani P, Samkumar RA, Satheesh V, Subashchandrabose SR, Ramadass K, Naidu R, et al. Microbes from mined sites: Harnessing their potential for reclamation of derelict mine sites. Environmental Pollution. 2017;230:495–505. https://doi.org/10.1016/j.envpol.2017.06.056.

79. Romano-Armada N, Yañez-Yazlle MF, Irazusta VP, Rajal VB, Moraga NB. Potential of bioremediation and PGP traits in *Streptomyces* as strategies for bio-reclamation of salt-affected soils for agriculture. Pathogens. 2020;9(2). https://doi.org/10.3390/pathogens9020117.

80. Martínez FL, Orce IG, Rajal VB, Irazusta VP. Salar del Hombre Muerto, source of lithium-tolerant bacteria. Environmental Geochemistry and Health. 2019;41(2):529–543. https://doi.org/10.1007/s10653-018-0148-2.

81. Laranjeira S, Fernandes-Silva A, Reis S, Torcato C, Raimundo F, Ferreira L, et al. Inoculation of plant growth promoting bacteria and arbuscular mycorrhizal fungi improve chickpea performance under water deficit conditions. Applied Soil Ecology. 2021;164. https://doi.org/10.1016/j.apsoil.2021.103927.

82. Toussaint J-P, Pham TTM, Barriault D, Sylvestre M. Plant exudates promote PCB degradation by a rhodococcal rhizobacteria. Applied Microbiology and Biotechnology. 2012;95(6):1589–1603. https://doi.org/10.1007/s00253-011-3824-z.

83. Pinter IF, Salomon MV, Berli F, Bottini R, Piccoli P. Characterization of the As(III) tolerance conferred by plant growth promoting rhizobacteria to *in vitro*-grown grapevine. Applied Soil Ecology. 2017;109:60–68. https://doi.org/10.1016/j.apsoil.2016.10.003.

84. Jiang J, Pan C, Xiao A, Yang X, Zhang G. Isolation, identification, and environmental adaptability of heavy-metal-resistant bacteria from ramie rhizosphere soil around mine refinery. 3 Biotech. 2017;7(1). https://doi.org/10.1007/s13205-017-0603-2.

85. Jiang Q-Y, Zhuo F, Long S-H, Zhao H-D, Yang D-J, Ye Z-H, et al. Can arbuscular mycorrhizal fungi reduce Cd uptake and alleviate Cd toxicity of *Lonicera japonica* grown in Cd-added soils? Scientific Reports. 2016;6. https://doi.org/10.1038/srep21805.

86. Yang X, Qin J, Li J, Lai Z, Li H. Upland rice intercropping with *Solanum nigrum* inoculated with arbuscular mycorrhizal fungi reduces grain Cd while promoting phytoremediation of Cd-contaminated soil. Journal of Hazardous Materials. 2021;406. https://doi.org/10.1016/j.jhazmat.2020.124325.

87. Mallick I, Bhattacharyya C, Mukherji S, Dey D, Sarkar SC, Mukhopadhyay UK, et al. Effective rhizoinoculation and biofilm formation by arsenic immobilizing halophilic plant growth promoting bacteria (PGPB) isolated from mangrove rhizosphere: A step towards arsenic rhizoremediation. Science of the Total Environment. 2018;610–611:1239–1250. https://doi.org/10.1016/j.scitotenv.2017.07.234.

88. Lyubun Y, Chernyshova M. Use of rhizobacteria to inoculate agricultural crops grown on arsenic-polluted soil. Journal of Biotechnology. 2010;150. https://doi.org/10.1016/J.JBIOTEC.2010.09.118.

89. Ju W, Liu L, Fang L, Cui Y, Duan C, Wu H. Impact of co-inoculation with plant-growth-promoting rhizobacteria and rhizobium on the biochemical responses of alfalfa-soil system in copper contaminated soil. Ecotoxicology and Environmental Safety. 2019;167:218–226. https://doi.org/10.1016/j.ecoenv.2018.10.016.

90. Shen G, Ju W, Liu Y, Guo X, Zhao W, Fang L. Impact of urea addition and rhizobium inoculation on plant resistance in metal contaminated soil. International Journal of Environmental Research and Public Health. 2019;16(11). https://doi.org/10.3390/ijerph16111955.

91. Li X, Feng C, Chen L, Liu F, Wang L, Luo K, et al. Cultivable rhizobacteria improve castor bean seedlings root and plant growth in Pb–Zn treated soil. Rhizosphere. 2021;19. https://doi.org/10.1016/j.rhisph.2021.100406.

92. Yadav KK, Gupta N, Kumar A, Reece LM, Singh N, Rezania S, et al. Mechanistic understanding and holistic approach of phytoremediation: A review on application and future prospects. Ecological Engineering. 2018;120:274–298. https://doi.org/10.1016/j.ecoleng.2018.05.039.

93. Kullu B, Patra DK, Acharya S, Pradhan C, Patra HK. AM fungi mediated bioaccumulation of hexavalent chromium in *Brachiaria mutica*-a mycorrhizal phytoremediation approach. Chemosphere. 2020;258. https://doi.org/10.1016/j.chemosphere.2020.127337.

ORCID IDs
Margarita Yu. Drozdova https://orcid.org/0000-0002-9499-9470
Anna V. Pozdnyakova https://orcid.org/0000-0002-6854-0850
Maria A. Osintseva https://orcid.org/0000-0002-4045-8054
Varvara I. Minina https://orcid.org/0000-0003-3485-9123

GUIDE FOR AUTHORS FORMATTING REQUIREMENTS FOR ARTICLES

We publish original, previously unpublished English language articles that possess scientific novelty in the field of food industry and related branches of science. The Journal publishes scientific papers, reports, peer reviews, brief scientific communications, letters to the editor, and related news items.

The main requirements for submitted articles are: validity of factual material, clarity and brevity, reproducibility of experimental data. The manuscript should meet the specified formatting standards. Please make sure that the section "Results and discussion" of your article states the novelty of your research.

All manuscripts submitted to the Foods and Raw Materials should be written in US English. The manuscript should contain no less than 10 pages in Microsoft Word text editor, abstract, tables, figures, and references included.

Format instructions

– 20 mm margins;
– single line spacing without automatic hyphenation;
– no extra interspaces between words or gaps between paragraphs;
– Times New Roman, size 10.

Structure

(1) **The type of your manuscript** should be clarified in the upper left corner (scientific article, review article, short message, note or letter, etc).

(2) **Title** (< 10 words) should be informative and reflect the main results of the research. The title of the article should be in lowercase letters, with the exception of the first letter and proper names. Please avoid abbreviations.

(3) **First and last names of the authors** are separated by commas. Paternal and middle names should be contracted to the first letter. Spelling should coincide with your ORCID id. Please mark the name of the author responsible for correspondence with an asterisk*.

(4) **Affiliation** is a formal name of the institution, city, postal address with postal code. The names and locations of institutions or companies should be given for all authors. If several institutions are listed, match the institution and the corresponding author with superscript numbers. Please include the e-mail address of the author responsible for correspondence.

(5) **Abstract** (200–250 words) cannot exceed 2000 characters with spaces. The abstract should be original and completely reflect the main results and novelty of the article. The best way to structure your abstract is to let it follow the structure of the article itself: relevance, tasks and objectives, methods, results, and conclusions. Please avoid meaningless introductory phrases and vague, general statements.

(6) **Keywords** provide < 10 keywords identifying the subject and the result of the research. Remember that it is key words that enable your potential readers to find your article on the Internet.

(7) **Introduction** gives a brief review of the publications related to the matter and proves its relevance. Referenced sources should be indexed in international scientific databases. In-text references should be given in square brackets and numbered [beginning with №1] in order of their appearance in the text. If several sources are quoted, they are given in chronological order. Make sure your introduction reflects the objectives of your research.

(8) **Study objects and methods:**

– Experimental research papers should contain a full description of the subject of the study, consecutive stages of the experiment, equipment, and reagents. Do not forget to specify the original company names of equipment and reagents manufacturers in brackets. If the method you use is not widely known or has been considerably modified, please provide a brief description.

– Theoretical research papers should specify objectives, approximations and assumptions, conclusions and equations. Please do not overload your text with intermediate data and description of well-known methods (such as numerical methods of solving equations) unless you have introduced some novelty into them.

(9) **Results and discussion** should provide a concise description of experimental data. Rather than repeating the data given in tables and graphs, the text should seek to reveal the principles detected. While describing your research results, it is recommended to use the Past Indefinite verb tense. The discussion should not reiterate the results. The discussion should contain an interpretation of the obtained research results (compliance of the results with the research hypothesis, generalisation of the research results, suggestions for practical application and future research).

Each **table** should be made in MS Word (Table – Add Table) or MS Excel and contain no less than three columns. Provide a number and a title for each table.

The Journal publishes color photographs and diagrams.

Mathematical equations should start with a separate line and be typed in the MathType frame as a whole. Mind that it is not allowed to compile formulae from composite elements (e.g. one part of the formula is a table, another part is a text, and some other part is an embedded frame). Please maintain the common settings for fonts, the size of characters and their placement in MathType formulas. Please avoid manual change for individual symbols or formula elements.

(10) **Conclusion** briefly summarises the main results of your research. Naturally, the conclusion should contain the answer to the question posed by the introduction.

(11) **Conflict of interest** should indicate a real or potential conflict of interest. If there is no conflict of interests, you should write that "the author declares that there is no conflict of interest".

(12) **Acknowledgements** contains expression of gratitude to those who contributed to the research.

(13) **Funding** indicates how the research and the publication of this article were funded. If the study was performed with the support of a grant, specify the number of the grant and its name. State the name of your employer if the study was performed as part of your routine work and did not receive additional funding.

(14) **References** should be formatted according to the standard defined by the editors. The references are given in the order of their appearance in the text. Make sure you have included the DOI, if available.

Please avoid references to publications that are not readily available, e.g. institutional regulations, state standards, technical requirements, unpublished works, proceedings of conferences, extended abstracts of dissertation, and dissertations. Make sure you do not cite unpublished articles. It is not recommended to use more than three references to web resources. Please avoid citing publications that are more than 10 years old.

Self-citation should be well-justified and cannot exceed 10% of the references. Please make sure that at least 50% of the works you cite are less than 5 years old and published in periodicals registered in such data bases as Scopus, Web of Science, etc.

If you mention no references to fresh, 2–3-year-old papers, it might reduce your chances for publication. The references should reflect the actual impact of representatives of the international scientific community on the issue.

The manuscript should be carefully checked and signed by all authors on the first page of the main text. The article will not be published if it fails to meet the requirements. All articles are subject to general editing.

Correspondence and submission of all documents is done by e-mail: fjournal@mail.ru or www.jfrm.ru/en

The editors expect to receive **the following documents**, in Russian or English:

(1) an e-version of your article in MS Word named by the first author's last name (e.g. SmithJ.doc).

(2) a scanned PDF version of your article, the first page signed by all the authors (SmithJ.pdf);

(3) a form with personal information about the author(s). Please do not forget to mark the name of the author responsible for correspondence with an asterisk*. Name the file by the first author's name, e.g., SmithJ_Form.doc;

(4) a scanned PDF version of a cover letter to the editor-in-chief from the responsible organisation with the conclusion about the relevance of the research and recommendations for its publishing. The document should contain the date, reference number, and the signature of the head of the organisation;

(5) a standard copyright agreement.

Please mind that all the files should contain a single document.

For submission instructions, subscription and all other information visit this journals online at www.jfrm.ru/en/

FRM
Foods and Raw Materials, 2021, vol. 9, no. 2
E-ISSN 2310-9599
ISSN 2308-4057
Available online at http://jfrm.ru/en/
DOI: http://doi.org/10.21603/2308-4057-2021-2

CONTENTS